frontiers | Research Topics

Tumor-promoting immune cells: Cancer immune escape and beyond

Edited by
Nicolas Larmonier, Charlotte Domblides and Darya Alizadeh

Published in
Frontiers in Immunology

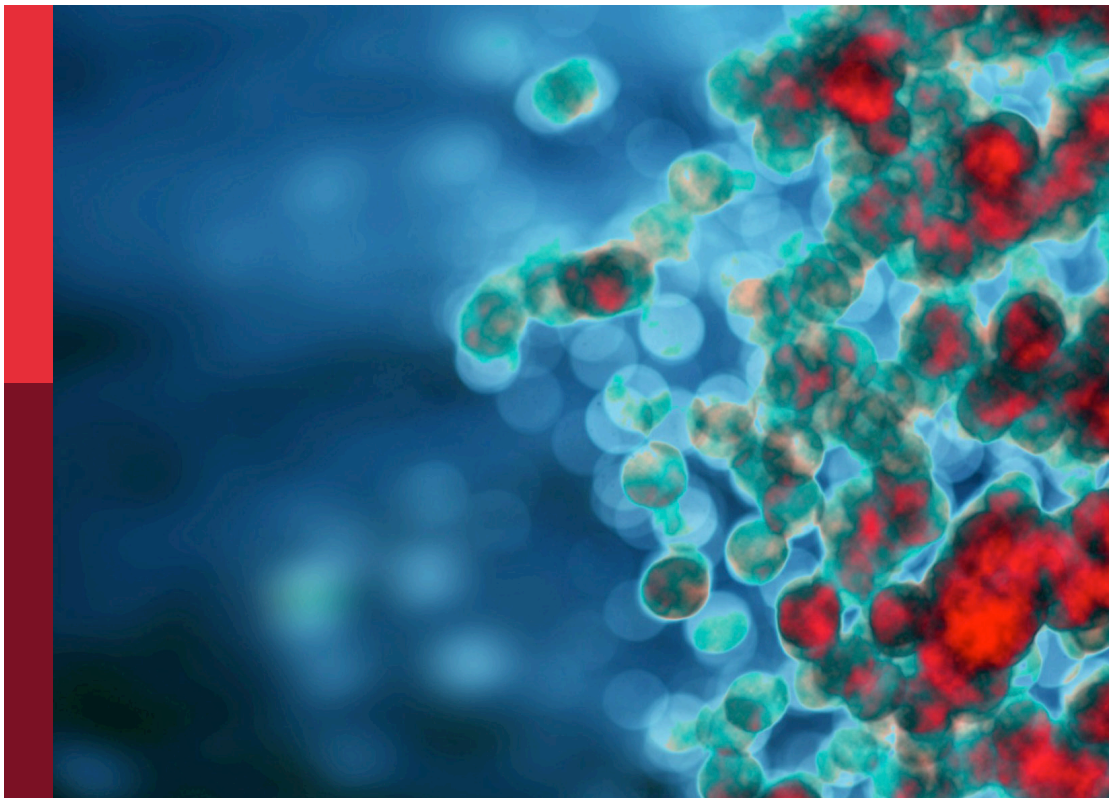

ISSN 1664-8714
ISBN 978-2-83251-950-9
DOI 10.3389/978-2-83251-950-9

About Frontiers

Frontiers is more than just an open access publisher of scholarly articles: it is a pioneering approach to the world of academia, radically improving the way scholarly research is managed. The grand vision of Frontiers is a world where all people have an equal opportunity to seek, share and generate knowledge. Frontiers provides immediate and permanent online open access to all its publications, but this alone is not enough to realize our grand goals.

Frontiers journal series

The Frontiers journal series is a multi-tier and interdisciplinary set of open-access, online journals, promising a paradigm shift from the current review, selection and dissemination processes in academic publishing. All Frontiers journals are driven by researchers for researchers; therefore, they constitute a service to the scholarly community. At the same time, the *Frontiers journal series* operates on a revolutionary invention, the tiered publishing system, initially addressing specific communities of scholars, and gradually climbing up to broader public understanding, thus serving the interests of the lay society, too.

Dedication to quality

Each Frontiers article is a landmark of the highest quality, thanks to genuinely collaborative interactions between authors and review editors, who include some of the world's best academicians. Research must be certified by peers before entering a stream of knowledge that may eventually reach the public - and shape society; therefore, Frontiers only applies the most rigorous and unbiased reviews. Frontiers revolutionizes research publishing by freely delivering the most outstanding research, evaluated with no bias from both the academic and social point of view. By applying the most advanced information technologies, Frontiers is catapulting scholarly publishing into a new generation.

What are Frontiers Research Topics?

Frontiers Research Topics are very popular trademarks of the *Frontiers journals series*: they are collections of at least ten articles, all centered on a particular subject. With their unique mix of varied contributions from Original Research to Review Articles, Frontiers Research Topics unify the most influential researchers, the latest key findings and historical advances in a hot research area.

Find out more on how to host your own Frontiers Research Topic or contribute to one as an author by contacting the Frontiers editorial office: frontiersin.org/about/contact

Tumor-promoting immune cells: Cancer immune escape and beyond

Topic editors

Nicolas Larmonier — Université de Bordeaux, France

Charlotte Domblides — Centre Hospitalier Universitaire de Bordeaux, France

Darya Alizadeh — Department of Hematology and Hematopoietic Cell Transplantation, United States

Citation

Larmonier, N., Domblides, C., Alizadeh, D., eds. (2023). *Tumor-promoting immune cells: Cancer immune escape and beyond.* Lausanne: Frontiers Media SA.

doi: 10.3389/978-2-83251-950-9

The authors declare that the research was conducted in the absence of any commercial or financial relationships that could be construed as a potential conflict of interest

Table of contents

frontiers | Frontiers in Immunology

TYPE Editorial
PUBLISHED 03 March 2023
DOI 10.3389/fimmu.2023.1168884

OPEN ACCESS

EDITED AND REVIEWED BY
Katy Rezvani,
University of Texas MD Anderson Cancer Center, United States

*CORRESPONDENCE
Nicolas Larmonier
nicolas.larmonier@u-bordeaux.fr
Darya Alizadeh
dalizadeh@coh.org
Charlotte Domblides
charlotte.domblides@chu.fr

†These authors have contributed equally to this work

SPECIALTY SECTION
This article was submitted to Cancer Immunity and Immunotherapy, a section of the journal Frontiers in Immunology

RECEIVED 18 February 2023
ACCEPTED 27 February 2023
PUBLISHED 03 March 2023

CITATION
Domblides C, Alizadeh D and Larmonier N (2023) Editorial: Tumor-promoting immune cells: Cancer immune escape and beyond. *Front. Immunol.* 14:1168884. doi: 10.3389/fimmu.2023.1168884

Editorial: Tumor-promoting immune cells: Cancer immune escape and beyond

Charlotte Domblides[1,2,3*†], Darya Alizadeh[4*†] and Nicolas Larmonier[1,3*†]

[1]Centre National de la Recherche Scientifique (CNRS) Unité Mixte de Recherche (UMR) 5164, ImmunoConcEpT, University of Bordeaux, Bordeaux, France, [2]Department of Medical Oncology, Bordeaux University Hospital, Bordeaux, France, [3]Biological and Medical Sciences Department, University of Bordeaux, Bordeaux, France, [4]T Cell Therapeutics Research Labs, Cellular Immunotherapy Center, Department of Hematology and Hematopoietic Cell Transplantation, City of Hope, Duarte, CA, United States

KEYWORDS

immunosuppression, cancer immune escape, myeloid cells, Treg - regulatory T cell, tumor microenvironment, immunosuppressive immune cells, immunotherapies

Editorial on the Research Topic
Tumor-promoting immune cells: Cancer immune escape and beyond

Most cancers emerge and develop in a dedicated tumor-promoting environment. Compelling evidence has been provided that immune cells critically contribute to, and shape this tumor landscape. Efficient protective innate and adaptive anti-tumoral immune responses, primarily attributed to diverse immune effector subsets, such as cytotoxic $CD8^+$ T lymphocytes (CTL), $CD4^+$ helper T lymphocytes (Th), γδ T cells, Natural Killer cells (NK), NKT, dendritic cells or anti-tumoral macrophages, are profoundly altered in this context. Conversely, many different populations of immunosuppressive immune cells play a central role in the mechanisms of cancer escape from anti-tumor immunity. These tumor-induced, tumor-promoting immune subsets include cells of the lymphoid lineage (a large variety of immunosuppressive $CD4^+$ and $CD8^+$ "regulatory T lymphocytes", Tregs), and of myeloid origin (primarily tumor-associated macrophages (TAMs), tumor-associated neutrophils (TANs), tolerogenic dendritic cells (tDC) and immature subsets of myeloid cells endowed with immunosuppressive properties that have collectively been termed "myeloid-derived suppressor cells" (MDSCs)). Induced by tumor-derived factors, these cells accumulate in the tumor microenvironment, but also at the sites of priming of anti-tumoral immune responses, in the bloodstream and in the metastatic niches. Increased frequency of these immune cell populations usually (but not always) correlates with a negative prognostic and relapse of many cancer patients. The modalities by which these cells impair the different steps of anti-tumoral immune responses have been extensively deciphered and involve very broad mechanisms, including the production of soluble and/or membrane-bound immunosuppressive factors such as Tumor Growth Factor (TGF)-β, and/or the expression of enzymes involved in amino acid metabolism such as indoleamine 2,3-dioxygénase (IDO) or arginase (Arg).

However, beyond their cardinal immunosuppressive properties, most of these immune lymphoid or myeloid subsets can also exhibit multiple "non-immunological" tumor-

promoting functions. Some of these populations can indeed directly enhance tumor cell survival and proliferation, contribute to the epithelial-to-mesenchymal transition (EMT) and to cancer cell stemness, participate to local tissue invasion, foster blood or lymphatic vessel intravasation and extravasation of migrating cancer cells. Additionally, it has been reported that some subsets of myeloid cells can associate with circulating tumor cells, protecting them in the bloodstream and can prepare the pre-metastatic niches thus enhancing malignant cell metastasis. In addition, the contribution of these cells to cancer resistance to chemotherapeutic agents and to endocrine therapies has also been widely described.

As these immunosuppressive T lymphocytes and myeloid cells significantly participate to most key processes responsible for tumor development and dissemination, their therapeutic targeting (elimination, inactivation or reprogramming) has consistently been associated with successful anti-tumor responses. Unfortunately, the extreme phenotypic and functional heterogeneity and the high degree of plasticity of these cells in time and space has prevented their systematic use as reliable biomarkers and represents a current challenge in the development of therapeutic approaches to selectively inhibit their generation, development, and multiple tumor-promoting functions. In this Research Topic of *Frontiers in Immunology*, contributing authors focus on the limits related to current classifications of suppressive myeloid cells based on their phenotype, functions and metabolic characteristics in different cancer types, on the contribution of recent single-cell technics to the identification of these cells and on the role and mechanisms of action and regulation of regulatory T lymphocytes and suppressive myeloid cell subsets in the tumor environment. Therapeutic interventions to overcome the tumor-promoting effects of these immune cells in cancers are further assessed and discussed.

In a systematic review assessing the multifaced tumor-promoting functions of dedicated subpopulations of myeloid cells in breast cancers, Blaye et al. highlight the challenges related to the heterogeneous nature of these cells and the phenotypical and functional overlaps between subsets. Current pitfalls preventing the unequivocal discrimination of distinct subsets of suppressive myeloid cells are discussed. This problem is particularly striking in the case of Polymorphonuclear (PMN)-MDSC and immunosuppressive neutrophils, prompting the authors to propose to globally name these cells IMCGL (immunosuppressive myeloid cells of the granulocytic lineage). The value of individual subsets as biomarkers and potential therapeutic targets, and whether distinct subsets may be endowed with one unique or with multiple specialized tumor-promoting functions, concomitantly or acquired over time remain important issues to be addressed in the future. Along these lines, Larkin et al. address the complexity of the myeloid landscape, a predominant element of glioblastoma (GBM) microenvironment, and particularly emphasize the origins and heterogeneity of macrophage subsets in GBM. The authors extensively analyze and discuss the main breakthroughs made by recent single-cell technologies (specifically scRNA-seq and CyTOF) at the transcriptomic and proteomic levels, towards a deeper and more precise characterization of myeloid cells in GBM. The authors also assess the possibilities to further harness these technologies before and after patient therapy to explore mechanisms of resistance or response to therapies. The limits and future improvements of these approaches are further discussed. Similarly, Lin et al. review the main myeloid elements of the glioma environment including glioma-associated macrophages/microglia, neutrophils, dendritic cells and MDSCs, with a specific emphasis on the cross-talks between these cells and malignant cells, and on their ambivalent roles (pro- *versus* anti-tumoral) in cancer development. Specific targeting of these glioma-associated myeloid cells is considered. In a focused review, Chen et al. provide an extensive description of the characteristics (composition in proteins and RNAs) and impact of exosomes produced by MDSC associated with different tumors on cancer immunity, angiogenesis, metastasis and resistance to therapies. The underlying mechanisms of action of these extracellular vesicles and their potential prognostic and therapeutic values are detailed and discussed. In an effort to further comprehend the implications of MDSC in immune escape mechanisms in melanomas, Marguier et al. extensively studied the characteristic of a novel subset of monocytic MDSC that overexpress the receptor for the pro-angiogenic factor angiopoietin 2 (Tie-2). The authors specifically demonstrate that Tie-2-expressing MDSC exhibiting immunosuppressive features are increased in melanoma patients, and that, interestingly, stimulation of Tie-2 signaling enhances the immunosuppressive functions of these cells. These results thus suggest that targeting Tie-2/angiopoietin axis may offer a potential new therapeutic option to improve immunotherapies. Using melanoma and lung cancer mouse models, Papafragkos et al. highlight the implication of the NLRP3 inflammasome in MDSC function, particularly showing that monocytic and granulocytic MDSC suppressive activity is impaired in NLRP3 KO mice. The authors further provide data suggesting that inhibition of NLRP3 using pharmacologic agents also alter MDSC activities, resulting in reduced tumor development and advocating for a possible interest in NLRP3 targeting to augment the efficacy of immune-based therapies.

Analyzing the lung microenvironment of non-small cell lung cancer patients (NSCLC), Heim et al. detected IL-9 and IL-21 production by both tumor-infiltrating T lymphocytes (TIL) and by malignant cells and demonstrate the presence of FoxP3-expressing Treg producing IL-9 in the lung microenvironment. Assessing the relevance of these findings in mouse lung cancer models, the authors establish that IL-9 deletion or IL-9 blockade using antibodies leads to inhibition of tumor development. Furthermore, IL-9 receptor-expressing tumor cells, TIL and Treg were identified as target of IL-9. These results thus provide further evidence for the role (and thereby potential targeting interest) of IL-9/IL-9 producing cells in the mechanisms of immune escape in NSCLC. In an analysis by immunohistochemistry of tissue microarrays from rectal cancer patients, Schnellhardt et al. described data further supporting the notion that immunosuppressive FoxP3$^+$ Treg are not always associated with negative prognostic but may conversely represent positive factors depending on the relative abundance of tumor-infiltrating CD8$^+$ T lymphocytes.

In additional articles, Jia et al. review, in the context of primary hepatic carcinoma, the composition, origin, formation, distribution and the controversial prognostic value of tertiary lymphoid structures (TLS), which correspond to ectopic lymphatic edifices containing lymphocytes, myeloid cells, and interstitial cells and involved in tumor immunity, while Wang et al. summarizes the role and modulation of the tumor immune landscape, including suppressive myeloid cells and Treg, in the response or resistance to checkpoint inhibitor anti-PD1 therapies. Yu et al. focus on the possible role and relevance of CD47 in ovarian cancer immune microenvironment and Liu et al. assess the implication of the complement regulatory protein CD55 (DAF, decay acceleration factor) in colon malignancies. Li and Liu discuss the possible prognostic relevance of activator of HSP90 ATPase activity 1 in relation with the tumor immune landscape in different cancer types, and finally, Song et al. review and discuss the regulation and immunosuppressive modes of action of the enzyme IDO1, as one out of many mechanisms of tumor-induced immunosuppression and tumor immune escape.

Author contributions

All authors have equally contributed to the design, structure, writting and proofreading of the manuscript.

Funding

Supported by the French National League Against Cancer (National and Dordogne Commitees), the SIRIC-BRIO (CD, NL), the Cancéropôle Grand-Sud-Ouest (CD, NL), The "Réseau Impulsion Newmoon" (CD, NL), an ITMO Aviesan grant (NL), The Ben and Catherine Ivy Foundation (DA), R01-CA236500 (DA), R01CA254271 (DA), and The Kenneth T. and Eileen L. Norris Foundation (DA).

Conflict of interest

The authors declare that the research was conducted in the absence of any commercial or financial relationships that could be construed as a potential conflict of interest.

Publisher's note

frontiers in Immunology

ORIGINAL RESEARCH
published: 13 December 2021
doi: 10.3389/fimmu.2021.768115

Significance of CD47 and Its Association With Tumor Immune Microenvironment Heterogeneity in Ovarian Cancer

Lan Yu[1,2†], *Yi Ding*[1†], *Ting Wan*[1], *Ting Deng*[1], *He Huang*[1*] *and Jihong Liu*[1*]

[1] *Department of Gynecologic Oncology, State Key Laboratory of Oncology in South China, Collaborative Innovation Center for Cancer Medicine, Sun Yat-Sen University Cancer Center, Guangzhou, China,* [2] *Department of Obstetrics and Gynecology, The First Affiliated Hospital of Guangzhou Medical University, Guangzhou, China*

OPEN ACCESS

Edited by:
Charlotte Domblides, Centre Hospitalier Universitaire de Bordeaux, France

Reviewed by:
Sukhbir Kaur, National Institutes of Health (NIH), United States
Gang Chen, Huazhong University of Science and Technology, China

***Correspondence:**
Jihong Liu
liujih@mail.sysu.edu.cn
He Huang
huangh@sysucc.org.cn

[†]*These authors share first authorship*

Specialty section:
This article was submitted to Cancer Immunity and Immunotherapy, a section of the journal Frontiers in Immunology

Received: *31 August 2021*
Accepted: *23 November 2021*
Published: *13 December 2021*

Citation:
Yu L, Ding Y, Wan T, Deng T, Huang H and Liu J (2021) Significance of CD47 and Its Association With Tumor Immune Microenvironment Heterogeneity in Ovarian Cancer. Front. Immunol. 12:768115. doi: 10.3389/fimmu.2021.768115

Background: It was reported that tumor heterogeneity and the surrounding tumor microenvironment (TME) in ovarian cancer affects immunotherapy efficacy and patient outcomes. And the TME of ovarian cancer is intrinsically heterogeneous. CD47 plays vital roles in cell functional behavior and immune homeostasis relating to cancer prognosis. But how it affects TME and its contribution to heterogeneity in ovarian cancer has not been fully illustrated. Therefore, we aimed to identify a prognostic biomarker which may help explain tumor immune microenvironment heterogeneity of ovarian cancer.

Methods: Cancer single-cell state atlas (CancerSEA) was used to evaluate functional role of CD47. Several bioinformatics database including Oncomine, Gene Expression Profiling Interaction Analysis (GEPIA), Tumor Immune Estimation Resource (TIMER), The Human Protein Atlas (HPA), Ualcan and Kaplan-Meier plotter (KM plotter) were applied to illustrate correlation of CD47 with ovarian cancer prognosis and immune infiltration. Tumor Immune Single-cell Hub (TISCH) single cell database was employed to evaluate correlation of CD47 with tumor microenvironment. GeneMANIA was implemented to identify regulation networks of CD47. Differentially expressed genes (DEGs) between CD47 high and low expression groups were analyzed with R package DESeq2. Kyoto encyclopedia of genes and genomes (KEGG) and Gene Set Enrichment Analysis (GSEA) were utilized to explore how CD47 affect the immune related cell signaling pathway.

Results: CD47 expression was upregulated and connected to worse OS and PFS in ovarian cancer. Close relation was found between CD47 expression level and immune infiltration in ovarian cancer, especially with Treg cells, Monocytes, Macrophages and T cell exhaustion ($P<0.05$). The CD47 expression level was relatively low in plasma cells, dendritic cells and Mono/Macro cells of OV_GSE115007, in myofibroblasts, fibroblasts and endothelial cells of OV_GSE118828, compared to malignant cells of OV_GSE118828 dataset. The cell components and distribution in primary and metastatic ovarian cancer are quite distinct, which may lead to TME heterogeneity of ovarian cancer.

Conclusion: Our results indicated that CD47 is closely correlated to ovarian cancer immune microenvironment and might induce ovarian cancer heterogeneity. Therefore, CD47 may be used as a candidate prognostic biomarker and provide us with new insights into potential immunotherapy in ovarian cancer patients.

Keywords: CD47, scRNA-seq, tumor microenvironment, heterogeneity, ovarian cancer

INTRODUCTION

Ovarian cancer is one of the most lethal malignancies among women worldwide. Even with bulk surgery and adjuvant chemotherapy, it shows a high fatality rate of 70% in late stage patients (1). Despite advances in maintenance therapy of bevacizumab or PARP inhibitors, most ovarian cancer patients have a high recurrence rate within 5 years of diagnosis (2). It was reported that immunotherapy efficacy and patient outcomes were closely related to the tumor heterogeneity and the surrounding tumor microenvironment (TME) in ovarian cancer (3, 4). Because TME of ovarian cancer patients is intrinsically heterogeneous, successful treatments towards ovarian cancer are challenging (4, 5). Therefore, we aimed to identify a prognostic biomarker which may help explain tumor immune microenvironment heterogeneity of ovarian cancer.

CD47 is a transmembrane protein which plays significant roles in cellular functions, such as proliferation, apoptosis, migration and immune homeostasis (6, 7). CD47 is a ligand for signal regulatory protein alpha (SIRPα) which exists on immune cells, for instance, macrophages and dendritic cells (8). SIRPα binds CD47 to initiate a signaling cascade and finally inhibit phagocytosis (9). Besides, CD47 is a receptor of secreted protein thrombospondin-1 (TSP-1). TSP-1 broadly regulates metabolism in TME and causes resistance to cancer treatment (10). Previous studies used CD47 antibody-B6H12 prevented interaction of TSP-1 and SIRPα with CD47 (10, 11). Blockade of CD47 signaling triggers the immune system, reactivates phagocytosis and promotes tumor eradication (12). Therefore, CD47 could be used as an immunologic protection for targeted therapies (6, 7). However, how CD47 might affect TME heterogeneity of ovarian cancer has not been fully investigated. Therefore, it is urgent to elucidate roles of CD47 in ovarian cancer and to illustrate its immune interactions in ovarian cancer microenvironment.

In this study, we investigated the function and heterogeneity expression pattern of CD47 in different immune cells at single-cell level using CancerSEA and TISCH (13, 14). Several other bioinformatics tools including Oncomine, GEPIA, TIMER were used for CD47 expression analysis. The relationship between CD47 and other parameters, for instance, tumor stage, tumor grade, patient's race, patient's age and TP53 mutation status were investigated using Ualcan. KM plotter was used to show how CD47 affect the prognosis of ovarian cancer patients. Moreover, we investigated the correlation of CD47 expression with immune-infiltrating cells in ovarian cancer using TIMER database. To better illustrate CD47 co-expression genes and its regulation networks, Genemania, KEGG and GSEA were further analyzed. This study aims to provide insights into prognosis and immune infiltration-related role of CD47 in ovarian cancer. This study might be a fresh perspective to disclose the reason of heterogeneity of ovarian cancer immune microenvironment.

Abbreviations: SIRPα, signal regulatory protein alpha; cancer single-cell state atlas (CancerSea); GEPIA, Gene Expression Profiling Interaction Analysis; TIMER, Tumor Immune Estimation Resource; KM plotter, Kaplan-Meier plotter; EMT, Epithelial-Mesenchymal Transition; HPA, The Human Protein Atlas; IHC, immunohistochemistry; PFS, progression-free survival; OS, overall survival; HRs, Hazard ratios; M1 cells, macrophage type1 cells; M2 cells, macrophage type2 cells; Treg, regulatory T cells; TAMs, Tumor-associated macrophages.

MATERIALS AND METHODS

Oncomine

Oncomine is a publicly available database (https://www.oncomine.org). It consists online cancer microarray data of 715 datasets, 86,733 cancer and normal tissue samples (15). The Oncomine database was used to illustrate the transcriptional level of CD47 in ovarian cancer. The thresholds were set as follow: *P*-value<1e-4, fold change >2, and gene rank in the top 10%.

GEPIA

The GEPIA database (http://gepia.cancer-pku.cn/) consists of RNA sequencing expression data of 9,736 tumors and 8,587 normal samples derived from the TCGA and GTEx database (16). CD47 expression level in different cancer types versus normal tissues were processed using GEPIA. $P<0.05$ was considered to be statistically significant.

CancerSEA

CancerSEA (http://biocc.hrbmu.edu.cn/CancerSEA/home.jsp) is the first dedicated database to analyze distinct functional states of different cancer cells at single-cell level (13). It involves 14 functional states of 41900 cancer single cells in 25 types of different cancers. Cellular functional states include angiogenesis, apoptosis, cell cycle, differentiation, DNA damage, DNA repair, Epithelial-Mesenchymal Transition (EMT), hypoxia, inflammation, invasion, metastasis, proliferation, quiescence and stemness. The CancerSEA database was used to analyze CD47 function in 14 different states using cancer single cell data.

UALCAN

Ualcan (http://ualcan.path.uab.edu/) is a comprehensive web portal for analyzing cancer OMICS data (17). In this study,

expression of CD47 in ovarian cancer was analyzed in Ualcan based on individual cancer stages, tumor grades, patient's race, patient's age and TP53 mutation status. The expression level of CD47 was normalized as transcript per million reads. $P<0.05$ was considered statistically significant.

The Human Protein Atlas

HPA (https://www.proteinatlas.org/) is an open access protein database (18). It is composed of proteomic data based on 26941 antibodies targeting 17165 unique proteins. CD47 protein expression level between ovarian cancer and normal ovary was verified using immunohistochemistry (IHC).

Kaplan-Meier Plotter

The KM plotter (http://kmplot.com) database evaluates survival of different genes in 21 cancer types including breast (n=6234), ovarian (n=2190), lung (n=3452) and gastric (n=1440) cancer (19). Prognostic values including PFS (progression-free survival) and OS (overall survival) of CD47 were evaluated in ovarian cancers. Four different probes were used to evaluate CD47 related PFS and OS in ovarian cancer. Hazard ratios (HRs) with 95% confidence intervals and logrank *P*-value were determined.

TISCH

TISCH collected data from Gene Expression Omnibus (GEO) (20) and ArrayExpress (21) to formulate its scRNA-seq atlas (14). TISCH includes 79 databases and 2045746 cells from both tumor patients and healthy donors. The datasets were uniformly processed to enable clarifying components of the TME at both single-cell and annotated cluster levels. In this work, we used datasets derived from TISCH to decipher the TME heterogeneity between primary and metastatic ovarian tumor sites at single cell level.

GeneMANIA

GeneMANIA (http://genemania.org/) is a flexible website for predicting protein-protein interactions based on gene functions (22). It indexes 2, 813 interactive functional association networks which includes 660, 443, 499 interactions derived from 9 organisms. In this work, we adopted GeneMANIA to construct the network of CD47 interactive proteins based on physical interactions, co-expression, predicted, co-localization, pathway, genetic interactions, and shared protein domains.

TIMER

TIMER (https://cistrome.shinyapps.io/timer/) is a database for comprehensive analysis of tumor-infiltrating immune cells (23). TIMER database consists of 10897 samples of 32 cancer types from the TCGA database to evaluate immune infiltrates abundance. CD47 expression correlation with six immune infiltrates (B cells, CD4+ T cells, CD8+ T cells, Neutrophils, Macrophages and Dendritic cells) were estimated using TIMER. The gene expression level was assessed using log2 TPM. CD47 was also evaluated with different gene markers of B cell, T cell, CD8+ T cell, Dendritic cell, macrophage type1 cells (M1), macrophage type2 cells (M2), Th1 cell, Th2 cell, regulatory T cells (Treg), monocyte, tumor-associated macrophages (TAM) and T cell exhaustion.

Pathway Analysis

We used TCGA OV RNA-Seq data to find DEGs between CD47 high and low expression groups with R package DESeq2. There are 376 patients in the TCGA OV RNA-Seq dataset. We used quartile method to divide patients into CD47 high and low group. We sorted descending CD47 TPM expression value in all patients, and chose top 94 patients as CD47 high group, and bottom 96 patients as CD47 low group. The genes with *P* value less than 0.05 and log fold change larger than 1 or lower than -1 were considered significant. They were showed in a volcano plot with R package ggplot2. These different up-expression genes were enrichment in KEGG pathways with KOBAS web tool (http://kobas.cbi.pku.edu.cn/), *P* value less than 0.05 was considered significant in statistic. Besides, we also analyzed pathways in GSEA software about CD47 high expression group.

Statistical Analysis

Results generated using CancerSEA was displayed with correlation and *P*-value. GEPIA and Ualcan results were calculated using *P*-value. KM plotter and log-rank tests were utilized to represent the survival curves. Results displayed using Oncomine was processed with *P*-values, fold changes and ranks. The correlation of CD47 with different immune infiltration levels was represented using *P*-value. The DEGs analyses were produced using R software (version 3.6.3). $P<0.05$ was considered statistically significant ($^{*}P<0.05$ $^{**}P<0.01$, $^{***}P<0.001$).

RESULTS

CD47 Expression Levels in Different Types of Cancers

Oncomine database was used to probe into CD47 differential expression at pan-cancer level. The results showed high CD47 expression in head and neck cancer, kidney cancer, myeloma, ovarian cancer, pancreatic cancer and sarcoma (**Figure 1A**). Meanwhile, GEPIA database was used to further validate the results. CD47 was highly expressed in bladder urothelial carcinoma (BLCA), BRCA, CESC, cholangiocarcinoma (CHOL), colon adenocarcinoma (COAD) and ovarian cancer (**Figure 1B**). The data was also evaluated using TIMER database, which showed significant difference ($P<0.05$) in BRCA (1093 tumor vs. 112 normal), CHOL, COAD (457 tumor vs. 41 normal), GBM, HNSC, LUAD (515 tumor vs. 59 normal), LUSC, PRAD, STAD, THCA and UCEC (545 tumor vs. 35 normal) (**Figure 1C**). The results showed that CD47 played different roles in distinct types of cancer. Although TIMER only investigated CD47 expression in 303 ovarian tumor samples but not in adjacent normal tissues, CD47 expression level in ovarian cancer was relatively high.

CD47 Functional States in scRNA-seq Datasets

To explore how CD47 might affect different cancers, we used CancerSEA single-cell database to analyze the correlation of CD47 with 14 distinct functions in 14 types of cancer.

As shown in **Supplementary Figure 1**, correlation of CD47 was analyzed using an interactive bubble chart. The upper bar represents the correlation of CD47 with 14 distinct functional states of all single-cell datasets. Expression of CD47 showed positive correlation with angiogenesis, apoptosis, cell cycle, differentiation, EMT, hypoxia, inflammation, metastasis, proliferation and quiescence. The data showed that CD47 might play a tumor activator role in several types of cancer.

Functional Characteristics of CD47 in Different Cancers

Functional relevance analysis showed that CD47 expression was positively correlated with metastasis in ovarian carcinoma (**Figure 2A**); with DNA repair in renal cell carcinoma (RCC) (**Supplementary Figure 2A**); with inflammation, cell cycle, DNA repair, and proliferation in breast cancer (BRCA) (**Supplementary Figure 2B**); with invasion, quiescence, proliferation, and angiogenesis in prostate cancer (PC) (**Supplementary Figure 2C**); with metastasis, invasion and EMT in head and neck cancer (**Supplementary Figure 2D**); with invasion, EMT, hypoxia and metastasis in glioblastoma (GBM) (**Supplementary Figure 2E**); with metastasis, cell cycle, proliferation and EMT in glioma (**Supplementary Figure 2F**); with inflammation, differentiation, quiescence and hypoxia in astrocytoma (AST) (**Supplementary Figure 2G**); with metastasis, EMT, inflammation and apoptosis in high-grade glioma (HGG) (**Supplementary Figure 2H**); with stemness, inflammation, differentiation and metastasis in Oligodendroglioma (ODG) (**Supplementary Figure 2I**); with no significant correlation in lung adenocarcinoma (LUAD) (**Supplementary Figure 2J**); with quiescence, inflammation, proliferation and differentiation in non-small cell lung cancer (NSCLC) (**Supplementary Figure 2K**); with metastasis, quiescence, apoptosis and inflammation in melanoma (MEL) (**Supplementary Figure 2L**).

However, CD47 is negatively correlated with invasion (R=-0.58; P<0.001) and DNA repair (R=-0.28; P<0.05) in ovarian cancer (**Figure 2A**); with differentiation (R=-0.19; P<0.01) in colorectal cancer (CRC) (**Figure 2B**). These data indicated that CD47 might play different functional roles in ovarian cancer and CRC. Therefore, in this study, we aimed to clarify functional role of CD47 in ovarian cancer.

CD47 Expression Level in Ovarian Cancer Patients

First, we used the HPA database to confirm CD47 expression in ovarian cancer and normal ovary tissue. CD47 expression level in ovarian cancer was significantly higher than that of normal ovary tissue (**Figures 3A, B**). CD47 expression level was notably higher

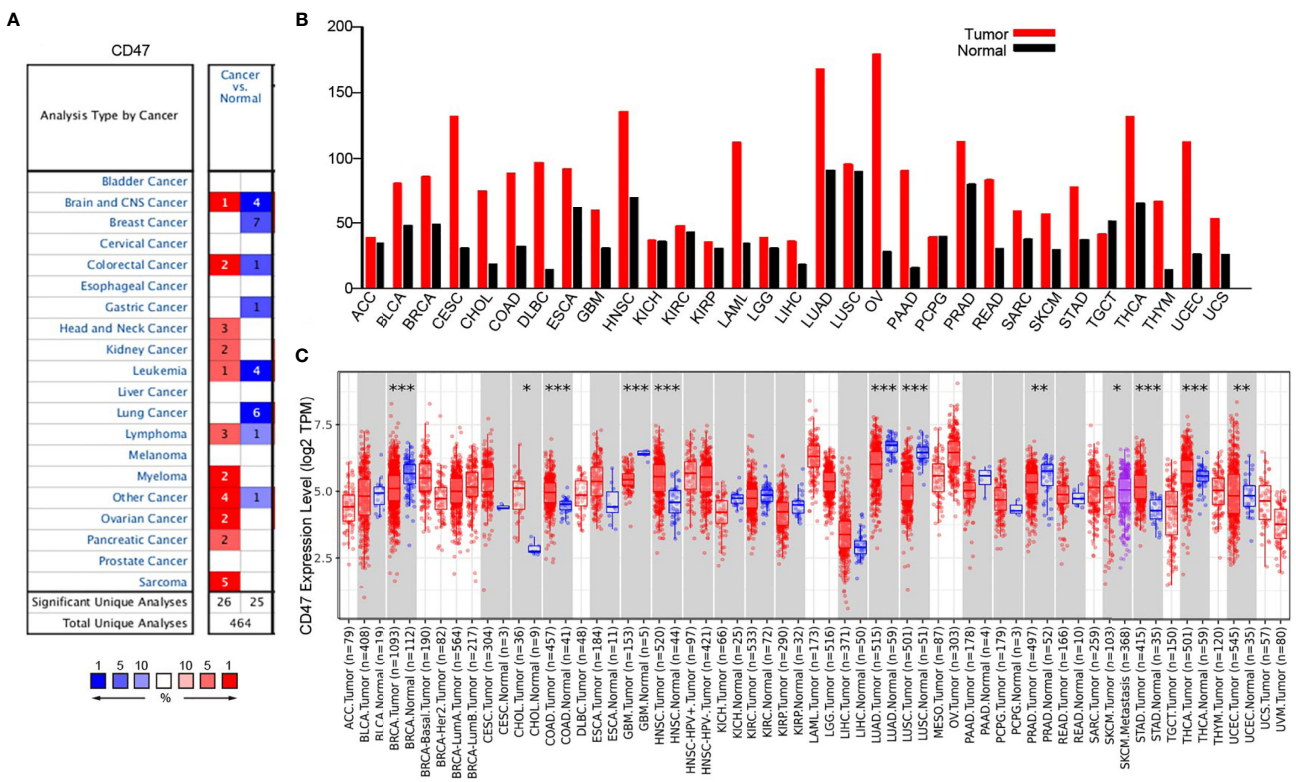

FIGURE 1 | CD47 expression at pan-cancer level. **(A)** CD47 expression level in datasets of distinct cancer types. **(B)** CD47 expression level in different cancers verified using GEPIA database. CD47 was highly expressed in several cancer types, for instance, BLCA, BRCA, CESC, CHOL, COAD and OV. **(C)** CD47 levels in different cancers from TCGA database was represented using TIMER. Significant difference was observed in BRCA, CHOL, COAD, GBM, HNSC, LUAD, LUSC, PRAD, STAD, THCA and UCEC (***p < 0.001, **p < 0.01, *p < 0.05).

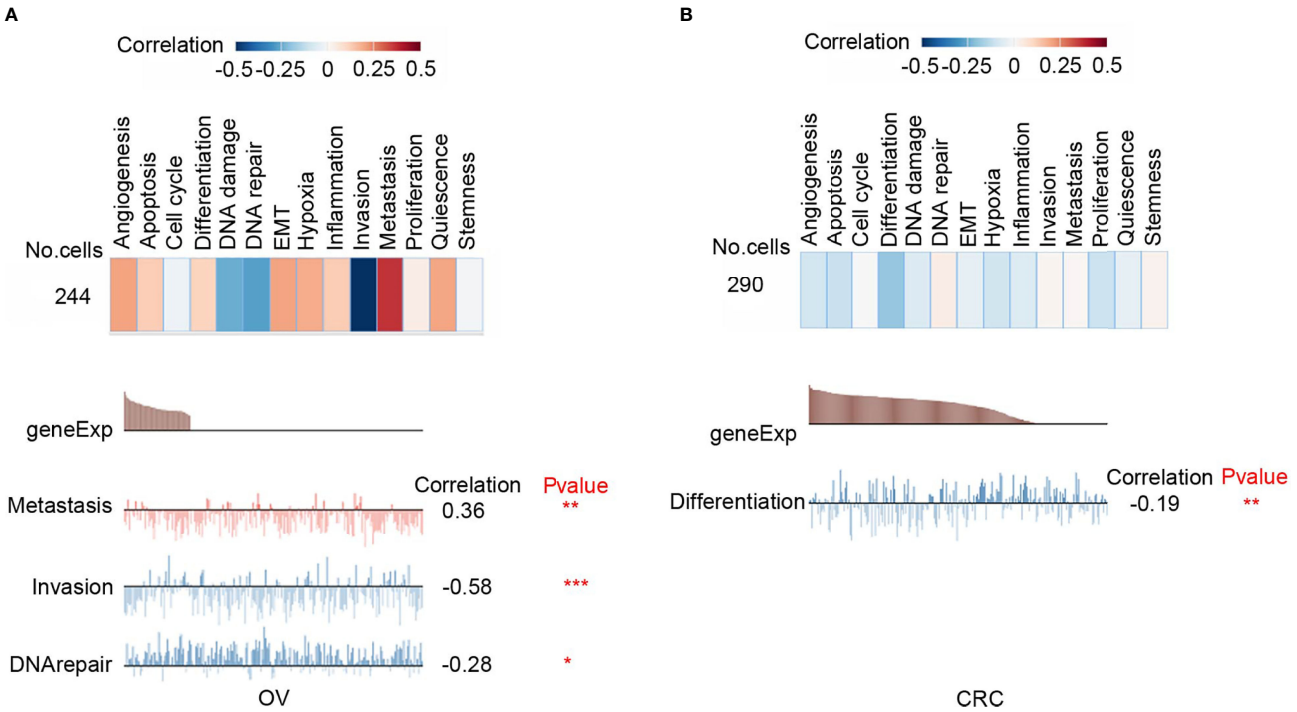

FIGURE 2 | Functional relevance of CD47 in cancers. **(A)** Functional relevance of CD47 in OV. **(B)** Functional relevance of CD47 in CRC. (***p < 0.001, **p < 0.01, *p < 0.05).

in ovarian cancer compared to normal ovarian tissues (P<0.05; num (T)=426; num (N)=88) (**Figure 3C**). Two independent datasets derived from oncomine showed that CD47 was highly expressed in ovarian cancer in Yoshihara Ovarian (P=3.66e-7) and Lu Ovarian (P=3.09e-8) (**Figures 3D, E**). GEPIA and Oncomine results were consistent with the HPA database.

We next investigated CD47 expression based on cancer stages using GEPIA database. Expression level of CD47 in ovarian cancer showed no significant difference among different stages (**Figure 3F**). Ualcan database demonstrated no correlation of CD47 expression with cancer stages, tumor grade, patient's race, patients' age or TP53 mutation status (**Figures 3G–K**). These results suggest that CD47 may serve as a diagnostic tumor marker in ovarian cancer regardless of different pathological parameters.

Prognostic Value of CD47 in Ovarian Cancers

The KM plotter was used as an indicator for evaluating prognostic value of CD47 expression based on Affymetrix microarrays. CD47 mRNA level correlated with overall survival (OS) and progression-free survival (PFS) in ovarian cancer patients. We found that CD47 mRNA expression level was positively correlated with worse OS among all ovarian cancer patients based on four different arrays (HR=1.16 (1.02-1.33), logrank P=0.025 for 211075_s_at; HR=1.18 (1.01-1.37), logrank P=0.033 for 213857_s_at; HR=1.33 (1.09-1.63), logrank P=0.0058 for 226016_at and HR = 1.23 (1-1.51), logrank P = 0.048 for 227259_at (**Figures 4A–D**). We found CD47 mRNA expression level reversely correlated with PFS of ovarian cancer patients with HR=1.29 (1.11-1.49), logrank P=0.00059 for 211075_s_at; HR=1.29 (1.11-1.49), logrank P=0.00078 for 213857_s_at; HR=1.51 (1.25-1.83), logrank P=1.7e-05 for 226016_at and HR=1.36 (1.13-1.65), logrank P=0.0013 for 227259_at (**Figures 4E–H**). The data suggested CD47 to be a potential biomarker for predicting ovarian cancer prognosis.

Correlation Between CD47 and the Tumor Immune Microenvironment Heterogeneity

We used two datasets (OV_GSE115007 and OV_GSE118828) of the TISCH database to evaluate CD47 expression in TME-related immune cells. As to different immune cell types, for instance, plasma cells, dendritic cells and Mono/Macro cells of OV_GSE115007, myofibroblasts, fibroblasts and endothelial cells of OV_GSE118828, the CD47 expression level was relatively low compared to expression level in malignant cells of OV_GSE118828 dataset (**Supplementary Figure 3A**). In OV_GSE118828 dataset, CD47 expression level remains the highest in malignant cells, suggesting high CD47 expression in malignant ovarian cancer cells (**Supplementary Figure 3A**). As to other components of the TME, relatively higher CD47 expression level was observed in CD4 T conventional cells and mono/macro cells of OV_GSE118828 dataset. Violin plot showed the same trend of CD47 expression in the ovarian cancer cell microenvironment (**Supplementary Figure 3B**). In OV_GSE115007, only three cell types were found, including plasma cells, dendritic cells and Mono/Macro cells, while DC cells exhibited the most abundant cell counts (n=3415) (**Figures 5A, B**). And all of the three cell types exhibited CD47

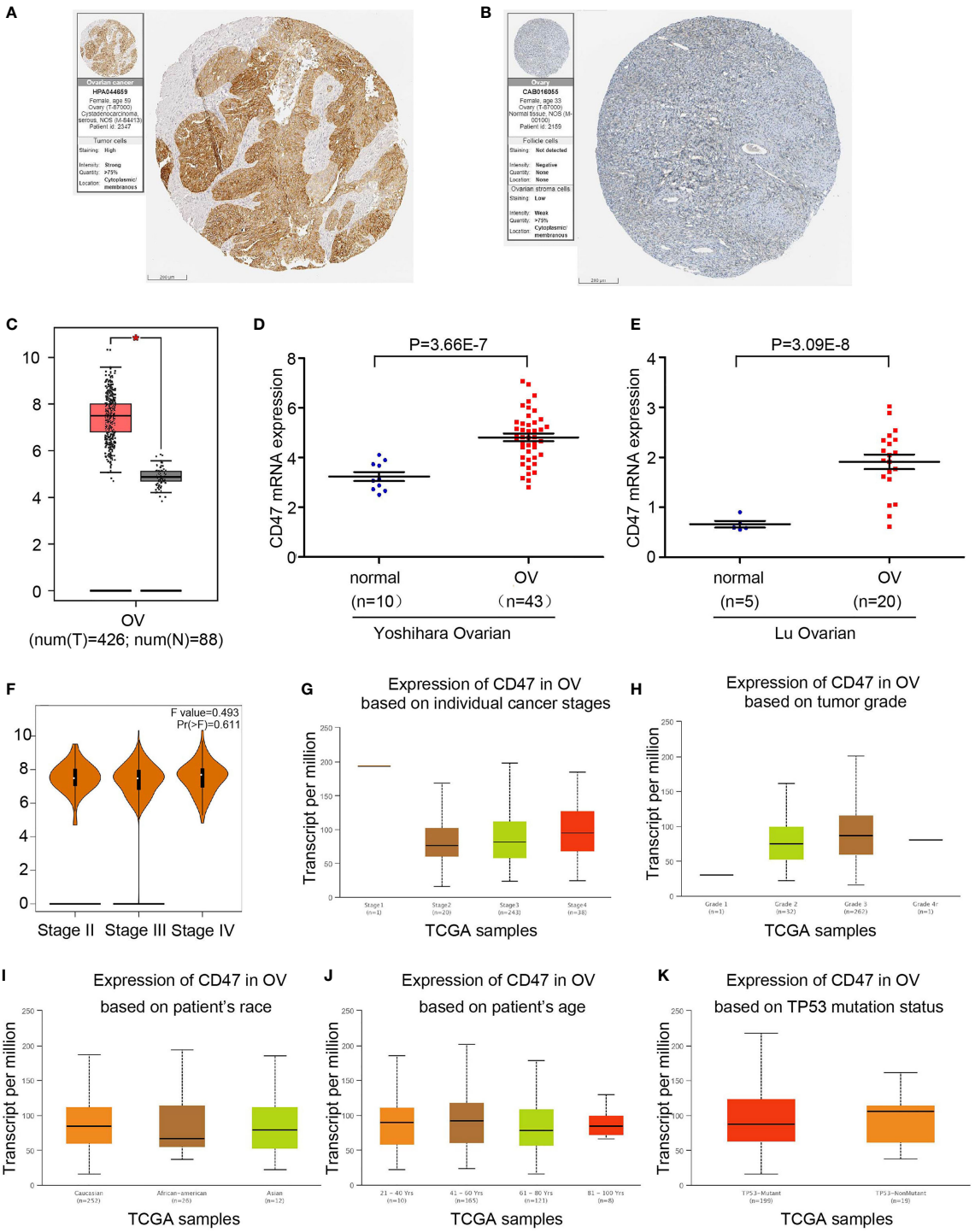

FIGURE 3 | CD47 transcription levels in ovarian cancer. **(A)** Protein levels of CD47 in ovarian cancer tissue. **(B)** Protein levels of CD47 in normal ovary. **(C)** Boxplot shows expression of CD47 in ovarian cancer using GEPIA. **(D)** Box plot shows CD47 mRNA levels in Yoshihara ovarian dataset. **(E)** Box plot shows CD47 mRNA levels in Lu ovarian dataset. **(F)** CD47 expression level has no correlation among different stages in OV. **(G)** Expression of CD47 based on individual cancer stages using Ualcan database. **(H)** Expression of CD47 based on tumor grades. **(I)** Expression of CD47 based on patient's race. **(J)** Expression of CD47 based on patient's age. **(K)** Expression of CD47 based on TP53 mutation status. For all the analysis, $p<0.05$ was considered statistically significant.

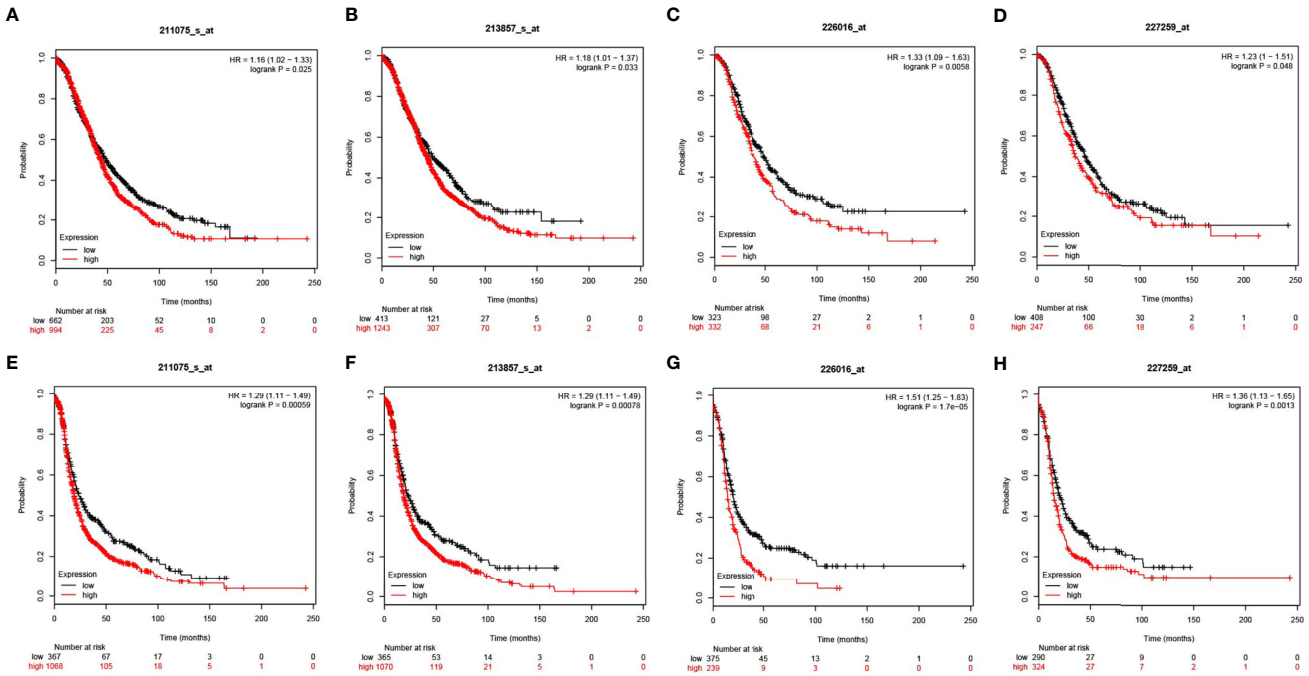

FIGURE 4 | Prognostic values of CD47 in OV using different probes. CD47 OS in OV using probes of **(A)** 211075_s_at, **(B)** 213857_s_at, **(C)** 226016_at, **(D)** 227259_at. CD47 PFS in OV using probes of **(E)** 211075_s_at, **(F)** 213857_s_at, **(G)** 226016_at, **(H)** 227259_at.

expression at a lower level compared to malignant cells in OV_GSE118828 dataset. While in OV_GSE118828 dataset, six cell types were found, with the highest number of 793 to malignant cells (**Figures 5C, D**). Because it was reported that the OV_GSE115007 contains only tumor ascites from primary ovarian cancer patients and OV_GSE118828 dataset contains both primary and metastatic tumor sites (24, 25), we got the fact that the cell components and distribution in primary ovarian cancer ascites and metastatic ovarian cancers are quite distinct. **Figures 5E, F** represented the distribution of various immune cells related to **Figures 5B, D**. These results suggest that CD47 expression level was quite different in distinct cell types with the highest in malignant ovarian cancer cells and the cell components of primary and metastatic patients are different, which might be the source of ovarian cancer microenvironment heterogeneity.

CD47 Expression Is Correlated With Immune Infiltration in Ovarian Cancer

To further clarify ovarian cancer microenvironment and how CD47 might affect ovarian cancer heterogeneity and prognosis, we investigated whether CD47 was related to immune infiltration. TIMER database was used to estimate immune infiltration levels in ovarian cancer. CD47 expression was positively correlated with CD8+ T cell infiltration (r=0.102, p=2.48e-02), CD4+ T cell (r=0.107, p=1.90e-02), Neutrophil (r=0.246, p=4.50e-08) and dendritic cell (r=0.162, p=3.71e-04), negatively correlated with tumor purity (r=-0.17, p=1.73e-04). No correlation was observed with B cell (r=0.074, p=1.04e-01) and macrophage (r=0.076, p=9.81e-02) (**Figure 6A**). In addition, we evaluated CD47 expression with other immune cells markers. The results showed that CD47 was not correlated with B cell (**Figure 6B**), CD8+ T cell (**Figure 6D**), dendritic cell (**Figure 6E**) and Th2 cell (**Figure 6I**), but correlated with other immune cells of T cell (**Figure 6C**), M1 cell (**Figure 6F**), M2 cell (**Figure 6G**), Th1 cell (**Figure 6H**), Treg cell (**Figure 6J**).

To illustrate whether CD47 is correlated with other immune infiltrating cells, we also analyzed its correlation with monocyte and TAM cells. CD47 expression was positively correlated with monocyte and TAM infiltration in ovarian cancer (**Supplementary Figures 4A, B**). We then evaluated correlation of T cell exhaustion biomarkers PD1 (PDCD1), CTLA4, LAG3 and HAVCR2 with the expression of CD47 in ovarian cancer (**Supplementary Figure 4C**). The results showed that CD47 was positively correlated with T cell exhaustion. In summary, the above results suggested that CD47 expression might affect the TME through regulating immune cell infiltration.

Interaction Networks Between CD47 and Its Interactive Genes

We analyzed the interactive networks of CD47 with its interactive genes using the GeneMANIA database (**Supplementary Figure 5**). The circle represented CD47 gene located at center of the interaction network. CD47 gene was surrounded by 20 circles representing genes showing close relation based on physical interactions, co-expression, predicted, co-localization, pathway, genetic interactions and shared protein domains. The top five genes included the signal regulatory protein gamma (SIRPG), SIRPα, src kinase associated

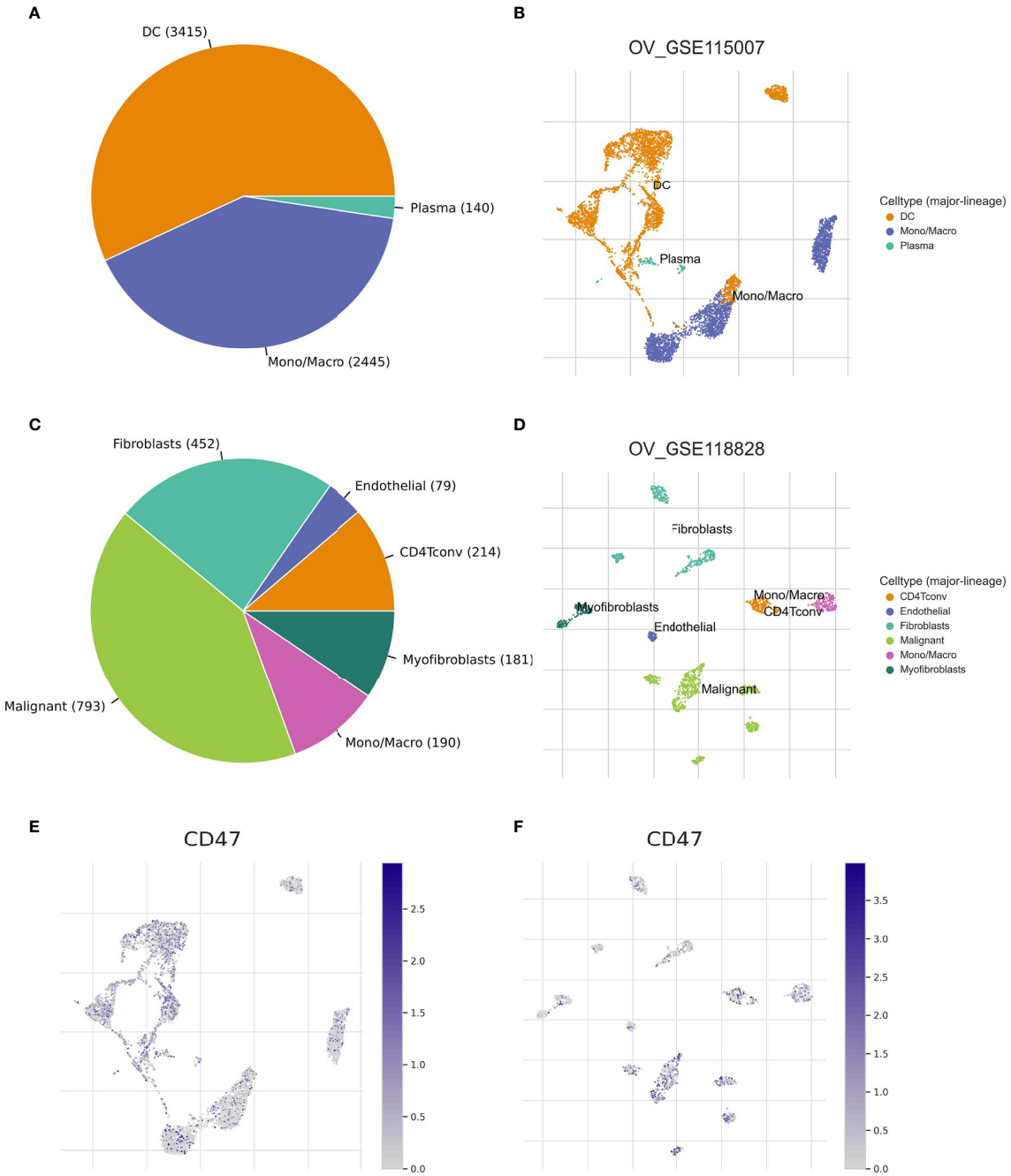

FIGURE 5 | CD47-related cell type distribution using scRNA seq database. **(A–D)** The cell types and their distribution in OV_GSE115007 and OV_GSE118828 datasets. **(E, F)** Distribution of CD47 in different cells in OV_GSE115007 and OV_GSE118828 datasets.

phosphoprotein2 (SKAP2), protein tyrosine kinase 2 beta (PTK2B) and the thrombosondin1 (THBS1) gene. The five genes displayed greatest correlation with the CD47 gene. Further analysis showed that these 20 closely correlated genes were related with functions of cell adhesion mediator activity, leukocyte migration, cell-substrate adhesion, regulation of reactive oxygen species metabolic process, leukocyte cell-cell adhesion, cellular extravasation and sulfur compound binding.

Immune-Related Pathways Regulated by CD47 in Ovarian Cancer

To explore the association of CD47 high expression with immune regulation, we performed KEGG and GSEA analysis. First, we found CD47 high expression associated DEGs in ovarian cancer (**Figure 7A**). Then, KEGG pathway enrichment was performed to explore the biological processes related to CD47 high expression in ovarian cancer. Biological processes

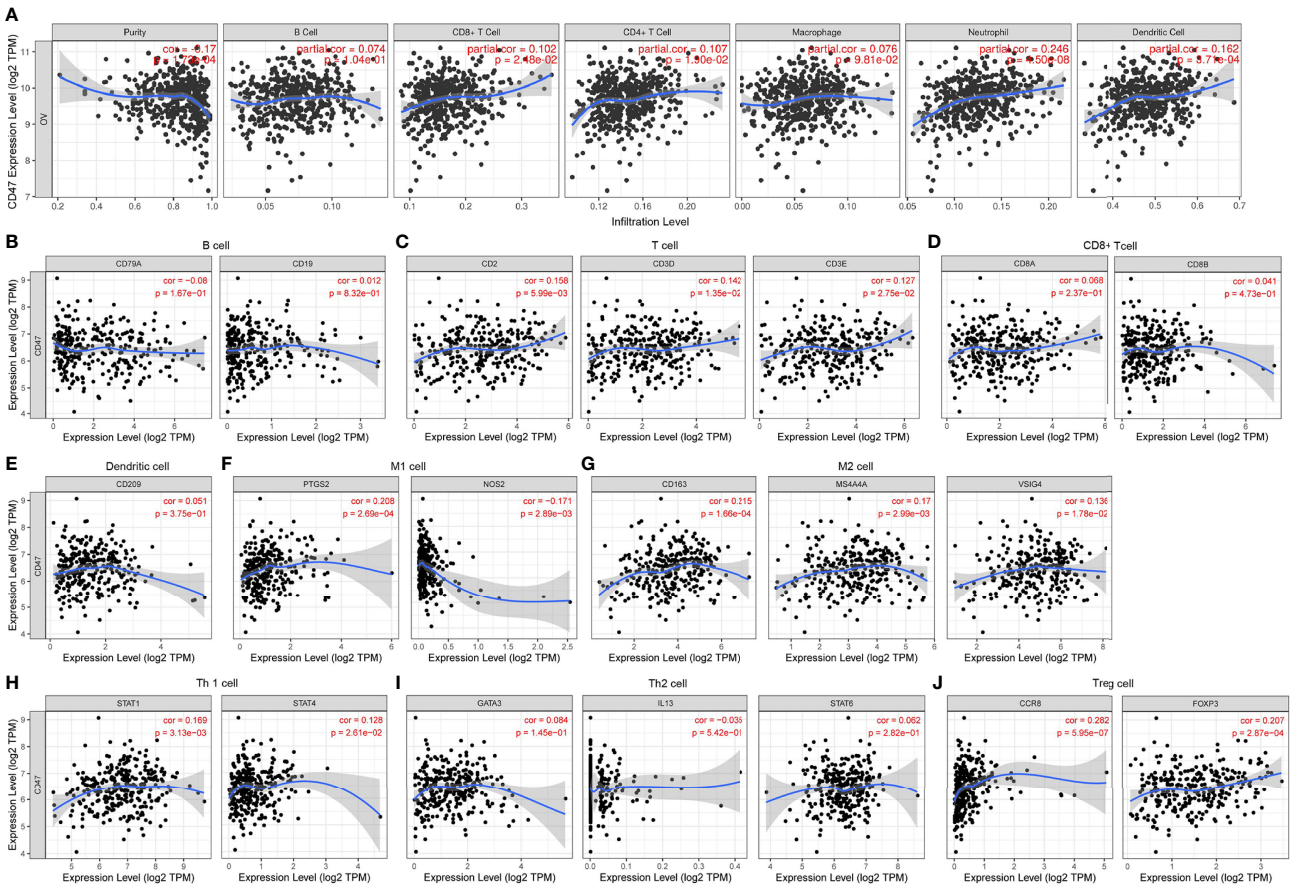

FIGURE 6 | Expression of CD47 is related to a panel of gene markers of immune cells. **(A)** The relation of CD47 expression and immune cell infiltration in OV using TIMER. Relation of CD47 is analyzed with gene markers of **(B)** B cell, **(C)** T cell, **(D)** CD8+ T cell, **(E)** Dendritic cell, **(F)** M1 cell, **(G)** M2 cell, **(H)** Th1 cell, **(I)** Th2 cell, **(J)** Treg cell.

were mainly involved in cytokine-cytokine receptor interaction, IL-17 signaling pathway, TNF signaling pathway, chemokine signaling pathway, NF-kappa B signaling pathway, NOD-like receptor signaling pathway, PI3K-Akt signaling pathway and Toll-like receptor signaling pathway (**Figure 7B**). According to GSEA analysis, high CD47 expression was mainly involved in the process of toll-like receptor signaling pathway (NES=2.05, p-value=0.0), NOD-like receptor signaling pathway (NES=2.01, p-value=0.0), chemokine-signaling pathway (NES=1.90, p-value=0.0) and cytokine-cytokine receptor interaction pathways (NES=1.86, p-value=0.0) (**Figure 7C**). Accordingly, these above data suggest that CD47 high expression is closely linked to ovarian cancer cell immune cell infiltration and thus might affect TME and induce ovarian cancer heterogeneity.

DISCUSSION

CD47 was reported to be involved in various biological processes, including neutrophil migration, macrophage phagocytosis, immune system homeostasis and other immune-related cellular processes (26, 27). Increased CD47 impression has been reported in ovarian cancer (28, 29). Blockade of CD47 signaling reactivates phagocytosis and promotes tumor eradication (6, 7). However, how CD47 might be correlated with ovarian cancer immune microenvironment and lead to tumor heterogeneity has not been fully studied.

Firstly, we used oncomine, GEPIA and TIMER databases to investigate CD47 expression at pan-cancer level. We found CD47 highly expressed in many types of cancers, including ovarian cancer (**Figure 1**). To illustrate functional roles of CD47, scRNA-seq database-CancerSEA was further implemented. We found CD47 positively connected to various functions in most cancer types. However, in ovarian cancer, CD47 was positively correlated to metastasis, negatively correlated to invasion and DNA repair (**Figure 2**). The distinct functional roles of CD47 in ovarian cancer might be due to inherent heterogeneity in ovarian cancer or the small amount of single cells collected using scRNA-seq data.

To further explain correlation of CD47 with prognosis of ovarian cancer, we used several bioinformatics database including HPA, oncomine, GEPIA, Ualcan and KM plotter.

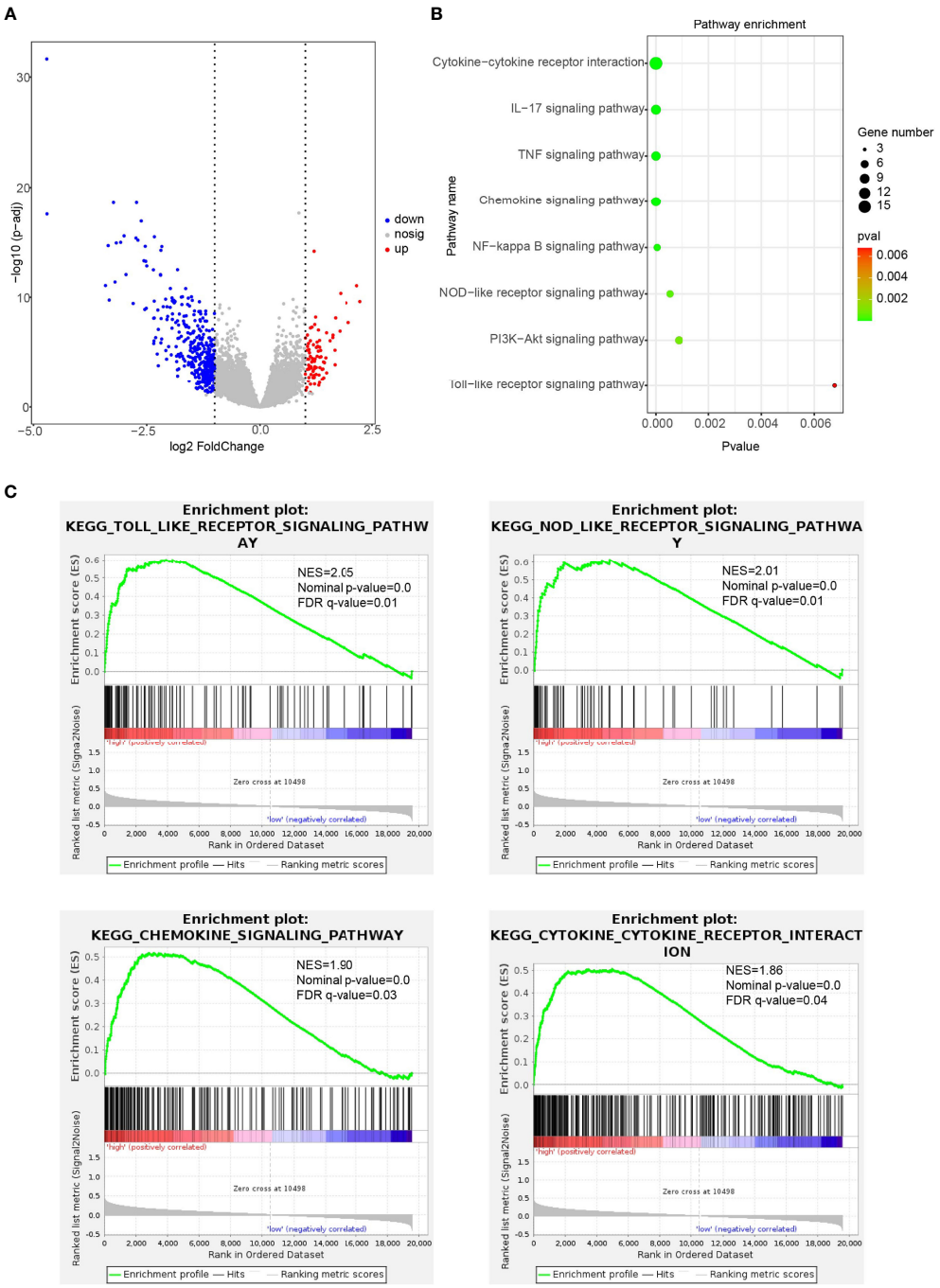

FIGURE 7 | Immune-related pathways regulated by CD47 in ovarian cancer detected using KEGG and GSEA analysis. **(A)** CD47 high expression associated DEGs in ovarian cancer. **(B)** Biological processes related to CD47 high expression in ovarian cancer. **(C)** GSEA analysis revealed CD47 expression involved in the process of different pathways.

The results showed that CD47 was highly expressed in ovarian cancer which was consistent with previous reports (12, 29). HPA database confirmed the result using immunohistochemistry. Ualcan concluded that CD47 expression level was independent of patients' stages, grades, age, race, or TP53 mutation status. Higher CD47 expression was connected to poorer OS and PFS in ovarian cancer. Together we found strong evidence that CD47 might be used as a prognostic biomarker in ovarian cancer patients.

It is well known that the TME of ovarian cancer is highly heterogeneous (30, 31). To clarify how CD47 might affect TME, we used TISCH single cell database. We observed different

immune cell distribution based on primary and primary to metastatic ovarian tumor sites. In OV_GSE115007 dataset, tumor ascites from primary ovarian cancer patients exhibited relatively low CD47 expression levels in plasma cells, dendritic cells and Mono/Macro cells compared to expression level in malignant cells of OV_GSE118828 dataset (**Supplementary Figure 3A**). In contrast, in primary to metastatic ovarian tumor sites, OV_GSE118828 exhibited more cell types, including CD4 T conventional cells, myofibroblasts, fibroblasts and endothelial cells. Higher CD47 expression was observed in mono/macro cells in OV_GSE118828 dataset compared to that of OV_GSE115007 dataset. And that CD47 expression was higher in malignant ovarian cells in OV_GSE118828 dataset. Therefore, the TME in primary and metastatic ovarian cancer might be different, leading to heterogeneity of ovarian cancer.

It was reported that tumor immune cell infiltration might be related to prognosis of cancers (32, 33). Presence of CD8+ T cells in ovarian cancer is associated with prolonged survival (34, 35). Zhou et al. reported the availability of considering immune cells in diagnosis and treatment of colon cancer (36). Burugu et al. suggested that both density and distribution of immune cells could affect prognosis of breast cancer (37). These researches highlight the role of immune infiltration in prognosis of cancers. However, there is limited research probing into the role of CD47 regarding immune infiltration in ovarian cancer. In our study, we used TIMER to investigate different tumor immune cell infiltration in ovarian cancer. The results showed that M2 and Tregs were increasingly infiltrated in high CD47 ovarian cancer microenvironment (**Figure 6**). M2 and Tregs were capable of making immunologic barriers against antitumor immune responses, indicating immune escape in CD47 high expression ovarian cancer (38).

Correlation between CD47 and biomarkers of PD1, CTLA4, LAG3, HAVCR2 showed that CD47 expression level was positively correlated with T cell exhaustion (**Supplementary Figure 4**). Because T cell exhaustion leads to immune escape, therefore, cancer cells get out of control from the immune system (39). In numerous models and clinical trials, CD47 has been blocked to promote phagocytosis. Blockade of CD47 reduced tumor burden both *in vitro* and *in vivo* (40, 41). Therefore, cancer therapies targeting CD47 might be used to treat ovarian cancer.

We next explored the gene networks correlated to CD47. We showed that CD47 expression interacted with SIRPG, SIRPA, SKAP2, PTK2B, TSP-1 and 15 other proteins. These proteins closely related with CD47 were mainly involved with functions of cell adhesion mediator activity, leukocyte migration and leukocyte cell-cell adhesion. These suggested that CD47 might affect ovarian cancer tumorigenesis and prognosis through regulating TME.

KEGG and GSEA analysis indicated that CD47 high expression in ovarian cancer was mainly involved in toll-like receptor signaling pathway, NOD-like receptor signaling pathway, chemokine-signaling pathway and cytokine-cytokine receptor interaction pathways. The results suggested that CD47 might be crucial in regulating tumorigenesis and progression. For instance, the Toll-like receptors (TLRs) are expressed in immune cells as well as tumor cells. Abnormal activation of TLRs can induce immune reaction in tumor cells and thereby modulate the TME (42). NOD-like receptors (NLRs) are reported to be capable of activating innate immune responses (43). NLRs play crucial roles in immune functions, metastasis and tumorigenesis (44, 45). As to chemokine-signaling pathway, chemokines are known to be involved with immune evasion and inflammatory reactions of many kinds of cancers. Chemokine-receptor interactions are reported to be connected to TME modification of cancers (46). Cytokine-cytokine receptor interaction is closely connected with immune reactions. And cytokines are intricately linked with prognosis of patients in various cancers (45, 47). The roles of CD47 might help clarify the mechanism and detailed processes of these pathways.

Accordingly, these above data suggest that CD47 high expression is closely linked to ovarian cancer cell immune infiltration and thus affect TME and might induce ovarian cancer heterogeneity. These findings underscore CD47 expression with different types of immune cell infiltration and T cell exhaustion. Therefore, CD47 high expression might contribute to immune escape, leading to worse prognosis of ovarian cancer.

CONCLUSIONS

In summary, our study showed that increased levels of CD47 could impact the ovarian cancer TME, indicating that CD47 might be used as a potential predictor of ovarian cancer heterogeneity. Moreover, our results demonstrated that CD47 expression level was correlated with ovarian cancer immune infiltration level. Therefore, CD47 might play vital roles in affecting immune infiltration in ovarian cancer microenvironment and be used as a potential target in reversing immune escape and provide insights into understanding the function of CD47 in ovarian cancer prognosis and tumor immunology.

DATA AVAILABILITY STATEMENT

The datasets presented in this study can be found in online repositories. The names of the repository/repositories and accession number(s) can be found in the article/**Supplementary Material**.

AUTHOR CONTRIBUTIONS

LY and YD conceived the idea for the paper and were major contributors in writing the manuscript. TW and TD participated in the design. HH and JL revised the manuscript. LY and JL provided fund. All authors contributed to the article and approved the submitted version.

FUNDING

This work was supported by the National Natural Science Foundation of China (No. 81772782 and No. 81972443), Key

scientific research platforms and research projects of universities in Guangdong Province (2018KQNCX204), the Guangdong basic and applied basic research fund project-regional joint fund (2019A1515110046), and the General guidance project of Health Science and technology in Guangzhou (20201A011074).

ACKNOWLEDGMENTS

We acknowledge all the public databases we used in the study for providing their platforms and contributors for uploading their meaningful datasets.

SUPPLEMENTARY MATERIAL

The Supplementary Material for this article can be found online at: https://www.frontiersin.org/articles/10.3389/fimmu.2021.768115/full#supplementary-material

Supplementary Figure 1 | Relevance of CD47 among 14 functional states in distinct cancers. The upper bar represents the correlation of CD47 with 14 distinct functional states of all single-cell datasets. Red and blue represent positive and negative correlation respectively.

Supplementary Figure 2 | Functional correlation of CD47 in distinct cancers. CD47 shows distinct functional relevance in twelve different cancers. (***p < 0.001, **p < 0.01, *p < 0.05, ns means p > 0.05).

Supplementary Figure 3 | Correlation between CD47 and the tumor immune microenvironment heterogeneity using TISCH. Average expression of CD47 in different cell types **(A)**. Distribution of CD47 expression in different cell types using violin plot **(B)**.

Supplementary Figure 4 | Expression of CD47 is related to immune infiltration of TME in ovarian cancer. Immune infiltration levels represented using gene markers of **(A)** monocyte, **(B)** TAM and **(C)** T cell exhaustion.

Supplementary Figure 5 | Interaction networks between CD47 and its interactive genes using GeneMANIA.

REFERENCES

1. Gorski JW, Ueland FR, Kolesar JM. CCNE1 Amplification as a Predictive Biomarker of Chemotherapy Resistance in Epithelial Ovarian Cancer. *Diagnostics* (2020) 10:279. doi: 10.3390/diagnostics10050279
2. Kuroki L, Guntupalli SR. Treatment of Epithelial Ovarian Cancer. *BMJ* (2020) 371:m3773. doi: 10.1136/bmj.m3773
3. Coukos G, Tanyi J, Kandalaft LE. Opportunities in Immunotherapy of Ovarian Cancer. *Ann Oncol* (2016) 27:11–5. doi: 10.1093/annonc/mdw084
4. Baci D, Bosi A, Gallazzi M, Rizzi M, Noonan DM, Poggi A, et al. The Ovarian Cancer Tumor Immune Microenvironment (TIME) as Target for Therapy: A Focus on Innate Immunity Cells as Therapeutic Effectors. *Int J Mol Sci* (2020) 21(9):3125. doi: 10.3390/ijms21093125
5. Jimenez-Sanchez A, Cybulska P, Mager KL, Koplev S, Cast O, Couturier DL, et al. Unraveling Tumor-Immune Heterogeneity in Advanced Ovarian Cancer Uncovers Immunogenic Effect of Chemotherapy. *Nat Genet* (2020) 52:582–93. doi: 10.1038/s41588-020-0630-5
6. Brightwell RM, Grzankowski KS, Lele S, Eng K, Arshad M, Chen H, et al. The CD47 "Don't Eat Me Signal" Is Highly Expressed in Human Ovarian Cancer. *Gynecol Oncol* (2016) 143:393–7. doi: 10.1016/j.ygyno.2016.08.325
7. Willingham SB, Volkmer JP, Gentles AJ, Sahoo D, Dalerba P, Mitra SS, et al. The CD47-Signal Regulatory Protein Alpha (SIRPa) Interaction Is a Therapeutic Target for Human Solid Tumors. *Proc Natl Acad Sci USA* (2012) 109:6662–7. doi: 10.1073/pnas.1121623109
8. Jiang P, Lagenaur CF, Narayanan V. Integrin-Associated Protein Is a Ligand for the P84 Neural Adhesion Molecule. *J Biol Chem* (1999) 274:559–62. doi: 10.1074/jbc.274.2.559
9. Barclay AN. Signal Regulatory Protein Alpha (SIRPalpha)/CD47 Interaction and Function. *Curr Opin Immunol* (2009) 21:47–52. doi: 10.1016/j.coi.2009.01.008
10. Kaur S, Bronson SM, Pal-Nath D, Miller TW, Soto-Pantoja DR, Roberts DD. Functions of Thrombospondin-1 in the Tumor Microenvironment. *Int J Mol Sci* (2021) 22(9):4570. doi: 10.3390/ijms22094570
11. Kaur S, Cicalese KV, Bannerjee R, Roberts DD. Preclinical and Clinical Development of Therapeutic Antibodies Targeting Functions of CD47 in the Tumor Microenvironment. *Antib Ther* (2020) 3:179–92. doi: 10.1093/abt/tbaa017
12. Liu R, Wei H, Gao P, Yu H, Wang K, Fu Z, et al. CD47 Promotes Ovarian Cancer Progression by Inhibiting Macrophage Phagocytosis. *Oncotarget* (2017) 8:39021–32. doi: 10.18632/oncotarget.16547
13. Yuan H, Yan M, Zhang G, Liu W, Deng C, Liao G, et al. CancerSEA: A Cancer Single-Cell State Atlas. *Nucleic Acids Res* (2019) 47:D900–8. doi: 10.1093/nar/gky939
14. Sun D, Wang J, Han Y, Dong X, Ge J, Zheng R, et al. TISCH: A Comprehensive Web Resource Enabling Interactive Single-Cell Transcriptome Visualization of Tumor Microenvironment. *Nucleic Acids Res* (2021) 49:D1420–30. doi: 10.1093/nar/gkaa1020
15. Rhodes DR, Yu J, Shanker K, Deshpande N, Varambally R, Ghosh D, et al. ONCOMINE: A Cancer Microarray Database and Integrated Data-Mining Platform. *Neoplasia* (2004) 6:1–6. doi: 10.1016/s1476-5586(04)80047-2
16. Tang Z, Li C, Kang B, Gao G, Li C, Zhang Z. GEPIA: A Web Server for Cancer and Normal Gene Expression Profiling and Interactive Analyses. *Nucleic Acids Res* (2017) 45:W98–W102. doi: 10.1093/nar/gkx247
17. Chandrashekar DS, Bashel B, Balasubramanya SAH, Creighton CJ, Ponce-Rodriguez I, Chakravarthi B, et al. UALCAN: A Portal for Facilitating Tumor Subgroup Gene Expression and Survival Analyses. *Neoplasia* (2017) 19:649–58. doi: 10.1016/j.neo.2017.05.002
18. Uhlen M, Zhang C, Lee S, Sjostedt E, Fagerberg L, Bidkhori G, et al. A Pathology Atlas of the Human Cancer Transcriptome. *Science* (2017) 357 (6352):eaan2507. doi: 10.1126/science.aan2507
19. Gyorffy B, Lanczky A, Szallasi Z. Implementing an Online Tool for Genome-Wide Validation of Survival-Associated Biomarkers in Ovarian-Cancer Using Microarray Data From 1287 Patients. *Endocr Relat Cancer* (2012) 19:197–208. doi: 10.1530/ERC-11-0329
20. Barrett T, Wilhite SE, Ledoux P, Evangelista C, Kim IF, Tomashevsky M, et al. NCBI GEO: Archive for Functional Genomics Data Sets–Update. *Nucleic Acids Res* (2013) 41:D991–995. doi: 10.1093/nar/gks1193
21. Athar A, Fullgrabe A, George N, Iqbal H, Huerta L, Ali A, et al. ArrayExpress Update - From Bulk to Single-Cell Expression Data. *Nucleic Acids Res* (2019) 47:D711–5. doi: 10.1093/nar/gky964
22. Warde-Farley D, Donaldson SL, Comes O, Zuberi K, Badrawi R, Chao P, et al. The GeneMANIA Prediction Server: Biological Network Integration for Gene Prioritization and Predicting Gene Function. *Nucleic Acids Res* (2010) 38: W214–220. doi: 10.1093/nar/gkq537
23. Li T, Fan J, Wang B, Traugh N, Chen Q, Liu JS, et al. TIMER: A Web Server for Comprehensive Analysis of Tumor-Infiltrating Immune Cells. *Cancer Res* (2017) 77:e108–10. doi: 10.1158/0008-5472.CAN-17-0307
24. Tang-Huau TL, Gueguen P, Goudot C, Durand M, Bohec M, Baulande S, et al. Human *In Vivo*-Generated Monocyte-Derived Dendritic Cells and Macrophages Cross-Present Antigens Through a Vacuolar Pathway. *Nat Commun* (2018) 9:2570. doi: 10.1038/s41467-018-04985-0
25. Shih AJ, Menzin A, Whyte J, Lovecchio J, Liew A, Khalili H, et al. Identification of Grade and Origin Specific Cell Populations in Serous Epithelial Ovarian Cancer by Single Cell RNA-Seq. *PLoS One* (2018) 13: e0206785. doi: 10.1371/journal.pone.0206785

26. Liu Y, Buhring HJ, Zen K, Burst SL, Schnell FJ, Williams IR, et al. Signal Regulatory Protein (SIRPalpha), a Cellular Ligand for CD47, Regulates Neutrophil Transmigration. *J Biol Chem* (2002) 277:10028–36. doi: 10.1074/jbc.M109720200
27. Chang CL, Wu CC, Hsu YT, Hsu YC. Immune Vulnerability of Ovarian Cancer Stem-Like Cells Due to Low CD47 Expression Is Protected by Surrounding Bulk Tumor Cells. *Oncoimmunology* (2020) 9:1803530. doi: 10.1080/2162402X.2020.1803530
28. Wang CL, Lin MJ, Hsu CY, Lin HY, Tsai HP, Long CY, et al. CD47 Promotes Cell Growth and Motility in Epithelial Ovarian Cancer. *BioMed Pharmacother* (2019) 119:109105. doi: 10.1016/j.biopha.2019.109105
29. Li Y, Lu S, Xu Y, Qiu C, Jin C, Wang Y, et al. Overexpression of CD47 Predicts Poor Prognosis and Promotes Cancer Cell Invasion in High-Grade Serous Ovarian Carcinoma. *Am J Transl Res* (2017) 9:2901–10.
30. Rodriguez-Garcia A, Lynn RC, Poussin M, Eiva MA, Shaw LC, O'Connor RS, et al. CAR-T Cell-Mediated Depletion of Immunosuppressive Tumor-Associated Macrophages Promotes Endogenous Antitumor Immunity and Augments Adoptive Immunotherapy. *Nat Commun* (2021) 12:877. doi: 10.1038/s41467-021-20893-2
31. Kostova I, Mandal R, Becker S, Strebhardt K. The Role of Caspase-8 in the Tumor Microenvironment of Ovarian Cancer. *Cancer Metastasis Rev* (2021) 40:303–18. doi: 10.1007/s10555-020-09935-1
32. Karn T, Jiang T, Hatzis C, Sanger N, El-Balat A, Rody A, et al. Association Between Genomic Metrics and Immune Infiltration in Triple-Negative Breast Cancer. *JAMA Oncol* (2017) 3:1707–11. doi: 10.1001/jamaoncol.2017.2140
33. Tanaka A, Sakaguchi S. Regulatory T Cells in Cancer Immunotherapy. *Cell Res* (2017) 27:109–18. doi: 10.1038/cr.2016.151
34. Le Saux O, Ray-Coquard I, Labidi-Galy SI. Challenges for Immunotherapy for the Treatment of Platinum Resistant Ovarian Cancer. *Semin Cancer Biol* (2020) S1044-579X(20)30193-0. doi: 10.1016/j.semcancer.2020.08.017
35. Ovarian Tumor Tissue Analysis C, Goode EL, Block MS, Kalli KR, Vierkant RA, Chen W, et al. Dose-Response Association of CD8+ Tumor-Infiltrating Lymphocytes and Survival Time in High-Grade Serous Ovarian Cancer. *JAMA Oncol* (2017) 3:e173290. doi: 10.1001/jamaoncol.2017.3290
36. Zhou R, Zhang J, Zeng D, Sun H, Rong X, Shi M, et al. Immune Cell Infiltration as a Biomarker for the Diagnosis and Prognosis of Stage I-III Colon Cancer. *Cancer Immunol Immunother* (2019) 68:433–42. doi: 10.1007/s00262-018-2289-7
37. Burugu S, Asleh-Aburaya K, Nielsen TO. Immune Infiltrates in the Breast Cancer Microenvironment: Detection, Characterization and Clinical Implication. *Breast Cancer* (2017) 24:3–15. doi: 10.1007/s12282-016-0698-z
38. Farhood B, Najafi M, Mortezaee K. CD8(+) Cytotoxic T Lymphocytes in Cancer Immunotherapy: A Review. *J Cell Physiol* (2019) 234:8509–21. doi: 10.1002/jcp.27782
39. Wang JC, Xu Y, Huang ZM, Lu XJ. T Cell Exhaustion in Cancer: Mechanisms and Clinical Implications. *J Cell Biochem* (2018) 119:4279–86. doi: 10.1002/jcb.26645
40. Chao MP, Alizadeh AA, Tang C, Myklebust JH, Varghese B, Gill S, et al. Anti-CD47 Antibody Synergizes With Rituximab to Promote Phagocytosis and Eradicate Non-Hodgkin Lymphoma. *Cell* (2010) 142:699–713. doi: 10.1016/j.cell.2010.07.044
41. Liu X, Pu Y, Cron K, Deng L, Kline J, Frazier WA, et al. CD47 Blockade Triggers T Cell-Mediated Destruction of Immunogenic Tumors. *Nat Med* (2015) 21:1209–15. doi: 10.1038/nm.3931
42. Angrini M, Varthaman A, Cremer I. Toll-Like Receptors (TLRs) in the Tumor Microenvironment (TME): A Dragon-Like Weapon in a Non-Fantasy Game of Thrones. *Adv Exp Med Biol* (2020) 1263:145–73. doi: 10.1007/978-3-030-44518-8_9
43. Sonnessa M, Cioffi A, Brunetti O, Silvestris N, Zito FA, Saponaro C, et al. NLRP3 Inflammasome From Bench to Bedside: New Perspectives for Triple Negative Breast Cancer. *Front Oncol* (2020) 10:1587. doi: 10.3389/fonc.2020.01587
44. Liu P, Lu Z, Liu L, Li R, Liang Z, Shen M, et al. NOD-Like Receptor Signaling in Inflammation-Associated Cancers: From Functions to Targeted Therapies. *Phytomedicine* (2019) 64:152925. doi: 10.1016/j.phymed.2019.152925
45. Yang Y, Zheng Y, Liu X, Ji R, Chen Z, Guo Q, et al. Comprehensive Analysis of Gene Regulation Network and Immune Signatures of Prognostic Biomarker YAP1 in Pancreatic Cancer. *J Cancer* (2020) 11:6960–9. doi: 10.7150/jca.49117
46. Caligiuri A, Pastore M, Lori G, Raggi C, Di Maira G, Marra F, et al. Role of Chemokines in the Biology of Cholangiocarcinoma. *Cancers (Basel)* (2020) 12(8):2215. doi: 10.3390/cancers12082215
47. Lippitz BE. Cytokine Patterns in Patients With Cancer: A Systematic Review. *Lancet Oncol* (2013) 14:e218–228. doi: 10.1016/S1470-2045(12)70582-X

Conflict of Interest: The authors declare that the research was conducted in the absence of any commercial or financial relationships that could be construed as a potential conflict of interest.

Publisher's Note: All claims expressed in this article are solely those of the authors and do not necessarily represent those of their affiliated organizations, or those of the publisher, the editors and the reviewers. Any product that may be evaluated in this article, or claim that may be made by its manufacturer, is not guaranteed or endorsed by the publisher.

frontiers in Immunology

REVIEW
published: 23 December 2021
doi: 10.3389/fimmu.2021.800630

Indoleamine 2,3-Dioxygenase 1: A Promising Therapeutic Target in Malignant Tumor

Xiaotian Song[1,2†], Qianqian Si[1,2†], Rui Qi[1,2], Weidan Liu[3], Miao Li[1,2], Mengyue Guo[1,2], Lin Wei[1,2] and Zhiyan Yao[1,2]*

[1] Department of Immunology, Hebei Medical University, Shijiazhuang, China, [2] Key Laboratory of Immune Mechanism and Intervention on Serious Disease in Hebei Province, Shijiazhuang, China, [3] Department of Clinical Laboratory, The People's Hospital, Pingxiang County, Xingtai, China

Tumorigenesis is a complex multifactorial and multistep process in which tumors can utilize a diverse repertoire of immunosuppressive mechanisms to evade host immune attacks. The degradation of tryptophan into immunosuppressive kynurenine is considered an important immunosuppressive mechanism in the tumor microenvironment. There are three enzymes, namely, tryptophan 2,3-dioxygenase (TDO), indoleamine 2,3-dioxygenase 1 (IDO1), and indoleamine 2,3-dioxygenase 2 (IDO2), involved in the metabolism of tryptophan. IDO1 has a wider distribution and higher activity in catalyzing tryptophan than the other two; therefore, it has been studied most extensively. IDO1 is a cytosolic monomeric, heme-containing enzyme, which is now considered an authentic immune regulator and represents one of the promising drug targets for tumor immunotherapy. Collectively, this review highlights the regulation of IDO1 gene expression and the ambivalent mechanisms of IDO1 on the antitumoral immune response. Further, new therapeutic targets *via* the regulation of IDO1 are discussed. A comprehensive analysis of the expression and biological function of IDO1 can help us to understand the therapeutic strategies of the inhibitors targeting IDO1 in malignant tumors.

Keywords: IDO1, tryptophan, kynurenine, tumor immune escape, immunotherapy

OPEN ACCESS

Edited by:
Charlotte Domblides, Centre Hospitalier Universitaire de Bordeaux, France

Reviewed by:
Lijie Zhai, Northwestern Medicine, United States
Giada Mondanelli, University of Perugia, Italy

***Correspondence:**
Zhiyan Yao
17800600@hebmu.edu.cn

[†]These authors have contributed equally to this work

Specialty section:
This article was submitted to Cancer Immunity and Immunotherapy, a section of the journal Frontiers in Immunology

Received: *23 October 2021*
Accepted: *03 December 2021*
Published: *23 December 2021*

Citation:
Song X, Si Q, Qi R, Liu W, Li M, Guo M, Wei L and Yao Z (2021) Indoleamine 2,3-Dioxygenase 1: A Promising Therapeutic Target in Malignant Tumor. Front. Immunol. 12:800630. doi: 10.3389/fimmu.2021.800630

INTRODUCTION

Tryptophan (Trp) depletion and kynurenine (Kyn) production promote immunosuppression in different tumor types (1, 2). Indoleamine 2,3-dioxygenase 1 (IDO1) catalyzes the first and rate-limiting enzyme of the essential amino acid Trp catabolism and degrades Trp along a pathway known as the Kyn pathway. In this cascade of enzymatic reactions, several biologically active metabolites are produced, such as Kyn, an immunosuppressive metabolite. Finally, nicotinamide adenine dinucleotide (NAD+) and adenosine triphosphate (ATP) in this process are produced to fuel cellular metabolism (3, 4). The main theory about the function of IDO1 is that Trp availability is locally reduced while bioactive metabolites such as Kyn are increased, which mediate immune regulation and immune tolerance involved in the pathological mechanisms of tumor immune escape. In recent years, with the deepening research, the IDO1 function is more complex than

initially assumed. IDO1 is not only an enzyme but also a mediator of a signaling pathway to sustain the regulatory phenotype of a specific set of immune cells (5), which may be associated with the protein conformations of IDO1 in the cells responding to the distinct context (6). Therefore, a full understanding of the expression of IDO1 and biological function may provide more effective immunotherapeutic approaches for a wide range of malignant tumors. Besides IDO1, it has been shown that the other two types of isoenzymes, tryptophan 2,3-dioxygenase (TDO) and indoleamine 2,3-dioxygenase 2 (IDO2), catalyze the same biochemical reaction. However, TDO and IDO2 show higher tissue specificity and much lower enzyme activity than IDO1 that significantly restrict their function in immune regulation. The main role of TDO is involved in maintaining the homeostasis of Trp level and plays a key modulator in brain disease (4, 7, 8). IDO2 was identified as its high homology with IDO1, but the expression and precise activity of IDO2 have not been well elaborated in human tissue due to lower enzyme activity and complexity of human IDO2 transcription (9). Accordingly, this review mainly describes the immunosuppressive mechanisms of IDO1 in tumors.

BASIC FEATURES OF INDOLEAMINE 2,3-DIOXYGENASE 1

IDO1, also known as IDO in the literatures (5, 10), was first identified in rabbit small intestines in 1967. In 1998, IDO1 was described as a molecule associated with immunosuppression in maternal–fetal tolerance (11). It was not until 2006 that the crystal structure of human IDO1 (hIDO1) was first reported (12). In 2017, Lewis-Ballester et al. reported that the crystal structure of the hIDO1–Trp complex and revealed interaction sites of hIDO1 with Trp substrate (13). The resolution of the crystal structure of hIDO1 has shown that it is folded into two domains, including a catalytic large C-terminal domain and a non-catalytic small N-terminal domain, which was connected by a long loop. IDO1 protein contains 403 amino acids, which are intracellular heme-containing dioxygenases (also known as metalloproteins) and encoded by INDO (human chromosome 8p22). Its catalytic activity requires the prosthetic group heme. Along with inactive heme-Fe^{3+} being reduced into active heme-Fe^{2+}, IDO1 catalyzes the oxidative cleavage of Trp to produce the intermediate product *N*-formylkynurenine, which is further hydrolyzed to Kyn. By using Trp depletion and Kyn production, IDO1 is considered as an immunomodulatory enzyme involved in anti-inflammation, tumor immune escape, and immunoregulation to promote maternal tolerance toward the allogeneic fetus, suppressing transplant rejection, regulating autoimmune disorders, and so on. In addition to its enzyme activity, a signaling function has recently been described for the phosphorylated form of immunoreceptor tyrosine-based inhibitory motifs (ITIM1 or ITIM2), located at sites in the small non-catalytic domain and the interconnecting loop of IDO1 protein. Albini et al. confirmed that ITIM-related phosphorylation could upregulate or downregulate IDO1 expression in interleukin-6 (IL-6) or transforming growth factor-β (TGF-β)-dominated environments, which suggest that the ITIMs in IDO1 not only control its own stability but also participate in a self-maintaining immunological modulation (14). Therefore, the appropriate regulation of the phosphorylation of ITIMs of IDO1, leading to either enhancing or terminating the expression of IDO1, may provide some innovative strategies in treating malignant tumors. Recently, a separate study confirmed that IDO1-dependent signaling events would activate class IA phosphoinositide 3-kinases (PI3Ks) to produce immunoregulatory phenotype in plasmacytoid dendritic cells (pDCs), accompanied by IDO1 shifting from the cytosol to early endosomes (15). In conclusion, the available evidences indicate that the IDO1 is not only an enzyme in the Kyn pathway but also a moonlighting protein that mediates non-catalytic functions through different mechanisms (16).

THE EXPRESSION AND ACTIVITY OF INDOLEAMINE 2,3-DIOXYGENASE 1

The Constitutive/Intrinsic Expression of Indoleamine 2,3-Dioxygenase 1

IDO1 is not or weakly expressed under physiological states. It is constitutively expressed in a restricted set of tissues, including the placenta, the mucosa, and lymphoid organs (https://www.proteinatlas.org/ENSG00000131203-IDO1/tissue). For example, IDO1 is mainly expressed in the endothelial cells of the placenta, epithelial cells of the fallopian tube, interstitial cells of the lymph node, and so on (17). Interestingly, some data confirmed that IDO1 expression was increased in select tissues with age (18).

Although IDO1 expression is often silent in normal tissues, the IDO1 expression/activity has been observed in malignant cells. The loss of Bridging Integrator 1 (BIN1; with the features of immunosuppression) or overexpression cyclooxygenase-2 (COX-2) in malignant cells is usually the reason for high constitutive/intrinsic expression of IDO1. The deletion or downregulation of BIN1 in malignant cells enhances IDO1 expression depending on signal transducer and activator of transcription 1 (STAT1) and nuclear factor-kappa B (NF-κB) (19). On the contrary, high BIN1 expression has a favorable prognosis in cancer (20). The up-expression of COX-2 increases its product prostaglandin E2 (PGE_2) binding to the EP receptor through the autocrine signaling pathway, which activates IDO1 *via* the protein kinase C (PKC) and PI3K pathways (21). Indeed, genetic studies of IDO1 in the mouse suggested there was genetic overlap between COX-2 and IDO1 (22). Litzenburger et al. suggested that constitutive IDO1 expression in human tumor cells was sustained by an autocrine aryl hydrocarbon receptor (AhR)-IL-6-STAT3 signaling loop (23), although the clinical data revealed that the upregulated expression of IDO1 in various human tumor tissues, such as esophageal cancer, thyroid carcinoma, and leiomyosarcoma, was considered to be a worse prognostic factor and a more aggressive tumor phenotype (24–26). However, there

was still controversy about the relationship between high expression of IDO1 in tumor-draining lymph nodes (TDLN) and poor clinical outcomes (17, 27).

In summary, there may be some discrepancies in IDO1 expression profiles in different tumor types. Nonetheless, constitutive IDO1 expression in tumor cells is still a key factor to mediate immune evasion, and thus exploring the mechanism of up-expression may guide and pre-evaluate the efficacy of therapeutic approaches by targeting IDO1.

The Induced/Extrinsic Expression of Indoleamine 2,3-Dioxygenase 1

As noted above, the IDO1 expression is constitutive in some tumor cells. However, it could be also induced to express in tumor cells and intratumoral cells, including DCs, macrophage, endothelial cells, cancer-associated fibroblasts (CAFs), and mesenchymal stem cells (MSCs) (28–34), by a variety of inflammatory stimuli, such as interferon-γ (IFN-γ), tumor necrosis factor-α (TNF-α), IL-32, and IL-6 (33, 35–37). Among the multiple mediators of IDO1 induction, IFN-γ is considered the main inducer of IDO1. Interestingly, tumor-infiltrating lymphocytes (TILs) of the tumor microenvironment (TME) represent the major source of IFN-γ secretion (38–40). IFN-γ inducing IDO1 expression has been extensively studied. For instance, IFN-γ mediates STAT1 to form a homodimer and then binds to the gamma activation sequence (GAS) in IDO1 gene. Meanwhile, IFN-γ also mediates NF-κB and STAT-1-dependent synthesis of IFN-γ-regulated factor 1 (IRF1), which binds to the IFN-stimulated elements (ISREs) in IDO1 gene promoter to induce the transcription of IDO1 (41).

In addition to IFN-γ, there are other cytokines involved in the induction of IDO1. Multiple myeloma cell-derived IL-32γ significantly induced the production of the IDO1 in macrophages through proteinase 3 (PR3) and the downstream STAT3 and NF-κB pathways (33). However, the role of IL-6 in inducing the expression of IDO1 is controversial. It was reported that constitutive IDO1 expression in SKOV-3 and NSCLC human cancer cell lines was sustained by autocrine IL-6 (23). Hepatic CAF-derived IL-6 also differentiated DCs into a regulatory subtype through STAT3 activation (42). In contrast, IL-6 induced IDO1 proteasomal degradation by selectively inducing the interaction between SOCS3 and ITIM of IDO1 in DCs (14, 43). The conflicting results of the IL-6 effect on IDO1 expression suggest that there are different signals in different cells or the complicated environment involved in its expression, which need to be well illustrated in the future.

So far, there are other factors and signaling events involved in IDO1 expression/activity in DCs that have been extensively analyzed. It was reported that tumor cells promote tolerization of DCs through paracrine Wnt5a-mediated signaling. Melanoma-derived Wnt5a promotes the transcriptional expression of IDO1 in nearby DCs by Wnt5a-β-catenin signaling and activates peroxisome proliferator-activated receptor-γ (PPAR-γ) signaling pathway, culminating in enhanced IDO1 activity to establish an immunosuppressive microenvironment (44). Cytotoxic T lymphocyte-associated protein-4-immunoglobulin (CTLA-4-Ig) interacts with B7 molecules as receptors to induce IDO1 expression in DCs (45). TGF-β could trigger immunoregulatory signaling in IDO1, which did not require the catalyst function of IDO1 to induce pDCs for long-term tolerance (5, 14). Interestingly, spermidine, a main arginase 1 (Arg1) product, is required for IDO1 expression and activity by TGF-β in DCs (46).

In addition to the inducers described above, type I IFNs (IFN-α and IFN-β), IL-10, soluble CD83 (sCD83), and toll-like receptor (TLR) ligands such as bacterial lipopolysaccharides (LPSs) are still involved in the modulation of IDO1 expression/activity (47–52). When mitochondrial Lon is overexpressed in oral cancer cells OEC-M1, mitochondrial DNA (mtDNA) is damaged, and then oxidized mtDNA is released into the cytosol to induce IFN-β signaling *via* cytosolic DNA sensors, which upregulates the programmed death ligand-1 (PD-L1) and IDO1 expression (50). Aside from all this, miRNAs are also involved in the regulation of IDO1 expression. *In vitro*, cervical cancer cells secreted exosomal miR-142-5p, which induces IDO1 expression *via* targeting lymphatic AT-rich interactive domain-containing protein 2 (ARID2) to enhance IFN-γ transcription by suppressing promoter methylation (53). On the contrary, miR-153 expression in bladder cancer cells could exert antitumor activity by targeting IDO1 3′-UTR and inhibiting cancer cell Trp metabolism subsequently (54).

Collectively, a great variety of stimuli can affect either directly or indirectly IDO1 expression and activity in different cell types in TME. However, the proportion of these cell types may differ in different tumors and tissues, the exact mechanisms for the distinct expression patterns of IDO1 are only partially revealed, and the functions of overexpressed IDO1 in these cell types are far from completely understood. It is notable that the complex interaction between tumors cells and other cells, especially immunity cells in TME, contributes substantially to exploring the strong IDO1 expression and its particular function.

Indoleamine 2,3-Dioxygenase 1 and Tryptophan Metabolism

Trp is one of the eight essential amino acids that cannot be synthesized in the human body. In addition to being a building block for proteins synthesis, Trp undergoes complex metabolic pathways, resulting in the production of many active compounds. Less than 2% of Trp is hydroxylated to produce 5-hydroxytryptophan, which is then decarboxylated by an aromatic amino acid decarboxylase to produce 5-hydroxytryptamine (5-HT), an essential neurotransmitter. A very small percentage of Trp can be decarboxylated to produce tryptamine to control the balance between excitatory and inhibitory functions of 5-HT. About more than 95% of the Trp is catalyzed by IDO1 or the other two isoenzymes (IDO2 or TDO), which catalyzes the Trp *via* the Kyn pathway to produce Kyn (55). Kyn is a key component in the synthesis of a number of metabolites, which could convert into 3-hydroxykynurenine (3-HK), 3-hydroxyanthranilic acid (3-HAA), and quinolinic acid. Quinolinic acid finally undergoes a series of chemical reactions to produce NAD+, an important cofactor for redox reactions in mitochondria, while excess carbon

skeletons from the Kyn pathway eventually participate in the citric acid cycle to produce ATP. The depletion of Trp and production of Kyn through the Kyn pathway affect the immune cell metabolism and tumor characteristics. It has been confirmed that the IDO1–Kyn–ligand-activated transcription factor (AhR) pathway in thyroid cancer cells would facilitate epithelial-to-mesenchymal transition (EMT) (56), while Kyn depletion *in vivo* would reverse IDO1-mediated cancer immune suppression in an animal model (57).

Although IDO1, IDO2, and TDO may catalyze the same biochemical reactions in the metabolism of Trp, they have different tissue distribution and physiological functions. Unlike IDO1, TDO is mainly found in the liver and neuronal cells and is regulated by glucocorticoid hormones and Trp levels. The main role of TDO is to maintain homeostasis of dietary Trp levels, and there is also evidence that TDO plays a role in immune-related diseases and central nervous system disorders (58, 59). Nevertheless, the recent studies revealed that TDO could be involved in modulating antitumor immune responses and the antitumor immunotherapy efficacy (60, 61), but it did not colocalize with IDO1, at least, in human glioblastoma (62). In most cancers, such as glioblastomas, melanomas, colon carcinomas, lung carcinomas, and endometrium carcinomas, TDO could be detected in pericytes that belonged to morphologically abnormal vessels in the intratumoral rather than tumor cells themselves (62), although the mechanism that triggers TDO expression in tumor pericytes and the relationship between TDO-expression pericytes and abnormal vessels are all unclear, which suggests that TDO may play a proangiogenic role depending on its expression site in certain cancer types. IDO2 is directly adjacent to IDO1 on the same chromosome, is more narrowly expressed, and has much less catalytic efficiency for Trp than IDO1 (63). Although IDO2 was also detected at high levels in some human tumors, the function of IDO2 in tumors is still far from being understood (64, 65). The available evidences support that IDO1, TDO, and IDO2 may be all involved in malignant tumor, but the three differ in the expression, regulatory mechanism, and the role in different TME.

INDOLEAMINE 2,3-DIOXYGENASE 1 IN MODULATING THE IMMUNOSUPPRESSIVE TUMOR MICROENVIRONMENT

Initially, the function of IDO1 was described as an innate mechanism of defense against microbial invasion (66, 67), because IDO1 could induce depletion of Trp, an essential amino acid for microbial and parasite proliferation (66–68). In 1998, Munn et al. performed a pioneering experiment showing that elevated IDO (namely, IDO1) expression at the maternal–fetal interface was crucial to prevent immune rejection of fetal allografts (11). Subsequently, extensive studies have demonstrated the immunological regulation role for IDO1 in physiological and pathological states including pregnancy, obesity, transplantation, infectious diseases, autoimmune diseases, neurological diseases, and neoplastic diseases (69–72). In clinical researches, the expression of IDO1 has been found in various tumors such as breast cancer, melanoma, and bladder cancer, which inactivates surrounding immune cells in TME primarily through abnormalities of Trp metabolism (54, 73, 74). Here, the mechanisms reported in the literatures are summarized about IDO1 in the establishment of tumor immune escape (**Figure 1**).

Dysfunction and Apoptosis of Effector T Cells and Differentiation and Activation of Regulatory T Cells

The effect of IDO1 on T cells is based on the Trp "starvation" theory. 1) T cells are especially sensitive to low Trp concentrations, which arrest T cells in the mid-G1 phase of the cell progression cycle (75). 2) The Trp depletion can inhibit T-cell proliferation through the activation of kinase general control non-derepressible 2 (GCN2), a molecular sensor of Trp deprivation, and its downstream phosphorylated eukaryotic initiation factor 2 (eIFα) (76). Furthermore, activation of GCN2 also promotes Treg differentiation, enhances Treg activity, and collaborates with phosphatase and tensin homolog (PTEN) signaling to maintain the suppressive phenotype of Tregs (77). Paradoxically, GCN2 does not mediate suppression of antitumor T-cell responses by Trp catabolism in experimental melanomas (78), and GCN2 is required for normal cytotoxic T-cell function (79), which suggests that the immune regulatory role of GCN2 in subsets of T cells may depend on the complex context in different types of tumors. 3) The Trp shortage can also inhibit the mTOR signaling pathway, which leads to impairment of T-cell function (80). In addition to the depletion of Trp, accumulation of Trp catabolite, including Kyn and downstream derivative metabolites, would also inhibit T effector cell activation and induce Treg differentiation. For instance, Kyn could promote AhR nuclear translocation and then increase the transcription of Foxp3, a marker of Tregs (81). And the activation in Tregs could modulate M2-like macrophage activity, which contributes to the establishment of a myeloid-enriched immunosuppressive TME (82).

Tolerance of Dendritic Cells and Myeloid-Derived Suppressor Cells and Suppression of Natural Killer Cells Proliferation and Functions

In addition to suppressing the immune effects of T cells, it is generally considered that IDO1 also exerts immunosuppressive effects by regulating the function of innate immune cells, such as DCs, myeloid-derived suppressor cells (MDSCs), and natural killer (NK) cells. IDO1 normally has low basal expression in DCs but is rapidly induced such as by IFN-γ in inflamed tissues, especially in mature, immunogenic myeloid DCs, which are involved in the regulation of immune homeostasis (83, 84). However, in the tumor region, there is a set of DCs highly expressed IDO1 with a high capacity to support immune tolerance. Especially, under the presence of TGF-β in TME, the ITIM1 motif of IDO1 is phosphorylated, which reprograms DCs

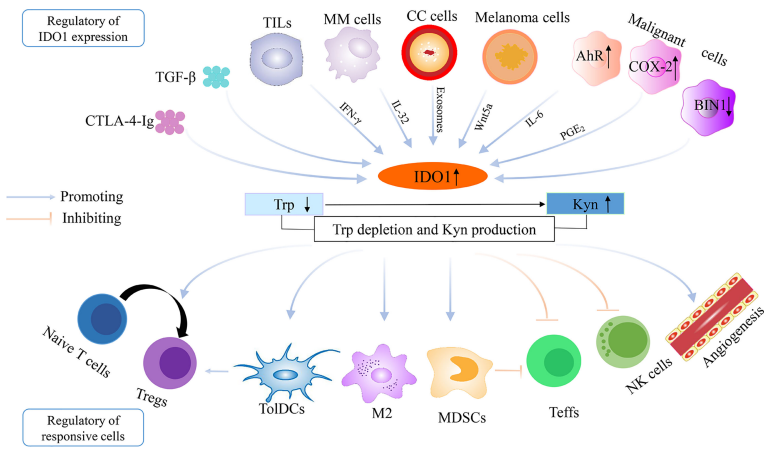

FIGURE 1 | The regulation of IDO1 overexpression and the establishment of immune escape in the tumor microenvironment. IDO1, indoleamine 2,3-dioxygenase 1; Trp, tryptophan; Kyn, kynurenine; TGF-β, transforming growth factor-β; CTLA-4-Ig, cytotoxic T lymphocyte-associated protein-4-immunoglobulin; TILs, tumor-infiltrating lymphocytes; COX-2, cyclooxygenase-2; BIN1, Bridging Integrator 1; AhR, aryl hydrocarbon receptor; IL-6, interleukin-6; CC cells, cervical cancer cells; MM cells, multiple myeloma cells; Teffs, effector T cells; Tregs, regulatory T cells; TolDCs, tolerogenic dendritic cells; MDSCs, myeloid-derived suppressor cells; NK cells, natural killer cells; M2, M2 macrophage.

to the immune tolerance phenotype and leads to sustained IDO1 expression through a positive feedback loop (14). And IDO1-expressing DCs also induce Treg proliferation (85). MDSCs are composed of multiple myeloid cells that are arrested at different stages of lineage development, which would be recruited to the TME by IDO1 overexpressing tumor cells, and then MDSCs inhibit T-cell function and reduce tumor response to immunotherapy in an IDO1-dependent manner (86–89).

NK cells are known as one of the most important innate immune cells with potent antitumor activity. In TME, however, tumor cells would suppress NK cell cytotoxicity and inhibit the expression of activating receptors on the surface of NK cells, such as NKG2D and NKp46, by IDO-induced Kyn production (90). But against this, Nafia et al. demonstrated that the proliferation and granzyme B production of NK cells were inhibited by GDC-0919 (an innovative IDO1 inhibitor) through upregulation of inhba (encoding for the inhibin—a member of the Tgfbeta signaling) (91). Certain IDO1 inhibitors unexpectedly impair NK cell-mediated killing in tumors, which suggests that we consider the inhibitory mechanisms of different IDO1 inhibitors and their effects on others cells, especially immune cells.

Neovascularization of Tumor

Tumor growth depends on continuous and extensive angiogenesis, which is a major pathway for tumor metastasis. Among them, vascular endothelial growth factor (VEGF) plays an important role in tumor angiogenesis. It has been found that IDO1 could increase angiogenesis through IL-6/STAT3/VEGF signaling (54). The expression of IDO1 in MDSCs has been implicated in promoting neovascularization through GCN2, which shifts the balance between the inflammatory cytokines IFN-γ and IL-6 (92). *In vivo* experiments also showed that the blood vessel density in the tumor was significantly reduced, and the tumor growth and metastases were impeded in IDO1-deficient mice (93, 94).

Furthermore, IDO1 can be induced in endothelial cells, CAFs, and MSCs, which could participate in mediating an immunosuppressive TME, for instance, supporting cancer cells to evade tumor dormancy (95), impairing NK cell function (96), and inducing Treg expansion (28). However, accumulating evidences about the mechanism of IDO1 action in immunosuppression indicate that not all immunosuppressive effects of IDO1 can be explained through the Trp depletion/Kyn accumulation theory (97). Besides, contrary to what is generally hypothesized in suppressing the immune effects of T cells, IDO1 would supply the required energy for T-cell survival and proliferation by increasing free fatty acid oxidation (98).

In conclusion, IDO1 is a key mediator in the establishment of tumor immune escape. Nonetheless, a greater understanding is needed about the exact mechanisms in the immunosuppressive effects of Trp catabolism by IDO1 derived from different cells in the different TME. Besides, detailed information about the differences related to the catalytic and non-catalytic functions of IDO1 is needed to elucidate this.

THE SIGNIFICANCE OF TARGETING INDOLEAMINE 2,3-DIOXYGENASE 1 IN TUMOR THERAPY

Recently, wide use of immune checkpoint inhibitors (ICIs), which mainly target CTLA-4 and the programmed death receptor/ligand 1 (PD-1/PD-L1) in cancer immunotherapies, improved durable responses in some advanced cancer patients (99). Nevertheless, these existing checkpoint inhibitors have

shown substantial benefit to only some of the patients, while the majority of patients do not respond to this approach, and even treatment-induced resistance would arise in the initial treatment responders, and life-threatening adverse effects would occur after ICI treatment (100–102). Therefore, it is very important to develop a reasonable immunotherapy strategy targeting different immunosuppressive points in TME. Several studies suggest there may be the non-T-cell-inflamed TME (so-called cold tumors) where checkpoint inhibitors are not effective in this group of patients (103). Brown et al. provided evidence of adaptive resistance to anti-CTLA-4 treatment due to upregulation of IDO1 in HCC (104). That is, ICIs in combination with inhibiting IDO1 may improve therapeutic benefit in tumors overexpressed IDO1, which could also drive inflammation in the TME and transform "cold" tumors to "hot" tumors.

So far, there are many small molecule compounds such as IDO1 inhibitors that have been reported to treat cancers alone or in combination with ICIs. 1-Methyl-D-tryptophan (D-1-MT), considered as a first-generation IDO1 enzyme inhibitor, is an analog of Trp. In addition to terminating immune tolerance, D-1-MT can also block the dormancy of tumor-repopulating cells (TRCs) and induce apoptosis through the IDO1-blocking/P53/reactive oxygen species (ROS)-mediated pathway (105). In a phase II trial, the combination of indoximod (D-1-MT) and pembrolizumab (PD-1 checkpoint inhibitor) showed encouraging safety and efficacy in patients with advanced melanoma (106). Controversially, in another independent phase III trial, the efficacy of epacadostat (direct inhibitor of IDO1 enzyme activity) in combination with pembrolizumab was not superior to pembrolizumab monotherapy in patients with unresectable or metastatic melanoma (107). In addition, a series of studies by Zhai et al. showed that in tumor cells, IDO1 suppressed the antitumor immune response by increasing the expression of complement factor H (CFH) and factor H-like protein 1 (FHL-1) instead of its association with Trp metabolism in human glioblastoma, and there was a survival advantage mediated by ICIs requiring non-tumor cell IDO1 enzyme activity in mouse glioblastoma. Oppositely, the combination of radiation and PD-1 antibody treatment efficacy required to inhibit IDO1 enzyme activity in non-tumor cells from another study of mouse glioblastoma model (97, 108, 109). The reason for the controversial conclusion may be that the immunosuppressive effects of IDO1 in the organism are not isolated, and there are multiple factors involved, such as the differentiation degree, the invasion degree, lymph node metastasis, clinical stage of the tumor, the different combinations of inhibitors, the infiltration of T effector cells in the tumor lesion, the host cell IDO1 origin, the enzyme activity versus non-enzyme effects of IDO1 in tumor lesion or TDLN, and age of the subject, all of which need to be considered comprehensively in order to better apply and develop IDO1-targeted drug and new combined therapeutic strategies in the clinical setting.

In addition to targeting IDO1 inhibiting, blocking the AhR pathway would overcome the limitation of single IDO1 targeting agents, particularly in combination with ICIs (82). Therefore, the targeted blockade of IDO1 or IDO1-driven metabolism pathway represents a promising therapeutic pathway. Meanwhile, IDO1 inhibitors combined with other therapies should be considered as an effective strategy in tumor immunotherapy, such as effectively suppressing tumor growth by synergizing photothermal therapy (PTT), radiotherapy, or chemotherapy (110–112). With the discovery of cancer tissue expression IDO1 or TDO or both, IDO1/TDO combined inhibitors have become a study focus (113–115). However, at odds with IDO1 inhibitors, TDO inhibitors are effective in synergistic immunotherapy with ICIs even though there is little or no TDO expression in cancers, which may be because the inhibitor of TDO could block hepatic TDO to increase systemic Trp levels (60, 113). More surprisingly, in viral hepatitis, the inhibition of TDO or IDO (both IDO1 and IDO2) separately leads to dichotomous outcomes. TDO could participate in the Kyn pathway as IDO1 does, but both also differ in mediating inflammation (116, 117). In regard to TDO in the tumor, although the mechanisms to regulate the TDO expression and its separate role in maintaining Trp homeostasis are all unclear as yet, TDO could be regarded as a candidate after resistance to IDO1 inhibitors, as well as the circulating level of Trp may be an indicator to evaluate the efficacy of inhibitors of TDO in tumor immunotherapy. Anyway, one thing should be confirmed that the mechanism of their expression and activation in the different cell types needs to be understood first, which could guide the development and applications of IDO1 inhibitors and IDO1/TDO combined inhibitors.

Due to the short half-life of small molecule inhibitors, the lack of patient stratification based on IDO1 expression, the option of combination with therapy ICIs, and inhibitors targeting IDO1 have so far failed to show therapeutic benefit in the animal model research or even in clinical trials (118–120). For instance, IDO1 inhibitor combination with PD-L1 blockade did not cause a synergistic effect in sarcoma (91). Therefore, more and more new strategies of inhibiting the expression of IDO1 have been explored. Phan et al. found that attenuated *Salmonella* typhimurium (ST) delivering an shRNA plasmid targeting IDO1 can reduce intratumoral IDO1 levels more effectively than epacadostat (121), while locked nucleic acid (LNA)-modified antisense oligonucleotides (ASOs) could inhibit IDO1 expression in cancer cells, exhibiting longer exposure times and more engaged targets than epacadostat (122). Besides, there may be other Trp metabolizing enzymes involved in tumor immune escape, such as interleukin-4-induced-1 (IL4i1), but at this point, the biology and expression of IL4i1 are still poorly understood (123).

In addition to being a target of antitumor therapy, targeted IDO1 can be considered as an independent prognostic value and predictive biomarker. High proportions of PD-L1+ and IDO1+ TAMs are associated with unfavorable outcomes in classical Hodgkin's lymphoma patients treated with standard chemotherapy (34). Moreover, there is clinical evidence that IDO1 gene expression in the urine of men indicates a high risk of prostate cancer development (36, 124). And in non-small cell

lung cancer, the high serum Kyn/Trp levels are also associated with early progression and a low prognosis (125). Even though, as mentioned above, the up-expression IDO1 has been described in various human tumor tissues not only in tumor cells but also in other components of the TME, and the IDO1 expression status in patients has also been explored in some clinical trials to assess its relevance with poor prognosis (126), not all tumor progression or poor prognosis has a positive correlation with high IDO1 expression (127, 128). Also, the current clinical trial data of IDO1 activity assessment are mainly derived from serum Kyn or Trp levels. In fact, the consumption of Trp and the accumulation of Kyn do not always happen simultaneously in human cancers, and the immunosuppression effects of IDO1 in TME do not just depend on its enzyme activity. On the contrary, its enzyme activity may also contribute to the response to ICI therapy (97, 108, 129, 130). Therefore, the high IDO1 expression is not a single indicator to decide whether to choose IDO1 inhibitors, and the IDO1 activity assessment may also need multiple factors, including the concentrations of Trp and Kyn as well as the Kyn/Trp ratio in human cancers.

CONCLUSION

Overall, the important role of IDO1 in tumoral immune escape renders the IDO1 pathway a potential target for adjuvant treatment. IDO1 inhibitors are widely studied in various cancers as monotherapy or in combination with other therapies in preclinical and clinical trials. It is remarkable, however, that the complex mechanism of regulating IDO1 expression and its different biological effects depending on the context or cell types may render its clinical development complicated. So more researches are needed to elucidate the mechanisms of immunotherapy against IDO1 and how IDO1 works in combination therapy. And further understanding of the immunobiological properties of IDO1, individual IDO1 expression levels, the optimal drugs targeting IDO1, and combination therapy strategies would lead to favorable treatment for patients with malignant tumors. Besides, it is important to explore the exact role of other Trp metabolizing enzymes, Kyn, and its downstream metabolites in tumoral immune escape.

AUTHOR CONTRIBUTIONS

XS, QS, and ZY edited the manuscript. ZY revised the whole manuscript about important intellectual content. XS, QS, ZY, RQ, WL, ML, MG, and LW wrote parts of the manuscript. All authors contributed to the article and approved the submitted version.

FUNDING

This work was supported by grants from the National Science Foundation of China (81702827, 81801560), the Science and Technology Planning Project of Hebei Province (H2019206614), and the Science and Technology Research Projects of the Colleges and Universities of Hebei Province (ZD2021071).

REFERENCES

1. Mor A, Tankiewicz-Kwedlo A, Pawlak D. Kynurenines as a Novel Target for the Treatment of Malignancies. *Pharm (Basel Switzerland)* (2021) 14(7):606. doi: 10.3390/ph14070606
2. Li C, Zhao H. Tryptophan and Its Metabolites in Lung Cancer: Basic Functions and Clinical Significance. *Front Oncol* (2021) 11:707277. doi: 10.3389/fonc.2021.707277
3. Bilir C, Sarisozen C. Indoleamine 2,3-Dioxygenase (IDO): Only an Enzyme or a Checkpoint Controller? *J Oncological Sci* (2017) 32:52–6. doi: 10.1016/j.jons.2017.04.001
4. Badawy A. Kynurenine Pathway of Tryptophan Metabolism: Regulatory and Functional Aspects. *Int J Tryptophan Res* (2017) 10:1178646917691938. doi: 10.1177/1178646917691938
5. Pallotta MT, Orabona C, Volpi C, Vacca C, Belladonna ML, Bianchi R, et al. Indoleamine 2,3-Dioxygenase Is a Signaling Protein in Long-Term Tolerance by Dendritic Cells. *Nat Immunol* (2011) 129:870–8. doi: 10.1038/ni.2077
6. Mammoli A, Coletti A, Ballarotto M, Riccio A, Carotti A, Grohmann U, et al. New Insights From Crystallographic Data: Diversity of Structural Motifs and Molecular Recognition Properties Between Groups of IDO1 Structures. *ChemMedChem* (2020) 1510:891–9. doi: 10.1002/cmdc.202000116
7. Kanai M, Funakoshi H, Takahashi H, Hayakawa T, Mizuno S, Matsumoto K, et al. Tryptophan 2,3-Dioxygenase Is a Key Modulator of Physiological Neurogenesis and Anxiety-Related Behavior in Mice. *Mol Brain* (2009) 2:8. doi: 10.1186/1756-6606-2-8
8. Yu C, Pan Z, Luo D. TDO as a Therapeutic Target in Brain Diseases. *Metab Brain Dis* (2016) 314:737–47. doi: 10.1007/s11011-016-9824-z
9. van Baren N, Van den Eynde BJ. Tryptophan-Degrading Enzymes in Tumoral Immune Resistance. *Front Immunol* (2015) 6:34. doi: 10.3389/fimmu.2015.00034
10. Zhai L, Bell A, Ladomersky E, Lauing K, Bollu L, Sosman J, et al. Immunosuppressive IDO in Cancer: Mechanisms of Action, Animal Models, and Targeting Strategies. *Front Immunol* (2020) 11:1185. doi: 10.3389/fimmu.2020.01185
11. Munn D, Zhou M, Attwood J, Bondarev I, Conway S, Marshall B, et al. Prevention of Allogeneic Fetal Rejection by Tryptophan Catabolism. *Sci (New York NY)* (1998) 2815380:1191–3. doi: 10.1126/science.281.5380.1191
12. Sugimoto H, Oda S, Otsuki T, Hino T, Yoshida T, Shiro Y. Crystal Structure of Human Indoleamine 2,3-Dioxygenase: Catalytic Mechanism of O2 Incorporation by a Heme-Containing Dioxygenase. *Proc Natl Acad Sci USA* (2006) 1038:2611–6. doi: 10.1073/pnas.0508996103
13. Lewis-Ballester A, Pham K, Batabyal D, Karkashon S, Bonanno J, Poulos T, et al. Structural Insights Into Substrate and Inhibitor Binding Sites in Human Indoleamine 2,3-Dioxygenase 1. *Nat Commun* (2017) 81:1693. doi: 10.1038/s41467-017-01725-8
14. Albini E, Rosini V, Gargaro M, Mondanelli G, Belladonna M, Pallotta M, et al. Distinct Roles of Immunoreceptor Tyrosine-Based Motifs in Immunosuppressive Indoleamine 2,3-Dioxygenase 1. *J Cell Mol Med* (2017) 211:165–76. doi: 10.1111/jcmm.12954
15. Iacono A, Pompa A, De Marchis F, Panfili E, Greco F, Coletti A, et al. Class IA PI3Ks Regulate Subcellular and Functional Dynamics of IDO1. *EMBO Rep* (2020) 2112:e49756. doi: 10.15252/embr.201949756
16. Jeffery CJ. Enzymes, Pseudoenzymes, and Moonlighting Proteins: Diversity of Function in Protein Superfamilies. *FEBS J* (2020) 28719:4141–9. doi: 10.1111/febs.15446

17. Theate I, van Baren N, Pilotte L, Moulin P, Larrieu P, Renauld JC, et al. Extensive Profiling of the Expression of the Indoleamine 2,3-Dioxygenase 1 Protein in Normal and Tumoral Human Tissues. *Cancer Immunol Res* (2015) 32:161–72. doi: 10.1158/2326-6066.CIR-14-0137
18. Ladomersky E, Zhai L, Gritsina G, Genet M, Lauing KL, Wu M, et al. Advanced Age Negatively Impacts Survival in an Experimental Brain Tumor Model. *Neurosci Lett* (2016) 630:203–8. doi: 10.1016/j.neulet.2016.08.002
19. Muller AJ, DuHadaway JB, Donover PS, Sutanto-Ward E, Prendergast GC. Inhibition of Indoleamine 2,3-Dioxygenase, an Immunoregulatory Target of the Cancer Suppression Gene Bin1, Potentiates Cancer Chemotherapy. *Nat Med* (2005) 113:312–9. doi: 10.1038/nm1196
20. Ahmadzada T, Lee K, Clarke C, Cooper WA, Linton A, McCaughan B, et al. High BIN1 Expression has a Favorable Prognosis in Malignant Pleural Mesothelioma and Is Associated With Tumor Infiltrating Lymphocytes. *Lung Cancer* (2019) 130:35–41. doi: 10.1016/j.lungcan.2019.02.005
21. Hennequart M, Pilotte L, Cane S, Hoffmann D, Stroobant V, Plaen E, et al. Constitutive IDO1 Expression in Human Tumors Is Driven by Cyclooxygenase-2 and Mediates Intrinsic Immune Resistance. *Cancer Immunol Res* (2017) 58:695–709. doi: 10.1158/2326-6066.Cir-16-0400
22. Prendergast G, Metz R, Muller A. Towards a Genetic Definition of Cancer-Associated Inflammation: Role of the IDO Pathway. *Am J Pathol* (2010) 1765:2082–7. doi: 10.2353/ajpath.2010.091173
23. Litzenburger U, Opitz C, Sahm F, Rauschenbach K, Trump S, Winter M, et al. Constitutive IDO Expression in Human Cancer Is Sustained by an Autocrine Signaling Loop Involving IL-6, STAT3 and the AHR. *Oncotarget* (2014) 54:1038–51. doi: 10.18632/oncotarget.1637
24. Rosenbaum M, Gigliotti B, Pai S, Parangi S, Wachtel H, Mino-Kenudson M, et al. PD-L1 and IDO1 Are Expressed in Poorly Differentiated Thyroid Carcinoma. *Endocr Pathol* (2018) 291:59–67. doi: 10.1007/s12022-018-9514-y
25. Kiyozumi Y, Baba Y, Okadome K, Yagi T, Ishimoto T, Iwatsuki M, et al. IDO1 Expression Is Associated With Immune Tolerance and Poor Prognosis in Patients With Surgically Resected Esophageal Cancer. *Ann Surg* (2019) 2696:1101–8. doi: 10.1097/sla.0000000000002754
26. Iwasaki T, Kohashi K, Toda Y, Ishihara S, Yamada Y, Oda Y. Association of PD-L1 and IDO1 Expression With JAK-STAT Pathway Activation in Soft-Tissue Leiomyosarcoma. *J Cancer Res Clin Oncol* (2021) 1475:1451–63. doi: 10.1007/s00432-020-03390-9
27. Munn D, Sharma M, Hou D, Baban B, Lee J, Antonia S, et al. Expression of Indoleamine 2,3-Dioxygenase by Plasmacytoid Dendritic Cells in Tumor-Draining Lymph Nodes. *J Clin Invest* (2004) 1142:280–90. doi: 10.1172/jci21583
28. Kadle R, Abdou S, Villarreal-Ponce A, Soares M, Sultan D, David J, et al. Microenvironmental Cues Enhance Mesenchymal Stem Cell-Mediated Immunomodulation and Regulatory T-Cell Expansion. *PloS One* (2018) 133:e0193178. doi: 10.1371/journal.pone.0193178
29. Seeber A, Klinglmair G, Fritz J, Steinkohl F, Zimmer K, Aigner F, et al. High IDO-1 Expression in Tumor Endothelial Cells Is Associated With Response to Immunotherapy in Metastatic Renal Cell Carcinoma. *Cancer Sci* (2018) 1095:1583–91. doi: 10.1111/cas.13560
30. Cui G, Li C, Xu G, Sun Z, Zhu L, Li Z, et al. Tumor-Associated Fibroblasts and Microvessels Contribute to the Expression of Immunosuppressive Factor Indoleamine 2, 3-Dioxygenase in Human Esophageal Cancers. *Pathol Oncol Res POR* (2018) 242:269–75. doi: 10.1007/s12253-017-0244-0
31. Meireson A, Chevolet I, Hulstaert E, Ferdinande L, Ost P, Geboes K, et al. Peritumoral Endothelial Indoleamine 2, 3-Dioxygenase Expression Is an Early Independent Marker of Disease Relapse in Colorectal Cancer and Is Influenced by DNA Mismatch Repair Profile. *Oncotarget* (2018) 938:25216–24. doi: 10.18632/oncotarget.25393
32. Kim D, Kim J, Kim J, Kim S, Kim K. Differential Expression and Clinicopathological Significance of HER2, Indoleamine 2,3-Dioxygenase and PD-L1 in Urothelial Carcinoma of the Bladder. *J Clin Med* (2020) 9 (5):1265. doi: 10.3390/jcm9051265
33. Yan H, Dong M, Liu X, Shen Q, He D, Huang X, et al. Multiple Myeloma Cell-Derived IL-32γ Increases the Immunosuppressive Function of Macrophages by Promoting Indoleamine 2,3-Dioxygenase (IDO) Expression. *Cancer Lett* (2019) 446:38–48. doi: 10.1016/j.canlet.2019.01.012
34. Karihtala K, Leivonen S, Brück O, Karjalainen-Lindsberg M, Mustjoki S, Pellinen T, et al. Prognostic Impact of Tumor-Associated Macrophages on Survival Is Checkpoint Dependent in Classical Hodgkin Lymphoma. *Cancers* (2020) 12(4):877. doi: 10.3390/cancers12040877
35. Zhao Q, Wang P, Huang Z, Peng L, Lin C, Gao Z, et al. Tumoral Indoleamine 2, 3-Dioxygenase 1 Is Regulated by Monocytes and T Lymphocytes Collaboration in Hepatocellular Carcinoma. *Oncotarget* (2016) 712:14781–90. doi: 10.18632/oncotarget.7438
36. Banzola I, Mengus C, Wyler S, Hudolin T, Manzella G, Chiarugi A, et al. Expression of Indoleamine 2,3-Dioxygenase Induced by IFN-γ and TNF-α as Potential Biomarker of Prostate Cancer Progression. *Front Immunol* (2018) 9:1051. doi: 10.3389/fimmu.2018.01051
37. Liang Y, Yu Z, Song Y, Wang T, Xiao B. Indoleamine 2,3-Dioxygenase Activation by Interferon Gamma in Vascular Endothelial Rat Cells Requires Noncanonical NF-κb Signaling. *Transplant Proc* (2019) 516:2141–5. doi: 10.1016/j.transproceed.2019.03.043
38. Mojic M, Takeda K, Hayakawa Y. The Dark Side of IFN-γ: Its Role in Promoting Cancer Immunoevasion. *Int J Mol Sci* (2017) 19(1):89. doi: 10.3390/ijms19010089
39. Deczkowska A, Baruch K, Schwartz M. Type I/II Interferon Balance in the Regulation of Brain Physiology and Pathology. *Trends Immunol* (2016) 373:181–92. doi: 10.1016/j.it.2016.01.006
40. Zhai L, Ladomersky E, Lauing K, Wu M, Genet M, Gritsina G, et al. Infiltrating T Cells Increase IDO1 Expression in Glioblastoma and Contribute to Decreased Patient Survival. *Clin Cancer Res* (2017) 2321:6650–60. doi: 10.1158/1078-0432.Ccr-17-0120
41. Du M, Sotero-Esteva W, Taylor M. Analysis of Transcription Factors Regulating Induction of Indoleamine 2,3-Dioxygenase by IFN-Gamma. *J Interferon Cytokine Res Off J Int Soc Interferon Cytokine Res* (2000) 202:133–42. doi: 10.1089/107999000312531
42. Cheng J, Deng Y, Yi H, Wang G, Fu B, Chen W, et al. Hepatic Carcinoma-Associated Fibroblasts Induce IDO-Producing Regulatory Dendritic Cells Through IL-6-Mediated STAT3 Activation. *Oncogenesis* (2016) 5:e198. doi: 10.1038/oncsis.2016.7
43. Orabona C, Pallotta M, Volpi C, Fallarino F, Vacca C, Bianchi R, et al. SOCS3 Drives Proteasomal Degradation of Indoleamine 2,3-Dioxygenase (IDO) and Antagonizes IDO-Dependent Tolerogenesis. *Proc Natl Acad Sci USA* (2008) 10552:20828–33. doi: 10.1073/pnas.0810278105
44. Zhao F, Xiao C, Evans KS, Theivanthiran T, DeVito N, Holtzhausen A, et al. Paracrine Wnt5a-Beta-Catenin Signaling Triggers a Metabolic Program That Drives Dendritic Cell Tolerization. *Immunity* (2018) 481:147–160 e7. doi: 10.1016/j.immuni.2017.12.004
45. Grohmann U, Orabona C, Fallarino F, Vacca C, Calcinaro F, Falorni A, et al. CTLA-4-Ig Regulates Tryptophan Catabolism *In Vivo*. *Nat Immunol* (2002) 311:1097–101. doi: 10.1038/ni846
46. Mondanelli G, Bianchi R, Pallotta M, Orabona C, Albini E, Iacono A, et al. A Relay Pathway Between Arginine and Tryptophan Metabolism Confers Immunosuppressive Properties on Dendritic Cells. *Immunity* (2017) 462:233–44. doi: 10.1016/j.immuni.2017.01.005
47. Xiong L, Wang D, Lin S, Wang Y, Luo M, Gao L. Soluble CD83 Inhibits Acute Rejection by Up Regulating TGF-β and IDO Secretion in Rat Liver Transplantation. *Transplant Immunol* (2021) 64:101351. doi: 10.1016/j.trim.2020.101351
48. Zhai L, Spranger S, Binder D, Gritsina G, Lauing K, Giles F, et al. Molecular Pathways: Targeting IDO1 and Other Tryptophan Dioxygenases for Cancer Immunotherapy. *Clin Cancer Res an Off J Am Assoc Cancer Res* (2015) 2124:5427–33. doi: 10.1158/1078-0432.Ccr-15-0420
49. Fujigaki S, Saito K, Sekikawa K, Tone S, Takikawa O, Fujii H, et al. Lipopolysaccharide Induction of Indoleamine 2,3-Dioxygenase Is Mediated Dominantly by an IFN-Gamma-Independent Mechanism. *Eur J Immunol* (2001) 318:2313–8. doi: 10.1002/1521-4141(200108)31:8<2313::aid-immu2313>3.0.co;2-s
50. Cheng A, Cheng L, Kuo C, Lo Y, Chou H, Chen C, et al. Mitochondrial Lon-Induced mtDNA Leakage Contributes to PD-L1-Mediated Immunoescape *via* STING-IFN Signaling and Extracellular Vesicles. *J Immunother Cancer* (2020) 8(2):e001372. doi: 10.1136/jitc-2020-001372
51. Bessede A, Gargaro M, Pallotta M, Matino D, Servillo G, Brunacci C, et al. Aryl Hydrocarbon Receptor Control of a Disease Tolerance Defence Pathway. *Nature* (2014) 5117508:184–90. doi: 10.1038/nature13323
52. Puccetti P. On Watching the Watchers: IDO and Type I/II IFN. *Eur J Immunol* (2007) 374:876–9. doi: 10.1002/eji.200737184

53. Zhou C, Zhang Y, Yan R, Huang L, Mellor AL, Yang Y, et al. Exosome-Derived miR-142-5p Remodels Lymphatic Vessels and Induces IDO to Promote Immune Privilege in the Tumour Microenvironment. *Cell Death Differ* (2021) 282:715–29. doi: 10.1038/s41418-020-00618-6
54. Zhang W, Mao S, Shi D, Zhang J, Zhang Z, Guo Y, et al. MicroRNA-153 Decreases Tryptophan Catabolism and Inhibits Angiogenesis in Bladder Cancer by Targeting Indoleamine 2,3-Dioxygenase 1. *Front Oncol* (2019) 9:619. doi: 10.3389/fonc.2019.00619
55. Richard D, Dawes M, Mathias C, Acheson A, Hill-Kapturczak N, Dougherty D. L-Tryptophan: Basic Metabolic Functions, Behavioral Research and Therapeutic Indications. *Int J tryptophan Res IJTR* (2009) 2:45–60. doi: 10.4137/ijtr.s2129
56. Moretti S, Nucci N, Menicali E, Morelli S, Bini V, Colella R, et al. The Aryl Hydrocarbon Receptor Is Expressed in Thyroid Carcinoma and Appears to Mediate Epithelial-Mesenchymal-Transition. *Cancers* (2020) 12(1):145. doi: 10.3390/cancers12010145
57. Triplett T, Garrison K, Marshall N, Donkor M, Blazeck J, Lamb C, et al. Reversal of Indoleamine 2,3-Dioxygenase-Mediated Cancer Immune Suppression by Systemic Kynurenine Depletion With a Therapeutic Enzyme. *Nat Biotechnol* (2018) 368:758–64. doi: 10.1038/nbt.4180
58. Hoglund E, Overli O, Winberg S. Tryptophan Metabolic Pathways and Brain Serotonergic Activity: A Comparative Review. *Front Endocrinol (Lausanne)* (2019) 10:158. doi: 10.3389/fendo.2019.00158
59. Wang H, Do DC, Liu J, Wang B, Qu J, Ke X, et al. Functional Role of Kynurenine and Aryl Hydrocarbon Receptor Axis in Chronic Rhinosinusitis With Nasal Polyps. *J Allergy Clin Immunol* (2018) 1412:586–600 e6. doi: 10.1016/j.jaci.2017.06.013
60. Schramme F, Crosignani S, Frederix K, Hoffmann D, Pilotte L, Stroobant V, et al. Inhibition of Tryptophan-Dioxygenase Activity Increases the Antitumor Efficacy of Immune Checkpoint Inhibitors. *Cancer Immunol Res* (2020) 81:32–45. doi: 10.1158/2326-6066.Cir-19-0041
61. Li S, Li L, Wu J, Song F, Qin Z, Hou L, et al. TDO Promotes Hepatocellular Carcinoma Progression. *OncoTargets Ther* (2020) 13:5845–55. doi: 10.2147/ott.S252929
62. Hoffmann D, Dvorakova T, Stroobant V, Bouzin C, Daumerie A, Solvay M, et al. Tryptophan 2,3-Dioxygenase Expression Identified in Human Hepatocellular Carcinoma Cells and in Intratumoral Pericytes of Most Cancers. *Cancer Immunol Res* (2020) 81:19–31. doi: 10.1158/2326-6066.Cir-19-0040
63. Ball H, Sanchez-Perez A, Weiser S, Austin C, Astelbauer F, Miu J, et al. Characterization of an Indoleamine 2,3-Dioxygenase-Like Protein Found in Humans and Mice. *Gene* (2007) 3961:203–13. doi: 10.1016/j.gene.2007.04.010
64. Mandarano M, Bellezza G, Belladonna M, Vannucci J, Gili A, Ferri I, et al. Indoleamine 2,3-Dioxygenase 2 Immunohistochemical Expression in Resected Human Non-Small Cell Lung Cancer: A Potential New Prognostic Tool. *Front Immunol* (2020) 11:839. doi: 10.3389/fimmu.2020.00839
65. Guastella A, Michelhaugh S, Klinger N, Fadel H, Kiousis S, Ali-Fehmi R, et al. Investigation of the Aryl Hydrocarbon Receptor and the Intrinsic Tumoral Component of the Kynurenine Pathway of Tryptophan Metabolism in Primary Brain Tumors. *J Neuro-Oncol* (2018) 1392:239–49. doi: 10.1007/s11060-018-2869-6
66. Gupta S, Carlin J, Pyati P, Dai W, Pfefferkorn E, Murphy M. Antiparasitic and Antiproliferative Effects of Indoleamine 2,3-Dioxygenase Enzyme Expression in Human Fibroblasts. *Infect Immun* (1994) 626:2277–84. doi: 10.1128/iai.62.6.2277-2284.1994
67. Thomas S, Garrity L, Brandt C, Schobert C, Feng G, Taylor M, et al. IFN-Gamma-Mediated Antimicrobial Response. Indoleamine 2,3-Dioxygenase-Deficient Mutant Host Cells No Longer Inhibit Intracellular Chlamydia Spp. Or Toxoplasma Growth. *J Immunol (Baltimore Md 1950)* (1993) 15012:5529–34.
68. Schmidt S, Schultze J. New Insights Into IDO Biology in Bacterial and Viral Infections. *Front Immunol* (2014) 5:384. doi: 10.3389/fimmu.2014.00384
69. Niinisalo P, Raitakari O, Kähönen M, Hurme M, Lehtimäki T, Magnussen C, et al. IDO Activity Forecasts Obesity in Males and Premenopausal Females in a 10-Year Follow-Up Study:The Cardiovascular Risk in Young Finns Study. *Atherosclerosis* (2021) 336:32–8. doi: 10.1016/j.atherosclerosis.2021.09.018
70. Lassiter R, Merchen T, Fang X, Wang Y. Protective Role of Kynurenine 3-Monooxygenase in Allograft Rejection and Tubular Injury in Kidney Transplantation. *Front Immunol* (2021) 12:671025. doi: 10.3389/fimmu.2021.671025
71. Marim F, Teixeira D, Queiroz-Junior C, Valiate B, Alves-Filho J, Cunha T, et al. ZikaInhibition of Tryptophan Catabolism Is Associated With Neuroprotection During Virus Infection. *Front Immunol* (2021) 12:702048. doi: 10.3389/fimmu.2021.702048
72. Silvano A, Seravalli V, Strambi N, Cecchi M, Tartarotti E, Parenti A, et al. Tryptophan Metabolism and Immune Regulation in the Human Placenta. *J Reprod Immunol* (2021) 147:103361. doi: 10.1016/j.jri.2021.103361
73. Smith C, Chang M, Parker K, Beury D, DuHadaway J, Flick H, et al. IDO Is a Nodal Pathogenic Driver of Lung Cancer and Metastasis Development. *Cancer Discov* (2012) 28:722–35. doi: 10.1158/2159-8290.Cd-12-0014
74. Li H, Bullock K, Gurjao C, Braun D, Shukla S, Bossé D, et al. Metabolomic Adaptations and Correlates of Survival to Immune Checkpoint Blockade. *Nat Commun* (2019) 101:4346. doi: 10.1038/s41467-019-12361-9
75. Munn D, Shafizadeh E, Attwood J, Bondarev I, Pashine A, Mellor A. Inhibition of T Cell Proliferation by Macrophage Tryptophan Catabolism. *J Exp Med* (1999) 1899:1363–72. doi: 10.1084/jem.189.9.1363
76. Munn D, Sharma M, Baban B, Harding H, Zhang Y, Ron D, et al. GCN2 Kinase in T Cells Mediates Proliferative Arrest and Anergy Induction in Response to Indoleamine 2,3-Dioxygenase. *Immunity* (2005) 225:633–42. doi: 10.1016/j.immuni.2005.03.013
77. Sharma M, Shinde R, McGaha T, Huang L, Holmgaard R, Wolchok J, et al. The PTEN Pathway in Tregs Is a Critical Driver of the Suppressive Tumor Microenvironment. *Sci Adv* (2015) 110:e1500845. doi: 10.1126/sciadv.1500845
78. Sonner JK, Deumelandt K, Ott M, Thome CM, Rauschenbach KJ, Schulz S, et al. The Stress Kinase GCN2 Does Not Mediate Suppression of Antitumor T Cell Responses by Tryptophan Catabolism in Experimental Melanomas. *Oncoimmunology* (2016) 512:e1240858. doi: 10.1080/2162402X.2016.1240858
79. Van de Velde L, Guo X, Barbaric L, Smith A, Oguin T, Thomas P, et al. Stress Kinase GCN2 Controls the Proliferative Fitness and Trafficking of Cytotoxic T Cells Independent of Environmental Amino Acid Sensing. *Cell Rep* (2016) 179:2247–58. doi: 10.1016/j.celrep.2016.10.079
80. Metz R, Rust S, Duhadaway J, Mautino M, Munn D, Vahanian N, et al. IDO Inhibits a Tryptophan Sufficiency Signal That Stimulates mTOR: A Novel IDO Effector Pathway Targeted by D-1-Methyl-Tryptophan. *Oncoimmunology* (2012) 19:1460–8. doi: 10.4161/onci.21716
81. Zhang X, Liu X, Zhou W, Du Q, Yang M, Ding Y, et al. Blockade of IDO-Kynurenine-AhR Axis Ameliorated Colitis-Associated Colon Cancer *via* Inhibiting Immune Tolerance. *Cell Mol Gastroenterol Hepatol* (2021) 12 (4):1179–99. doi: 10.1016/j.jcmgh.2021.05.018
82. Campesato L, Budhu S, Tchaicha J, Weng C, Gigoux M, Cohen I, et al. Blockade of the AHR Restricts a Treg-Macrophage Suppressive Axis Induced by L-Kynurenine. *Nat Commun* (2020) 111:4011. doi: 10.1038/s41467-020-17750-z
83. Wolf B, Posnick D, Fisher J, Lewis L, Ernstoff M. Indoleamine-2,3-Dioxygenase Enzyme Expression and Activity in Polarized Dendritic Cells. *Cytotherapy* (2009) 118:1084–9. doi: 10.3109/14653240903271230
84. Chung D, Rossi M, Romano E, Ghith J, Yuan J, Munn D, et al. Indoleamine 2,3-Dioxygenase-Expressing Mature Human Monocyte-Derived Dendritic Cells Expand Potent Autologous Regulatory T Cells. *Blood* (2009) 1143:555–63. doi: 10.1182/blood-2008-11-191197
85. Chen W, Liang X, Peterson A, Munn D, Blazar B. The Indoleamine 2,3-Dioxygenase Pathway Is Essential for Human Plasmacytoid Dendritic Cell-Induced Adaptive T Regulatory Cell Generation. *J Immunol* (2008) 1818:5396–404. doi: 10.4049/jimmunol.181.8.5396
86. Holmgaard R, Zamarin D, Lesokhin A, Merghoub T, Wolchok J. Targeting Myeloid-Derived Suppressor Cells With Colony Stimulating Factor-1 Receptor Blockade Can Reverse Immune Resistance to Immunotherapy in Indoleamine 2,3-Dioxygenase-Expressing Tumors. *EBioMedicine* (2016) 6:50–8. doi: 10.1016/j.ebiom.2016.02.024
87. Yu J, Du W, Yan F, Wang Y, Li H, Cao S, et al. Myeloid-Derived Suppressor Cells Suppress Antitumor Immune Responses Through IDO Expression and Correlate With Lymph Node Metastasis in Patients With Breast Cancer. *J Immunol (Baltimore Md 1950)* (2013) 1907:3783–97. doi: 10.4049/jimmunol.1201449

88. Li F, Zhao Y, Wei L, Li S, Liu J. Tumor-Infiltrating Treg, MDSC, and IDO Expression Associated With Outcomes of Neoadjuvant Chemotherapy of Breast Cancer. *Cancer Biol Ther* (2018) 198:695–705. doi: 10.1080/15384047.2018.1450116
89. Holmgaard RB, Zamarin D, Li Y, Gasmi B, Munn DH, Allison JP, et al. Tumor-Expressed IDO Recruits and Activates MDSCs in a Treg-Dependent Manner. *Cell Rep* (2015) 132:412–24. doi: 10.1016/j.celrep.2015.08.077
90. Park A, Yang Y, Lee Y, Kim M, Park Y, Jung H, et al. Indoleamine-2,3-Dioxygenase in Thyroid Cancer Cells Suppresses Natural Killer Cell Function by Inhibiting NKG2D and NKp46 Expression *via* STAT Signaling Pathways. *J Clin Med* (2019 8(6):842. doi: 10.3390/jcm8060842
91. Nafia I, Toulmonde M, Bortolotto D, Chaibi A, Bodet D, Rey C, et al. IDO Targeting in Sarcoma: Biological and Clinical Implications. *Front Immunol* (2020) 11:274. doi: 10.3389/fimmu.2020.00274
92. Dey S, Mondal A, DuHadaway JB, Sutanto-Ward E, Laury-Kleintop LD, Thomas S, et al. IDO1 Signaling Through GCN2 in a Subpopulation of Gr-1 (+) Cells Shifts the IFNgamma/IL6 Balance to Promote Neovascularization. *Cancer Immunol Res* (2021) 95:514–28. doi: 10.1158/2326-6066.CIR-20-0226
93. Pan J, Yuan K, Peng S, Huang Y, Zhang Y, Hu Y, et al. Gene Silencing of Indoleamine 2,3-Dioxygenase Hinders Tumor Growth Through Angiogenesis Inhibition. *Int J Oncol* (2017) 506:2136–44. doi: 10.3892/ijo.2017.3975
94. Yuan W, Su C, Yang X, Li Y, Cao Y, Liang X, et al. Biological and Anti-Vascular Activity Evaluation of Ethoxy-Erianin Phosphate as a Vascular Disrupting Agent. *J Cell Biochem* (2019) 120(10):16978–89. doi: 10.1002/jcb.28959
95. Lopes-Bastos B, Jin L, Ruge F, Owen S, Sanders A, Cogle C, et al. Association of Breast Carcinoma Growth With a Non-Canonical Axis of Ifnγ/Ido1/Tsp1. *Oncotarget* (2017) 849:85024–39. doi: 10.18632/oncotarget.18781
96. Li T, Yang Y, Hua X, Wang G, Liu W, Jia C, et al. Hepatocellular Carcinoma-Associated Fibroblasts Trigger NK Cell Dysfunction *via* PGE2 and IDO. *Cancer Lett* (2012) 3182:154–61. doi: 10.1016/j.canlet.2011.12.020
97. Zhai L, Ladomersky E, Dostal C, Lauing K, Swoap K, Billingham L, et al. Non-Tumor Cell IDO1 Predominantly Contributes to Enzyme Activity and Response to CTLA-4/PD-L1 Inhibition in Mouse Glioblastoma. *Brain Behav Immun* (2017) 62:24–9. doi: 10.1016/j.bbi.2017.01.022
98. Eleftheriadis T, Pissas G, Liakopoulos V, Stefanidis I. IDO Decreases Glycolysis and Glutaminolysis by Activating GCN2K, While It Increases Fatty Acid Oxidation by Activating AhR, Thus Preserving CD4+ T−cell Survival and Proliferation. *Int J Mol Med* (2018) 421:557–68. doi: 10.3892/ijmm.2018.3624
99. Schadendorf D, Hodi FS, Robert C, Weber JS, Margolin K, Hamid O, et al. Pooled Analysis of Long-Term Survival Data From Phase II and Phase III Trials of Ipilimumab in Unresectable or Metastatic Melanoma. *J Clin Oncol* (2015) 3317:1889–94. doi: 10.1200/JCO.2014.56.2736
100. Sharma P, Hu-Lieskovan S, Wargo J, Ribas A. Primary, Adaptive, and Acquired Resistance to Cancer Immunotherapy. *Cell* (2017) 1684:707–23. doi: 10.1016/j.cell.2017.01.017
101. Serafini M, Torre E, Aprile S, Grosso E, Gesù A, Griglio A, et al. *In Vivo* Discovery of Highly Potent Benzimidazole Derivatives as Indoleamine 2,3-Dioxygenase-1 (IDO1) Inhibitors: From Structure-Based Virtual Screening to Pharmacodynamic Activity. *J Med Chem* (2020) 636:3047–65. doi: 10.1021/acs.jmedchem.9b01809
102. Cheong J, Sun L. Targeting the IDO1/TDO2-KYN-AhR Pathway for Cancer Immunotherapy - Challenges and Opportunities. *Trends Pharmacol Sci* (2018) 393:307–25. doi: 10.1016/j.tips.2017.11.007
103. Spranger S. Mechanisms of Tumor Escape in the Context of the T-Cell-Inflamed and the Non-T-Cell-Inflamed Tumor Microenvironment. *Int Immunol* (2016) 288:383–91. doi: 10.1093/intimm/dxw014
104. Brown Z, Yu S, Heinrich B, Ma C, Fu Q, Sandhu M, et al. Indoleamine 2,3-Dioxygenase Provides Adaptive Resistance to Immune Checkpoint Inhibitors in Hepatocellular Carcinoma. *Cancer Immunol Immunother CII* (2018) 678:1305–15. doi: 10.1007/s00262-018-2190-4
105. Liu Y, Lv J, Liu J, Liang X, Jin X, Xie J, et al. STAT3/p53 Pathway Activation Disrupts IFN-Beta-Induced Dormancy in Tumor-Repopulating Cells. *J Clin Invest* (2018) 1283:1057–73. doi: 10.1172/JCI96329
106. Zakharia Y, McWilliams RR, Rixe O, Drabick J, Shaheen MF, Grossmann KF, et al. Phase II Trial of the IDO Pathway Inhibitor Indoximod Plus Pembrolizumab for the Treatment of Patients With Advanced Melanoma. *J Immunother Cancer* (2021) 9(6):e002057. doi: 10.1136/jitc-2020-002057
107. Long G, Dummer R, Hamid O, Gajewski T, Caglevic C, Dalle S, et al. Epacadostat Plus Pembrolizumab Versus Placebo Plus Pembrolizumab in Patients With Unresectable or Metastatic Melanoma (ECHO-301/KEYNOTE-252): A Phase 3, Randomised, Double-Blind Study. *Lancet Oncol* (2019) 208:1083–97. doi: 10.1016/s1470-2045(19)30274-8
108. Zhai L, Bell A, Ladomersky E, Lauing K, Bollu L, Nguyen B, et al. Tumor Cell IDO Enhances Immune Suppression and Decreases Survival Independent of Tryptophan Metabolism in Glioblastoma. *Clin Cancer Res an Off J Am Assoc Cancer Res* (2021) 27(23):6514–28. doi: 10.1158/1078-0432.Ccr-21-1392
109. Ladomersky E, Zhai L, Lenzen A, Lauing K, Qian J, Scholtens D, et al. IDO1 Inhibition Synergizes With Radiation and PD-1 Blockade to Durably Increase Survival Against Advanced Glioblastoma. *Clin Cancer Res an Off J Am Assoc Cancer Res* (2018) 2411:2559–73. doi: 10.1158/1078-0432.Ccr-17-3573
110. Guo YX, Liu Y, Wu W, Ling DS, Zhang Q, Zhao P, et al. Indoleamine 2,3-Dioxygenase (Ido) Inhibitors and Their Nanomedicines for Cancer Immunotherapy. *Biomaterials* (2021) 276:121018. doi: 10.1016/j.biomaterials.2021.121018
111. Low H, Lee Y, Lee Y, Wang H, Chen Y, Chien P, et al. Reciprocal Regulation Between Indoleamine 2,3-Dioxigenase 1 and Notch1 Involved in Radiation Response of Cervical Cancer Stem Cells. *Cancers* (2020) 12(6):1547. doi: 10.3390/cancers12061547
112. Zhang Y, Feng Y, Huang Y, Wang Y, Qiu L, Liu Y, et al. Tumor-Targeted Gene Silencing IDO Synergizes PTT-Induced Apoptosis and Enhances Anti-Tumor Immunity. *Front Immunol* (2020) 11:968. doi: 10.3389/fimmu.2020.00968
113. Pilotte L, Larrieu P, Stroobant V, Colau D, Dolusic E, Frédérick R, et al. Reversal of Tumoral Immune Resistance by Inhibition of Tryptophan 2,3-Dioxygenase. *Proc Natl Acad Sci USA* (2012) 1097:2497–502. doi: 10.1073/pnas.1113873109
114. Du L, Xing Z, Tao B, Li T, Yang D, Li W, et al. Both IDO1 and TDO Contribute to the Malignancy of Gliomas *via* the Kyn-AhR-AQP4 Signaling Pathway. *Signal Transduct Target Ther* (2020) 51:10. doi: 10.1038/s41392-019-0103-4
115. Li H, Ning S, Ghandi M, Kryukov GV, Gopal S, Deik A, et al. The Landscape of Cancer Cell Line Metabolism. *Nat Med* (2019) 255:850–60. doi: 10.1038/s41591-019-0404-8
116. Duhalde Vega M, Aparício J, Retegui L. Levo-1-Methyl Tryptophan Aggravates the Effects of Mouse Hepatitis Virus (MHV-A59) Infection. *Int Immunopharmacol* (2015) 242:377–82. doi: 10.1016/j.intimp.2014.12.031
117. Duhalde Vega M, Aparicio J, Mandour M, Retegui L. The Autoimmune Response Elicited by Mouse Hepatitis Virus (MHV-A59) Infection Is Modulated by Liver Tryptophan-2,3-Dioxygenase (TDO). *Immunol Lett* (2020) 217:25–30. doi: 10.1016/j.imlet.2019.11.004
118. Muller A, Manfredi M, Zakharia Y, Prendergast G. Inhibiting IDO Pathways to Treat Cancer: Lessons From the ECHO-301 Trial and Beyond. *Semin immunopathol* (2019) 411:41–8. doi: 10.1007/s00281-018-0702-0
119. Opitz C, Somarribas Patterson L, Mohapatra S, Dewi D, Sadik A, Platten M, et al. The Therapeutic Potential of Targeting Tryptophan Catabolism in Cancer. *Br J Cancer* (2020) 1221:30–44. doi: 10.1038/s41416-019-0664-6
120. Ozturk S, Kalter V, Roessner PM, Sunbul M, Seiffert M. IDO1-Targeted Therapy Does Not Control Disease Development in the Emicro-TCL1 Mouse Model of Chronic Lymphocytic Leukemia. *Cancers (Basel)* (2021) 13(8):1899. doi: 10.3390/cancers13081899
121. Phan T, Nguyen VH, D'Alincourt MS, Manuel ER, Kaltcheva T, Tsai W, et al. Salmonella-Mediated Therapy Targeting Indoleamine 2, 3-Dioxygenase 1 (IDO) Activates Innate Immunity and Mitigates Colorectal Cancer Growth. *Cancer Gene Ther* (2020) 273-4:235–45. doi: 10.1038/s41417-019-0089-7
122. Klar R, Michel S, Schell M, Hinterwimmer L, Zippelius A, Jaschinski F. A Highly Efficient Modality to Block the Degradation of Tryptophan for Cancer Immunotherapy: Locked Nucleic Acid-Modified Antisense Oligonucleotides to Inhibit Human Indoleamine 2,3-Dioxygenase 1/Tryptophan 2,3-Dioxygenase Expression. *Cancer Immunol Immunother* (2020) 691:57–67. doi: 10.1007/s00262-019-02438-1
123. Fiore A, Murray P. Tryptophan and Indole Metabolism in Immune Regulation. *Curr Opin Immunol* (2021) 70:7–14. doi: 10.1016/j.coi.2020.12.001

124. Thüring M, Knuchel R, Picchetta L, Keller D, Schmidli T, Provenzano M. The Prognostic Value of Indoleamine-2,3-Dioxygenase Gene Expression in Urine of Prostate Cancer Patients Undergoing Radical Prostatectomy as First Treatment of Choice. *Front Immunol* (2020) 11:1244. doi: 10.3389/fimmu.2020.01244
125. Botticelli A, Mezi S, Pomati G, Cerbelli B, Cerbelli E, Roberto M, et al. Tryptophan Catabolism as Immune Mechanism of Primary Resistance to Anti-PD-1. *Front Immunol* (2020) 11:1243. doi: 10.3389/fimmu.2020.01243
126. Yu C, Fu S, Chen X, Ye J, Ye Y, Kong L, et al. The Clinicopathological and Prognostic Significance of IDO1 Expression in Human Solid Tumors: Evidence From a Systematic Review and Meta-Analysis. *Cell Physiol Biochem Int J Exp Cell Physiol Biochem Pharmacol* (2018) 491:134–43. doi: 10.1159/000492849
127. Riesenberg R, Weiler C, Spring O, Eder M, Buchner A, Popp T, et al. Expression of Indoleamine 2,3-Dioxygenase in Tumor Endothelial Cells Correlates With Long-Term Survival of Patients With Renal Cell Carcinoma. *Clin Cancer Res an Off J Am Assoc Cancer Res* (2007) 1323:6993–7002. doi: 10.1158/1078-0432.Ccr-07-0942
128. Ishio T, Goto S, Tahara K, Tone S, Kawano K, Kitano S. Immunoactivative Role of Indoleamine 2,3-Dioxygenase in Human Hepatocellular Carcinoma. *J Gastroenterol Hepatol* (2004) 193:319–26. doi: 10.1111/j.1440-1746.2003.03259.x
129. Masaki A, Ishida T, Maeda Y, Suzuki S, Ito A, Takino H, et al. Prognostic Significance of Tryptophan Catabolism in Adult T-Cell Leukemia/Lymphoma. *Clin Cancer Res an Off J Am Assoc Cancer Res* (2015) 2112:2830–9. doi: 10.1158/1078-0432.Ccr-14-2275
130. Zhai L, Dey M, Lauing K, Gritsina G, Kaur R, Lukas R, et al. The Kynurenine to Tryptophan Ratio as a Prognostic Tool for Glioblastoma Patients Enrolling in Immunotherapy. *J Clin Neurosci Off J Neurosurgical Soc Australasia* (2015) 2212:1964–8. doi: 10.1016/j.jocn.2015.06.018

Conflict of Interest: The authors declare that the research was conducted in the absence of any commercial or financial relationships that could be construed as a potential conflict of interest.

frontiers in Immunology

REVIEW
published: 23 December 2021
doi: 10.3389/fimmu.2021.773168

What Happens to the Immune Microenvironment After PD-1 Inhibitor Therapy?

Qingyi Wang[1,2], *Bin Xie*[1], *Shuang Liu*[1,2], *Ying Shi*[1,2], *Yongguang Tao*[1,2,3,4*], *Desheng Xiao*[1,2*] *and Wenxiang Wang*[5*]

[1] Department of Pathology, Xiangya Hospital, Central South University, Changsha, China, [2] Department of Pathology, School of Basic Medicine, Key Laboratory of Carcinogenesis and Cancer Invasion (Ministry of Education), Central South University, Changsha, China, [3] National Health Commission (NHC) Key Laboratory of Carcinogenesis (Central South University), Cancer Research Institute and School of Basic Medicine, Central South University, Changsha, China, [4] Hunan Key Laboratory of Early Diagnosis and Precision Therapy, Second Xiangya Hospital, Central South University, Changsha, China, [5] Department of the 2nd Department of Thoracic Surgery, Hunan Cancer Hospital and The Affiliated Cancer Hospital of Xiangya School of Medicine, Central South University, Changsha, China

OPEN ACCESS

Edited by:
Nicolas Larmonier,
Université de Bordeaux, France

Reviewed by:
Jaya Lakshmi Thangaraj,
University of California, San Diego, United States
Maite Alvarez,
University of Navarra, Spain

***Correspondence:**
Yongguang Tao
taoyong@csu.edu.cn
Desheng Xiao
xdsh96@csu.edu.cn
Wenxiang Wang
wwx78@foxmail.com

Specialty section:
This article was submitted to Cancer Immunity and Immunotherapy, a section of the journal Frontiers in Immunology

Received: 09 September 2021
Accepted: 23 November 2021
Published: 23 December 2021

Citation:
Wang Q, Xie B, Liu S, Shi Y, Tao Y, Xiao D and Wang W (2021) What Happens to the Immune Microenvironment After PD-1 Inhibitor Therapy? Front. Immunol. 12:773168. doi: 10.3389/fimmu.2021.773168

The fruitful results of tumor immunotherapy establish its indispensable status in the regulation of the tumorous immune context. It seems that the treatment of programmed cell death receptor 1 (PD-1) blockade is one of the most promising approaches for cancer control. The significant efficacy of PD-1 inhibitor therapy has been made in several cancer types, such as breast cancer, lung cancer, and multiple myeloma. Even so, the mechanisms of how anti-PD-1 therapy takes effect by impacting the immune microenvironment and how partial patients acquire the resistance to PD-1 blockade have yet to be studied. In this review, we discuss the cross talk between immune cells and how they promote PD-1 blockade efficacy. In addition, we also depict factors that may underlie tumor resistance to PD-1 blockade and feasible solutions in combination with it.

Keywords: immunotherapy, PD-1 inhibitor, tumor microenvironment, cytotoxic T lymphocytes (CTLs), immunotherapy resistance, combined immunotherapy

BACKGROUND

Immune surveillance functions of innate and adaptive immune cells can be suppressed by multiple mechanisms in the tumor microenvironment (TME); the most noted one is the programmed cell death receptor 1 (PD-1)/programmed cell death ligand 1 (PD-L1) pathway. For example, PD-L1, as the ligand of PD-1, could overexpress on tumor cells to evade the antitumor immune response by repressing the activation and function of CD8+T cells (1). Anti-PD-1 is one of the most promising attractive anticancer immune checkpoint blockers (ICB). Growing evidence shows that not only T cells but also other immune cells can be promoted by anti-PD-1 directly or indirectly, to suppress the progression of tumors (2–5). However, despite PD-1 blockade therapies having durable responses for a minority of patients in clinical trials, there is still an unmet clinical need for the majority of patients who do not respond to anti-PD-1 (6). Thus, we firstly summarize the cross talk between immune cells and their possible transformation in the TME after PD-1 blockade therapy. In the second part, we discuss the primary impact factors of resistance to PD-1 inhibitors,

such as tumor immune recognition, oncogenic signal pathways, interferon (IFN), immune contexture, angiogenesis, immunometabolism, intestinal microbiota, and new immune checkpoints. We also highlight feasible combined therapy strategies to re-sensitize tumors to PD-1 blockade.

THE ROLE OF PD-1 AND PD-1 INHIBITORS IN IMMUNE RESPONSE

PD-1

PD-1, a member of the B7-CD28 receptor family, is a transmembrane protein and widely expressed in B cells, T cells, natural killer (NK) cells, and myeloid cells (7). As the ligand of PD-1, programmed cell death ligand 1 (PD-L1) can be expressed in dendritic cells (DCs), macrophages, T cells, NK cells (8, 9), and tumor cells (10). Generally, when PD-L1 binds to PD-1 in the presence of the T cell receptor (TCR) signaling complex, PD-1 delivers a co-inhibitory signal, leading to the termination of TCR signaling and inhibition of T cell proliferation (11). PD-1 often uses mono-tyrosine signaling motifs which present in its cytoplasmic tail, such as immunoreceptor tyrosine-based inhibitory motif (ITIM) and immunoreceptor tyrosine-based switch motif (ITSM) (12), to end the CD28/TCR signal by PD-1 phosphorylation and the recruitment of SHP-2 and SHP-1 (13–15). In the tumor immune context, antigen-presenting cells (APCs) and tumor cells highly express PD-L1, and they can interact with PD-1-overexpressed T cells, leading to T-cell anergy or exhaustion (16, 17). Programmed cell death ligand 2 (PD-L2) is the second ligand for the PD-1 molecule, which is expressed predominantly by DCs, macrophages, B cells, and cancer cell populations, depending on microenvironmental stimulation (18, 19). Similar to PD-L1, PD-L2 plays a crucial role in evading antitumor immunity. The engagement of PD-1 and PD-L2 can lead to the downregulation of T cell responses, which inhibits TCR-mediated proliferation and cytokine production by CD4+ T cells by blocking cell cycle progression (18). Although PD-1/PD-L2 blockade must be considered for optimal immunotherapy in antitumor immunity (20), since most of the research results are focused on the PD-1/PD-L1 pathway, we mainly discuss the PD-1/PD-L1 axis in this article.

PD-1 Inhibitors

As surface molecules, the activity of PD-1 and PD-L1 can be easily inhibited by blocking antibodies. Anti-PD-1 therapy is one of the most successful immune checkpoint blockade therapies that have been approved to treat a wide variety of cancer types (**Table 1**). PD-1 inhibitors competitively bind to PD-1 and block PD-1/PD-L1 interactions, which subsequently regulate negative signals on the T cell surface to enhance the functions of effector T cells and promote the proliferation of T cells (54). Nivolumab and pembrolizumab are the primary clinically approved PD-1 inhibitors. They are humanized IgG4 antibodies targeting PD-1 with high affinity (55). To ensure that they elicit their inhibitory effects of PD-1/PD-L1 interactions primarily by direct occupancy and steric blockade of the PD-L1-binding site of PD-1 (56), they minimize the function of effector cells engaging other antibodies.

Pembrolizumab was initially approved for refractory unresectable melanoma in 2014 (57), known as the first PD-1-targeted therapy to gain Food and Drug Administration (FDA) approval. Not long, in 2015, it becomes the first immune checkpoint inhibitor to be approved as a first-line treatment, also in melanoma therapy (21). Pembrolizumab is thus approved to treat a wide variety of cancer types. To date, pembrolizumab therapy has been licensed in many cancers (27, 30, 58, 59) and was often conducted primarily in patients with PD-L1-positive disease (31, 34). In general, a higher level of PD-L1 expression is associated with a more effective clinic outcome of pembrolizumab. However, in some cancer types, such as non-small cell lung cancer (NSCLC) (60), classical Hodgkin's lymphoma (cHL) (25), and urothelial carcinoma (UC) (61), PD-L1 expression did not explicitly correlate with response to pembrolizumab.

Nivolumab also displays a good response and favorable safety profile, particularly in melanoma and NSCLC. Nivolumab was approved by FDA following its showing a clear advantage in response over chemotherapy in refractory unresectable melanoma (62). Soon after, the FDA approved nivolumab for the treatment of NSCLC after progression on a platinum-based chemotherapy regimen (41, 63). Also, nivolumab has been demonstrated durable effects in other cancers (47, 64, 65), and it appears that combination therapy may further improve them (50, 66). Nevertheless, research has demonstrated a low response rate in some hematological tumors, such as follicular lymphoma (FL) (67) and diffuse large B cell lymphoma (DLBCL) (68). It may appear to correlate positively with 9p24.1 translocation and increased PD-L1 expression (69). In addition to nivolumab and pembrolizumab, cemiplimab is also approved by FDA for the treatment of advanced cutaneous squamous cell carcinoma (70) and first-line NSCLC (53). Up till now, more than 1,500 clinical trials involving PD-1 inhibition are currently supported by the National Cancer Institute (NCI).

IMMUNE MICROENVIRONMENT

Immunotherapies based on PD-L1/PD-1 blockade have revolutionized the treatment paradigm for several cancer types. Their interaction regulates the activation of immune responses and specifically of T cell responses in physiological conditions. In the last years, increasing evidence has demonstrated that the elimination of tumor cells is mainly mediated by cytotoxic T lymphocytes (CTLs) (71). Several types of immune cells in the TME, such as tumor-associated macrophages (TAMs), DCs, NK cells, and immunosuppressive cells, can also interact with each other to promote or repress tumor progression in direct and indirect mechanisms by secreting cytokines and chemokines (71). Indeed, there is a complex picture of the relationship between checkpoint blockade and immune context. The precise molecular mechanisms of how PD-1 inhibitors function by stimulation/inhibition of immune-related cells remain to be fully

TABLE 1 | Summary of FDA-approved PD-1 inhibitors in advanced/metastatic cancers.

Agent(s)	Pathology	Indications	Clinical trial	Reference
Pembrolizumab	Melanoma	First-line/ Second-line	KEYNOTE-006 phase 3/KEYNOTE-002 phase 2	(21, 22)
	NSCLC	First-line (TPS ≥1%, ALK/EGFR wt) Second-line (TPS ≥1%)	KEYNOTE-042 phase 3/KEYNOTE-010 phase 2/3	(23, 24)
	HL	Relapsed after ≥ third-line	KEYNOTE-087 phase 2	(25)
	PMBCL	Relapsed after ≥ second-line	KEYNOTE-170 phase 2	(26)
	MCC	First-line	KEYNOTE-017 phase 2	(27)
	UC	First-line cisplatin-ineligible/recurrent after platinum-based treatment	KEYNOTE-052 phase 2/KEYNOTE-045 phase 3	(28, 29)
	HCC	Second-line after sorafenib	KEYNOTE-224 phase 2	(30)
	GC	Progression on or after ≥ second-line (CPS ≥1%)	KEYNOTE-059 phase 2	(31)
	Non-colorectal MSI-H/ dMMR cancer	Previously treated	KEYNOTE-158 phase 2	(32)
	HNSCC	First-line (CPS ≥1%)/ Second-line	KEYNOTE-048 phase 3 KEYNOTE-012 phase 1b	(33)
	CC	Previously treated (CPS ≥1%)	KEYNOTE-158 phase 2	(34)
	EC	Progression after first-line (CPS ≥10%)	KEYNOTE-181 phase 3	(35)
Pembrolizumab + chemotherapy	NSCLC	First-line	KEYNOTE-021 phase 2/KEYNOTE-407 phase 3	(36, 37)
	EC	First-line	KEYNOTE-590 phase 3	(38)
Nivolumab	Melanoma	First-line/second-line	CheckMate-037/066 phase 3	(39, 40)
	NSCLC	Second-line	CheckMate-017/057 phase 3	(41, 42)
	HL	Progressed after ASCT or brentuximab	CheckMate-039 phase 1 CheckMate-205 phase 2	(43)
	UC	Recurrent after platinum-based treatment	CheckMate-275 phase 2	(44)
	HCC	Previously treated with sorafenib	CheckMate-040 phase 1/2	(45)
	MSI-H/dMMR colorectal cancer	Treatment-refractory to all standard therapies	CheckMate-142 phase 2	(46)
	HNSCC	Platinum-refractory, recurrent	CheckMate-141 phase 3	(47)
	SCLC	Third-line	CheckMate-032 phase 1/2	(48)
Nivolumab+ Ipilimumab	MSI-H and dMMR	Treatment-refractory to all standard therapies	CheckMate-142 phase 2	(49)
	RCC	First-line	CheckMate-214 phase 3	(50)
	NSCLC	First-line (PD-L1 ≥1%)	CheckMate-227 phase 3	(51)
Cemiplimab	CSCC	First-line	NCT02383212/ NCT02760498 phase 3	(52)
	NSCLC	First-line (TPS ≥50% EGFR, ALK, or ROS1 wt)	NCT03088540 phase 3	(53)

Tumor types: NSCLC, non-small cell lung carcinoma; HL, Hodgkin lymphoma; PMLBCL, primary mediastinal large B cell lymphoma; MCC, Merkel cell carcinoma; UC, urothelial carcinoma; HCC, hepatocellular carcinoma; GC, gastric cancer; MSI, microsatellite instability; dMMR, mismatch repair-deficient; HNSCC, head and neck squamous cell carcinoma; CC, cervical cancer; EC, esophageal cancer; SCLC, small cell lung carcinoma; RCC, renal cell carcinoma; CSCC, cutaneous squamous cell carcinoma. wt, wild-type; TPS, tumor proportion score; CPS, combined positive score; ASCT, autologous hematopoietic stem cell transplantation.

understood. Here, we will attempt to discuss in detail the cross talk between immune cells and the critical role of some immune cells in the efficacy of PD-1 inhibitors therapy (**Figure 1**).

T Cells

CD8+T Cells

CD8+T cells are a subset of lymphocytes developing in the thymus. They recognize antigen-presented cells expressing major histocompatibility complex (MHC) class I molecules and in turn exert antitumor function (3, 71). Initiation of a response from CD8+T cells against an antigen requires corroboration work between CD4+T cells with NK cells and DCs (3, 72). Activated, antigen-loaded DCs can launch the differentiation of CD8+T cells into CTLs by cross-presenting MHC class I molecules to cells (73). CD4+T cells can secrete cytokines following the interaction with antigens to simulate the optimal proliferation and activation of CD8+ T cells (74). On the other hand, NK cells and CD4+T cells can produce chemokines which indirectly induce the activation of CD8+ T cells by promoting the differentiation and maturation of DC cells (72, 75). Due to such cross talk, CTLs can initiate the antitumor effect through releasing IFN-γ and tumor necrosis factor α (TNF-α) to induce cytotoxicity in the cancer cells (76).

However, PD-1, as a coinhibitory receptor, could overexpress on activated CD8+ T cells (77). Once this happens, signals downstream of TCR may be attenuated and may cause the exhaustion of CD8+ T cells and ultimately contribute to the restriction of T cell activation and cytokine production (78). PD-1 blockade therapy seems to counteract tumor-induced T cell dysfunctionality by interfering with PD-1/PD-L1 signals; it releases the negative regulation of T cells and promotes T cells which produced higher levels of IFN-γ to activate antitumor immune response (79–81). Besides, PD-1 inhibitors reinvigorate preexisting CD8+T cells within the tumor and promote systemic T cell immunity priming. Nevertheless, the study revealed that preexisting tumor-specific T cells may have limited

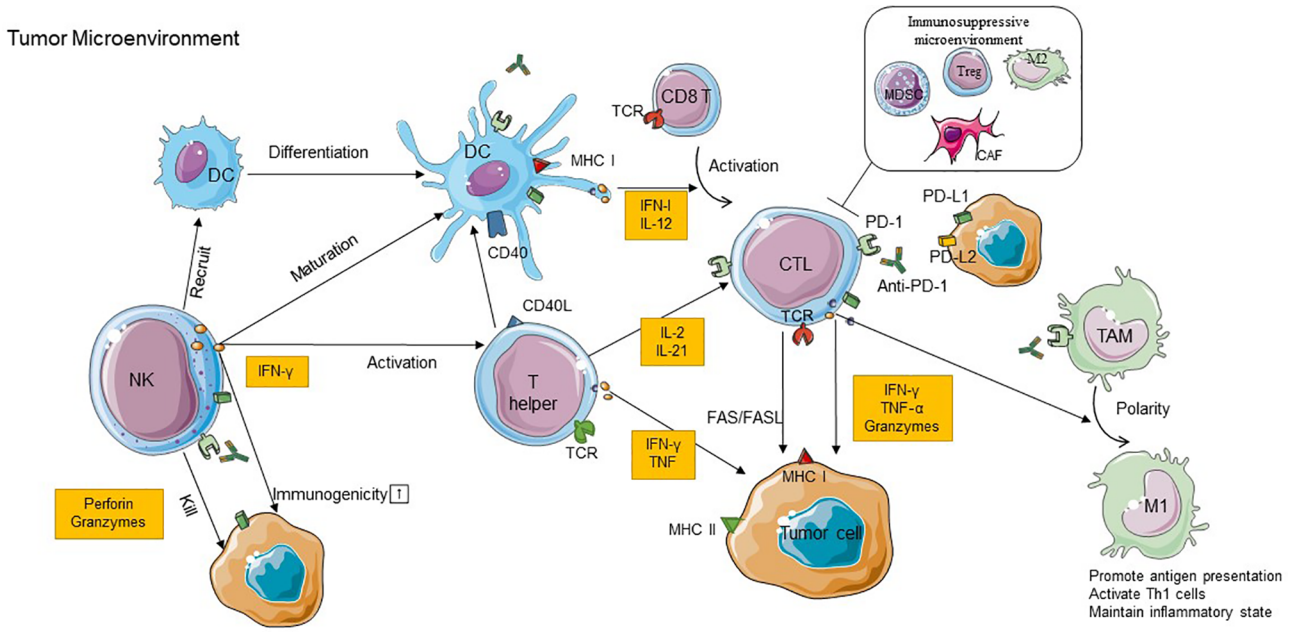

FIGURE 1 | The cross talk between immune cells in TME and the role of immune cells in the efficacy of PD-1 inhibitor therapy. CD8+T cells recognize antigens requiring a corroboration work between CD4+T cells with NK cells and DCs, and M1 TAM can exert antitumoral effects due to the stimulation of IFN-γ produced by CD8+ T cells. In addition to these immunostimulatory cells, the immunoinhibitory cells including CAFs, Tregs, M2 TAMs, and MDSCs can construct an immunosuppressive microenvironment to restrict the antitumor effect. Anti-PD-1 binds to PD-1 on immune cells which can block PD-1/PD-L1 interactions and recover the antitumor function of those cells. PD-1, programmed cell death protein 1; PD-L1, programmed death-ligand 1; PD-L2, programmed death-ligand 2; IFN-γ, interferon gamma; TNF, tumor necrosis factor; CTL, cytotoxic T lymphocyte; DC, dendritic cell; NK, natural killer cell; MDSC, myeloid-derived suppressor cell; Treg, regulatory T cell; CAF, cancer-associated fibroblast; TAM, tumor-associated macrophage; M1, type 1 macrophage cell; M2, type 2 macrophage cell; MHC, major histocompatibility complex; TCR, T cell receptor; TME, tumor microenvironment.

reinvigoration capacity and that the T cell response to checkpoint blockade derives from a distinct repertoire of T cell clones that may have just recently entered the tumor (82). The priming of antitumor T-cell immunity in lymphatic drainage might explain such consequence, which is further explained in another study. This study showed that tumor-draining lymph nodes (TDLNs) are enriched for tumor-specific PD-1^{+}T cells which are closely associated with PD-L1^{+}DCs (83). Suppression of DCs, accompanied by excess PD-L1 surface expression, may lead to restrained T cell priming and deviated CD8+ T cell differentiation in the TDLN. Therefore, it suggests that progenitor-exhausted T cells can be rescued by immune checkpoint blockade and then home to the tumor and populate the TME, to improve tumor control (83). However, the exact contribution of TDLN versus TME during PD-1/PD-L1 checkpoint blockade therapy remains to be elucidated.

On the other hand, the report found that PD-L1 can also be upregulated on T cells (84). PD-L1-expressing T cells can suppress immunity on neighboring T cells and polarize macrophages toward a tolerogenic phenotype *via* the PD-L1–PD-1 axis in the TME, which in turn both suppresses T cell activation and promotes tumor growth (84). It is still not clear whether PD-1 inhibitors also play a role based on this theory. Accordingly, the precise molecular mechanisms of T cell function stimulated by PD-1 inhibitors remain to be clarified.

CD4+T Cells (T Helper Cells)

CD4+T cells participate in the activation and expansion of CD8+T effectors; they induce an antitumor response by providing regulatory signals (85–87). In the tumor context, MHC class II molecules can present antigenic peptides recognized by CD4+T cells (88, 89). MHC-class II+ tumors can be directly killed by CD4+ CTLs. For the MHC-class II-negative tumor cells, CD4+ T cells can produce a vast range of cytokines that mediate inflammatory and effector immune responses (90, 91); TNF and IFN-γ are the most important cytokines that are mainly produced by T helper (Th) 1 cells. Additionally, CD4 Th1 cells also display antitumor responses by activating NK cells (90) and M1 TAM (92, 93), inhibition of angiogenesis (94), and/or induction of tumor senescence (95).

To date, the specific contribution of CD4 immunity to PD-1 blockade therapy efficacy is still unknown. In NSCLC, proliferation and low PD-1/LAG-3 co-expression of CD4 at baseline were responsive to PD-1 blockade *ex vivo* and *in vivo* (96). In cHL, PD-1 blockade therapy has strong antitumor effects on MHC-II-expressing tumors mediated by cytotoxic CD4+ T cells in murine models (97). These provide strong evidence that CD4 immunity might be an entry point to achieve efficacious clinical responses under PD-1 blockade therapies. Further research is needed to reveal the specific contribution of CD4+ T cells.

NK Cells

NK cells can spontaneously kill cells and thus are presumed to be key innate immune effectors in cancer immunosurveillance; it belongs to the family of innate lymphoid cells (ILCs) (98). IFN-γ produced by NK cells during early-phase immune responses can directly kill tumor cells and promote the differentiation of naive CD4+ T cells toward Th1 cells to facilitate cell-mediated immunity (99). Thus, NK cells are critical components both in humoral immunity and in cellular immunity.

As an inhibitory receptor, PD-1 can express on NK cells (100, 101) and prevent the activation of NK cell function when engaging with its ligand which is expressed on the surface of target tumor cells or APC (102). PD-1$^+$ NK cells may be inhibited in killing tumor cells instead of being anergic in PD-L1$^+$ tumors, which means that PD-1 is an important checkpoint for NK activation and PD-1 blockade might elicit an antitumor NK cell response (102). In high PD-L1 expression head and neck cancer (HNC) patients, the study observed that PD-1 blockade increased cetuximab-mediated NK cell activation and cytotoxicity (103). Besides, tumors might drive the development of PD-L1-expressing NK cells that acquire immunoregulatory functions; such cell population can directly inhibit CD8+ T cell proliferation in a PD-L1-dependent manner (104). These results show the importance of the PD-1/PD-L1 axis in inhibiting NK cell responses *in vivo*, and future research is needed to determine the specific mechanism of the PD-1 pathway in the antitumor response of NK cells.

DCs

DCs, known as specialized APC, transport tumor antigens to draining lymph nodes and cross-present antigens *via* MHC I and II to activate cytotoxic T lymphocytes (105). DC maturation is necessary to T cell proliferation and differentiation; the final antitumor immunity is also associated with co-stimulatory molecules and cytokines which are expressed as the mature markers on DCs, such as CD80/CD86 and IL-12 (106).

DCs are necessary for anti-PD-1 efficacy. Anti-PD-1-activated T cells secrete IFN-γ, which in turn primes a transcriptomic shift in DC phenotype; DCs produce IL-12 upon sensing IFN-γ to stimulate effector T cell responses (107–109). The activation of the non-canonical nuclear factor kappa-light-chain enhancer of the activated B cell (NF-κB) pathway is also required for checkpoint efficacy, for it can enrich IL-12-producing DCs (107). Additionally, evidence of direct regulation is still emerging. PD-1 expression has recently been identified on DCs in the specific tumor context (110, 111). The result of an ovarian study demonstrated that PD-1 expressed on the tumor-associated DC can suppress NF-κB activation and the release of immune regulatory cytokines and restrict the upregulation of co-stimulatory molecules (111), which mediate immune suppression. PD-1 inhibition seems to increase the co-stimulatory molecule expression of DCs (112). In addition, the specific ablation of PD-1 on intratumoral DCs resulted in enhanced priming of tumor-specific CD8+ T cells to secrete IL-2 and IFN-γ (110). While DCs are the major antigen-presenting cells for cross-presenting tumor antigens to T cells and promoting antitumor response, PD-L1 expression on DCs can be upregulated by inflammatory cytokines, especially IFNs. Such upregulation is likely to prevent the overexpansion of tumor-infiltrating lymphocytes and eventually dampen the antitumor responses (113, 114). These results might provide additional insights into the role PD-1/PD-L1 plays on DCs to facilitate antitumor response and the mechanisms of immune checkpoint blockade therapy efficacy.

TAMs

TAMs are major components of infiltrated leukocytes in tumors, which dominantly orchestrate cancer-related inflammation (115). They can be divided into two subtypes: M1 and M2. Anti-tumorigenic M1 macrophages express high levels of TNFα, inducible nitric oxide synthase (iNOS), and MHC class II molecules. They exert antitumoral effects due to the stimulation of IFN-γ produced by CD8+ T cells and CD4+T cells (71). Inversely, pro-tumorigenic M2 macrophages are marked with a high level of arginase 1 (ARG1) and CD206 expression (116). M2 cells can secrete STAT3 to the TME for impairing responses from CTLs when their number increases in the stroma (117). Besides, M2 cells can express inhibitory ligands PD-L1, which bind to inhibitory receptor PD-1 constitutively expressed in T cells to activate them, directly inhibiting TCR signals to restrain the antitumor function of T cells (118).

Primary macrophages transform into the M1 or M2 phenotype which can be induced by PD-1 signaling pathways (119). TAMs display detectable PD-1 levels in the tumor microenvironment; PD-1 blockade therapy contributed to both a direct and an indirect impact on TAMs. Indirectly, checkpoint blockade-activated T cells can accumulate TAMs by secrete factors (such as IFN-γ) to remodel the TME toward a tumor hostile environment rich in iNOS+ TAMs (119). In direct regulation, PD-1 deficiency in TAMs shifts their phenotype toward an antitumor profile, with higher levels of TNF-α, iNOS, and MHC II (120). Myeloid-specific PD-1 deletion was as effective at limiting tumor growth as global PD-1 deletion and more effective than selective ablation of PD-1 in T cells (121). TAM PD-1 expression negatively correlates with phagocytic potency against tumor cells; TAM infiltration is skewed toward high CD206 and ARG1 macrophages dampening antitumor immune responses (122, 123). Anti-PD-1 therapy can surprisingly reverse this trend, increasing the expression of iNOS, TNF-α, and IL-6, which may augment antitumor immunity (124). Accordingly, the inhibition of PD-1 expressed on TAMs can shift them to the M1 phenotype and form an antitumor TME.

Immunosuppressive Cells

Immunosuppressive cells, unlike immune cells, have a positive effect on antitumoral immunity. There are some immunoinhibitory cells that display negative cross talking in TME, including cancer-associated fibroblasts (CAFs), regulatory T cells (Tregs), myeloid-derived suppressor cells (MDSCs), and M2 TAMs

(mentioned above). Tregs repress the proliferation of both CD8+ and CD4+T cells through releasing transforming growth factor β (TGF-β) (125). CAFs promote the rate of glycolytic metabolism and further constitute a glucose-deficient TME. CTLs tend to decrease their number when encountered with such conditions (126). It is not yet known whether these have a role in promoting the efficacy of PD-1, but studies have shown that they are crucial in immune resistance, which will be discussed in detail in a subsequent paragraph.

DRUG RESISTANCE AND COMBINED THERAPY

Anti-PD-1 therapy has shown significant efficacy in clinical trials and has been approved for treating several cancers in clinic therapy. However, the occurrence of primary or acquired drug resistance will cause the patient to be ineffective to PD-1 blockade therapy or eventually the recurrence of malignant tumors (127). There are internal and external causes of tumor resistance to PD-1 blockade. The internal causes focus on the inherent characteristics of tumor cells; these include defective tumor immunorecognition, epigenetic regulation, abnormal oncogenic signaling, and IFN-γ signal pathway, while the external causes are mainly emanated from the tumor microenvironment, such as exhaustion of T cells, immunosuppressive cells and cytokines, tumor metabolites, new immune checkpoints, and intestinal microflora (128). Here, we summarize the primary resistant mechanisms to anti-PD-1 (**Figure 2**). In addition, we highlight emerging combined treatment strategies that might prolong the efficacy of PD-1 blockade or enable immunotherapy to impinge on previously intractable cancer types.

Defective Tumor Immunorecognition

Some studies have shown that carcinomas with robust T cell immunosurveillance can evade recognition through diverse genetic and immune-related mechanisms, including loss of tumor neoantigens and defect in antigen presentation.

Loss of Tumor Neoantigens

Despite that cancer immunoediting can suppress tumor growth, it can establish favorable conditions within the tumor microenvironment to facilitate tumor outgrowth of the immune system which no longer recognizes the tumor (129). A neoantigen is an antigen encoded by the mutant gene of tumor cells. It is cross-presented *via* DCs and recognized by mature activated T cells. Emerging research supports the critical role of neoantigens in response to PD-1 blockade therapy. For instance, it highlights that neoantigen-specific CD8+T-cell responses were parallel to tumor regression in a responder of NSCLC patients treated with pembrolizumab (130), indicating that anti-PD-1 therapy enhances tumor neoantigen-specific T cell responses. In addition, in NSCLC patients who developed acquired drug resistance after single anti-PD-1 or anti-PD-1 combined with anti-CTLA-4 therapy, the loss of neoantigens has been found based on complete exome sequencing of tumor cells (131). It means that the PD-1-blocking therapy may be less effective if the tumor does not contain a mutation that can be a target. Despite the underlying mechanism being still unclear, evidence highlights that the combination of radiotherapy (RT) and anti-PD-1 is considered a promising strategy (132). Most likely, it is dependent on RT-induced cell damage that may express somatic mutations that generate neo-antigens, which have the potential to serve as targets for a more robust immune response (133). In preclinical triple-negative breast tumor models, data show that radiotherapy can enrich tumors of functionally active. Curative capacity has been enhanced when radiotherapy is combined with immunostimulatory and α-PD-1 monoclonal antibodies (mAbs) (134). Similarly, cancer cell death induced by chemotherapy is thought to promote tumor antigen release and antigen presentation and stimulate immune effectors. Combining checkpoint inhibitors with standard-of-care chemotherapy has been successful in non-small cell lung carcinoma (135, 136) and triple-negative breast cancer (137). Besides, individualized mutanome vaccines, an RNA-based poly-neo-epitope approach to mobilize immunity against a spectrum of cancer mutations, were applied to patients in melanoma and obtained a complete response to vaccination in combination with PD-1 blockade therapy (138). These results mean that the combination of PD-1 blockade with an agent that can facilitate tumor cells to generate neo-antigen may increase antitumor immunity.

Defective Antigen Presentation

Effective tumor antigen presentation to CD8+T cells relies on class I MHC (139, 140). Loss of heterozygosity and genetic deficiencies of β2-microglobulin (B2M) are both crucial ways that lead to the loss of MHC molecules (140–142), which promote resistance to PD-1 blockade due to the inability of CD8+T cells to recognize tumor antigens and specifically kill tumor cells (143). Thus, to recover the ability of antigen presentation may represent potential avenues that can be combined with immunotherapy.

The impairment of antigen presentation can be induced by epigenetic regulation. DNA methylation is thought to regulate the expression of tumor-associated antigens by downregulating the level of MHC class I. Studies have shown that the capability of DNA methyltransferase inhibitors (DNMTi) to upregulate MHC class I and MHC class II has appeared in many cancers (144, 145). Enhancer of zeste homolog 2 (EZH2), a catalytic component in the polycomb repressive complex 2 (PRC2), plays a crucial role in the mediation of histone h3 lysine 27 tri-methylation (H3K27me3) (146). Research revealed a negative correlation between the expression levels of EZH2 and MHC I antigen presentation molecules (147). The study also found that tumor progression of an anti-PD-1-resistant head and neck squamous cell carcinoma (HNSCC) model can be suppressed by combinatorial treatment of an EZH2 inhibitor and anti-PD-1. Paradoxically, in ovarian cancer models, EZH2 inhibition has nothing to do with the alteration of the class I antigen presentation of ovarian cancer cells (148), indicating that the regulation of EZH2 on antigen presentation may be cancer-type specific. Therefore, the impairment of antigen presentation may

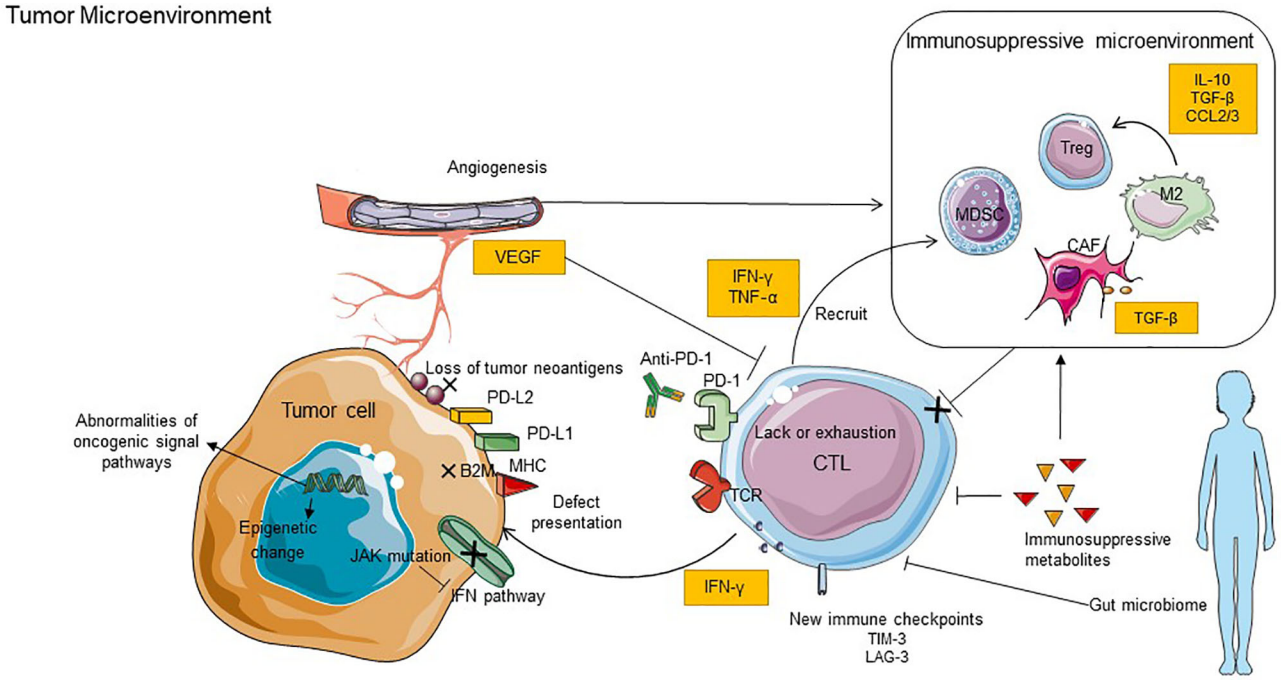

FIGURE 2 | Key mechanisms of resistance to anti-PD-1 inhibitors. The mechanisms of resistance including internal and external causes. The internal causes focus on the inherent characteristics of tumor cells, it includes defective tumor immunorecognition, epigenetic regulation, abnormal oncogenic signaling, and IFN-γ signal pathway. The external causes are mainly emanated from the tumor microenvironment, such as exhaustion of T cells, immunosuppressive cells and cytokines, tumor metabolites, new immune checkpoints, and intestinal microflora. B2M, B2-microglobulin; LAG3, lymphocyte-activation gene 3; TIM3, T cell immunoglobulin and mucin domain-containing molecule 3; VEGF, vascular endothelial growth factor; JAK, Janus kinase.

promote tumor immune escape while providing a potential strategy to overcome resistance to PD-1 inhibitor therapy.

Oncogenic Signal Pathways

Cancer is a genetic disease that can be induced by multiple genetic alterations, which are commonly caused by abnormalities of several key oncogenic pathways (149), like the phosphatase and tensin homolog (PTEN) signal pathway and mitogen-activated protein kinase (MAPK) signal pathway. Here, we mainly describe the two most common pathways, which have been proven to be closely related to PD-1 inhibitor resistance.

Research found that loss of PTEN in tumor cells in clinical patients of melanoma correlates with decreased T-cell infiltration, expansion, and inferior outcomes with PD-1 inhibitor therapy (150). PTEN loss-of-function mutations in tumors were significantly increased in non-responders who were treated with anti-PD-1 antibodies (151). Additionally, one of the most common pathways activated by loss of expression of the tumor suppressor PTEN is the phosphatidylinositol 3-kinase (PI3K) pathway, which plays a critical role in cancer by regulating several critical cellular processes. Thus, the PI3Kβ inhibitor, which is thought to regulate AKT activity in tumors with PTEN loss, has been applied to PTEN-deficient melanoma mouse models and demonstrated to enhance the efficacy of both PD-1 and CTLA-4 inhibitors (150). Accordingly, the regime that anti-PD-1 combined with PI3K-AKT pathway inhibitors may benefit cancer patients in the future.

The RAF/MEK/ERK pathway which is the classic routine in the MAPK pathway is also critical for human cancer; the pathway can be primed by activated RAS interacting with RAF kinase (152–154). Furthermore, RAS, RAF, and MEK are also frequently amplified or mutated in various cancers, accompanied by the activated MEK-ERK signaling pathway (155). KRAS, the component of RAS, is one of the most frequently mutated oncogenes in human cancers and participates in the mechanism of PD-1 inhibitor resistance (156). Similarly, BRAF, another mutated oncogene, has the vast majority in number harboring an activating point mutation (V600E) (157). This oncogenic mutation leads to constitutive activation of the MAPK signaling pathway and increased oncogenic potential through a variety of mechanisms, including reduced apoptosis, increased invasiveness, and increased metastatic behavior (158). Recent *in vitro* data suggest that BRAF V600E could also contribute to immune escape (157, 159). Based on these, selective inhibition of BRAF has been shown to induce an activated CD8+ T cell infiltrate, as well as increase melanoma MHC expression and melanoma antigen presentation early during treatment both in preclinical models and in human melanoma tissue samples (159–161). The study also suggested that combined BRAF and MEK inhibition with PD-1 blockade immunotherapy in BRAF-mutant melanoma

can increase the frequency of long-lasting antitumor responses (162). Thus, the inhibition of the RAF/MEK/ERK signaling pathway may be a promising therapeutic strategy for cancer dysregulated in this pathway.

IFNs

IFN-γ, effector cytokines of T cells, can directly exert an effective antitumor immune response by recognizing the corresponding receptors on tumor cells or indirectly promote the cross-activation of CD8+ T cells by upregulating antigen-presenting machinery to attack tumor cells (163). Classically, IFN-γ inhibits the proliferation of tumor cells and promotes their apoptosis, as it can activate signal transducer and activator of transcription 1 (STAT1) through using the Janus kinase (JAK) signal transducer and activator of the transcription pathway (127). Recent studies have implicated that defects in such pathways involved in IFN-receptor signaling and antigen presentation are associated with primary and acquired resistance to PD-1 blockades, such as inactivating mutations in JAK1 and JAK2 (143, 164). It may result in PD-L1 not being able to be reactively expressed and failing to attract T cell infiltration due to lack of chemokine production which is controlled by the IFN-γ pathway downstream of JAK1/2 (165). Considering that preexisting T cells in the tumor are a requisite for response to anti-PD-1 therapy (166), the absence of reactive PD-L1 expression may implicate a poor response to PD-1 blockade therapy, because of the impairment of tumor-infiltrating T cells (164).

IFN-β, belonging to type I IFN that is associated with innate immune responses (167), was proved to be suppressed by lysine-specific histone demethylase 1 (LSD1) (168). Ablation of LSD1 in cancer cells increases repetitive element expression; this leads to dsRNA stress and activation of type 1 IFN, which promotes antitumor T cell immunity and sensitizes refractory tumors to PD-1 blockade in a melanoma mouse model (168). The remarkable ability of LSD1 inhibition to convert a tumor resistant to PD-1 blockade to a tumor responsive to PD-1 blockade provides a means to increase the efficacy of anti-PD-1 cancer therapy and potentially turn "cold" tumors "hot" (169). It may suggest LSD1 inhibition combined with PD-1 blockade as a novel cancer treatment strategy. In addition, long-term IFN-β transcription can also promote the occurrence of resistance to anti-PD-1 therapy by inducing intratumoral augment of Tregs and myeloid cells, which cause T cell depletion and immunosuppression (170). Thus, IFNs display the consequence of resulting in T cell depletion and immunosuppression, although they can also promote the effect of tumor-specific CD8+T cells.

Immune Contexture

As noted, research of immune checkpoint blockade therapy was concentrated on reversing tumor-specific T cell dysfunction. CD8+T cells play an essential role in the scope of T cell-directed immunotherapy. Thus, the exhaustion of CD8+T cells induced by several factors can also be a crucial reason for PD-1 blockade resistance (143).

Epigenomic modifications might underlie CD8+T cell exhaustion. These long-lasting, exhaustion-associated epigenetic programs limit the rejuvenation of antigen-specific CD8 T cells during PD-1 blockade therapy. A study displayed that initial DNA-methylation programs could restrict T-cell expansion and clonal diversity during PD-1 blockade treatment (171). The administration of DNA-demethylating agents before ICB therapy reversed these programs and enhanced the reinvigoration of antitumor CD8 T cells. Moreover, the latest clinic trials concerning epigenetic therapies also suggest that histone deacetylase inhibitors may synergize with PD-1 blockade to overcome resistance (172, 173). What they found highlights epigenetic programs among exhausted T-cells as a potential mechanism to explain PD-1 blockade therapeutic failures. Besides, research found that co-stimulatory molecules like CD28 can also suppress the function of effector T cells and reduce the response to anti-PD-1 therapy by blocking the CD28-B7 co-stimulatory pathway (13). In addition to the regulation of epigenetic change and co-stimulatory pathway over CD8+T cells, other immune-suppressive cells also have more or less indirect effects on it, impacting drug resistance of anti-PD-1 therapy.

MDSCs are defined as immature myeloid cells, which can be induced to expand by tumor progression and play an immunosuppressive role in multiple cancers (174, 175). The recruitment of immunosuppressive MDSCs has shown complex protumorigenic outcomes following anti-PD-1 therapy (176). One mechanism of this recruitment may be driven by anti-PD-1-activated T cells, which partially trigger a tumor-intrinsic NLRP3 inflammasome signaling cascade (176, 177). This signaling cascade constitutes an adaptive resistance pathway, the genetic and pharmacological inhibition of which can enhance the efficacy of anti-PD-1 immunotherapy by inhibiting the tumor infiltration of MDSCs (176). On the other hand, checkpoint-activated CD8+ T cells can induce the differentiation and survival of protumorigenic TAMs and MDSCs by stimulating tumor production of CSF1 by secreting more TNF-α (178). These prompt us to hypothesize that neutralizing MDSCs and preserving T cell function may elicit robust immunotherapy responses by the combined actions of ICB agents together with targeted agents (179). Paradoxically, in HNSCC, it demonstrates reduced granulocytic MDSC infiltration post-PD-1 blockade (180). Thus, it is still unclear whether this model involves different mechanisms of MDSC recruitment or whether blockade of PD-1 inhibits MDSC proliferation directly.

TAM is another type of myeloid cells. It can impact the response to immunotherapy by activating triggering receptors expressed on myeloid cells 2 (TREM2) (181). TREM2 deficiency was associated with the transformation of macrophage subsets and an increase of intratumoral $CD8^+$ T cells, some of which expressed PD-1. The observation found that tumor macrophage infiltrates enhanced T-cell-mediated control of tumor growth after the anti-TREM2 therapy; the anti-TREM2 mAb to tumor-bearing mice blunted tumor growth and strongly enhanced the efficacy of anti-PD-1 immunotherapy (181). Efforts are currently ongoing to complement checkpoint blockade with treatment targeting myeloid cells (115), including depletion of myeloid cells from tumors, blocking their pro-tumoral

functions, or restoring their immunostimulatory properties (182, 183). These results may be applied as a theoretical basis to clinical trials.

Tregs can inhibit TCR-mediated activation and proliferation of CD4+/CD8+T cells to promote tumor immune evasion. Simultaneously, EZH2 has a critical role in maintaining the identity and function of Tregs; it has been proved that Ezh2 deficiency in Tregs stimulates antitumor immunity with enhanced T cell infiltration and elevated effector function (147). Mechanistically, Ezh2 functioned in regulating the stability of Foxp3 protein which is specifically expressed by Tregs. Based on these, the synergistic impact of the combination of EZH2 inhibition and anti-PD-1 has been found in an anti-PD-1-resistant model of HNSCC. It is explained that EZH2 inhibition can enhance tumor cell Class I MHC expression *in vivo* including in highly resistant models (147). Thus, it is promising that try to improve the efficacy of anti-PD-1 therapy by combining it with Ezh2 inhibitors.

CAFs are activated fibroblast cells during cancer development, contributing to the establishment of an immunosuppressive TME (184). Despite T cells being recovered from the capability against tumor cells following anti-PD-1 therapy, CAFs can act as a formidable barrier to T cells by secreting-related factors, resulting in T cell exclusion from tumor nests (185). TGF-β, a factor released by CAFs, promotes T-cell exclusion and blocks Th1 effector phenotype acquisition, which eventually results in resistance to PD-1 blockade therapy (186, 187). Inhibition of TGF-β unleashed a potent, enduring cytotoxic T-cell against tumor cells to prevent refractory. In mice with progressive liver metastatic disease, blockade of TGF-β signaling improves the susceptibility to anti-PD-1 therapy and suggests that TGF-β inhibition could prevent, but not reverse, CAF differentiation (186). NOX 4 is a specific downstream target of TGF-β. Inhibition of NOX 4 can "normalize" CAF to a quiescent phenotype and promote intratumoral CD8+ T-cell infiltration, overcoming the exclusion effect (185). These trials show that the regulation of CAFs through repressing the related downstream pathway or factors may have a synergistic effect on the anti-PD-1 therapy.

As mentioned above, one of the major obstacles that remain to be overcome is the restriction of T cells' function in the immunosuppressive microenvironment formed by Tregs, MDSCs, and TAMs. The adoptive cell therapy (ACT) with chimeric antigen receptor (CAR)-redirected T cells is an attractive anticancer strategy. The breakthrough with CAR-T cell therapy was achieved, targeting B-cell hematologic tumors (188–191), while there is less efficacy in solid tumors. Research shows that TGF-β can be produced in most human tumors and markedly inhibits tumor antigen-specific cellular immunity. CAR-T lymphocytes have generated the resistance to TGF-β suppression, which expresses dominant-negative TGF-β receptors, to counteract these immunomodulatory activities (192). Such a result demonstrates their superior antitumor activity in animal models. Thus, combining engineered CAR-T cells with PD-1 antagonists makes a great deal of sense. There are promising results in both the pre-clinic model and case report (193, 194), presenting a large opportunity for the field of cellular engineering and immune checkpoint therapy.

Accordingly, the abovementioned studies indicate that the resistance to PD-1 inhibitors is directly related to the dysfunction of T cells caused by its epigenetic change, while other immune-related cells can also indirectly result in immune evasion *via* impacting the antitumor immunity progression of T cells.

Angiogenesis

The angiogenic tumor vasculature plays a vital role in regulating the response to cancer immunotherapy. Vascular abnormalities restrict T cell trafficking into the intratumor *via* upregulating vascular endothelial growth factor (VEGF) and gene-related to proangiogenic (195). Study has suggested that the VEGF signal induces the expression of the factor-related apoptosis antigen ligand (FasL)-mediated cell death on vascular endothelial cells, which in turn poses a formidable physical barrier to vascular material exchange (195). Additionally, the tumor neovasculature also decreases immature DCs and expands Treg cells and MDSC populations (195, 196). The modulation of tumor vasculature includes anti-angiogenesis and vascular normalization, which can induce the depletion of Tregs and regulatory B cells, enhancement of M1 TAMs, and activation of T cells, to reduce immunosuppression. The modulation can make favorable conditions for the infiltration of CD8+ cells and allow the effectiveness of immune checkpoint blockade (197). Immune checkpoint inhibitors have also shown promise in combination with anti-angiogenic in solid tumors (198), such as NSCLC and colorectal cancer (199). Thus, anti-angiogenesis and immunotherapy are documented to work synergistically together, showing promise for the resistance of PD-1 inhibitors.

Deregulation of Immunometabolism

Immune cells undergo complex shifts in metabolic states; immunosuppressive metabolites in TME can inhibit antitumor immunity by inhibiting immune cell infiltration (200–203).

Aerobic glycolysis is indispensable to CD8+T effector cells. It can be restricted by tumor cells that outcompete T cells for glucose uptake (81). In pretreatment of melanoma tumors, hypoxia-associated genes are highly expressed in the tumors that are subsequently resistant to PD-1 blockade compared with those from responding tumors (204). A high concentration of lactic acid can also blunt aerobic glycolysis of CD8+T cells and correlate with primary resistance on PD-1 blockade (205). A database analysis of patients with melanoma revealed strong negative associations between tumor lactate dehydrogenase expression and markers of CTL activation (201). Separately, indoleamine 2,3-dioxygenase (IDO), generated by tumors and immune cells, can enhance Treg and MDSC production and activity and inhibit the effect on T-cell immunity (206). IDO is the initial and rate-limiting enzyme in the degradation of tryptophan through the kynurenine pathway. A report found a significantly higher kynurenine/tryptophan ratio in NSCLC patients with early progression on nivolumab, suggesting that IDO might contribute to primary resistance to anti-PD-1 monoclonal antibodies (207). Despite that, the following

clinical studies have shown that the efficacy of the IDO1 selective inhibitor plus PD-1 inhibitor is not as good as that of PD-1 blockade treatment alone (208). The combination therapy of IDO inhibitors and PD-1 antibodies may become a study direction for overcoming immunotherapy resistance. In addition, adenosine also is an immunosuppressive molecule that can suppress effector T cells and NK cells and increase Treg numbers (209, 210). Accordingly, metabolic disorders can encumber proper T cell activation and effector functions, which is a potential mechanism of resistance to PD-1 blockade. It is believed that the combined strategy based on this can bring gratifying results.

Disorder of Intestinal Microbiota

The gastrointestinal microbiome has been demonstrated to play an essential role in regulating the immune response function during cancer therapy (211–214). There is a group of active microorganisms that live in symbiosis with the host in the human intestinal tract and may cause tumor resistance to anti-PD-1 when it gets disordered (215, 216). Concordantly, a result has displayed that the responders to PD-1 blockade had a differential composition of gut bacteria (217). It has shown an "unfavorable" gut microbiome with low diversity and high relative abundance. Such a population may impair systemic and antitumor immune responses mediated by the limited intratumoral T cells, myeloid infiltration, and weakened antigen presentation capacity (211). Enhanced responses of anti-PD-1 therapy have been observed in mice that accepted fecal microbiome transplantation of the responder to PD-1 blockade. On the other hand, the efficacy of anti-PD-1 in mice receiving a non-responder could be restored by administration of specific genera enriched in responding patients in these mice. In addition, these specific genera were associated with increased intratumoral immune infiltrates mediated by the recruitment of $CD4^+$T cells into the tumor bed and increased ratio of $CD4^+$T cells to Tregs in response to PD-1 blockade (217). Besides, fecal microbiota transplant also overcomes resistance to anti-PD-1 therapy in melanoma patients (218). This suggests that regulating the gut microbiota may potentially enhance antitumor immune responses as well as response to immune checkpoint blockade.

New Immune Checkpoints

During checkpoint blockade with anti-PD-1 inhibitors, other inhibitory checkpoints might become coordinately upregulated and in turn lead to therapeutic failure (219). T-cell immunoglobulin mucin 3 (TIM-3), a member of the TIM family of immunomodulatory proteins, has been identified as a critical regulator of CTL exhaustion with co-expression of PD-1 (220). Such co-expression means that the most dysfunctional subgroup of T cells does not produce IL-2 and IFN-γ and eventually causes adaptive resistance. The mechanism has demonstrated that the increased Tim-3-mediated escape of exhausted TIL from PD-1 inhibition was mediated by PI3K/Akt complex downstream of TCR signaling in HNSCC (219). *In vitro*, the anti-Tim-3-blocking antibody reverses resistance to anti-PD-1 in PBMC from lung cancer patients (221). On the other hand, significant antitumor activity was observed after sequential addition of anti-Tim-3 mAb to overcome adaptive resistance to anti-PD-1 mAb in a murine HNSCC model (219). Thus, combination therapy targeting TIM-3 and PD-1 signaling pathways might be effective against the resistance of mono-immunotherapy.

Lymphocyte activation gene 3 (LAG-3) can selectively be expressed on activated T cells, NK cells, DCs and may get compensatory upregulation. The regulatory function of LAG-3 on T cells is similar to that of PD-1, which delivers suppressive signaling to hinder antitumor response (222). LAG-3 also competes for binding to MHC class II, which leads to decreased efficacy of MHC class II-mediated antigen presentation (223). The upregulation of LAG-3 in tumors of melanoma and lung cancer patients with acquired resistance to anti-PD-1 therapy has been demonstrated (223). There appeared to be a synergistic benefit of anti-LAG-3/anti-PD-1 combinatorial immunotherapy compared with anti-PD-1 monotherapy. In addition, a higher proportion of effector T cells were observed in mice treated with anti-LAG-3/anti-PD-1 than in PD-1 monotherapy groups. These suggest that anti-LAG-3/anti-PD-1 combinatorial immunotherapy may act synergistically (224). The roles of other checkpoints are still unconfirmed in anti-PD-1 resistance, such as TIGIT. Thus, a more particular knowledge of these new immune checkpoints may provide a rationale for designing combination treatments in the future.

CONCLUSIONS

In this review, we primarily describe a complex story of the relationship between anti-PD-1 and TME. The initiation of the antitumor effect depends on the cross talk between immune cells (**Figure 1**). Besides T cells, other immune-activating cells, like NK cells, DCs, and M1 TAMs, also contribute to anti-PD-1 efficacy through direct or indirect mechanisms. Furthermore, PD-1 blockade can target PD-1 expressed on these cells directly or reactivate CD8+ T cells to induce these immune-activating cell responses indirectly within the TME. Also, the review briefly displays the mechanisms that possibly contribute to primary or acquired resistance to PD-1 blockade, including the internal and external causes; the former focuses on the inherent characteristics of tumor cells while the other is mainly emanated from the tumor microenvironment (**Figure 2**). Due to the different reasons for drug resistance, the appropriate combination immunotherapy is also different, which is also discussed in detail in this article. It means that using a combination of such strategies is more suitable than using one approach alone for stimulating an antitumor immune response in some situations. A future challenge for researchers and clinicians is to achieve the satisfactory efficacy of immunotherapy. It means that the mechanisms of tumor immune evasion and immune drug resistance should be clarified as much as possible. It also plays a crucial role in the exploration of predictive markers, which are associated with the response rate of immunotherapy and improved clinical outcomes.

AUTHOR CONTRIBUTIONS

QW wrote the manuscript; all authors were involved in the amendments and improvements in the text. All authors contributed to the article and approved the submitted version.

FUNDING

This work was supported by the National Natural Science Foundation of China [82072594 (YT), 82073097 (SL), 82073136 (DX), 81874139 (SL), and 81872285 (YS)], Shenzhen Science and Technology Program [KQTD20170810160226082 (YT)], Shenzhen Municipal Government of China [JCYJ20180507184647104 (YT)], and the Hunan Provincial Key Area R&D Program [2019SK2253 (YT)].

ACKNOWLEDGMENTS

The authors want to give the sincerest thanks to the other lab members of YT and DX for their helpful comments and suggestions.

REFERENCES

1. Baumeister SH, Freeman GJ, Dranoff G, Sharpe AH. Coinhibitory Pathways in Immunotherapy for Cancer. *Annu Rev Immunol* (2016) 34 (February):539–73. doi: 10.1146/annurev-immunol-032414-112049
2. Liu X, Hogg GD, DeNardo DG. Rethinking Immune Checkpoint Blockade: "Beyond the T Cell". *J Immunother Cancer* (2021) 9(1):e001460. doi: 10.1136/jitc-2020-001460
3. Borst J, Ahrends T, Bąbała N, Melief CJM, Kastenmüller W. CD4(+) T Cell Help in Cancer Immunology and Immunotherapy. *Nat Rev Immunol* (2018) 18(10):635–47. doi: 10.1038/s41577-018-0044-0
4. Wculek SK, Cueto FJ, Mujal AM, Melero I, Krummel MF, Sancho D. Dendritic Cells in Cancer Immunology and Immunotherapy. *Nat Rev Immunol* (2020) 20(1):7–24. doi: 10.1038/s41577-019-0210-z
5. Peterson EE, Barry KC. The Natural Killer–Dendritic Cell Immune Axis in Anti-Cancer Immunity and Immunotherapy. *Front Immunol* (2021) 11:621254. doi: 10.3389/fimmu.2020.621254
6. Yan Y, Zhang L, Zuo Y, Qian H, Liu C. Immune Checkpoint Blockade in Cancer Immunotherapy: Mechanisms, Clinical Outcomes, and Safety Profiles of PD-1/PD-L1 Inhibitors. *Archivum Immunologiae Therapiae Experimentalis* (2020) 68(6):1–15. doi: 10.1007/s00005-020-00601-6
7. Quezada SA, Peggs KS. Exploiting CTLA-4, PD-1 and PD-L1 to Reactivate the Host Immune Response Against Cancer. *Br J Cancer* (2013) 108(8):1560–5. doi: 10.1038/bjc.2013.117
8. Herbst RS, Soria JC, Kowanetz M, Fine GD, Hamid O, Gordon MS, et al. Predictive Correlates of Response to the Anti-PD-L1 Antibody MPDL3280A in Cancer Patients. *Nature* (2014) 515(7528):563–7. doi: 10.1038/nature14011
9. Alvarez M, Simonetta F, Baker J, Morrison AR, Wenokur AS, Pierini A, et al. Indirect Impact of PD-1/PD-L1 Blockade on a Murine Model of NK Cell Exhaustion. *Front Immunol* (2020) 11:7. doi: 10.3389/fimmu.2020.00007
10. Juneja VR, McGuire KA, Manguso RT, LaFleur MW, Collins N, Nicholas Haining W, et al. PD-L1 on Tumor Cells Is Sufficient for Immune Evasion in Immunogenic Tumors and Inhibits CD8 T Cell Cytotoxicity. *J Exp Med* (2017) 214(4):895–904. doi: 10.1084/jem.20160801
11. Okazaki T, Maeda A, Nishimura H, Kurosaki T, Honjo T. PD-1 Immunoreceptor Inhibits B Cell Receptor-Mediated Signaling by Recruiting Src Homology 2-Domain-Containing Tyrosine Phosphatase 2 to Phosphotyrosine. *Proc Natl Acad Sci USA* (2001) 98(24):13866–71. doi: 10.1073/pnas.231486598
12. He X, Xu C. Immune Checkpoint Signaling and Cancer Immunotherapy. *Cell Res* (2020) 30(8):660–9. doi: 10.1038/s41422-020-0343-4
13. Hui E, Cheung J, Zhu J, Su X, Taylor MJ, Wallweber HA, et al. T Cell Costimulatory Receptor CD28 Is a Primary Target for PD-1-Mediated Inhibition. *Sci (New York NY)* (2017) 355(6332):1428–33. doi: 10.1126/science.aaf1292
14. Yokosuka T, Takamatsu M, Kobayashi-Imanishi W, Hashimoto-Tane A, Azuma M, Saito T. Programmed Cell Death 1 Forms Negative Costimulatory Microclusters That Directly Inhibit T Cell Receptor Signaling by Recruiting Phosphatase SHP2. *J Exp Med* (2012) 209 (6):1201–17. doi: 10.1084/jem.20112741
15. Chemnitz JM, Parry RV, Nichols KE, June CH, Riley JL. SHP-1 and SHP-2 Associate With Immunoreceptor Tyrosine-Based Switch Motif of Programmed Death 1 Upon Primary Human T Cell Stimulation, But Only Receptor Ligation Prevents T Cell Activation. *J Immunol* (2004) 173 (2):945–54. doi: 10.4049/jimmunol.173.2.945
16. Zhao Y, Harrison DL, Song Y, Ji J, Huang J, Hui E. Antigen-Presenting Cell-Intrinsic PD-1 Neutralizes PD-L1 in Cis to Attenuate PD-1 Signaling in T Cells. *Cell Rep* (2018) 24(2):379–90.e6. doi: 10.1016/j.celrep.2018.06.054
17. Patsoukis N, Brown J, Petkova V, Liu F, Li L, Boussiotis VA. Selective Effects of PD-1 on Akt and Ras Pathways Regulate Molecular Components of The Cell Cycle and Inhibit T Cell Proliferation. *Sci Signaling* (2012) 5(230):ra46. doi: 10.1126/scisignal.2002796
18. Latchman Y, Wood CR, Chernova T, Chaudhary D, Borde M, Chernova I, et al. PD-L2 Is a Second Ligand for PD-1 and Inhibits T Cell Activation. *Nat Immunol* (2001) 2(3):261–8. doi: 10.1038/85330
19. Sharpe AH, Pauken KE. The Diverse Functions of the PD1 Inhibitory Pathway. *Nat Rev Immunol* (2018) 18(3):153–67. doi: 10.1038/nri.2017.108
20. Tanegashima T, Togashi Y, Azuma K, Kawahara A, Ideguchi K, Sugiyama D, et al. Immune Suppression by PD-L2 Against Spontaneous and Treatment-Related Antitumor Immunity. *Clin Cancer Res* (2019) 25(15):4808–19. doi: 10.1158/1078-0432.CCR-18-3991
21. Robert C, Schachter J, Long GV, Arance A, Grob JJ, Mortier L, et al. Pembrolizumab Versus Ipilimumab in Advanced Melanoma. *N Engl J Med* (2015) 372(26):2521–32. doi: 10.1056/NEJMoa1503093
22. Ribas A, Puzanov I, Dummer R, Schadendorf D, Hamid O, Robert C, et al. Pembrolizumab Versus Investigator-Choice Chemotherapy for Ipilimumab-Refractory Melanoma (KEYNOTE-002): A Randomised, Controlled, Phase 2 Trial. *Lancet Oncol* (2015) 16(8):908–18. doi: 10.1016/S1470-2045(15)00083-2
23. Mok TSK, Wu YL, Kudaba I, Kowalski DM, Cho BC, Turna HZ, et al. Pembrolizumab Versus Chemotherapy for Previously Untreated, PD-L1-Expressing, Locally Advanced or Metastatic Non-Small-Cell Lung Cancer (KEYNOTE-042): A Randomised, Open-Label, Controlled, Phase 3 Trial. *Lancet (London England)* (2019) 393(10183):1819–30. doi: 10.1016/S0140-6736(18)32409-7
24. Herbst RS, Baas P, Kim DW, Felip E, Pérez-Gracia JL, Han J-Y, et al. Pembrolizumab Versus Docetaxel for Previously Treated, PD-L1-Positive, Advanced Non-Small-Cell Lung Cancer (KEYNOTE-010): A Randomised Controlled Trial. *Lancet (London England)* (2016) 387(10027):1540–50. doi: 10.1016/S0140-6736(15)01281-7
25. Chen R, Zinzani PL, Fanale MA, Armand P, Johnson NA, Brice P, et al. Phase II Study of the Efficacy and Safety of Pembrolizumab for Relapsed/Refractory Classic Hodgkin Lymphoma. *J Clin Oncol: Off J Am Soc Clin Oncol* (2017) 35(19):2125–32. doi: 10.1200/JCO.2016.72.1316
26. Armand P, Rodig S, Melnichenko V, Thieblemont C, Bouabdallah K, Tumyan G, et al. Pembrolizumab in Relapsed or Refractory Primary Mediastinal Large B-Cell Lymphoma. *J Clin Oncol: Off J Am Soc Clin Oncol* (2019) 37(34):3291–9. doi: 10.1200/JCO.19.01389
27. Nghiem P, Bhatia S, Lipson EJ, Sharfman WH, Kudchadkar RR, Brohl AS, et al. Durable Tumor Regression and Overall Survival in Patients With Advanced Merkel Cell Carcinoma Receiving Pembrolizumab as First-Line Therapy. *J Clin Oncology: Off J Am Soc Clin Oncol* (2019) 37(9):693–702. doi: 10.1200/JCO.18.01896
28. Balar AV, Castellano D, O'Donnell PH, Grivas P, Vuky J, Powles T, et al. First-Line Pembrolizumab in Cisplatin-Ineligible Patients With Locally

Advanced and Unresectable or Metastatic Urothelial Cancer (KEYNOTE-052): A Multicentre, Single-Arm, Phase 2 Study. *Lancet Oncol* (2017) 18 (11):1483–92. doi: 10.1016/S1470-2045(17)30616-2
29. Fradet Y, Bellmunt J, Vaughn DJ, Lee JL, Fong L, Vogelzang NJ, et al. Randomized Phase III KEYNOTE-045 Trial of Pembrolizumab Versus Paclitaxel, Docetaxel, or Vinflunine in Recurrent Advanced Urothelial Cancer: Results of >2 Years of Follow-Up. *Ann Oncol: Off J Eur Soc Med Oncol* (2019) 30(6):970–6. doi: 10.1093/annonc/mdz127
30. Zhu AX, Finn RS, Edeline J, Cattan S, Ogasawara S, Palmer D, et al. Pembrolizumab in Patients With Advanced Hepatocellular Carcinoma Previously Treated With Sorafenib (KEYNOTE-224): A Non-Randomised, Open-Label Phase 2 Trial. *Lancet Oncol* (2018) 19(7):940–52. doi: 10.1016/S1470-2045(18)30351-6
31. Fuchs CS, Doi T, Jang RW, Muro K, Satoh T, Machado M, et al. Safety and Efficacy of Pembrolizumab Monotherapy in Patients With Previously Treated Advanced Gastric and Gastroesophageal Junction Cancer: Phase 2 Clinical KEYNOTE-059 Trial. *JAMA Oncol* (2018) 4(5):e180013. doi: 10.1001/jamaoncol.2018.0013
32. Marabelle A, Le DT, Ascierto PA, Di Giacomo AM, De Jesus-Acosta A, Delord J-P, et al. Efficacy of Pembrolizumab in Patients With Noncolorectal High Microsatellite Instability/Mismatch Repair-Deficient Cancer: Results From the Phase II KEYNOTE-158 Study. *J Clin Oncol: Off J Am Soc Clin Oncol* (2020) 38(1):1–10. doi: 10.1200/JCO.19.02105
33. Burtness B, Harrington KJ, Greil R, Soulières D, Tahara M, de Castro GJ, et al. Pembrolizumab Alone or With Chemotherapy Versus Cetuximab With Chemotherapy for Recurrent or Metastatic Squamous Cell Carcinoma of the Head and Neck (KEYNOTE-048): A Randomised, Open-Label, Phase 3 Study. *Lancet (London England)* (2019) 394(10212):1915–28. doi: 10.1016/S0140-6736(19)32591-7
34. Chung HC, Ros W, Delord JP, Perets R, Italiano A, Shapira-Frommer R, et al. Efficacy and Safety of Pembrolizumab in Previously Treated Advanced Cervical Cancer: Results From the Phase II KEYNOTE-158 Study. *J Clin Oncology: Off J Am Soc Clin Oncol* (2019) 37(17):1470–8. doi: 10.1200/JCO.18.01265
35. Kojima T, Shah MA, Muro K, Francois E, Adenis A, Hsu C-H, et al. Randomized Phase III KEYNOTE-181 Study of Pembrolizumab Versus Chemotherapy in Advanced Esophageal Cancer. *J Clin Oncology: Off J Am Soc Clin Oncol* (2020) 38(35):4138–48. doi: 10.1200/JCO.20.01888
36. Langer CJ, Gadgeel SM, Borghaei H, Papadimitrakopoulou VA, Patnaik A, Powell SF, et al. Carboplatin and Pemetrexed With or Without Pembrolizumab for Advanced, Non-Squamous Non-Small-Cell Lung Cancer: A Randomised, Phase 2 Cohort of the Open-Label KEYNOTE-021 Study. *Lancet Oncol* (2016) 17(11):1497–508. doi: 10.1016/S1470-2045(16)30498-3
37. Paz-Ares L, Luft A, Vicente D, Tafreshi A, Gümüş M, Mazières J, et al. Pembrolizumab Plus Chemotherapy for Squamous Non-Small-Cell Lung Cancer. *N Engl J Med* (2018) 379(21):2040–51. doi: 10.1056/NEJMoa1810865
38. Kato K, Shah MA, Enzinger P, Bennouna J, Shen L, Adenis A, et al. KEYNOTE-590: Phase III Study of First-Line Chemotherapy With or Without Pembrolizumab for Advanced Esophageal Cancer. *Future Oncol (London England)* (2019) 15(10):1057–66. doi: 10.2217/fon-2018-0609
39. Weber JS, D'Angelo SP, Minor D, Hodi FS, Gutzmer R, Neyns B, et al. Nivolumab Versus Chemotherapy in Patients With Advanced Melanoma Who Progressed After Anti-CTLA-4 Treatment (CheckMate 037): A Randomised, Controlled, Open-Label, Phase 3 Trial. *Lancet Oncol* (2015) 16(4):375–84. doi: 10.1016/S1470-2045(15)70076-8
40. Larkin J, Minor D, D'Angelo S, Neyns B, Smylie M, Miller WHJ, et al. Overall Survival in Patients With Advanced Melanoma Who Received Nivolumab Versus Investigator's Choice Chemotherapy in CheckMate 037: A Randomized, Controlled, Open-Label Phase III Trial. *J Clin Oncol: Off J Am Soc Clin Oncol* (2018) 36(4):383–90. doi: 10.1200/JCO.2016.71.8023
41. Brahmer J, Reckamp KL, Baas P, Crinò L, Eberhardt WEE, Poddubskaya E, et al. Nivolumab Versus Docetaxel in Advanced Squamous-Cell Non-Small-Cell Lung Cancer. *N Engl J Med* (2015) 373(2):123–35. doi: 10.1056/NEJMoa1504627
42. Borghaei H, Paz-Ares L, Horn L, Spigel DR, Steins M, Ready NE, et al. Nivolumab Versus Docetaxel in Advanced Nonsquamous Non-Small-Cell Lung Cancer. *N Engl J Med* (2015) 373(17):1627–39. doi: 10.1056/NEJMoa1507643
43. Younes A, Santoro A, Shipp M, Zinzani PL, Timmerman JM, Ansell S, et al. Nivolumab for Classical Hodgkin's Lymphoma After Failure of Both Autologous Stem-Cell Transplantation and Brentuximab Vedotin: A Multicentre, Multicohort, Single-Arm Phase 2 Trial. *Lancet Oncol* (2016) 17(9):1283–94. doi: 10.1016/S1470-2045(16)30167-X
44. Sharma P, Retz M, Siefker-Radtke A, Baron A, Necchi A, Bedke J, et al. Nivolumab in Metastatic Urothelial Carcinoma After Platinum Therapy (CheckMate 275): A Multicentre, Single-Arm, Phase 2 Trial. *Lancet Oncol* (2017) 18(3):312–22. doi: 10.1016/S1470-2045(17)30065-7
45. El-Khoueiry AB, Sangro B, Yau T, Crocenzi TS, Kudo M, Hsu C, et al. Nivolumab in Patients With Advanced Hepatocellular Carcinoma (CheckMate 040): An Open-Label, Non-Comparative, Phase 1/2 Dose Escalation and Expansion Trial. *Lancet (London England)* (2017) 389 (10088):2492–502. doi: 10.1016/S0140-6736(17)31046-2
46. Overman MJ, McDermott R, Leach JL, Lonardi S, Lenz H-J, Morse MA, et al. Nivolumab in Patients With Metastatic DNA Mismatch Repair-Deficient or Microsatellite Instability-High Colorectal Cancer (CheckMate 142): An Open-Label, Multicentre, Phase 2 Study. *Lancet Oncol* (2017) 18(9):1182–91. doi: 10.1016/S1470-2045(17)30422-9
47. Ferris RL, Blumenschein GJ, Fayette J, Guigay J, Colevas AD, Licitra L, et al. Nivolumab for Recurrent Squamous-Cell Carcinoma of the Head and Neck. *N Engl J Med* (2016) 375(19):1856–67. doi: 10.1056/NEJMoa1602252
48. Antonia SJ, López-Martin JA, Bendell J, Ott PA, Taylor M, Eder JP, et al. Nivolumab Alone and Nivolumab Plus Ipilimumab in Recurrent Small-Cell Lung Cancer (CheckMate 032): A Multicentre, Open-Label, Phase 1/2 Trial. *Lancet Oncol* (2016) 17(7):883–95. doi: 10.1016/S1470-2045(16)30098-5
49. Overman MJ, Lonardi S, Wong KYM, Lenz H-J, Gelsomino F, Aglietta M, et al. Durable Clinical Benefit With Nivolumab Plus Ipilimumab in DNA Mismatch Repair-Deficient/Microsatellite Instability-High Metastatic Colorectal Cancer. *J Clin Oncol: Off J Am Soc Clin Oncol* (2018) 36 (8):773–9. doi: 10.1200/JCO.2017.76.9901
50. Motzer RJ, Tannir NM, McDermott DF, Arén Frontera O, Melichar B, Choueiri TK, et al. Nivolumab Plus Ipilimumab Versus Sunitinib in Advanced Renal-Cell Carcinoma. *N Engl J Med* (2018) 378(14):1277–90. doi: 10.1056/NEJMoa1712126
51. Hellmann MD, Paz-Ares L, Bernabe Caro R, Zurawski B, Kim S-W, Carcereny Costa E, et al. Nivolumab Plus Ipilimumab in Advanced Non-Small-Cell Lung Cancer. *N Engl J Med* (2019) 381(21):2020–31. doi: 10.1056/NEJMoa1910231
52. Rischin D, Migden MR, Lim AM, Schmults CD, Khushalani NI, Hughes BGM, et al. Phase 2 Study of Cemiplimab in Patients With Metastatic Cutaneous Squamous Cell Carcinoma: Primary Analysis of Fixed-Dosing, Long-Term Outcome of Weight-Based Dosing. *J Immunother cancer* (2020) 8(1):e000775. doi: 10.1136/jitc-2020-000775
53. Sezer A, Kilickap S, Gümüş M, Bondarenko I, Özgüroğlu M, Gogishvili M, et al. Cemiplimab Monotherapy for First-Line Treatment of Advanced Non-Small-Cell Lung Cancer With PD-L1 of at Least 50%: A Multicentre, Open-Label, Global, Phase 3, Randomised, Controlled Trial. *Lancet (London England)* (2021) 397(10274):592–604. doi: 10.1016/S0140-6736(21)00228-2
54. Wong RM, Scotland RR, Lau RL, Wang C, Korman AJ, Kast WM, et al. Programmed Death-1 Blockade Enhances Expansion and Functional Capacity of Human Melanoma Antigen-Specific CTLs. *Int Immunol* (2007) 19(10):1223–34. doi: 10.1093/intimm/dxm091
55. Fessas P, Lee H, Ikemizu S, Janowitz T. A Molecular and Preclinical Comparison of the PD-1–Targeted T-Cell Checkpoint Inhibitors Nivolumab and Pembrolizumab. *Semin Oncol* (2017) 44(2):136–40. doi: 10.1053/j.seminoncol.2017.06.002
56. Lee JY, Lee HT, Shin W, Chae J, Choi J, Kim SH, et al. Structural Basis of Checkpoint Blockade by Monoclonal Antibodies in Cancer Immunotherapy. *Nat Commun* (2016) 7:1–10. doi: 10.1038/ncomms13354
57. Robert C, Ribas A, Wolchok JD, Hodi FS, Hamid O, Kefford R, et al. Anti-Programmed-Death-Receptor-1 Treatment With Pembrolizumab in Ipilimumab-Refractory Advanced Melanoma: A Randomised Dose-Comparison Cohort of a Phase 1 Trial. *Lancet (London England)* (2014) 384(9948):1109–17. doi: 10.1016/S0140-6736(14)60958-2

58. Robert C, Ribas A, Schachter J, Arance A, Grob J-J, Mortier L, et al. Pembrolizumab Versus Ipilimumab in Advanced Melanoma (KEYNOTE-006): Post-Hoc 5-Year Results From an Open-Label, Multicentre, Randomised, Controlled, Phase 3 Study. *Lancet Oncol* (2019) 20(9):1239–51. doi: 10.1016/S1470-2045(19)30388-2
59. Rini BI, Plimack ER, Stus V, Gafanov R, Hawkins R, Nosov D, et al. Pembrolizumab Plus Axitinib Versus Sunitinib for Advanced Renal-Cell Carcinoma. *N Engl J Med* (2019) 380(12):1116–27. doi: 10.1056/NEJMoa1816714
60. Gandhi L, Rodríguez-Abreu D, Gadgeel S, Esteban E, Felip E, De Angelis F, et al. Pembrolizumab Plus Chemotherapy in Metastatic Non-Small-Cell Lung Cancer. *N Engl J Med* (2018) 378(22):2078–92. doi: 10.1056/NEJMoa1801005
61. Bellmunt J, de Wit R, Vaughn DJ, Fradet Y, Lee J-L, Fong L, et al. Pembrolizumab as Second-Line Therapy for Advanced Urothelial Carcinoma. *N Engl J Med* (2017) 376(11):1015–26. doi: 10.1056/NEJMoa1613683
62. Wolchok JD, Chiarion-Sileni V, Gonzalez R, Rutkowski P, Grob J-J, Cowey CL, et al. Overall Survival With Combined Nivolumab and Ipilimumab in Advanced Melanoma. *N Engl J Med* (2017) 377(14):1345–56. doi: 10.1056/NEJMoa1709684
63. Vokes EE, Ready N, Felip E, Horn L, Burgio MA, Antonia SJ, et al. Nivolumab Versus Docetaxel in Previously Treated Advanced Non-Small-Cell Lung Cancer (CheckMate 017 and CheckMate 057): 3-Year Update and Outcomes in Patients With Liver Metastases. *Ann oncology: Off J Eur Soc Med Oncol* (2018) 29(4):959–65. doi: 10.1093/annonc/mdy041
64. Antonia SJ, Lopez-Martin JA, Bendell JC, Ott PA, Taylor MH, Eder JP, et al. Checkmate 032: Nivolumab (N) Alone or in Combination With Ipilimumab (I) for the Treatment of Recurrent Small Cell Lung Cancer (SCLC). *J Clin Oncol* (2016) 34(15_suppl):100. doi: 10.1200/JCO.2016.34.15_suppl.100
65. Siefker-Radtke A, Baron A, Necchi A, Plimack E, Pal S, Bedke J, et al. Nivolumab Monotherapy in Patients With Advanced Platinum-Resistant Urothelial Carcinoma: Efficacy and Safety Update From CheckMate 275. *J Clin Oncol* (2019) 37:4524. doi: 10.1200/JCO.2019.37.15_suppl.4524
66. Overman MJ, Kopetz S, Lonardi S, McDermott R, Leone F, Leach J, et al. Nivolumab ± Ipilimumab Treatment (Tx) Efficacy, Safety, and Biomarkers in Patients (Pts) With Metastatic Colorectal Cancer (mCRC) With and Without High Microsatellite Instability (MSI-H): Results From the CheckMate-142 Study. *Ann Oncol* (2016) 27:vi158. doi: 10.1093/annonc/mdw370.27
67. Herrera AF, Goy A, Mehta A, Ramchandren R, Pagel JM, Svoboda J, et al. Safety and Activity of Ibrutinib in Combination With Durvalumab in Patients With Relapsed or Refractory Follicular Lymphoma or Diffuse Large B-Cell Lymphoma. *Am J Hematology* (2020) 95(1):18–27. doi: 10.1002/ajh.25659
68. Ansell SM, Minnema MC, Johnson P, Timmerman JM, Armand P, Shipp MA, et al. Nivolumab for Relapsed/Refractory Diffuse Large B-Cell Lymphoma in Patients Ineligible for or Having Failed Autologous Transplantation: A Single-Arm, Phase II Study. *J Clin Oncol: Off J Am Soc Clin Oncol* (2019) 37(6):481–9. doi: 10.1200/JCO.18.00766
69. Roemer MGM, Redd RA, Cader FZ, Pak CJ, Abdelrahman S, Ouyang J, et al. Major Histocompatibility Complex Class II and Programmed Death Ligand 1 Expression Predict Outcome After Programmed Death 1 Blockade in Classic Hodgkin Lymphoma. *J Clin Oncol* (2018) 36(10):942–50. doi: 10.1200/JCO.2017.77.3994
70. Migden MR, Rischin D, Schmults CD, Guminski A, Hauschild A, Lewis KD, et al. PD-1 Blockade With Cemiplimab in Advanced Cutaneous Squamous-Cell Carcinoma. *N Engl J Med* (2018) 379(4):341–51. doi: 10.1056/NEJMoa1805131
71. Farhood B, Najafi M, Mortezaee K. CD8+ Cytotoxic T Lymphocytes in Cancer Immunotherapy: A Review. *J Cell Physiol* (2019) 234(6):8509–21. doi: 10.1002/jcp.27782
72. Böttcher JP, Bonavita E, Chakravarty P, Blees H, Cabeza-Cabrerizo M, Sammicheli S, et al. NK Cells Stimulate Recruitment of Cdc1 Into the Tumor Microenvironment Promoting Cancer Immune Control. *Cell* (2018) 172(5):1022–37.e14. doi: 10.1016/j.cell.2018.01.004
73. Palucka K, Banchereau J. Cancer Immunotherapy *via* Dendritic Cells. *Nat Rev Cancer* (2012) 12(4):265–77. doi: 10.1038/nrc3258
74. Topalian SL, Taube JM, Anders RA, Pardoll DM. Mechanism-Driven Biomarkers to Guide Immune Checkpoint Blockade in Cancer Therapy. *Nat Rev Cancer* (2016) 16(5):275–87. doi: 10.1038/nrc.2016.36
75. Peng X, He Y, Huang J, Tao Y, Liu S. Metabolism of Dendritic Cells in Tumor Microenvironment: For Immunotherapy. *Front Immunol* (2021) 12:613492. doi: 10.3389/fimmu.2021.613492
76. Thomas DA, Massagué J. TGF-Beta Directly Targets Cytotoxic T Cell Functions During Tumor Evasion of Immune Surveillance. *Cancer Cell* (2005) 8(5):369–80. doi: 10.1016/j.ccr.2005.10.012
77. Ahmadzadeh M, Johnson LA, Heemskerk B, Wunderlich JR, Dudley ME, White DE, et al. Tumor Antigen-Specific CD8 T Cells Infiltrating the Tumor Express High Levels of PD-1 and Are Functionally Impaired. *Blood* (2009) 114(8):1537–44. doi: 10.1182/blood-2008-12-195792
78. Sfanos KS, Bruno TC, Meeker AK, De Marzo AM, Isaacs WB, Drake CG. Human Prostate-Infiltrating CD8+ T Lymphocytes Are Oligoclonal and PD-1+. *Prostate* (2009) 69(15):1694–703. doi: 10.1002/pros.21020
79. Pardoll DM. The Blockade of Immune Checkpoints in Cancer Immunotherapy. *Nat Rev Cancer* (2012) 12(4):252–64. doi: 10.1038/nrc3239
80. Topalian SL, Drake CG, Pardoll DM. Immune Checkpoint Blockade: A Common Denominator Approach to Cancer Therapy. *Cancer Cell* (2015) 27(4):450–61. doi: 10.1016/j.ccell.2015.03.001
81. Chang CH, Qiu J, O'Sullivan D, Buck MD, Noguchi T, Curtis JD, et al. Metabolic Competition in the Tumor Microenvironment Is a Driver of Cancer Progression. *Cell* (2015) 162(6):1229–41. doi: 10.1016/j.cell.2015.08.016
82. Yost KE, Satpathy AT, Wells DK, Qi Y, Wang C, Kageyama R, et al. Clonal Replacement of Tumor-Specific T Cells Following PD-1 Blockade. *Nat Med* (2019) 25(8):1251–9. doi: 10.1038/s41591-019-0522-3
83. Dammeijer F, van Gulijk M, Mulder EE, Lukkes M, Klaase L, van den Bosch T, et al. The PD-1/PD-L1-Checkpoint Restrains T Cell Immunity in Tumor-Draining Lymph Nodes. *Cancer Cell* (2020) 38(5):685–700.e8. doi: 10.1016/j.ccell.2020.09.001
84. Diskin B, Adam S, Cassini MF, Sanchez G, Liria M, Aykut B, et al. PD-L1 Engagement on T Cells Promotes Self-Tolerance and Suppression of Neighboring Macrophages and Effector T Cells in Cancer. *Nat Immunol* (2020) 21(4):442–54. doi: 10.1038/s41590-020-0620-x
85. Zuazo M, Arasanz H, Bocanegra A, Fernandez G, Chocarro L, Vera R, et al. Systemic CD4 Immunity as a Key Contributor to PD-L1/PD-1 Blockade Immunotherapy Efficacy. *Front Immunol* (2020) 11:586907. doi: 10.3389/fimmu.2020.586907
86. Marzo AL, Kinnear BF, Lake RA, Frelinger JJ, Collins EJ, Robinson BW, et al. Tumor-Specific CD4+ T Cells Have a Major "Post-Licensing" Role in CTL Mediated Anti-Tumor Immunity. *J Immunol (Baltimore Md: 1950)* (2000) 165(11):6047–55. doi: 10.4049/jimmunol.165.11.6047
87. Hung K, Hayashi R, Lafond-Walker A, Lowenstein C, Pardoll D, Levitsky H. The Central Role of CD4(+) T Cells in the Antitumor Immune Response. *J Exp Med* (1998) 188(12):2357–68. doi: 10.1084/jem.188.12.2357
88. Oh DY, Kwek SS, Raju SS, Li T, McCarthy E, Chow E, et al. Intratumoral CD4+ T Cells Mediate Anti-Tumor Cytotoxicity in Human Bladder Cancer. *Cell* (2020) 181(7):1612–25.e13. doi: 10.1016/j.cell.2020.05.017
89. Quezada SA, Simpson TR, Peggs KS, Merghoub T, Vider J, Fan X, et al. Tumor-Reactive CD4(+) T Cells Develop Cytotoxic Activity and Eradicate Large Established Melanoma After Transfer Into Lymphopenic Hosts. *J Exp Med* (2010) 207(3):637–50. doi: 10.1084/jem.20091918
90. Perez-Diez A, Joncker NT, Choi K, Chan WFN, Anderson CC, Lantz O, et al. CD4 Cells can be More Efficient at Tumor Rejection Than CD8 Cells. *Blood* (2007) 109(12):5346–54. doi: 10.1182/blood-2006-10-051318
91. Mumberg D, Monach PA, Wanderling S, Philip M, Toledano AY, Schreiber RD, et al. CD4(+) T Cells Eliminate MHC Class II-Negative Cancer Cells *In Vivo* by Indirect Effects of IFN-Gamma. *Proc Natl Acad Sci USA* (1999) 96(15):8633–8. doi: 10.1073/pnas.96.15.8633
92. Eisel D, Das K, Dickes E, König R, Osen W, Eichmüller SB. Cognate Interaction With CD4(+) T Cells Instructs Tumor-Associated Macrophages to Acquire M1-Like Phenotype. *Front Immunol* (2019) 10:219. doi: 10.3389/fimmu.2019.00219
93. Fauskanger M, Haabeth OAW, Skjeldal FM, Bogen B, Tveita AA. Tumor Killing by CD4(+) T Cells Is Mediated *via* Induction of Inducible Nitric

Oxide Synthase-Dependent Macrophage Cytotoxicity. *Front Immunol* (2018) 9:1684. doi: 10.3389/fimmu.2018.01684
94. Qin Z, Blankenstein T. CD4+ T Cell–Mediated Tumor Rejection Involves Inhibition of Angiogenesis That Is Dependent on IFN Gamma Receptor Expression by Nonhematopoietic Cells. *Immunity* (2000) 12(6):677–86. doi: 10.1016/s1074-7613(00)80218-6
95. Braumüller H, Wieder T, Brenner E, Aßmann S, Hahn M, Alkhaled M, et al. T-Helper-1-Cell Cytokines Drive Cancer Into Senescence. *Nature* (2013) 494(7437):361–5. doi: 10.1038/nature11824
96. Zuazo M, Arasanz H, Fernández-Hinojal G, García-Granda MJ, Gato M, Bocanegra A, et al. Functional Systemic CD4 Immunity Is Required for Clinical Responses to PD-L1/PD-1 Blockade Therapy. *EMBO Mol Med* (2019) 11(7):e10293. doi: 10.15252/emmm.201910293
97. Nagasaki J, Togashi Y, Sugawara T, Itami M, Yamauchi N, Yuda J, et al. The Critical Role of CD4+ T Cells in PD-1 Blockade Against MHC-II-Expressing Tumors Such as Classic Hodgkin Lymphoma. *Blood advances* (2020) 4 (17):4069–82. doi: 10.1182/bloodadvances.2020002098
98. Diefenbach A, Colonna M, Romagnani C. The ILC World Revisited. In: Immunity. *Cell Press* (2017) 46:327–32. doi: 10.1016/j.immuni.2017.03.008
99. Castro F, Cardoso AP, Gonçalves RM, Serre K, Oliveira MJ. Interferon-Gamma at the Crossroads of Tumor Immune Surveillance or Evasion. *Front Immunol* (2018) 9:847. doi: 10.3389/fimmu.2018.00847
100. Pesce S, Greppi M, Tabellini G, Rampinelli F, Parolini S, Olive D, et al. Identification of a Subset of Human Natural Killer Cells Expressing High Levels of Programmed Death 1: A Phenotypic and Functional Characterization. *J Allergy Clin Immunol* (2017) 139(1):335–46.e3. doi: 10.1016/j.jaci.2016.04.025
101. Vari F, Arpon D, Keane C, Hertzberg MS, Talaulikar D, Jain S, et al. Immune Evasion *via* PD-1/PD-L1 on NK Cells and Monocyte/Macrophages Is More Prominent in Hodgkin Lymphoma Than DLBCL. *Blood* (2018) 131 (16):1809–19. doi: 10.1182/blood-2017-07-796342
102. Hsu J, Hodgins JJ, Marathe M, Nicolai CJ, Bourgeois-Daigneault M-C, Trevino TN, et al. Contribution of NK Cells to Immunotherapy Mediated by PD-1/PD-L1 Blockade. *J Clin Invest* (2018) 128(10):4654–68. doi: 10.1172/JCI99317
103. Concha-Benavente F, Kansy B, Moskovitz J, Moy J, Chandran U, Ferris RL. PD-L1 Mediates Dysfunction in Activated PD-1 Þ NK Cells in Head and Neck Cancer Patients. *Cancer Immunol Res* (2018) 6(12):1548–60. doi: 10.1158/2326-6066.CIR-18-0062
104. Sierra JM, Secchiari F, Nuñez SY, Iraolagoitia XLR, Ziblat A, Friedrich AD, et al. Tumor-Experienced Human NK Cells Express High Levels of PD-L1 and Inhibit CD8+ T Cell Proliferation. *Front Immunol* (2021) 12:745939. doi: 10.3389/fimmu.2021.745939
105. Gardner A, Ruffell B. Dendritic Cells and Cancer Immunity. *Trends Immunol* (2016) 37(12):855–65. doi: 10.1016/j.it.2016.09.006
106. Mellman I, Steinman RM. Dendritic Cells: Specialized and Regulated Antigen Processing Machines. *Cell* (2001) 106(3):255–8. doi: 10.1016/S0092-8674(01)00449-4
107. Garris CS, Arlauckas SP, Kohler RH, Trefny MP, Garren S, Piot C, et al. Successful Anti-PD-1 Cancer Immunotherapy Requires T Cell-Dendritic Cell Crosstalk Involving the Cytokines IFN-γ and IL-12. *Immunity* (2018) 49 (6):1148–61.e7. doi: 10.1016/j.immuni.2018.09.024
108. Frasca L, Nasso M, Spensieri F, Fedele G, Palazzo R, Malavasi F, et al. IFN-Gamma Arms Human Dendritic Cells to Perform Multiple Effector Functions. *J Immunol (Baltimore Md: 1950)* (2008) 180(3):1471–81. doi: 10.4049/jimmunol.180.3.1471
109. He T, Tang C, Xu S, Moyana T, Xiang J. Interferon Gamma Stimulates Cellular Maturation of Dendritic Cell Line DC2.4 Leading To Induction of Efficient Cytotoxic T Cell Responses and Antitumor Immunity. *Cell Mol Immunol* (2007) 4(2):105–11. doi: 10.1016/j.cellimm.2007.07.001
110. Lim TS, Chew V, Sieow JL, Goh S, Yeong JP-S, Soon AL, et al. PD-1 Expression on Dendritic Cells Suppresses CD8(+) T Cell Function and Antitumor Immunity. *Oncoimmunology* (2016) 5(3):e1085146. doi: 10.1080/2162402X.2015.1085146
111. Krempski J, Karyampudi L, Behrens MD, Erskine CL, Hartmann L, Dong H, et al. Tumor-Infiltrating Programmed Death Receptor-1+ Dendritic Cells Mediate Immune Suppression in Ovarian Cancer. *J Immunol (Baltimore Md: 1950)* (2011) 186(12):6905–13. doi: 10.4049/jimmunol.1100274
112. Karyampudi L, Lamichhane P, Krempski J, Kalli KR, Behrens MD, Vargas DM, et al. PD-1 Blunts the Function of Ovarian Tumor-Infiltrating Dendritic Cells by Inactivating NF-κb. *Cancer Res* (2016) 76(2):239–50. doi: 10.1158/0008-5472.CAN-15-0748
113. Chen L, Azuma T, Yu W, Zheng X, Luo L, Chen L. B7-H1 Maintains the Polyclonal T Cell Response by Protecting Dendritic Cells From Cytotoxic T Lymphocyte Destruction. *Proc Natl Acad Sci USA* (2018) 115(12):3126–31. doi: 10.1073/pnas.1722043115
114. Peng Q, Qiu X, Zhang Z, Zhang S, Zhang Y, Liang Y, et al. PD-L1 on Dendritic Cells Attenuates T Cell Activation and Regulates Response to Immune Checkpoint Blockade. *Nat Commun* (2020) 11(1):4835. doi: 10.1038/s41467-020-18570-x
115. Mantovani A, Marchesi F, Malesci A, Laghi L, Allavena P. Tumour-Associated Macrophages as Treatment Targets in Oncology. *Nat Rev Clin Oncol* (2017) 14(7):399–416. doi: 10.1038/nrclinonc.2016.217
116. Waqas SFH, Ampem G, Röszer T. Analysis of IL-4/STAT6 Signaling in Macrophages. *Methods Mol Biol (Clifton NJ)* (2019) 1966:211–24. doi: 10.1007/978-1-4939-9195-2_17
117. Tan B, Shi X, Zhang J, Qin J, Zhang N, Ren H, et al. Inhibition of Rspo-Lgr4 Facilitates Checkpoint Blockade Therapy by Switching Macrophage Polarization. *Cancer Res* (2018) 78(17):4929–42. doi: 10.1158/0008-5472.CAN-18-0152
118. Bloch O, Crane CA, Kaur R, Safaee M, Rutkowski MJ, Parsa AT. Gliomas Promote Immunosuppression Through Induction of B7-H1 Expression in Tumor-Associated Macrophages. *Clin Cancer Res* (2013) 19(12):3165–75. doi: 10.1158/1078-0432.CCR-12-3314
119. Gubin MM, Esaulova E, Ward JP, Malkova ON, Runci D, Wong P, et al. High-Dimensional Analysis Delineates Myeloid and Lymphoid Compartment Remodeling During Successful Immune-Checkpoint Cancer Therapy. *Cell* (2018) 175(4):1014–30.e19. doi: 10.1016/j.cell.2018.09.030
120. Yao A, Liu F, Chen K, Tang L, Liu L, Zhang K, et al. Programmed Death 1 Deficiency Induces the Polarization of Macrophages/Microglia to The M1 Phenotype After Spinal Cord Injury in Mice. *Neurotherapeutics: J Am Soc Exp NeuroTherapeutics* (2014) 11(3):636–50. doi: 10.1007/s13311-013-0254-x
121. Strauss L, Mahmoud MAA, Weaver JD, Tijaro-Ovalle NM, Christofides A, Wang Q, et al. Targeted Deletion of PD-1 in Myeloid Cells Induces Antitumor Immunity. *Sci Immunol* (2020) 5(43):eaay1863. doi: 10.1126/sciimmunol.aay1863
122. Gordon SR, Maute RL, Dulken BW, Hutter G, George BM, McCracken MN, et al. PD-1 Expression by Tumour-Associated Macrophages Inhibits Phagocytosis and Tumour Immunity. *Nature* (2017) 545(7655):495–9. doi: 10.1038/nature22396
123. Rashidian M, LaFleur MW, Verschoor VL, Dongre A, Zhang Y, Nguyen TH, et al. Immuno-PET Identifies the Myeloid Compartment as a Key Contributor to the Outcome of The Antitumor Response Under PD-1 Blockade. *Proc Natl Acad Sci USA* (2019) 116(34):16971–80. doi: 10.1073/pnas.1905005116
124. Dhupkar P, Gordon N, Stewart J, Kleinerman ES. Anti-PD-1 Therapy Redirects Macrophages From an M2 to an M1 Phenotype Inducing Regression of OS Lung Metastases. *Cancer Med* (2018) 7(6):2654–64. doi: 10.1002/cam4.1518
125. Maj T, Wang W, Crespo J, Zhang H, Wang W, Wei S, et al. Oxidative Stress Controls Regulatory T Cell Apoptosis and Suppressor Activity and PD-L1-Blockade Resistance in Tumor. *Nat Immunol* (2017) 18(12):1332–41. doi: 10.1038/ni.3868
126. Kato T, Noma K, Ohara T, Kashima H, Katsura Y, Sato H, et al. Cancer-Associated Fibroblasts Affect Intratumoral CD8(+) and FoxP3(+) T Cells Via IL6 in the Tumor Microenvironment. *Clin Cancer Research: An Off J Am Assoc Cancer Res* (2018) 24(19):4820–33. doi: 10.1158/1078-0432.CCR-18-0205
127. Syn NL, Teng MWL, Mok TSK, Soo RA. De-Novo and Acquired Resistance to Immune Checkpoint Targeting. *Lancet Oncol* (2017) 18(12):e731–41. doi: 10.1016/S1470-2045(17)30607-1
128. Huang Q, Lei Y, Li X, Guo F, Liu M. A Highlight of the Mechanisms of Immune Checkpoint Blocker Resistance. *Front Cell Dev Biol* (2020) 8:580140. doi: 10.3389/fcell.2020.580140

129. Matsushita H, Vesely MD, Koboldt DC, Rickert CG, Uppaluri R, Magrini VJ, et al. Cancer Exome Analysis Reveals a T-Cell-Dependent Mechanism of Cancer Immunoediting. *Nature* (2012) 482(7385):400–4. doi: 10.1038/nature10755
130. Rizvi NA, Hellmann MD, Snyder A, Kvistborg P, Makarov V, Havel JJ, et al. Cancer Immunology. Mutational Landscape Determines Sensitivity to PD-1 Blockade in Non-Small Cell Lung Cancer. *Sci (New York NY)* (2015) 348 (6230):124–8. doi: 10.1126/science.aaa1348
131. Anagnostou V, Smith KN, Forde PM, Niknafs N, Bhattacharya R, White J, et al. Evolution of Neoantigen Landscape During Immune Checkpoint Blockade in Non-Small Cell Lung Cancer. *Cancer Discov* (2017) 7(3):264–76. doi: 10.1158/2159-8290.CD-16-0828
132. Trommer M, Yeo SY, Persigehl T, Bunck A, Grüll H, Schlaak M, et al. Abscopal Effects in Radio-Immunotherapy-Response Analysis of Metastatic Cancer Patients With Progressive Disease Under Anti-PD-1 Immune Checkpoint Inhibition. *Front Pharmacol* (2019) 10:511. doi: 10.3389/fphar.2019.00511
133. Formenti SC, Demaria S. Combining Radiotherapy and Cancer Immunotherapy: A Paradigm Shift. *J Natl Cancer Institute* (2013) 105 (4):256–65. doi: 10.1093/jnci/djs629
134. Verbrugge I, Hagekyriakou J, Sharp LL, Galli M, West A, McLaughlin NM, et al. Radiotherapy Increases the Permissiveness of Established Mammary Tumors to Rejection by Immunomodulatory Antibodies. *Cancer Res* (2012) 72(13):3163–74. doi: 10.1158/0008-5472.CAN-12-0210
135. Gadgeel SM, Garassino MC, Esteban E, Speranza G, Felip E, Hochmair MJ, et al. KEYNOTE-189: Updated OS and Progression After the Next Line of Therapy (PFS2) With Pembrolizumab (Pembro) Plus Chemo With Pemetrexed and Platinum vs Placebo Plus Chemo for Metastatic Nonsquamous NSCLC. *J Clin Oncol* (2019) 37(15_suppl):9013. doi: 10.1200/JCO.2019.37.15_suppl.9013
136. Paz-Ares L, Luft A, Vicente D, Tafreshi A, Gümüş M, Mazières J, et al. Pembrolizumab Plus Chemotherapy for Squamous Non–Small-Cell Lung Cancer. *N Engl J Med* (2018) 379(21):2040–51. doi: 10.1056/nejmoa1810865
137. Cortes J, Cescon DW, Rugo HS, Nowecki Z, Im SA, Yusof MM, et al. Pembrolizumab Plus Chemotherapy Versus Placebo Plus Chemotherapy for Previously Untreated Locally Recurrent Inoperable or Metastatic Triple-Negative Breast Cancer (KEYNOTE-355): A Randomised, Placebo-Controlled, Double-Blind, Phase 3 Clinical Trial. *Lancet* (2020) 396 (10265):1817–28. doi: 10.1016/S0140-6736(20)32531-9
138. Sahin U, Derhovanessian E, Miller M, Kloke B-P, Simon P, Löwer M, et al. Personalized RNA Mutanome Vaccines Mobilize Poly-Specific Therapeutic Immunity Against Cancer. *Nature* (2017) 547(7662):222–6. doi: 10.1038/nature23003
139. Schumacher TN, Schreiber RD. Neoantigens in Cancer Immunotherapy. *Science* (2015) 348(6230):69–74. doi: 10.1126/science.aaa4971
140. Gettinger S, Choi J, Hastings K, Truini A, Datar I, Sowell R, et al. Impaired HLA Class I Antigen Processing and Presentation as a Mechanism of Acquired Resistance to Immune Checkpoint Inhibitors in Lung Cancer. *Cancer Discov* (2017) 7(12):1420–35. doi: 10.1158/2159-8290.CD-17-0593
141. McGranahan N, Rosenthal R, Hiley CT, Rowan AJ, Watkins TBK, Wilson GA, et al. Allele-Specific HLA Loss and Immune Escape in Lung Cancer Evolution. *Cell* (2017) 171(6):1259–71.e11. doi: 10.1016/j.cell.2017.10.001
142. Pereira C, Gimenez-Xavier P, Pros E, Pajares MJ, Moro M, Gomez A, et al. Genomic Profiling of Patient-Derived Xenografts for Lung Cancer Identifies B2M Inactivation Impairing Immunorecognition. *Clin Cancer research: an Off J Am Assoc Cancer Res* (2017) 23(12):3203–13. doi: 10.1158/1078-0432.CCR-16-1946
143. Zaretsky JM, Garcia-Diaz A, Shin DS, Escuin-Ordinas H, Hugo W, Hu-Lieskovan S, et al. Mutations Associated With Acquired Resistance to PD-1 Blockade in Melanoma. *N Engl J Med* (2016) 375(9):819–29. doi: 10.1056/nejmoa1604958
144. Dubovsky JA, McNeel DG, Powers JJ, Gordon J, Sotomayor EM, Pinilla-Ibarz JA. Treatment of Chronic Lymphocytic Leukemia With a Hypomethylating Agent Induces Expression of NXF2, an Immunogenic Cancer Testis Antigen. *Clin Cancer Res: An Off J Am Assoc Cancer Res* (2009) 15(10):3406–15. doi: 10.1158/1078-0432.CCR-08-2099
145. Fonsatti E, Nicolay HJM, Sigalotti L, Calabrò L, Pezzani L, Colizzi F, et al. Functional Up-Regulation of Human Leukocyte Antigen Class I Antigens Expression by 5-Aza-2'-Deoxycytidine in Cutaneous Melanoma: Immunotherapeutic Implications. *Clin Cancer Res: An Off J Am Assoc Cancer Res* (2007) 13(11):3333–8. doi: 10.1158/1078-0432.CCR-06-3091
146. Zhou L, Xu N, Shibata H, Saloura V, Uppaluri R. Epigenetic Modulation of Immunotherapy and Implications in Head and Neck Cancer. *Cancer Metastasis Rev* (2021) 40(1):141–52. doi: 10.1007/s10555-020-09944-0
147. Zhou L, Mudianto T, Ma X, Riley R, Uppaluri R. Targeting EZH2 Enhances Antigen Presentation, Antitumor Immunity, and Circumvents Anti-PD-1 Resistance in Head and Neck Cancer. *Clin Cancer research: an Off J Am Assoc Cancer Res* (2020) 26(1):290–300. doi: 10.1158/1078-0432.CCR-19-1351
148. Peng D, Kryczek I, Nagarsheth N, Zhao L, Wei S, Wang W, et al. Epigenetic Silencing of TH1-Type Chemokines Shapes Tumour Immunity and Immunotherapy. *Nature* (2015) 527(7577):249–53. doi: 10.1038/nature15520
149. Kobayashi Y, Lim SO, Yamaguchi H. Oncogenic Signaling Pathways Associated With Immune Evasion and Resistance to Immune Checkpoint Inhibitors in Cancer. *Semin Cancer Biol* (2020) 65:51–64. doi: 10.1016/j.semcancer.2019.11.011
150. Peng W, Chen JQ, Liu C, Malu S, Creasy C, Tetzlaff MT, et al. Loss of PTEN Promotes Resistance to T Cell-Mediated Immunotherapy. *Cancer Discov* (2016) 6(2):202–16. doi: 10.1158/2159-8290.CD-15-0283
151. Zhao J, Chen AX, Gartrell RD, Silverman AM, Aparicio L, Chu T, et al. Immune and Genomic Correlates of Response to Anti-PD-1 Immunotherapy in Glioblastoma. *Nat Med* (2019) 25(3):462–9. doi: 10.1038/s41591-019-0349-y
152. Roberts PJ, Der CJ. Targeting the Raf-MEK-ERK Mitogen-Activated Protein Kinase Cascade for the Treatment Of Cancer. *Oncogene* (2007) 26(22):3291–310. doi: 10.1038/sj.onc.1210422
153. Katz M, Amit I, Yarden Y. Regulation of MAPKs by Growth Factors and Receptor Tyrosine Kinases. *Biochim Biophys Acta* (2007) 1773(8):1161–76. doi: 10.1016/j.bbamcr.2007.01.002
154. Dhillon AS, Hagan S, Rath O, Kolch W. MAP Kinase Signalling Pathways in Cancer. *Oncogene* (2007) 26(22):3279–90. doi: 10.1038/sj.onc.1210421
155. Simanshu DK, Nissley DV, McCormick F. RAS Proteins and Their Regulators in Human Disease. *Cell* (2017) 170(1):17–33. doi: 10.1016/j.cell.2017.06.009
156. Liao W, Overman MJ, Boutin AT, Shang X, Zhao D, Dey P, et al. KRAS-IRF2 Axis Drives Immune Suppression and Immune Therapy Resistance in Colorectal Cancer. *Cancer Cell* (2019) 35(4):559–72.e7. doi: 10.1016/j.ccell.2019.02.008
157. Sosman JA, Kim KB, Schuchter L, Gonzalez R, Pavlick AC, Weber JS, et al. Survival in BRAF V600–Mutant Advanced Melanoma Treated With Vemurafenib. *N Engl J Med* (2012) 366(8):707–14. doi: 10.1056/nejmoa1112302
158. Singh M, Lin J, Hocker TL, Tsao H. Genetics of Melanoma Tumorigenesis. *Br J Dermatol* (2008) 158(1):15–21. doi: 10.1111/j.1365-2133.2007.08316.x
159. Boni A, Cogdill AP, Dang P, Udayakumar D, Njauw CNJ, Sloss CM, et al. Selective BRAFV600E Inhibition Enhances T-Cell Recognition of Melanoma Without Affecting Lymphocyte Function. *Cancer Res* (2010) 70(13):5213–9. doi: 10.1158/0008-5472.CAN-10-0118
160. Frederick DT, Piris A, Cogdill AP, Cooper ZA, Lezcano C, Ferrone CR, et al. BRAF Inhibition Is Associated With Enhanced Melanoma Antigen Expression and a More Favorable Tumor Microenvironment in Patients With Metastatic Melanoma. *Clin Cancer Res* (2013) 19(5):1225–31. doi: 10.1158/1078-0432.CCR-12-1630
161. Hirata E, Girotti MR, Viros A, Hooper S, Spencer-Dene B, Matsuda M, et al. Intravital Imaging Reveals How BRAF Inhibition Generates Drug-Tolerant Microenvironments With High Integrin β1/FAK Signaling. *Cancer Cell* (2015) 27(4):574–88. doi: 10.1016/j.ccell.2015.03.008
162. Ribas A, Lawrence D, Atkinson V, Agarwal S, Miller WHJ, Carlino MS, et al. Combined BRAF and MEK Inhibition With PD-1 Blockade Immunotherapy in BRAF-Mutant Melanoma. *Nat Med* (2019) 25(6):936–40. doi: 10.1038/s41591-019-0476-5
163. Kammertoens T, Friese C, Arina A, Idel C, Briesemeister D, Rothe M, et al. Tumour Ischaemia by Interferon-γ Resembles Physiological Blood Vessel Regression. *Nature* (2017) 545(7652):98–102. doi: 10.1038/nature22311
164. Shin DS, Zaretsky JM, Escuin-Ordinas H, Garcia-Diaz A, Hu-Lieskovan S, Kalbasi A, et al. Primary Resistance to PD-1 Blockade Mediated by JAK1/2

Mutations. *Cancer Discov* (2017) 7(2):188–201. doi: 10.1158/2159-8290.CD-16-1223
165. Fish EN, Platanias LC. Interferon Receptor Signaling in Malignancy: A Network of Cellular Pathways Defining Biological Outcomes. *Mol Cancer Res* (2014) 12(12):1691–703. doi: 10.1158/1541-7786.MCR-14-0450
166. Tumeh PC, Harview CL, Yearley JH, Shintaku IP, Taylor EJM, Robert L, et al. PD-1 Blockade Induces Responses by Inhibiting Adaptive Immune Resistance. *Nature* (2014) 515(7528):568–71. doi: 10.1038/nature13954
167. Parker BS, Rautela J, Hertzog PJ. Antitumour Actions of Interferons: Implications for Cancer Therapy. *Nat Rev Cancer* (2016) 16(3):131–44. doi: 10.1038/nrc.2016.14
168. Sheng W, LaFleur MW, Nguyen TH, Chen S, Chakravarthy A, Conway JR, et al. LSD1 Ablation Stimulates Anti-Tumor Immunity and Enables Checkpoint Blockade. *Cell* (2018) 174(3):549–63.e19. doi: 10.1016/j.cell.2018.05.052
169. Sharma P, Hu-Lieskovan S, Wargo JA, Ribas A. Primary, Adaptive, and Acquired Resistance to Cancer Immunotherapy. *Cell* (2017) 168(4):707–23. doi: 10.1016/j.cell.2017.01.017
170. Jacquelot N, Yamazaki T, Roberti MP, Duong CPM, Andrews MC, Verlingue L, et al. Sustained Type I Interferon Signaling as a Mechanism of Resistance to PD-1 Blockade. *Cell Res* (2019) 29(10):846–61. doi: 10.1038/s41422-019-0224-x
171. Ghoneim HE, Fan Y, Moustaki A, Abdelsamed HA, Dash P, Dogra P, et al. *De Novo* Epigenetic Programs Inhibit PD-1 Blockade-Mediated T Cell Rejuvenation. *Cell* (2017) 170(1):142–57.e19. doi: 10.1016/j.cell.2017.06.007
172. Sheng W, Liu Y, Chakraborty D, Debo B, Shi Y. Simultaneous Inhibition of LSD1 and TGF-B Enables Eradication of Poorly Immunogenic Tumors With Anti-PD-1 Treatment. *Cancer Discov* (2021) 11(8):1970–81. doi: 10.1158/2159-8290.CD-20-0017
173. Hellmann MD, Jänne PA, Opyrchal M, Hafez N, Raez LE, Gabrilovich DI, et al. Entinostat Plus Pembrolizumab in Patients With Metastatic NSCLC Previously Treated With Anti-PD-(L)1 Therapy. *Clin Cancer Res: An Off J Am Assoc Cancer Res* (2021) 27(4):1019–28. doi: 10.1158/1078-0432.CCR-20-3305
174. Gabrilovich DI, Ostrand-Rosenberg S, Bronte V. Coordinated Regulation of Myeloid Cells by Tumours. *Nat Rev Immunol* (2012) 12(4):253–68. doi: 10.1038/nri3175
175. Weber J, Gibney G, Kudchadkar R, Yu B, Cheng P, Martinez AJ, et al. Phase I/II Study of Metastatic Melanoma Patients Treated With Nivolumab Who Had Progressed After Ipilimumab. *Cancer Immunol Res* (2016) 4(4):345–53. doi: 10.1158/2326-6066.CIR-15-0193
176. Theivanthiran B, Evans KS, DeVito NC, Plebanek M, Sturdivant M, Wachsmuth LP, et al. A Tumor-Intrinsic PD-L1/NLRP3 Inflammasome Signaling Pathway Drives Resistance to Anti-PD-1 Immunotherapy. *J Clin Invest* (2020) 130(5):2570–86. doi: 10.1172/JCI133055
177. van Deventer HW, Burgents JE, Wu QP, Woodford RMT, Brickey WJ, Allen IC, et al. The Inflammasome Component Nlrp3 Impairs Antitumor Vaccine by Enhancing the Accumulation of Tumor-Associated Myeloid-Derived Suppressor Cells. *Cancer Res* (2010) 70(24):10161–9. doi: 10.1158/0008-5472.CAN-10-1921
178. Neubert NJ, Schmittnaegel M, Bordry N, Nassiri S, Wald N, Martignier C, et al. T Cell-Induced CSF1 Promotes Melanoma Resistance to PD1 Blockade. *Sci Trans Med* (2018) 10(436):eaan3311. doi: 10.1126/scitranslmed.aan3311
179. Lu X, Horner JW, Paul E, Shang X, Troncoso P, Deng P, et al. Effective Combinatorial Immunotherapy for Castration-Resistant Prostate Cancer. *Nature* (2017) 543(7647):728–32. doi: 10.1038/nature21676
180. Yu GT, Bu LL, Huang CF, Zhang W-F, Chen W-J, Gutkind JS, et al. PD-1 Blockade Attenuates Immunosuppressive Myeloid Cells Due to Inhibition of CD47/Sirpα Axis in HPV Negative Head and Neck Squamous Cell Carcinoma. *Oncotarget* (2015) 6(39):42067–80. doi: 10.18632/oncotarget.5955
181. Molgora M, Esaulova E, Vermi W, Hou J, Chen Y, Luo J, et al. TREM2 Modulation Remodels the Tumor Myeloid Landscape Enhancing Anti-PD-1 Immunotherapy. *Cell* (2020) 182(4):886–900.e17. doi: 10.1016/j.cell.2020.07.013
182. Hughes R, Qian BZ, Rowan C, Muthana M, Keklikoglou I, Olson OC, et al. Perivascular M2 Macrophages Stimulate Tumor Relapse After Chemotherapy. *Cancer Res* (2015) 75(17):3479–91. doi: 10.1158/0008-5472.CAN-14-3587
183. Barkal AA, Brewer RE, Markovic M, Kowarsky M, Barkal SA, Zaro BW, et al. CD24 Signalling Through Macrophage Siglec-10 Is a Target for Cancer Immunotherapy. *Nature* (2019) 572(7769):392–6. doi: 10.1038/s41586-019-1456-0
184. Ziani L, Chouaib S, Thiery J. Alteration of the Antitumor Immune Response by Cancer-Associated Fibroblasts. *Front Immunol* (2018) 9:414. doi: 10.3389/fimmu.2018.00414
185. Ford K, Hanley CJ, Mellone M, Szyndralewiez C, Heitz F, Wiesel P, et al. NOX4 Inhibition Potentiates Immunotherapy by Overcoming Cancer-Associated Fibroblast-Mediated CD8 T-Cell Exclusion From Tumors. *Cancer Res* (2020) 80(9):1846–60. doi: 10.1158/0008-5472.CAN-19-3158
186. Tauriello DVF, Palomo-Ponce S, Stork D, Berenguer-Llergo A, Badia-Ramentol J, Iglesias M, et al. Tgfβ Drives Immune Evasion in Genetically Reconstituted Colon Cancer Metastasis. *Nature* (2018) 554(7693):538–43. doi: 10.1038/nature25492
187. Li MO, Flavell RA. TGF-β: A Master of All T Cell Trades. *Cell* (2008) 134 (3):392–404. doi: 10.1016/j.cell.2008.07.025
188. Lee DW, Kochenderfer JN, Stetler-Stevenson M, Cui YK, Delbrook C, Feldman SA, et al. T Cells Expressing CD19 Chimeric Antigen Receptors for Acute Lymphoblastic Leukaemia In Children and Young Adults: A Phase 1 Dose-Escalation Trial. *Lancet (London England)* (2015) 385(9967):517–28. doi: 10.1016/S0140-6736(14)61403-3
189. Turtle CJ, Hanafi LA, Berger C, Gooley TA, Cherian S, Hudecek M, et al. CD19 CAR-T Cells of Defined CD4+:CD8+ Composition in Adult B Cell ALL Patients. *J Clin Invest* (2016) 126(6):2123–38. doi: 10.1172/JCI85309
190. Maude SL, Frey N, Shaw PA, Aplenc R, Barrett DM, Bunin NJ, et al. Chimeric Antigen Receptor T Cells for Sustained Remissions in Leukemia. *N Engl J Med* (2014) 371(16):1507–17. doi: 10.1056/NEJMoa1407222
191. Davila ML, Riviere I, Wang X, Bartido S, Park J, Curran K, et al. Efficacy and Toxicity Management of 19-28z CAR T Cell Therapy in B Cell Acute Lymphoblastic Leukemia. *Sci Trans Med* (2014) 6(224):224ra25. doi: 10.1126/scitranslmed.3008226
192. Foster AE, Dotti G, Lu A, Khalil M, Brenner MK, Heslop HE, et al. Antitumor Activity of EBV-Specific T Lymphocytes Transduced With a Dominant Negative TGF-β Receptor. *J Immunother* (2008) 31(5):500–5. doi: 10.1097/CJI.0b013e318177092b
193. John LB, Devaud C, Duong CPM, Yong CS, Beavis PA, Haynes NM, et al. Anti-PD-1 Antibody Therapy Potently Enhances the Eradication of Established Tumors by Gene-Modified T Cells. *Clin Cancer Res: An Off J Am Assoc Cancer Res* (2013) 19(20):5636–46. doi: 10.1158/1078-0432.CCR-13-0458
194. Chong EA, Melenhorst JJ, Lacey SF, Ambrose DE, Gonzalez V, Levine BL, et al. PD-1 Blockade Modulates Chimeric Antigen Receptor (CAR)-Modified T Cells: Refueling The CAR. *Blood* (2017) 129(8):1039–41. doi: 10.1182/blood-2016-09-738245
195. Motz GT, Santoro SP, Wang LP, Garrabrant T, Lastra RR, Hagemann IS, et al. Tumor Endothelium FasL Establishes a Selective Immune Barrier Promoting Tolerance in Tumors. *Nat Med* (2014) 20(6):607–15. doi: 10.1038/nm.3541
196. Gabrilovich D, Ishida T, Oyama T, Ran S, Kravtsov V, Nadaf S, et al. Vascular Endothelial Growth Factor Inhibits the Development of Dendritic Cells and Dramatically Affects the Differentiation of Multiple Hematopoietic Lineages. *vivo Blood* (1998) 92(11):4150–66. doi: 10.1016/S0950-3536(98)80044-9
197. Newport EL, Pedrosa AR, Njegic A, Hodivala-Dilke KM, Muñoz-Félix JM. Improved Immunotherapy Efficacy by Vascular Modulation. *Cancers* (2021) 13(20):5207. doi: 10.3390/cancers13205207
198. Fukumura D, Kloepper J, Amoozgar Z, Duda DG, Jain RK. Enhancing Cancer Immunotherapy Using Antiangiogenics: Opportunities and Challenges. *Nat Rev Clin Oncol* (2018) 15(5):325–40. doi: 10.1038/nrclinonc.2018.29
199. Ren S, Xiong X, You H, Shen J, Zhou P. The Combination of Immune Checkpoint Blockade and Angiogenesis Inhibitors in the Treatment of Advanced Non-Small Cell Lung Cancer. *Front Immunol* (2021) 12:689132. doi: 10.3389/fimmu.2021.689132

200. Delgoffe GM. Filling the Tank: Keeping Antitumor T Cells Metabolically Fit for the Long Haul. *Cancer Immunol Res* (2016) 4(12):1001–6. doi: 10.1158/2326-6066.CIR-16-0244
201. Brand A, Singer K, Koehl GE, Kolitzus M, Schoenhammer G, Thiel A, et al. LDHA-Associated Lactic Acid Production Blunts Tumor Immunosurveillance by T and NK Cells. *Cell Metab* (2016) 24(5):657–71. doi: 10.1016/j.cmet.2016.08.011
202. Young A, Mittal D, Stagg J, Smyth MJ. Targeting Cancer-Derived Adenosine: New Therapeutic Approaches. *Cancer Discov* (2014) 4(8):879–88. doi: 10.1158/2159-8290.CD-14-0341
203. Li T, Mao C, Wang X, Shi Y, Tao Y. Epigenetic Crosstalk Between Hypoxia and Tumor Driven by HIF Regulation. *J Exp Clin Cancer Res: CR* (2020) 39 (1):224. doi: 10.1186/s13046-020-01733-5
204. Gide TN, Quek C, Menzies AM, Tasker AT, Shang P, Holst J, et al. Distinct Immune Cell Populations Define Response to Anti-PD-1 Monotherapy and Anti-PD-1/Anti-CTLA-4 Combined Therapy. *Cancer Cell* (2019) 35(2):238–55.e6. doi: 10.1016/j.ccell.2019.01.003
205. Fischer K, Hoffmann P, Voelkl S, Meidenbauer N, Ammer J, Edinger M, et al. Inhibitory Effect of Tumor Cell-Derived Lactic Acid on Human T Cells. *Blood* (2007) 109(9):3812–9. doi: 10.1182/blood-2006-07-035972
206. Puccetti P, Grohmann U. IDO and Regulatory T Cells: A Role for Reverse Signalling and Non-Canonical NF-kappaB Activation. *Nat Rev Immunol* (2007) 7(10):817–23. doi: 10.1038/nri2163
207. Botticelli A, Cerbelli B, Lionetto L, Zizzari I, Salati M, Pisano A, et al. Can IDO Activity Predict Primary Resistance to Anti-PD-1 Treatment in NSCLC? *J Trans Med* (2018) 16(1):219. doi: 10.1186/s12967-018-1595-3
208. Long G v, Dummer R, Hamid O, Gajewski TF, Caglevic C, Dalle S, et al. Epacadostat Plus Pembrolizumab Versus Placebo Plus Pembrolizumab in Patients With Unresectable or Metastatic Melanoma (ECHO-301/KEYNOTE-252): A Phase 3, Randomised, Double-Blind Study. *Lancet Oncol* (2019) 20(8):1083–97. doi: 10.1016/S1470-2045(19)30274-8
209. Liu H, Kuang X, Zhang Y, Ye Y, Li J, Liang L, et al. ADORA1 Inhibition Promotes Tumor Immune Evasion by Regulating the ATF3-PD-L1 Axis. *Cancer Cell* (2020) 37(3):324–339.e8. doi: 10.1016/j.ccell.2020.02.006
210. Sun X, Wu Y, Gao W, Enjyoji K, Csizmadia E, Müller CE, et al. CD39/ENTPD1 Expression by CD4+Foxp3+ Regulatory T Cells Promotes Hepatic Metastatic Tumor Growth in Mice. *Gastroenterology* (2010) 139(3):1030–40. doi: 10.1053/j.gastro.2010.05.007
211. Gopalakrishnan V, Spencer CN, Nezi L, Reuben A, Andrews MC, Karpinets T v, et al. Gut Microbiome Modulates Response to Anti-PD-1 Immunotherapy in Melanoma Patients. *Science* (2018) 359(6371):97–103. doi: 10.1126/science.aan4236
212. Gopalakrishnan V, Helmink BA, Spencer CN, Reuben A, Wargo JA. The Influence of the Gut Microbiome on Cancer, Immunity, and Cancer Immunotherapy. *Cancer Cell* (2018) 33(4):570–80. doi: 10.1016/j.ccell.2018.03.015
213. Si W, Liang H, Bugno J, Xu Q, Ding X, Yang K, et al. Lactobacillus Rhamnosus GG Induces cGAS / STING- Dependent Type I Interferon and Improves Response to Immune Checkpoint Blockade. *Gut* (2021) (2021):gutjnl-2020-323426. doi: 10.1136/gutjnl-2020-323426
214. Zhang Z, Tang H, Chen P, Xie H, Tao Y. Demystifying the Manipulation of Host Immunity, Metabolism, and Extraintestinal Tumors by the Gut Microbiome. *Signal Transduction Targeted Ther* (2019) 4:41. doi: 10.1038/s41392-019-0074-5
215. Derosa L, Routy B, Enot D, Baciarello G, Massard C, Loriot Y, et al. Impact of Antibiotics on Outcome in Patients With Metastatic Renal Cell Carcinoma Treated With Immune Checkpoint Inhibitors. *J Clin Oncol* (2017) 35:462. doi: 10.1200/JCO.2017.35.6_suppl.462
216. Gopalakrishnan V, Spencer CN, Reuben A, Karpinets T, Hutchinson D, Hoffman K, et al. Association of Diversity and Composition of the Gut Microbiome With Differential Responses to PD-1 Based Therapy in Patients With Metastatic Melanoma. *J Clin Oncol* (2017) 35:2. doi: 10.1200/JCO.2017.35.7_suppl.2
217. Routy B, le Chatelier E, Derosa L, Duong CPM, Alou MT, Daillère R, et al. Gut Microbiome Influences Efficacy of PD-1-Based Immunotherapy Against Epithelial Tumors. *Science* (2018) 359(6371):91–7. doi: 10.1126/science.aan3706
218. Davar D, Dzutsev AK, McCulloch JA, Rodrigues RR, Chauvin J-M, Morrison RM, et al. Fecal Microbiota Transplant Overcomes Resistance to Anti-PD-1 Therapy in Melanoma Patients. *Sci (New York NY)* (2021) 371(6529):595–602. doi: 10.1126/science.abf3363
219. Shayan G, Srivastava R, Li J, Schmitt N, Kane LP, Ferris RL. Adaptive Resistance to Anti-PD1 Therapy by Tim-3 Upregulation Is Mediated by the PI3K-Akt Pathway in Head and Neck Cancer. *Oncoimmunology* (2017) 6(1):e1261779. doi: 10.1080/2162402X.2016.1261779
220. Koyama S, Akbay EA, Li YY, Herter-Sprie GS, Buczkowski KA, Richards WG, et al. Adaptive Resistance to Therapeutic PD-1 Blockade Iis Associated With Upregulation of Alternative Immune Checkpoints. *Nat Commun* (2016) 7:10501. doi: 10.1038/ncomms10501
221. Limagne E, Richard C, Thibaudin M, Fumet JD, Truntzer C, Lagrange A, et al. Tim-3/Galectin-9 Pathway and mMDSC Control Primary and Secondary Resistances to PD-1 Blockade in Lung Cancer Patients. *OncoImmunology* (2019) 8(4):e1564505. doi: 10.1080/2162402X.2018.1564505
222. Lui Y, Davis SJ. LAG-3: A Very Singular Immune Checkpoint. *Nat Immunol* (2018) 19(12):1278–9. doi: 10.1038/s41590-018-0257-1
223. Johnson DB, Nixon MJ, Wang Y, Wang DY, Castellanos E, Estrada M v, et al. Tumor-Specific MHC-II Expression Drives a Unique Pattern of Resistance to Immunotherapy via LAG-3/FCRL6 Engagement. *JCI Insight* (2018) 3(24):e120360. doi: 10.1172/jci.insight.120360
224. Woo SR, Turnis ME, Goldberg M v, Bankoti J, Selby M, Nirschl CJ, et al. Immune Inhibitory Molecules LAG-3 and PD-1 Synergistically Regulate T-Cell Function To Promote Tumoral Immune Escape. *Cancer Res* (2012) 72 (4):917–27. doi: 10.1158/0008-5472.CAN-11-1620

Conflict of Interest: The authors declare that the research was conducted in the absence of any commercial or financial relationships that could be construed as a potential conflict of interest.

GLOSSARY

APC	antigen-presenting cell
ARG1	Arginase 1
B2M	β2-microglobulin
cHL	classical Hodgkin's lymphoma
CTL	cytotoxic T lymphocyte
CAF	cancer-associated fibroblast
DC	dendritic cell
DLBCL	diffuse large B cell lymphoma
DNMTi	DNA methyltransferase inhibitor
EZH2	enhancer of zeste homolog 2
FDA	Food and Drug Administration
FasL	factor-related apoptosis antigen ligand
FL	follicular lymphoma
HNC	head and neck cancer
HNSCC	head and neck squamous cell carcinoma
H3K27me3	histone h3 lysine 27 tri-methylation
ICB	immune checkpoint blocker
ITIM	immunoreceptor tyrosine-based inhibitory motif
ITSM	immunoreceptor tyrosine-based switch motif
ILC	innate lymphoid cell
IDO	indoleamine 2,3-dioxygenase
IFN	interferon
iNOS	inducible nitric oxide synthase
JAK	Janus kinase
LSD1	lysine-specific histone demethylase 1
LAG-3	lymphocyte activation gene 3
MHC	major histocompatibility complex
MAPK	mitogen-activated protein kinase
mCRPC	metastatic castration-resistant prostate cancer
mAb	monoclonal antibody
MDSC	myeloid-derived suppressor cell
NK	natural killer cell
NSCLC	non-small cell lung cancer
NCI	National Cancer Institute
NF-κB	nuclear factor kappa-light-chain-enhancer of activated B cells
PD-1	programmed cell death receptor 1
PD-L1	programmed cell death ligand 1
PD-L2	programmed cell death ligand 2
PRC2	polycomb repressive complex 2
PTEN	phosphatase and tensin homolog
RT	radiotherapy
STAT1	signal transducer and activator of transcription 1
TDLNs	tumor-draining lymph nodes
TME	tumor microenvironment
TCR	T cell receptor
TAM	tumor-associated macrophage
TNF-α	tumor necrosis factor α
Th1 cell	T helper 1 cell
Treg	regulatory T cell
TGF-β	transforming growth factor β
TREM2	triggering receptor expressed on myeloid cells 2
TIM-3	T-cell immunoglobulin mucin 3
UC	urothelial carcinoma
VEGF	vascular endothelial growth factor

frontiers in Immunology

ORIGINAL RESEARCH
published: 24 January 2022
doi: 10.3389/fimmu.2022.781222

The Prognostic Value of FoxP3+ Tumour-Infiltrating Lymphocytes in Rectal Cancer Depends on Immune Phenotypes Defined by CD8+ Cytotoxic T Cell Density

Sören Schnellhardt[1,2], *Johannes Hirneth*[1,2], *Maike Büttner-Herold*[2,3], *Christoph Daniel*[2,3], *Marlen Haderlein*[1,2], *Arndt Hartmann*[2,4], *Rainer Fietkau*[1,2] *and Luitpold Distel*[1,2]*

[1] Department of Radiation Oncology, Universitätsklinikum Erlangen, Friedrich-Alexander-Universität Erlangen-Nürnberg, Erlangen, Germany, [2] Comprehensive Cancer Center Erlangen-Europäische Metropolregion Nürnberg (CCC ER-EMN), Erlangen, Germany, [3] Department of Nephropathology, Institute of Pathology, Universitätsklinikum Erlangen, Friedrich-Alexander-Universität Erlangen-Nürnberg, Erlangen, Germany, [4] Institute of Pathology, Universitätsklinikum Erlangen, Friedrich-Alexander-Universität Erlangen-Nürnberg, Erlangen, Germany

OPEN ACCESS

Edited by:
Nicolas Larmonier, Université de Bordeaux, France

Reviewed by:
Gerhard Grabenbauer, Coburg Cancer Center, Germany
Pierpaolo Correale, Azienda ospedaliera 'Bianchi-Melacrino-Morelli', Italy

***Correspondence:**
Luitpold Distel
Luitpold.Distel@uk-erlangen.de

Specialty section:
This article was submitted to Cancer Immunity and Immunotherapy, a section of the journal Frontiers in Immunology

Received: 22 September 2021
Accepted: 04 January 2022
Published: 24 January 2022

Citation:
Schnellhardt S, Hirneth J, Büttner-Herold M, Daniel C, Haderlein M, Hartmann A, Fietkau R and Distel L (2022) The Prognostic Value of FoxP3+ Tumour-Infiltrating Lymphocytes in Rectal Cancer Depends on Immune Phenotypes Defined by CD8+ Cytotoxic T Cell Density. Front. Immunol. 13:781222. doi: 10.3389/fimmu.2022.781222

Tumour-infiltrating FoxP3+ regulatory T cells have been identified as both positive and negative prognostic factors in colorectal cancer (CRC) and rectal cancer (RC). In this study we investigated whether immune phenotypes, defined by CD8+ cytotoxic T cell density, may influence the prognostic association of FoxP3+ T cell densities in RC. Tissue microarrays from 154 rectal cancer resections were immunohistochemically double stained for CD8 and FoxP3. CD8+ and FoxP3+ cell densities were measured in the stromal and intraepithelial compartment. Stromal FoxP3+ cell densities were not associated with 10-year overall survival (OS). In the "immune-desert" phenotype, defined by very low stromal CD8+ cell density, a high density of stromal FoxP3+ T cells displayed a tendency towards an association with decreased 10-year OS ($p = 0.179$). In "inflamed" tumours, defined by high intraepithelial CD8+ T cell infiltration, the opposite was the case and high stromal FoxP3+ T cell densities were a positive prognostic factor ($p = 0.048$). Additionally, patients with an increased FoxP3/CD8 cell density ratio demonstrated a strong trend towards decreased 10-year OS ($p = 0.066$). These contrasting findings suggest functional heterogeneity within the group of FoxP3+ T cells. They are consistent with experimental studies which reported suppressive and non-suppressive populations of FoxP3+ T cells in CRC. Furthermore, our study demonstrates that CD8 immunohistochemistry may act as an instrument to identify tumours infiltrated by possibly functionally differing FoxP3+ T cell subtypes.

Keywords: Foxp3, CD8, regulatory T cells, rectal cancer, tumour-infiltrating lymphocytes, TILs, immune phenotypes, prognosis

INTRODUCTION

The relevant relationship of immune cell infiltration in colorectal and rectal carcinomas (CRC) and patient prognosis has been established in numerous studies (1–4). Yet, our understanding of the complex causal links between immune response and disease progression remains limited. Various molecular subtypes have been identified and their immunological importance is becoming more apparent (5–7). A crucial role in influencing and controlling the local immune response is attributed to tumour-infiltrating FoxP3+ regulatory T cells (Treg) (8). Treg are an important element of immunological tolerance, both for self-tolerance in healthy tissue and locally in tumours (9, 10). Targeting this cell type is regarded as a promising approach for improving the response rate of current immunotherapies (11). However, in order not to cross the fine line between the induction of immunity in tumours and fatal systemic autoimmunity, a profound understanding of the role of Treg in cancer is necessary (12). But even the fundamental question of whether increased Treg infiltration in CRC is a favourable or unfavourable prognostic factor is still undecided and several studies have reported conflicting results (13, 14). In this immunohistochemical study we investigated the prognostic relevance of FoxP3+ T cell density in the context of different degrees of intratumoural inflammation as signified by CD8+ T cell infiltration. Our results offer a possible explanation for inconsistent findings on the role of Treg in previous studies and give insights into the intricacies of Treg functionality in cancers.

MATERIALS AND METHODS

Patients and Samples

Between 2006 and 2013, a total of 154 patients with advanced rectal cancer were treated at Universitätsklinikum Erlangen (University Hospital Erlangen) (**Table 1**). Tissue samples were obtained from surgical resection specimens after neoadjuvant treatment (**Figure 1**). The prognostic relevance of FoxP3+ and CD8+ T cell densities in general, cell-to-cell distances and distances to the epithelial-stromal interface have previously been reported in this cohort (15, 16).

The use of formalin-fixed paraffin-embedded material from the Archive of the Institute of Pathology was approved by the Ethics Committee of the Friedrich-Alexander-University of Erlangen-Nuremberg on 24 January 2005 (21_ 19 B), waiving the need for consent for using the existing archived material. Written informed consent was obtained "front door" from all patients allowing the collection of their tissue and clinical data.

TABLE 1 | Clinical characteristics of the studied patient cohort.

Gender:	**male: 118 (76.6%) female: 36 (23.4%)**
Age (years):	mean: 63,8± 11,1; min.: 32 max.: 88
Primary tumour:	T1: 3 (1.9%) T2: 17 (11%) T3: 113 (73.4%) T4: 21 (13.6%)
Regional lymph nodes:	N0: 49 (31.8%) N1: 80 (51.9%) N2: 25 (16.2%)
Distant metastasis:	M0: 129 (83.8%) M1: 25 (16.2%)
UICC stage:	I: 11 (7.1%) II: 46 (29.9%) III: 72 (46.8%) IV: 25 (16.2%)
Grading:	G1: 3 (1.9%) G2: 121 (78.6%) G3: 30 (19.5%)
Chemotherapy:	5-FU: 48 (31.2%) 5-FU + Oxaliplatin: 89 (57.8%) other: 17 (11%)

Treatment Protocol

All patients underwent neoadjuvant radiochemotherapy (RCT). A total radiation dose of 50.4 Gy was applied in 28 fractions of 1.8 Gy and 5-fluorouracil based chemotherapy as described earlier (17). After a period of 8 weeks treatment response was assessed and total mesorectal excision was performed to surgically remove the residual tumour. Additionally, 5-FU based adjuvant chemotherapy was administered.

Tissue Microarray Construction and Immunohistochemistry

Two formalin-fixed, paraffin-embedded tissue cores of 2 mm diameter from the tumour centre of resection specimens of each patient were arranged in tissue microarrays (TMA). The tumour centre was identified and marked by a pathologist on a section of the whole tissue block prior to extraction of the cores. Samples of patients with pathologic complete response after neoadjuvant RCT were not included in this study.

An immunohistochemical double-staining with anti-FoxP3- and anti-CD8-specific antibodies was performed on the sections of the TMA to identify CD8+ and FoxP3+ T cells. As described previously, sections were deparaffinised and rehydrated and antigen retrieval was performed in a steam cooker for 5 minutes (16). The FoxP3-specific antibody (1:100, Ab20034, abcam, Cambridge, United Kingdom) was applied overnight and detected with a Polymer-Kit (Fa Zytomed POLAP-100) and Fast Red as a chromogen. Then, the CD8-specific antibody (1:50, M7103, Agilent, Santa Clara, CA United States) was added for 60 minutes and detection was performed with the Polymer-Kit and Fast Blue as a chromogen.

Quantification of Cell Densities

Following immunohistochemical double-staining a high throughput scanner was used to scan sections at a magnification of 1:200 (Zeiss, Mirax MIDI Scan, Göttingen, Germany). Digital images of each tissue core were analysed using an image analysis software (Biomas, Erlangen, Germany). Stained cells were counted in a two-step process of automatic detection and manual correction by the examiner. Colour, shape, localization (nuclear for FoxP3 and membranous for CD8) and size were criteria for inclusion of stained cells. Cell densities (cells/mm^2) were then calculated after measurement of the area of the stromal and intraepithelial compartment, respectively. For each patient the average cell density was determined by calculating the arithmetic mean of cell densities measured in the two cores.

Statistical Analysis

Kaplan-Meier plots and the log-rank test were used to describe and compare overall survival rates (OS) and no-evidence-of-disease survival rates (NED) of different groups. Optimized

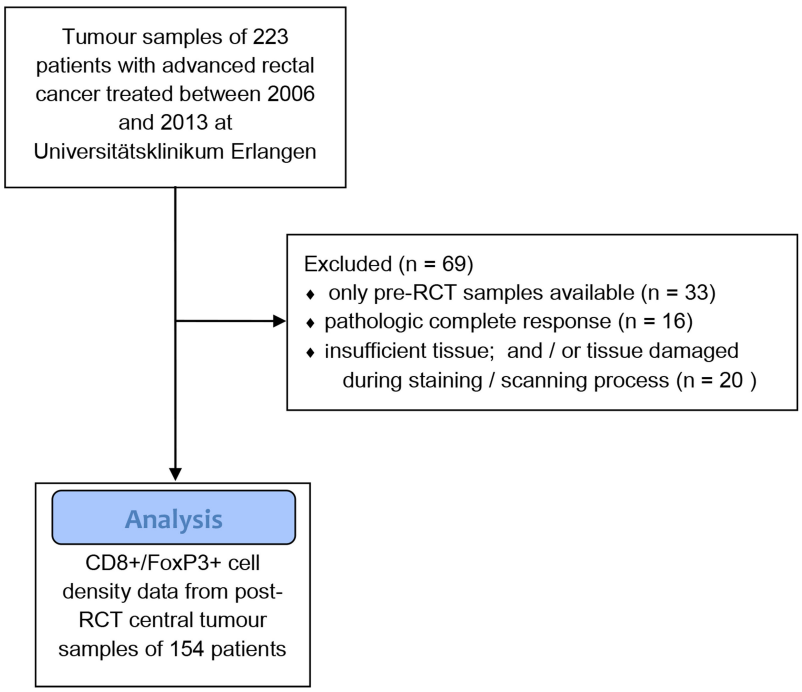

FIGURE 1 | Flow diagram of the patient and tissue sample selection process.

cut-off values for prognostic groups were determined through receiver operating characteristic curve analysis and X-tile software (Version 3.6.1, Yale University, New Haven, Connecticut, USA) (18). Student's t-Test and one-way analysis of variance (ANOVA) were used to compare means of two or more groups, respectively. Frequency distributions of categorical variables in contingency tables were compared with chi-squared test and Fisher's exact test. SPSS (Version 26, IBM, Chicago, Illinois, USA) and Microsoft Excel (Version 16, Microsoft, Redmond, Washington, USA) were used to perform statistical analyses.

RESULTS

Among 154 patients suffering from rectal cancer, the respective OS and NED were 45% and 60% at 10 years (**Figure 2A**). Overall stromal FoxP3+ cell densities were not associated with 10-year OS (**Figure 2B**). In the intraepithelial compartment high densities of FoxP3+ cells were associated with improved 10-year OS ($p = 0.018$) (**Figure 2C**).

Three groups defined by different "immune phenotype" were established based on stromal and intraepithelial CD8+ cell densities (**Figure 3A**). Cut-off values of these groups were defined by serial comparison of different CD8+ cell density thresholds for their impact on the prognostic significance of stromal FoxP3+ cell densities on OS and NED. Accordingly, "immune-desert" tumours were defined by stromal CD8+ cell densities of less than 40 cells/mm², which was accompanied by very low levels of intraepithelial CD8+ cell densities (**Figure 3B**). In this subgroup stromal FoxP3+ cell density displayed a tendency towards an association with decreased 10-year OS (52% vs 40% 10-year OS, $p = 0.179$) (**Figure 3C**). Tumours with stromal CD8+ cell densities of equal to or more than 40 cells/mm² in combination with intraepithelial CD8+ cell densities of less than 170 cells/mm² were assigned to the "immune-excluded" group, indicating a phenotype characterized by stromal accumulations of cytotoxic T cells with a simultaneous lack of intraepithelial infiltration (**Figure 3D**). 10-year OS was not associated with FoxP3+ cell densities in this group (**Figure 3E**). "Inflamed" tumours were defined by intraepithelial CD8+ cell densities of ≥170 cells/mm². With stromal and intraepithelial median values of CD8+ cell densities of 237 and 415 cells/mm², respectively, this group was characterized by high levels of cytotoxic T cell infiltration (**Figure 3F**). Here, increased stromal FoxP3+ cell densities were associated with significantly improved 10-year OS (33% vs. 74% 10-year OS, $p = 0.048$ (**Figure 3G**).

The prognostic value of intraepithelial FoxP3+ T cell densities also changed from negative to positive comparing "immune-desert" and "inflamed" tumours, but this relationship was less pronounced than in stromal FoxP3+ T cells (**Supplementary Figure 1**). FoxP3+ cell density levels correlated with those of CD8+ cells and were distinctly higher in "inflamed" tumours than in those classified as "immune-desert" (**Figure 3H**).

Stromal FoxP3+ and CD8+ cell densities were moderately positively correlated in both "immune-desert" (Spearman correlation coefficient = 0.59, $p = 0.001$, $n = 43$) and "inflamed"

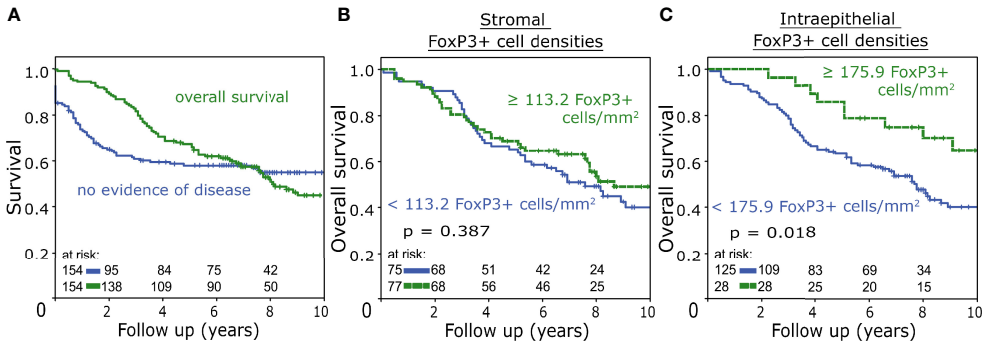

FIGURE 2 | **(A)** Overall survival and no-evidence-of-disease survival rate of the studied patient cohort analysed with the Kaplan-Meier method and log-rank test. **(B, C)** Overall survival analysed with the Kaplan-Meier method and log-rank test according to FoxP3+ tumour-infiltrating T cell densities in the stromal **(B)** and intraepithelial **(C)** compartment.

tumours (Spearman correlation coefficient = 0.407, p = 0.014, n = 36).

There were no significant differences concerning the type of chemotherapy used between immune phenotype groups (p = 0.067, **Supplementary Table 1**).

Comparing patients with different immune phenotypes, the 10-year OS was identical (**Figure 4A**). NED status on the other hand was significantly longer in the "inflamed" group compared to "immune-desert" (52% vs. 41% 10-year NED, p = 0.049) (**Figure 4B**). The only clinicopathological categories with significant differences between the analysed groups were age at diagnosis and nodal status: Patients with an "inflamed" tumour phenotype were older than those with "immune-excluded" and "immune-desert" tumours (median age at diagnosis: 69 vs. 67 vs. 60 years, respectively) and were more often lymph node positive at diagnosis (N+: 86% vs. 65% vs. 59%, respectively). The phenotype with the highest ratio of FoxP3+ to CD8+ cell densities was "immune-desert" (**Figure 4C**). An increased FoxP3/CD8 ratio was moderately associated with decreased 10-year OS (p = 0.066) (**Figure 4D**).

DISCUSSION

One of the most commonly used markers for self-tolerance promoting regulatory T cells (Treg) is the transcription factor forkhead box protein P3 (FoxP3) (19). The prognostic relevance of FoxP3+ tumour-infiltrating Treg in colorectal cancer (CRC) and rectal cancer (RC) has been a frequently studied albeit controversial subject. While Treg are generally assumed to have an immunosuppressive and thus adverse prognostic effect, there is ample evidence that high densities of intratumoural FoxP3+ T cells can be indicative of improved prognosis in CRC and other types of cancer (14, 20–22). There are, however, also numerous studies that reported the opposite, linking increased FoxP3+ T cell densities with an unfavourable prognosis (23–25). Some of these inconsistencies were most likely the result of variations in measurement methods and treatment modalities. But the apparent prognostic ambivalence is also indicative of the possibility that there may be multiple subpopulations of FoxP3+ T cells in CRC, or that Treg may have different and at times opposing functions depending on other environmental factors (10).

In the present study, we investigated the prognostic relevance of FoxP3+ T cell density in RC depending on the degree of inflammation within the tumour. To this end we established immune phenotypes defined by the density of tumour infiltrating CD8+ T cells. The phenotypes "immune-desert", "immune-excluded" and "inflamed" have previously been described as archetypical immune constellations in tumours (26). Chen et al. explained tumoural immunological tolerance for each of these constellations with different underlying causes. "Immune-desert" tumours were defined as immunologically cold tumours attracting only very few inflammatory cells. Here, an immunosuppressive environment as well as a lack of antigens or antigen presentation were assumed to be main factors promoting immunological tolerance. One of several possible immunosuppressive elements in this context were FoxP3+ Tregs, which were thus regarded as an unfavourable prognostic factor in "immune-desert" tumours. In the "immune-excluded" phenotype, the cellular immune response was limited to surrounding stromal tissue only. Infiltration of the intraepithelial compartment by inflammatory cells did not occur. Consequently, lack of T cell migration into the tumour was presumed to be the tolerance promoting factor in this setting. Lastly, tumours with ubiquitous high densities of immune cells were designated to the "inflamed" group: Inflammatory cells were numerous but rendered ineffective by local factors like, for example, the PD-1/PD-L1 pathway. As suppression of a cellular immune response obviously failed in this setting, a different and possibly prognostically favourable function was assumed for FoxP3+ T cells.

In head and neck squamous cell carcinoma (HNSCC) we were able to use stromal and intraepithelial CD8+ T cell densities as surrogate markers for the above-defined phenotypes and could demonstrate that the prognostic relevance of FoxP3+ T cell density depended on the degree of intratumoural inflammation (27). The results of the present work confirm

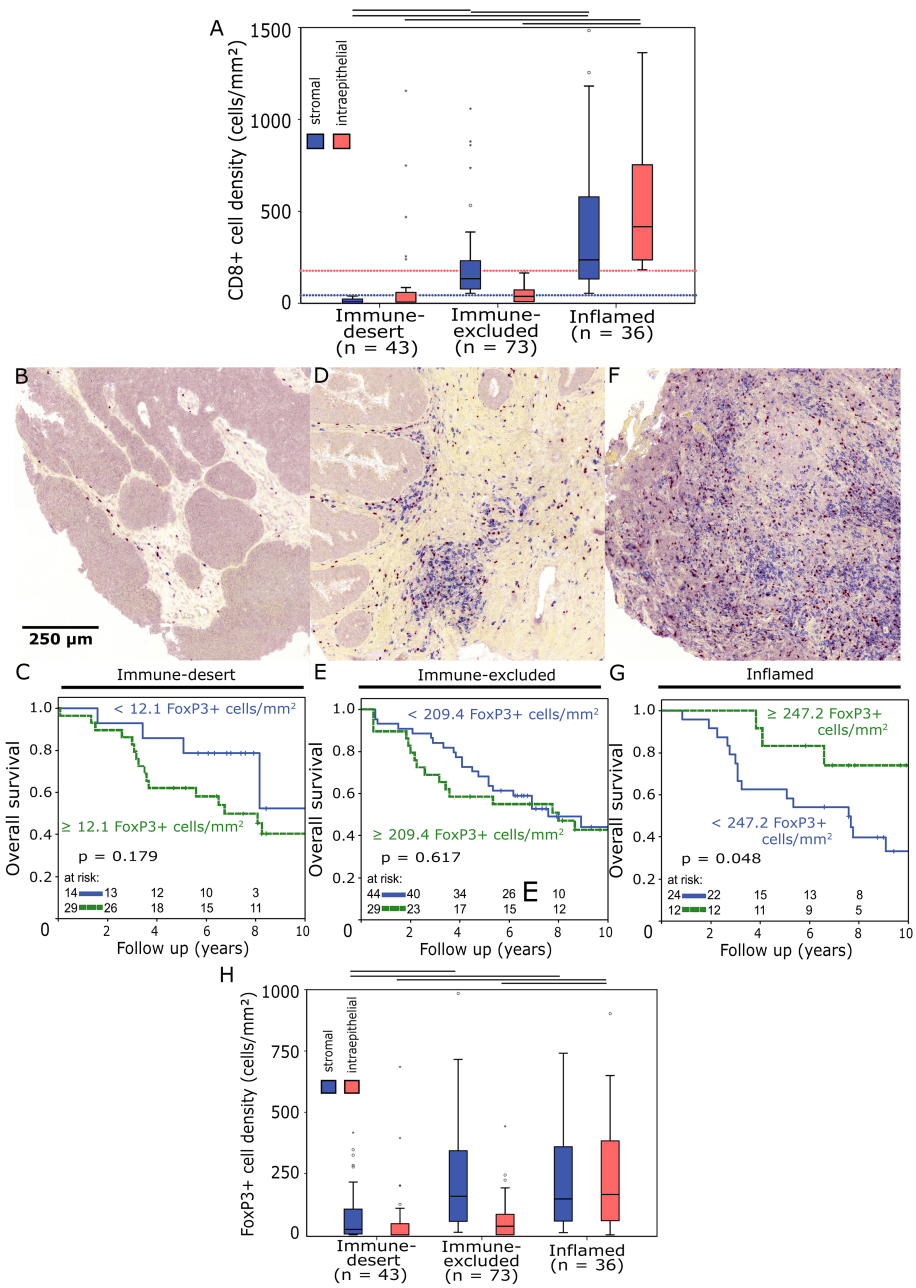

FIGURE 3 | **(A)** Boxplots of stromal and intraepithelial CD8+ cell density distributions in different immune phenotypes. Outliers are marked with an asterisk (*). Horizontal black bars signify $p < 0.05$ in Student's t-test. The "immune-desert" group was defined by stromal CD8+ cell densities < 40 cells/mm² (dotted blue line), "inflamed" tumours had intraepithelial CD8+ cell densities ≥ 170 cells/mm² (dotted red line). **(B, D, F)** Representative images of tissue microarray core sections from "immune-desert" **(B)**, "immune-excluded" **(D)** and "inflamed" **(F)** tumours double stained for FoxP3 (red)/CD8 (blue) (200x magnification). **(C, E, G)** Overall survival analysed with the Kaplan-Meier method and log-rank test according to stromal FoxP3+ tumour-infiltrating T cell densities in "immune-desert" **(C)**, "immune-excluded" **(E)** and "inflamed" **(G)** tumours. **(H)** Boxplots of stromal and intraepithelial FoxP3+ cell density distributions in different immune phenotypes.

that this phenomenon can also be observed in RC. High overall stromal FoxP3+ T cell densities had no prognostic impact, whereas in the "immune-desert" and "inflamed" subgroups they correlated with decreased and improved survival, respectively. Similar observations were also made in other types of cancer: A large immunohistochemical study reported that high densities of FoxP3+ TIL were only indicative of improved survival in HER2+/estrogen receptor negative (ER-) breast cancer if they coincided with accumulations of CD8+ TIL. Simultaneously, the negative prognostic significance of FoxP3+ TIL densities in ER+ breast cancer depended on the absence of CD8+ T cells (28). Another parameter that underlines this

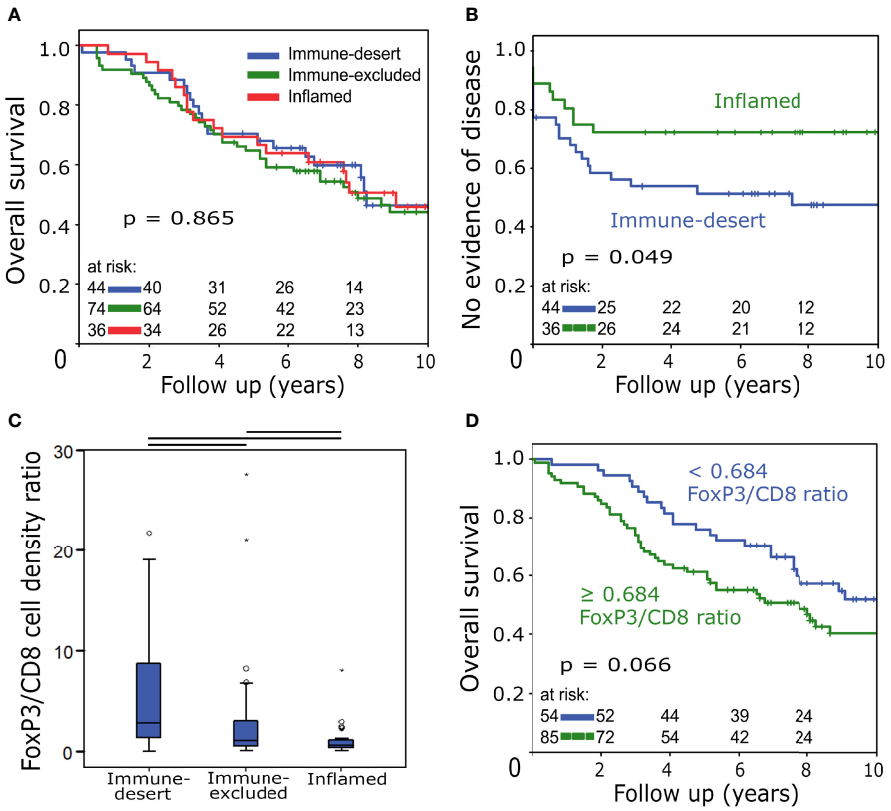

FIGURE 4 | **(A)** Overall survival analysed with the Kaplan-Meier method and log-rank test according to immune phenotypes. **(B)** No evidence of disease status analysed with the Kaplan-Meier method and log-rank test according to immune phenotypes. **(C)** Boxplots of stromal FoxP3+/CD8+ cell density ratio distributions in different immune phenotypes. Horizontal black bars signify $p < 0.05$ in Student's t-test. **(D)** Overall survival analysed with the Kaplan-Meier method and log-rank test according to the FoxP3+/CD8+ cell density ratio.

relationship is the ratio of FoxP3+ and CD8+ cell density, which was significantly increased in "immune-desert" tumours compared to the remaining two phenotypes. An increased FoxP3/CD8 ratio was a predictor of reduced survival in this study as well as in cervical cancer, esophageal cancer and lung cancer (29–31). Although the calculation of a ratio is less complicated than the proposed classification into immune phenotypes, it does not adequately express the prognostic ambivalence of FoxP3+ TILs observed here. Nonetheless, all the previous reports suggest functional and prognostic heterogeneity within the group of FoxP3+ TILs, which could be an innate feature of this cell type not limited to specific cancer entities (11, 32).

Conclusions drawn from our cohort regarding the functional heterogeneity of FoxP3+ T cells in RC are limited by the size of the cohort and methodology as an immunohistochemical association study. One possible rationale for the observed results could be a suppressive function of FoxP3+ TILs in "immune-desert" tumours and a lack of function in "inflamed" tumours. Correlations between FoxP3+ and CD8+ TIL densities in the inflammatory phenotype could mean that the former are simply a concomitant phenomenon of cytotoxic T cell infiltration. An extensive work by Saito et al., however, provided a different and very reasonable explanation to distinguish FoxP3+ T cells in "immune-desert" tumours from those in "inflamed" tumours. They postulated that two types of activated FoxP3+CD4+ cells exist in CRC: suppression-competent Fraction II effector Tregs (Fr-II eTregs) and non-suppressive, pro-inflammatory Fr-III non-Treg FoxP3+ T cells (33). Based on the frequency of non-suppressive Fr-III FoxP3+ T cells, they subdivided CRC into type A and B tumours. Type A CRC were characterized by low numbers of Fr-III non-Treg FoxP3+ T cells and increased numbers of immunosuppressive genes expressed. Increased levels of FoxP3 transcripts in quantitative real-time PCR were associated with poor prognosis in this CRC subtype. This is consistent with our "immune-desert" phenotype, in which immunosuppression was reflected by very low densities of cytotoxic T cells and in which high FoxP3+ T cell densities were a negative prognostic factor. In type B CRC on the other hand, high FoxP3 expression was associated with an improved prognosis, an inflammatory environment prevailed and overall FoxP3 expression levels were described as significantly higher than in type A. The authors hypothesised that this could also be associated with an increased density of CD8+ cytotoxic T cells. Again, all this applies to our "inflamed" subtype: FoxP3+ T cell densities were significantly

higher than in "immune-desert/type A-like" tumours and they were positively associated with survival. Additionally, highly increased densities of CD8+ cytotoxic T cells indicated a state of intratumoural inflammation. The lack of prognostic relevance of FoxP3+ T cells in the "immune-excluded" phenotype in our study can be explained in several ways. FoxP3+ T cells could be without prognostic relevance since, as stated earlier, lack of T cell migration into the tumour was assumed to be the main immune tolerance promoting factor in this phenotype. Alternatively, "immune-excluded" could also be an intermediate "type A/B" subtype in which neither Fr-II eTregs nor Fr-III non-Treg FoxP3 + cells predominate.

With regard to the prognostic relevance of the three immune phenotypes, the "inflamed/type B-like" group exhibited a significantly improved NED status in contrast to "immune-desert/type A-like", which is again consistent with the results of Saito et al. The fact that this benefit does not translate to overall survival can be attributed to the fact that patients of the former group were considerably older and had a higher proportion of lymph node involvement.

Going forward we are planning to further characterise not only FoxP3+ Treg, but also CD8+ cytotoxic T cells, by evaluating the simultaneous expression of other important immunomodulatory factors in the phenotypes described here. The prognostically favourable "inflamed" phenotype with high Treg density could, for example, very likely contain a high percentage of CCR7+CD8+ T cells, which were described as a positive prognostic factor in CRC by Correale et al., especially in combination with increased Treg infiltration (34, 35).

In summary, our findings suggest that the prognostic relevance of FoxP3+ T cell density in RC depends on immune phenotypes defined by CD8+ cytotoxic T cell infiltration. In the context of our immunohistochemical study we can only speculate what distinguished FoxP3+ T cells in these individual subgroups. However, our findings are consistent with phenomena described by Saito et al. supporting the conclusion that there are suppressive and non-suppressive subpopulations of FoxP3+ T cells in CRC. The fact that it was possible to achieve very similar results with a completely different experimental approach underlines the possible role of two FoxP3+ T cell subtypes. These findings imply that the immunohistochemical detection of CD8+ T cells could serve as an inexpensive and widely available surrogate marker for identifying RC, which are predominated by either suppressive or non-suppressive FoxP3+ T cells. Clinically, this could become relevant for deciding whether a patient would benefit from a strategy of Treg depletion. Furthermore, other types of cancer like HNSCC or breast cancer should also be investigated more closely for functionally heterogenous FoxP3+ T cell subpopulations, as this feature and its prognostic relevance might not be limited to RC.

DATA AVAILABILITY STATEMENT

The raw data supporting the conclusions of this article will be made available by the authors, without undue reservation.

ETHICS STATEMENT

The studies involving human participants were reviewed and approved by Ethics Committee of the Friedrich-Alexander-University of Erlangen-Nuremberg. The patients/participants provided their written informed consent to participate in this study.

AUTHOR CONTRIBUTIONS

Conceptualisation: LD, MB-H, CD, and SS. Resources: RF, AH, MB-H, CD, MH, and LD. Data Collection: SS, JH, and MH. Data Analysis & Interpretation: SS, LD, and JH. Writing - Original Draft: SS and LD. Writing - Review & Editing: LD, MB-H, CD, and SS. Supervision: LD, RF, MB-H, and CD. All authors contributed to the article and approved the submitted version.

ACKNOWLEDGMENTS

We thank the Tumour Centre at the Friedrich-Alexander University Erlangen-Nürnberg, Erlangen, Germany for providing us with patient data.

SUPPLEMENTARY MATERIAL

The Supplementary Material for this article can be found online at: https://www.frontiersin.org/articles/10.3389/fimmu.2022.781222/full#supplementary-material

REFERENCES

1. Huang A, Xiao Y, Peng C, Liu T, Lin Z, Yang Q, et al. 53BP1 Expression and Immunoscore Are Associated With the Efficacy of Neoadjuvant Chemoradiotherapy for Rectal Cancer. *Strahlenther Onkol* (2020) 196 (5):465–73. doi: 10.1007/s00066-019-01559-x
2. Angell HK, Bruni D, Barrett JC, Herbst R, Galon J. The Immunoscore: Colon Cancer and Beyond. *Clin Cancer Res* (2020) 26(2):332–9. doi: 10.1158/1078-0432.CCR-18-1851
3. Galon J, Costes A, Sanchez-Cabo F, Kirilovsky A, Mlecnik B, Lagorce-Pages C, et al. Type, Density, and Location of Immune Cells Within Human Colorectal Tumors Predict Clinical Outcome. *Science* (2006) 313 (5795):1960–4. doi: 10.1126/science.1129139
4. Pages F, Berger A, Camus M, Sanchez-Cabo F, Costes A, Molidor R, et al. Effector Memory T Cells, Early Metastasis, and Survival in Colorectal Cancer. *N Engl J Med* (2005) 353(25):2654–66. doi: 10.1056/NEJMoa051424
5. Roelands J, Kuppen PJK, Vermeulen L, Maccalli C, Decock J, Wang E, et al. Immunogenomic Classification of Colorectal Cancer and Therapeutic Implications. *Int J Mol Sci* (2017) 18:2229. doi: 10.3390/ijms18102229
6. Guinney J, Dienstmann R, Wang X, de Reynies A, Schlicker A, Soneson C, et al. The Consensus Molecular Subtypes of Colorectal Cancer. *Nat Med* (2015) 21(11):1350–6. doi: 10.1038/nm.3967

7. Angelova M, Charoentong P, Hackl H, Fischer ML, Snajder R, Krogsdam AM, et al. Characterization of the Immunophenotypes and Antigenomes of Colorectal Cancers Reveals Distinct Tumor Escape Mechanisms and Novel Targets for Immunotherapy. *Genome Biol* (2015) 16:64. doi: 10.1186/s13059-015-0620-6
8. Salama P, Phillips M, Grieu F, Morris M, Zeps N, Joseph D, et al. Tumor-Infiltrating FOXP3+ T Regulatory Cells Show Strong Prognostic Significance in Colorectal Cancer. *J Clin Oncol* (2009) 27(2):186–92. doi: 10.1200/JCO.2008.18.7229
9. Josefowicz SZ, Lu LF, Rudensky AY. Regulatory T Cells: Mechanisms of Differentiation and Function. *Annu Rev Immunol* (2012) 30:531–64. doi: 10.1146/annurev.immunol.25.022106.141623
10. Savage PA, Malchow S, Leventhal DS. Basic Principles of Tumor-Associated Regulatory T Cell Biology. *Trends Immunol* (2013) 34(1):33–40. doi: 10.1016/j.it.2012.08.005
11. Tanaka A, Sakaguchi S. Regulatory T Cells in Cancer Immunotherapy. *Cell Res* (2017) 27(1):109–18. doi: 10.1038/cr.2016.151
12. Shimizu J, Yamazaki S, Sakaguchi S. Induction of Tumor Immunity by Removing CD25+CD4+ T Cells: A Common Basis Between Tumor Immunity and Autoimmunity. *J Immunol* (1999) 163(10):5211–8.
13. Ladoire S, Martin F, Ghiringhelli F. Prognostic Role of FOXP3+ Regulatory T Cells Infiltrating Human Carcinomas: The Paradox of Colorectal Cancer. *Cancer Immunol Immunother* (2011) 60(7):909–18. doi: 10.1007/s00262-011-1046-y
14. Idos GE, Kwok J, Bonthala N, Kysh L, Gruber SB, Qu C. The Prognostic Implications of Tumor Infiltrating Lymphocytes in Colorectal Cancer: A Systematic Review and Meta-Analysis. *Sci Rep* (2020) 10(1):3360. doi: 10.1038/s41598-020-60255-4
15. Rudolf J, Buttner-Herold M, Erlenbach-Wunsch K, Posselt R, Jessberger J, Haderlein M, et al. Regulatory T Cells and Cytotoxic T Cells Close to the Epithelial-Stromal Interface are Associated With a Favorable Prognosis. *Oncoimmunology* (2020) 9(1):1746149. doi: 10.1080/2162402X.2020.1746149
16. Posselt R, Erlenbach-Wunsch K, Haas M, Jessberger J, Buttner-Herold M, Haderlein M, et al. Spatial Distribution of FoxP3+ and CD8+ Tumour Infiltrating T Cells Reflects Their Functional Activity. *Oncotarget* (2016) 7(37):60383–94. doi: 10.18632/oncotarget.11039
17. Sauer R, Becker H, Hohenberger W, Rodel C, Wittekind C, Fietkau R, et al. Preoperative Versus Postoperative Chemoradiotherapy for Rectal Cancer. *N Engl J Med* (2004) 351(17):1731–40. doi: 10.1056/NEJMoa040694
18. Camp RL, Dolled-Filhart M, Rimm DL. X-Tile: A New Bio-Informatics Tool for Biomarker Assessment and Outcome-Based Cut-Point Optimization. *Clin Cancer Res* (2004) 10(21):7252–9. doi: 10.1158/1078-0432.CCR-04-0713
19. Hori S, Nomura T, Sakaguchi S. Control of Regulatory T Cell Development by the Transcription Factor Foxp3. *Science* (2003) 299(5609):1057–61. doi: 10.1126/science.1079490
20. Zhao Y, Ge X, He J, Cheng Y, Wang Z, Wang J, et al. The Prognostic Value of Tumor-Infiltrating Lymphocytes in Colorectal Cancer Differs by Anatomical Subsite: A Systematic Review and Meta-Analysis. *World J Surg Oncol* (2019) 17(1):85. doi: 10.1186/s12957-019-1621-9
21. Tsuchiya T, Someya M, Takada Y, Hasegawa T, Kitagawa M, Fukushima Y, et al. Association Between Radiotherapy-Induced Alteration of Programmed Death Ligand 1 and Survival in Patients With Uterine Cervical Cancer Undergoing Preoperative Radiotherapy. *Strahlenther Onkol* (2020) 196(8):725–35. doi: 10.1007/s00066-019-01571-1
22. Correale P, Rotundo MS, Del Vecchio MT, Remondo C, Migali C, Ginanneschi C, et al. Regulatory (FoxP3+) T-Cell Tumor Infiltration Is a Favorable Prognostic Factor in Advanced Colon Cancer Patients Undergoing Chemo or Chemoimmunotherapy. *J Immunother* (2010) 33(4):435–41. doi: 10.1097/CJI.0b013e3181d32f01
23. McCoy MJ, Hemmings C, Miller TJ, Austin SJ, Bulsara MK, Zeps N, et al. Low Stromal Foxp3+ Regulatory T-Cell Density Is Associated With Complete Response to Neoadjuvant Chemoradiotherapy in Rectal Cancer. *Br J Cancer* (2015) 113(12):1677–86. doi: 10.1038/bjc.2015.427
24. Ye L, Zhang T, Kang Z, Guo G, Sun Y, Lin K, et al. Tumor-Infiltrating Immune Cells Act as a Marker for Prognosis in Colorectal Cancer. *Front Immunol* (2019) 10:2368. doi: 10.3389/fimmu.2019.02368
25. Xu X, Ma J, Yu G, Qiu Q, Zhang W, Cao F. Effective Predictor of Colorectal Cancer Survival Based on Exclusive Expression Pattern Among Different Immune Cell Infiltration. *J Histochem Cytochem* (2021) 69(4):271–86. doi: 10.1369/0022155421991938
26. Chen DS, Mellman I. Elements of Cancer Immunity and the Cancer-Immune Set Point. *Nature* (2017) 541(7637):321–30. doi: 10.1038/nature21349
27. Echarti A, Hecht M, Buttner-Herold M, Haderlein M, Hartmann A, Fietkau R, et al. CD8+ and Regulatory T Cells Differentiate Tumor Immune Phenotypes and Predict Survival in Locally Advanced Head and Neck Cancer. *Cancers (Basel)* (2019) 11:1398. doi: 10.3390/cancers11091398
28. Liu S, Foulkes WD, Leung S, Gao D, Lau S, Kos Z, et al. Prognostic Significance of FOXP3+ Tumor-Infiltrating Lymphocytes in Breast Cancer Depends on Estrogen Receptor and Human Epidermal Growth Factor Receptor-2 Expression Status and Concurrent Cytotoxic T-Cell Infiltration. *Breast Cancer Res* (2014) 16(5):432. doi: 10.1186/s13058-014-0432-8
29. Liang Y, Lu W, Zhang X, Lu B. Tumor-Infiltrating CD8+ and FOXP3+ Lymphocytes Before and After Neoadjuvant Chemotherapy in Cervical Cancer. *Diagn Pathol* (2018) 13(1):93. doi: 10.1186/s13000-018-0770-4
30. Zhu Y, Li M, Mu D, Kong L, Zhang J, Zhao F, et al. CD8+/FOXP3+ Ratio and PD-L1 Expression Associated With Survival in Pt3n0m0 Stage Esophageal Squamous Cell Cancer. *Oncotarget* (2016) 7(44):71455–65. doi: 10.18632/oncotarget.12213
31. Kinoshita F, Takada K, Yamada Y, Oku Y, Kosai K, Ono Y, et al. Combined Evaluation of Tumor-Infiltrating CD8 + and FoxP3 + Lymphocytes Provides Accurate Prognosis in Stage IA Lung Adenocarcinoma. *Ann Surg Oncol* (2020) 27(6):2102–9. doi: 10.1245/s10434-019-08029-9
32. Miyara M, Yoshioka Y, Kitoh A, Shima T, Wing K, Niwa A, et al. Functional Delineation and Differentiation Dynamics of Human CD4+ T Cells Expressing the FoxP3 Transcription Factor. *Immunity* (2009) 30(6):899–911. doi: 10.1016/j.immuni.2009.03.019
33. Saito T, Nishikawa H, Wada H, Nagano Y, Sugiyama D, Atarashi K, et al. Two FOXP3(+)CD4(+) T Cell Subpopulations Distinctly Control the Prognosis of Colorectal Cancers. *Nat Med* (2016) 22(6):679–84. doi: 10.1038/nm.4086
34. Correale P, Rotundo MS, Botta C, Del Vecchio MT, Ginanneschi C, Licchetta A, et al. Tumor Infiltration by T Lymphocytes Expressing Chemokine Receptor 7 (CCR7) Is Predictive of Favorable Outcome in Patients With Advanced Colorectal Carcinoma. *Clin Cancer Res* (2012) 18(3):850–7. doi: 10.1158/1078-0432.CCR-10-3186
35. Correale P, Rotundo MS, Botta C, Del Vecchio MT, Tassone P, Tagliaferri P. Tumor Infiltration by Chemokine Receptor 7 (CCR7)(+) T-Lymphocytes Is a Favorable Prognostic Factor in Metastatic Colorectal Cancer. *Oncoimmunology* (2012) 1(4):531–2. doi: 10.4161/onci.19404

Conflict of Interest: The authors declare that the research was conducted in the absence of any commercial or financial relationships that could be construed as a potential conflict of interest.

frontiers in Immunology

REVIEW
published: 27 January 2022
doi: 10.3389/fimmu.2022.817942

Roles of the Exosomes Derived From Myeloid-Derived Suppressor Cells in Tumor Immunity and Cancer Progression

Zhuang Chen†, Rui Yuan†, Shengyun Hu, Weitang Yuan and Zhenqiang Sun**

Department of Colorectal Surgery, The First Affiliated Hospital of Zhengzhou University, Zhengzhou, China

Tumor immunity is involved in malignant tumor progression. Myeloid-derived suppressor cells (MDSCs) play an irreplaceable role in tumor immunity. MDSCs are composed of immature myeloid cells and exhibit obvious immunomodulatory functions. Exosomes released by MDSCs (MDSCs-Exos) have similar effects to parental MDSCs in regulating tumor immunity. In this review, we provided a comprehensive description of the characteristics, functions and mechanisms of exosomes. We analyzed the immunosuppressive, angiogenesis and metastatic effects of MDSCs-Exos in different tumors through multiple perspectives. Immunotherapy targeting MDSCs-Exos has demonstrated great potential in cancers and non-cancerous diseases.

Keywords: myeloid-derived suppressor cells, exosome, tumor immunity, cancer, immune escape

OPEN ACCESS

Edited by:
Nicolas Larmonier, Université de Bordeaux, France

Reviewed by:
Serena Meraviglia, University of Palermo, Italy
Tomer Cooks, Ben-Gurion University of the Negev, Israel

****Correspondence:***
Zhenqiang Sun
fccsunzq@zzu.edu.cn
Weitang Yuan
yuanweitang@zzu.edu.cn

†These authors have contributed equally to this work

Specialty section:
This article was submitted to Cancer Immunity and Immunotherapy, a section of the journal Frontiers in Immunology

Received: *18 November 2021*
Accepted: *12 January 2022*
Published: *27 January 2022*

Citation:
Chen Z, Yuan R, Hu S, Yuan W and Sun Z (2022) Roles of the Exosomes Derived From Myeloid-Derived Suppressor Cells in Tumor Immunity and Cancer Progression. Front. Immunol. 13:817942. doi: 10.3389/fimmu.2022.817942

INTRODUCTION

Malignant tumors are considered a major threat to human health (1). Studying the contribution of tumor immunity in tumor progression may improve the extremely narrow therapeutic strategy regarding cancer. Myeloid-derived suppressor cells (MDSCs) are immature cells consisting of myeloid progenitor cells, immature macrophages, immature granulocytes and immature dendritic cells. They are closely related to patients' poor prognosis due to its powerful effects on tumor immune suppression, tumor angiogenesis, drug resistance, and tumor metastases (2–4). For example, The interaction between MDSCs and macrophages can reduce the production of IL-12 by macrophages and increase the production of IL-10 by MDSCs, which promotes tumor progression (5).

Exosomes are 40- to 100-nm small vesicles that are released by the vast majority of cells and distributed in all body fluids (6, 7). Exosomes derived from different cells perform variable

Abbreviations: Bv8, bombina variegata peptide 8; C4B-bp, C4B-binding proteins; CSCs, cancer stem cells; MDSCs, Myeloid-derived suppressor cells; MDSCs-Exos, exosomes released by MDSCs; G-MDSCs, granulocytic MDSCs; M-MDSCs, monocytic MDSCs; mRNAs, messenger RNAs; ncRNAs, noncoding RNAs; MIF, migration inhibition factor; PF-4, platelet factor-4; STAT, signal transducer and activator of transcription; TDEs, tumor-derived exosomes; PGE2, Prostaglandin E2; TGF-β1, transforming growth factor-β1; Th17, helper T cell 17; TME, tumor microenvironment; Tregs, regulatory T cells; NSCLC, in non-small cell lung cancer; G-CSF, granulocyte colony–stimulating factor; VEGF, vascular endothelial growth factor; Tsp1, thrombospondin1.

functions. Exosomes carry proteins, DNA, messenger RNAs (mRNAs), noncoding RNAs(ncRNAs), and lipids (8). Exosomes exert cancer-inhibiting or cancer-promoting effects. For example, exosomal miR-19a is delivered to osteoblasts to promote bone metastasis in breast cancer (9). While human umbilical cord mesenchymal stem cell -derived exosomal miR-320a inhibits lung cancer cell growth *via* SOX4/Wnt/β-catenin axis (10). In addition, emerging studies have shown that exosomes have potential clinical applications as biomarkers for disease diagnosis and prognosis (11–14).

The exosomes derived from MDSCs (MDSCs-Exos) are involved in the function of immunosuppression, promoting tumor angiogenesis, tumor metastasis, drug resistance of malignant tumors (15–17). Here, we summarized linkages and differences between MDSCs-Exos and parental cells, as well as regulatory roles and possible diagnostic and prognostic values in tumor immunity.

MDSCs IN TUMOR IMMUNITY

MDSCs are a special kind of cells that have important tumor immunomodulatory effects, composed of several immature heterogeneous cells originating from myeloid cells (18). Normally, immature myeloid cells differentiate into mature immediately after entering the peripheral organs (19). Under a variety of pathological conditions, MDSCs expand and can be detected in blood, cancer tissue, inflammatory sites, lymph nodes and spleen (20). In the tumor microenvironment (TME), the differentiation and amplification of MDSCs is mediated by a variety of molecules, such as: granulocyte-macrophage colony–stimulating factor, granulocyte colony–stimulating factor (G-CSF), macrophage colony–stimulating factor, stem cell factor, vascular endothelial growth factor (VEGF), and polyunsaturated fatty acids (21–23). Activation of MDSCs is dependent on the following cytokines: IFN-γ, IL-1β, TNF, IL-4, IL-6, IL-13 and high mobility group box protein 1 which function through NF-κB, STAT1 and STAT6 pathways (24). According to different surface markers, MDSCs are divided into two subtypes: granulocytic MDSCs (G-MDSCs, $CD11b^{+}Ly6G^{+}Ly6C^{low}$), termed polymorphonuclear MDSCs (PMN-MDSCs) simultaneously, and monocytic MDSCs (M-MDSCs, $CD11b^{+}Ly6G^{-}Ly6C^{hi}$) (23, 25, 26). The number of G-MDSCs is far outweighed by that of M-MDSCs, and a majority of current studies have focused on investigating the capabilities of G-MDSCs, while the role of M-MDSCs remains to be further investigated (27). Their immunosuppressive abilities and mechanisms also differ (23, 28). G-MDSCs inhibit T-cell responses mainly through the production of reactive oxygen species (ROS) by antigen-specific methods. M-MDSCs produce large amounts of NO, arginase 1 (Arg-1) and immunosuppressive cytokines, such as IL-10, which inhibit both antigen-specific and non-specific T-cell responses. M-MDSCs have a higher inhibitory activity than G-MDSCs (29–33).

MDSCs exert their immunosuppressive effect by promoting the expansion of regulatory T cells (Tregs) (34–36), promoting the production of helper T cell 17 (Th17) (35), inducing macrophage differentiation into the M2 phenotype (2, 37, 38) and inhibiting of immune response of NK cells (39) and B cells (40). In addition to suppressing the immune response, MDSCs also accelerate tumor progression by remodeling tumor microenvironment (22). MDSCs promote tumor angiogenesis through up-regulating VEGF, matrix metallopeptidase 9 (MMP9) and bombina variegata peptide 8 (Bv8) (41). MDSCs also promote tumor metastases by infiltrating primary tumors and facilitating the formation of premetastatic niches (42).

In conclusion, MDSCs exhibit great prospect in the treatment of cancer by blocking T cells, B cells and NK cells activity and bolstering Tregs expansion and mobilization.

EXOSOME

Extracellular vesicles (EVs) were initially considered to be "platelet dust" by Peter Wolf in 1967 (43). EVs transport proteins, nucleic acids, lipids, cytokines, metabolites, and enable intercellular information communication (44). Depending on their origin, markers, properties and functions, EVs are classified into two main groups: ectosomes and exosomes (45). Ectosomes are vesicles formed by outward budding of the plasma membrane, whereas exosomes are intraluminal vesicles formed by plasma membrane invagination, the release of the latter involves the fusion of multivesicular bodies with the plasma membrane (46–48). Recent studies suggest that CD63 is the signature exosome-specific protein, while CD9 and CD81 are not specific (49). Statistically, the cargoes that have been identified in exosomes include 9769 proteins, 3408 mRNAs, 2838 miRNAs and 1116 lipids [data from http://www.exocarta.org (a database collecting many studies)]. These components are involved in cellular signaling pathways, regulation of lipid metabolism, tumor progression, recurrence and metastasis (50–53).

After exosomes are released outside the cell, they participate in information transmission with the target cells through membrane fusion, endocytosis and binding to the receptors on the surface of the target cells (54). Currently, it is becoming increasingly evident that exosomes play an essential role in disease, especially in tumors by promoting the reprogramming of receptor cells (55–57). In non-small cell lung cancer(NSCLC), tumor-derived exosomes(TDEs) polarize macrophages to an immunosuppressive phenotype that increases programmed death ligand-1 expression through NF-kB-dependent, glycolysis-dominated metabolic reprogramming, triggering the formation of pre-metastatic niche (58). Exosomal lncARSR propagates sunitinib resistance through competitive binding of miR-34/miR-449 in renal cell carcinoma (59).

In briefly, exosomes participate in the physiopathological processes of coagulation, inflammation, angiogenesis and immune response (12). Exosomes are widely distributed and easy to modulate, can be used as a promising minimally invasive tool for diagnosis and treatment (7, 60–62).

CHARACTERIZATION OF EXOSOMES DERIVED FROM MDSCs

It is now known that exosomes carry proteins, DNA, messenger RNAs(mRNAs), noncoding RNAs(ncRNAs), and lipids. MDSCs-Exos exert a unique function due to the specificity of the cargoes carried. MDSCs-Exos are also rich in proteins, RNA and DNA. We next discuss the properties of exosomes in five dimensions.

Protein Differences Between MDSCs and Their Exosomes

It is well known that protein is the material basis of life activities (63). The same protein exists in different structures and performs different biological functions due to post-translational modifications (64). Current studies have shown that the cargoes carried by MDSCs-Exos are mainly involved in the immunosuppressive effect of MDSCs (65). S100A8/A9 (calcium binding protein, with chemotactic activity) is present in both MDCSs and MDSC-EXO. Chronic inflammation increased S100A8/A9 content in MDSCs (66), with insignificant changes in exosomes (65). At present, numerous studies on exosomes in tumor-bearing mice are mainly focused on the differences of cargoes (especially ubiquitination protein (67), glycoprotein (68, 69) and RNA (70, 71) carried by exosomes and parental cells.

A study identified 1726 proteins in MDSCs and their exosomes, of which 58% were identified in MDSCs and their exosomes simultaneously. Regardless of inflammation, 30% of the proteins in MDSCs are enriched in their exosomes, especially those involved in exosome formation and protein sorting as well as proteins that load miRNAs into exosomes. Through this selective sorting mechanism, MDSCs-Exos may mediate some functions different from those of MDSCs (15). Similar to other exosomes, MDSCs-Exos enrich many characteristic components, such as tetraspanins (including CD9, CD177), Hsp70, Hsp90α, Hsp90β, Alix, and the ESCRT complex, which are involved in exosome formation and protein sorting. Compared with parental cells, the abundance of CD9 was 89-fold increased regardless of inflammatory status (15, 65). MDSCs-Exos also contain many other protein cargoes, including many nucleic acid binding proteins, numerous histone variants and several elongation factors. It has been reported that these proteins can bind to nucleic acids and induce changes in nucleic acids expression and the protein spectrum of receptor cells (72). Some chemotactic proteins are enriched in MDSCs-Exos, such as the pro-inflammatory proteins S100A8/9, CD47 and thrombospondin-1. These proteins mediate the aggregation of MDSCs and enhance the immunosuppressive function of MDSCs. The relative abundance of the pro-inflammatory proteins S100A8/9, which are secreted by MDSCs and mediate >90% of the chemotactic effect on MDSCs, are not affected by inflammatory conditions. The cytokine macrophage migration inhibition factor and the chemokine platelet factor-4 are also enriched in exosomes, and these proteins exhibit chemotactic activity on leukocytes (15). Regardless of inflammatory conditions, transforming growth factor-β1(TGF-β1) is 4.3-fold more abundant in the exosomes compared with parental cells (15). TGF-β1 participates in the expansion of T cells and the inhibition of NK cells (73, 74). Immunoglobulins, complement regulatory factor H and C4B-binding proteins(C4B-bp) are enriched in exosomes. They may also be involved in the regulation of immune system by MDSCs and their exosomes (15).

The above results indicated that the cancer-promoting effects of MDCSs are partially achieved by exosomes. Targeting MDSCs-Exos holds a bright future for cancer treatment.

Differences Roles of the Exosomes Released by G-MDSCs and M-MDSCs in Tumor

As we mentioned earlier, MDSCs are distinguished into two subtypes. Interestingly, the exosomes derived from different subtypes of MDSCs also differ in their impacts on tumor. Rab27a controls exosomes biogenesis (75). The expression of Rab27a was significantly reduced by transfecting siRNA. In a tumor sphere formation assay, after inhibiting of exosome derived from G-MDSCs, the tumor sphere numbers, CD44+ cell percentages and CD133+ cell percentages were decreased. But the CD44+ cell percentages was not decreased when exosomes were inhibited in M-MDSCs (76). This indicated that G-MDSCs-Exos and M-MDSCs-Exos have different effects on cancer cell stemness.

Currently, researchers have mainly focused on investigating the role of G-MDSCs-Exos on tumor progression, and studies on M-MDSCs-Exos are very rare. Although there is an evidence that M-MDSCs-Exos affects tumor immunity. However, researchers have mainly focused on investigating the role of G-MDSCs-Exos on tumor progression, and studies on M-MDSCs-Exos are very rare. To some extent, an insight into the role of M-MDSCs-Exos may lead to new immunotherapeutic approaches. Distinguishing the role differences between M-MDSCs-Exos and G-MDSCs-Exos may be a new research hotspot.

Differences in Proteins Carried by MDSCs-Exos Under Different Inflammatory Conditions

As inflammation increases, an increasing number of MDSCs were identified, and stronger immunosuppressive effect was observed (77). MDSCs play a key role in the control of experimental necrotizing small intestinal colitis in neonatal mice by suppressing T-cell function (78). Immunosuppressive proteins and miRNAs are increased in EVs during chronic inflammation and aging (79). In one study, the researchers identified 412 proteins, of which the abundance of 63 proteins changed greater than 2-fold in an inflammatory environment. It is worth noting that there was no obvious difference in quantity of exosomes shed per MDSC isolated from low-inflammation or high-inflammation environments. Compared with conventional conditions, inflammatory conditions reduced the abundance of 33 proteins, such as C4B-bp, complement C3 and ficolin-1, which participate in the innate immune response. Several

cytoskeletal proteins and chemotactic proteins are found to be reduced in an inflammatory environment, which are related to the migration of exosomes. In addition, a highly inflammatory environment increased the abundance of 30 proteins, including Leukocyte elastase inhibitor A, DBF4-type zinc finger-containing protein 2 homologue and Cathepsin G, etc (65).

Reducing inflammation may expand new horizons for cancer treatment by weakening MDCSs in TME. In the future, the majority of cancer patients may be able to benefit from this.

Ubiquitin Proteins and Glycoproteins Carried by MDSCs-Exos

Ubiquitin is a common post-translational modification (80), which affects protein function by influencing protein stability, turnover, cellular localization, and regulating cellular signaling cascade responses (81). The imbalance between ubiquitination and deubiquitination is closely related to the occurrence of human immune diseases, cancer, infection and neuropathy (82). In NSCLC, deubiquitination of PDL-1 promotes immune escape by suppressing $CD8^+$T cell responses (83). NLRC3, a member of the innate immune receptor, impaired $CD4^+$ T cell signaling and metabolism by limiting NF-κB activation, reducing glycolysis and oxidative phosphorylation *via* decreased K63-linked ubiquitination of TNF-receptor-associated factor 6 (84). Therefore, it is urgently needed to investigate whether MDCSs and MDSCs-Exos carry ubiquitin protein, which will help to develop new treatment strategies based on exosomes. Protein blot analysis demonstrated that the parental cells and their exosomes contained different ubiquitinated protein profiles (85). Initially, 10 ubiquitinated proteins in MDSCs-Exos were identified (65). With the application of mass spectrometry-based bottom-up proteomics technology, scholars isolated and identified 50 ubiquitinated proteins from MDSCs-Exos (86). Specifically, the ubiquitinated nuclear proteins include several histones, ribosomal proteins and nucleic acid binding proteins. The ubiquitinated histones in these exosomes may possess active pro-inflammatory properties (87, 88). Interestingly, the pro-inflammatory high mobility group box protein 1 is ubiquitinated, promotes the accumulation of MDSCs, and enhances the immunosuppressive effect of MDSCs (89). Sorting nexin 13 has been identified to be involved in endosomal transport of ubiquitinated proteins (90). Two ubiquitinated keratins were revealed to play an active role in plasma membrane invagination during the initial phase of EVs formation (91, 92). Other ubiquitinated proteins leucine zipper EF hand-containing transmembrane protein 1 and endoplasmin, which participate in the formation of endosomes and exosomes (65).

Similarly, glycosylation is an important protein modification that determines protein folding and transport and is crucial for mammalian survival (93, 94). Until 2018, 21 N-glycoproteins on the surface of MDCS-Exos exosomes were identified using proteomic methods, including CD44, CD47, CD321, CD157, CD11b, CD97, thrombospondin1 (Tsp1), fibronectin, cytoskeletal krt, fibrinogen, etc (95). Of special interest is CD47, donor CD47 plays an important role in the control of T cell allogeneic response and tolerance induction after hepatocyte transplantation (96, 97). It mediates the chemotaxis and migration of MDSCs by combining with Tsp1 on MDSCs. When CD47 on tumor cells binds to CD172a (signal regulatory protein α or SIRP α), it can prevent macrophages from phagocytosing tumors (98) and maintain acquired immune tolerance (97). Therefore, CD47 is a potential drug target (99). In addition, it is worth noting that MDSCs-Exos may transport immunosuppressive cargoes to T cells through the binding of CD321 to TLFA-1 of T cells (95).

Both ubiquitinated and glycosylated proteins are present in MDSC and its derived exosomes, respectively, which supports the idea that exosomes have an analog to parental cells.

mRNAs and miRNAs Carried by MDSCs-Exos

In addition to carrying protein cargo, MDSCs-Exos also carry a large number of RNAs, including mRNAs and miRNAs (15), similar to the results of previous studies, almost no ribosomal RNA was found (100–102). The mRNAs carried by exosomes is also transferred to recipient cells and translated into functionally active proteins, which produces more lasting effects than proteins. Compared with parental cells, 45% of mRNA transcripts in exosomes exhibited statistically differences in abundance regardless of the inflammatory conditions. The transcripts of these mRNAs took part in several signaling pathways including "calcium signaling pathway", "cAMP signaling pathway" and "hippo signaling pathway". In addition, only approximately 3.5% of the mRNA transcripts differ in abundance under inflammatory conditions compared with parental cells. These mRNA transcripts played role in the signaling pathway associated with TGF-β and VEGF. Compared with conventional exosomes, several biological processes were identified enriched in inflammatory exosomes, including "cell-cell signaling", "macrophage differentiation" (15).

Simultaneously, the study identified approximately 1500 differentially expressed miRNAs in MDSCs-Exos, and approximately half of them exhibited increased abundance in inflammatory exosomes. According to the prediction of these miRNA targets, if these miRNAs are transferred to the target cells and bind to mRNA targets, they will affect the proliferation, differentiation and apoptosis of target cells. These miRNAs can regulate the immune system and tumor microenvironment and thus affect tumor progression and metastasis.

The miRNAs enriched in inflammatory exosomes include miRNA-704, miRNA-5134, miRNA-7022 and miRNA-7062, which bind to the target mRNA taking part in the apoptosis pathway, including Fas. Compared to parental cells, miRNA-690 and miRNA-155 are enriched in exosomes and may be delivered to MDSCs. MiRNA-690 promotes MDSCs expansion through regulating the cell cycle of myeloid cells. MiRNA-155 increases the production of IL-10. IL-10 induces the proliferation of regulatory T cells and causes the transformation of macrophages to tumor growth-promoting M2-Mϕ. Interestingly, miR-146a negatively regulates the activation of the NF-κB pathway and subsequently controls inflammation by targeting the IL-1

receptor-associated kinase 1 and TNF receptor-associated factor 6 mRNAs (15, 103). In contrast to miRNA-690 and miRNA-155, miR-146a suppresses the development of malignant tumors (15).

We have realized that MDSCs-Exos regulate the signaling pathways and biological processes of target cells through the carried proteins and RNAs. At present, it is necessary to further clarify the type and abundance of cargoes contained in MDSCs and their exosomes, and compare the similarities and differences of cargoes carried by MDSCs and exosomes under different conditions. It is helpful to predict the function of MDSCs-Exos according to the existing research on the composition and function of MDSCs.

EFFECTS OF MDSCs-EXOS ON TUMOR IMMUNITY IN VARIOUS CANCERS

Tumor immunosuppression is a feature of malignant tumors (104). MDSCs-Exos play an irreplaceable role in tumor immunity, similar to parental MDSCs. Here, we summarized the role of MDSCs-Exos in cancer immunity.

Immune Suppression Induced by MDSCs-Exos in Cancers

MDSCs are one of the components of TME and are involved in tumor progression mainly by suppressing the function of T cells (26). MDSCs-Exos, as the immunosuppressive factor in the TME, carry many bioactive substances from MDCSs. In tumor-bearing mice, MDSCs-Exos were significantly higher in tumor tissue than at the spleen and bone marrow. MDSCs-Exos activate CD8+ T cells and drive them to produce more IFN-γ, but MDSCs-Exos increase ROS production, activate the Fas/FasL pathway in T cells, and trigger so-called activation-induced cell death (AICD) (105, 106). In tumor patients, this process is induced by the high expression of S100A8/9 (20). TDEs-provided membrane-associated Hsp72 triggers the activation of TLR2/MyD88-dependent STAT3 pathway in MDSCs through autocrine IL-6, which triggers significant immunosuppressive activity (107). The miRNAs carried by TDEs are also involved in enhancing the expansion and immunosuppression of MDSCs. For example, hypoxia-inducible miRNA-21 in TDEs enhances MDSC expansion and activation by targeting RORα and PTEN (108).

MDSCs-Exos regulate tumor immunity by carrying differential bioactive contents that mainly act on MDSCs and other target cells in the immune system. The pro-inflammatory S100A8/9 heterodimer carried by MDSCs-Exos is chemotactic for MDSCs and plays the primary role in promoting the aggregation of MDSCs to the tumor tissue and pre-metastatic niche (109). Other chemotactic proteins enriched in MDSCs-Exos include CD47 and TSP1, which mediate the immunosuppressive function of MDSCs together with S100A8/9 (65). Similar to MDSCs, MDSCs-Exos can also transform macrophages into tumor growth-promoting M2 macrophages by reducing the production of IL12 from macrophages (65). TGF-β1 enriched in MDSCs-Exos induces Tregs or Th17 cells and impair the cytotoxicity of natural killer (NK) cells, which enhances the immunosuppressive effect of MDSCs-Exos (15).

Contribution of MDSCs-Exos to Tumor Progression and Metastasis

MDSCs and their exosomes participate in the entire process of tumor progression through immunosuppression, angiogenesis, invasion and metastasis, the formation of a premetastatic niche and the stemness of tumor cells. G-MDSCs gathered in lung cancer tissue secreted a large amount of miRNA-143-3p. MiRNA-143-3p promotes tumor cell proliferation by inhibiting integral membrane protein 2B and activating PI3K/Akt pathway (110).

Angiogenesis is fundamental for the growth and metastasis of solid tumors (111). Tumors can induce the upregulation of growth factors, including VEGF, ANG, PDGF, TGF and EGF, which disrupt the balance between proangiogenic and antiangiogenic signals. Growth factors also induce the "angiogenic switch" and subsequently promote the proliferation of vascular endothelial cells and the formation of capillaries (112). In addition, hypoxia in the tumor microenvironment aggravates this process by increasing the expression of proangiogenic factors (113). Several recent studies demonstrated that MDSCs and their exosomes also participate in tumor angiogenesis by recruiting MDSCs to the tumor site with several chemokines. MDSCs can secrete proangiogenic factors, including BV8 (bombina variegata peptide 8), VEGF, and basic fibroblast growth factor, by activating the STAT3 signaling pathway (41). MDSCs can also produce MMP-9, a protease that degrades extracellular matrix, which triggers the release of VEGF deposited in the matrix and increases its bioavailability (114). Moreover, the production of CCL2 in the TME is another important mechanism by which MDSCs promote tumor angiogenesis (115). Notably, splenic MDSCs can differentiate into endothelial progenitor cells that directly participate in tumor angiogenesis (116). It has been reported that miR-126a +MDSCs induced by doxorubicin (DOX) treatment in breast tumor-bearing mice interact with IL-13+Th2 cells in a positive feedback loop manner, increasing the production of Th2 cells and miR-126a+MDSC-Exo. Consequently, the increased level of miR-126a+MDSC-Exo lead to lung metastasis by promoting tumor angiogenesis (17).

One of the negative features of malignant tumors is their unlimited proliferation ability, and cancer stem cells (CSCs) endow them with this ability (117). CSCs have been considered a significant supporter of tumor progression and chemoresistance, and emerging evidence suggests that MDSCs and their exosomes exert crucial influence on the stemness of tumor cells. In patients with ovarian cancer, MDSCs induce ovarian cancer cells to express microRNA101. MicroRNA101 increases the expression of stem cell genes, including OCT3/4, SOX2, and NANOG, *via* inhibiting the expression of C-terminal binding protein-2 in ovarian cancer cells. As a result, MDSCs promote the stemness of ovarian cancer cells (118). In breast cancer patients, MDSCs promote cancer cell stemness by activating the NO/NOTCH and

IL-6/STAT3 signaling pathways (119). New evidence in cervical cancer patients indicates that MDSCs induced by tumor-derived G-CSF enhance the stemness of cancer cells *via* producing Prostaglandin E2(PGE2) (120). MDSCs infiltrate into PTEN null prostate cancer cells and induce the stemness of prostate cancer cells *via* producing IL-1Ra and blocking the IL-1α/IL-1R axis (121). In addition, MDSCs promote the stemness and induce mesenchymal characteristics of pancreatic cancer cells by upregulating the levels of p-STAT3 (122). In A549 transplantation tumors treated with endostatin, MDSCs and MDSC-derived TGF-β1 and hypoxia enhanced the stemness of A549 cells and their resistance to endostatin (123). A new study of colorectal cancer revealed that hypoxia can promote G-MDSCs to generate more MDSCs-Exos by up-regulating HIF-1α. MDSCs-Exos aggravate the stemness of colorectal cancer cells through exosomal S100A9. Blocking S100A9 expression in MDSCs-Exos can inhibit the stemness of colorectal cancer cells and prevent the occurrence of colon cancer in mice with colitis (76) (**Figure 1**).

The Role of MDSCs in Tumor Chemoresistance

Chemotherapy is one of the most important treatments for malignant tumors, but chemoresistance is a crucial obstacle impeding clinical treatment (124). At present, the mechanism underlying chemoresistance has not been well elucidated, but several emerging lines of evidence suggest that MDSCs induce reduced tumor cell sensitivity to chemotherapy. In mice with colorectal cancer, oxaliplatin leads to chemoresistance by restraining the polarization of MDSCs into M1-like macrophages. In addition, MDSCs and their differentiated M2-like macrophages promote immunosuppression, angiogenesis and chemoresistance by producing protumorigenic cytokines (IL-10, TGF-β, VEGF and proteases) and suppressping the function of CD8+ T cells (125).

Tumor-derived G-CSF increases the production of MDSCs and attenuates the spontaneous apoptosis of MDSCs by activating the STAT3 pathway. Then, the increased G-MDSCs induce angiogenesis through Bv8, which leads to chemoresistance in cervical cancer. The study also showed that treating mice with depleting MDSCs enhances the effect of chemotherapy for cervical cancer (126). It has been reported that IL-6 released by drug-resistant hepatocellular cancer promotes the expansion and activity of MDSCs, and the interactions between IL-6 and MDSCs promote the chemoresistance of hepatocellular cancer. The sensitivity to chemotherapy can be enhanced *via* depleting MDSCs or blocking IL-6 (127). Similarly, PMN-MDSCs promote multiple myeloma survival in response to chemotherapies, such as doxorubicin and melphalan, and the process is mediated by soluble factors, including IL-6 (128). Benzyl butyl phthalate exposure aggravates the resistance of breast cancer to doxorubicin. Mechanically, it promotes MDSCs to infiltrate into tumors and increases the secretion of S100A8/A9 by MDSCs (129). A study shows that MDSCs promote Tregs infiltrate into lung tumors and trigger CD8T cells depletion, which strongly induces immunosuppression and chemoresistance (130).

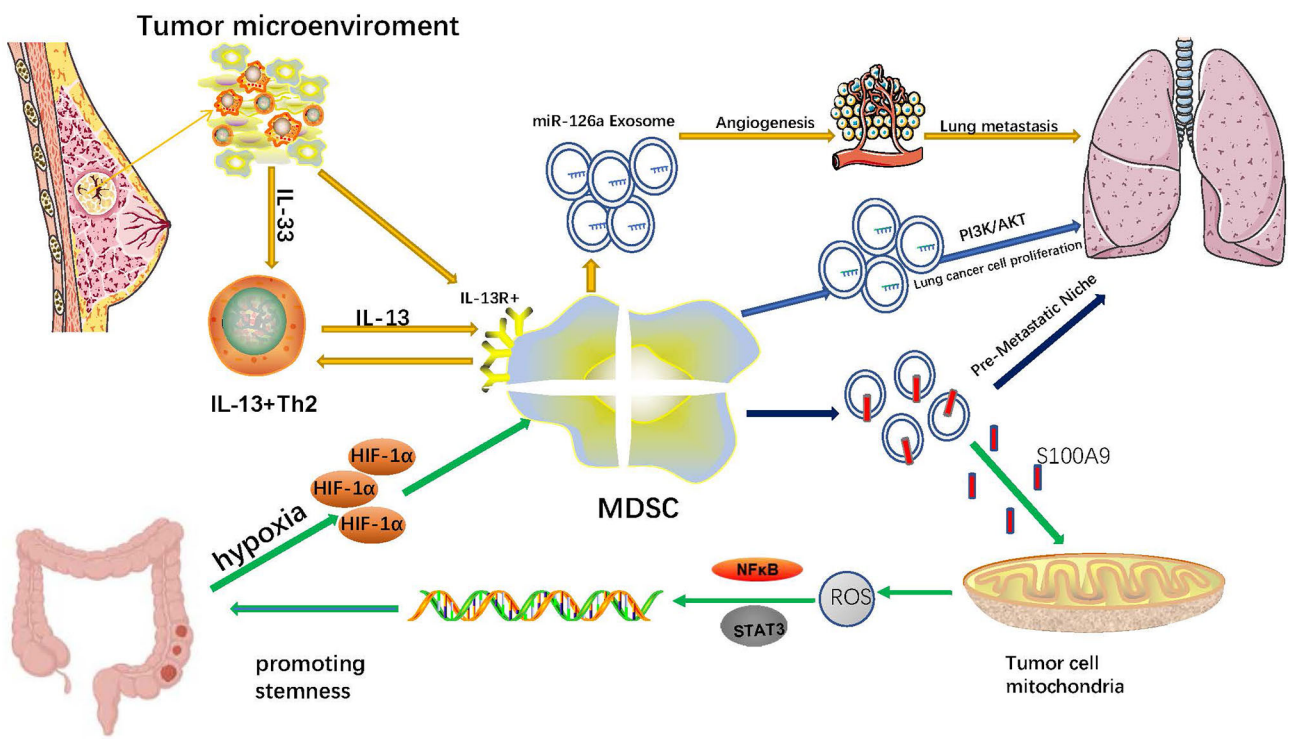

FIGURE 1 | Immunoregulator effects of MDSCs-Exos in cancers.

In numerous studies, MDSCs-Exos exhibit a highly similar role to MDSCs, but whether they play a role in tumor drug resistance has not been explored. In-depth studies on the role of MDSCs-Exos in drug resistance may provide new perspectives for anti-cancer treatment strategies.

EFFECTS OF MDSCs-EXO IN NON-ONCOLOGIC DISEASES

Except in tumors, the massive expansion of MDSCs is always accompanied by non-oncologic diseases, especially in autoimmune diseases. Unlike their role in tumors, MDSCs and MDSCs-Exos can alleviate autoimmune diseases (131). Exosomes derived from MDSCs carry a variety of bioactive contents, including proteins and RNAs, which play a similar role as MDSCs. MDSCs play an irreplaceable role in maternal-fetal tolerance in normal pregnancy. The isolation and identification of exosomes from maternal peripheral blood G-MDSCs revealed that G-MDSCs-Exos inhibited $CD4^+$T cells and $CD8^+$T cells, induced Tregs production, Th2 cell differentiation, and this effect was preserved under frozen conditions (132). (**Figure 2B**). This is very beneficial for application in clinical treatment. G-MDSCs-Exos attenuated the damage of inflammatory cell infiltration and reduced the activity index of DSS-induced colitis in mice, thus significantly alleviating the severity of the disease. This effect was mainly achieved *via* repressing the proliferation of Th1 cells, promoting the expansion of Tregs, and reducing the levels of serum IFN-γ and TNF-α in mice (133) (**Figure 2A**). In the mouse model of autoimmune alopecia areata (AA), MDSCs-Exos reversed the progression of the disease and promoted hair regeneration. MDSCs-Exos accumulated in the draining lymph nodes and cells near residual hair follicles. They are absorbed by T cells, macrophages and NK cells, especially Tregs. As a result, MDSCs-Exos significantly alleviated the disease by amplifying Tregs, weakening the cytotoxic activity of T cells, reducing the proliferation of T helper cells and increasing lymphocyte apoptosis (134) (**Figure 2C**). In mice with collagen-induced arthritis, G-MDSC-derived exosomes attenuated joint destruction efficiently by reducing the number of Th1 and Th17 cells. Mechanistically, miR-29a-3p carried by G-MDSCs-Exos targets T-bet to suppress the differentiation of Th1 cells, and miR-93-5p carried by G-MDSCs-Exos targets STAT3 to suppress the differentiation of Th17 cells (16). There is no such ability in M-MDSCs exosomes. Under hypoxic conditions, the higher levels of miR-29a-3p and miR-93-5p in G-MDSCs-Exos more effectively inhibited the proliferation of $CD4^+$T cells and thus more effectively attenuate arthropathy (135). In addition, PGE2 in MDSCs-Exos upregulated the phosphorylation levels of GSK-3β and CREB to promote IL-10+ Breg cell production to attenuate CIA in mice. This effect was blocked by celecoxib (136). (**Figure 2D**)

Although the understanding of the relationship between MDSCs and autoimmune diseases has become increasingly

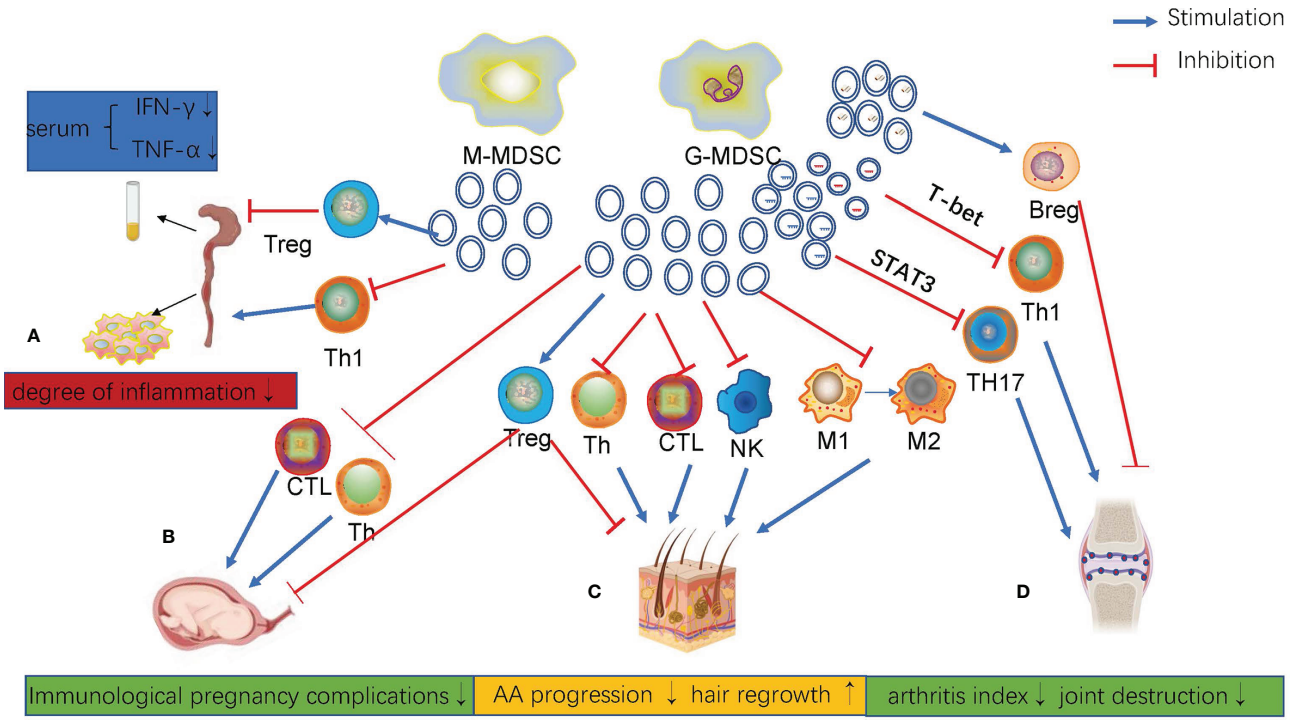

FIGURE 2 | **(A)** In DSS-induced colitis, G-MDSCs-Exos inhibited the proliferation of Th1 cells, promoted the proliferation of Treg cells, and decreased serum IFN-g and TNF-AIN levels in mice. **(B)** Maternal peripheral blood G-MDSCs-Exos regulated different subtypes of T cell differentiation and function. **(C)** MDSCs-Exos inhibited AA progression and promoted hair regrowth. **(D)** G-MDSCs-Exos attenuated CIA in mice by regulating Th1, Th17 and Breg cells.

clear, research on the role of MDSCs-Exos in autoimmune diseases remains limited. Because abundant bioactive molecules overlap in MDSCs and MDSCs-Exos, the function of MDSCs-Exos can be predicted and verified according to known research on MDSCs. Related researches will provide fresh insight into the diagnosis and treatment of autoimmune diseases.

CLINICAL APPLICATIONS OF MDSCs-EXOS

Given the crucial role of MDSC-mediated immunosuppression in tumor progression, several studies have explored a number of therapeutic strategies by targeting MDSCs. These treatments mainly include two aspects. On one hand, the number of MDSCs are reduced by using chemotherapeutic drugs (137), inhibiting the expansion of MDSCs (138) and promoting the differentiation of myeloid cells (139). On the other hand, the functions of MDSCs are suppressed. For example, nitroaspirin is used as an ROS inhibitor (140), and cyclooxygenase 2 inhibitors are used to restrain the production of arginase 1 (141). In addition, phosphodiesterase 5 inhibitors are used to suppress the production of iNOS (142).

In recent years, research on the clinical application of exosomes has become a hot topic. In terms of diagnosis, proteins and ncRNAs expressed in exosomes can be used as markers for early diagnosis, drug sensitivity and prognosis of many cancers (143). In terms of treatment, exosomes are used in tumor immunotherapy and as a new carrier for loading drugs, proteins and ncRNAs (144). When exosomes contact with the extracellular matrix or membrane of the target cells, the exosome contents will be directly transported into the target cells. According to these phenomena, drugs can be loaded into exosomes to target specific areas to treat the disease. At present, there are only a few attempts on the clinical application of MDSCs-Exos. The level of plasma S100A9 expressed in exosomes in patients with colorectal cancer is significantly increased compared with that in normal controls, and the serum level in patients with recurrent tumors is increased compared with that in patients with successful resection of colorectal cancer. Consequently, MDSC-Exo S100A9 can be used as a marker to predict the occurrence and development of colorectal cancer (76). In addition, respiratory hyperoxia inhibits the stemness of colorectal cancer cells by reducing the production of G-MDSCs-Exos, which may be used to assist in the treatment of colorectal cancer. Similarly, breast cancer patients who are resistant to DOX chemotherapy exhibit high levels of circulating miR-126a+ MDSCs-Exos in their serum. Therefore, miR-126a+MDSC-Exo can be used as a potential biomarker of chemotherapy resistance to DOX in breast cancer and to guide the use of DOX in the treatment of breast cancer patients. Moreover, the systematic application of miR-126a inhibitor can improve the chemotherapeutic efficiency of DOX against lung metastasis by inhibiting tumor angiogenesis, which provides a basis for targeting MDSCs-Exos (17).

Non-steroidal anti-inflammatory drugs, glucocorticoids, and immunosuppressants have always been the main treatments of autoimmune diseases, and now MDSCs-Exos may be used as a new treatment strategy. Exosomes derived from G-MDSCs relieved collagen-induced arthritis by inhibiting the proliferation of Th1 and Th17 cells (16) and inducing $IL10^{+}$Breg cells (136). Furthermore, high expression of miR-29a-3p and miR-93-5p induced by hypoxia in exosomes improved the condition (135). In addition, the application of G-MDSC-derived exosomes attenuated DSS-induced colitis by decreasing the percentages of Th1 cells and promoting the expansion of Tregs (133). MDSCs-Exos were also used in the treatment of autoimmune alopecia areata, which reversed the progression of the disease and promoted hair regeneration (134). Relay transfer of MDSCs protected pregnant mice from miscarriage, and exosomes exhibited similar effects, making MDSCs-Exos a possible target for the treatment of immune pregnancy complications. However, its safety as well as reliability still need to be further explored in depth (132).

There are still many blank areas in related research, and it is a demanding task to gain insight. However, future research on the characteristics, mechanism and clinical application of MDSCs-Exos will offer promising information.

CONCLUSION

In summary, MDSCs-Exos play multiple roles in the tumor immunity. MDSCs-Exos exhibit tumor immunosuppressive, angiogenic and metastatic effects similar to parental cells due to similar substances to parental cells. However, research on functions, mechanisms, and contribution rates of MDSCs-Exos in tumor immunity is limited. Thus, the scientific questions that require urgent exploration include: 1. What other specific substances in MDSCs-Exos are highly effective in affecting tumor immunity? 2. Whether these substances regulate each other and subsequently affect tumor immunity? 3. How to apply MDSCs-Exos to advanced cancer patients as soon as possible?4. How to ensure the safety of MDSCs-Exos in clinical applications?

To conclude, MDSCs-Exos play an essential role in the tumor immunity. Further investigation of MDSCs-Exos in tumor immunity will be beneficial for overcoming tumor progression, recurrence, metastasis and drug resistance, providing potential biomarkers and targets for immunotherapy of cancers. Therefore, people no longer turn pale at the mention of a "cancer" in the future.

AUTHOR CONTRIBUTIONS

ZS and WY provided direction and guidance throughout the preparation of this manuscript. ZC and RY wrote and edited the manuscript. SH reviewed and made significant revisions to the manuscript. All authors read and approved the final manuscript.

FUNDING

This study was supported by The National Natural Science Foundation of China (82173055, 81972663, U2004112), Key Scientific Research Projects of Institutions of Higher Education in Henan Province (19A310024) and The National Natural Science Foundation of Henan Province (212300410074).

REFERENCES

1. Fan CM, Wang JP, Tang YY, Zhao J, He SY, Xiong F, et al. Circman1a2 Could Serve as a Novel Serum Biomarker for Malignant Tumors. *Cancer Sci* (2019) 110(7):2180–8. doi: 10.1111/cas.14034
2. Gabrilovich DI, Nagaraj S. Myeloid-Derived Suppressor Cells as Regulators of the Immune System. *Nat Rev Immunol* (2009) 9(3):162–74. doi: 10.1038/nri2506
3. Zhao Y, Shao Q, Zhu H, Xu H, Long W, Yu B, et al. Resveratrol Ameliorates Lewis Lung Carcinoma-Bearing Mice Development, Decreases Granulocytic Myeloid-Derived Suppressor Cell Accumulation and Impairs Its Suppressive Ability. *Cancer Sci* (2018) 109(9):2677–86. doi: 10.1111/cas.13720
4. Safarzadeh E, Hashemzadeh S, Duijf PHG, Mansoori B, Khaze V, Mohammadi A, et al. Circulating Myeloid-Derived Suppressor Cells: An Independent Prognostic Factor in Patients With Breast Cancer. *J Cell Physiol* (2019) 234(4):3515–25. doi: 10.1002/jcp.26896
5. Tan Z, Liu L, Chiu MS, Cheung KW, Yan CW, Yu Z, et al. Virotherapy-Recruited PMN-MDSC Infiltration of Mesothelioma Blocks Antitumor CTL by IL-10-Mediated Dendritic Cell Suppression. *Oncoimmunology* (2019) 8 (1):e1518672. doi: 10.1080/2162402X.2018.1518672
6. Vlassov AV, Magdaleno S, Setterquist R, Conrad R. Exosomes: Current Knowledge of Their Composition, Biological Functions, and Diagnostic and Therapeutic Potentials. *Biochim Biophys Acta* (2012) 1820(7):940–8. doi: 10.1016/j.bbagen.2012.03.017
7. Boukouris S, Mathivanan S. Exosomes in Bodily Fluids Are a Highly Stable Resource of Disease Biomarkers. *Proteomics Clin Appl* (2015) 9(3-4):358–67. doi: 10.1002/prca.201400114
8. Morini M, Cangelosi D, Segalerba D, Marimpietri D, Raggi F, Castellano A, et al. Exosomal microRNAs From Longitudinal Liquid Biopsies for the Prediction of Response to Induction Chemotherapy in High-Risk Neuroblastoma Patients: A Proof of Concept SIOPEN Study. *Cancers (Basel)* (2019) 11(10):1476. doi: 10.3390/cancers11101476
9. Wu K, Feng J, Lyu F, Xing F, Sharma S, Liu Y, et al. Exosomal miR-19a and IBSP Cooperate to Induce Osteolytic Bone Metastasis of Estrogen Receptor-Positive Breast Cancer. *Nat Commun* (2021) 12(1):5196. doi: 10.1038/s41467-021-25473-y
10. Xie H, Wang J. MicroRNA-320a-Containing Exosomes From Human Umbilical Cord Mesenchymal Stem Cells Curtail Proliferation and Metastasis in Lung Cancer by Binding to SOX4. *J Recept Signal Transduct Res* (2021), 1–11. doi: 10.1080/10799893.2021.1918166
11. Kourembanas S. Exosomes: Vehicles of Intercellular Signaling, Biomarkers, and Vectors of Cell Therapy. *Annu Rev Physiol* (2015) 77:13–27. doi: 10.1146/annurev-physiol-021014-071641
12. Lin J, Li J, Huang B, Liu J, Chen X, Chen XM, et al. Exosomes: Novel Biomarkers for Clinical Diagnosis. *Sci World J* (2015) 2015:657086. doi: 10.1155/2015/657086
13. Wang J, Yan F, Zhao Q, Zhan F, Wang R, Wang L, et al. Circulating Exosomal miR-125a-3p as a Novel Biomarker for Early-Stage Colon Cancer. *Sci Rep* (2017) 7(1):4150. doi: 10.1038/s41598-017-04386-1
14. Zhao R, Zhang Y, Zhang X, Yang Y, Zheng X, Li X, et al. Exosomal Long Noncoding RNA HOTTIP as Potential Novel Diagnostic and Prognostic Biomarker Test for Gastric Cancer. *Mol Cancer* (2018) 17(1):68. doi: 10.1186/s12943-018-0817-x
15. Geis-Asteggiante L, Belew AT, Clements VK, Edwards NJ, Ostrand-Rosenberg S, El-Sayed NM, et al. Differential Content of Proteins, mRNAs, and miRNAs Suggests That MDSC and Their Exosomes May Mediate Distinct Immune Suppressive Functions. *J Proteome Res* (2018) 17 (1):486–98. doi: 10.1021/acs.jproteome.7b00646
16. Zhu D, Tian J, Wu X, Li M, Tang X, Rui K, et al. G-MDSC-Derived Exosomes Attenuate Collagen-Induced Arthritis by Impairing Th1 and Th17 Cell Responses. *Biochim Biophys Acta Mol Basis Dis* (2019) 1865 (12):165540. doi: 10.1016/j.bbadis.2019.165540
17. Deng Z, Rong Y, Teng Y, Zhuang X, Samykutty A, Mu J, et al. Exosomes miR-126a Released From MDSC Induced by DOX Treatment Promotes Lung Metastasis. *Oncogene* (2017) 36(5):639–51. doi: 10.1038/onc.2016.229
18. Solito S, Falisi E, Diaz-Montero CM, Doni A, Pinton L, Rosato A, et al. A Human Promyelocytic-Like Population Is Responsible for the Immune Suppression Mediated by Myeloid-Derived Suppressor Cells. *Blood* (2011) 118(8):2254–65. doi: 10.1182/blood-2010-12-325753
19. Trac NT, Chung EJ. Peptide-Based Targeting of Immunosuppressive Cells in Cancer. *Bioact Mater* (2020) 5(1):92–101. doi: 10.1016/j.bioactmat.2020.01.006
20. Condamine T, Gabrilovich DI. Molecular Mechanisms Regulating Myeloid-Derived Suppressor Cell Differentiation and Function. *Trends Immunol* (2011) 32(1):19–25. doi: 10.1016/j.it.2010.10.002
21. Zhao Y, Wu T, Shao S, Shi B, Zhao Y. Phenotype, Development, and Biological Function of Myeloid-Derived Suppressor Cells. *Oncoimmunology* (2016) 5(2):e1004983. doi: 10.1080/2162402X.2015.1004983
22. Veglia F, Perego M, Gabrilovich D. Myeloid-Derived Suppressor Cells Coming of Age. *Nat Immunol* (2018) 19(2):108–19. doi: 10.1038/s41590-017-0022-x
23. Bronte V, Brandau S, Chen SH, Colombo MP, Frey AB, Greten TF, et al. Recommendations for Myeloid-Derived Suppressor Cell Nomenclature and Characterization Standards. *Nat Commun* (2016) 7:12150. doi: 10.1038/ncomms12150
24. Jin S, Yang Z, Hao X, Tang W, Ma W, Zong H. Roles of HMGB1 in Regulating Myeloid-Derived Suppressor Cells in the Tumor Microenvironment. *biomark Res* (2020) 8:21. doi: 10.1186/s40364-020-00201-8
25. Zhang Y, Xu J, Zhang N, Chen M, Wang H, Zhu D. Targeting the Tumour Immune Microenvironment for Cancer Therapy in Human Gastrointestinal Malignancies. *Cancer Lett* (2019) 458:123–35. doi: 10.1016/j.canlet.2019.05.017
26. Yang Z, Guo J, Weng L, Tang W, Jin S, Ma W. Myeloid-Derived Suppressor Cells-New and Exciting Players in Lung Cancer. *J Hematol Oncol* (2020) 13 (1):10. doi: 10.1186/s13045-020-0843-1
27. Kostlin N, Kugel H, Spring B, Leiber A, Marme A, Henes M, et al. Granulocytic Myeloid Derived Suppressor Cells Expand in Human Pregnancy and Modulate T-Cell Responses. *Eur J Immunol* (2014) 44 (9):2582–91. doi: 10.1002/eji.201344200
28. Damuzzo V, Pinton L, Desantis G, Solito S, Marigo I, Bronte V, et al. Complexity and Challenges in Defining Myeloid-Derived Suppressor Cells. *Cytometry B Clin Cytom* (2015) 88(2):77–91. doi: 10.1002/cyto.b.21206
29. Youn JI, Nagaraj S, Collazo M, Gabrilovich DI. Subsets of Myeloid-Derived Suppressor Cells in Tumor-Bearing Mice. *J Immunol* (2008) 181(8):5791–802. doi: 10.4049/jimmunol.181.8.5791
30. Movahedi K, Guilliams M, Van den Bossche J, Van den Bergh R, Gysemans C, Beschin A, et al. Identification of Discrete Tumor-Induced Myeloid-Derived Suppressor Cell Subpopulations With Distinct T Cell-Suppressive Activity. *Blood* (2008) 111(8):4233–44. doi: 10.1182/blood-2007-07-099226
31. Safarzadeh E, Orangi M, Mohammadi H, Babaie F, Baradaran B. Myeloid-Derived Suppressor Cells: Important Contributors to Tumor Progression and Metastasis. *J Cell Physiol* (2018) 233(4):3024–36. doi: 10.1002/jcp.26075
32. Kumar V, Patel S, Tcyganov E, Gabrilovich DI. The Nature of Myeloid-Derived Suppressor Cells in the Tumor Microenvironment. *Trends Immunol* (2016) 37(3):208–20. doi: 10.1016/j.it.2016.01.004
33. Tian X, Ma J, Wang T, Tian J, Zhang Y, Mao L, et al. Long Non-Coding RNA HOXA Transcript Antisense RNA Myeloid-Specific 1-HOXA1 Axis Downregulates the Immunosuppressive Activity of Myeloid-Derived Suppressor Cells in Lung Cancer. *Front Immunol* (2018) 9:473. doi: 10.3389/fimmu.2018.00473
34. Shu CC, Pan SW, Feng JY, Wang JY, Chan YJ, Yu CJ, et al. The Clinical Significance of Programmed Death-1, Regulatory T Cells and Myeloid Derived Suppressor Cells in Patients With Nontuberculous Mycobacteria-Lung Disease. *J Clin Med* (2019) 8(5):736. doi: 10.3390/jcm8050736
35. Ji J, Xu J, Zhao S, Liu F, Qi J, Song Y, et al. Myeloid-Derived Suppressor Cells Contribute to Systemic Lupus Erythaematosus by Regulating Differentiation of Th17 Cells and Tregs. *Clin Sci (Lond)* (2016) 130(16):1453–67. doi: 10.1042/CS20160311
36. Park MJ, Lee SH, Kim EK, Lee EJ, Baek JA, Park SH, et al. Interleukin-10 Produced by Myeloid-Derived Suppressor Cells Is Critical for the Induction of Tregs and Attenuation of Rheumatoid Inflammation in Mice. *Sci Rep* (2018) 8(1):3753. doi: 10.1038/s41598-018-21856-2

37. Han X, Shi H, Sun Y, Shang C, Luan T, Wang D, et al. CXCR2 Expression on Granulocyte and Macrophage Progenitors Under Tumor Conditions Contributes to Mo-MDSC Generation *via* SAP18/ERK/Stat3. *Cell Death Dis* (2019) 10(8):598. doi: 10.1038/s41419-019-1837-1
38. Kumar V, Cheng P, Condamine T, Mony S, Languino LR, McCaffrey JC, et al. CD45 Phosphatase Inhibits STAT3 Transcription Factor Activity in Myeloid Cells and Promotes Tumor-Associated Macrophage Differentiation. *Immunity* (2016) 44(2):303–15. doi: 10.1016/j.immuni.2016.01.014
39. Bruno A, Mortara L, Baci D, Noonan DM, Albini A. Myeloid Derived Suppressor Cells Interactions With Natural Killer Cells and Pro-Angiogenic Activities: Roles in Tumor Progression. *Front Immunol* (2019) 10:771. doi: 10.3389/fimmu.2019.00771
40. Wang Y, Schafer CC, Hough KP, Tousif S, Duncan SR, Kearney JF, et al. Myeloid-Derived Suppressor Cells Impair B Cell Responses in Lung Cancer Through IL-7 and STAT5. *J Immunol* (2018) 201(1):278–95. doi: 10.4049/jimmunol.1701069
41. Qu X, Zhuang G, Yu L, Meng G, Ferrara N. Induction of Bv8 Expression by Granulocyte Colony-Stimulating Factor in CD11b+Gr1+ Cells: Key Role of Stat3 Signaling. *J Biol Chem* (2012) 287(23):19574–84. doi: 10.1074/jbc.M111.326801
42. Hanahan D, Coussens LM. Accessories to the Crime: Functions of Cells Recruited to the Tumor Microenvironment. *Cancer Cell* (2012) 21(3):309–22. doi: 10.1016/j.ccr.2012.02.022
43. Wolf P. The Nature and Significance of Platelet Products in Human Plasma. *Br J Haematol* (1967) 13(3):269–88. doi: 10.1111/j.1365-2141.1967.tb08741.x
44. S ELA, Mager I, Breakefield XO, Wood MJ. Extracellular Vesicles: Biology and Emerging Therapeutic Opportunities. *Nat Rev Drug Discov* (2013) 12(5):347–57. doi: 10.1038/nrd3978
45. Weng Z, Zhang B, Wu C, Yu F, Han B, Li B, et al. Therapeutic Roles of Mesenchymal Stem Cell-Derived Extracellular Vesicles in Cancer. *J Hematol Oncol* (2021) 14(1):136. doi: 10.1186/s13045-021-01141-y
46. Akers JC, Gonda D, Kim R, Carter BS, Chen CC. Biogenesis of Extracellular Vesicles (EV): Exosomes, Microvesicles, Retrovirus-Like Vesicles, and Apoptotic Bodies. *J Neurooncol* (2013) 113(1):1–11. doi: 10.1007/s11060-013-1084-8
47. Colombo M, Raposo G, Thery C. Biogenesis, Secretion, and Intercellular Interactions of Exosomes and Other Extracellular Vesicles. *Annu Rev Cell Dev Biol* (2014) 30:255–89. doi: 10.1146/annurev-cellbio-101512-122326
48. van Niel G, D'Angelo G, Raposo G. Shedding Light on the Cell Biology of Extracellular Vesicles. *Nat Rev Mol Cell Biol* (2018) 19(4):213–28. doi: 10.1038/nrm.2017.125
49. Mathieu M, Nevo N, Jouve M, Valenzuela JI, Maurin M, Verweij FJ, et al. Specificities of Exosome Versus Small Ectosome Secretion Revealed by Live Intracellular Tracking of CD63 and CD9. *Nat Commun* (2021) 12(1):4389. doi: 10.1038/s41467-021-24384-2
50. Choi DS, Yang JS, Choi EJ, Jang SC, Park S, Kim OY, et al. The Protein Interaction Network of Extracellular Vesicles Derived From Human Colorectal Cancer Cells. *J Proteome Res* (2012) 11(2):1144–51. doi: 10.1021/pr200842h
51. Rana S, Yue S, Stadel D, Zoller M. Toward Tailored Exosomes: The Exosomal Tetraspanin Web Contributes to Target Cell Selection. *Int J Biochem Cell Biol* (2012) 44(9):1574–84. doi: 10.1016/j.biocel.2012.06.018
52. Skotland T, Sandvig K, Llorente A. Lipids in Exosomes: Current Knowledge and the Way Forward. *Prog Lipid Res* (2017) 66:30–41. doi: 10.1016/j.plipres.2017.03.001
53. Sato-Kuwabara Y, Melo SA, Soares FA, Calin GA. The Fusion of Two Worlds: Non-Coding RNAs and Extracellular Vesicles–Diagnostic and Therapeutic Implications (Review). *Int J Oncol* (2015) 46(1):17–27. doi: 10.3892/ijo.2014.2712
54. Tian T, Zhu YL, Hu FH, Wang YY, Huang NP, Xiao ZD. Dynamics of Exosome Internalization and Trafficking. *J Cell Physiol* (2013) 228(7):1487–95. doi: 10.1002/jcp.24304
55. Lo Cicero A, Stahl PD, Raposo G. Extracellular Vesicles Shuffling Intercellular Messages: For Good or for Bad. *Curr Opin Cell Biol* (2015) 35:69–77. doi: 10.1016/j.ceb.2015.04.013
56. Abd Elmageed ZY, Yang Y, Thomas R, Ranjan M, Mondal D, Moroz K, et al. Neoplastic Reprogramming of Patient-Derived Adipose Stem Cells by Prostate Cancer Cell-Associated Exosomes. *Stem Cells* (2014) 32(4):983–97. doi: 10.1002/stem.1619
57. Subramanian A, Gupta V, Sarkar S, Maity G, Banerjee S, Ghosh A, et al. Exosomes in Carcinogenesis: Molecular Palkis Carry Signals for the Regulation of Cancer Progression and Metastasis. *J Cell Commun Signal* (2016) 10(3):241–9. doi: 10.1007/s12079-016-0338-6
58. Morrissey SM, Zhang F, Ding C, Montoya-Durango DE, Hu X, Yang C, et al. Tumor-Derived Exosomes Drive Immunosuppressive Macrophages in a Pre-Metastatic Niche Through Glycolytic Dominant Metabolic Reprogramming. *Cell Metab* (2021) 33(10):2040–58.e10. doi: 10.1016/j.cmet.2021.09.002
59. Qu L, Ding J, Chen C, Wu ZJ, Liu B, Gao Y, et al. Exosome-Transmitted lncARSR Promotes Sunitinib Resistance in Renal Cancer by Acting as a Competing Endogenous RNA. *Cancer Cell* (2016) 29(5):653–68. doi: 10.1016/j.ccell.2016.03.004
60. Jia S, Zocco D, Samuels ML, Chou MF, Chammas R, Skog J, et al. Emerging Technologies in Extracellular Vesicle-Based Molecular Diagnostics. *Expert Rev Mol Diagn* (2014) 14(3):307–21. doi: 10.1586/14737159.2014.893828
61. Johnsen KB, Gudbergsson JM, Skov MN, Pilgaard L, Moos T, Duroux M. A Comprehensive Overview of Exosomes as Drug Delivery Vehicles - Endogenous Nanocarriers for Targeted Cancer Therapy. *Biochim Biophys Acta* (2014) 1846(1):75–87. doi: 10.1016/j.bbcan.2014.04.005
62. Kotmakci M, Bozok Cetintas V. Extracellular Vesicles as Natural Nanosized Delivery Systems for Small-Molecule Drugs and Genetic Material: Steps Towards the Future Nanomedicines. *J Pharm Pharm Sci* (2015) 18(3):396–413. doi: 10.18433/j36w3x
63. Jin S, Zeng X, Xia F, Huang W, Liu X. Application of Deep Learning Methods in Biological Networks. *Brief Bioinform* (2021) 22(2):1902–17. doi: 10.1093/bib/bbaa043
64. Liu Y, Cheng A, Wang M, Mao S, Ou X, Yang Q, et al. Duck Hepatitis A Virus Type 1 Induces Eif2alpha Phosphorylation-Dependent Cellular Translation Shutoff *via* PERK/Gcn2. *Front Microbiol* (2021) 12:624540. doi: 10.3389/fmicb.2021.624540
65. Burke M, Choksawangkarn W, Edwards N, Ostrand-Rosenberg S, Fenselau C. Exosomes From Myeloid-Derived Suppressor Cells Carry Biologically Active Proteins. *J Proteome Res* (2014) 13(2):836–43. doi: 10.1021/pr400879c
66. Choksawangkarn W, Graham LM, Burke M, Lee SB, Ostrand-Rosenberg S, Fenselau C, et al. Peptide-Based Systems Analysis of Inflammation Induced Myeloid-Derived Suppressor Cells Reveals Diverse Signaling Pathways. *Proteomics* (2016) 16(13):1881–8. doi: 10.1002/pmic.201500102
67. Lee HD, Kim YH, Kim DS. Exosomes Derived From Human Macrophages Suppress Endothelial Cell Migration by Controlling Integrin Trafficking. *Eur J Immunol* (2014) 44(4):1156–69. doi: 10.1002/eji.201343660
68. Batista BS, Eng WS, Pilobello KT, Hendricks-Munoz KD, Mahal LK. Identification of a Conserved Glycan Signature for Microvesicles. *J Proteome Res* (2011) 10(10):4624–33. doi: 10.1021/pr200434y
69. Shimoda A, Tahara Y, Sawada SI, Sasaki Y, Akiyoshi K. Glycan Profiling Analysis Using Evanescent-Field Fluorescence-Assisted Lectin Array: Importance of Sugar Recognition for Cellular Uptake of Exosomes From Mesenchymal Stem Cells. *Biochem Biophys Res Commun* (2017) 491(3):701–7. doi: 10.1016/j.bbrc.2017.07.126
70. Hegde VL, Tomar S, Jackson A, Rao R, Yang X, Singh UP, et al. Distinct microRNA Expression Profile and Targeted Biological Pathways in Functional Myeloid-Derived Suppressor Cells Induced by Delta9-Tetrahydrocannabinol *In Vivo*: Regulation of CCAAT/enhancer-Binding Protein Alpha by microRNA-690. *J Biol Chem* (2013) 288(52):36810–26. doi: 10.1074/jbc.M113.503037
71. Chen S, Zhang Y, Kuzel TM, Zhang B. Regulating Tumor Myeloid-Derived Suppressor Cells by MicroRNAs. *Cancer Cell Microenviron* (2015) 2(1):e637. doi: 10.14800/ccm.637
72. Geis-Asteggiante L, Dhabaria A, Edwards N, Ostrand-Rosenberg S, Fenselau C. Top-Down Analysis of Low Mass Proteins in Exosomes Shed by Murine

Myeloid-Derived Suppressor Cells. *Int J Mass Spectrom* (2015) 378:264–9. doi: 10.1016/j.ijms.2014.08.035
73. Parker KH, Beury DW, Ostrand-Rosenberg S. Myeloid-Derived Suppressor Cells: Critical Cells Driving Immune Suppression in the Tumor Microenvironment. *Adv Cancer Res* (2015) 128:95–139. doi: 10.1016/bs.acr.2015.04.002
74. Li H, Han Y, Guo Q, Zhang M, Cao X. Cancer-Expanded Myeloid-Derived Suppressor Cells Induce Anergy of NK Cells Through Membrane-Bound TGF-Beta 1. *J Immunol* (2009) 182(1):240–9. doi: 10.4049/jimmunol.182.1.240
75. Ramadass M, Johnson JL, Catz SD. Rab27a Regulates GM-CSF-Dependent Priming of Neutrophil Exocytosis. *J Leukoc Biol* (2017) 101(3):693–702. doi: 10.1189/jlb.3AB0416-189RR
76. Wang Y, Yin K, Tian J, Xia X, Ma J, Tang X, et al. Granulocytic Myeloid-Derived Suppressor Cells Promote the Stemness of Colorectal Cancer Cells Through Exosomal S100a9. *Adv Sci (Weinh)* (2019) 6(18):1901278. doi: 10.1002/advs.201901278
77. Zhou L, Miao K, Yin B, Li H, Fan J, Zhu Y, et al. Cardioprotective Role of Myeloid-Derived Suppressor Cells in Heart Failure. *Circulation* (2018) 138(2):181–97. doi: 10.1161/CIRCULATIONAHA.117.030811
78. He YM, Li X, Perego M, Nefedova Y, Kossenkov AV, Jensen EA, et al. Transitory Presence of Myeloid-Derived Suppressor Cells in Neonates Is Critical for Control of Inflammation. *Nat Med* (2018) 24(2):224–31. doi: 10.1038/nm.4467
79. Salminen A, Kaarniranta K, Kauppinen A. Exosomal Vesicles Enhance Immunosuppression in Chronic Inflammation: Impact in Cellular Senescence and the Aging Process. *Cell Signal* (2020) 75:109771. doi: 10.1016/j.cellsig.2020.109771
80. Sun T, Liu Z, Yang Q. The Role of Ubiquitination and Deubiquitination in Cancer Metabolism. *Mol Cancer* (2020) 19(1):146. doi: 10.1186/s12943-020-01262-x
81. Zhang Y, Chen C, Yu T, Chen T. Proteomic Analysis of Protein Ubiquitination Events in Human Primary and Metastatic Colon Adenocarcinoma Tissues. *Front Oncol* (2020) 10:1684. doi: 10.3389/fonc.2020.01684
82. Popovic D, Vucic D, Dikic I. Ubiquitination in Disease Pathogenesis and Treatment. *Nat Med* (2014) 20(11):1242–53. doi: 10.1038/nm.3739
83. Liu Z, Wang T, She Y, Wu K, Gu S, Li L, et al. N(6)-Methyladenosine-Modified Circigf2bp3 Inhibits CD8(+) T-Cell Responses to Facilitate Tumor Immune Evasion by Promoting the Deubiquitination of PD-L1 in Non-Small Cell Lung Cancer. *Mol Cancer* (2021) 20(1):105. doi: 10.1186/s12943-021-01398-4
84. Uchimura T, Oyama Y, Deng M, Guo H, Wilson JE, Rampanelli E, et al. The Innate Immune Sensor NLRC3 Acts as a Rheostat That Fine-Tunes T Cell Responses in Infection and Autoimmunity. *Immunity* (2018) 49(6):1049–1061 e6. doi: 10.1016/j.immuni.2018.10.008
85. Buschow SI, Liefhebber JM, Wubbolts R, Stoorvogel W. Exosomes Contain Ubiquitinated Proteins. *Blood Cells Mol Dis* (2005) 35(3):398–403. doi: 10.1016/j.bcmd.2005.08.005
86. Burke MC, Oei MS, Edwards NJ, Ostrand-Rosenberg S, Fenselau C. Ubiquitinated Proteins in Exosomes Secreted by Myeloid-Derived Suppressor Cells. *J Proteome Res* (2014) 13(12):5965–72. doi: 10.1021/pr500854x
87. Vidal M, Mangeat P, Hoekstra D. Aggregation Reroutes Molecules From a Recycling to a Vesicle-Mediated Secretion Pathway During Reticulocyte Maturation. *J Cell Sci* (1997) 110(Pt 16):1867–77. doi: 10.1242/jcs.110.16.1867
88. Janig E, Stumptner C, Fuchsbichler A, Denk H, Zatloukal K. Interaction of Stress Proteins With Misfolded Keratins. *Eur J Cell Biol* (2005) 84(2-3):329–39. doi: 10.1016/j.ejcb.2004.12.018
89. Parker KH, Sinha P, Horn LA, Clements VK, Yang H, Li J, et al. HMGB1 Enhances Immune Suppression by Facilitating the Differentiation and Suppressive Activity of Myeloid-Derived Suppressor Cells. *Cancer Res* (2014) 74(20):5723–33. doi: 10.1158/0008-5472.CAN-13-2347
90. Gilthorpe JD, Oozeer F, Nash J, Calvo M, Bennett DL, Lumsden A, et al. Extracellular Histone H1 Is Neurotoxic and Drives a Pro-Inflammatory Response in Microglia. *F1000Res* (2013) 2:148. doi: 10.12688/f1000research.2-148.v1
91. Wen Z, Liu Y, Li F, Ren F, Chen D, Li X, et al. Circulating Histones Exacerbate Inflammation in Mice With Acute Liver Failure. *J Cell Biochem* (2013) 114(10):2384–91. doi: 10.1002/jcb.24588
92. Allam R, Kumar SV, Darisipudi MN, Anders HJ. Extracellular Histones in Tissue Injury and Inflammation. *J Mol Med (Berl)* (2014) 92(5):465–72. doi: 10.1007/s00109-014-1148-z
93. Gandini R, Reichenbach T, Tan TC, Divne C. Structural Basis for Dolichylphosphate Mannose Biosynthesis. *Nat Commun* (2017) 8(1):120. doi: 10.1038/s41467-017-00187-2
94. Xiao H, Suttapitugsakul S, Sun F, Wu R. Mass Spectrometry-Based Chemical and Enzymatic Methods for Global Analysis of Protein Glycosylation. *Acc Chem Res* (2018) 51(8):1796–806. doi: 10.1021/acs.accounts.8b00200
95. Chauhan S, Danielson S, Clements V, Edwards N, Ostrand-Rosenberg S, Fenselau C. Surface Glycoproteins of Exosomes Shed by Myeloid-Derived Suppressor Cells Contribute to Function. *J Proteome Res* (2017) 16(1):238–46. doi: 10.1021/acs.jproteome.6b00811
96. Zhang M, Wang H, Tan S, Navarro-Alvarez N, Zheng Y, Yang YG. Donor CD47 Controls T Cell Alloresponses and Is Required for Tolerance Induction Following Hepatocyte Allotransplantation. *Sci Rep* (2016) 6:26839. doi: 10.1038/srep26839
97. Pengam S, Durand J, Usal C, Gauttier V, Dilek N, Martinet B, et al. SIRPalpha/CD47 Axis Controls the Maintenance of Transplant Tolerance Sustained by Myeloid-Derived Suppressor Cells. *Am J Transplant* (2019) 19(12):3263–75. doi: 10.1111/ajt.15497
98. Lv Z, Bian Z, Shi L, Niu S, Ha B, Tremblay A, et al. Loss of Cell Surface CD47 Clustering Formation and Binding Avidity to SIRPalpha Facilitate Apoptotic Cell Clearance by Macrophages. *J Immunol* (2015) 195(2):661–71. doi: 10.4049/jimmunol.1401719
99. Tseng D, Volkmer JP, Willingham SB, Contreras-Trujillo H, Fathman JW, Fernhoff NB, et al. Anti-CD47 Antibody-Mediated Phagocytosis of Cancer by Macrophages Primes an Effective Antitumor T-Cell Response. *Proc Natl Acad Sci USA* (2013) 110(27):11103–8. doi: 10.1073/pnas.1305569110
100. Ekstrom K, Valadi H, Sjostrand M, Malmhall C, Bossios A, Eldh M, et al. Characterization of mRNA and microRNA in Human Mast Cell-Derived Exosomes and Their Transfer to Other Mast Cells and Blood CD34 Progenitor Cells. *J Extracell Vesicles* (2012) 1. doi: 10.3402/jev.v1i0.18389
101. Ji H, Chen M, Greening DW, He W, Rai A, Zhang W, et al. Deep Sequencing of RNA From Three Different Extracellular Vesicle (EV) Subtypes Released From the Human LIM1863 Colon Cancer Cell Line Uncovers Distinct miRNA-Enrichment Signatures. *PloS One* (2014) 9(10):e110314. doi: 10.1371/journal.pone.0110314
102. Xiao D, Ohlendorf J, Chen Y, Taylor DD, Rai SN, Waigel S, et al. Identifying mRNA, microRNA and Protein Profiles of Melanoma Exosomes. *PloS One* (2012) 7(10):e46874. doi: 10.1371/journal.pone.0046874
103. Taganov KD, Boldin MP, Chang KJ, Baltimore D. NF-kappaB-Dependent Induction of microRNA miR-146, an Inhibitor Targeted to Signaling Proteins of Innate Immune Responses. *Proc Natl Acad Sci USA* (2006) 103(33):12481–6. doi: 10.1073/pnas.0605298103
104. Feng J, Byrne NM, Al Jamal W, Coulter JA. Exploiting Current Understanding of Hypoxia Mediated Tumour Progression for Nanotherapeutic Development. *Cancers (Basel)* (2019) 11(12):1989. doi: 10.3390/cancers11121989
105. Hildeman DA, Mitchell T, Kappler J, Marrack P. T Cell Apoptosis and Reactive Oxygen Species. *J Clin Invest* (2003) 111(5):575–81. doi: 10.1172/JCI18007
106. Rashid MH, Borin TF, Ara R, Piranlioglu R, Achyut BR, Korkaya H, et al. Critical Immunosuppressive Effect of MDSCderived Exosomes in the Tumor Microenvironment. *Oncol Rep* (2021) 45(3):1171–81. doi: 10.3892/or.2021.7936
107. Chalmin F, Ladoire S, Mignot G, Vincent J, Bruchard M, Remy-Martin JP, et al. Membrane-Associated Hsp72 From Tumor-Derived Exosomes Mediates STAT3-Dependent Immunosuppressive Function of Mouse and Human Myeloid-Derived Suppressor Cells. *J Clin Invest* (2010) 120(2):457–71. doi: 10.1172/jci40483
108. Guo X, Qiu W, Liu Q, Qian M, Wang S, Zhang Z, et al. Immunosuppressive Effects of Hypoxia-Induced Glioma Exosomes Through Myeloid-Derived Suppressor Cells *via* the miR-10a/Rora and miR-21/Pten Pathways. *Oncogene* (2018) 37(31):4239–59. doi: 10.1038/s41388-018-0261-9

109. Eisenblaetter M, Flores-Borja F, Lee JJ, Wefers C, Smith H, Hueting R, et al. Visualization of Tumor-Immune Interaction - Target-Specific Imaging of S100A8/A9 Reveals Pre-Metastatic Niche Establishment. *Theranostics* (2017) 7(9):2392–401. doi: 10.7150/thno.17138
110. Zhou JH, Yao ZX, Zheng Z, Yang J, Wang R, Fu SJ, et al. G-MDSCs-Derived Exosomal miRNA-143-3p Promotes Proliferation *via* Targeting of ITM2B in Lung Cancer. *Onco Targets Ther* (2020) 13:9701–19. doi: 10.2147/ott.s256378
111. Li X, Li Y, Lu W, Chen M, Ye W, Zhang D. The Tumor Vessel Targeting Strategy: A Double-Edged Sword in Tumor Metastasis. *Cells* (2019) 8 (12):1602. doi: 10.3390/cells8121602
112. Qiang W, Zhou T, Lan X, Zhang X, Guo Y, Noman M, et al. A New Nanoscale Transdermal Drug Delivery System: Oil Body-Linked oleosin-hEGF Improves Skin Regeneration to Accelerate Wound Healing. *J Nanobiotechnol* (2018) 16(1):62. doi: 10.1186/s12951-018-0387-5
113. Condamine T, Ramachandran I, Youn JI, Gabrilovich DI. Regulation of Tumor Metastasis by Myeloid-Derived Suppressor Cells. *Annu Rev Med* (2015) 66:97–110. doi: 10.1146/annurev-med-051013-052304
114. Motallebnezhad M, Jadidi-Niaragh F, Qamsari ES, Bagheri S, Gharibi T, Yousefi M. The Immunobiology of Myeloid-Derived Suppressor Cells in Cancer. *Tumour Biol* (2016) 37(2):1387–406. doi: 10.1007/s13277-015-4477-9
115. Boelte KC, Gordy LE, Joyce S, Thompson MA, Yang L, Lin PC. Rgs2 Mediates Pro-Angiogenic Function of Myeloid Derived Suppressor Cells in the Tumor Microenvironment *via* Upregulation of MCP-1. *PloS One* (2011) 6(4):e18534. doi: 10.1371/journal.pone.0018534
116. Yang L, DeBusk LM, Fukuda K, Fingleton B, Green-Jarvis B, Shyr Y, et al. Expansion of Myeloid Immune Suppressor Gr+CD11b+ Cells in Tumor-Bearing Host Directly Promotes Tumor Angiogenesis. *Cancer Cell* (2004) 6 (4):409–21. doi: 10.1016/j.ccr.2004.08.031
117. Zhang Z, Zhang C, Miao J, Wang Z, Wang Z, Cheng Z, et al. A Tumor-Targeted Replicating Oncolytic Adenovirus Ad-TD-Nsil12 as a Promising Therapeutic Agent for Human Esophageal Squamous Cell Carcinoma. *Cells* (2020) 9(11):2438. doi: 10.3390/cells9112438
118. Cui TX, Kryczek I, Zhao L, Zhao E, Kuick R, Roh MH, et al. Myeloid-Derived Suppressor Cells Enhance Stemness of Cancer Cells by Inducing Microrna101 and Suppressing the Corepressor Ctbp2. *Immunity* (2013) 39 (3):611–21. doi: 10.1016/j.immuni.2013.08.025
119. Peng D, Tanikawa T, Li W, Zhao L, Vatan L, Szeliga W, et al. Myeloid-Derived Suppressor Cells Endow Stem-Like Qualities to Breast Cancer Cells Through IL6/STAT3 and NO/NOTCH Cross-Talk Signaling. *Cancer Res* (2016) 76(11):3156–65. doi: 10.1158/0008-5472.CAN-15-2528
120. Kuroda H, Mabuchi S, Yokoi E, Komura N, Kozasa K, Matsumoto Y, et al. Prostaglandin E2 Produced by Myeloid-Derived Suppressive Cells Induces Cancer Stem Cells in Uterine Cervical Cancer. *Oncotarget* (2018) 9 (91):36317–30. doi: 10.18632/oncotarget.26347
121. Di Mitri D, Toso A, Chen JJ, Sarti M, Pinton S, Jost TR, et al. Tumour-Infiltrating Gr-1+ Myeloid Cells Antagonize Senescence in Cancer. *Nature* (2014) 515(7525):134–7. doi: 10.1038/nature13638
122. Panni RZ, Sanford DE, Belt BA, Mitchem JB, Worley LA, Goetz BD, et al. Tumor-Induced STAT3 Activation in Monocytic Myeloid-Derived Suppressor Cells Enhances Stemness and Mesenchymal Properties in Human Pancreatic Cancer. *Cancer Immunol Immunother* (2014) 63 (5):513–28. doi: 10.1007/s00262-014-1527-x
123. Wang Y, Jiang M, Li Z, Wang J, Du C, Yanyang L, et al. Hypoxia and TGF-Beta1 Lead to Endostatin Resistance by Cooperatively Increasing Cancer Stem Cells in A549 Transplantation Tumors. *Cell Biosci* (2015) 5:72. doi: 10.1186/s13578-015-0064-4
124. Shen Q, Xu Z, Xu S. Long Noncoding RNA LUCAT1 Contributes to Cisplatin Resistance by Regulating the Mir514a3p/ULK1 Axis in Human Nonsmall Cell Lung Cancer. *Int J Oncol* (2020) 57(4):967–79. doi: 10.3892/ijo.2020.5106
125. Liu Z, Xie Y, Xiong Y, Liu S, Qiu C, Zhu Z, et al. TLR 7/8 Agonist Reverses Oxaliplatin Resistance in Colorectal Cancer *via* Directing the Myeloid-Derived Suppressor Cells to Tumoricidal M1-Macrophages. *Cancer Lett* (2020) 469:173–85. doi: 10.1016/j.canlet.2019.10.020
126. Kawano M, Mabuchi S, Matsumoto Y, Sasano T, Takahashi R, Kuroda H, et al. The Significance of G-CSF Expression and Myeloid-Derived Suppressor Cells in the Chemoresistance of Uterine Cervical Cancer. *Sci Rep* (2015) 5:18217. doi: 10.1038/srep18217
127. Xu M, Zhao Z, Song J, Lan X, Lu S, Chen M, et al. Interactions Between Interleukin-6 and Myeloid-Derived Suppressor Cells Drive the Chemoresistant Phenotype of Hepatocellular Cancer. *Exp Cell Res* (2017) 351(2):142–9. doi: 10.1016/j.yexcr.2017.01.008
128. Ramachandran IR, Condamine T, Lin C, Herlihy SE, Garfall A, Vogl DT, et al. Bone Marrow PMN-MDSCs and Neutrophils Are Functionally Similar in Protection of Multiple Myeloma From Chemotherapy. *Cancer Lett* (2016) 371(1):117–24. doi: 10.1016/j.canlet.2015.10.040
129. Hsu YL, Hung JY, Tsai EM, Wu CY, Ho YW, Jian SF, et al. Benzyl Butyl Phthalate Increases the Chemoresistance to Doxorubicin/Cyclophosphamide by Increasing Breast Cancer-Associated Dendritic Cell-Derived CXCL1/GROalpha and S100A8/A9. *Oncol Rep* (2015) 34(6):2889–900. doi: 10.3892/or.2015.4307
130. Anestakis D, Petanidis S, Domvri K, Tsavlis D, Zarogoulidis P, Katopodi T. Carboplatin Chemoresistance Is Associated With CD11b(+)/Ly6C(+) Myeloid Release and Upregulation of TIGIT and LAG3/CD160 Exhausted T Cells. *Mol Immunol* (2020) 118:99–109. doi: 10.1016/j.molimm.2019.11.008
131. Cripps JG, Gorham JD. MDSC in Autoimmunity. *Int Immunopharmacol* (2011) 11(7):789–93. doi: 10.1016/j.intimp.2011.01.026
132. Dietz S, Schwarz J, Ruhle J, Schaller M, Fehrenbacher B, Marme A, et al. Extracellular Vesicles Released by Myeloid-Derived Suppressor Cells From Pregnant Women Modulate Adaptive Immune Responses. *Cell Immunol* (2021) 361:104276. doi: 10.1016/j.cellimm.2020.104276
133. Wang S, Tang X. Exosomes Released by Granulocytic Myeloid-Derived Suppressor Cells Attenuate DSS-Induced Colitis in Mice. *Oncotarget* (2015) 7(13):15356–68. doi: 10.18632/oncotarget.7324
134. Zoller M, Zhao K, Kutlu N, Bauer N, Provaznik J, Hackert T, et al. Immunoregulatory Effects of Myeloid-Derived Suppressor Cell Exosomes in Mouse Model of Autoimmune Alopecia Areata. *Front Immunol* (2018) 9:1279. doi: 10.3389/fimmu.2018.01279
135. Chu X, Chen L, Zhang Y. Exosomes Derived From PMN-MDSCs Preconditioned by Hypoxia Attenuate Arthropathy of Collagen-Induced Arthritis Mice. *Xi Bao Yu Fen Zi Mian Yi Xue Za Zhi* (2021) 37(8):728–35.
136. Wu X, Zhu D, Tian J, Tang X, Guo H, Ma J, et al. Granulocytic Myeloid-Derived Suppressor Cell Exosomal Prostaglandin E2 Ameliorates Collagen-Induced Arthritis by Enhancing IL-10(+) B Cells. *Front Immunol* (2020) 11:588500:588500. doi: 10.3389/fimmu.2020.588500
137. Suzuki E, Kapoor V, Jassar AS, Kaiser LR, Albelda SM. Gemcitabine Selectively Eliminates Splenic Gr-1+/CD11b+ Myeloid Suppressor Cells in Tumor-Bearing Animals and Enhances Antitumor Immune Activity. *Clin Cancer Res* (2005) 11(18):6713–21. doi: 10.1158/1078-0432.ccr-05-0883
138. Melani C, Sangaletti S, Barazzetta FM, Werb Z, Colombo MP. Amino-Biphosphonate-Mediated MMP-9 Inhibition Breaks the Tumor-Bone Marrow Axis Responsible for Myeloid-Derived Suppressor Cell Expansion and Macrophage Infiltration in Tumor Stroma. *Cancer Res* (2007) 67 (23):11438–46. doi: 10.1158/0008-5472.can-07-1882
139. Hengesbach LM, Hoag KA. Physiological Concentrations of Retinoic Acid Favor Myeloid Dendritic Cell Development Over Granulocyte Development in Cultures of Bone Marrow Cells From Mice. *J Nutr* (2004) 134(10):2653–9. doi: 10.1093/jn/134.10.2653
140. De Santo C, Serafini P, Marigo I, Dolcetti L, Bolla M, Del Soldato P, et al. Nitroaspirin Corrects Immune Dysfunction in Tumor-Bearing Hosts and Promotes Tumor Eradication by Cancer Vaccination. *Proc Natl Acad Sci USA* (2005) 102(11):4185–90. doi: 10.1073/pnas.0409783102
141. Talmadge JE, Hood KC, Zobel LC, Shafer LR, Coles M, Toth B. Chemoprevention by Cyclooxygenase-2 Inhibition Reduces Immature Myeloid Suppressor Cell Expansion. *Int Immunopharmacol* (2007) 7 (2):140–51. doi: 10.1016/j.intimp.2006.09.021
142. Serafini P, Meckel K, Kelso M, Noonan K, Califano J, Koch W, et al. Phosphodiesterase-5 Inhibition Augments Endogenous Antitumor Immunity by Reducing Myeloid-Derived Suppressor Cell Function. *J Exp Med* (2006) 203(12):2691–702. doi: 10.1084/jem.20061104
143. Li M, Xia B, Wang Y, You MJ, Zhang Y. Potential Therapeutic Roles of Exosomes in Multiple Myeloma: A Systematic Review. *J Cancer* (2019) 10 (24):6154–60. doi: 10.7150/jca.31752

144. Yong T, Zhang X, Bie N, Zhang H, Zhang X, Li F, et al. Tumor Exosome-Based Nanoparticles Are Efficient Drug Carriers for Chemotherapy. *Nat Commun* (2019) 10(1):3838. doi: 10.1038/s41467-019-11718-4

Conflict of Interest: The authors declare that the research was conducted in the absence of any commercial or financial relationships that could be construed as a potential conflict of interest.

Publisher's Note: All claims expressed in this article are solely those of the authors and do not necessarily represent those of their affiliated organizations, or those of the publisher, the editors and the reviewers. Any product that may be evaluated in this article, or claim that may be made by its manufacturer, is not guaranteed or endorsed by the publisher.

frontiers in Immunology

REVIEW
published: 03 March 2022
doi: 10.3389/fimmu.2022.838040

Beyond Immunosuppression: The Multifaceted Functions of Tumor-Promoting Myeloid Cells in Breast Cancers

Céline Blaye[1,2], *Thomas Boyer*[1], *Florent Peyraud*[1], *Charlotte Domblides*[1,3] *and Nicolas Larmonier*[1,4]*

[1] Centre National de la Recherche Scientific (CNRS) Unité Mixte de Recherche (UMR) 5164, ImmunoConcEpT, Bordeaux, France, [2] Department of Medical Oncology, Institut Bergonié, Bordeaux, France, [3] Service d'Oncologie Médicale, Centre Hospitalo-Universitaire (CHU) Bordeaux, Bordeaux, France, [4] Department of Biological and Medical Sciences, University of Bordeaux, Bordeaux, France

OPEN ACCESS

Edited by:
Giovanna Schiavoni,
National Institute of Health (ISS), Italy

Reviewed by:
Keehoon Jung,
Seoul National University, South Korea
Linda Schuler,
University of Wisconsin-Madison, United States

***Correspondence:**
Nicolas Larmonier
nicolas.larmonier@u-bordeaux.fr

Specialty section:
This article was submitted to Cancer Immunity and Immunotherapy, a section of the journal Frontiers in Immunology

Received: 17 December 2021
Accepted: 02 February 2022
Published: 03 March 2022

Citation:
Blaye C, Boyer T, Peyraud F, Domblides C and Larmonier N (2022) Beyond Immunosuppression: The Multifaceted Functions of Tumor-Promoting Myeloid Cells in Breast Cancers. Front. Immunol. 13:838040. doi: 10.3389/fimmu.2022.838040

Breast cancers are commonly associated with an immunosuppressive microenvironment responsible for tumor escape from anti-cancer immunity. Cells of the myeloid lineage account for a major part of this tumor-promoting landscape. These myeloid cells are composed of heterogeneous subsets at different stages of differentiation and have traditionally been described by their cardinal ability to suppress innate and adaptive anticancer immunity. However, evidence has accumulated that, beyond their immunosuppressive properties, breast cancer-induced myeloid cells are also equipped with a broad array of "non-immunological" tumor-promoting functions. They therefore represent major impediments for anticancer therapies, particularly for immune-based interventions. We herein analyze and discuss current literature related to the versatile properties of the different myeloid cell subsets engaged in breast cancer development. We critically assess persisting difficulties and challenges in unequivocally discriminate dedicated subsets, which has so far prevented both the selective targeting of these immunosuppressive cells and their use as potential biomarkers. In this context, we propose the concept of IMCGL, "pro-tumoral immunosuppressive myeloid cells of the granulocytic lineage", to more accurately reflect the contentious nature and origin of granulocytic cells in the breast tumor microenvironment. Future research prospects related to the role of this myeloid landscape in breast cancer are further considered.

Keywords: breast cancer, tumor-promoting myeloid cells, immunosuppression, immunotherapies, tumor microenvironment

HIGHLIGHTS

Beyond their cardinal immunosuppressive properties, many subsets of myeloid cells are equipped with multiple tumor-promoting functions impacting most steps of cancer development.

INTRODUCTION

Centered for years on the intrinsic characteristics of tumor cells, the field of cancer research has evolved toward the notion that cancers emerge and develop in a dedicated tumor-promoting environment. The cross-talks between malignant cells and components of this tumor-specific landscape dictate the fate of cancer (persistence or elimination) and further shape the nature of this microenvironment (1, 2). In this context, the influence of the immune system on cancer development has been widely evidenced, and many strategies have been developed to induce, restore and enhance anti-cancer immunity. Successes of these immune-based approaches in inducing efficient anti-tumor responses and improving cancer patient survival have brought some of them to the forefront of cancer therapeutics in recent years (3). However, it has also become clear that cancers can escape from immune detection and destruction by many mechanisms resulting in the establishment of an immunosuppressive tumor environment, which represents a major obstacle for efficient immunotherapies. Compelling evidences have indicated that inhibition of these immunosuppressive networks is an important prerequisite to uncover the full potential of immune-based interventions. It is noteworthy that, although several immunotherapies provide clinical benefits in melanoma, lung, bladder and colon cancers, breast cancer patients have yet to fully experience these breakthroughs. Indeed, except for triple-negative cancers which are more immunogenic and have obtained FDA approval of immunotherapies in the neo-adjuvant (4) and metastatic (5) settings, most immune-based therapeutic attempts in breast cancers have ended in failure.

For many years, the environment of breast tumors has been described as "immunologically cold", as defined by the sparsity or absence of tumor-infiltrating lymphocytes (TILs) (6). This description is somewhat inaccurate insofar as it usually does not take into account cells of myeloid origin, despite their many diverse roles in the environment of mammary cancers. The lack of anti-tumoral immune response in breast cancers has indeed been associated with a hostile immuno-inhibitory microenvironment, the major components of which being cells of myeloid origin (7). Tumor-associated macrophages (TAMs), tumor-associated neutrophils (TANs), tolerogenic dendritic cells (tDC) and immature subsets of myeloid cells endowed with immunosuppressive properties termed "myeloid-derived suppressor cells" (MDSCs) have been identified as such myeloid subpopulations, present not only within the tumor environment, but also at the sites of priming of antitumoral immune responses (secondary lymphoid organs), in the bloodstream and in the pre-metastatic and metastatic sites.

Besides their ability to impair anti-tumor immunity at different steps of immune responses (initiation, priming, effector stages), these myeloid cells are also endowed with a large array of "non-immunologic" tumor-promoting functions. They can indeed contribute to the epithelial-to-mesenchymal transition (EMT), participate to local tissue invasion at the primary tumor site, foster blood or lymphatic vessel intravasation and extravasation of migrating cancer cells, associate with circulating tumor cells protecting them in the bloodstream, and prepare the pre-metastatic niches thus enhancing metastatic processes. Furthermore, these myeloid cells can also directly promote primary tumor cell survival and proliferation and foster tumor neoangiogenesis and cancer cell stemness (**Figure 1**). The role of breast cancer-induced myeloid cells in resistance to chemotherapy as well as endocrine therapy has also been described, making them potential targets for the development of new immunotherapies.

Recently, major advances in the characterization of the phenotypes, functions and origins of myeloid cell subpopulations in breast cancers have been made, particularly by single cell RNA sequencing approaches. In this review, we discuss the equivocal identify of some subsets, particularly "polymorphonuclear-MDSCs" ("PMN-MDSCs") and "immunosuppressive neutrophils", and examine and discuss the polyvalent tumor-promoting functions of these myeloid cells in the breast cancer environment in light of recent literature, with a specific emphasis on the "non-immunologic" pro-tumoral properties of these multitasking cells.

MACROPHAGES IN BREAST CANCERS: A MULTIFUNCTIONAL IMPACT ON TUMOR PROMOTION

Macrophage Phenotype and Function in the Context of Breast Cancer

Macrophages have been one of the most widely studied population of myeloid cells in cancer, specifically in the context of breast malignancies. In breast cancer patients, tumor-associated macrophages (TAM) have been associated with aggressive features (size ≥ 2 cm, higher tumor grade, higher Ki67) and estrogen receptor (ER) negative breast cancers (8). However, the prognostic value of these cells remains controversial and depends on the cancer subtype, the macrophage subset (M1 *vs* M2, see below) and their localization (9). Indeed, some authors have described an improved survival of ER^- or triple-negative breast cancer (TNBC) patients with a $CD163^+CD68^+$ macrophage infiltrate (10), while others correlated the presence of tumor-infiltrating $CD163^+$ macrophages with a worse prognosis of TNBC patients (11). In a gene-expression based study using a CIBERSORT deconvolution method, macrophages have been associated with a significant poorer outcome in both ER^+ and ER^- BC patients, and were predictive of a worse response to chemotherapy in ER^- patients (12). Independently of BC subtype, immune population clustering identified 2 clusters enriched in pro-tumorigenic macrophages, which have been associated with significantly worse outcome in BC patients (12).

The polyvalent functions and the high degree of plasticity of macrophages are partly responsible for these conflicting results. Macrophages have originally been broadly discriminated in two

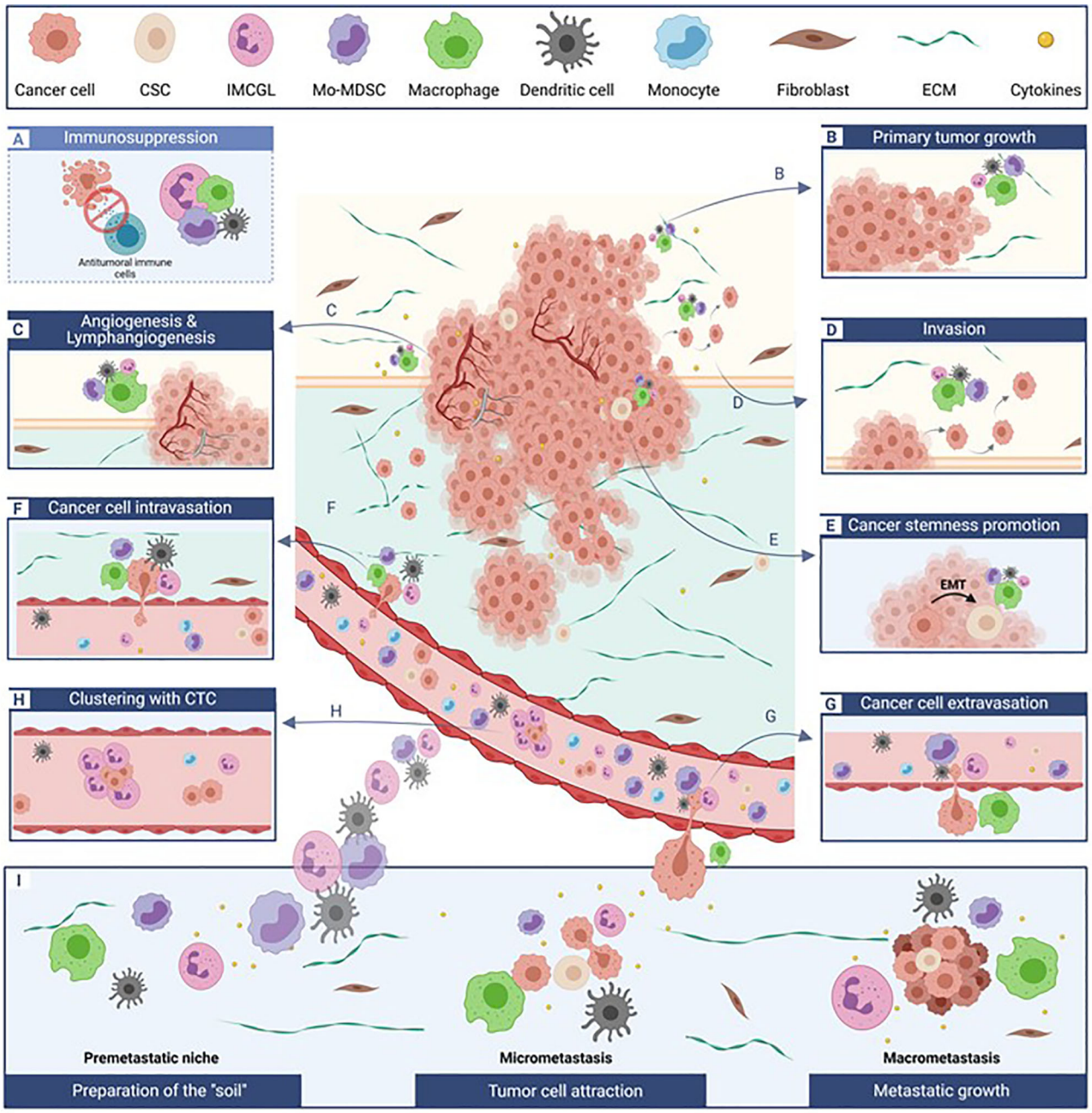

FIGURE 1 | Tumor-promoting myeloid cells critically affect multiple and distinct steps of cancer development. Besides impairing anti-tumor immunity. **(A)**, dedicated subpopulations of myeloid cells differentially impact primary tumor survival and growth **(B)**, tumor vascularization **(C)**, local tissue invasion **(D)** cancer stemness **(E)**, tumor cell intra- **(F)** and extravasation **(G)** in and from blood vessels, associate with circulation tumor as beneficial clusters **(H)**, and participate to metastatic site preparation and development **(I)**. The relative contribution of each myeloid cell subset to a specific process (each illustrated in a separate box) is depicted by the differential size of the cells. CSC, cancer stem cells; CTC, circulating tumor cells; ECM, extra-cellular matrix; EMT, epithelial-to-mesenchymal transition; IMCGL, immunosuppressive myeloid cells from granulocytic lineage; Mo-MDSCs, monocytic myeloid-derived suppressor cells.

different types with opposite roles. "M1" macrophages have been described as classically activated, pro-inflammatory, anti-tumoral effectors, whereas "M2" macrophages correspond to alternatively activated cells endowed with "wound-healing" and tumor-promoting functions. M1 and M2 represent in fact two extreme polarization states of a highly plastic differentiation program controlled by environmental cues (13). M1 macrophages can be induced by TLRs ligands such as LPS, and/or IFNγ. Their differentiation is driven by STAT1, IRF5, NF-kB (14). M2 macrophages are primarily induced by IL-4 and/

or IL-13 (+/- IL-10) *via* the IL-4Rα receptor and their differentiation depend mainly on STAT3, STAT6, IRF4 activation. Different markers have been used to distinguish between M1 and M2 macrophages, but most of these molecules are expressed by both types, although at different levels (14). In immunohistochemical studies, CD68 is often used as a "pan-macrophages" marker. M1 are described as iNOS-expressing cells, with high expression of MHC class II and detectable co-stimulatory molecules CD80 and CD86. M2 macrophages conventional markers include CD163, the scavenger receptor CD204 and mannose receptors CD206, as well as a high expression of Arg1 (9). However, this M1/M2 dichotomy has been challenged and it may not be fully relevant in the context of chronic, non resolutive inflammation such as cancer (14). In fact, recent transcriptomic data, RNA sequencing and mass-cytometry analyses argue for a more complex and heterogeneous phenotypic identity of breast cancer-associated macrophages. A single-cell RNA-seq analysis of 8 tumors (matched to healthy tissues from the same patients) uncovered numerous clusters of immune cells. Among them, three different clusters of TAMs were described (15). Whether TAM may originate from bone-marrow-derived monocytes or from tissue-resident macrophages, which derive from embryonic macrophages that colonize developing organs during the process of embryogenesis and that persist in mature developed adult organs, has been debated. The abovementioned study indicated that the three identified distinct TAM clusters originate either from monocytes or from resident macrophages. Interestingly, among these TAMs, the M1 gene signature correlated with that of M2, advocating for a simultaneous activation of these different genes (15). Along these lines, a mass-cytometry analysis of 144 breast tumors (compared with 46 matched juxta-tumoral tissue and four mammoplasties from cancer-free individuals) defined 19 clusters of myeloid cells and highlighted a frequent co-expression (although at different levels) of phenotypic markers of both M1 and M2 by TAMs such as CD169, CD86, CD204, CD206 and CD163 (16). Consistent with these studies, a RNA-seq analysis indicated that TAMs from breast and endometrial cancers did not exhibit typical M2 gene signatures (17). In this study, TAMs from these two different types of cancers revealed very small similarities, emphasizing the crucial role of the TME in differentially shaping macrophage phenotype and function (17). These data thus indicate that TAMs in breast cancers exhibit complex overlapping phenotypic and functional characteristics and cannot be simplistically categorized as conventional M1 *vs* M2. With regard to the origin of TAMs in breast cancers, the aforementioned single-cell RNA-seq analysis indicated that these cells can originate either from resident macrophages or from monocyte differentiation (15).

TAMs at the Primary Tumor Site

At the primary tumor site, crosstalks between macrophages and cancer cells contribute to the recruitment and activation of TAMs, which in turn foster tumor progression through many mechanisms. Particularly, the immunosuppressive activity of these cells has been extensively described. Indeed, macrophages can suppress anti-tumoral T lymphocytes responses *via* their catabolism of L-arginine and/or tryptophan (expression of iNOS, IDO, arginase), production of immunosuppressive cytokines such as IL-10, IL-4, IL-17, CXCL1, or the expression of ligands for immune checkpoint inhibitory receptors such as PD-L1. They also produce chemoattractant chemokines that further recruit immunosuppressive cells such as neutrophils, immature DCs and/or Tregs [reviewed in (18)]. Along these lines, IL-1ß production by TAM has been shown to participate to the recruitment of immunosuppressive cells and thus to overall suppression of adaptive immune responses (19, 20). In mice, specific targeting of these immunosuppressive macrophages or inhibition of their immunoinhibitory functions can restore anti-tumor immune responses (21).

However, tumor-associated macrophages can also display pro-angiogenic functions and can promote cancer cell stemness. For instance, the transcription factor POU class 1 homeobox 1 (POU1F1, also known as Pit-1), a protein expressed by breast cancer cells, has been reported to increase macrophage recruitment and to promote their polarization towards VEGFA-expressing tumor-promoting macrophages. In turn, these macrophages foster tumor growth, angiogenesis and extravasation of breast cancer cells in a CXCL12-dependent manner *in vitro* (22). Likewise, the expression by breast cancer cells of the ID4 protein (a member of inhibitors of differentiation family of proteins), which is associated with a basal, stem-like phenotype and poor prognosis in TNBC, induces the activation of a pro-angiogenic program in macrophages with upregulation of angiogenesis-related transcripts (23). It is noteworthy that pro-tumorigenic TAM infiltration is more prominent in inflammatory breast cancer (IBC), a disease with a very poor prognosis, compared to other breast cancer subtypes. These macrophages are recruited and polarized into a pro-tumoral phenotype (upregulation of CD206, CD163 and CD209) by CSF-1, CXCL2, VEGFA and CCL18 produced by cancer cells (24). In hypoxic zones, breast cancer cells produce Oncostatin M (OSM) that induces macrophage polarization toward a tumor-promoting phenotype (higher expression of CD163, CD206, Arg1 and Cox-2) (25). Hypoxia enhances TAM expression of galectin-3, a ß-galactoside binding protein modulating TAM apoptosis, migratory and adhesive properties. These macrophages have been shown to promote the proliferation, invasion and migration of MDA-MB-231 breast cancer cells and angiogenesis *in vitro*. Furthermore, *in vivo* experiments in Balb/c mice exposed to hypoxia indicate that targeting Galectin-3 decreases lung metastasis burden and reduces endothelial cell in the primary tumor (26). The presence of sexual steroids in the TME, particularly the presence of estrogens, is a specificity of breast malignancies as breasts are made of adipose tissues producing sexual steroids in the environment. ER+ breast cancers arising in this environment are uniquely capable of responding to these signals and grow. Interestingly, it has been reported that in BC patients, estrogens induce the production of CCL2 and CCL5 within the tumor beds, leading to the recruitment and polarization of macrophages towards a pro-

tumorigenic phenotype (27). The reversal of estrogen effects using Tamoxifen led to a reduced infiltration of these pro-tumoral macrophages in the primary tumor, a finding further confirmed in murine models (28).

Macrophages recruited and accumulating at the tumor site also contribute to tumor development through the promotion of cancer cell stemness *via* secretion of IL-8 and CXCL1, 2 and 3 (24). Cancer stem cells (CSCs) are described as "tumor-initiating cells" with the capability of self-renewal and asymmetric proliferation, and are characterized by a reduced sensitivity to drugs and irradiation compared to non-CSCs. These CSCs are critical for cancer dissemination and metastasis (29). The acquisition of stemness properties by cancer cells has been associated with the induction of the EMT (epithelial-to-mesenchymal transition) program. EMT is controlled by transcription factors such as *TWIST, ZEB1, SNAIL, or SLUG*, and is characterized by specific phenotypic changes whereby epithelial cancer cells acquire a mesenchymal-like phenotype, which increases their invasive and migratory potency (29). CCL2 and CXCL12 produced by breast cancer-associated fibroblasts and tumor cells promote the recruitment and differentiation of monocytes into immunosuppressive TAMs. In turn, these TAMs upregulate the expression of Vimentin, decrease the expression of E-cadherin, and induce *Twists*, *Snail* and *Slug* expression by breast cancer cells, thereby promoting the acquisition of mesenchymal and stemness properties by the latter (30). In a xenograft mouse model, $CD68^+$ TAMs have been demonstrated to promote breast cancer cell stemness through expression of the transmembrane protein LSECtin, which engaged BTN3A3 (B7 family member) on breast tumor cells (31). In the same study, the authors have found a co-localization between LSECtin-expressing macrophages and breast cancer cells expressing CD90 – a stemness marker in breast cancer (31). The role of CD90 in the anchorage of monocytes/macrophages to cancer cells had previously been highlighted in a previous study (32). This CD90-dependent bound leads to the production of cytokines such as IL-6, IL-8, GM-CSF by cancer stem cells which further support cancer stemness (32). Finally, in the inflammatory context of obesity, mammary adipose tissue macrophages can be reprogrammed into a pro-inflammatory metabolically activated phenotype (MMe), which can promote tumor initiation and triple negative breast cancer stem-like properties through an IL-6/GP130-dependent mechanism (33).

TAMs in the Metastatic Process

TAMs also play an essential role at most steps of breast cancer metastasis. As outlined above, these myeloid cells contribute to breast cancer EMT and stemness, two essential initial steps required for tumor systemic dissemination (24, 30–32). TAMs located in the tumor beds or at their vicinity have also been reported to promote intravasation of migrating cancer cells from the primary tumor in blood vessels, while TAMs at the metastatic sites may contribute to the preparation of the pre-metastatic niches before colonization by cancer cells, and enhance breast cancer cell extravasation from blood capillaries in distal metastatic tissues (9).

Many reports have described the influence of TAMs in breast cancer cells intravasation, but the underlying mechanisms *in vivo* have not been extensively studied. A real-time imaging analysis in the MMTV-PyMT mouse model has indicated that VEGF-A produced by Tie2-expressing macrophages induced the loss of vascular junctions and transient vascular permeability, allowing for breast tumor cell intravasation (34). More recent studies have identified proteins involved in pro-tumoral macrophage promotion of cancer cell invasion *in vitro* assays. Chitinase 3-like protein 1 (CHI3L1, a glycoprotein highly expressed in solid tumors) secreted by macrophages has been shown to enhance breast cancer cell invasion, migration and adhesion. CHI3L1 has been detected in the sera of patients with breast carcinomas but not in healthy individuals. Analysis of GEO databases has indicated that CHI3L1 is associated with a worse prognosis in breast cancer patients (35). Use of 2D, 3D and Transwell migration assays have also underlined the role of pro-tumorigenic macrophage-secreted CCL-18 in promoting breast cancer cell migration (36). TAMs can also indirectly foster tumor dissemination by promoting the expansion of pro-metastatic neutrophils by an IL-1ß-dependent mechanism (see neutrophil section below) (37). Even in early and non-invasive breast cancers (*in situ* carcinomas) in mice, CCL2-recruited tumor-infiltrating macrophages with pro-tumorigenic features ($CD206^+$/$Tie2^+$), downregulate expression of E-cadherin by malignant cells, thus destabilizing cell-cell junctions, which leads to cancer dissemination and metastasis. These data advocate further for a decisive role of these cells in the establishment of metastatic disease (38).

Macrophages can also contribute to the preparation of the pre-metastatic niches and the promotion of breast cancer cell extravasation from blood vessels in distant sites. Indeed, monocytes, recruited to pre-metastatic niches by the CCL2, have been reported to quickly differentiate into pro-metastatic macrophages, which contribute to metastatic disease (9, 18). More recently, the presence of CYP4A-expressing TAMs in uninvolved tumor draining lymph nodes has significantly been correlated with the expression of markers associated with pre-metastatic niche formation (VEGFR1, S100A8 and fibronectin), and with a reduced overall and relapse-free survival of patients. In the same study, the specific targeting of CYP4A using pharmacological approaches in 4T1 breast tumor-bearing mice reprogrammed tumor-infiltrated TAMs with a $F4/80^+CD206^+$ phenotype into TAM with a $F4/80^+iNOS^+$ "anti-tumor" phenotype, and reduced lung metastatic burden by impairing the preparation of the pre-metastatic niches (39). At the metastatic sites, macrophages further promote metastatic disease development by fostering vessel formation and directly enhancing cancer cell growth and survival, through the expression of VEGFA and downstream upregulation of MMP-9 (40).

TAMs have been recently described to promote lymphangiogenesis by two different mechanisms. First, expression of podoplanin, a transmembrane glycoprotein implicated in cell motility and adhesion, has been detected on TAMs at the vicinity of lymphatic vessels in the breast TME. The

binding of podoplanin to the galectin 8 protein, a secreted glycan-binding protein expressed by lymphatic endothelial cells, promotes the secretion of the pro-migratory integrin ß1 by macrophages, which in turn fosters their migration and binding to lymphatics vessels where they induce matrix remodeling and promote vessel growth and lymphoinvasion. In the same study, podoplanin-expressing TAMs were associated with lymph node invasion and organ metastasis in a small cohort of breast cancer patients (41). Second, signaling through the sphingolipid sphingosine-1-phosphate receptor 1 (S1PR1) expressed on TAMs induced macrophage NLRP3 inflammasome expression, leading to the production of IL-1ß, which in turn directly acted on lymphatic endothelial cells to promote lymphangiogenesis. In mice deficient in S1PR1 in macrophages, lymphangiogenesis and metastatic growth are impaired. In human, NLRP3 expression in macrophages correlated with lymph nodes invasion and distant metastasis (42). Consistent with the aforementioned observations, *in vitro* experiments confirmed the role of macrophage-derived IL-1ß in the promotion of breast cancer cell adhesion to human lymphatic endothelial cells (43).

BREAST CANCER PROMOTION BY "MYELOID-DERIVED SUPPRESSOR CELLS (MDSCS)": BEYOND THE SUPPRESSION OF ANTI-TUMOR IMMUNITY

"MDSCs": A Functional Definition Rather Than a True Biological Subtype

The term "myeloid-derived suppressor cells (MDSCs)" was initially proposed by Gabrilovich et al. in 2007 in an effort to globally describe a heterogeneous population of myeloid cells exhibiting an immature phenotype and endowed with immunosuppressive functions (ability to suppress T lymphocytes), which accumulate in large numbers in the context of cancer (44). These cells have drawn intense scrutiny over the last 20 years and a considerable amount of data has been provided related to their participation to the complex immunoregulatory networks responsible for tumor immune escape. It has also become clear that they contribute to tumor development and dissemination through many different "immune-unrelated" mechanisms. "MDSCs", in the context of cancer, derive from bone marrow hematopoietic precursors through aberrant myelopoiesis induced by tumor-derived factors (45). Many chemokines have been involved in MDSCs generation and recruitment to primary tumor sites or pre-metastatic niches, such as CXCL1, CXCL2, CXCL5, CXCL12, GM-CSF, G-CSF, M-CSF, VEGF, IL-6, IL-1ß or ß-FGF (46). More recently, breast cancer cells-derived exosomes have been shown to induce "MDSCs" from bone marrow myeloid progenitors (47), or to lead to their recruitment (48). In the specific estrogen-rich environment of breast cancer, these hormones have been shown to induce "MDSCs" recruitment *via* the activation of cancer associated fibroblasts, which in turn secrete CXCL12 (49). "MDSCs" have been defined as myeloid cells blocked at different stages in their differentiation toward mature terminally differentiated subsets such as macrophages and are thus associated with different degree of immaturity. This hallmark is however not always explored in many studies on "MDSCs". The immunosuppressive capabilities of these cells, enabling them to block innate and adaptive anti-tumoral immune responses, represent their primary characteristic which must be systematically investigated for their identification as such (50).

If the term "MDSCs" was designed to globally encompass immature myeloid cells with many common features, it has nonetheless become confusing, particularly because it has contributed to consider these cells as a unique population of myeloid cells. However, "MDSCs" are made of highly heterogeneous populations, including cells from the monocytic and granulocytic lineage. In human, monocytic (M)-MDSCs have been defined as $Lin^-CD33^+CD11b^+HLA\text{-}DR^{low/-}CD14^+CD15^-$, granulocytic (G) or polymorphonuclear (PMN)-MDSCs as $CD33^+CD11b^+HLA\text{-}DR^{low/-}CD14^-CD15^+CD66b^+$, and "early stage" (more immature MDSC) (eMDSCs) as $CD33^+HLA\text{-}DR^-Lin^-$ (Lin: CD3, CD19, CD20, CD56, CD14, CD15) (50). In mice, MDSCs are $CD11b^+/Gr1^+$ cells, with Gr1 composed of two molecules, Ly6C (expressed on monocytic cells/M-MDSCs), and Ly6G (expressed on granulocytic cells/PMN-MDSCs) (51). As a main pitfall in the field, in many preclinical studies the phenotypical characterization of "MDSCs" has been limited to $CD11b^+Gr1^+$, which does not allow to discriminate between monocytic and granulocytic myeloid cells, each subset being endowed with distinct functions (52).

Granulocytic MDSC or "PMN-MDSC" constitute the majority of the MDSC pool in many cancers. However, phenotypically and functionally, these "PMN-MDSC" can hardly be distinguished from pro-tumoral immunosuppressive neutrophils and share the same phenotype as differentiated granulocytes. For these reasons, and since this overlap between PMN-MDSC and tumor-associated neutrophils remains a significant challenge in the field, we will discuss their phenotype and function together with that of cells of the granulocytic lineage in a dedicated section hereafter.

M-MDSCs and conventional monocytes share a similar phenotype, with however as main differences, lower expression of MHC Class II molecules and immunosuppressive capability for M-MDSC (53). However, "classical" $CD14^{hi}CD16^{lo}$ monocytes may also exhibit low expression of HLA-DR, which is further reduced in the context of inflammation, sepsis, or cancer. In fact, cells with such a monocyte/M-MDSCs phenotype in the context of cancer have been shown to be immunosuppressive, blocking antitumoral T cell responses (54). In addition, both cell types have been reported to differentiate into pro-tumorigenic TAMs. This suggests a change of function of monocytes induced in the context of cancer (or other pathological conditions), rather than the occurrence of two different cell subtypes. Therefore, immunosuppressive monocytes and M-MDSC substantially overlap phenotypically and functionally. It is also noteworthy

that some cells of myeloid origin exhibiting phenotypic characteristics that do not meet the classical definition of MDSC because they lack expression of specific MDSC markers (but which are nonetheless immunosuppressive and pro-tumoral) are excluded by this current MDSC terminology and may thus be overlooked. This is for instance the case of non-classical monocytes described in different cancers (55–58).

Overall, the "MDSCs" terminology is a conceptual approach, which was indispensable fifteen years ago to provide a comprehensive picture of a particular phenomenon observed in many cancers: the expansion of a myeloid cell population, more or less mature, with immunosuppressive properties. With the evolution of detection technologies such as scRNAseq, new knowledge of these cells has been brought, and it appears today as an essential requirement to regroup these myeloid cells according to their refined phenotype, in order to better identify and ultimately target them. However, since many studies do not allow such a discrimination (because of the use of an incomplete phenotype to identify these cells), in the next section, we will discuss the "all" MDSCs population ($CD11b^+/Gr1^+$ in mice, $CD33^+$ in humans), the "early MDSCs" and the monocytic fraction (monocytes and M-MDSCs).

"MDSCs" in Breast Cancer Patients

In breast cancer patients, while some studies have reported that immunosuppressive monocytic cell number is increased compared to control patients (54), others did not observe this expansion (59). These cells have been associated with more advanced disease (60), and with a worse survival (61). Increased eMDSC numbers have also been correlated with a worse response to neo-adjuvant chemotherapy in TNBC patients (62). In breast cancer tissues, many reports have described, with various degree of accuracy, myeloid cells exhibiting an immature phenotype ($CD33^+CD13^+CD14^-CD15^-$) and immunosuppressive properties, which have been associated with adverse prognostic features (higher tumor grade, positive lymph nodes) (63). The composition of this myeloid infiltrate was different among studies, composed either with a majority of $CD14^+$ monocytic immunosuppressive cells (64), or with granulocytic myeloid cells and early MDSCs (59). Together, these studies consistently advocate for the presence and role of suppressive myeloid cells in the tumor microenvironment, but their contradictory findings related to the exact phenotype of these cells highlights the extreme heterogeneity of this myeloid landscape, as further outlined more recently in scRNAseq and cytometry by time of flight (CyTOF) studies discussed in the next sections (15, 16).

Direct Effects of "MDSCs" on Tumor Cells

In primary tumor sites, suppressive myeloid cells recruited by cancer cells play an important role in inhibiting anti-tumor immune responses using many mechanisms extensively reviewed elsewhere (expression of ARG1, production of NO, ROS, and prostaglandin E2) (50, 51). However, many studies have also lent support to the notion that, besides their role as potent suppressor of cancer immunity, "MDSC" may also play an important role in breast cancer cell invasion, activate other stromal cells such as fibroblasts, and promote angiogenesis. Recruited at the hypoxic tumor sites, $CD11b^+Gr1^+$ MDSCs produce S100A8, an alarmin not only involved in the recruitment of additional MDSCs, but also implicated in the activation of endothelial cells. This activation led to the modification of tight junctions, leading to vascular leakage (65).

MDSCs also participate to breast cancer resistance to chemotherapy. It has indeed been shown that immunosuppressive $CD33^+$ cells isolated from breast cancers patients are able to induce a stemness phenotype (associated with cancer cell chemoresistance) in the breast cancer cell line MCF-7 (64). Furthermore, the chemotherapeutic agent doxorubicin has been found to increase the levels of monocyte chemoattractant proteins (MCPs) 1 to 3 and particularly MCP1/CCL2 (48, 66). This chemotherapy-induced expression of CCL2 has also been reported in the metastatic sites such as the lungs. It results from the release of extracellular vesicles enriched in annexin-6 by chemoresistant cancer cells, which induced the recruitment of $Ly6C^+CCR2^+$ monocytes that participate to the pre-metastatic niche formation (48).

Preparation of the Metastatic Niche by Recruited "MDSCs"

$CD11b^+Gr1^+$ granulocytic and monocytic myeloid cells critically contribute to the metastatic dissemination of breast cancer cells (52). It has been observed that in the mouse 4T1.2 mammary cancer model, pro-inflammatory monocytes with MDSCs features (IL4R, CD49b, CD62L, CD11b) can be recruited by the chemokine CCL2 in the pre-metastatic lungs where they foster metastasis. CCL2 promotes the release of the alarmin S100A8/9 which further increases MDSC recruitment (67). $CD11b^+Gr1^+$ cells have been reported to progressively accumulate in the lungs of 4T1 tumor-bearing mice before the arrival of cancer cells, and to prepare the lung environment for seeding by metastatic cells *via* vascular remodeling and production of MMP9 (68). Interestingly, this recruitment of $CCR2^+$ cells induced by inflammatory signals can be mediated by other sources of inflammation than tumors. Indeed, myocardial infarction represent a major cause of systemic stress and is accompanied by systemic monocytosis. It has been shown to be associated with a higher risk of relapse and cancer-specific mortality in early breast cancer patients (69). In tumor-bearing mice, myocardial infarction results in an important recruitment of $Ly6C^+$ monocytes with immunosuppressive functions, which can differentiate into pro-tumorigenic macrophages at the tumor sites and accelerate primary tumor growth and metastasis (69). It has also been reported in the 4T1 triple negative mouse breast cancer model that $Gr1^+$ cells primarily promote the metastatic cascade by facilitating extravasation of malignant cells at the distant metastatic lungs through IL1β and matrix metalloproteinase secretion (70). Along these lines, CXCR4-dependent mechanisms were involved in $Gr1^+$ cell-mediated metastasis promotion in a mouse breast cancer model (71)

At the future metastatic site, MDSCs are implicated in the angiogenic switch. In two different studies in 4T1-bearing mice, $CD11b^+Gr1^+$ cells recruited in the lungs have been demonstrated to upregulate many pro-angiogenic factors such as *Il1ß, Mmp9, Tnf, Tie2* (72), or to secrete platelet-derived growth factor-BB (PDGF-BB), which mediates angiogenesis (73).

Differentiation of "MDSCs" Into Other Cell Types in the Context of Breast Cancer

"MDSC" are endowed with a particularly high degree of plasticity. Indeed, many reports indicate that monocytes/M-MDSCs often differentiate into pro-tumorigenic macrophages at the tumor site or in the metastatic organs. This phenomenon has been tracked *in vivo* with the use of GFP^+ expressing myeloid cells, transferred into E0771-bearing C57BL/6 mice: few hours after the transfer, classical monocytes were recruited in the metastatic lungs, where they differentiated into macrophages precursors, before becoming metastasis-associated macrophages (74). Exosomes derived from mesenchymal stem cells can promote the differentiation of M-MDSCs into highly immunosuppressive pro-tumorigenic macrophages (75).

Bone is one of the most important metastatic sites in breast cancer patients, with up to 70% of metastatic patients facing bone metastasis. MDSCs and monocytic cells play a major role in the formation of this metastatic site. Indeed, it has been demonstrated that MDSCs (defined as $CD11b^+Gr1^+$) cells can differentiate into osteoclasts *in vitro* and *in vivo*. These osteoclasts are capable of bone resorption (76, 77).

IMMUNOSUPPRESSIVE MYELOID CELLS OF THE GRANULOCYTIC LINEAGE: VERSATILE TUMOR-PROMOTING FUNCTIONS IN BREAST CANCERS

Granulocytic Cells in the Breast TME: Phenotypes, Functions and Controversies

Neutrophils constitute the more prominent leucocytes, primarily participating to the first lines of defense against infectious agents. They are produced in the bone marrow from granulocyte-monocyte myeloid progenitors (GMPs), which originate from lymphoid-primed multipotent progenitors, themselves derived from hematopoietic stem cells. Their maturation and differentiation depend on G-CSF and STAT3 activation.

In the context of cancer, and particularly in the context of breast cancers, it has been demonstrated that malignant cells could disrupt neutrophil homeostasis, hijacking their production and functions to their advantage through the production of TDFs such as G-CSF (78). The phenotypic characterization of tumor-associated neutrophils and the identification of specific subsets have remained the matter of intensive debates for the past few years. As mentioned in the previous section, the discrimination and possible relationship between tumor-associated neutrophils and polymorphonuclear (PMN)-MDSCs (MDSCs with a granulocyte phenotype) has remained an outstanding question in the field. Whether PMN-MDSC and tumor-associated neutrophils represent the same cell populations or are different subsets remains highly questionable. Indeed, in human, both are commonly identified as SSC^{high}, $CD33^{+/medium}$, $CD11b^{high}$, $CD16^+$, $CD15^+$, $CD66b^+$, $HLA\text{-}DR^{neg}$. Furthermore, many preclinical studies, primarily in mouse cancer models, on which most of our understandings of tumor-associated neutrophils have been based, do not clearly distinguish between neutrophils and PMN-MDSC. In these studies, cells with a $CD11b^+Gr1^+$ $Ly6G^+LY6C^{med/low}$ phenotype have been shown to expand over the course of cancer progression, and functional assays to assess their immunosuppressive properties have not always been performed (79, 80).. Although some markers have been proposed to discriminate between PMN-MDSC and "classical neutrophils" such as LOX-1 (81), CD84 and JAML (82), or sometimes the alarmins S100A8 or S100A9 (50), PMN-MDSC have mainly been defined by their immunosuppressive properties. Along these lines, because neutrophil density is higher than that of MDSC, it has also been proposed that density gradients may be used to separate physically tumor-associated neutrophils and tumor-induced PMN-MDSC. However, mature neutrophils have also been shown to exhibit immunosuppressive and pro-tumorigenic features in the TIME, and activated neutrophils fall in the "low-density" section of density gradients. Some authors also tried to establish a "N1/N2" dichotomy similar to that proposed for macrophages, N2 being pro-tumorigenic, immunosuppressive neutrophils (83). However, to date no reliable marker allow for a clear distinction of neutrophil different differentiation stages, and neutrophils in cancer are likely present as a heterogenous population, with cells at various activation states (84).

Recent reports have attempted to address this equivocal identity of PMN-MDSC and tumor-associated neutrophils. A single-cell transcriptomic analysis of the myeloid compartment in the splenocytes from two tumor-bearing mice (PyMT tumor model) and 2 tumor-free control animals has suggested that PMN-MDSCs differ from their normal myeloid counterparts and may originate from neutrophil progenitor cells undergoing an aberrant differentiation path (82). Data from another recent study have suggested that peripheral PMN-MDSCs from patients with metastatic breast cancer are more closely related to healthy donors' neutrophils than to MDSCs induced in another pathological condition (Gram-positive sepsis) (85). Further mass-cytometry analysis revealed that unique subpopulations of these granulocytic cells were specifically present in cancer patients, with a majority of low density mature activated neutrophils and a minority of immature neutrophils lacking maturation markers (CD10, CD13, CD45) at different maturation stages. These cells were collectively referred to by the authors as "G-MDSCs" and proposed to constitute neutrophils at various differentiation stages (85). These data thus advocate for a differential differentiation and activation profile of neutrophils in the context of cancer.

Considering this significant phenotypic and functional overlap between so-called "PMN-MDSC" and "immunosuppressive neutrophils" we propose to refer to these cells more accurately using the term "immunosuppressive myeloid cells of the granulocytic lineage" or "IMCGL" until definitive phenotypic markers or functional assays are available to unequivocally distinguish them. (**Figure 2**). We believe that, compared to the terms "immunosuppressive neutrophils" or "PMN-MDSC", the denomination ""IMCGL" allows to group these highly overlapping cell types to better study them and partly address

the current controversies and challenges in distinguishing between immunosuppressive neutrophils and PMN-MDSC (**Table 1**). The physiological relevance and clinical usefulness of discriminating these cells also remains to be addressed.

IMCGL in Breast Cancer Patients

In breast cancers, IMCGL have historically been considered as a major obstacle to anti-cancer immunity because of their immunosuppressive activities, a concept supported by recent findings in triple-negative breast cancer mouse models, where IMCGL-infiltrated tumors do not respond to immunotherapy (86). In breast cancer patients, tumor-induced expansion of circulating IMCGL has been corelated with a worst prognosis (87, 88). Interestingly, IMCGL are more frequently found in the tumor beds than in "healthy" adjacent tissues (59), and in most studies IMCGL have been associated with a higher tumor stage (89), or with a worse prognosis and an impaired response to chemotherapy (90). Tumor-induced IMCGL have been reported

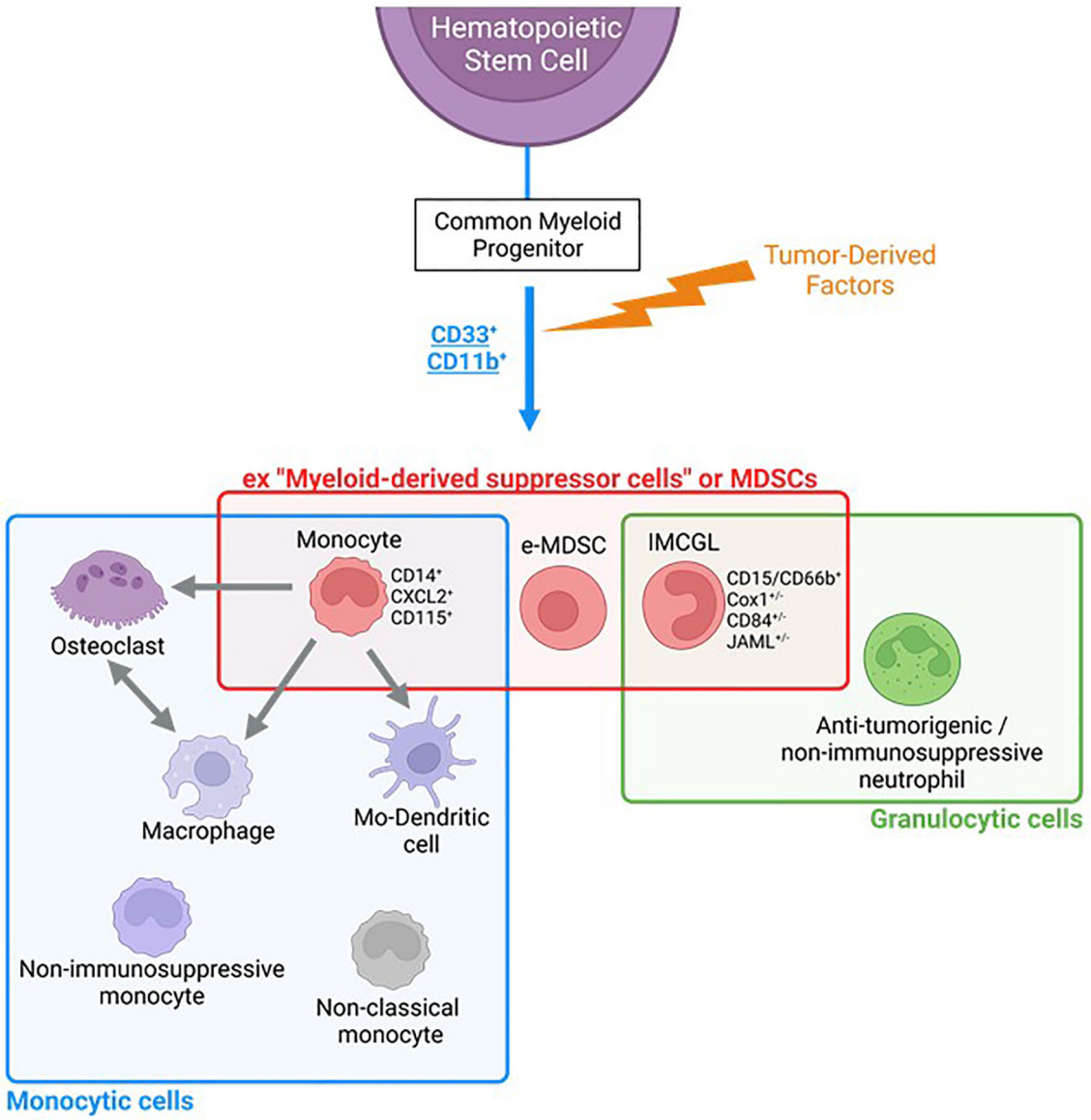

FIGURE 2 | Overlaps between subsets of tumor-promoting myeloid cells (monocytic vs gralulocytic origine). Cells formerly referred to as "Myeloid-Derived Suppressor Cells, MDSCs" encompass undifferentiated $CD33^{+}CD11b^{+}$ ("early-MDSCs"), immunosuppressive cells of the granulocytic lineage that we propose to call "immunosuppressive Myeloid Cell of the Granulocytic lineage, IMCGL" ("formal PMN-MDSCs"), and monocytes endowed with pro-tumoral properties. These tumor-promoting monocytes ("formal m-MDSCs") can differentiate into pro-tumoral macrophages, Mo-dendritic cells or osteoclasts, each endowed with multiple dedicated tumor-promoting activities. IMCG, immunosuppressive myeloid cells from granulocytic lineage; e-MDSCs, early-myeloid-derived suppressor cells; Mo-Dendritic cell, monocyte-derived dendritic cells.

TABLE 1 | IMCGL terminology, phenotype and non-immunological functions.

Study	BC subtype	Model	Cell line	IMCGL name in original article	Phenotype	Functions	Additional findings in patients
Ouzounova et al., Nat Commun 2017 (52)	TNBC	Mice	4T1	MDSCs	$CD11b^+$ $Ly6G^+$ $Ly6C^{lo}$	MDSCs promote primary and disseminated tumor cell growth and promote the formation of lungs metastasis.	
Kim et al., Nat Cell Biology 2019 (86)	TNBC	Mice	2208L, PyMT-N, 4T1, AT3, PyMT-M, E0771, 67NR	TINs (encompass both neutrophils and MDSCs)	$CD45^+$, $CD11b^+$, $Ly6G^+$,$Ly6C^{med\text{-}low}$	Creation of an immunosuppressive environment which impairs response to ICI	
Wang et al. CCR 2019 (90)	HR+, TNBC, HR+/HER2+	Human (*in vitro*)	MCF-7, MB-231, BT-474	Neutrophils isolated from patients tumors	$CD11b^+$ $CD66b^+$	Promotion of migration and invasion, + induction of EMT (tried on MCF7 cells only)	Prognosis: stromal CD66b+ cells (IHC) are associated with poor prognosis, advanced histologic grade, tumor size, LN metastasis, high TNM stage, TNBC and distant metastasis
	TNBC	Mice	4T1	Neutrophils	$Ly6G^+$	Promotion of metastasis. Use of an anti Ly6G+ antibody prevented the formation of lungs and liver metastasis.	
Liang et al, PNAS 2018 (92)	TNBC	Mice	4T1	Neutrophils	$Ly6G^+$	Promotion of tumor growth and metastasis (via transferrin secretion)	Peripheral neutrophils from breast cancer patients with metastatic disease, isolated by an immunomagnetic negative selection, promoted tumor cell growth of MDA-MB-231 cells *in vitro*.
Xiao et al, Cancer Cell 2021 (93)	TNBC	Mice	4T1, 4T07	Neutrophils	$CD11b^+$ $Ly6G^+$	Via the formation of NETs, neturophils recruited at the metastatic niche promote cancer cell proliferation	NETs and neutrophil infiltration are higher in lung metastases than in primary tumors (neutrophils: MPO in IHC). This infiltration is higher in TNBC than in HR+ tumors.
Kumar et al., JCI 2018 (96)	TNBC	*In vitro*	HCC1806, SUM159	MDSCs	$CD45^+$, $CD11b^+$, $Ly6G^+$/$Ly6C^{lo}$	Addition of MDSCs in turmospheres assay significantly increased the number of tumorspheres	MDSCs infiltration is higher in TNBC cancers ($CD11b^+$ $CD33^+$ $S100A9^+$ $CD15^+$ $LOX1^+$)
Luo et al., J Breast Cancer 2020 (97)	HR+, TNBC	*In vitro*	MCF-7, MDA-MB-231	MDSCs	$CD33^+HLA\text{-}DR^-CD15^+$ in PBMCs from BC pts	MDSCs promote migration and invasion of BCC *via* induction of EMT	The frequency of MDSCs increases in peripheral blood of patients with breast cancer. This was higher in high stage patients (III/IV), with extensive tumor burden, lymph node metastases, distant metastases, poorly differentiated tumors.
Vazquez Rodriguez et al., Cancer Immunol Res 2017 (102)	HR+	Zebrafish	MCF-7	Neutrophils	LFA-1 (neutrophils from HD, obtained by Ficoll)	Neutrophils promoted migration and invasion at tumor site, and intra/extravasation. They comigrated with cancer cells	
Szczerba et al., Nature 2019 (103)	HR+, TNBC, HER2+	Mice (immunocompetent and nude)	BR16, LM2, 4T1, PyMT	Neutrophils	$Ly6G^+$	Neutrophils directly interact with CTCs to support cell cycle progression in circulation and to accelerate metastasis seeding	Clusters of neutrophils and circulating tumor cells were also found in breast cancer patients blood samples. These clusters were associated with a significantly worse prognosis.
Sprouse et al., Int J Mol Sci 2019 (104)	HR+, TNBC, HER2+	Human	Isolated from patients	MDSCs	$CD45^+$/$CD33^+$/ $CD11b^+$/$CD14^-$/$CD15^+$	MDSCs from patients formed clusters with CTCs, as seen in	High number of MDSCs is correlated with metastasis in BC patients. PMN-

(Continued)

TABLE 1 | Continued

Study	BC subtype	Model	Cell line	IMCGL name in original article	Phenotype	Functions	Additional findings in patients
						patients and reproduced *in vitro*. This companionship promoted migration and proliferation of cancer cells.	MDSCs are responsible for higher ROS levels in the plasma of these patients.
Hsu et al., Cell Rep 2019 (106)	TNBC	Mice	4T1	"low-density" neutrophils	Low fraction of Ficoll, $CD11b^{+}Ly6G^{+}$	Promotion of liver metastasis formation, *via* NETosis	
Sangaletti et al., Front Immunol 2019 (107)	HER2+	Mice	SN25A, N3D + co-isogenic transfected with LXSPARCSH	MDSCs	$CD45^{+}$, $CD11b^{+}$, $Ly6G^{+}$	MDSCs promote tumor growth, angiogenesis and EMT in cancer cells.	
Albrengues et al., Science 2018 (110)	HR+	Mice (immunocompetent and nude)	D2.0R, MCF-7	Neutrophils	$Ly6G^{+}$ and/or MPO and/or Ficoll density gradient	Neutrophils promoted awakening of dormant cancer cells	
Park et al., Sci Transl Med 2016 (111)	TNBC	Mice	4T1, tumors from C3 (1)-Tag mice	Neutrophils	Ficoll + $CD45^{+}$, $Ly6G^{+}$, $CD11b^{+}$	Neutrophils are recruited by cancer cells at the metastatic sites where they promote tumor cells growth, migration and invasion *via* the formation of NETs.	NETs are detectable in human breast cancers and are more frequent in more agressive cancers (TNBC vs HR+).
Yang et al., Nature 2020 (112)	TNBC	Mice	4T1, MDA-MB-231	Neutrophils	MPO (IHC)	NETs at metastatic site promote migration and adhesion of cancer cells, and the formation of metastasis.	NETs are present in metastatic lesions of breast cancers such as liver, lungs, bones and brain, liver metastases having the most abundant infiltration (IHC: MPO and H3Cit stainings). Serum NETs level (detection of MPO/DNA complex) are significantly higher in patients with liver metastases. High levels of MPO/DNA was an independent variable associated with metastasis to the liver.
Teijeira et al, Immunity 2020 (113)	TNBC	Mice	4T1	Both	$Ly6G^{+}$	NETs formed by neutrophils and/or MDSCs shield tumor cells from NK cells and help them avoid immune destruction, thus leading to the formation of more metastasis.	
Ouzounova et al., Nat Commun 2017 (52)	TNBC	Mice	4T1	MDSCs	$CD11b^{+}$ $Ly6G^{+}$ $Ly6C^{lo}$	MDSCs promote primary and disseminated tumor cell growth and promote the formation of lungs metastasis.	

BC, breast cancers; EMT, epithelial-to-mesenchymal transition; ICI, immune checkpoint inhibitors; HR+, hormone receptor positive; IHC, immunohistochemistry; IMCGL, immunosuppressive myeloid cells of granulocytic lineage; LN, lymph node; MDSCs, myeloid-derived suppressor cells; MPO, myeloperoxydase; NETs, neutrophils extracellular traps; PBMCs, peripheral blood mononuclear cells; TINs, tumor-infiltrating neutrophils; TNBC, triple-negative breast cancer; TNM.

to impair T cell activation, particularly in advanced tumors, through increased production of ROS, NO or ARG1 or expression of immunoinhibitory ligands such as PDL1 (91).

IMCGL at the Primary Tumor Sites

IMCGL expansion and recruitment is directly promoted by breast cancer cells by various mechanisms. GM-CSF secretion by malignant cells induces the production of transferrin in $Ly6G^+$ cells from 4T1-bearing mice that, in turn significantly enhances primary tumor growth *in vivo* and *in vitro*. In humans, the transferrin, *TFR1* gene has been found to be up-regulated in breast cancers, and higher levels of this protein have been associated with higher tumor grades/stages, but also with a significantly worse survival (92). It has been shown that G-CSF production by breast cancer cells induces the recruitment of IMCGL that accumulate in the periphery of tumor-bearing PyMT mice (78). Cathepsin C (CTSC) produced by cancer cells has also been reported to induce recruitment and activation of IMCGL in 4T1 tumor bearing-mice. CTSC expression in human breast cancer is associated with metastasis and IMCGL occurrence (93). IMCGL recruitment can also be indirectly promoted by IL-1ß-secreting TAMs, which are recruited by Wnt ligands in p53-deficient cancer cells (94), or by cancer cell secretion of CCL2 (37).

Besides being equipped with immunosuppressive properties, IMCGL are also endowed with versatile tumor-promoting functions. Indeed, IMCGL can also induce and promote angiogenesis, participate to the remodeling of the extracellular matrix, contribute to tumor cell invasion, and participate to metastatic dissemination (84). IMCGL have also been shown to form Neutrophil Extracellular Traps (NETs) involved in tumor cell capture and growth as detailed hereafter (95).

IMCGL have been reported to display direct effects on breast cancer cells. Recent studies have indeed demonstrated that these cells participate to the acquisition of a stem-cell phenotype by malignant cells. Breast cancer cells expressing the ΔNp63 protein secrete CCL22 and CXCL2 that recruit IMCGL, which, in tumorsphere assays, promote the stemness phenotype of breast tumor cells *via* the secretion of CHI3L1 and MMP9 (96). Along these lines, it has also been reported that tumor-infiltrating IMCGL from breast cancer patients induce EMT in the MCF-7 cancer cell line, and promoted migration and invasion in *in vitro* assays (90). Consistent with these data, CCL3-recruited IMCGL have been observed to foster the EMT in breast cancer cells and enhance their proliferation, migratory and invasive properties through the PI3K/Akt/mTOR pathway (97).

IMCGL in the Metastatic Process

Most studies in the field have however shown that, primarily, IMCGL foster the process of breast cancer invasion and metastasis, with limited effects on primary tumor growth. Indeed, the elimination of these cells in pre-clinical models resulted mainly in dampening metastatic dissemination, with limited influence on primary tumor development (90, 94, 98–101). In zebrafish injected with MCF-7 cells, IMCGL from healthy human donors are capable of promoting cancer cell migration and intravasation at the tumor injection site in an Estradiol-dependent manner. In this model, IMCGL have been shown to migrate together with circulating cancer cells and to extravasate together in distant sites, thereby supporting disseminated tumor cell establishment in new metastatic niches (102). Two recent reports have brought substantial new insights into this joint migration of IMCGL with cancer cells. Indeed, evidence has emerged that some subpopulations of IMCGL can form companionship clusters with circulating tumor cells (CTC), and chaperone these CTC, protecting them in the circulating blood. Furthermore, IMCGL may foster CTC seeding at distant sites. CTC primarily circulate alone in the peripheral blood where the vast majority die in this environment. Only a limited number of these CTC (2-4%) have been detected as circulating homotypic or heterotypic clusters (103). These clusters have been associated with a significantly worse prognosis in breast cancer patients (103, 104). Heterotypic clusters are composed of CTC with white blood cells, most of them being myeloid cells of the granulocytic lineage (103, 104). Sprouse et al. have recently explored the cross-talks in these clusters between CTC and $CD33^+CD11b^+CD15^+$ IMCGL cells (defined by the authors as PMC-MDSC) in the PBMC fraction of the peripheral blood (104). IMCGL induce upregulation of Notch1 receptor expression in CTCs through the ROS-NRF2-ARE axis, while CTCs induce pro-tumorigenic differentiation of IMCGL through paracrine Nodal signaling. Importantly, in mice, co-injection of breast cancer cells with IMCGL leads to an early dissemination of malignant cells to the lungs and brain (104). Szczerba et al. have also studied the interactions between CTC and IMCGL in heterotypic clusters from breast-cancer patients and from mammary tumor-bearing mice (103). Within these clusters, CTC exhibit a marked enrichment in positive regulators of cell cycle and DNA replication programs. Furthermore, RNA sequencing analysis has identified cytokines implicated in these cellular cross-talks and determined that IMCGL secrete TNFα, OSM, IL-1ß and IL-6, while CTC express CSF1, CSF3 (G-CSF), TGF-ß and IL-15 (103). However, the exact identity of each cellular partners within these clusters, the nature and importance of their interactions as it relates to the metastatic process, and the mechanisms underlying the promotion of CTC seeding and development at the metastatic niches remain to be fully uncovered. Along these lines, not only do IMCGL represent the main immune cells present at the metastatic site (105), but they also critically participate to the preparation of pre-metastatic niches. In tumor-bearing mice, myeloid cells accumulating in distant tissues are essentially composed of $Ly6G^+$ immunosuppressive IMCGL (78). In 4T1 tumor-bearing mice, accumulation of IMCGL in the lungs (52) or in the liver (106) promotes metastatic cancer growth, and disseminated malignant cell proliferation. Importantly, depletion of IMCGL with an anti-Ly6G antibody suppresses metastasis in both studies (52, 106). It is noteworthy that although Ly6G has been used to deplete granulocytic cells, whether this approach results in the elimination of all IMCGL subsets remains to be determined.

Importance of NETs in Breast Cancer

Neutrophils have been described for their capacity of releasing neutrophil extra-cellular traps or "NETs", a function that has also been described for PMN-MDSCs (107). NETosis is the process by which neutrophils release large web-like structures composed of cytosolic and granule proteins assembled on de-condensed chromatin. NETosis has been proposed to be a specific defense mechanism harbored by neutrophils against some pathogens like funga. The phenomenon of NETosis has also been observed in cancer where it can be triggered in part by G-CSF produced by many malignant cells (95). The impact of this process on cancer progression and on disease-associated complications such as thrombosis is being increasingly acknowledged (95, 108). A recent breakthrough in breast cancer was the findings that NETs may contribute to the awakening of dormant cancer cells. Reactivation of dormant cancer cells is of utmost importance in breast cancers, since half of patient relapses occur more than 5 years after the initial diagnosis, and in some cases even up to 20 years (109). Using breast cancer models that usually do not metastasize in mice, Albrengues et al. have demonstrated that neutrophil-derived NETs, induced by inflammatory conditions such as prolonged tobacco exposure or LPS instillations, lead to dormant cancer cell awakening and development into aggressive lungs metastases. In this setting, inflammation triggers NETs extrusion, which forms a scaffold allowing the sequential cleavage of laminin by neutrophil elastase (NE) and MMP9, as well as thrombospondin 1 (TSP-1). This laminin cleavage activates an $\alpha 3\beta 1$-associated signaling in dormant cancer cells, leading to their reactivation (110). TSP-1 is a key matricellular protein that has been reported to inhibit metastasis. As outlined hereabove, CTSC secreted by cancer cells promotes the recruitment and activation of neutrophils in the metastatic niches, which upon activation form NETs that degrade the extracellular matrix, in part by cleavage of TSP-1, thereby allowing cancer cell proliferation and establishment (93). Other reports have indicated that in the context of breast cancers, NETs actively contribute to the formation of the pre-metastatic niches (111, 112). Indeed, these structures have been observed in the lungs of mice early after injection of 4T1 cells, thus before arrival and seeding of breast cancer cells. Furthermore, evidence has been provided that, *in vitro*, NETs stimulate invasion and migration of cancer cells. Consistently, NETs digestion with deoxyribonuclease I (DNase I) has been reported to significatively reduce the occurrence of lung metastasis (111). In humans, NETs have been detected in large amount in the metastatic lungs, and circulating NETs levels are higher in metastatic breast cancer patients compared to early-stage cancer patients (93). Suggesting a role of NETs in metastatic tumor cell organotropism regulation, Yang et al. have demonstrated that NETs contribute to the formation of metastases in the liver but not in the lungs. Furthermore, the authors have identified the protein CCDC25 expressed at the surface of cancer cells as a specific sensor of NETs DNA, and responsible for malignant cells migration, adhesion and proliferation induced by NETs. In breast cancer patients, CCDC25 has been detected in cancer cells with a clear membrane staining at the border of the tumor, and higher levels of CCDC25 in the primary tumors have correlated with a reduced survival (112).

Finally, NETs act as "shields" for cancer cells, wrapping them to avoid destruction by cytotoxic CD8 T cells of NK cells, adding to their multiple tumor-promoting functions (113).

ROLES OF "TOLEROGENIC/ REGULATORY" DENDRITIC CELLS IN BREAST CANCER DEVELOPMENT

Dendritic Cell Alterations in Breast Cancers

Dendritic cells (DC) play a central role in cancer immunosurveillance. They capture antigenic material from neoplastic cells, process tumor-specific antigens and present the derived peptides onto MHC class I or class II. Upon migration to the secondary lymphoid tissues, they activate effector tumor-specific $CD8^+$ CTL and $CD4^+$ Th lymphocytes. DC can also promote the anti-tumoral functions of NK, NKT and $\gamma\delta$ T cells (114). However, in most cancers, DC are phenotypically and functionally impaired leading to dampened anti-cancer immunity (115). Although the nature of the microenvironment of breast cancers greatly varies depending on the tumor subtype and stage of the disease, in most cases it negatively influences DC capability to induce and sustain anti-tumor immunity. These DC alterations in breast malignancies have been attributed: a) to DC elimination; b) to the blockade of the generation of these cells from DC precursors; c) to the triggering of functional deficiency in DC (reduced antigen capture, processing, presentation and ability to activate T lymphocytes); and d) to the generation of immunosuppressive and tolerogenic DC capable of blocking anti-cancer T cells, inducing T lymphocyte anergy or inducing tumor-promoting regulatory T cells (Treg) (116–118). These defects are induced by different tumor-derived factors [extensively reviewed in (116, 117)], among which are VEGF (119), TGFβ (120), IL10 (121), PGE2 (122) or tumor-produced polyamines (123), and are responsible for a deficient induction of anti-cancer T lymphocyte proliferation and activation, thus contributing to breast cancer evasion from immunosurveillance.

In addition, different studies have demonstrated that breast malignancies are associated with the induction of different subpopulations of DC (myeloid, mDC or plasmacytoid, pDC) at different stages of maturation in the tumor, lymph nodes or blood, which actively promote T cell anergy and suppression and/or which trigger tumor-promoting Treg induction by a variety of mechanisms such as L-Arginine depletion (124), PD-L1 (125), TGFβ, IDO (126) or ICOS-ligand (127). Breast cancer-derived thymic stromal lymphopoietin (TSLP) has been identified as an inducer of OX40L on DC infiltrating primary breast cancer (128). These $OX40L^+$ DC participate to the induction of IL-13- and TNF- producing Th2 cells thus contributing to the promotion of an environment permissible for breast tumor growth (128).

Role of DC in Breast Cancer Angiogenesis and Metastasis

Although many studies have extensively reported on the immune-modulatory role of tolerogenic/regulatory DC in breast cancers, much sparser reports are available as it relates to the tumor-promoting pro-angiogenic, pro-invasive and pro-metastatic properties of these cells. In this context, a study has correlated the presence of immature DC in highly angiogenic tumors (129), but the mechanistic bases underlying neoangiogenesis promotion remains to be determined. Similarly, the role of DC in breast cancer metastasis remains incompletely elucidated. A recent report indicates that $CD303^+$ pDC accumulating in human breast cancer beds of patients with positive lymph nodes promote CXCR4 expression by cancer cells, suggesting that these tumor-associated pDC may participate to malignant cell metastasis to lymph nodes expressing SDF-1 through a CXCR4/SDF-1-dependent mechanism (130). Since DC conditioned by the tumor microenvironments can produce TGFβ, these cells may also contribute to the epithelial-mesenchymal transition (EMT) precluding tumor cell migration from primary tissues to metastatic sites, but a formal demonstration of this effect in breast cancer remains to be provided. Likewise, the possibility that DC may contribute to the preparation of pre-metastatic niches, before seeding of metastasizing cancer cells has yet to be formally demonstrated. In this context, a recent study has suggested that, in the mouse breast cancer model E0771, glucose-regulated protein 78 (GRP78) produced by tumor reduces DC MHC class II expression in the liver in the early stage of metastasis. However, the actual role of DC in the preparation of the pre-metastatic liver has not been demonstrated (131). Along these lines, recent data have also indicated that $CD11c^+$ DC exposed to conditioned medium of $RANKL^+$ T cells from the bone marrow of 4T1 mammary tumor-bearing mice can differentiate into osteoclast-like cells, suggesting that DC may participate to the osteolytic process occurring in metastatic breast cancer patients (132).

CONCLUSION, PERSPECTIVES AND CHALLENGES

The critical contribution of immune cells of the myeloid lineage to the mechanisms of cancer escape from immune detection and elimination is now widely recognized, and many studies have deciphered the various modes of action underlying the immunosuppressive properties of these cells. The notion that, beside this cardinal role in antitumor immunity, different myeloid cell populations are also endowed with a variety of "non-immunologic" tumor-promoting functions has drawn less scrutiny, until recently.

The heterogeneous nature of tumor-promoting myeloid cells, with some likely phenotypical and functional overlaps between subsets (illustrated in **Figure 2**) remains a major challenge preventing the unequivocal identification of distinct subpopulations. This current problem is probably best illustrated by the difficulty to draw a clear line between PMN-MDSC and immunosuppressive neutrophils in breast cancer patients or in mammary tumor models. Recent extensive studies, which have attempted to establish dedicated genomic, proteomic and biochemical profiles to better characterize these cells, have actually highlighted further the complexity and the high degree of plasticity of this myeloid landscape, advocating for instance that PMN-MDSC may actually correspond to neutrophils at different maturation stages in breast malignancies. These considerations have prompted us to refer to these tumor-promoting granulocytic cells occurring in cancer as "immunosuppressive myeloid cells of the granulocytic lineage, IMCGL", which, we believe, better depicts their origins and functions. It would be clinically relevant to clearly decipher whether IMCGL are constituted of different subsets with dedicated properties and predictive or prognostic values. Better identification of these cells is a prerequisite to further determining whether they may serve as useful biomarkers and therapeutic targets, which warrants the urgent need to discover novel marker(s) and/or strategies allowing for a clear discrimination of the multiple subsets of these myeloid cells.

An additional outstanding question that still needs to be fully addressed relates to the "division of labor" among these tumor-promoting myeloid cell populations. As outlined in the previous section, it appears that all the main myeloid populations, TAM, MDSCs, IMCGL, and to some extend DC, are endowed with the capacity to exert many pro-tumoral activities. Recent single cell transcriptomic analysis suggest that, within each of these populations, a dedicated subset or even a single cell, may be equipped with concomitant multitasking activities (through the co-expression of factors involved for instance in immunosuppression, extracellular matrix remodeling, metastasis promotion…). The possibility that dedicated subsets or individual cells may sequentially acquire and lose one of these properties at a given time and depending on the nature of their environment and therefore on their location and on tumor stage is also conceivable, but remains to be clearly demonstrated. This functional plasticity of tumor-associated myeloid cells over time and space may be essential to fulfill the specific needs of growing tumors at each of the sequential stages of their development in the primary tumor sites (promotion of tumor growth, EMT, invasion, angiogenesis, intravasation, immunosuppression, production of chemokines involved in the recruitment of tumor-promoting cells), as CTC in the bloodstream (shielding in heterophilic clusters), and in the pre-metastatic and metastatic niches (soil preparation, ECM remodeling, extravasation, chemoattraction, immunosuppression).

Lastly, questions remain concerning the differences between breast cancer subtypes. Few studies have studied precisely the myeloid landscape and compared the different subtypes. Recent RNAseq findings show that myeloid infiltration is present in all main subtypes ("luminal" or HR positive BC, HER2+, TNBC) at different levels (133). A majority of studies discussed in this review focus on the TNBC subtype, some showing a higher infiltration of IMCGL in the tumors of these patients (90, 93, 96, 111). Macrophages are very represented across the different subtypes (133), though their role and exact phenotype in each subtype is unclear.

As these myeloid cells are essential contributors to many tumor-promoting networks, their therapeutic targeting (elimination, inactivation, reprogramming) has logically led to promising anti-tumor responses. However, the high phenotypic and functional heterogeneity and plasticity of these cells over time and depending on their tissue location has, to date, been a major hurdle for both their use as definitive biomarkers and the development of therapeutic strategies that would specifically interfere with their generation, development and multifaced tumor-promoting functions, which underlines the need to further characterize this myeloid landscape.

AUTHOR CONTRIBUTIONS

CB and NL conceived and wrote the article. TB drew figures and wrote the article. FP and CD wrote the article. All authors contributed to the article and approved the submitted version.

FUNDING

Supported by the French national league against cancer and the SIRIC-BRIO (NL), and the Fondation ARC (CB).

REFERENCES

1. Rondeau E, Larmonier N, Pradeu T, Bikfalvi A. Characterizing Causality in Cancer. *Elife* (2019) 8:1–6. doi: 10.7554/eLife.53755
2. Laplane L, Duluc D, Bikfalvi A, Larmonier N, Pradeu T. Beyond the Tumour Microenvironment. *Int J Cancer* (2019) 145(10):2611–8. doi: 10.1002/ijc.32343
3. Sharma P, Siddiqui BA, Anandhan S, Yadav SS, Subudhi SK, Gao J, et al. The Next Decade of Immune Checkpoint Therapy. *Cancer Discov* (2021) 11 (4):838–57. doi: 10.1158/2159-8290.CD-20-1680
4. Schmid P, Cortes J, Pusztai L, McArthur H, Kummel S, Bergh J, et al. Pembrolizumab for Early Triple-Negative Breast Cancer. *N Engl J Med* (2020) 382(9):810–21. doi: 10.1056/NEJMoa1910549
5. Cortes J, Cescon DW, Rugo HS, Nowecki Z, Im SA, Yusof MM, et al. Pembrolizumab Plus Chemotherapy Versus Placebo Plus Chemotherapy for Previously Untreated Locally Recurrent Inoperable or Metastatic Triple-Negative Breast Cancer (KEYNOTE-355): A Randomised, Placebo-Controlled, Double-Blind, Phase 3 Clinical Trial. *Lancet* (2020) 396 (10265):1817–28. doi: 10.1016/S0140-6736(20)32531-9
6. Vonderheide RH, Domchek SM, Clark AS. Immunotherapy for Breast Cancer: What Are We Missing? *Clin Cancer Res* (2017) 23(11):2640–6. doi: 10.1158/1078-0432.CCR-16-2569
7. Tekpli X, Lien T, Rossevold AH, Nebdal D, Borgen E, Ohnstad HO, et al. An Independent Poor-Prognosis Subtype of Breast Cancer Defined by a Distinct Tumor Immune Microenvironment. *Nat Commun* (2019) 10(1):5499. doi: 10.1038/s41467-019-13329-5
8. Klingen TA, Chen Y, Aas H, Wik E, Akslen LA. Tumor-Associated Macrophages are Strongly Related to Vascular Invasion, non-Luminal Subtypes, and Interval Breast Cancer. *Hum Pathol* (2017) 69:72–80. doi: 10.1016/j.humpath.2017.09.001
9. Qiu SQ, Waaijer SJH, Zwager MC, de Vries EGE, van der Vegt B, Schroder CP. Tumor-Associated Macrophages in Breast Cancer: Innocent Bystander or Important Player? *Cancer Treat Rev* (2018) 70:178–89. doi: 10.1016/j.ctrv.2018.08.010
10. Pelekanou V, Villarroel-Espindola F, Schalper KA, Pusztai L, Rimm DL. CD68, CD163, and Matrix Metalloproteinase 9 (MMP-9) Co-Localization in Breast Tumor Microenvironment Predicts Survival Differently in ER-Positive and -Negative Cancers. *Breast Cancer Res* (2018) 20(1):154. doi: 10.1186/s13058-018-1076-x
11. Zhang WJ, Wang XH, Gao ST, Chen C, Xu XY, Sun Q, et al. Tumor-Associated Macrophages Correlate With Phenomenon of Epithelial-Mesenchymal Transition and Contribute to Poor Prognosis in Triple-Negative Breast Cancer Patients. *J Surg Res* (2018) 222:93–101. doi: 10.1016/j.jss.2017.09.035
12. Ali HR, Chlon L, Pharoah PD, Markowetz F, Caldas C. Patterns of Immune Infiltration in Breast Cancer and Their Clinical Implications: A Gene-Expression-Based Retrospective Study. *PloS Med* (2016) 13(12):e1002194. doi: 10.1371/journal.pmed.1002194
13. Mosser DM, Edwards JP. Exploring the Full Spectrum of Macrophage Activation. *Nat Rev Immunol* (2008) 8(12):958–69. doi: 10.1038/nri2448
14. Murray PJ. Macrophage Polarization. *Annu Rev Physiol* (2017) 79:541–66. doi: 10.1146/annurev-physiol-022516-034339
15. Azizi E, Carr AJ, Plitas G, Cornish AE, Konopacki C, Prabhakaran S, et al. Single-Cell Map of Diverse Immune Phenotypes in the Breast Tumor Microenvironment. *Cell* (2018) 174(5):1293–308.e36. doi: 10.1016/j.cell.2018.05.060
16. Wagner J, Rapsomaniki MA, Chevrier S, Anzeneder T, Langwieder C, Dykgers A, et al. A Single-Cell Atlas of the Tumor and Immune Ecosystem of Human Breast Cancer. *Cell* (2019) 177(5):1330–45.e18. doi: 10.1016/j.cell.2019.03.005
17. Cassetta L, Fragkogianni S, Sims AH, Swierczak A, Forrester LM, Zhang H, et al. Human Tumor-Associated Macrophage and Monocyte Transcriptional Landscapes Reveal Cancer-Specific Reprogramming, Biomarkers, and Therapeutic Targets. *Cancer Cell* (2019) 35(4):588–602.e10. doi: 10.1016/j.ccell.2019.02.009
18. Williams CB, Yeh ES, Soloff AC. Tumor-Associated Macrophages: Unwitting Accomplices in Breast Cancer Malignancy. *NPJ Breast Cancer* (2016) 2:1–12. doi: 10.1038/npjbcancer.2015.25
19. Bent R, Moll L, Grabbe S, Bros M. Interleukin-1 Beta-A Friend or Foe in Malignancies? *Int J Mol Sci* (2018) 19(8):1–34. doi: 10.3390/ijms19082155
20. Mantovani A, Barajon I, Garlanda C. IL-1 and IL-1 Regulatory Pathways in Cancer Progression and Therapy. *Immunol Rev* (2018) 281(1):57–61. doi: 10.1111/imr.12614
21. Racioppi L, Nelson ER, Huang W, Mukherjee D, Lawrence SA, Lento W, et al. CaMKK2 in Myeloid Cells is a Key Regulator of the Immune-Suppressive Microenvironment in Breast Cancer. *Nat Commun* (2019) 10 (1):2450. doi: 10.1038/s41467-019-10424-5
22. Seoane S, Martinez-Ordonez A, Eiro N, Cabezas-Sainz P, Garcia-Caballero L, Gonzalez LO, et al. POU1F1 Transcription Factor Promotes Breast Cancer Metastasis via Recruitment and Polarization of Macrophages. *J Pathol* (2019) 249(3):381–94. doi: 10.1002/path.5324
23. Donzelli S, Milano E, Pruszko M, Sacconi A, Masciarelli S, Iosue I, et al. Expression of ID4 Protein in Breast Cancer Cells Induces Reprogramming of Tumour-Associated Macrophages. *Breast Cancer Res* (2018) 20(1):59. doi: 10.1186/s13058-018-0990-2
24. Valeta-Magara A, Gadi A, Volta V, Walters B, Arju R, Giashuddin S, et al. Inflammatory Breast Cancer Promotes Development of M2 Tumor-Associated Macrophages and Cancer Mesenchymal Cells Through a Complex Chemokine Network. *Cancer Res* (2019) 79(13):3360–71. doi: 10.1158/0008-5472.CAN-17-2158
25. Shrivastava R, Asif M, Singh V, Dubey P, Ahmad Malik S, Lone MU, et al. M2 Polarization of Macrophages by Oncostatin M in Hypoxic Tumor Microenvironment is Mediated by Mtorc2 and Promotes Tumor Growth and Metastasis. *Cytokine* (2019) 118:130–43. doi: 10.1016/j.cyto.2018.03.032
26. Wang L, Li YS, Yu LG, Zhang XK, Zhao L, Gong FL, et al. Galectin-3 Expression and Secretion by Tumor-Associated Macrophages in Hypoxia Promotes Breast Cancer Progression. *Biochem Pharmacol* (2020) 178:114113. doi: 10.1016/j.bcp.2020.114113
27. Trenti A, Tedesco S, Boscaro C, Trevisi L, Bolego C, Cignarella A. Estrogen, Angiogenesis, Immunity and Cell Metabolism: Solving the Puzzle. *Int J Mol Sci* (2018) 19(3):2–16. doi: 10.3390/ijms19030859
28. Svensson S, Abrahamsson A, Rodriguez GV, Olsson AK, Jensen L, Cao Y, et al. CCL2 and CCL5 Are Novel Therapeutic Targets for Estrogen-Dependent Breast Cancer. *Clin Cancer Res* (2015) 21(16):3794–805. doi: 10.1158/1078-0432.CCR-15-0204

29. Dittmer J. Breast Cancer Stem Cells: Features, Key Drivers and Treatment Options. *Semin Cancer Biol* (2018) 53:59–74. doi: 10.1016/j.semcancer.2018.07.007
30. Gok Yavuz B, Gunaydin G, Gedik ME, Kosemehmetoglu K, Karakoc D, Ozgur F, et al. Cancer Associated Fibroblasts Sculpt Tumour Microenvironment by Recruiting Monocytes and Inducing Immunosuppressive PD-1(+) TAMs. *Sci Rep* (2019) 9(1):3172. doi: 10.1038/s41598-019-39553-z
31. Liu D, Lu Q, Wang X, Wang J, Lu N, Jiang Z, et al. LSECtin on Tumor-Associated Macrophages Enhances Breast Cancer Stemness via Interaction With its Receptor BTN3A3. *Cell Res* (2019) 29(5):365–78. doi: 10.1038/s41422-019-0155-6
32. Lu H, Clauser KR, Tam WL, Frose J, Ye X, Eaton EN, et al. A Breast Cancer Stem Cell Niche Supported by Juxtacrine Signalling From Monocytes and Macrophages. *Nat Cell Biol* (2014) 16(11):1105–17. doi: 10.1038/ncb3041
33. Tiwari P, Blank A, Cui C, Schoenfelt KQ, Zhou G, Xu Y, et al. Metabolically Activated Adipose Tissue Macrophages Link Obesity to Triple-Negative Breast Cancer. *J Exp Med* (2019) 216(6):1345–58. doi: 10.1084/jem.20181616
34. Harney AS, Arwert EN, Entenberg D, Wang Y, Guo P, Qian BZ, et al. Real-Time Imaging Reveals Local, Transient Vascular Permeability, and Tumor Cell Intravasation Stimulated by TIE2hi Macrophage-Derived VEGFA. *Cancer Discovery* (2015) 5(9):932–43. doi: 10.1158/2159-8290.CD-15-0012
35. Chen Y, Zhang S, Wang Q, Zhang X. Tumor-Recruited M2 Macrophages Promote Gastric and Breast Cancer Metastasis via M2 Macrophage-Secreted CHI3L1 Protein. *J Hematol Oncol* (2017) 10(1):36. doi: 10.1186/s13045-017-0408-0
36. Little AC, Pathanjeli P, Wu Z, Bao L, Goo LE, Yates JA, et al. IL-4/IL-13 Stimulated Macrophages Enhance Breast Cancer Invasion Via Rho-GTPase Regulation of Synergistic VEGF/CCL-18 Signaling. *Front Oncol* (2019) 9:456. doi: 10.3389/fonc.2019.00456
37. Kersten K, Coffelt SB, Hoogstraat M, Verstegen NJM, Vrijland K, Ciampricotti M, et al. Mammary Tumor-Derived CCL2 Enhances Pro-Metastatic Systemic Inflammation Through Upregulation of IL1beta in Tumor-Associated Macrophages. *Oncoimmunology* (2017) 6(8):e1334744. doi: 10.1080/2162402X.2017.1334744
38. Linde N, Casanova-Acebes M, Sosa MS, Mortha A, Rahman A, Farias E, et al. Macrophages Orchestrate Breast Cancer Early Dissemination and Metastasis. *Nat Commun* (2018) 9(1):21. doi: 10.1038/s41467-017-02481-5
39. Chen XW, Yu TJ, Zhang J, Li Y, Chen HL, Yang GF, et al. CYP4A in Tumor-Associated Macrophages Promotes Pre-Metastatic Niche Formation and Metastasis. *Oncogene* (2017) 36(35):5045–57. doi: 10.1038/onc.2017.118
40. Celus W, Di Conza G, Oliveira AI, Ehling M, Costa BM, Wenes M, et al. Loss of Caveolin-1 in Metastasis-Associated Macrophages Drives Lung Metastatic Growth Through Increased Angiogenesis. *Cell Rep* (2017) 21(10):2842–54. doi: 10.1016/j.celrep.2017.11.034
41. Bieniasz-Krzywiec P, Martin-Perez R, Ehling M, Garcia-Caballero M, Pinioti S, Pretto S, et al. Podoplanin-Expressing Macrophages Promote Lymphangiogenesis and Lymphoinvasion in Breast Cancer. *Cell Metab* (2019) 30(5):917–936 e10. doi: 10.1016/j.cmet.2019.07.015
42. Weichand B, Popp R, Dziumbla S, Mora J, Strack E, Elwakeel E, et al. S1PR1 on Tumor-Associated Macrophages Promotes Lymphangiogenesis and Metastasis via NLRP3/IL-1beta. *J Exp Med* (2017) 214(9):2695–713. doi: 10.1084/jem.20160392
43. Storr SJ, Safuan S, Ahmad N, El-Refaee M, Jackson AM, Martin SG. Macrophage-Derived Interleukin-1beta Promotes Human Breast Cancer Cell Migration and Lymphatic Adhesion In Vitro. *Cancer Immunol Immunother* (2017) 66(10):1287–94. doi: 10.1007/s00262-017-2020-0
44. Gabrilovich DI, Bronte V, Chen SH, Colombo MP, Ochoa A, Ostrand-Rosenberg S, et al. The Terminology Issue for Myeloid-Derived Suppressor Cells. *Cancer Res* (2007) 67(1):425.doi: 10.1158/0008-5472.CAN-06-3037
45. Gabrilovich DI, Ostrand-Rosenberg S, Bronte V. Coordinated Regulation of Myeloid Cells by Tumours. *Nat Rev Immunol* (2012) 12(4):253–68. doi: 10.1038/nri3175
46. Condamine T, Ramachandran I, Youn JI, Gabrilovich DI. Regulation of Tumor Metastasis by Myeloid-Derived Suppressor Cells. *Annu Rev Med* (2015) 66:97–110. doi: 10.1146/annurev-med-051013-052304
47. Liu QW, Chen Y, Li JY, Xiao L, Zhang WJ, Zhao JL, et al. Bone Marrow Cells are Differentiated Into MDSCs by BCC-Ex Through Down-Regulating the Expression of CXCR4 and Activating STAT3 Signalling Pathway. *J Cell Mol Med* (2021) 25(12):5497–510. doi: 10.1111/jcmm.16559
48. Keklikoglou I, Cianciaruso C, Guc E, Squadrito ML, Spring LM, Tazzyman S, et al. Chemotherapy Elicits Pro-Metastatic Extracellular Vesicles in Breast Cancer Models. *Nat Cell Biol* (2019) 21(2):190–202. doi: 10.1038/s41556-018-0256-3
49. Ouyang L, Chang W, Fang B, Qin J, Qu X, Cheng F. Estrogen-Induced SDF-1alpha Production Promotes the Progression of ER-Negative Breast Cancer via the Accumulation of MDSCs in the Tumor Microenvironment. *Sci Rep* (2016) 6:39541. doi: 10.1038/srep39541
50. Bronte V, Brandau S, Chen SH, Colombo MP, Frey AB, Greten TF, et al. Recommendations for Myeloid-Derived Suppressor Cell Nomenclature and Characterization Standards. *Nat Commun* (2016) 7:12150. doi: 10.1038/ncomms12150
51. Veglia F, Perego M, Gabrilovich D. Myeloid-Derived Suppressor Cells Coming of Age. *Nat Immunol* (2018) 19(2):108–19. doi: 10.1038/s41590-017-0022-x
52. Ouzounova M, Lee E, Piranlioglu R, El Andaloussi A, Kolhe R, Demirci MF, et al. Monocytic and Granulocytic Myeloid Derived Suppressor Cells Differentially Regulate Spatiotemporal Tumour Plasticity During Metastatic Cascade. *Nat Commun* (2017) 8:14979. doi: 10.1038/ncomms14979
53. Thomas GD, Hamers AAJ, Nakao C, Marcovecchio P, Taylor AM, McSkimming C, et al. Human Blood Monocyte Subsets: A New Gating Strategy Defined Using Cell Surface Markers Identified by Mass Cytometry. *Arterioscler Thromb Vasc Biol* (2017) 37(8):1548–58. doi: 10.1161/ATVBAHA.117.309145
54. Bergenfelz C, Larsson AM, von Stedingk K, Gruvberger-Saal S, Aaltonen K, Jansson S, et al. Systemic Monocytic-MDSCs Are Generated From Monocytes and Correlate With Disease Progression in Breast Cancer Patients. *PloS One* (2015) 10(5):e0127028. doi: 10.1371/journal.pone.0127028
55. Jung K, Heishi T, Incio J, Huang Y, Beech EY, Pinter M, et al. Targeting CXCR4-Dependent Immunosuppressive Ly6C(low) Monocytes Improves Antiangiogenic Therapy in Colorectal Cancer. *Proc Natl Acad Sci U.S.A.* (2017) 114(39):10455–60. doi: 10.1073/pnas.1710754114
56. Jung K, Heishi T, Khan OF, Kowalski PS, Incio J, Rahbari NN, et al. Ly6Clo Monocytes Drive Immunosuppression and Confer Resistance to Anti-VEGFR2 Cancer Therapy. *J Clin Invest* (2017) 127(8):3039–51. doi: 10.1172/JCI93182
57. Jeong J, Suh Y, Jung K. Context Drives Diversification of Monocytes and Neutrophils in Orchestrating the Tumor Microenvironment. *Front Immunol* (2019) 10:1817. doi: 10.3389/fimmu.2019.01817
58. Jeong J, Kim DK, Park JH, Park DJ, Lee HJ, Yang HK, et al. Tumor-Infiltrating Neutrophils and Non-Classical Monocytes May Be Potential Therapeutic Targets for HER2(negative) Gastric Cancer. *Immune Netw* (2021) 21(4):e31. doi: 10.4110/in.2021.21.e31
59. Toor SM, Syed Khaja AS, El Salhat H, Faour I, Kanbar J, Quadri AA, et al. Myeloid Cells in Circulation and Tumor Microenvironment of Breast Cancer Patients. *Cancer Immunol Immunother* (2017) 66(6):753–64. doi: 10.1007/s00262-017-1977-z
60. Safarzadeh E, Mohammadi A, Mansoori B, Duijf PHG, Hashemzadeh S, Khaze V, et al. STAT3 Silencing and TLR7/8 Pathway Activation Repolarize and Suppress Myeloid-Derived Suppressor Cells From Breast Cancer Patients. *Front Immunol* (2020) 11:613215. doi: 10.3389/fimmu.2020.613215
61. Wang PF, Song SY, Wang TJ, Ji WJ, Li SW, Liu N, et al. Prognostic Role of Pretreatment Circulating MDSCs in Patients With Solid Malignancies: A Meta-Analysis of 40 Studies. *Oncoimmunology* (2018) 7(10):e1494113. doi: 10.1080/2162402X.2018.1494113
62. Salvador-Coloma C, Santaballa A, Sanmartin E, Calvo D, Garcia A, Hervas D, et al. Immunosuppressive Profiles in Liquid Biopsy at Diagnosis Predict Response to Neoadjuvant Chemotherapy in Triple-Negative Breast Cancer. *Eur J Cancer* (2020) 139:119–34. doi: 10.1016/j.ejca.2020.08.020
63. Yu J, Du W, Yan F, Wang Y, Li H, Cao S, et al. Myeloid-Derived Suppressor Cells Suppress Antitumor Immune Responses Through IDO Expression and Correlate With Lymph Node Metastasis in Patients With Breast Cancer. *J Immunol* (2013) 190(7):3783–97. doi: 10.4049/jimmunol.1201449

64. Peng D, Tanikawa T, Li W, Zhao L, Vatan L, Szeliga W, et al. Myeloid-Derived Suppressor Cells Endow Stem-Like Qualities to Breast Cancer Cells Through IL6/STAT3 and NO/NOTCH Cross-Talk Signaling. *Cancer Res* (2016) 76(11):3156–65. doi: 10.1158/0008-5472.CAN-15-2528
65. Bauer R, Udonta F, Wroblewski M, Ben-Batalla I, Santos IM, Taverna F, et al. Blockade of Myeloid-Derived Suppressor Cell Expansion With All-Trans Retinoic Acid Increases the Efficacy of Antiangiogenic Therapy. *Cancer Res* (2018) 78(12):3220–32. doi: 10.1158/0008-5472.CAN-17-3415
66. Liu L, Yang L, Yan W, Zhai J, Pizzo DP, Chu P, et al. Chemotherapy Induces Breast Cancer Stemness in Association With Dysregulated Monocytosis. *Clin Cancer Res* (2018) 24(10):2370–82. doi: 10.1158/1078-0432.CCR-17-2545
67. Eisenblaetter M, Flores-Borja F, Lee JJ, Wefers C, Smith H, Hueting R, et al. Visualization of Tumor-Immune Interaction - Target-Specific Imaging of S100A8/A9 Reveals Pre-Metastatic Niche Establishment. *Theranostics* (2017) 7(9):2392–401. doi: 10.7150/thno.17138
68. Yan HH, Pickup M, Pang Y, Gorska AE, Li Z, Chytil A, et al. Gr-1+CD11b+ Myeloid Cells Tip the Balance of Immune Protection to Tumor Promotion in the Premetastatic Lung. *Cancer Res* (2010) 70(15):6139–49. doi: 10.1158/0008-5472.CAN-10-0706
69. Koelwyn GJ, Newman AAC, Afonso MS, van Solingen C, Corr EM, Brown EJ, et al. Myocardial Infarction Accelerates Breast Cancer via Innate Immune Reprogramming. *Nat Med* (2020) 26(9):1452–8. doi: 10.1038/s41591-020-0964-7
70. Spiegel A, Brooks MW, Houshyar S, Reinhardt F, Ardolino M, Fessler E, et al. Neutrophils Suppress Intraluminal NK Cell-Mediated Tumor Cell Clearance and Enhance Extravasation of Disseminated Carcinoma Cells. *Cancer Discovery* (2016) 6(6):630–49. doi: 10.1158/2159-8290.CD-15-1157
71. Hiratsuka S, Duda DG, Huang Y, Goel S, Sugiyama T, Nagasawa T, et al. C-X-C Receptor Type 4 Promotes Metastasis by Activating P38 Mitogen-Activated Protein Kinase in Myeloid Differentiation Antigen (Gr-1)-Positive Cells. *Proc Natl Acad Sci U.S.A.* (2011) 108(1):302–7. doi: 10.1073/pnas.1016917108
72. Ghouse SM, Vadrevu SK, Manne S, Reese B, Patel J, Patel B, et al. Therapeutic Targeting of Vasculature in the Premetastatic and Metastatic Niches Reduces Lung Metastasis. *J Immunol* (2020) 204(4):990–1000. doi: 10.4049/jimmunol.1901208
73. Hsu YL, Yen MC, Chang WA, Tsai PH, Pan YC, Liao SH, et al. CXCL17-Derived CD11b(+)Gr-1(+) Myeloid-Derived Suppressor Cells Contribute to Lung Metastasis of Breast Cancer Through Platelet-Derived Growth Factor-BB. *Breast Cancer Res* (2019) 21(1):23. doi: 10.1186/s13058-019-1114-3
74. Kitamura T, Doughty-Shenton D, Cassetta L, Fragkogianni S, Brownlie D, Kato Y, et al. Monocytes Differentiate to Immune Suppressive Precursors of Metastasis-Associated Macrophages in Mouse Models of Metastatic Breast Cancer. *Front Immunol* (2017) 8:2004. doi: 10.3389/fimmu.2017.02004
75. Biswas S, Mandal G, Roy Chowdhury S, Purohit S, Payne KK, Anadon C, et al. Exosomes Produced by Mesenchymal Stem Cells Drive Differentiation of Myeloid Cells Into Immunosuppressive M2-Polarized Macrophages in Breast Cancer. *J Immunol* (2019) 203(12):3447–60. doi: 10.4049/jimmunol.1900692
76. Sawant A, Deshane J, Jules J, Lee CM, Harris BA, Feng X, et al. Myeloid-Derived Suppressor Cells Function as Novel Osteoclast Progenitors Enhancing Bone Loss in Breast Cancer. *Cancer Res* (2013) 73(2):672–82. doi: 10.1158/0008-5472.CAN-12-2202
77. Danilin S, Merkel AR, Johnson JR, Johnson RW, Edwards JR, Sterling JA. Myeloid-Derived Suppressor Cells Expand During Breast Cancer Progression and Promote Tumor-Induced Bone Destruction. *Oncoimmunology* (2012) 1(9):1484–94. doi: 10.4161/onci.21990
78. Casbon AJ, Reynaud D, Park C, Khuc E, Gan DD, Schepers K, et al. Invasive Breast Cancer Reprograms Early Myeloid Differentiation in the Bone Marrow to Generate Immunosuppressive Neutrophils. *Proc Natl Acad Sci U.S.A.* (2015) 112(6):E566–75. doi: 10.1073/pnas.1424927112
79. Gustafson MP, Lin Y, Maas ML, Van Keulen VP, Johnston PB, Peikert T, et al. A Method for Identification and Analysis of non-Overlapping Myeloid Immunophenotypes in Humans. *PloS One* (2015) 10(3):e0121546. doi: 10.1371/journal.pone.0121546
80. Lakschevitz FS, Hassanpour S, Rubin A, Fine N, Sun C, Glogauer M. Identification of Neutrophil Surface Marker Changes in Health and Inflammation Using High-Throughput Screening Flow Cytometry. *Exp Cell Res* (2016) 342(2):200–9. doi: 10.1016/j.yexcr.2016.03.007
81. Condamine T, Dominguez GA, Youn JI, Kossenkov AV, Mony S, Alicea-Torres K, et al. Lectin-Type Oxidized LDL Receptor-1 Distinguishes Population of Human Polymorphonuclear Myeloid-Derived Suppressor Cells in Cancer Patients. *Sci Immunol* (2016) 1(2):1–32. doi: 10.1126/sciimmunol.aaf8943
82. Alshetaiwi H, Pervolarakis N, McIntyre LL, Ma D, Nguyen Q, Rath JA, et al. Defining the Emergence of Myeloid-Derived Suppressor Cells in Breast Cancer Using Single-Cell Transcriptomics. *Sci Immunol* (2020) 5(44):1–28. doi: 10.1126/sciimmunol.aay6017
83. Fridlender ZG, Sun J, Kim S, Kapoor V, Cheng G, Ling L, et al. Polarization of Tumor-Associated Neutrophil Phenotype by TGF-Beta: "N1" Versus "N2" TAN. *Cancer Cell* (2009) 16(3):183–94. doi: 10.1016/j.ccr.2009.06.017
84. Coffelt SB, Wellenstein MD, de Visser KE. Neutrophils in Cancer: Neutral No More. *Nat Rev Cancer* (2016) 16(7):431–46. doi: 10.1038/nrc.2016.52
85. Mehmeti-Ajradini M, Bergenfelz C, Larsson AM, Carlsson R, Riesbeck K, Ahl J, et al. Human G-MDSCs are Neutrophils at Distinct Maturation Stages Promoting Tumor Growth in Breast Cancer. *Life Sci Alliance* (2020) 3 (11):1–19. doi: 10.26508/lsa.202000893
86. Kim IS, Gao Y, Welte T, Wang H, Liu J, Janghorban M, et al. Immuno-Subtyping of Breast Cancer Reveals Distinct Myeloid Cell Profiles and Immunotherapy Resistance Mechanisms. *Nat Cell Biol* (2019) 21(9):1113–26. doi: 10.1038/s41556-019-0373-7
87. Huszno J, Kolosza. Prognostic Value of the Neutrophil-Lymphocyte, Platelet-Lymphocyte and Monocyte-Lymphocyte Ratio in Breast Cancer Patients. *Oncol Lett* (2019) 18(6):6275–83. doi: 10.3892/ol.2019.10966
88. Ethier JL, Desautels D, Templeton A, Shah PS, Amir E. Prognostic Role of Neutrophil-To-Lymphocyte Ratio in Breast Cancer: A Systematic Review and Meta-Analysis. *Breast Cancer Res: BCR* (2017) 19(1):1–13. doi: 10.1186/s13058-016-0794-1
89. Wu L, Saxena S, Goel P, Prajapati DR, Wang C, Singh RK. Breast Cancer Cell-Neutrophil Interactions Enhance Neutrophil Survival and Pro-Tumorigenic Activities. *Cancers (Basel)* (2020) 12(10):1–18. doi: 10.3390/cancers12102884
90. Wang Y, Chen J, Yang L, Li J, Wu W, Huang M, et al. Tumor-Contacted Neutrophils Promote Metastasis by a CD90-TIMP-1 Juxtacrine-Paracrine Loop. *Clin Cancer Res* (2019) 25(6):1957–69. doi: 10.1158/1078-0432.CCR-18-2544
91. Jaillon S, Ponzetta A, Di Mitri D, Santoni A, Bonecchi R, Mantovani A. Neutrophil Diversity and Plasticity in Tumour Progression and Therapy. *Nat Rev Cancer* (2020) 20(9):485–503. doi: 10.1038/s41568-020-0281-y
92. Liang W, Li Q, Ferrara N. Metastatic Growth Instructed by Neutrophil-Derived Transferrin. *Proc Natl Acad Sci USA* (2018) 115(43):11060–5. doi: 10.1073/pnas.1811717115
93. Xiao Y, Cong M, Li J, He D, Wu Q, Tian P, et al. Cathepsin C Promotes Breast Cancer Lung Metastasis by Modulating Neutrophil Infiltration and Neutrophil Extracellular Trap Formation. *Cancer Cell* (2020) 39(3):423–37.e7. doi: 10.1016/j.ccell.2020.12.012
94. Wellenstein MD, Coffelt SB, Duits DEM, van Miltenburg MH, Slagter M, de Rink I, et al. Loss of P53 Triggers WNT-Dependent Systemic Inflammation to Drive Breast Cancer Metastasis. *Nature* (2019) 572(7770):538–42. doi: 10.1038/s41586-019-1450-6
95. Papayannopoulos V. Neutrophil Extracellular Traps in Immunity and Disease. *Nat Rev Immunol* (2018) 18(2):134–47. doi: 10.1038/nri.2017.105
96. Kumar S, Wilkes DW, Samuel N, Blanco MA, Nayak A, Alicea-Torres K, et al. DeltaNp63-Driven Recruitment of Myeloid-Derived Suppressor Cells Promotes Metastasis in Triple-Negative Breast Cancer. *J Clin Invest* (2018) 128(11):5095–109. doi: 10.1172/JCI99673
97. Luo A, Meng M, Wang G, Han R, Zhang Y, Jing X, et al. Myeloid-Derived Suppressor Cells Recruited by Chemokine (C-C Motif) Ligand 3 Promote the Progression of Breast Cancer via Phosphoinositide 3-Kinase-Protein Kinase B-Mammalian Target of Rapamycin Signaling. *J Breast Cancer* (2020) 23(2):141–61. doi: 10.4048/jbc.2020.23.e26
98. Janiszewska M, Tabassum DP, Castano Z, Cristea S, Yamamoto KN, Kingston NL, et al. Subclonal Cooperation Drives Metastasis by Modulating Local and Systemic Immune Microenvironments. *Nat Cell Biol* (2019) 21(7):879–88. doi: 10.1038/s41556-019-0346-x
99. Robichaud N, Hsu BE, Istomine R, Alvarez F, Blagih J, Ma EH, et al. Translational Control in the Tumor Microenvironment Promotes Lung

Metastasis: Phosphorylation of Eif4e in Neutrophils. *Proc Natl Acad Sci U.S.A.* (2018) 115(10):E2202–9. doi: 10.1073/pnas.1717439115
100. Coffelt SB, Kersten K, Doornebal CW, Weiden J, Vrijland K, Hau CS, et al. IL-17-Producing γδ T Cells and Neutrophils Conspire to Promote Breast Cancer Metastasis. *Nature* (2015) 522(7556):345–8. doi: 10.1038/nature14282
101. Li P, Lu M, Shi J, Hua L, Gong Z, Li Q, et al. Dual Roles of Neutrophils in Metastatic Colonization are Governed by the Host NK Cell Status. *Nat Commun* (2020) 11(1):4387. doi: 10.1038/s41467-020-18125-0
102. Vazquez Rodriguez G, Abrahamsson A, Jensen LD, Dabrosin C. Estradiol Promotes Breast Cancer Cell Migration via Recruitment and Activation of Neutrophils. *Cancer Immunol Res* (2017) 5(3):234–47. doi: 10.1158/2326-6066.CIR-16-0150
103. Szczerba BM, Castro-Giner F, Vetter M, Krol I, Gkountela S, Landin J, et al. Neutrophils Escort Circulating Tumour Cells to Enable Cell Cycle Progression. *Nature* (2019) 566(7745):553–7. doi: 10.1038/s41586-019-0915-y
104. Sprouse ML, Welte T, Boral D, Liu HN, Yin W, Vishnoi M, et al. PMN-MDSCs Enhance CTC Metastatic Properties Through Reciprocal Interactions via ROS/Notch/Nodal Signaling. *Int J Mol Sci* (2019) 20(8):1–20. doi: 10.3390/ijms20081916
105. Ombrato L, Nolan E, Kurelac I, Mavousian A, Bridgeman VL, Heinze I, et al. Metastatic-Niche Labelling Reveals Parenchymal Cells With Stem Features. *Nature* (2019) 572(7771):603–8. doi: 10.1038/s41586-019-1487-6
106. Hsu BE, Tabaries S, Johnson RM, Andrzejewski S, Senecal J, Lehuede C, et al. Immature Low-Density Neutrophils Exhibit Metabolic Flexibility That Facilitates Breast Cancer Liver Metastasis. *Cell Rep* (2019) 27(13):3902–3915 e6. doi: 10.1016/j.celrep.2019.05.091
107. Sangaletti S, Talarico G, Chiodoni C, Cappetti B, Botti L, Portararo P, et al. SPARC Is a New Myeloid-Derived Suppressor Cell Marker Licensing Suppressive Activities. *Front Immunol* (2019) 10:1369. doi: 10.3389/fimmu.2019.01369
108. Snoderly HT, Boone BA, Bennewitz MF. Neutrophil Extracellular Traps in Breast Cancer and Beyond: Current Perspectives on NET Stimuli, Thrombosis and Metastasis, and Clinical Utility for Diagnosis and Treatment. *Breast Cancer Res* (2019) 21(1):145. doi: 10.1186/s13058-019-1237-6
109. Pan H, Gray R, Braybrooke J, Davies C, Taylor C, McGale P, et al. 20-Year Risks of Breast-Cancer Recurrence After Stopping Endocrine Therapy at 5 Years. *N Engl J Med* (2017) 377(19):1836–46. doi: 10.1056/NEJMoa1701830
110. Albrengues J, Shields MA, Ng D, Park CG, Ambrico A, Poindexter ME, et al. Neutrophil Extracellular Traps Produced During Inflammation Awaken Dormant Cancer Cells in Mice. *Science* (2018) 361(6409):1–30. doi: 10.1126/science.aao4227
111. Park J, Wysocki RW, Amoozgar Z, Maiorino L, Fein MR, Jorns J, et al. Cancer Cells Induce Metastasis-Supporting Neutrophil Extracellular DNA Traps. *Sci Transl Med* (2016) 8(361):361ra138. doi: 10.1126/scitranslmed.aag1711
112. Yang L, Liu Q, Zhang X, Liu X, Zhou B, Chen J, et al. DNA of Neutrophil Extracellular Traps Promotes Cancer Metastasis via CCDC25. *Nature* (2020) 583(7814):133–8. doi: 10.1038/s41586-020-2394-6
113. Teijeira A, Garasa S, Gato M, Alfaro C, Migueliz I, Cirella A, et al. CXCR1 and CXCR2 Chemokine Receptor Agonists Produced by Tumors Induce Neutrophil Extracellular Traps That Interfere With Immune Cytotoxicity. *Immunity* (2020) 52(5):856–871 e8. doi: 10.1016/j.immuni.2020.03.001
114. Hanke N, Alizadeh D, Katsanis E, Larmonier N. Dendritic Cell Tumor Killing Activity and its Potential Applications in Cancer Immunotherapy. *Crit Rev Immunol* (2013) 33(1):1–21. doi: 10.1615/CritRevImmunol.2013006679
115. Wculek SK, Cueto FJ, Mujal AM, Melero I, Krummel MF, Sancho D. Dendritic Cells in Cancer Immunology and Immunotherapy. *Nat Rev Immunol* (2020) 20(1):7–24. doi: 10.1038/s41577-019-0210-z
116. Zong J, Keskinov AA, Shurin GV, Shurin MR. Tumor-Derived Factors Modulating Dendritic Cell Function. *Cancer Immunol Immunother* (2016) 65(7):821–33. doi: 10.1007/s00262-016-1820-y
117. Gabrilovich D. Mechanisms and Functional Significance of Tumour-Induced Dendritic-Cell Defects. *Nat Rev Immunol* (2004) 4(12):941–52. doi: 10.1038/nri1498
118. Janikashvili N, Bonnotte B, Katsanis E, Larmonier N. The Dendritic Cell-Regulatory T Lymphocyte Crosstalk Contributes to Tumor-Induced Tolerance. *Clin Dev Immunol* (2011) 2011:430394. doi: 10.1155/2011/430394
119. Long J, Hu Z, Xue H, Wang Y, Chen J, Tang F, et al. Vascular Endothelial Growth Factor (VEGF) Impairs the Motility and Immune Function of Human Mature Dendritic Cells Through the VEGF Receptor 2-RhoA-Cofilin1 Pathway. *Cancer Sci* (2019) 110(8):2357–67. doi: 10.1111/cas.14091
120. Sisirak V, Vey N, Goutagny N, Renaudineau S, Malfroy M, Thys S, et al. Breast Cancer-Derived Transforming Growth Factor-Beta and Tumor Necrosis Factor-Alpha Compromise Interferon-Alpha Production by Tumor-Associated Plasmacytoid Dendritic Cells. *Int J Cancer* (2013) 133 (3):771–8. doi: 10.1002/ijc.28072
121. Ruffell B, Chang-Strachan D, Chan V, Rosenbusch A, Ho CM, Pryer N, et al. Macrophage IL-10 Blocks CD8+ T Cell-Dependent Responses to Chemotherapy by Suppressing IL-12 Expression in Intratumoral Dendritic Cells. *Cancer Cell* (2014) 26(5):623–37. doi: 10.1016/j.ccell.2014.09.006
122. Pockaj BA, Basu GD, Pathangey LB, Gray RJ, Hernandez JL, Gendler SJ, et al. Reduced T-Cell and Dendritic Cell Function is Related to Cyclooxygenase-2 Overexpression and Prostaglandin E2 Secretion in Patients With Breast Cancer. *Ann Surg Oncol* (2004) 11(3):328–39. doi: 10.1245/ASO.2004.05.027
123. Gervais A, Leveque J, Bouet-Toussaint F, Burtin F, Lesimple T, Sulpice L, et al. Dendritic Cells are Defective in Breast Cancer Patients: A Potential Role for Polyamine in This Immunodeficiency. *Breast Cancer Res* (2005) 7(3): R326–35. doi: 10.1186/bcr1001
124. Norian LA, Rodriguez PC, O'Mara LA, Zabaleta J, Ochoa AC, Cella M, et al. Tumor-Infiltrating Regulatory Dendritic Cells Inhibit CD8+ T Cell Function via L-Arginine Metabolism. *Cancer Res* (2009) 69(7):3086–94. doi: 10.1158/0008-5472.CAN-08-2826
125. Ning Y, Shen K, Wu Q, Sun X, Bai Y, Xie Y, et al. Tumor Exosomes Block Dendritic Cells Maturation to Decrease the T Cell Immune Response. *Immunol Lett* (2018) 199:36–43. doi: 10.1016/j.imlet.2018.05.002
126. Hanks BA, Holtzhausen A, Evans KS, Jamieson R, Gimpel P, Campbell OM, et al. Type III TGF-Beta Receptor Downregulation Generates an Immunotolerant Tumor Microenvironment. *J Clin Invest* (2013) 123 (9):3925–40. doi: 10.1172/JCI65745
127. Faget J, Bendriss-Vermare N, Gobert M, Durand I, Olive D, Biota C, et al. ICOS-Ligand Expression on Plasmacytoid Dendritic Cells Supports Breast Cancer Progression by Promoting the Accumulation of Immunosuppressive CD4+ T Cells. *Cancer Res* (2012) 72(23):6130–41. doi: 10.1158/0008-5472.CAN-12-2409
128. Pedroza-Gonzalez A, Xu K, Wu TC, Aspord C, Tindle S, Marches F, et al. Thymic Stromal Lymphopoietin Fosters Human Breast Tumor Growth by Promoting Type 2 Inflammation. *J Exp Med* (2011) 208(3):479–90. doi: 10.1084/jem.20102131
129. Fainaru O, Almog N, Yung CW, Nakai K, Montoya-Zavala M, Abdollahi A, et al. Tumor Growth and Angiogenesis are Dependent on the Presence of Immature Dendritic Cells. *FASEB J* (2010) 24(5):1411–8. doi: 10.1096/fj.09-147025
130. Gadalla R, Hassan H, Ibrahim SA, Abdullah MS, Gaballah A, Greve B, et al. Tumor Microenvironmental Plasmacytoid Dendritic Cells Contribute to Breast Cancer Lymph Node Metastasis via CXCR4/SDF-1 Axis. *Breast Cancer Res Treat* (2019) 174(3):679–91. doi: 10.1007/s10549-019-05129-8
131. Chen L, Zheng H, Yu X, Liu L, Li H, Zhu H, et al. Tumor-Secreted GRP78 Promotes the Establishment of a Pre-Metastatic Niche in the Liver Microenvironment. *Front Immunol* (2020) 11:584458. doi: 10.3389/fimmu.2020.584458
132. Monteiro AC, Bonomo A. Dendritic Cells Development Into Osteoclast-Type APCs by 4T1 Breast Tumor T Cells Milieu Boost Bone Consumption. *Bone* (2020) 143:115755. doi: 10.1016/j.bone.2020.115755
133. Pal B, Chen Y, Vaillant F, Capaldo BD, Joyce R, Song X, et al. A Single-Cell RNA Expression Atlas of Normal, Preneoplastic and Tumorigenic States in the Human Breast. *EMBO J* (2021) 40(11):e107333. doi: 10.15252/embj.2020107333

Conflict of Interest: The authors declare that the research was conducted in the absence of any commercial or financial relationships that could be construed as a potential conflict of interest.

this article, or claim that may be made by its manufacturer, is not guaranteed or endorsed by the publisher.

frontiers | Frontiers in Immunology

ORIGINAL RESEARCH
published: 20 April 2022
doi: 10.3389/fimmu.2022.859738

IL-9 Producing Tumor-Infiltrating Lymphocytes and Treg Subsets Drive Immune Escape of Tumor Cells in Non-Small Cell Lung Cancer

Lisanne Heim[1†], Zuqin Yang[1†], Patrick Tausche[1], Katja Hohenberger[1], Mircea T. Chiriac[2], Julia Koelle[1], Carol-Immanuel Geppert[3‡], Katerina Kachler[1], Sarah Miksch[1], Anna Graser[1], Juliane Friedrich[1], Rakshin Kharwadkar[4], Ralf J. Rieker[3‡], Denis I. Trufa[5‡], Horia Sirbu[5‡], Markus F. Neurath[2‡§], Mark H. Kaplan[4] and Susetta Finotto[1†]*

[1] Department of Molecular Pneumology, Friedrich-Alexander-Universität Erlangen-Nürnberg (FAU), Erlangen, Germany,
[2] Department of Internal Medicine 1, Friedrich-Alexander-Universität Erlangen-Nürnberg (FAU), Erlangen, Germany,
[3] Institute of Pathology, Friedrich-Alexander-Universität Erlangen-Nürnberg (FAU), Erlangen, Germany,
[4] Department of Microbiology and Immunology, Indiana University School of Medicine, Indianapolis, IN, United States,
[5] Department of Thoracic Surgery, Friedrich-Alexander-Universität Erlangen-Nürnberg (FAU), Erlangen, Germany

Although lung cancer is the leading cause of cancer deaths worldwide, the mechanisms how lung cancer cells evade the immune system remain incompletely understood. Here, we discovered IL-9-dependent signaling mechanisms that drive immune evasion in non-small cell lung cancer (NSCLC). We found increased IL-9 and IL-21 production by T cells in the tumoral region of the lung of patients with NSCLC, suggesting the presence of Th9 cells in the lung tumor microenvironment. Moreover, we noted IL-9 producing Tregs in NSCLC. IL-9 target cells in NSCLC consisted of IL-9R+ tumor cells and tumor-infiltrating lymphocytes. In two murine experimental models of NSCLC, and *in vitro*, IL-9 prevented cell death and controlled growth of lung adenocarcinoma cells. Targeted deletion of IL-9 resulted in successful lung tumor rejection *in vivo* associated with an induction of IL-21 and reduction of Treg cells. Finally, anti-IL-9 antibody immunotherapy resulted in suppression of tumor development even in established experimental NSCLC and was associated with reduced IL-10 production in the lung. In conclusion, our findings indicate that IL-9 drives immune escape of lung tumor cells *via* effects on tumor cell survival and tumor infiltrating T cells. Thus, strategies blocking IL-9 emerge as a new approach for clinical therapy of lung cancer.

Keywords: IL-9, immune escape, NSCLC, TIL, tumor immunotherapy

OPEN ACCESS

Edited by:
Nicole Joller,
University of Zurich, Switzerland

Reviewed by:
Davide Mangani,
Harvard Medical School, United States
Carsten Krieg,
Medical University of South Carolina, United States

****Correspondence:***
Susetta Finotto
susetta.finotto@uk-erlangen.de

[†]These authors have contributed equally to this work and share first authorship

[‡]Comprehensive Cancer Center Erlangen-EMN (CCC ER-EMN), Erlangen, Germany

[§]Deutsches Zentrum Immuntherapie DZI

Specialty section:
This article was submitted to Cancer Immunity and Immunotherapy, a section of the journal Frontiers in Immunology

Received: *21 January 2022*
Accepted: *10 March 2022*
Published: *20 April 2022*

Citation:
Heim L, Yang Z, Tausche P, Hohenberger K, Chiriac MT, Koelle J, Geppert C-I, Kachler K, Miksch S, Graser A, Friedrich J, Kharwadkar R, Rieker RJ, Trufa DI, Sirbu H, Neurath MF, Kaplan MH and Finotto S (2022) IL-9 Producing Tumor-Infiltrating Lymphocytes and Treg Subsets Drive Immune Escape of Tumor Cells in Non-Small Cell Lung Cancer. Front. Immunol. 13:859738. doi: 10.3389/fimmu.2022.859738

INTRODUCTION

Lung cancer (small and non-small cell lung cancer) represents the leading cause of cancer deaths worldwide (1, 2). In non-small cell lung cancer (NSCLC), growth and progress of the disease is associated with a local expansion of regulatory T cells (Treg) that suppress anti-tumor immune responses thus creating an immunosuppressive environment facilitating immune escape of tumor

cells. Recent studies suggest that immunotherapy with PD1/PDL1 checkpoint inhibitors could be a promising approach to activate anti-tumor immune responses and to improve the prognosis for this disease (3, 4). However, the role of cytokines in controlling anti-tumor immune responses in NSCLC remains incompletely understood (5). This aspect is relevant since only 20% of the patients with NSCLC respond to current immunotherapies (6).

Interleukin-9 (IL-9) is a cytokine with pleiotropic functions that was first purified and characterized as a T cell and mast cell growth factor (7). T lymphocytes have been identified as a major source of IL-9 (8–11). However, different T cell subsets, mast cells and innate lymphoid cells-type 2 (ILC2) have the common capability to produce this cytokine (8, 12). Regarding the development of T cells producing IL-9 (Th9) it is known that naïve T-cells in the presence of TGF-beta and interleukin-4 (IL-4) produce IL-9 (13). These cytokines also induce IL-9 production in activated T cells. Hereby, IL-4 activates intracellularly several transcription factors like signal transducer and activator of transcription 6 (STAT6), interferon regulatory factor 4 (IRF4), GATA-binding protein 3 (GATA3), basic leucine zipper transcription factor ATF-like (BATF) and nuclear factor of activated T cells (NFAT) (13, 14). Moreover, the transcription factor PU1 binds to a purine-rich sequence known as the PU-box found on enhancers of target genes. PU1 is a transcription factor of the Erythroblast Transformation Specific (ETS)- family of transcription factors, activated downstream of Transforming growth factor beta (TGF-beta) receptor signaling, that has been demonstrated to bind to the IL-9 promoter in T cells and induces IL-9 production after TGF-beta and IL-4 stimulation in cell culture (11, 15). In addition, several other transcription factors seem to play an important role in the development of Th9 cells including the SMA ("small" worm phenotype) and MAD family ("Mothers Against Decapentaplegic") of genes known as SMAD proteins as well as the members of the signal transducers and activators of transcription family STAT5 and STAT6 (16). STAT5 is activated downstream of IL-2 and IL-9 signaling and controls IL-9 production in T cells (17). In addition to STAT5, IL-9 activates STAT3 resulting in Th17 and T regulatory cell induction (18). By contrast, STAT6 is the major component of the IL-4-receptor signaling pathway and is therefore also involved in controlling the Th9 phenotype (8). STAT6 is also able to suppress expression of the Th1-associated transcription factor T-box expressed in T cells (T-bet), a known inducer of IFN-ɣ production that inhibits TGFβ-induced expression of Foxp3 (8, 19, 20). It has also been demonstrated that, T cell receptor (TCR) signaling and co-stimulatory molecules regulate IL-9 production. On the one hand, TCR and CD28-mediated co-stimulation leads to the activation of Nuclear Factor of Activated T-cells (NFAT), while on the other hand TCR signaling and OX40 co-stimulation result in activation of nuclear factor-κB (NF-κB) (21).

In agreement with its pleiotropic functions, IL-9 has been demonstrated to influence various different cell types expressing IL-9 receptor (IL-9R) (8, 22, 23). The IL9R consists of 2 subunits: an IL-9R specific alpha chain (IL9R-alpha) and the common gamma chain of the receptor that is shared by other cytokine receptors including receptors for IL-2, IL-4 and IL-7 (23). The IL-9R is expressed on T effector cells rather than in naïve T cells (24). Furthermore, IL-9R is expressed on airway epithelial cells and smooth muscle cells suggesting that several target cell populations for IL-9 exist in lung tissue.

In this study, we determined the expression and function of IL-9 in NSCLC. We demonstrate that IL-9 expression is augmented in NSCLC and plays an important functional role in regulating tumor cell growth. Our findings suggest new avenues for tailored immunotherapy in NSCLC.

MATERIALS AND METHODS

Human Study

Our human study was performed at the Friedrich-Alexander-University Erlangen-Nürnberg, Germany, after being approved by the ethics review board of the University of Erlangen (Re-No: 56-12B; DRKS-ID: DRKS00005376). To date more than one hundred and seventy (170) patients that suffered from primary NSCLC and three metastatic patients underwent surgery and gave their approval to be enrolled in this study in an informed written consent. The patient studies were conducted in accordance with the ethical guidelines of the Declaration of Helsinki. Patients enrolled in this study did not receive any therapy. The confidentiality of the patients was maintained.

Lung cancer diagnosis was based on pathological confirmation. The histological types of lung cancer were classified according to the World Health Organization (WHO) in 2004. Staging was based on the Cancer TNM Staging Manual formulated by the International Association for the Study of Lung Cancer (IASLC), issued in 2010. Clinical data including histological classification, TNM stage, age, gender and smoking status were provided by the Department of Thoracic Surgery and the Institute of Pathology and are summarized in **Table S1**. Clinical data of the control cohort are shown in **Tables S2–S4**.

Immediately after surgery, lung tissue samples were taken from three different regions: the tumoral region (TU: solid tumor tissue), peri-tumoral region (PT: 2-3 cm away from the solid tumor) and the tumor-free control region (CTR: > 5 cm away from the solid tumor). The post-surgery tissue samples were used for RNA and protein isolation as well as for total cell isolation followed by cell culture and FACS analysis. Paraffin-embedded lung tissue arrays were generated as previously described (25) and applied for immunohistochemistry (IHC).

Antibodies

Antibodies used in this study are listed in the **Supplementary Material**.

Immunohistochemistry (IHC)

Immunohistochemistry was performed on paraffin-embedded histological sections. Before staining, paraffin was removed from the slides by incubation at 72°C for 30 min and treatment with Roti-Histol (Carl Roth) two times for 10 min. The tissue sections

were then rehydrated by immersion in ethanol-series in descending concentrations (100%, 95%, 70%) for 3 min each and in deionized water for 1 min, followed by blocking endogeneous peroxidase in 3% H_2O_2 (in methanol) for 20 min. For heat-induced antigen retrieval, slides were placed into a rack containing 50 ml 1 mM Tris-EDTA buffer which was transferred into a pressure cooker followed by incubation at 120°C for 5 min. Slides were then cooled down for 30 min at room temperature (RT) followed by incubation for 1 min in deionized water. Tissue was surrounded with a hydrophobic barrier using a barrier pen. In a next step, slides were stained with the respective primary antibody against CD3, Foxp3, IL-9 or IL-9R **(Table S5)** using the ZytoChem-Plus AP Polymer-Kit (Zytomed Systems GmbH) according to the manufactures instructions. For IHC single stainings, nuclei were stained with hematoxylin solution (Carl Roth) and slides were covered with coverslips using Aquatex (Merck). For IHC double staining, the second antibody against IL-9 (**Table S5**) was applied and detected according to the manufacture instructions of the Dako EnVision Detection System Kit (Dako Deutschland GmbH). Negative controls were not treated with the primary antibody; the other steps remained the same. Stained slides were scanned using the digital slide scanner (Scan 150) at the Institute of Pathology. Whole slide images were visualized by the CaseViewer software (Version 2.0, 3D Histech Ltd). IL-9 single staining was quantified using the Definiens Tissue Studio 4.1 software (Definiens) while the IL-9R single and the IL-9/Foxp3 double staining have been evaluated using the ImageJ Cell Counter (Version 1.46).

Cell Isolation and Culture From Lung Tissue

Human tissue samples were cut into small pieces (1-3 mm^2) using scalpels and digested with Collagenase (2700 U/ml, Sigma-Aldrich: Collagenase from Clostridium histolyticum, Cat# C98991-500MG) and 150µl DNase (10 mg/ml, Roche Diagnostics GmbH: DNase I, Cat#10104159001) diluted in 10 ml R10 medium (500 ml RPMI1640, anprotec, Cat# AC-LM-0060; 50 ml heat-inactivated fetal bovine serum (FCS), Sigma-Aldrich, Cat# S0615; 2mM L-Glutamine, anprotec, Cat# AC-AS-0001; 5 ml Penicillin-Streptomycin (Pen/Strep), anprotec, Cat# AC-AB-0024) in a shaker at 37°C for 1 h. After incubation, the samples were passed through a cell-strainer (100 µm, Greiner Bio-One GmbH: EASYstrainer; Cat# 542000), single-cell suspensions were washed with RPMI1640 and centrifuged at 300g for 7 min at 4°C. The supernatant was removed, and red blood cells (RBC) were lysed in ACK lysis buffer (0,15M NH4Cl, Carl Roth GmbH + Co. KG, Cat# P726.2; 0,01M KHCO3, Carl Roth GmbH + Co. KG, Cat#P748.1; 100M Na2EDTA, GERBU Biotechnik GmbH, Cat# 1034.1000; dissolved and steril filtered in deionized H2O; pH=7.2-7.4) with subsequent centrifugation at 1500rpm for 5 min at 4°C. The cell pellets were washed with Washing Buffer I (500 ml PBS EDTA pH 7.5, BioWhittaker, Cat# BE02-017F; 5 ml Pen/Strep), centrifuged again and resuspended in Washing Buffer II (500 ml PBS EDTA pH 7.5; 5 ml Pen/Strep; 25 ml FCS). Cells were centrifuged at 800rpm for 15 min at 4°C with a low deceleration mode 1. Supernatant was discarded and cells were taken up in Tumor tissue medium (500 ml RPMI1640; 50 ml FCS; 2mM L-Glutamine; 5 ml Pen/Strep; 1mM Sodium-Pyruvate, anprotec, Cat# 11360-070; 5 ml Non-Essential Amino Acids, Gibco, Cat# 11140-035). Cell numbers were determined using Trypan-blue staining in a Neubauer counting chamber. Cells were cultured in Tumor tissue medium at 37°C and 5% CO2.

Isolation of Peripheral Blood Mononuclear Cells (PBMCs)

PBMCs were freshly isolated using LeucoSep Tubes (Greiner Bio-One, Cat# 227290) according to the manufacturer´s protocol. After cell counting with Trypan-blue in a Neubauer counting chamber, PBMCs were cultured for 4-5 days with $5x10^5$ cells per condition as shown in **Figure 2E**.

Experimental Skewing Conditions for Foxp3+Treg and IL-9 Producing T Cells in PBMCs

Freshly isolated PBMCs from NSCLC patients and healthy control subjects were cultured in 1ml R10 medium at 5 x 10^5 cells/well for 4-5 days with plate bound anti-CD3 (1µg/well) and soluble anti-CD28 antibodies (10µg/ml) in a 48 well cell culture plate (Greiner Bio-One, Cat# 677180) at 37°C and 5% CO_2 (**Figure 2E**). For skewing of IL-9 producing T cells, TGFβ (20ng/ml) and IL-4 (20ng/ml) were added, while the Treg skewing condition included TGFβ (20ng/ml) and IL-2 (2ng/ml). The respective cytokine information are listed in the Table below:

Cytokine/Antibody	Company	Catalog number
aCD3	BD Biosciences	Cat# 555329
aCD28	BD Biosciences	Cat# 555725
rhIL-2	ImmunoTools	Cat# 11340025
rhIL-4	ImmunoTools	Cat# 11340043
hTGFβ	Miltenyi Biotec	Cat# 130-095-067

Flow Cytometric Analysis

To prevent unspecific binding of antibodies to Fc receptors, single cell suspensions were incubated with unlabeled antibodies against IgG Fc receptors CD16/32 (human: 1:100, BD Biosciences Cat# 564220; murine: 1:100, BD Biosciences Cat# 553142) in FACS Buffer (500 ml PBS, anprotec Cat# AC-BS-0002; 10 ml FCS) for 5 min at 4°C. Cells were washed with FACS Buffer and centrifuged. Pellets were resuspended with FACS Buffer containing antigen-specific fluorochrome-conjugated antibodies in appropriate concentrations and incubated for 15 minutes at 4°C in the dark. After cells were washed with FACS Buffer and centrifuged, pellets were either resuspended in FACS Buffer to measure directly the surface stained cells or proceeded to intracellular staining. Therefore, the FoxP3 staining kit (Thermo Fisher Scientific Cat# 00-5523-00) was applied according to the manufacturer's protocol. Permeabilized cells were stained for intracellular proteins in a volume of 50 µl

PermWash Buffer supplemented with antibodies in appropriate concentrations. Cells were washed, taken up in FACS Buffer and analyzed immediately **(Table S6).** Flow cytometric analyses were obtained with the FACS Canto II and the BD FACS Diva software (both BD Biosciences) for compensation. Data were analyzed with Flow-Jo v10.2 (FlowJo) software always gating for singlets using the forward scatter and for living cells using forward scatter vs. sideward scatter before specific analysis (also shown in **Supplementary Material**).

Cells were first stained with Zombie (1:500, Biolegend, Cat#423101/423102) for 15 min at room temperature prior to Fc blocking and washed twice with FACS buffer. The staining of surface proteins was then continued as described above.

Data of applied FMOs (Fluorescence minus one) are shown in **Supplementary Material**.

RNA Isolation and cDNA Synthesis

Lung tissue samples were homogenized using Precellys Lysing Kits (Bertin Technologies, Cat# P000918-LYSK0-A) and the benchtop homogenizer Minilys (Bertin Technologies) as described in the manufacturer's protocol. RNA of homogenized samples or single cell suspensions was isolated using peqGold RNA Pure (Peqlab, Cat# 30-1010) or Qiazol Lysis Reagent (Qiagen, Cat# 79306) according to the manufacturer´s instructions. RNA was reversely transcribed into cDNA using the RevertAid First Strand cDNA Synthesis Kit (ThermoFisher Scientific, Cat# K1622) according to the manufacturer's protocol.

Quantitative Real-Time PCR (qPCR)

qPCR of synthesized cDNA was performed by using iTaq Universal SYBR Green Supermix (Bio-Rad Laboratories, Cat# 1725124) in a total volume of 20 µl. Primer sequences for murine and human qPCR analyzes are depicted in **Supplementary Table S7** which were purchased from Eurofins-Genomics Germany. qPCR Reactions (50 cycles, initial activation 98°C, 2 min, denaturation 95°C, 5 min, hybridization/elongation 60°C, 10 min) were performed using the CFX-96 Real-Time PCR Detection System and analyzed by the respective CFX Manager Software (both Bio-Rad Laboratories). Data were analyzed using the relative quantification $2^{-\Delta\Delta CT}$ method by normalization to the housekeeping-gene hypoxanthine-guanine-phosphoribosyltransferase (Hprt).

ELISA

The enzyme-linked immunosorbent assay (ELISA) technique was utilized to analyze the cytokine concentration in cell culture supernatants, BALF and Serum. ELISA was performed in accordance with the manufacturer's instructions. Human ELISA Sets were purchased as followed: IL-9 ELISA (Human IL-9 DuoSet ELISA, R&D Systems, Cat# DY209-05), IL-21 ELISA (Human IL-21 DuoSet ELISA, R&D Systems, Cat# DY8879-05), IFNγ ELISA (BD OptEIA™ Human IFN-γ ELISA Set, BD Biosciences, Cat# 555142). Murine samples were analyzed by: IL-21 ELISA (Mouse IL-21 DuoSet ELISA, R&D Systems, Cat# DY594), IFNγ ELISA (BD OptEIA™ Mouse IFNγ ELISA Set, BD Biosciences, Cat# 555138), IL-10 ELISA (BD OptEIA™ Mouse IL-10 ELISA Set, BD Biosciences, Cat# 555252).

Protein Extraction and Western Blot Analysis

Lung tissue samples from patients were lysed with RIPA Buffer (Thermo Fisher Scientific, Cat# 89900) and inhibitor cocktail (complete Mini EDTA-free, Roche Diagnostics, Cat# 11836170 001) then homogenized with SpeedMill PLUS (Analytik Jena) in innuSPEED lysis Tubes P (Analytik Jena, Cat# 845-CS-1020250) and centrifuged (3000rpm, 5min, 4°C). The supernatant was incubated for 30 minutes on ice and centrifuged again (2000g, 5min, 4°C). Final extraction was done by another centrifugation step of the supernatant (45min, maximum speed, 4°C) and measured with Bradford Assay (Protein Assay Dye Reagent Concentrate, Bio-Rad, Cat# 5000006), followed by protein denaturation (95°C, 5 min) in a mix of reducing loading buffer (4xLDS Sample Buffer, Thermo Fisher Scientific, Cat# NP0007) and DTT (1M, Thermo Fisher Scientific, Cat# P2325). A mini-PROTEAN TGX Stain-Free Gel (Bio- Rad, Cat# 4568086) was used with 20µg of proteins per well and at 120V, 150mA for 1h. Proteins were then transferred to a 0,2µm nitrocellulose membrane (Trans-Blot Turbo Transfer Pack, Bio-Rad, Cat# 1704158) by using a western blot trans-blot turbo system (Bio-Rad). Transfer and protein load was assessed and recorded by using a ChemiDoc Imaging System (Bio-Rad). After washing and blocking (3% powdered milk (Carl Roth GmbH, Cat# T145.3) in Tween SDS buffer) the membrane for 1h at room temperature, the primary antibody was applied and incubated over night at 4°C. After that, the membrane was washed and incubated with the compatible secondary antibody in blocking buffer, for 1h at room temperature. Respective antibody information are listed in **Table S8**. After final washing steps, detection was performed using SuperSignal™ West Femto Maximum Sensitivity Substrate (Thermo Scientific, Cat# 34095). Visualization of the western blot results was done by using the ChemiDoc Imaging System. Protein bands and total protein levels were analysed with the ImageLab software (Bio-Rad).

Cell Lines

The human A549 (ATCC® CCL-185™) cell line was purchased authenticated from the ATCC bank (Manassas, Virginia, USA). Cells were cultured in F-12K Nut mix medium (Thermo Fisher Scientific, Cat# 21127-022) supplemented with 10% FCS, 1% Pen/Strep and 1% L-Glu at 37°C and 5% of CO_2.

The murine LL/2-luc-M38 (LL/2) cell line was purchased and authenticated from Caliper LifeScience (Bioware cell line, Caliper LifeScience, Waltham, Massachussets, USA). All Caliper Life Sciences cell lines are confirmed to be pathogen-free by the IMPACT profile I (PCR) at the University of Missouri Research Animal Diagnostic and Investigative Laboratory. LL/2 cells were cultured in D10 medium (anprotec, Cat# AC-LM-0012; 50 ml heat-inactivated fetal bovine serum (FCS), Sigma-Aldrich, Cat# S0615; 2mM L-Glutamine, anprotec, Cat# AC-AS-0001; 5 ml Penicillin-Streptomycin (Pen/Strep), anprotec, Cat# AC-AB-0024) at 37°C and 5% of CO_2.

The murine bronchoalveolar carcinoma cell line L1C2 (Dubinett et al. https://pubmed.ncbi.nlm.nih.gov/8382559/) was obtained from Prof R. Wiewrodt. Cells were cultured in R10 Medium at 37°C and 5% CO2.

Cell Line Experiments

$3x10^5$ A549 were cultured overnight in 6-well plates (Greiner Bio-One, Cat#657160) in supplemented F-12K Nut mix or R10 medium with or without 50 ng/ml IL-9 (ImmunoTools, Cat# 11340093) for 72h. Other different experimental conditions were described in the respective figure. For the Fas agonistic challenge, we incubated A549 with 2 µg/mL anti-CD95 (Biolegend, Clone DX2, Cat# 305655) or IgG1, k (Biolegend, Clone MOPC-21, Cat# 400153).

$1.25x10^5$ LL/2 cells were cultured in 24-well cell culture plates (Greiner Bio-One, Cat# 662160) for 24h at 37°C and 5% CO2 in D10 medium with 30 ng/ml or 100 ng/ml IL-9 or left untreated. Cells were harvested and counted for live and dead cells using trypan blue staining.

$5x10^5$ LL/2 or L1C2 cells were cultured overnight in 6-well plates in D10 or R10 medium, respectively. After the first 24h the cells were stimulated with 30 ng/ml or 100 ng/ml IL-9 or left untreated for another 24h.

Apoptosis Analysis by Flow Cytometry

Determination of apoptotic cells was performed using Annexin V/PI staining according to the manufacturer's protocol (BD Bioscience; Cat#550474 and #556463). Briefly, $1x10^5$ cells were stained with 5 µl AnnexinV-APC and 5 µl PI in 100 µl 1x AnnexinV binding buffer for a total volume of 110 µl and incubated for 15 min at RT in the dark. Reaction was stopped by adding 200 µl 1x AnnexinV binding buffer and samples were immediately analyzed with the FACSCanto II. Data sets were evaluated by Flow-Jo v10.2.

Proliferation Analysis by Flow Cytometry

Determination of proliferating cells was performed using Ki67 staining according to the manufacturer's protocol (BD Bioscience, Cat# 556026). For Ki67 analysis, $1x10^6$ LL/2 or L1C2 cells were fixed with 75% ethanol and incubated for at least 2 hours at -20°C. After washing the cells with FACS buffer the cells were stained with 20 µl Ki67-FITC diluted in FACS buffer for a total volume of 120 µl and incubated for 30 min at RT in the dark. Reaction was stopped by adding 1 ml PBS, centrifuged and resuspended in 250 µl PBS. Cells were immediately analyzed using the FACSCanto II. Data sets were evaluated by Flow-Jo v10.2.

Experimental Mice Models

All mice were bred and maintained under specific-pathogen-free (SPF) conditions in our animal facility (University Hospital Erlangen, Hartmannstraße 14, Erlangen). All experiments were performed in accordance with the German and European laws for animal protection and were approved by the local ethics committees of the Regierung Unterfranken (Az 55.2-2532-2-1286-20). IL-$9^{-/-}$ mice were bred on Balb/c and C57BL/6 genetic backgrounds. And they were kindly presented by PD Dr. Benno Weigmann and PD Dr. med. Andreas Ramming from University Hospital Erlangen Medicine 1 and Medicine 3, respectively (26).

LL/2 Induced Lung Adenocarcinoma Model and Antibody Treatment

For lung tumor induction, $5x10^5$ cells resuspended in 200 µl DMEM medium (without supplements) were injected into the tail vein of 6-8 weeks old female mice. At the indicated time points, mice were weighed and injected intraperitoneally (i.p.) with luciferin (0.15 mg per 1 g body weight; Promega, Cat#P1043). Luciferase activity was measured after 20 min by the IVIS Spectrum *In Vivo* Imaging System (PerkinElmer) as previously described (5). Briefly, mice were anaesthetized using isoflurane and luciferase activity was measured by detecting luminescence intensity (photons per second). Analyses were performed in a logarithmic scale mode. Mice were sacrificed at day 14-23 after tumor cell injection. For the inhibition of IL-9 *in vivo*, we used two different protocols. In the first protocol, mice were treated i.p. with 200 µg of anti-IL9 antibody (BioXCell, Clone 9C1, Cat# BE0181) or IgG2a Isotype control (BioXCell, Clone C1.18.4, Cat# BE0085) dissolved in 100 µl PBS at day 1, 3, 6, 9, 13 and 16 after tumor induction with an experiment termination at day 21 to 23 depending on the lung tumor load. In the second protocol, mice were treated i.p. with 20 µg anti-IL9 antibody or IgG2a Isotype control resolved in 200 µl PBS at day 6, 9, 10 and 13 after tumor induction with an experiment termination at day 20.

L1C2 Induced Lung Adenocarcinoma Model

For lung tumor induction by L1C2, $2x10^5$ cells resuspended in 200 µl DMEM or RPMI medium (without supplements) were injected into the tail vein of 6-8 weeks old female mice. Mice were sacrificed at day 14-23 after tumor cell injection, as indicated.

Hematoxylin and Eosin (H&E) Staining on Murine Paraffin-Embedded Lung Sections and Analysis of Tumor Load

Representative parts of the sectioned mouse lung were fixed in 10% formalin-PBS solution, dehydrated, and embedded in paraffin. Five-micrometer-thick lung sections cut from paraffin blocks were stained with hematoxylin and eosin for visualization of lung tumors. Stained slides were scanned using a digital slide scanner (Scan 150, 3D Histech Ltd) and slide images were visualized using the CaseViewer software (Version 2.0, 3D Histech Ltd). Staining and scanning of slides was performed in cooperation with the Institute of Pathology in Erlangen

To analyze the tumor load in the lung for each mouse, the lung sections were histologically evaluated after Hematoxylin and Eosin staining. A pathologist analysed in a blinded codified manner the tumor load of the murine lungs. Moreover, each section was analyzed by means of area [μm^2] and number of foci. The sections were investigated under the microscope with an object magnified 10 times (Carl Zeiss, AxioCam MRC) and live pictures were directly transmitted to the Zen 2 blue edition

software (Carl Zeiss Microscopy GmbH). With the help of the graphic tool, the foci were localized, circled and automatically measured by means of area. The obtained data corresponding to each mouse was used for comparisons as well as correlation analyzes and transferred into graphs (GraphPad Prism 8).

Isolation of Total Murine Lung Cells

Dissected lungs were cut into small pieces using scalpels and digested with Collagenase (2700 U/ml; Sigma-Aldrich: Collagenase from Clostridium histolyticum; Cat# C98991-500MG) and 1,5 mg DNase (10 mg/ml; Roche Diagnostics GmbH: DNase I; Cat#10104159001) diluted in 10 ml R10 medium in a shaker at 37°C for 1 h. After incubation the samples were passed through a cell-strainer (40 µm, Company, Cat#542040), single-cell suspensions were washed with RPMI1640 and centrifuged at 1500rpm for 10 min at 4°C. The supernatant was removed and RBC were lysed in 10 ml ACK lysis buffer with subsequent centrifugation at 1500rpm for 5 min at 4°C. The cell pellets were washed with 10 ml PBS and centrifuged at 1500rpm for 5 min at 4°C. After removal of the supernatant, the cells were taken up in 10 ml R10 medium and cell numbers were determined using Trypan-blue staining in a Neubauer counting chamber.

Isolation of Murine Lung CD4+ T Cells

CD4+T cells were isolated from the lungs of tumor-bearing mice by magnetic cell separation using anti-CD4 MicroBeads (Miltenyi Biotec) according to the manufactures protocol. The purity of isolated CD4+ T cells was confirmed by FACS analysis. Isolated T cells were then cultured in RPMI medium supplemented with 10% FCS, 1% Pen/Strep and 1% L-Glu at 37°C and 5% CO_2, in the presence plate-bound anti-CD3 (5 µg/ml, BD Biosciences, Cat#) and soluble anti-CD28 (1 µg/ml, Biolegend, Cat#) antibodies. Supernatants and cells were harvested after 24h of cell culture for further analyses.

Mouse CD4+ T Cell Isolation and *In Vitro* Differentiation

Naïve CD4 T cells were isolated from mouse spleens using the $CD4^+CD62L^+$ T cell isolation kit according to the manufacturer's protocol (Miltenyi Biotec). Cells were cultured in R10 medium on anti-CD3 (2 µg/ml; BioXCell) coated cell culture plates with soluble anti-CD28 (2 µg/ml; BioXcell). Cells were cultured under Treg polarizing conditions including hTGF-β1 (2 ng/ml), hIL-2 (50 U/ml), anti-IFN-γ (XMG; 10 mg/ml) and anti-IL-4 (11B11; 10mg/ml). Th9 cells were cultured with hTGF- β1 (2 ng/ml), IL-4 (20 ng/ml), hIL-2 (50 U/ml) and anti-IFN-γ (10 mg/ml). Th0 cells were cultured with hIL-2 (50 U/ml), anti-IFN-γ (XMG; 10 mg/ml) and anti-IL-4 (11B11; 10mg/ml). On day 3, cells were expanded into fresh media containing the original concentrations of cytokines in the absence of co-stimulatory signals for additional 2 days. On day 5, mature T cell subsets were harvested for further analysis.

Flow Cytometric Analysis of Cultured Treg Cells

For transcription factor staining in Treg cells from different culture conditions were harvested on day 5 of differentiation whereas for cytokine staining, CD4+ T cells were stimulated with Phorbol 12-myristate 13-acetate (PMA, 5ng/ml, Sigma-Aldrich) and ionomycin (500ng/ml, Sigma-Aldrich) for 3 hours followed by monensin (2µM, Biolegend) for total 6 hours at 37°C. Cells were washed with FACS buffer (PBS with 0.5% BSA). CD4+ T cell subsets were then stained with a fixable viability dye (eBioscience) and surface markers (CD4, RM4-4, Biolegend; CD25, PC61, Biolegend) for 30 min at 4°C followed by washing and fixation with 4% formaldehyde for 10 min at room temperature. For transcription factor staining, after surface staining, cells were fixed with Fixation & Permeabilization Buffer (FoxP3 staining kit, Thermo Fisher Scientific, Cat# 00-5523-00) for 2 hours at 4°C, and then permeabilized with permeabilization buffer. Cells were stained with Foxp3 antibody (Foxp3, FJK-16s, eBioscience) for 30 min at 4°C followed by flow-cytometry. For cytokine staining, after fixation cells were then permeabilized with permeabilization buffer, and stained for cytokines (IL-9; RM9A4, Biolegend).

Gene Expression and IL-9 Analysis in Cultured Treg Cells

Total RNA was isolated from cells using TRIzol (Life Technologies). RNA was reverse transcribed according to manufactures directions (Quantabio, Beverly, MA). Quantitative Reverse Transcriptase (qRT-PCR) was performed with commercially available primers (Life Technologies) with a 7500 Fast-PCR machine (Life Technologies). Gene expression was normalized to housekeeping gene expression (β2-microglobulin).

For measurement of IL-9 secretion, on day 5, $1x10^6$ cells were re-stimulated with anti-CD3 coated on 12 well cell culture (Greiner Bio-One, Cat# 665180) plates for 12 hours. Supernatants were collected and IL-9 secretion was measured using IL-9 ELISA MAX™ kit provided by BioLegend (Cat#442704).

Th1-*In Vitro* Differentiation

Naïve $CD4^+CD62L^+$ T cells were isolated from the spleens of naïve mice by magnetic cell sorting using the $CD4^+CD62L^+$ T Cell Isolation Kit II (Miltenyi Biotec). The purity of the cell isolation was confirmed by FACS analysis.

For T cell differentiation, $CD4^+CD62L^+$ T cell were cultured in RPMI medium supplemented with 10% FCS, 1% Pen/Strep and 1% L-Glu, at 37 °C and 5 % CO_2 in the presence of plate-bound anti-CD3 (5 µg/ml, BD Biosciences) and soluble anti-CD28 (1 µg/ml, Biolegend) antibodies.

For Th1 differentiation, cells were additionally treated with 5 µg/ml anti-IL-4 antibody (BioLegend) and 12 ng/ml recombinant IL-12 (PeproTech).

Afterwards ACK lysis buffer was applied as previously described (27).

Statistical Analysis

All data analysis was done using Prims software version 8 (Graphpad Software) using a Student's test, ordinary one-way ANOVA or two-way ANOVA. *Post hoc* Tukey test was used for multiple comparisons. Simple linear regression was used for the correlation. $P<0.05$ was considered statistically significant.

RESULTS

Increased IL-9 Production by T Cells in the Tumoral Region of the Lung of Patients With NSCLC

In this study, we aimed for characterizing the expression and function of IL-9, a cytokine with immune-regulatory functions (28, 29), in non-small cell lung cancer (NSCLC).

To investigate the IL-9 expression in the lung of patients with NSCLC, we did immunohistochemistry for IL-9 on post-surgery lung samples collected on tissue arrays and compared IL-9 production from the tumoral region (TU: solid tumor tissue), and the tumor-free control region (CTR: > 5cm away from the solid tumor) in NSCLC (see *Materials and Methods* and **Figure 1A**). The clinical data of these patients as well as the healthy subjects whose post-surgery lung samples were analyzed in this study, are reported in **Tables S1, S2**, respectively. This analysis showed induction of IL-9+ cells in the tumoral region of the lung as compared to the control region in these lung sections derived from patients with NSCLC **(Figure 1B** and **Supplementary Figure 1A).** Patients included in this study were not treated with any immunotherapy before undergoing surgery analysis. To further analyze the IL-9 induction in the tumoral region of these patients, we next analyzed interleukin 9 expression in proteins extracted from the control and tumoral regions of the lung of NSCLC patients. Furthermore, we analyzed the lung of 3 healthy controls (CN) and one subject with lung inflammation (Lu-infl.) by using Western blot analysis **(Figures 1C–E** and **Supplementary Figure 1B).** Here, we confirmed upregulation of IL-9 in the tumoral region of the lung of patients with NSCLC **(Figures 1C, D)**.

We next started to investigate the cellular sources of IL-9 in NSCLC. Since IL-9 was induced in the tumoral region of the lung, we asked whether the tumor cells themselves would produce IL-9. To do so, we cultured the lung tumor adenocarcinoma cell line A549 and extracted proteins for performing Western blot analysis for IL-9. We found that A549 cells produce IL-9 although not as high as control healthy lungs when corrected for GAPDH expression **(Figure 1E).**

We further investigated IL-9 in epithelial cells isolated from the lung of one NSCLC patient and found decreased numbers of epithelial cells (EpCAM+) producing IL-9 (IL-9+ cells) in the tumoral region as compared to the control region by flow cytometric analysis **(Figure 1F).** Furthermore, we found few epithelial cells expressing IL-9 distributed in the different regions of the lung of the patients with NSCLC by immunohistochemistry (IHC) **(Supplementary Figure 1A)**. We next further characterized the cellular source of IL-9 in lung tissue from NSCLC patients and focused our analysis on IL-9 production by tumor infiltrating T cells (TIL) and performed double immunohistochemistry with anti-IL-9 and anti-CD3 antibodies in lung tissue arrays as in **Figure 1B**. An example of this staining is shown in **Figure 1G**. Here, we found double positive cells, indicating the presence of lung CD3+ T cells producing IL-9, which infiltrated the tumoral regions of the lung in NSCLC. Accordingly, we analyzed IL-9 production of total lung cells from the three lung tumor regions after T cell stimulation with anti-CD3/CD28 antibodies in a cohort of NSCLC patients by ELISA **(Figure 1H)**. Here, we noted significantly augmented IL-9 production by cultured lung cells stimulated with aCD3/28 antibodies from the TU region in NSCLC as compared to the CTR and PT regions of these patients. As IL-9 from T cells is mainly produced by Th9 cells which also produce IL-21 (20, 28), we next determined IL-21 concentration in the same cell supernatants where IL-9 was detected. We found a significant upregulation of IL-21 production in the supernatants of aCD3/aCD28 antibodies cultured total lung cells from the TU region of patients with NSCLC as compared to the CTR region **(Figure 1I).** This finding indicates higher T cell infiltration as the possible cause for the increased IL-9 levels found in the tumoral area of the lung of NSCLC patients (30). By contrast, the anti-tumoral cytokine IFN-ɣ was found, by trend, downregulated in these lung cells isolated from the tumoral region **(Figure 1J)**. In confirmation of decreased anti-tumoral cells infiltrating the tumoral region of NSCLC patients, we found significantly less TNF-alpha mRNA levels in mRNA isolated from the lung tumoral regions as compared to the respective control region **(Figure 1K).**

In conclusion, we found that TIL in the tumoral region of NSCLC patients produced IL-9 while challenged with anti-CD3/CD28 antibodies. Moreover, in addition to tumor infiltrating lymphocytes, also lung tumoral cells have the capacity to produce IL-9.

Increased IL-9 Production by T Regulatory Cells in the Tumoral Region of the Lung of Patients With NSCLC

We previously described induced immunosuppression in the tumoral region of the lung of patients with NSCLC (31, 32). To determine whether regulatory T (Treg) cells would produce IL-9 in the lung of patients with NSCLC, we performed double immunohistochemistry for IL-9 and Foxp3 in tissue array slides **(Figures 2A, B).** Here, we found an increased number of double positive cells for Foxp3 and IL-9 in the tumoral region compared to the control region of the lung of NSCLC patients suggesting that lung Treg cells may produce IL-9 in NSCLC. Consistently, we found a positive correlation between the Foxp3 mRNA levels and IL-9+ T cells in the tumoral area in NSCLC **(Figure 2C).**

Treg cells are known to be induced by low levels of IL-2, hereby competing with TIL for IL-2 induced survival (33, 34). By having a view on IL-2, we noted reduced IL-2 mRNA expression in the tumoral region compared to the control region **(Figure 2D),** indicating that low levels of IL-2 and the presence of other immunosuppressive cytokines like TGF-beta and IL-10 in the tumor microenvironment may contribute to augmented Treg numbers in NSCLC (31, 35).

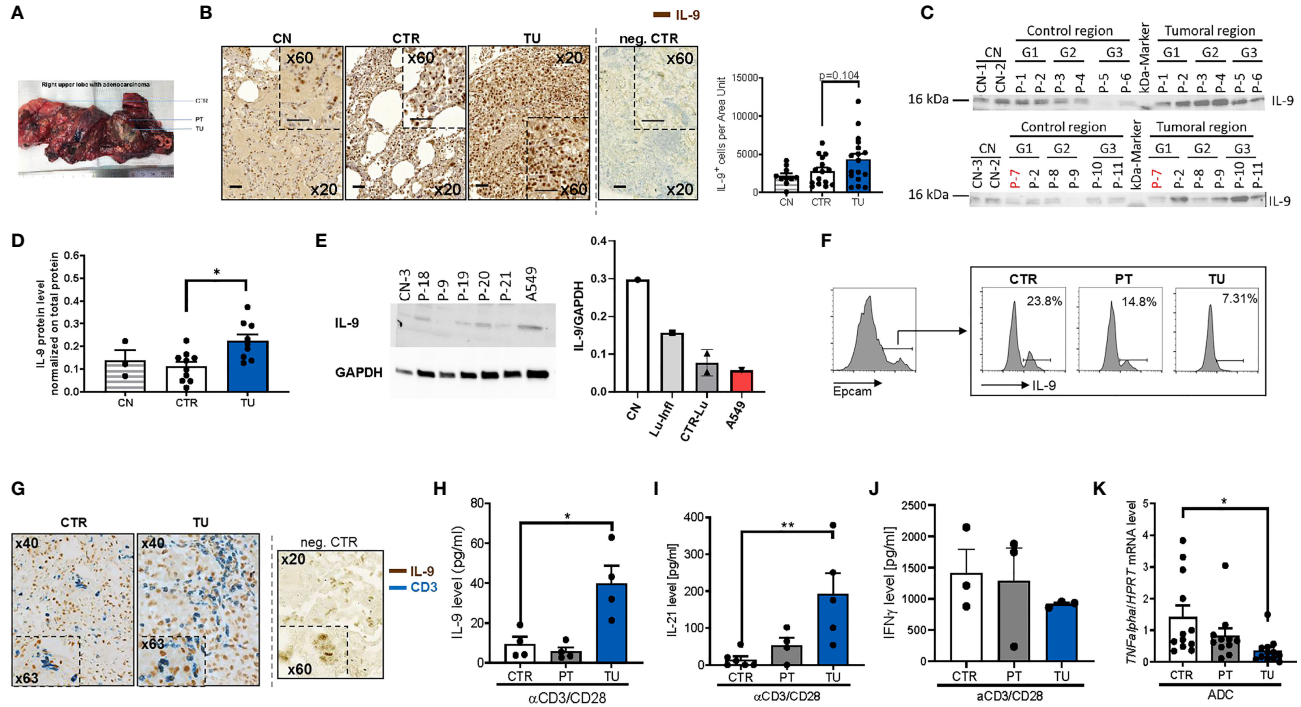

FIGURE 1 | Increased IL-9 production by T cells in the tumoral lung region of NSCLC patients. **(A)** Representative photographic image of the resected lung of one NSCLC patient as a showcase of defined regions implemented for our human study cohort. Lung tissue samples were dissected from the tumoral area (TU), the peri-tumoral area (PT) surrounding the tumor and from the control area (CTR) consisting out of healthy lung tissue. **(B)** IL-9 immunohistochemistry (IHC) on paraffin-embedded tissue arrays obtained from the lung of tumor-free control patients (CN) or the CTR and TU lung regions of non-small cell lung cancer (NSCLC) patients (nCN=10; nCTR=15; nTU=17) (scale bar=50 µm). **(C, D)** Proteins were isolated from lung tissue samples of control patients (CN), the CTR and the TU of NSCLC ADC patients (classified by grading of tumor cell differentiation (G1, G2 and G3) and Western blot was performed. Detected protein levels of IL-9 were normalized on total protein of the samples (CN: n=3, CTR: n=10, TU:n=10). **(E)** Proteins were isolated from tissue samples of control patients that underwent surgery due to disease unrelated to tumor and from cells of the adenocarcinoma cell line A549. Analysed data are shown as mean ± SEM (nCN=1; nLu-Infl (Lung inflammation)=1; CTR-Lu=CTR, n=2; nA549 = 1) or single values. **(F)** Flow cytometry analysis of IL-9+ cells (shown in percentage) gated on Epcam+ cells of cells isolated from the CTR, the PT and the TU of a NSCLC patient. **(G)** Double IHC for IL-9 (brown) and CD3 (blue) on lung tissue obtained from the CTR and TU regions of an adenocarcinoma **(**ADC) patient (scale bar=50 µm**). (H)** ELISA analysis of IL-9 levels (pg/ml), **(I)** IL-21 levels (pg/ml), **(J)** IFNγ (pg/ml) in supernatants obtained from total cells isolated from the control (CTR), peri-tumoral (PT) and tumoral (TU) region of adenocarcinoma (ADC) patients and cultured with anti(α)-CD3/CD28 antibodies for 24h (IL-21: nCTR=6, nPT=4, nTU=5; IFNγ: nCTR=3; nPT=3; nTU=3). **(K)** TNF-alpha mRNA level from total lung cells was normalized on HPRT mRNA level (nCTR=12, nPT=11, nTU=12). N values are given per group. Bar charts indicate mean values +/- s.e.m. using student´s two-tailed t-test *P,0.05; **P,0.01; ***P,0.001.

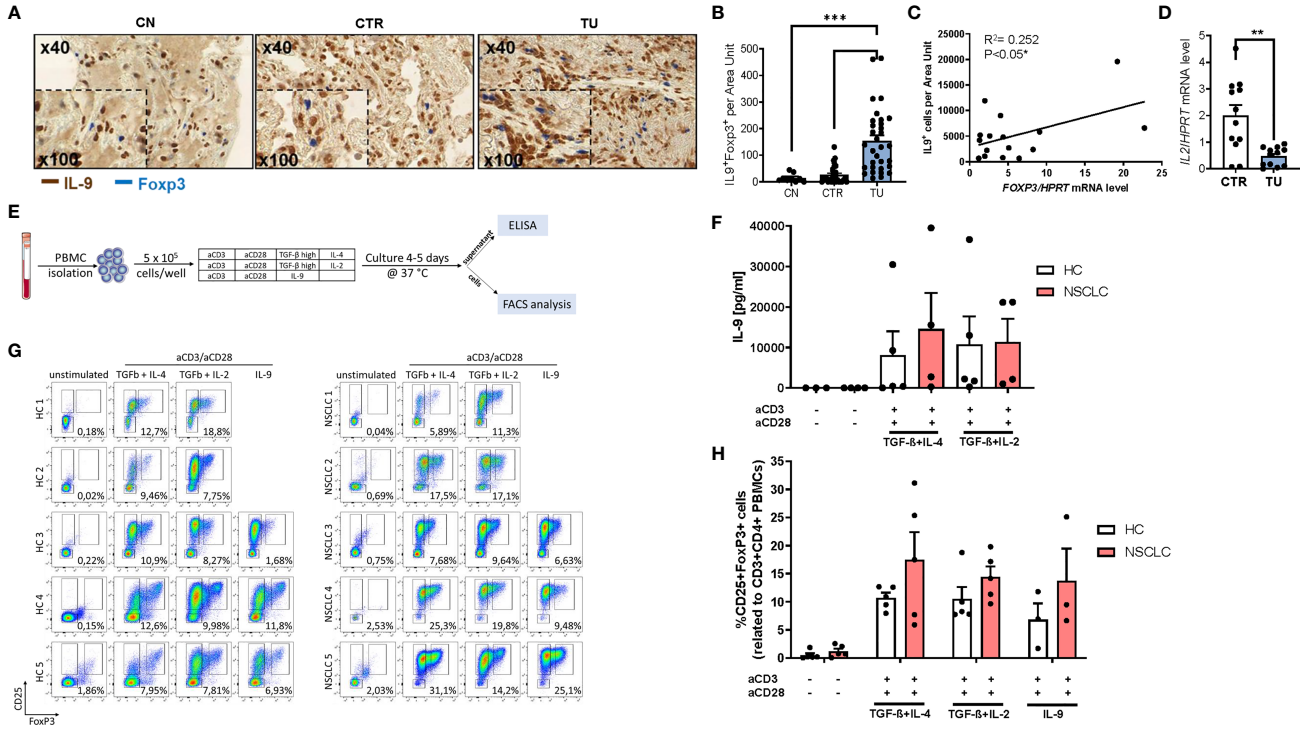

FIGURE 2 | Increased IL-9 production by regulatory T cells (Tregs) of patients with NSCLC. **(A)** Immunohistochemistry staining of lung tissue sections for IL-9 (colored in brown) and Foxp3 (colored in blue). Representative microscopy images are shown for one healthy control patient (CN) and the CTR and TU lung region from one NSCLC patient. Images were taken at a 40x magnification while inserts show a magnification of 100x. **(B)** Total IL-9 and FoxP3 double-positive cells per area are shown for CN (n=10) and NSCLC CTR (n=35) and NSCLC TU (n=34) Data are shown as mean + SEM. using student's two-tailed t-test *P,0.05; **P,0.01; ***P,0.001. **(C)** Correlation of IL-9$^+$ cells and FoxP3 mRNA levels from the tumoral region of NSCLC patients. Correlation was done with IL-9$^+$ cells from the TU of immunohistochemistry staining analysis and FoxP3 mRNA levels of the TU from the same patient. mRNA levels were detected by RT-qPCR and set in relation to HPRT mRNA level (n=16). **(D)** qPCR based analysis of IL-2 mRNA levels of CTR and TU set in relation to HPRT mRNA level (nCTR=12; nTU=11). **(E)** Experimental design for the *in vitro* culture of PBMCs. PBMCs from NSCLC patients or healthy control patients were isolated and cultured with different conditions for 4-5 days at 37°C and 5% CO_2 (500.000 cells/well). After harvesting the cells, the supernatant was used to perform ELISA and the cells were analyzed by flow cytometry. **(F)** Analysis of IL-9 concentration (pg/ml) in the supernatant of PBMC cell culture from healthy controls (n=3-5) and NSCLC patients by ELISA (n=4. **(G)** Representative flow cytometry analysis of CD25^{high}FoxP3$^+$ cells (%) gated on CD3$^+$CD4$^+$ lymphocytes (n=5). Representative dot-plots showing CD25 and FoxP3 staining of PBMCs from control patients and NSCLC patients after cell culture with different conditions (unstimulated; IL-4 (20 ng/ml) and TGFβ (20 ng/ml); Treg: IL-2 (2 ng/ml) and TGFβ (20 ng/ml); IL-9 (20 ng/ml)). **(H)** Quantification of CD25^{high}FoxP3$^+$ Tregs (n_{HC}=5, n_{NSCLC}=5; IL9-condition: n_{HC}=3, n_{NSCLC}=3). For statistical analysis One-way ANOVA test was applied. *p < 0.05.

PBMCs From NSCLC Patients Release Augmented Amounts of IL-9 Upon Specific Skewing Conditions

To determine the capacity of Treg cells to produce IL-9, we isolated peripheral blood mononuclear cells (PBMCs) from five NSCLC patients and five healthy control subjects. Next, the PBMCs were cultured under T cell producing IL-9 and Treg skewing conditions with anti-CD3 and anti-CD28 antibodies. After 4-5 days of cell culture, we performed FACS analysis and measured IL-9 in the supernatant by ELISA (**Figures 2E, F** and **Figure S2A**). In the cell supernatants from PBMCs derived from both healthy controls as well as NSCLC patients, we observed an induction of IL-9 under conditions inducing IL-9 (TGF-beta +IL-4) as well as under immunosuppressive conditions (TGF-beta+ low IL-2) **(Figure 2F).** Moreover, we could detect induced CD3+CD4+CD25+Foxp3+ T regulatory cells both in Treg and IL-9 inducing conditions in PBMCs from both healthy control subjects and from NSCLC patients (**Figures 2G, H).** Thereby the NSCLC group showed an enhanced induction of Treg frequency. These data indicate that factors present in the tumor microenvironment like TGF-beta and low IL-2, can induce IL-9 in TILs from patients with NSCLC and simultaneously induce Foxp3+ T regulatory cells. In addition, our results from the peripheral blood demonstrate that immunosuppression can drive IL-9 both in healthy and in NSCLC subjects.

Human NSCLC Tumor Cells and TILs Express IL-9R

Lung cancer immunosuppression is mediated *via* effects of tumor cells on TILs resulting in T cells expressing Foxp3+ and IL-10 (35). To determine whether this concept is also relevant for tumor cells and TILs in NSCLC patients, we next assessed the distribution of IL-9R in patient samples. To this end, we performed immunohistochemistry for IL9R on the lung tissue arrays of our cohort of NSCLC patients and found an upregulation of IL-9R in the tumoral region as compared to the control region and healthy controls **(Figure 3A**).

Flow cytometric analysis of TILs from lungs of NSCLC patients revealed an upregulation of IL-9R expression in the CD3+ T cells localized in the peritumoral and tumoral region of the lung as compared to control regions **(Figure 3B**, upper graph). We next addressed IL-9R expression in epithelial cells, as this is developed in lung tumors upon epithelial transformation. We found that IL-9R expression was increased by trend in Epcam+ epithelial cells in the lung tumoral region, as compared to the control and the peri-tumoral regions in patients with lung adenocarcinoma, indicating

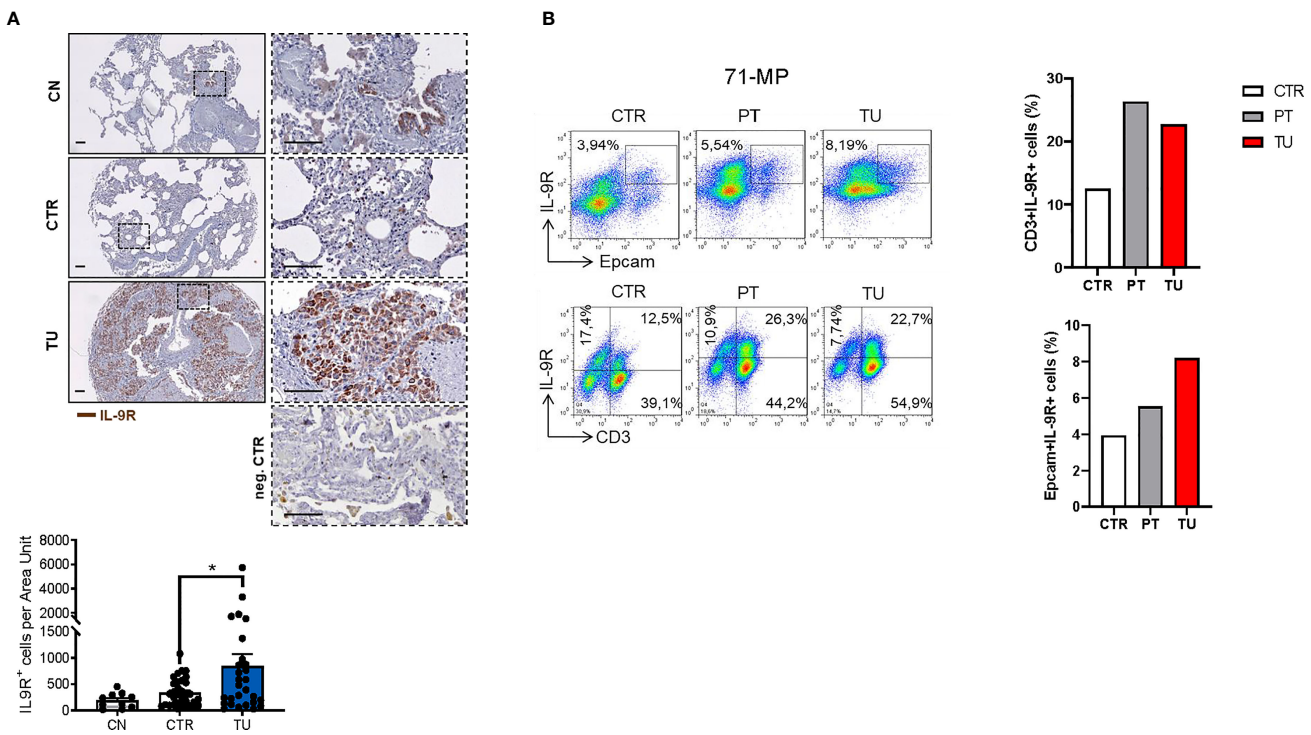

FIGURE 3 | Increased IL-9 Receptor expression in the lung of NSCLC patients. **(A)** Immunohistochemistry staining of lung tissue sections for IL-9R (colored in brown). Representative microscopy images are shown for one healthy control patient (CN), the CTR and TU from one NSCLC patient and a negative Control. Images were taken at a 20x magnification while squared areas are shown below at a magnification of 60x. Quantification of the data is shown below as mean ± SEM using ordinary one-way ANOVA (nCN=10, nCTR=33, nTU=28), *P,0.05; **P,0.01; ***P,0.001. **(B)** Flow cytometry analysis of IL-9R$^+$ cells (%) in association with Epcam$^+$ and CD3$^+$ lung tissue cells derived from the CTR, the PT and the TU from a representative patient with NSCLC (patient ID: 71-MP). Percentage of CD3+IL-9R+ and EpCAM+IL-9R+ cells is shown in the right.

that normal epithelial cells as well as tumor cells express comparable amounts of IL-9R **(Figure 3B).**

Finally, we performed FACS analysis in the human adenocarcinoma lung cancer cell line A549 to understand if IL-9R is expressed in these tumor cells and detected IL9R expression **(Figures 4A, B)** in A549 cells. The gating strategy for FACS staining is shown in **Supplementary Figure 3A**. In summary, subsets of tumor infiltrating lymphocytes in the lung as well as lung adenocarcinoma cells express IL9R and may thus be targets for immunomodulatory and cancer promoting effects of IL-9.

IFN-ɣ Inhibited IL-9R on A549 but IL-9 Did Not Inhibit IFN-ɣ Induced Lung Tumor Apoptosis

We next asked if IFN-γ would regulate IL-9 signaling. Here we found that, IFN-ɣ, but not IL-21 and TNF-α treatment significantly downregulated IL-9R expression on A549 cells (**Figure 4B**). Moreover, independently from IL-9, we found that, TNF-alpha induced IFN-ɣ receptor (CD119) levels on A549 cells (**Figure 4C**), indicating an opposite role of IFN-ɣ and TNF-alpha as compared to IL-9 on lung tumor cells.

It has been reported that IL-9 induced A549 proliferation (36). Therefore, we investigated if IL-9 would influence the tumor cell survival and death. Here we found that, as opposed to the anti-tumoral cytokine IFN-ɣ, IL-9 suppressed lung tumor cell apoptosis (**Figure 4D**). Furthermore, pre-treatment of A549 cells with IFN-ɣ reversed the anti-apoptotic effect of IL-9 **(Figure 4D).** Taken together these data indicate a pro-tumoral role of IL-9 in lung cancer.

IFN-ɣ Induced and IL-9 Inhibited Fas Receptors (FAS-R) on Lung Cancer Cells

In search of the molecular mechanism of IFN-ɣ's apoptotic effect on lung tumor cells, we discovered FAS-R (CD95) induction on A549 cells mediated by IFN-ɣ and an inhibition of FAS-R expression by IL-9 treatment (**Figure 5A**).

We next treated A549 cells either with IFN-ɣ or pretreated them with IL-9 and use agonistic antibodies to activate FAS-R (CD95). Here we could confirm that IFN-ɣ induced specifically FAS-R (**Figures 5B, C**). Moreover, treatment with agonistic anti-CD95 antibodies resulted in induction of IFN-ɣ mediated A549 cell death (**Figure 5D**).

By contrast, agonistic FAS-R treatment did not affect the effect of IL-9 on apoptosis demonstrating that IFN-ɣ-FAS mediated apoptosis is not influenced by IL-9. To prove that IFN-ɣ mediated A549 apoptosis, but not IL-9 induced tumor apoptosis *via* FAS-R.

IL-9R Is Induced in CD4+CD25+ Foxp3+ Treg Cells During T Regulatory Cell Development

To further explore the effects of IL-9 on Treg cells, we analyzed IL-9 production and IL-9R expression by T regulatory cells differentiated *in vitro* in naïve mice. In addition, we added IL-9 and anti-IL-9 antibodies to see their effects on Tregs. As comparison we also set up Th9 skewing conditions. It was found that IL-9 is produced by Treg skewed lymphocytes although at lower levels as compared to Th9 cells (**Figure S4A, B**). Moreover, Treg skewing conditions did not result in increased Th9 cells (**Figure S4C**). In addition, Th9 skewing conditions induced Foxp3+ Treg cells (**Figure S4D**) although at lower levels as compared to Treg skewing conditions. IL-9 did not further induce Treg development upon IL-2 and TGF-beta stimulation (**Figure S4D**). Finally, when naive T cells were differentiated into Treg cells, IL-9R expression mRNA was upregulated at day 5 as compared to day 3 (**Figure S4E**). These findings suggest that Treg cells produce lower levels of IL-9 as compared to Th9 cells but may have increased capability to respond to IL-9 signaling as they differentiate. We then analyzed levels of IFN-ɣ, an anti-tumor Th1 cytokine released by different immunocompetent cells such as CD8+ T cells that play a key role in anti-tumor mediated immune responses (27, 37, 38). To this aim, we first skewed naïve spleen CD4+CD62L+ T cells under Th1 skewing conditions. As IL-9 production of naive CD4+ T cells is inhibited by IFN-ɣ (9, 39), we induced Th1 development in naïve spleen T cells by incubating naïve cells with IL-12, a cytokine produced by dendritic cells and macrophages that induces IFN-ɣ production in naive T cells (40), and anti-IL-4 antibodies. In these studies, we found that Th1 skewing conditions inhibited IL-9 while inducing IFN-ɣ levels in the supernatants **(Figure S4F).**

In a Syngenic Model of Lung Cancer With LL/2 Cells IL-9 Deficiency Resulted in Decreased Tumor Load Associated With Increased IL-21 Levels

In subsequent experiments, we performed studies in the syngenic LL/2 model and analyzed the direct anti-tumoral function of IL-9 on the tumor cell line LL/2 by using Ki67 and AnnexinV/PI as proliferation and apoptosis markers, respectively **(Figures 6A, B)**. By using Ki67 staining we found that, IL-9 stimulation did not induce tumor cell proliferation of LL/2 cells **(Figure 6A).** In addition, IL-9 significantly reduced late apoptosis in LL/2 cells at the lower concentration analyzed, as determined by Annexin/PI staining, suggesting that IL-9 may directly regulate apoptosis of LL/2 lung tumor cells in a dose dependent manner **(Figure 6B).** The overall survival of LL/2 was induced by higher concentrations of IL-9 at 100ng/ml **(Figure 6C).**

We next induced lung tumor in a syngenic model of disease in C57Bl/6 mice. As the transcription factor PU1 has been implicated in controlling IL-9 production by T cells (16), we then asked if levels of PU1 (*Spi1* mRNA) are upregulated in lung T cells of wild-type mice bearing tumors. In fact, *Spi1* mRNA levels were significantly induced in tumor infiltrating T cells in WT mice as compared to lung T cells from mice lacking tumors **(Figure 6D)**. In addition, we demonstrated that these lung T cells may respond to IL-9 stimulation because they express the IL-9R **(Figure 6E).** However, we could not find any difference in IL-9R expression between tumor infiltrating T cells and lung T cells from naïve mice.

In this syngenic model **(Figures 6F–J)**, we found that, targeted deletion of IL-9, resulted in induced body weight as compared to the wild type littermates bearing tumor **(Figures 6F, G).** Moreover, by assessing the tumor load, we

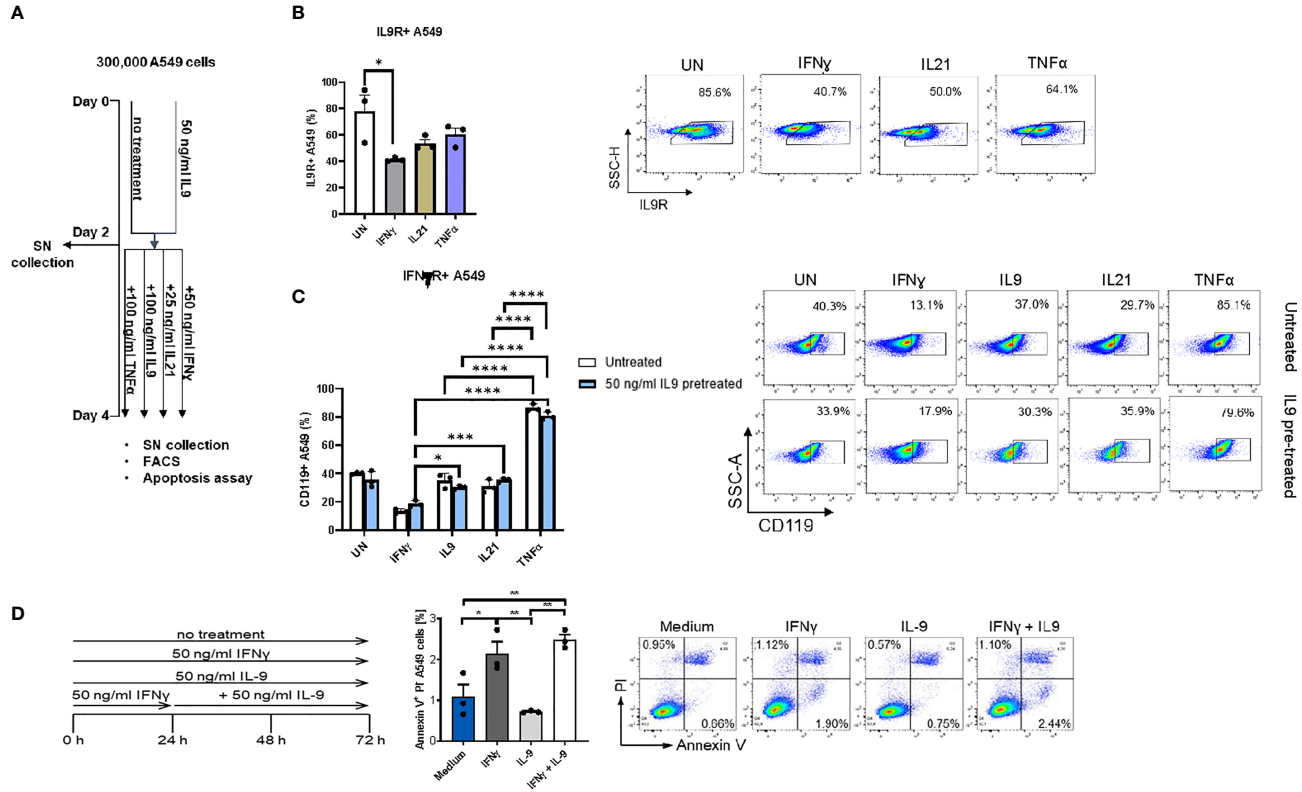

FIGURE 4 | Analysis of IL9 effects on cell surface receptors IL-9R and IFNγ-R expression *in vitro* on A549 cell line. **(A)** Experimental design of A549 cell line culture for 4 days. A549 cells were pretreated with or without IL9 (50 ng/ml) for two days. On day 2, supernatants were collected and cells were further cultured for two days with IFNɣ (50 ng/ml), IL9 (100 ng/ml), IL21 (25 ng/ml) or TNFα (100 ng/ml) in new medium, respectively. Cells were harvested for flow cytometry analysis and apoptosis assay on day 4. **(B)** Flow cytometry analysis of the percentage of IL9R expressing A549 cells unstimulated, or stimulated with IFNɣ, IL21 or TNFα, respectively. A representative dot plot is shown for each group. **(C)** Flow cytometry analysis of the percentage of IFNɣR (CD119) expression A549 cells unstimulated or stimulated with IFNɣ, IL9, IL21 or TNFα, respectively. Both IL9 pretreated and untreated A549 cells were analyzed. A representative dot plot is shown for each group. **(D)** Experimental design of A549 cell line culture for 72 hours. A549 cells were untreated, or treated with IFNɣ (50 ng/ml) or IL9 (50 ng/ml) for 72 hours. In addition, one group was first pretreated with IFNɣ (50 ng/ml) for 24 hours, then stimulated with IL9 (50 ng/ml) for 48 hours. After 72 hours, all cells were harvested for flow cytometry analysis for cell apoptosis. Flow cytometry analysis of the percentage of A549 early apoptosis (Annexin V+PI- cells) in unstimulated cell culture condition or in condition of IFNɣ, IL9, IFNɣ+IL9, respectively. A representative dot plot is shown for each group. All data were statistically analyzed with ordinary one-way ANOVA or two-way ANOVA, and showed with mean ± SEM. n=3 per group. *P < 0.05; **P < 0.01; ***P < 0.001; ****P < 0.0001.

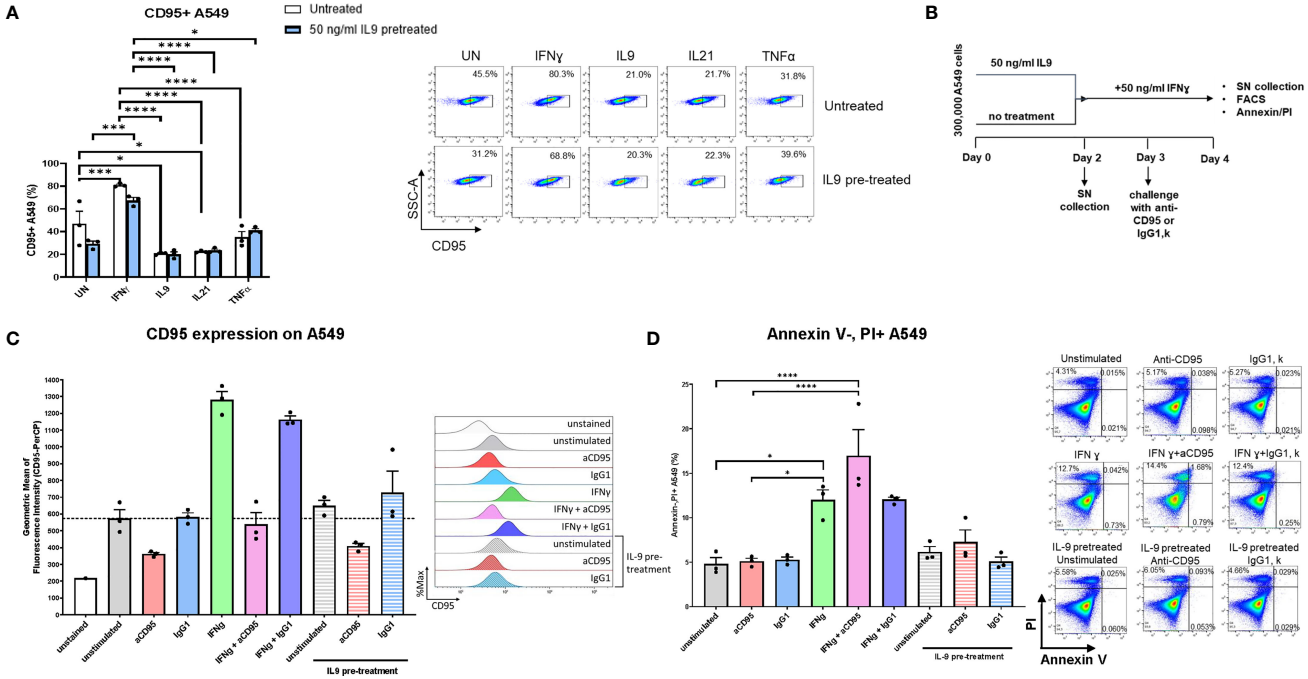

FIGURE 5 | Analysis of IL9 effects on tumor cell survival *in vitro* on A549 cell line. **(A)** Flow cytometry analysis of the percentage of CD95 (Fas) expressing A549 cells unstimulated or stimulated with IFNɣ, IL9, IL21 or TNFα, respectively. Both IL9 pretreated and untreated A549 cells were analyzed**. (B)** Experimental design of A549 cell line culture for 4 days. **(C)** Flow cytometry analysis of the geometric mean of CD95 (Fas) expressing A549 cells unstimulated or stimulated with aCD95, IgG1, IFNγ and a combination of aCD95 or IgG1 with IFNγ, respectively. Furthermore, aCD95 and IgG1 stimulated cells were analyzed after IL-9 pre-treatment. **(D)** Flow cytometry analysis of the percentage of A549 necrotic cells (Annexin V-PI+ cells) in unstimulated cell culture condition or in condition of aCD95, IgG1, IFNγ and a combination of aCD95 or IgG1 with IFNγ, respectively. Furthermore, aCD95 and IgG1 stimulated cells were analyzed after IL-9 pre-treatment. A representative histogram (c) or dot plot (d) is shown for each group. The data were statistically analyzed with two-way ANOVA, and showed with mean ± SEM. n=3 per group. *P < 0.05; **P < 0.01; ***P < 0.001; ****P < 0.0001.

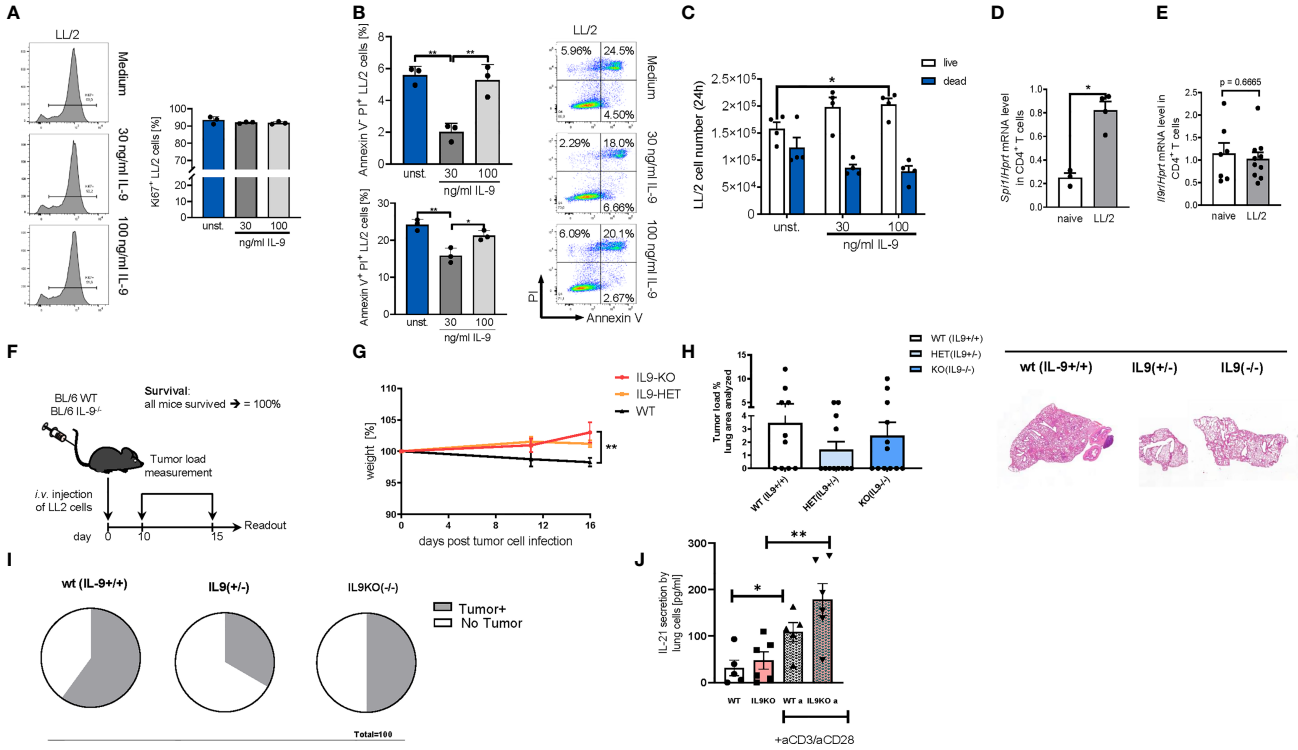

FIGURE 6 | Targeted deletion of IL-9 resulted in lung tumor rejection in BL6 syngenic mice. **(A)** *In vitro* studies of murine LL/2-luc-M38 (LL/2) lung carcinoma cells treated with/out recombinant IL-9 for 24h. Flow cytometry analysis of the percentage of Ki67 expressing LL/2 cells after stimulation with or without IL-9 for 24h and representative histograms (left) (n unst. = 3; n30 ng/ml=3; n100 ng/ml=3). **(B)** Annexin V/PI flow cytometry analysis of LL/2 cells after stimulation with or without IL-9 for 24h and representative dot plots (n unst. = 3; n30 ng/ml=3; n100 ng/ml=3). **(C)** Cell count by using Neubauer chamber. Bar charts indicate mean values ± SEM using student´s two-tailed *t*-test (b–g) or ordinary one-way ANOVA (i–j) (*p<0.05, **p<0.01, ***p<0.001). **(D)** qPCR based analysis of *Spi1* encoding PU.1 (n_{naive}=3; $n_{LL/2\ =}$ 4) and **(E)** *Il9r* (n_{naive}=7; $n_{LL/2\ =}$ 10) in relation to Hprt mRNA level in $CD4^+$ T cells isolated cells from the lung of naïve and lung tumor-bearing (LL/2) WT mice. **(F)** Experimental design for the induction of lung tumor development in BL/6 WT, BL/6-IL-$9^{+/-}$ and BL/6 IL-$9^{-/-}$ mice which were intravenously (i.v.) with LL/2-luc-M38 (LL/2) lung carcinoma cells on day 0. The experiment ended on day 16. **(G)** Monitored body weight during tumor development. **(H)** Quantification of the tumor-infiltrated area of the lung (left) and representative H&E staining of the lung of WT, IL-$9^{+/-}$ and IL-$9^{-/-}$ mice (right) (n_{WT}=10; $n_{IL\text{-}9+/-=}$10 $n_{IL\text{-}9-/-}$=10). **(I)** Circles represent mice per group tumor free (circle sectors in white) and mice with lung bearing tumor (sectors in grey). **(J)** ELISA analysis of IL-21 levels (pg/ml) in supernatant obtained from cells isolated from the lung of wild-type and IL-$9^{-/-}$ tumor-bearing mice. Lung cells were cultured for 4 days unstimulated or re-stimulated with aCD3/aCD28 antibodies (n_{WT}=5, $n_{IL9\text{-}/\text{-}}$=6).

found that both the IL-9 deficient and the IL-9 heterozygous mice had a decreased (but not statistically significant) tumor load as compared to wild type littermates (**Figure 6H**). More importantly, 67% of the IL-9 heterozygous and 50% of the IL-9 knockout mice were tumor free as opposed to 40% in the wild type mice group, indicating an anti-tumoral effect of IL-9 deficient mice (**Figure 6I**). By looking into the mechanism we found that consistent with the presence of Th9 cells in the tumor of NSCLC patients, targeted deletion of IL-9 resulted in significant upregulation of IL-21, a cytokine produced by Th9 cells that may regulate anti-tumor effects of Th9 cells in lung cancer (**Figure 6J**).

Targeted Deletion of IL-9 Reduced Tumor Load and Induced Tumor Free Lungs in a Second Syngenic Model of Lung Cancer

We next asked if the presence of IL-9 affects tumor development in a second syngenic model of lung cancer after intravenous injection of L1C2 lung tumor cell line in a Balb/c genetic background (**Figure 7**). Consistent with the other models of disease, we confirmed significant upregulation of body weight in the absence of IL-9 during tumor development as compared to wild type littermates (**Figures 7A, B).** We observed a reduction of the tumor load, by trend (**Figures 7C–E**). Similar to the LL/2 model, we observed in additional experiments that the number of mice with no tumor was induced in the absence of IL-9 (**Figure 7E**). Moreover, the immunosuppressive FoxP3+CD4+ CD25+ T regulatory cells were reduced in the absence of IL-9 (**Figure 7F**), consistent with our finding that Treg cells express IL-9R. Finally, we directly analyzed the pro-tumoral function of IL-9 on the tumor cell line L1C2 by using cell counts (**Figure 7G**), Ki67 (**Figure 7H**) and AnnexinV/PI (**Figure 7I**) as proliferation and apoptosis markers, respectively. By using cell counts, we found that IL-9 did not influence the tumor cell count, while IFN-ɣ and TNF-alpha decreased the overall tumor cell count (**Figure 7G**). By Ki67 staining, we detected that IL-9 stimulation significantly induced L1C2 tumor cell proliferation in a dose dependent manner (**Figure 7H).** In addition, IL-9 significantly reduced early apoptosis in L1C2 cells at lower concentrations, as determined by Annexin/PI staining, suggesting that IL-9 may directly regulate both apoptosis and proliferation of L1C2 lung tumor cells (**Figure 7H**).

Anti-IL-9 Antibodies Inhibit Lung Tumor Growth in the Syngenic LL/2 Model *In Vivo*

The above findings are consistent with a model in which IL-9 derived by TIL cells directly favours tumor cell survival and suppresses anti-tumor immune responses by effects back on TILs. Therefore, we asked if targeting of IL-9 function might be therapeutically useful in lung cancer. To explore this concept under *in vivo* conditions, we next studied the effects of neutralizing anti-IL-9 antibodies in our experimental lung cancer model induced by LL/2 cells *in vivo*. To this aim, we blocked IL-9 repeatedly during lung tumor development in WT mice *via* intraperitoneal injection of anti-IL-9 antibodies (**Figure 8A**). Consistent with the phenotype discovered for IL-9 deficient mice, intraperitoneal anti-IL-9 antibody treatment in WT mice resulted in increased body weight and an increased tumor rejection (**Figures 8B–D**) as compared to control IgG-treated WT animals. Moreover, we found that IgG control treatment in tumor model resulted in decreased number of CD4+ and CD8+ T-bet+TNF-α+ T cells which were induced by the anti-IL-9 antibody treatment (**Figures 8E, F**). Finally, we pretreated LL/2 cells with IL-9 for 48 hours and then challenge LL/2 cells with different cytokines. Shown is flow cytometric analysis of the percentage of necrotic cells (Annexin V-PI+ cells) after IL9 (100 ng/ml) pretreatment of LL/2 cells following 48h unstimulated cell culture condition or in conditions with IFNɣ, IL9, IL21, TNFα treatment, respectively. Under these conditions only TNF-α showed a pro-apoptotic function on LL/2 tumor cells (**Figure 8G**).

Blockade of IL-9 at Later Time Points in Established Tumors Resulted in Tumor Rejection in the Two Syngenic LL/2 and L1C2 Mediated Models of Experimental NSCLC in Mice

In subsequent studies on the effects of anti-IL-9 antibodies in experimental NSCLC, we explored the effects of these antibodies at later time points of tumor induction in the two models of disease in syngenic mice. In the LL/2 model we started the treatment at day 6 after tumor cell injection (**Figure 9A).** Here we observed that, blocking IL-9 at later time points during tumor development resulted in a significant tumor reduction as compared to IgG treatment (**Figures 9B, C).** pSTAT5 is activated downstream of IL-9 and thus we looked at pSTAT5 in lung CD4+CD25+ T cells and found that this cell population was down-regulated by anti-IL-9 antibody treatment (**Figure 9D).** By trend, we also found induction of IFN-ɣ after anti IL-9 treatment (**Figure 9E).**

We next analyzed a second syngenic model of disease using the cell line L1C2 in a BALB/c genetic background and started treatment at a later time point at day 9 when the tumor was already present in the lung (**Figure 9F**). In this model we found a reduction of the number of pre-tumoral lesions in the anti-IL-9 antibody treated mice (**Figure 9G).** Additionally, we studied the number of activated CD4+CD25 (IL2Ralpha)+ T cells and found them to be induced in the lung of anti-IL-9 antibody treated mice (**Figure 9I**). Moreover, the immunosuppressive cytokine IL-10 was downregulated upon anti-IL-9 treatment (**Figure 9J**), suggesting that IL-9 controls the balance between inflammatory and immunosuppressive cytokines in NSCLC.

DISCUSSION

In this study, we investigated the functional role of IL-9 in NSCLC. We observed an induction of IL-9 production by tumor infiltrating lymphocytes (TIL) and a subset of FoxP3+ regulatory T cells in the tumoral region of NSCLC patients and identified tumor infiltrating T cells, FoxP3+ Treg cells and tumor cells as IL-9R expressing target cells for IL-9 signaling. The functional relevance of IL-9 signaling in lung cancer was underlined by

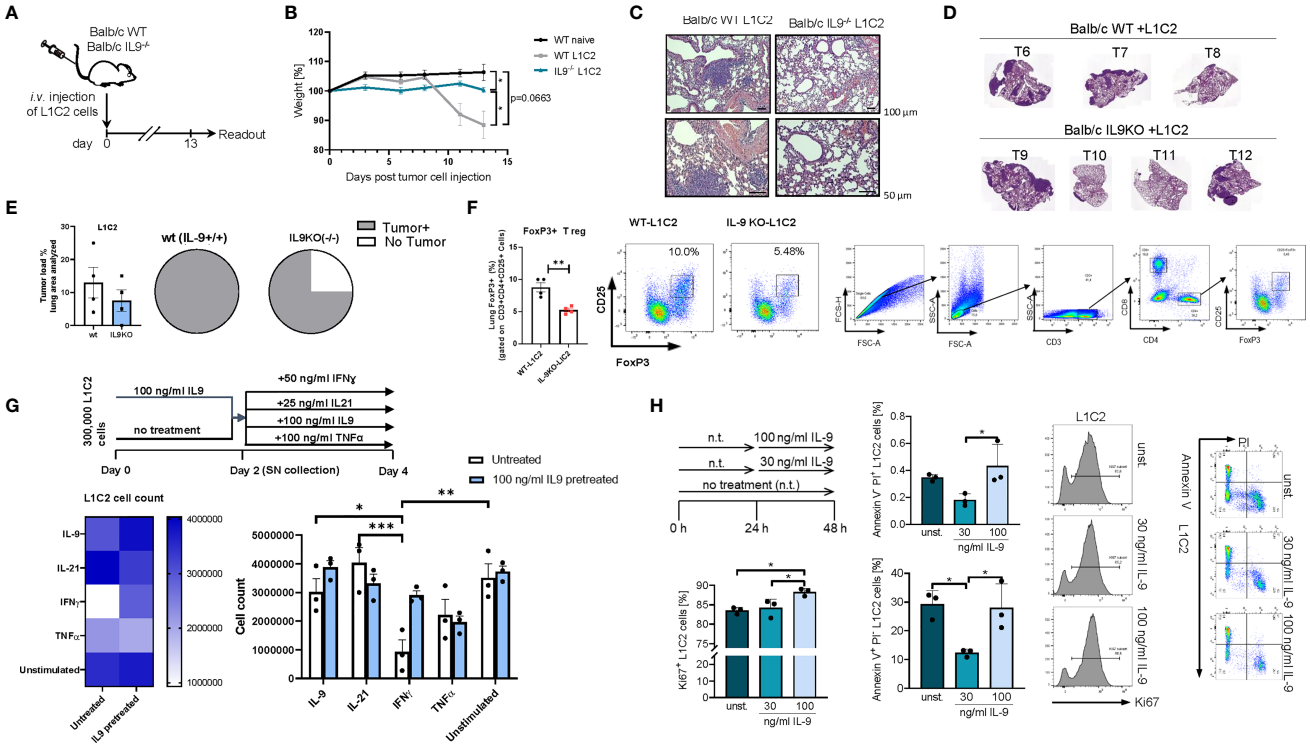

FIGURE 7 | Targeted deletion of IL-9 resulted in lung tumor rejection Balb/c syngenic mice. **(A)** Experimental design for the induction of lung tumor development in Balb/c wild-type (WT) and Balb/c IL9$^{-/-}$ mice. Tumor growth was induced *via* intravenous (i.v.) injection of L1C2 lung carcinoma cells. The experiment ended on day 14. **(B)** Body weight changes of Balb/c IL9$^{-/-}$ mice and Balb/c control littermates (injected i.v. with/out L1C2 cells) 0 to 14 days after tumor induction ($n_{IL9-/-}$=4; $n_{balb/c\ L1C2}$ = 3; $n_{balb/c\ naive}$=2). **(C)** Representative H&E staining of the lung of WT and IL-9$^{-/-}$ mice (top, scale bar=100 µm; bottom, scale bar=50 µm) and **(D, E)** additional mice were evaluated by a pathologist in a blind manner (n=4 per group). Circles represent mice per group tumor free (sectors in white) and mice with lung bearing tumor (sectors in grey). **(F)** FACS analysis of Foxp3+ CD25+ T regulatory cells in total lung cells of 4 wt and 4 IL9 ko mice after gating on CD3+CD4+ T cells. **(G)** Experimental design is similar to the A549 cell line culture whereby L1C2 were pre-cultured or not for 2 days of IL9 (100 ng/ml) and then further cultured for 2 days unstimulated or cultured with either IFNɣ, or IL9, IL21 or TNFα, respectively. The data were statistically analyzed with two-way ANOVA, and showed with mean ± SEM. n=3 per group. *, P<0.05; **, P<0.01; ***, P<0.001; ****, P<0.0001. **(H)** Flow cytometry analysis of the percentage of Ki67 expressing L1C2 cells after stimulation with or without IL-9 for 24h and representative histograms (n-unst. = 3; n30 ng/ml=3; n100 ng/ml=3). Annexin V/PI flow cytometry analysis of L1C2 cells after stimulation with or without IL-9 for 24h and representative dot plots (n-unst. = 3; n30 ng/ml=3; n100 ng/ml=3). Bar charts indicate mean values ± SEM using student´s two-tailed t-test (b-g) or ordinary one-way ANOVA (i-j) (*p < 0.05, **p < 0.01, ***p < 0.001).

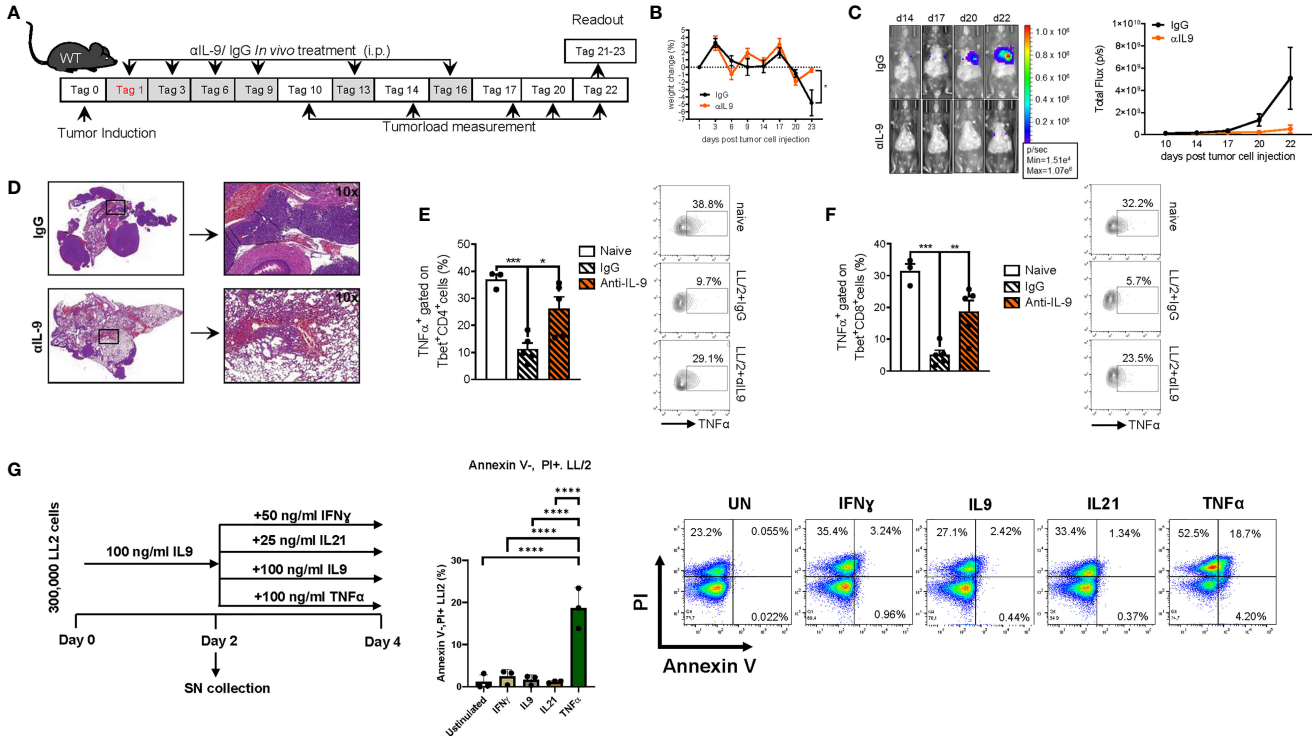

FIGURE 8 | Anti-IL9 antibody treatment inhibits lung tumor development. **(A)** Experimental design: BL/6 WT mice were intravenously injected with LL/2 cells on day 0. Mice were then treated intraperitoneally (i.p.) with anti (α)-IL9 antibody or IgG2a isotype control on days 1, 3, 6, 9, 13 and 16 after tumor induction. Overall survival rate of αIL9 antibody or IgG2a isotype control treated mice. Survival rate on the right handside. **(B)** Monitoring of body weight changes of BL/6 WT mice injected i.v. with LL/2 cells). **(C)** Tumor load was analyzed *via* bioluminescence-based imaging system on the indicated days. The experiment ended on day 23. Representative *in vivo* images of lung tumor load analysis at days 14, 17, 20 and 22 in WT mice treated with αIL9 antibody or IgG2a isotype control (representative of 3 independent experiments) are shown. and lung tumor load (Total flux=photons/second) (Day10-20 $n_{IgG2a+LL/2\ =}$ 5, $n_{\alpha IL\text{-}9+LL/2\ =}$ 5; day22 $n_{IgG2a+LL/2\ =}$ 5, $n_{\alpha IL\text{-}9+LL/2\ =}$ 4) were quantified. **(D)** Representative H&E staining of WT mice treated with αIL9 antibody or IgG2a isotype control (scale bar=200 μm). **(E)** Flow cytometry analysis of TNFα positive cells (%) gated on Tbet and CD4 co-expressing cells (nnaive=3; nIgG2a+LL/2 = 5; nαIL-9+LL/2 = 5). **(F)** Flow cytometry analysis of TNFα positive cells (%) gated on Tbet and CD8 co-expressing cells (nnaive=3; nIgG2a+LL/2 = 5; nαIL-9+LL/2 = 5). **(G)** Experimental design is similar to the A549 cell line culture whereby LL/2 were pre-cultured for 2 days of IL9 (100 ng/ml) and then further cultured for 2 days unstimulated or cultured with either IFNɣ, or IL9, IL21 or TNFα, respectively. Annexin V(AnnV)/PI flow cytometry analysis of IL9 pre-treated LL/2 cells at the end of the cell culture, A representative dot plot is showed for each group. The data were statistically analyzed with one-way ANOVA, and showed with mean ± SEM. n=3 per group. *P < 0.05; **P < 0.01; ***P < 0.001; ****P < 0.0001.

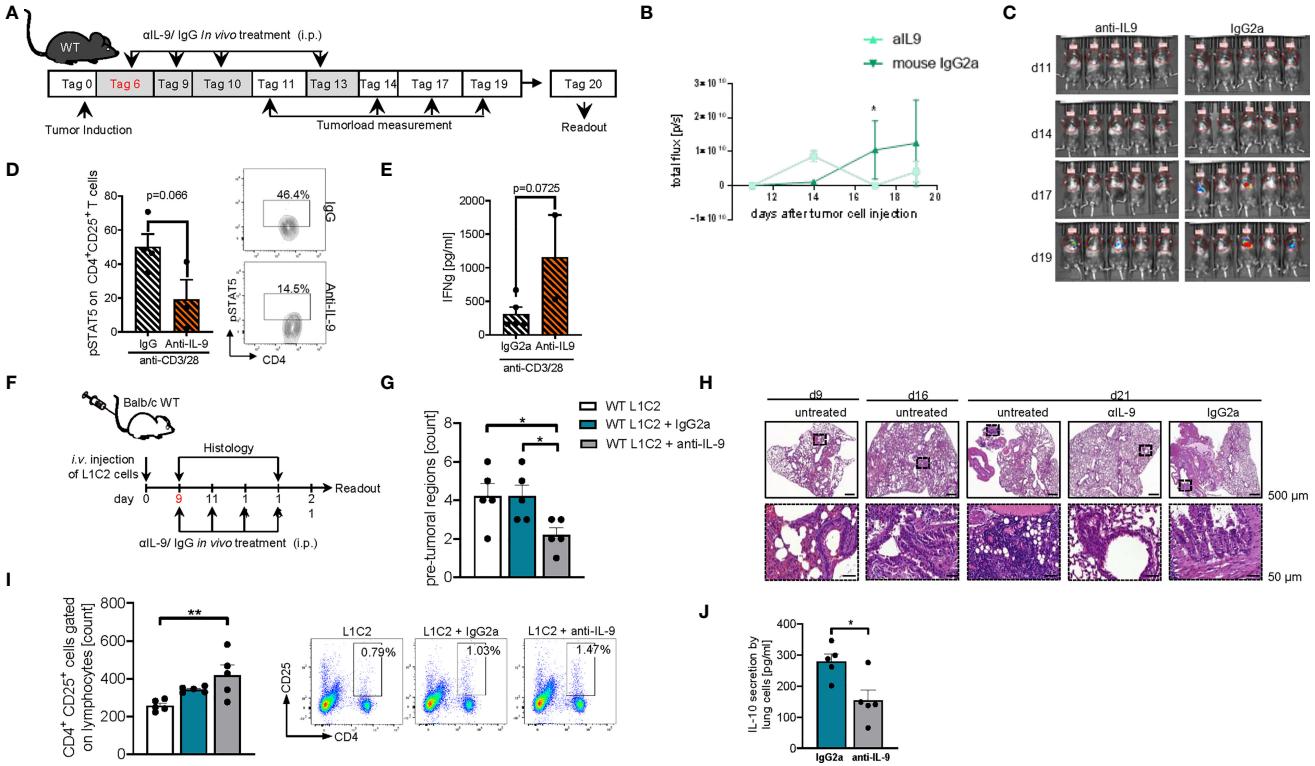

FIGURE 9 | Later treatment with anti-IL9 antibodies during tumor development, protected from experimental induced tumor. **(A)** Experimental design: BL/6 WT mice were intravenously injected with LL/2 cells on day 0. Mice were then treated intraperitoneally (i.p.) with anti (α)-IL9 antibody or IgG2a isotype control on day 6, 9, 10 and 13 after tumor induction. The experiment ended on day 20. **(B, C)** Tumor load was analyzed *via* bioluminescence-based imaging system on the indicated days. Representative *in vivo* images of lung tumor load analysis at day 11, 14, 17 and 19 in WT mice treated with αIL9 antibody or IgG2a isotype control (c). (b)Quantification of lung tumor load (Total flux=photons/second) (Day10-20 $n_{\alpha IL\text{-}9+LL/2\ =}$ 5; $n_{IgG2a+LL/2\ =}$ 5). **(D)** FACS analysis of lung pSTAT5+CD4+CD25+ lung cells after 24 hours culture with anti_CD3/CD28 antibodies (n-αIL-9+LL/2 = 5; n-IgG2a+LL/2 = 5). **(E)** ELISA analysis of IFNγ levels (pg/ml) in supernatants obtained from cells isolated from the lung of wild-type (WT) lung tumor-bearing mice treated with/out anti(α)-IL9 antibody or IgG2a isotype control and cultured for 24h at 37°C (nIgG2a= 5; nαIL-9 = 5). N values are given per group. Bar charts indicate mean values ± SEM using student´s two-tailed t-test *p<0.05, **p<0.01, ***p<0.001. **(F)** Experimental design: Balb/c WT mice were intravenously injected with L1C2 cells on day 0. Mice were then treated intraperitoneally (i.p.) with anti (α)-IL9 antibody or IgG2a isotype control on day 9, 11, 14 and 16 after tumor induction. Tumor load was analyzed *via* immune histology on the indicated days. The experiment ended on day 21. **(G, H)** Representative H&E staining of WT mice untreated or treated with αIL9 antibody or IgG2a isotype control on day 9, 16 and 21 (top, scale bar=500 µm; bottom, scale bar=50 µm) and quantification of the number of pre-tumoral lesions in the in the lung on day 21 (n_{IgG2a}= 5; $n_{\alpha IL\text{-}9\ =}$ 5). **(I)** Flow cytometry analysis of percentage of CD4+CD25+ cells gated on lymphocytes in non-treated or with αIL9 antibody or IgG2a isotype control treated mice. **(J)** ELISA analysis of IL-10 levels (pg/ml) in supernatant obtained from cells isolated from the lung of wild-type (WT) lung tumor-bearing mice treated with/out anti(α)-IL9 antibody cultured for 24h at 37°C ($n_{untr.\ =}$ 5; n_{IgG2a}= 5; $n_{\alpha IL\text{-}9\ =}$ 5). N values are given per group. Bar charts indicate mean values ± SEM using student´s two-tailed *t*-test *p < 0.05, **p < 0.01, ***p < 0.001.

studies in several independent murine NSCLC models of lung adenocarcinoma where IL-9 deficiency resulted in suppression of tumor growth. Finally, antibodies to IL-9 inhibited tumor growth *in vivo* in two syngenic models of disease. These findings suggest that targeting of IL-9 function may be useful for immunotherapy of NSCLC.

In an initial series of studies on the role of IL-9 in NSCLC, we analyzed samples from a large cohort of NSCLC patients. In the lung of patients with NSCLC, we found IL-9+ cells induced in the tumoral region of the lung as compared to the control region **(Figure 1B).** While no induction of epithelial cells expressing IL-9 was noted in NSCLC patients, we identified tumor infiltrating T cells in NSCLC as important IL-9 producers **(Figures 1G, H)**. Thus, we determined IL-9 production in different T cell subsets **(Figure 2).** Upon antigen binding, naïve $CD4^+$ T cells can differentiate into distinct subtypes, such as Th1, Th2, Th9, and Th17 cells but also regulatory T cells (Tregs) (41–43). The development of each T cell subtype can be induced by a specific cytokine milieu and is characterized by the expression of lineage specific hallmark transcription factors, such as Tbet, Gata3, Rorγt or STAT5 and Foxp3 (44–48). Here, we noted that IL-9 is increasingly produced by TIL **(Figures 1G, H)** and a subset of Foxp3 expressing Treg cells **(Figures 2A–D**) in lung tissues of NSCLC patients. Although IL-9 producing Treg cells have been described in inflammatory conditions such as nephritis (49), they have not been observed in cancer tissue so far. However, we found that such Foxp3+ T cells are located in lung cancer tissue of NSCLC patients. As FoxP3+ Treg cells are known to suppress anti-tumor immunity in NSCLC (50), these findings suggested that IL-9 derived from Treg cells and TIL might control immune responses and tumor growth. As TIL in NSCLC patients produced elevated amounts of the Th9 cytokine IL-21 (7, 22) and expressed the Th9 associated transcription factor PU.1 (15, 28), our findings suggested that Th9 cells as well as Tregs are an important source of IL-9. Future studies on the relative contribution and functional relevance of these IL-9 producing T cell subsets (for instance, by using conditional IL-9 deficient animals) are warranted.

Further studies suggested that IL-9 derived from tumor infiltrating T cells (TILs) as well as the tumor cells themselves might influence the T regulatory cells infiltrating the tumor. In fact, TILs were found to release induced IL-9 upon antiCD3/CD28 antibody treatment **(Figure 1H),** and T regulatory cells had increased levels of IL-9R *ex vivo* **(Figure S4)**. Mechanistic studies in a murine model of lung adenocarcinoma highlighted the functional relevance of IL-9 signaling for cancer growth *in vivo*. Specifically, we found that the absence of IL-9 inhibits lung carcinoma growth and drives tumor rejection in two independent murine models of NSCLC.

These findings led to further mechanistic studies showing decreased numbers of T regulatory cells expressing Foxp3 in the absence of IL-9 in one model of disease **(Figure 7F)** confirming the predominant effects of IL-9 on the presence and function of immunosuppressive T cells that facilitate cancer growth. Altogether, these data support a pro-tumoral function of IL-9 in TILs that may be considered for the design of new immunotherapies against NSCLC. In fact, we demonstrated here that anti-IL-9 antibodies given intraperitoneally during tumor development resulted in increased survival rates and enhanced tumor rejection **(Figures 8**, **9)**. Remarkably, anti-IL9 treatment was even effective in mice with already established lesions in both models suggesting a key function role of IL-9 in controlling tumor growth *in vivo*. In the syngenic L1C2 model, IL-9 blockade resulted in a downregulation of IL-10 **(Figure 9J)**. As IL-10 and TGF-beta expressing T cells are known to play a crucial role for inducing Foxp3+ T regulatory cells and controlling immune responses in NSCLC (31, 35), these results suggest that IL-9 plays an important role in regulating immune responses in lung cancer *in vivo*.

Further studies on the effects of IL-9 blockade in experimental lung cancer identified direct effects of IL-9 on tumor cells. Specifically, human lung cancer cells expressed the IL-9R **(Figures 4A, B)**. Furthermore, IL-9 treatment prevented the induction of tumor cell death in lung adenocarcinoma cells indicating a pro-tumoral role of IL-9 signaling. Experimental studies in NSCLC cell lines identified effects of IL-9 on cell proliferation or apoptosis suggesting that this cytokine drives tumor growth in NSCLC both in human **(Figure 5A)** and in murine tumor cells **(Figure 7H).** Consistently, a previous study showed that IL-9 promoted the proliferation of A549 lung cancer cells (36). Moreover, IL-9 facilitated intercellular adhesion of these cancer cells to pleural mesothelial cell monolayers suggesting that this cytokine may be involved in malignant pleural effusion and pleural metastasis (36).

Reports on the role of IL-9 and Th9 cells in tumor immunity have yielded partially controversial results (51–54). While an important anti-tumoral role of IL-9 was found in melanoma, we observed here a key pro-tumoral role of IL-9 in NSCLC. One possible explanation for these differences relates to IL-9 target cells in different tumor types. In fact, we noted here that IL-9 controls tumor cell growth in NSCLC *via* direct effects on IL-9R expressing cancer cells. In contrast, IL-9 effects on anti-cancer immunity *via* the tumor micromilieu rather than direct effects on tumor cells were noted in melanoma. Additional differences could be due to discrepancies in the tumor microenvironment between melanoma and NSCLC or the analysis of IL-9- versus Th9-dependent effects, as many studies used Th9 cell transfer-models rather than IL-9 single cytokine targeting to determine the functional relevance of IL-9. However, Th9 cells produce IL-21 in addition to IL-9, a cytokine with anti-tumor function. Recently, it was report that T follicular helper cells producing IL-21 play crucial roles in lung adenocarcinoma, because these cells were able to induce the effect function of tumor-infiltrating CD8 *via* IL-21/IL-21R signaling (55). Moreover, it has been reported that the transcription factor IRF1 enhanced the effector function of Th9 cells and dictated their anticancer properties. Consistent with this, IRF1 inhibits IRF4 effects on the IL-9 promoter (23). These observations raise the possibility that selective targeting of IL-9 may yield different results as compared to Th9 cell targeting, as the anti-tumor effect of the Th9 cytokine IL-21 is not targeted by anti-IL-9 antibodies. This possibility was also confirmed by the upregulation of IL-21 in a second syngenic model of disease

in IL-9 ko mice bearing tumor **(Figure 6J).** Thus, the role of IL-9 must be revised and analyzed independent from Th9 cells. Taken together, our findings indicate effects of IL-9 on growth of lung cancer cells. This concept is in agreement with the finding that IL-9 promotes the development of many hematological human tumors, including Hodgkin's lymphoma and B cell lymphoma (56) suggesting the presence of pro-tumoral effects of IL-9 in several tumor entities.

In summary, the present study has uncovered an important pro-tumoral role of IL-9 in NSCLC *via* direct effects on tumor cells and modulation of cytokine production by tumor infiltrating T cells. This observation in NSCLC is not consistent to the previously reported anti-tumoral role of IL-9 in melanoma where decreased IL-9 levels were associated with tumor growth (54, 57). Although the precise reasons for these differences remain currently unclear, they may be related to the specific microenvironment provided by lung TILs in NSCLC or to the question whether the targeted tumor cell type expresses the IL-9R. The expression of IL-9R on lung adenocarcinoma cells may permit direct effects of IL-9 on tumor cell proliferation or apoptosis. Consistent with these data, we noted that IL-9 treatment augments tumor cell proliferation or prevented cell death of human NSCLC cell lines in cell culture. Moreover, our findings demonstrate that anti-IL-9 antibodies markedly suppress tumor growth *in vivo* and identify IL-9R+ TILs and lung adenocarcinoma cells as targets for IL-9 signaling. Our findings provide new insights into the regulatory role of IL-9 for lung cancer growth and suggest new avenues for therapy of NSCLC by targeting of IL-9 function.

DATA AVAILABILITY STATEMENT

The raw data supporting the conclusions of this article will be made available by the authors, without undue reservation.

ETHICS STATEMENT

The studies involving human participants were reviewed and approved by the ethics review board of the University of Erlangen (Re-No: 56_12B; DRKS-ID: DRKS00005376). The patients/participants provided their written informed consent to participate in this study. The animal study was reviewed and approved by Ethics committees of the Regierung Unterfranken (Az 55.2-2532-2-1286-20).

AUTHOR CONTRIBUTIONS

SF designed the experiments, supervised the research, performed western blot and analysis for Human IL-9 in **Figure 1E**, murine 6I and **7E**, helped with set up human IHC, WB and their analysis, helped with data analysis and wrote this manuscript. LH analysed most of the human lung data, contributed to the murine anti-IL-9 therapy, and to the writing of the manuscript. ZY reanalyzed all the human data, generated the A549, LL/2 and L1C2 figures, except for **Figures 4D**, generated by SM and **Figures 6A–C** and **7H** which were generated by JK and helped with the manuscript writing and generation of the figures. PT and KH did all the FACS and ELISA analysis in human PBMCs samples, contributed to western blot and IL9 -/- mice analysis as well as to revisioning the manuscript. PT contributed to the anti-FAS mediated A549 apoptosis and relative FACS analysis and set up tumor load analysis in murine model. C-IG is the pathologist that digitalized all the histological sections (murine and human) and contributed to the tumor load analysis. KK, AG, JF, and SM helped with the murine anti IL-9 therapy (LL/2) and the human NSCLC lung FACS and IHC data. MTC injected the murine tumor cells i.v. JK helped with the anti IL9 therapy on Balb/c and did murine cell line culture and assisted to the generations of figures and material and methods. RK generated the Figure on murine TH9 and T reg differentiation. MK and MFN contributed to the writing of the manuscript. DIT and HS are the thoracic surgeons that performed human lung tumor surgery and RJR is the pathologist that generated the lung tissues arrays from NSCLC patients, as well as lung tissues from controls. In addition, he made the histopathologic definition of tumor free tissue (Control region) and Tumor cell containing tissue (Tumoral tissue) in the lung tissue arrays. All authors performed experiments, discussed the results or provided help with regard to the writing of the manuscript. All authors contributed to the article and approved the submitted version.

FUNDING

This work was supported by the DFG-FI817-5/3 grants and by the Molecular Pneumology department in Erlangen. MC was supported by the DFG CH1428/2-1 and MK was supported by NIH grant AI057459. PT is supported by the Sander Stiftung 2020.016.1 awarded to SF, and ZY is supported by the SFB CRC1181 Project B08 N awarded to SF.

ACKNOWLEDGMENTS

The authors thank the whole team of the Molecular Pneumology Department at the University of Erlangen-Nürnberg for their excellent technical support: Adriana Geiger for animal care and RNA extraction, Susanne Mittler for performing human IHC and helping the pathologists with tissue arrays, Eveldina Nendel for performing human and murine ELISAs and sectioning all the murine lung slides, and Sonja Trump for performing all RNA extraction and qPCR in humans and murine samples, for help with all cell culture enclosing preparing cells before injection, as

well as for extraction of human proteins and contributing to Western Blot performance. We also thank the Pathology Institute team at the Uniklinikum Erlangen for providing us with the human patient diagnosis and the human and murine histology including digitalization.

SUPPLEMENTARY MATERIAL

The Supplementary Material for this article can be found online at: https://www.frontiersin.org/articles/10.3389/fimmu.2022.859738/full#supplementary-material

REFERENCES

1. Rogers TK, Hamilton W, Tod A, Neal R. Response to: What Characteristics of Primary Care and Patients Are Associated With Early Death in Patients With Lung Cancer in the UK? *Thorax* (2015) 70(2):184. doi: 10.1136/thoraxjnl-2014-206514
2. van Klaveren RJ. Lung Cancer Screening With Low Dose Computed Tomography: Where Do We Stand Today? *Eur J Cancer* (2009) 45(Suppl 1):375–6. doi: 10.1016/S0959-8049(09)70054-1
3. Mazzaschi G, Facchinetti F, Missale G, Canetti D, Madeddu D, Zecca A, et al. The Circulating Pool of Functionally Competent NK and CD8+ Cells Predicts the Outcome of Anti-PD1 Treatment in Advanced NSCLC. *Lung Cancer* (2019) 127:153–63. doi: 10.1016/j.lungcan.2018.11.038
4. Liu J, Zhong Y, Peng S, Zhou X, Gan X. Efficacy and Safety of PD1/PDL1 Blockades Versus Docetaxel in Patients With Pretreated Advanced Non-Small-Cell Lung Cancer: A Meta-Analysis. *Onco Targets Ther* (2018) 11:8623–32. doi: 10.2147/OTT.S181413
5. Reppert S, Boross I, Koslowski M, Tureci O, Koch S, Lehr HA, et al. A Role for T-Bet-Mediated Tumour Immune Surveillance in Anti-IL-17A Treatment of Lung Cancer. *Nat Commun* (2011) 2:600. doi: 10.1038/ncomms1609
6. Ayati N, Lee ST, Zakavi SR, Cheng M, Lau E, Parakh S, et al. Response Evaluation and Survival Prediction Following PD-1 Immunotherapy in Patients With Non-Small-Cell Lung Cancer: Comparison of Assessment Methods. *J Nucl Med* (2020) 62(7):926-33. doi: 10.2967/jnumed.120.254508
7. Kaplan MH, Hufford MM, Olson MR. The Development and *In Vivo* Function of T Helper 9 Cells. *Nat Rev Immunol* (2015) 15(5):295–307. doi: 10.1038/nri3824
8. Goswami R, Kaplan MH. A Brief History of IL-9. *J Immunol* (2011) 186 (6):3283–8. doi: 10.4049/jimmunol.1003049
9. Schmitt E, Germann T, Goedert S, Hoehn P, Huels C, Koelsch S, et al. IL-9 Production of Naive CD4+ T Cells Depends on IL-2, Is Synergistically Enhanced by a Combination of TGF-Beta and IL-4, and is Inhibited by IFN-Gamma. *J Immunol* (1994) 153(9):3989–96.
10. Gerlach K, Hwang Y, Nikolaev A, Atreya R, Dornhoff H, Steiner S, et al. TH9 Cells That Express the Transcription Factor PU.1 Drive T Cell-Mediated Colitis *via* IL-9 Receptor Signaling in Intestinal Epithelial Cells. *Nat Immunol* (2014) 15(7):676–86. doi: 10.1038/ni.2920
11. Finotto S. B Lymphocyte-Induced Maturation Protein 1 (Blimp-1), a Negative Regulator of TH9 Development, Orchestrates the Resolution of Airway Inflammation in Patients With Allergic Asthma. *J Allergy Clin Immunol* (2018) 143(3):1119-30. doi: 10.1016/j.jaci.2018.07.039
12. Vely F, Barlogis V, Vallentin B, Neven B, Piperoglou C, Ebbo M, et al. Evidence of Innate Lymphoid Cell Redundancy in Humans. *Nat Immunol* (2016) 17(11):1291–9. doi: 10.1038/ni.3553
13. Jabeen R, Goswami R, Awe O, Kulkarni A, Nguyen ET, Attenasio A, et al. Th9 Cell Development Requires a BATF-Regulated Transcriptional Network. *J Clin Invest* (2013) 123(11):4641-53. doi: 10.1172/JCI69489
14. Jash A, Sahoo A, Kim GC, Chae CS, Hwang JS, Kim JE, et al. Nuclear Factor of Activated T Cells 1 (NFAT1)-Induced Permissive Chromatin Modification Facilitates Nuclear Factor-kappaB (NF-Kappab)-Mediated Interleukin-9 (IL-9) Transactivation. *J Biol Chem* (2012) 287(19):15445–57. doi: 10.1074/jbc.M112.340356
15. Chang HC, Sehra S, Goswami R, Yao W, Yu Q, Stritesky GL, et al. The Transcription Factor PU.1 Is Required for the Development of IL-9-Producing T Cells and Allergic Inflammation. *Nat Immunol* (2010) 11 (6):527–34. doi: 10.1038/ni.1867
16. Koh B, Abdul Qayum A, Srivastava R, Fu Y, Ulrich BJ, Janga SC, et al. A Conserved Enhancer Regulates IL9 Expression in Multiple Lineages. *Nat Commun* (2018) 9(1):4803. doi: 10.1038/s41467-018-07202-0
17. Olson MR, Verdan FF, Hufford MM, Dent AL, Kaplan MH. STAT3 Impairs STAT5 Activation in the Development of IL-9-Secreting T Cells. *J Immunol* (2016) 196(8):3297–304. doi: 10.4049/jimmunol.1501801
18. Elyaman W, Bradshaw EM, Uyttenhove C, Dardalhon V, Awasthi A, Imitola J, et al. IL-9 Induces Differentiation of TH17 Cells and Enhances Function of FoxP3+ Natural Regulatory T Cells. *Proc Natl Acad Sci USA* (2009) 106 (31):12885–90. doi: 10.1073/pnas.0812530106
19. Dardalhon V, Awasthi A, Kwon H, Galileos G, Gao W, Sobel RA, et al. IL-4 Inhibits TGF-Beta-Induced Foxp3+ T Cells and, Together With TGF-Beta, Generates IL-9+ IL-10+ Foxp3(-) Effector T Cells. *Nat Immunol* (2008) 9 (12):1347–55. doi: 10.1038/ni.1677
20. Veldhoen M, Uyttenhove C, van Snick J, Helmby H, Westendorf A, Buer J, et al. Transforming Growth Factor-Beta 'Reprograms' the Differentiation of T Helper 2 Cells and Promotes an Interleukin 9-Producing Subset. *Nat Immunol* (2008) 9(12):1341–6. doi: 10.1038/ni.1659
21. Xiao X, Balasubramanian S, Liu W, Chu X, Wang H, Taparowsky EJ, et al. OX40 Signaling Favors the Induction of T(H)9 Cells and Airway Inflammation. *Nat Immunol* (2012) 13(10):981–90. doi: 10.1038/ni.2390
22. Vegran F, Berger H, Boidot R, Mignot G, Bruchard M, Dosset M, et al. The Transcription Factor IRF1 Dictates the IL-21-Dependent Anticancer Functions of TH9 Cells. *Nat Immunol* (2014) 15(8):758–66. doi: 10.1038/ni.2925
23. Knoops L, Louahed J, Renauld JC. IL-9-Induced Expansion of B-1b Cells Restores Numbers But Not Function of B-1 Lymphocytes in Xid Mice. *J Immunol* (2004) 172(10):6101–6. doi: 10.4049/jimmunol.172.10.6101
24. Demoulin JB, Renauld JC. Interleukin 9 and its Receptor: An Overview of Structure and Function. *Int Rev Immunol* (1998) 16(3-4):345–64. doi: 10.3109/08830189809043001
25. Eisenhut F, Heim L, Trump S, Mittler S, Sopel N, Andreev K, et al. FAM13A is Associated With Non-Small Cell Lung Cancer (NSCLC) Progression and Controls Tumor Cell Proliferation and Survival. *Oncoimmunol* (2017) 6(1): e1256526. doi: 10.1080/2162402X.2016.1256526
26. Cui Y, Riedlinger G, Miyoshi K, Tang W, Li C, Deng CX, et al. Inactivation of Stat5 in Mouse Mammary Epithelium During Pregnancy Reveals Distinct Functions in Cell Proliferation, Survival, and Differentiation. *Mol Cell Biol* (2004) 24(18):8037–47. doi: 10.1128/MCB.24.18.8037-8047.2004
27. Andreev K, Trufa DI, Siegemund R, Rieker R, Hartmann A, Schmidt J, et al. Impaired T-Bet-Pstat1alpha and Perforin-Mediated Immune Responses in the Tumoral Region of Lung Adenocarcinoma. *Br J Cancer* (2015) 113(6):902–13. doi: 10.1038/bjc.2015.255
28. Kaplan MH. Th9 Cells: Differentiation and Disease. *Immunol Rev* (2013) 252 (1):104–15. doi: 10.1111/imr.12028
29. Campos Carrascosa L, Klein M, Kitagawa Y, Luckel C, Marini F, Konig A, et al. Reciprocal Regulation of the Il9 Locus by Counteracting Activities of Transcription Factors IRF1 and IRF4. *Nat Commun* (2017) 8:15366. doi: 10.1038/ncomms15366
30. Andreev K, Trufa DI, Siegemund R, Rieker R, Hartmann A, Schmidt J, et al. Impaired T-Bet-Pstat1alpha and Perforin-Mediated Immune Responses in the Tumoral Region of Lung Adenocarcinoma. *Br J Cancer* (2016) 115(9):e11. doi: 10.1038/bjc.2016.299
31. Kachler K, Holzinger C, Trufa DI, Sirbu H, Finotto S. The Role of Foxp3 and Tbet Co-Expressing Treg Cells in Lung Carcinoma. *Oncoimmunol* (2018) 7 (8):e1456612. doi: 10.1080/2162402X.2018.1456612
32. Heim L, Kachler K, Siegmund R, Trufa DI, Mittler S, Geppert CI, et al. Increased Expression of the Immunosuppressive Interleukin-35 in Patients With Non-Small Cell Lung Cancer. *Br J Cancer* (2019) 120(9):903–12. doi: 10.1038/s41416-019-0444-3
33. Shimbara A, Christodoulopoulos P, Soussi-Gounni A, Olivenstein R, Nakamura Y, Levitt RC, et al. IL-9 and Its Receptor in Allergic and Nonallergic Lung Disease: Increased Expression in Asthma. *J Allergy Clin*

Immunol (2000) 105(1 Pt 1):108–15. doi: 10.1016/S0091-6749(00)90185-4
34. Hartemann A, Bensimon G, Payan CA, Jacqueminet S, Bourron O, Nicolas N, et al. Low-Dose Interleukin 2 in Patients With Type 1 Diabetes: A Phase 1/2 Randomised, Double-Blind, Placebo-Controlled Trial. *Lancet Diabetes endocrinol* (2013) 1(4):295–305. doi: 10.1016/S2213-8587(13)70113-X
35. Vahl JM, Friedrich J, Mittler S, Trump S, Heim L, Kachler K, et al. Interleukin-10-Regulated Tumour Tolerance in Non-Small Cell Lung Cancer. *Br J Cancer* (2017) 117(11):1644–55. doi: 10.1038/bjc.2017.336
36. Ye ZJ, Zhou Q, Yin W, Yuan ML, Yang WB, Xiong XZ, et al. Differentiation and Immune Regulation of IL-9-Producing CD4+ T Cells in Malignant Pleural Effusion. *Am J Respir Crit Care Med* (2012) 186(11):1168–79. doi: 10.1164/rccm.201207-1307OC
37. Heim L, Friedrich J, Engelhardt M, Trufa DI, Geppert CI, Rieker RJ, et al. NFATc1 Promotes Antitumoral Effector Functions and Memory CD8(+) T-Cell Differentiation During Non-Small Cell Lung Cancer Development. *Cancer Res* (2018) 78(13):3619–33. doi: 10.1158/0008-5472.CAN-17-3297
38. Thommen DS, Koelzer VH, Herzig P, Roller A, Trefny M, Dimeloe S, et al. A Transcriptionally and Functionally Distinct PD-1(+) CD8(+) T Cell Pool With Predictive Potential in Non-Small-Cell Lung Cancer Treated With PD-1 Blockade. *Nat Med* (2018) 24(7):994–1004. doi: 10.1038/s41591-018-0057-z
39. Murtas D, Maric D, De Giorgi V, Reinboth J, Worschech A, Fetsch P, et al. IRF-1 Responsiveness to IFN-Gamma Predicts Different Cancer Immune Phenotypes. *Br J Cancer* (2013) 109(1):76–82. doi: 10.1038/bjc.2013.335
40. Zundler S, Neurath MF. Interleukin-12: Functional Activities and Implications for Disease. *Cytokine Growth Factor Rev* (2015) 26(5):559–68. doi: 10.1016/j.cytogfr.2015.07.003
41. Neurath MF, Finotto S, Glimcher LH. The Role of Th1/Th2 Polarization in Mucosal Immunity. *Nat Med* (2002) 8(6):567–73. doi: 10.1038/nm0602-567
42. Hwang SM, Sharma G, Verma R, Byun S, Rudra D, Im SH. Inflammation-Induced Id2 Promotes Plasticity in Regulatory T Cells. *Nat Commun* (2018) 9 (1):4736. doi: 10.1038/s41467-018-07254-2
43. Hasan Z, Koizumi SI, Sasaki D, Yamada H, Arakaki N, Fujihara Y, et al. JunB is Essential for IL-23-Dependent Pathogenicity of Th17 Cells. *Nat Commun* (2017) 8:15628. doi: 10.1038/ncomms15628
44. Lazarevic V, Chen X, Shim JH, Hwang ES, Jang E, Bolm AN, et al. T-Bet Represses T(H)17 Differentiation by Preventing Runx1-Mediated Activation of the Gene Encoding RORgammat. *Nat Immunol* (2011) 12(1):96–104. doi: 10.1038/ni.1969
45. Lazarevic V, Glimcher LH, Lord GM. T-Bet: A Bridge Between Innate and Adaptive Immunity. *Nat Rev Immunol* (2013) 13(11):777–89. doi: 10.1038/nri3536
46. Zhang F, Meng G, Strober W. Interactions Among the Transcription Factors Runx1, RORgammat and Foxp3 Regulate the Differentiation of Interleukin 17-Producing T Cells. *Nat Immunol* (2008) 9(11):1297–306. doi: 10.1038/ni.1663
47. Zhou L, Chong MM, Littman DR. Plasticity of CD4+ T Cell Lineage Differentiation. *Immun* (2009) 30(5):646–55. doi: 10.1016/j.immuni.2009.05.001
48. Zhu J, Jankovic D, Oler AJ, Wei G, Sharma S, Hu G, et al. The Transcription Factor T-Bet is Induced by Multiple Pathways and Prevents an Endogenous Th2 Cell Program During Th1 Cell Responses. *Immun* (2012) 37(4):660–73. doi: 10.1016/j.immuni.2012.09.007
49. Eller K, Wolf D, Huber JM, Metz M, Mayer G, McKenzie AN, et al. IL-9 Production by Regulatory T Cells Recruits Mast Cells That are Essential for Regulatory T Cell-Induced Immune Suppression. *J Immunol* (2011) 186 (1):83–91. doi: 10.4049/jimmunol.1001183
50. Schreiber TH, Wolf D, Bodero M, Podack E. Tumor Antigen Specific Itreg Accumulate in the Tumor Microenvironment and Suppress Therapeutic Vaccination. *Oncoimmunol* (2012) 1(5):642–8. doi: 10.4161/onci.20298
51. Tan H, Wang S, Zhao L. A Tumour-Promoting Role of Th9 Cells in Hepatocellular Carcinoma Through CCL20 and STAT3 Pathways. *Clin Exp Pharmacol Physiol* (2017) 44(2):213–21. doi: 10.1111/1440-1681.12689
52. Xiao X, Shi X, Fan Y, Zhang X, Wu M, Lan P, et al. GITR Subverts Foxp3(+) Tregs to Boost Th9 Immunity Through Regulation of Histone Acetylation. *Nat Commun* (2015) 6:8266. doi: 10.1038/ncomms9266
53. Rivera Vargas T, Humblin E, Vegran F, Ghiringhelli F, Apetoh L. TH9 Cells in Anti-Tumor Immunity. *Semin Immunopathol* (2017) 39(1):39–46. doi: 10.1007/s00281-016-0599-4
54. Lu Y, Hong S, Li H, Park J, Hong B, Wang L, et al. Th9 Cells Promote Antitumor Immune Responses *In Vivo*. *J Clin Invest* (2012) 122(11):4160–71. doi: 10.1172/JCI65459
55. Cui C, Wang J, Fagerberg E, Chen PM, Connolly KA, Damo M, et al. Neoantigen-Driven B Cell and CD4 T Follicular Helper Cell Collaboration Promotes Anti-Tumor CD8 T Cell Responses. *Cell* (2021) 184(25):6101–18.e13. doi: 10.1016/j.cell.2021.11.007
56. Demoulin JB, Uyttenhove C, Lejeune D, Mui A, Groner B, Renauld JC. STAT5 Activation Is Required for Interleukin-9-Dependent Growth and Transformation of Lymphoid Cells. *Cancer Res* (2000) 60(14):3971–7.
57. Purwar R, Schlapbach C, Xiao S, Kang HS, Elyaman W, Jiang X, et al. Robust Tumor Immunity to Melanoma Mediated by Interleukin-9-Producing T Cells. *Nat Med* (2012) 18(8):1248-53. doi: 10.1038/nm.2856

Conflict of Interest: The authors declare that the research was conducted in the absence of any commercial or financial relationships that could be construed as a potential conflict of interest.

Publisher's Note: All claims expressed in this article are solely those of the authors and do not necessarily represent those of their affiliated organizations, or those of the publisher, the editors and the reviewers. Any product that may be evaluated in this article, or claim that may be made by its manufacturer, is not guaranteed or endorsed by the publisher.

frontiers | Frontiers in Immunology

REVIEW
published: 31 May 2022
doi: 10.3389/fimmu.2022.887781

The Role of Myeloid Cells in GBM Immunosuppression

Ya-Jui Lin[1,2], *Caren Yu-Ju Wu*[2,3], *Janet Yuling Wu*[2] *and Michael Lim*[2*]

[1] Department of Neurosurgery, Chang Gung Medical Foundation, Linkou Medical Center, Taoyuan, Taiwan, [2] Department of Neurosurgery, Stanford University School of Medicine, Stanford, CA, United States, [3] Department of Neurosurgery, Chang Gung Medical Foundation, Keelung Chang Gung Memorial Hospital, Keelung, Taiwan

Gliomas are intrinsic brain tumors that originate from glial cells. Glioblastoma (GBM) is the most aggressive glioma type and resistant to immunotherapy, mainly due to its unique immune environment. Dimensional data analysis reveals that the intra-tumoral heterogeneity of immune cell populations in the glioma microenvironment is largely made up of cells of myeloid lineage. Conventional therapies of combined surgery, chemotherapy and radiotherapy have achieved limited improvements in the prognosis of glioma patients, as myeloid cells are prominent mediators of immune and therapeutic responses—like immunotherapy resistance—in glioma. Myeloid cells are frequently seen in the tumor microenvironment (TME), and they are polarized to promote tumorigenesis and immunosuppression. Reprogramming myeloid cells has emerged as revolutionary, new types of immunotherapies for glioma treatment. Here we detail the current advances in classifying epigenetic, metabolic, and phenotypic characteristics and functions of different populations of myeloid cells in glioma TME, including myeloid-derived suppressor cells (MDSCs), glioma-associated microglia/macrophages (GAMs), glioma-associated neutrophils (GANs), and glioma-associated dendritic cells (GADCs), as well as the mechanisms underlying promotion of tumorigenesis. The final goal of this review will be to provide new insights into novel therapeutic approaches for specific targeting of myeloid cells to improve the efficacy of current treatments in glioma patients.

Keywords: glioma, myeloid cells, immunosuppression, immunotherapy, macrophage, neutrophil, dendritic cell

OPEN ACCESS

Edited by:
Charlotte Domblides, Centre Hospitalier Universitaire de Bordeaux, France

Reviewed by:
Robert Adam Harris, Karolinska Institutet (KI), Sweden
Katayoun Ayasoufi, Mayo Clinic, United States

***Correspondence:**
Michael Lim
mklim@stanford.edu

Specialty section:
This article was submitted to Cancer Immunity and Immunotherapy, a section of the journal Frontiers in Immunology

Received: *02 March 2022*
Accepted: *25 April 2022*
Published: *31 May 2022*

Citation:
Lin Y-J, Wu CY-J, Wu JY and Lim M (2022) The Role of Myeloid Cells in GBM Immunosuppression. Front. Immunol. 13:887781. doi: 10.3389/fimmu.2022.887781

INTRODUCTION

Due to advanced diagnostic imaging tools including of computed tomography (CT) and magnetic resonance imaging (MRI), the incidence of brain tumors has increased recently (1). Brain tumors greatly affect the neurological function, psychological health, and quality of life of patients (1, 2). Gliomas are intrinsic tumors that originate from neuroglial progenitor cells. Glioblastoma (GBM), a grade IV glioma, is the most common primary malignant brain tumor (49.1%) with male predominance in United States (3). Based on the 2021 WHO classification, gliomas include adult-type diffuse gliomas, pediatric-type diffuse low-grade gliomas, pediatric-type diffuse high-grade gliomas, circumscribed astrocytic gliomas (4). Previously, glioblastomas were diagnosed based on the histologic findings of microvascular proliferation and/or necrosis and included both IDH-mutated (10%) and IDH wild-type (90%) tumors with very different prognoses. In WHO CNS5,

GBMs will comprise only IDH wild-type tumors. Otherwise, IDH-mutant GBM is now referred to as IDH-mutant astrocytoma, WHO grade 4. In 2021, in response to modifications of diagnostic algorithms and mature results of many large clinical trials, the European Association of Neuro-Oncology (EANO) provide updated guidelines for the diagnosis and management of adult-type diffuse gliomas including GBMs (5). The standard of care for patients with GBM aged <70 years and with a KPS >70 is maximal resection with neurologic function preservation or biopsy followed by concurrent chemo-radiation and maintenance adjuvant chemotherapy (temozolomide, TMZ) (6). Elderly patients could be treated with low-dose radiotherapy or TMZ alone (7, 8). Once recurrence, no consensus for treatment is defined. Re-operation, radiotherapy (re-boost), nitrosourea regimens, TMZ re-challenges, and bevacizumab are all options, but benefit remained unclear on overall survival. On the other hand, recruitment into appropriate clinical trials should be considered when available. The new treatment modality, tumor-treating fields (TTF), demonstrated superior progression-free survival and overall survival outcomes in all patients and across all tumor subgroups when in addition to maintenance TMZ in patients with newly diagnosed GBM (9). However, the feasibility and cost-effectiveness of TTF are still concerned and remain controversial as a standard of care (10). In summary, the prognosis of GBM is still very poor, and effective therapies are urgently needed.

The aim of cancer immunotherapy is to overcome tumor immune resistance to promote tumor eradication. This strategy has demonstrated great progress and excellent results in recent years, especially since immune checkpoint inhibitors (ICIs) in melanoma and lung cancer (11). However, recent clinical trials of ICIs and vaccine therapies have shown negative results in GBM patients (12). Several obstacles, which include natures of heterogeneity and low mutation burden, and local/systemic immunosuppressive microenvironment, impede the success to GBM immunotherapies (13). Therefore, the tumor microenvironment (TME) is emerging as a critical regulator of cancer progression in glioma. Besides cancer cells, there are many different noncancerous cell types residing in TME, including endothelial cells, pericytes, fibroblasts, and immune cells (14). There is mounting evidence, however, that the TME alters myeloid cells—the most abundant nucleated hematopoietic cells in the human body—by converting them into potent immunosuppressive cells, including myeloid-derived suppressor cells (MDSCs), tumor-associated macrophages and microglia (TAMs), tumor-associated neutrophils (TANs), and tumor-associated dendritic cells (TADCs) (15). Here, we review the current understanding of the roles of myeloid-derived suppressor cells (MDSCs), glioma-associated macrophages (GAMs), glioma-associated neutrophils (GANs), and glioma-associated dendritic cells (GADCs) (**Table 1**). By developing a comprehensive understanding of the complex interactions of myeloid cells in glioma TME (**Figure 1**), we will greatly expand the range of therapeutic strategies available to target GBM, a devastating disease.

MYELOID-DERIVED SUPPRESSOR CELLS (MDSC)

Myeloid-derived suppressor cells (MDSCs) are a heterogeneous group of bone marrow-derived immature myeloid cells comprising of either monocytic or granulocytic at different

TABLE 1 | Summary of tumor promotion function in myeloid cells.

Cell	Origin	Surface marker		Tumor promoting features
MDSC	Myeloblast (bone marrow)	G-MDSC	$CD11b^+CD14^-CD33^+HLA\text{-}DR^{low/-}CD15^+$ (or $CD66^+$)	• Loss of MHC class II from MDSCs interferes with T-cell mediated immune responses, leading to immunosuppressive TME.
	Monocyte/macrophage and dendritic cell precursor (bone marrow)	M-MDSC	$CD11b^+CD14^+CD33^+HLA\text{-}DR^{low/-}CD15^-$	
GAM (Glioma-associated macrophage)	CNS resident microglia (York sac)	$CD11b^+CD45^{low/int}$ or $CD11b^+CD206^{low/-}CD163^-$		• Mediate immunosuppression by upregulation of Arg-1, IL-10, TGF-β, CD206, CD163, CCL17, and CCL22, inhibitory immune checkpoints (PD-1, CTLA-4 and TIM-3).
	monocyte/macrophage and dendritic cell precursor (bone marrow)	$CD11b^+CD45^{hi}$ or $CD11b^+CD206^{hi}CD163^+$		
GAN (Glioma-associated neutrophil)	Myeloblasts (bone marrow)	N1	$CD66b^+$, $CD11b^+$, $CD101^+$, $CD170^{low}$, $CD54^+$, HLA-DR^+, $CD86^+$, $CD15^{high}$	• N2 GANs suppress T cell immunity and induce genetic instability, tumor cell proliferation, angiogenesis, and metastasis • NETs induce the IL-8 expression, which is correlated with tumor burden and prognosis through a HMGB1- and RAGE/ERK/NF-kB axis-dependent manner.
		N2	$CD66b^+$, $CD11b^+$, $CD170^{high}$, PDL1	
GADC (Glioma associated dendritic cell)	monocyte/macrophage and dendritic cell precursor (bone marrow)	cDC	$CD45^{hi}$, $CD11b^+$, $CD11c^+$, $CD103^+$, $CD205^+$, MHC II^+	• FGL2 and CCL2 induce Treg to inhibit antigen presentation • MIF decreased GADC migration and maturation • Inhibit GADC maturation by STAT3 signaling pathway • Inhibit costimulatory factors CD80 and CD86 by VEGF, expressed VEGF is expressed by tumor cells and influenced by mutant IDH1 and IDH2

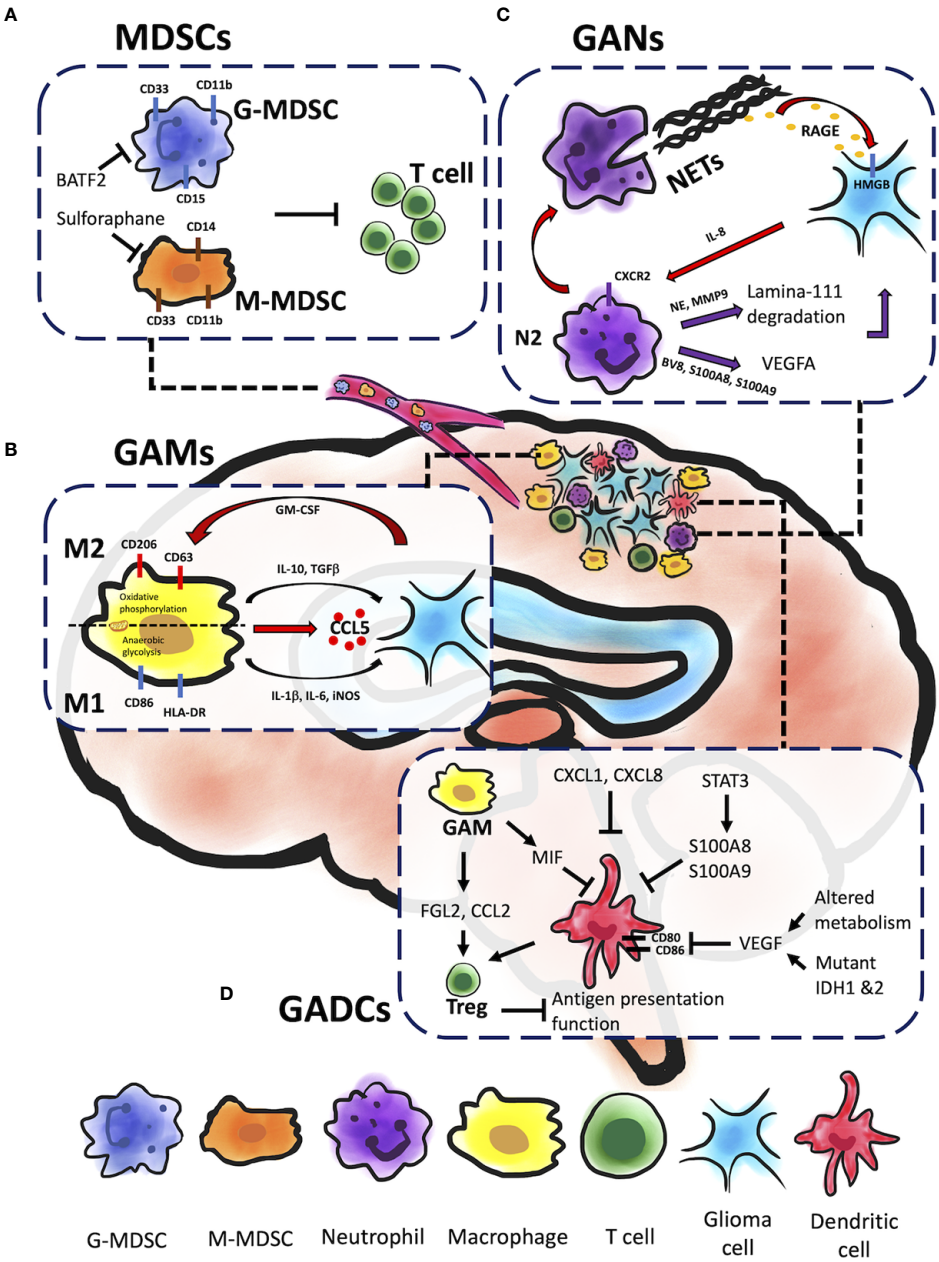

FIGURE 1 | Myeloid cells within glioma microenvironment. Gliomas are composed of different types of myeloid immune cells which promote tumor progression, including MDSCs, GAMs, GANs, and GADCs. Each of these cell types contributes to glioma progression in unique ways. **(A)** Both G-MDSC and M-MDSC recruitments contribute to T cell inactivation and inhibition cytotoxicity of glioma cells. BATF-2 on G-MDSC and sulforaphane on M-MDSC could cause inhibitory effect and further prevent from T cell inactivation and glioma progression. **(B)** GAMs engage in significant bidirectional crosstalk with glioma cells. Glioma cells release cytokines and chemoattractants to recruit GAMs to the glioma microenvironment, and M2 GAMs in turn supply pro-tumorigenic and pro-survival factors. In addition, GM-CSF promote GAMs' mitochondrial reprograming that sway between M1 and M2 inflammatory response leading to glioma resistance. **(C)** GANs can be reprogrammed to express pro-tumor phenotype (N2) with TGFβ signaling in the TME to facilitate tumor growth through NE and MMP9 secretion. The release of the pro-angiogenic factors BV8 and the S100 proteins (S100A8 and S100A9) by N2 GANs activate VEGFA to promote tumor growth. Glioma cells can induce NETs formation *via* IL-8 production. NETs are correlated with glioma progression and prognosis through a HMGB1/RAGE/IL-8 axis. **(D)** A variety of signaling molecules alter GADC migration, infiltration of the TME, maturation, and function. FGL2 and CCL2 secreted by GAMs and GADCs induce Treg activity, which suppresses antigen presentation function of GADCs. MIF, also secreted by GAMs, inhibits GADC maturation as well as migration and infiltration to the TME. The STAT3 signaling pathway inhibits GADC maturation, as does VEGF through inhibition of costimulatory factors CD80 and CD86. VEGF is expressed by tumor cells and influenced by mutant IDH1 and IDH2, as well as altered metabolism in the TME.

stages of differentiation (16). There are three major types of MDSCs: granulocytic or polymorphic nuclear MDSCs (G/PMN-MDSCs), mononuclear MDSCs (M-MDSCs), and early-stage MDSCs (eMDSCs). Human G-MDSCs are characterized as $CD11b^+CD14^-CD33^+HLA\text{-}DR^{low/-}CD15^+$ (or $CD66^+$), M-MDSCs as $CD11b^+CD14^+CD33^+HLA\text{-}DR^{low/-}CD15^-$, and eMDSCs as Lin^- ($CD3^-$, $CD14^-$, $CD15^-$, $CD19^-$, $CD56^-$, HLA-DR^-, and $CD33^+$) (17). In healthy conditions, immature myeloid cells (IMCs) quickly differentiate into mature macrophages, granulocytes, or dendritic cells (DCs). Under pathological conditions such as glioma, inflammatory conditions prevent immature myeloid cells differentiation into mature myeloid cells resulting in MDSC accumulation (18). For example, IMCs from tumor-bearing mice had a significantly higher level of reactive oxygen species (ROS) than from tumor-free mice. Hydrogen peroxide (H_2O_2) but not superoxide radical anions were found to be the major component of ROS that prevents MDSCs differentiation of antigen-presenting cells (18). In human cancer patients, MDSCs are identified as HLA-DR^- $CD11b^+CD14^-CD33^+$ cells that co-express the myeloid differentiation markers, CD11b and CD33, while lacking mature lymphoid and myeloid cell markers, such as HLA-DR, an MHC class II molecule (19). This MHC class II molecule is normally found on antigen-presenting cells (APCs) and regulated by CIITA, a transactivator (20). Loss of MHC class II from MDSCs interferes with T-cell mediated immune responses, leading to immunosuppressive TME, and is correlated with poor clinical outcomes in glioma (20–22). Accumulating evidence has shown that glioma-released factors promote the recruitment of MDSCs, inhibiting T cell proliferation and leading to glioma growth (23). Sulforaphane treatment has been shown to prevent transformation of normal monocytes to M-MDSCs (23), and BATF2 inhibitor was shown to prevent glioma progression by inhibiting G-MDSCs recruitment (**Figure 1A**) (24). Immune checkpoints such as TIGIT, CTLA-4, PD-1 on T cells are thought to cause T cell exhaustion and associate with glioma recurrence (25, 26). Dual treatment of anti-PD-1 and anti-TIGIT was shown to increase effector T cell function and downregulate suppressive regulatory T cells (Tregs). However, a recent phase I clinical trial has revealed although neoadjuvant PD-1 blockade increases T cell function, these cells eventually transit into an exhausted stated and are inhibited by the myeloid suppressor population (25). A preclinical study also revealed sexual dimorphism: M-MDSCs were enriched in the male tumors whereas G-MDSCs were elevated in the females' peripheral blood, both of which can be leveraged for therapeutic management (27).

GLIOMA-ASSOCIATED MICROGLIA/ MACROPHAGES (GAMS)

The central nervous system (CNS) is considered to be immune-privileged environment. The blood-brain barrier (BBB) prevents activated T cells from entering CNS under steady-state and healthy conditions. Diseased states, such as glioma, cause BBB leaks, leading to immune cell infiltration from the periphery (28). However, such a belief has been amended as mouse and human studies revealed that tissue $CD4^+$ and $CD8^+$ cells patrol in the cerebrospinal fluid or brain parenchyma and can interact with ACPs (29, 30). Brain $CD8^+$ T cells that were $CD103^+$ associated with increased expression of tissue-homing chemokine receptors compared to those that were $CD103^-$ (29), and CXCL12 was shown to promote T cell transmigration across BBB (31). Microglia, the major APC subset within the CNS, are functionally compromised in the glioma microenvironment, which decreases the effectiveness of tumor eradication at the initial stage, as well as later T-cell-dependent immune responses (20). Last but not least, microglia exhibit suppression of MHC class II (MHC-II) molecules, which limits T cell-dependent antitumor immunity (20, 22). The MHC-II molecules were thought to mediate antigen presentation whereas the mechanism of antigen presentation is complicated. Although MHC-II was muted in GAMs, this may be just a compiled factor contributing to GAM poorly activate T cells (32). In addition, Toll-like receptor 2 (TLR2) activation is prevailing found in GAMs that can downregulate MHC class II molecules in GAMs and prevents T cell proliferation and activation (20). The study has shown that glioma induces chronic inflammation in microglia and activates Toll-like receptor 2 (TLR2), triggering downstream MAPK/ERK signaling, and responses associated to loss of histone H3 acetylation at CIITA promoters (20). In the glioma microenvironment, various endogenous TLRs ligands, such as heat shock proteins, high-mobility-group box 1 (HMBG1), and damage-associated molecular patterns (DAMPs), are upregulated by necrotic cells. This upregulation is correlated with CIITA inhibition, contributing to glioma immune evasion (33, 34).

GAMs belong to myeloid lineages that are defined as CNS resident microglia and bone marrow-derived macrophages; they populate the TME and promote tumor progression (35). GAMs are the most prominent cell sub-type of the tumor mass (~30-50%). Tumor size is positively correlated to the number of GAMs shown to inversely correlate with overall survival in patients with recurrent GBM (35–37). Glioma-derived Granulocyte-macrophage colony-stimulating factor (GM-CSF) promotes activation of GAMs and production of CCL5 (**Figure 1B**), which further induce a series of calcium-dependent pathways such as p-PYK2 and p-CAMKII that lead to glioma progression (35). Generally, microglia are recognized as $CD11b^+CD45^{low/int}$ or $CD11b^+CD206^{low/-}CD163^-$, whereas macrophages are recognized as $CD11b^+CD45^{hi}$ or $CD11b^+CD206^{hi}CD163^+$ (38, 39). Common activation markers observed in microglia and macrophages include CD68, CD86, CD45, CX3CR1, and HLA-DR, though TMEM119, P2RY12 and CD49D (encoded by ITGA4) expression levels are higher in microglia and macrophages in the human brain (39–41). GAMs express molecules associated with M2 anti-inflammatory phenotype in mouse GBM models that include upregulation of Arginase-1 (Arg-1), IL-10, transforming growth factor-β (TGFβ), CD206, CD163, CCL17, and CCL22, and NF-κB activation associated with M2 differentiation (39, 42, 43). M2 GAMs have been shown

to mediate immunosuppression within the TME and promote tumor progression (44, 45). Activation of MerTK, a receptor tyrosine kinase, polarizes GAMs to an immunosuppressive phenotype, but inhibition of MerTK from GAMs decreases immunosuppressive $CD206^+$ GAM phenotype, leading to prolonged survival in GBM mouse models (**Figure 1B**) (46).

Several studies have advocated that pro-inflammatory M1 phenotype—associated with upregulation of CD115 and Siglec and consecutive production of IL-1β, IL-6, or IFN-γ—is critical for tumor eradication (39), especially since M1 phenotype has been reported to correlate with favorable survival outcomes in many human cancers (47). However, this trend appears inconsistent in glioma as inhibitory immune checkpoints such as PD-1, CTLA-4 and TIM-3 are consistently upregulated in M1/M2 GAMs which have been shown to significantly decrease patient prognosis (48, 49). Mice study has revealed that disruption of GBM-derived IL-6, known to induce myeloid PD-L1, reduces local and systemic myeloid-driven immunosuppression (50). In addition, GAMs in the TME are highly heterogeneous, with dynamic phenotypes and functions that are continuously shaped in response to the tumor. The binary M1/M2 classification appears too simplistic to explain the phenotype and functions of GAMs in tumors; dimensional data analysis from scRNA-seq reveals that GAMs possess multi-genomic phenotypes that encompass various M1 and M2 genes (41). Blood-derived macrophages, more so than resident microglia, have been reported to upregulate immunosuppressive cytokines and display an oxidative metabolism of M2 phenotype in the glioma microenvironment (41). A recent study further demonstrated regional differences of inflammatory responses in GAMs. GAMs in tumor core evolve toward pro-inflammation and are negatively correlated with PD-1 signaling, whereas GAMs in tumor periphery evolve toward anti-inflammation (37).

It has been previously recognized that GAMs undergo constant epigenetic and metabolic reprogramming regarding oxidative phosphorylation and anaerobic glycolysis, swinging between pro- and anti-inflammatory responses for growth-promoting or tumor-killing activity (51–54). Anti-inflammatory GAMs use the tricarboxylic acid (TCA) cycle in mitochondria to produce electrons that are essential for oxidative phosphorylation of glucose to generate high amounts of adenosine triphosphate (ATP) (55). This process fuels the mitochondrial electron transport chain and generates ROS, NADPH, and NO (56). Pro-inflammatory GAMs tend utilize anaerobic glycolysis, converting pyruvate into lactate (54, 57). Increased levels of lactate and TCA intermediates further upregulate histone hyperacetylation for IL-1β, TNF-α and IL-6 gene transcription (58, 59). In addition, gliomas are discovered to facilitate metabolic reprograming driven by mutations in the genes for the isocitrate dehydrogenase (IDH) and receptor tyrosine kinase (RTK) pathways (60). At present, even though signature mutations in known metabolic enzymes are recognized as being important, the metabolic landscape of gliomas is not incorporated with GAM pro- and anti-inflammatory environmental cues and patient prognosis.

GLIOMA/TUMOR-INFILTRATING NEUTROPHILS

Neutrophils with short life span are the most populous circulating leukocytes (61). In contrast to macrophages, neutrophils were traditionally considered bystanders in the TME. However, recent studies have uncovered distinct capabilities of neutrophils throughout each step of carcinogenesis from tumor initiation to primary tumor growth to metastasis. The degree of neutrophil infiltration in gliomas is significantly correlated with pathologic grade (62). Recently, new tools for genetic analysis further discovered the importance of tumor-associated neutrophils in the TME (63, 64). Thus, the efficacy of either traditional or novel strategies for treating cancers is likely determined by the phenotype of neutrophils in TME (61, 65).

In general, neutrophils play complex roles in tumor progression and metastases. Neutrophils are polarized to anti-tumor (N1) phenotype with IFNβ signaling or pro-tumor (N2) phenotype with TGFβ signaling in the TME (66, 67). This diversity of neutrophil behavior includes polar opposite functions in mediating tumor immunity (68). Additionally, TAMs and tumor-infiltrating lymphocytes (TIL), which are critical components in the TME, can be modulated by neutrophils to influence tumor development and T cell-dependent antitumor immunity. Neutrophils can be reprogrammed to express pro-tumor phenotype from intrinsic anti-tumor activity when recruited to the tumor (from N1 to N2) (66, 68). The N2 TANs can then facilitate tumor growth by suppressing T cell immunity and inducting genetic instability, tumor cell proliferation, angiogenesis, and metastasis (**Figure 1C**). Production of ROS and the release of microparticles (microRNAs miR-23A and miR-155) by neutrophils can downregulate molecules that maintain nuclear integrity and further lead to genetic instability (69–71). In addition, the epidermal growth factor (EGF), hepatocyte growth factor (HGF) and platelet- derived growth factor (PDGF) produced by neutrophils can facilitate tumor progression (72, 73). Neutrophil elastase (NE) and matrix metalloproteinase 9 (MMP9) (secreted by neutrophils) that cleaves laminin 111 (74, 75) lead to trigger cancer cell proliferation *via* activation of integrin signaling (74). In addition, pro-angiogenic factors including BV8, S100 proteins (S100A8, S100A9), and MMP9 released by neutrophils lead to activation of vascular endothelial growth factor A (VEGF A). Thus far, most studies demonstrated protumor roles of neutrophils (76, 77). Therefore, targeting TANs in immunotherapy for cancers, especially reprogramming of neutrophils from pro-tumor to anti-tumor phenotypes, holds promise to improve the efficacy of cancer treatments and possibly become the next-generation immunotherapy (78). Preclinical studies have shown positive results combining neutrophil depletion (anti-Ly6G antibody) and anti-PD-1 antibody treatment on glioma bearing mice (79). Additionally, there are currently several clinical trials targeting neutrophils. For example, clinical trials of Galunisertib (TGFβ receptor 1

kinase inhibitor) alone or combined with lomustine or temozolomide are ongoing in patients with recurrent glioblastoma (NCT01582269, NCT01682187, NCT01220271).

Neutrophil extracellular traps, NETs, are formed in response to extracellular pathogens and are specialized formation of fibrous decondensed chromatin with associated histones, MPO, and various cytoplasmic proteins, such as neutrophil elastase, cathepsin G, and lactoferrin. NETs have been shown to have diverse roles. Aggregated NETs can isolate immunostimulatory materials, which leads to limited immune activity and inflammation (80–82), but high density of NETs can cause organ or tissue damage (80, 83, 84). However, the role of NETs in the TME is an interesting unknown for cancer researchers. In theory, NETs can trap cancer cells and facilitate cytotoxic effects using ROS (84, 85). However, NETs can promote cancer metastasis by isolating circulating tumor cells (86). In glioma cells, NETs are thought to induce the IL-8 expression, which is correlated with tumor burden and prognosis through a HMGB1- and RAGE/ERK/NF-kB axis-dependent manner (**Figure 1C**) (87). Furthermore, glioma cells can induce NETs formation *via* IL-8 production by glioma (87). T-cell immunoglobulin and mucin domain-3 (TIM-3) interact with HMBG1 in TADCs and have an inhibitory, antitumor effect (88–90). A recent study has reported that TIM-3 can suppress the uptake of extracellular DNA in TADCs, which may influence the NETs production (91). Toll-like receptor 2, one of the HMGB receptors, is believed as correlation with NETs production, and HMGB1-mediated TLR2 signaling plays a critical role in eliciting glioblastoma regression, However, further studies are still needed to clarify the protumor and antitumor functions of NETs in glioma.

GLIOMA/TUMOR-INFILTRATING DENDRITIC CELLS

Dendritic cells (DCs) are professional antigen-presenting cells in the myeloid lineage that signal with and activate $CD4^+$ and $CD8^+$ T lymphocytes and natural killer (NK) cells to target the specific antigens presented (22, 92, 93). Since DCs usually confer protection against pathogens and disease, they are critical mediators of anti-tumor immunity and can be pulsed with peptide epitopes of tumor antigens to prime CD8+ T cells for an anti-tumor response (94). With induced activation and IL-12 signaling, mature GADs can then activate T lymphocytes against tumor antigens, even in the presence of the immunosuppressive TME induced by TGF-β2 signaling (95). However, DCs are manipulated by tumors to promote tumor growth and cancer disease progression.

There are many signaling pathways and secretory factors in the glioma TME that promote tumorigenesis (**Figure 1D**). STAT3 signaling in mouse glioma tumor-associated myeloid progenitor cells induces S100A8 and S100A9, which are inflammatory factors that arrest myeloid cell maturation, including DCs (19). This leads to a decrease in tumor-infiltrating and GADCs in the TME as well as the peripheral blood circulation, leading to a cyclic effect culminating in widespread immune suppression, a condition that favors tumor growth (19, 22, 96). CXC chemokines are also used by glioma cells to manipulate DC-mediated T cell immunity (96). CXCL1 and CXCL8 are enhanced in GBM patients, biomarkers for poorer prognosis, and positively correlated with DC and negatively correlated with $CD8^+$ T cell infiltration in the TME (97). GADCs, along with FGL2 and CCL2 expressed by tumor cells and GAMs, also induce T_{regs} to suppress anti-tumor responses by inhibiting DC antigen presentation (22, 96). Furthermore, macrophage migration inhibitory factor (MIF) correlates with decreased GAD migration as well as decreased maturation, likely contributing to the tumor-tolerant immune state observed in GBM (98).

Vascular Endothelial Growth Factor (VEGF) is another immune-modulating factor expressed and secreted by tumor cells that acts as a double-edged sword. It promotes tumor growth *via* angiogenesis and inhibits GADC maturation by downregulating costimulatory factors CD80 and CD86, which are necessary to produce robust anti-tumor immune responses (**Figure 1D**) (5, 8). Glioma cells that express VEGF also have altered metabolomes (96). Upregulated hexokinase 2, phosphoglycerate dehydrogenase (PGHDH), 3-hydroxy-3-methylglutaryl-CoA reductase (HMGCR), cyclooxygenase 2 (COX-2), prostaglandin E synthase (PGES), and mutated IDH1 and IDH2 increase VEGF expression, which exacerbate suppressive effects on GADCs (96). Altered glycolysis and lactic acid homeostasis in glioma cells further contribute to tolerant GADC phenotypes (96, 99, 100). Upregulated glycolytic enzymes and GLUT1/3 transporters increase lactic acid uptake by GAMs and GADCs, which contributes to expression of inhibitory phenotypes (96). Additionally, expression of indoleamine 2,3-dioxygenase (IDO)-1/2 by glioma cells has been shown to be proportional to tumor grade; IDO is expressed by DCs within the TME and helps to recruit T_{regs}, which further exacerbate and maintain the immunosuppressive state (96).

An additional subset of human DCs include plasmacytoid DCs (pDCs), which normally produce type 1 interferons in response to viral infections (101). However, in glioma patients, IFN-α and TLR7/9 signaling are downregulated, leading to a TME favoring tumorigenesis and a tolerogenic T cell response (101). pDCs have been previously shown to be the major subtype of DCs and antigen presenting cells at-large in glioma models and help recruit T_{regs} to the TME *via* TGF-β, secreted by glioma cells (101),. CXCL9, CXCL10, and CXCL12 signaling by glioma cells also help recruit pDCs to the TME (101). This flexibility in function—ranging from immunogenic to tolerogenic—makes this subset of DCs particularly exploitable by tumors for establishing an immunosuppressive TME, but it also makes them potential targets for effective anti-tumor therapies (101).

Because DCs can be manipulated to induce anti-tumor immunity, there have been many investigations and clinical trials for DC vaccine treatments. A meta-analysis of several phase II DC vaccine clinical trials revealed significant increases in overall and progression-free survival for GBM patients receiving DC vaccines in addition to standard of care (surgery, chemotherapy, and radiation therapy) (102). Research on the mechanisms of immunogenic cell death-based DC vaccines

showed that their efficacy relied upon ROS and danger signals stimulated by the vaccine, as well as functioning DCs and $CD8^+$ T cells (103). They also demonstrated that DC vaccines modified T cell homeostasis in the TME from the immune tolerant or suppressive T_{regs} to T_H1, T_H17, and cytotoxic $CD8^+$ T cells that mediate anti-tumor immune responses, even overcoming immune disruptions caused by chemotherapy (103). There are also promising preliminary results from the first phase III trial of DC vaccines against GBM (104). Though there was crossover in the treatment design, so that about 90% of the intent-to-treat population eventually received DCVax-L, median overall survival (mOS) was 23.1 months after surgery—increased to 34.7 months for MGMT methylated patients—and there was also a group with extended survival (mOS of 40.5 months) (104). While the mOS for MGMT unmethylated patients was approximately 19 months, these mOS are improvements compared to the standard 15-16 months (105). These developments show exciting promise for immunotherapies for GBM patients that target and manipulate DC functions and interactions.

CONCLUSIONS

In the past decades, emerging evidence showed the important role of myeloid cells in TME through great progress in fundamental and translational researches. Macrophages, neutrophils, and DCs have the dual functions of both pro-tumor and antitumor phenotypes within the TME, and this diverse function is probably a reflection of their plasticity in response to environmental cues. Therefore, based on understanding complex interaction between immune cells and glioma cells, various immunotherapeutic approaches, especially combination strategies, have been investigated and shown efficacious against glioma in some preclinical studies. However, conflicting research findings indicate the necessity of performing additional studies to assess efficacy in specific patient groups.

AUTHOR CONTRIBUTIONS

Y-JL, CW, and JW wrote the manuscript. Y-JL drew the figures. ML initiated the concept and supervised the writing. All authors contributed to the article and approved the submitted version.

ACKNOWLEDGMENTS

The authors thank Li-Ting Huang for drawing the figures.

REFERENCES

1. Lin YJ, Chiu HY, Chiou MJ, Huang YC, Wei KC, Kuo CF, et al. Trends in the Incidence of Primary Malignant Brain Tumors in Taiwan and Correlation With Comorbidities: A Population-Based Study. *Clin Neurol Neurosurg* (2017) 159:72–82. doi: 10.1016/j.clineuro.2017.05.021
2. Liu R, Page M, Solheim K, Fox S, Chang SM. Quality of Life in Adults With Brain Tumors: Current Knowledge and Future Directions. *Neuro Oncol* (2009) 11(3):330–9. doi: 10.1215/15228517-2008-093
3. Ostrom QT, Cioffi G, Waite K, Kruchko C, Barnholtz-Sloan JS. CBTRUS Statistical Report: Primary Brain and Other Central Nervous System Tumors Diagnosed in the United States in 2014-2018. *Neuro Oncol* (2021) 23(12 Suppl 2):iii1–iii105. doi: 10.1093/neuonc/noab200
4. Louis DN, Perry A, Wesseling P, Brat DJ, Cree IA, Figarella-Branger D, et al. The 2021 WHO Classification of Tumors of the Central Nervous System: A Summary. *Neuro Oncol* (2021) 23(8):1231–51. doi: 10.1093/neuonc/noab106
5. Weller M, van den Bent M, Preusser M, Le Rhun E, Tonn JC, Minniti G, et al. EANO Guidelines on the Diagnosis and Treatment of Diffuse Gliomas of Adulthood. *Nat Rev Clin Oncol* (2021) 18(3):170–86. doi: 10.1038/s41571-020-00447-z
6. Stupp R, Mason WP, van den Bent MJ, Weller M, Fisher B, Taphoorn MJ, et al. Radiotherapy Plus Concomitant and Adjuvant Temozolomide for Glioblastoma. *N Engl J Med* (2005) 352(10):987–96. doi: 10.1056/NEJMoa043330
7. Wick A, Kessler T, Platten M, Meisner C, Bamberg M, Herrlinger U, et al. Superiority of Temozolomide Over Radiotherapy for Elderly Patients With RTK II Methylation Class, MGMT Promoter Methylated Malignant Astrocytoma. *Neuro Oncol* (2020) 22(8):1162–72. doi: 10.1093/neuonc/noaa033
8. Wick W, Platten M, Meisner C, Felsberg J, Tabatabai G, Simon M, et al. Temozolomide Chemotherapy Alone Versus Radiotherapy Alone for Malignant Astrocytoma in the Elderly: The NOA-08 Randomised, Phase 3 Trial. *Lancet Oncol* (2012) 13(7):707–15. doi: 10.1016/S1470-2045(12)70164-X
9. Stupp R, Taillibert S, Kanner A, Read W, Steinberg D, Lhermitte B, et al. Effect of Tumor-Treating Fields Plus Maintenance Temozolomide vs Maintenance Temozolomide Alone on Survival in Patients With Glioblastoma: A Randomized Clinical Trial. *JAMA* (2017) 318(23):2306–16. doi: 10.1001/jama.2017.18718
10. Bernard-Arnoux F, Lamure M, Ducray F, Aulagner G, Honnorat J, Armoiry X. The Cost-Effectiveness of Tumor-Treating Fields Therapy in Patients With Newly Diagnosed Glioblastoma. *Neuro Oncol* (2016) 18(8):1129–36. doi: 10.1093/neuonc/now102
11. Ribas A, Wolchok JD. Cancer Immunotherapy Using Checkpoint Blockade. *Science* (2018) 359(6382):1350–5. doi: 10.1126/science.aar4060
12. Medikonda R, Dunn G, Rahman M, Fecci P, Lim M. A Review of Glioblastoma Immunotherapy. *J Neurooncol* (2021) 151(1):41–53. doi: 10.1007/s11060-020-03448-1
13. Lin YJ, Wei KC, Chen PY, Lim M, Hwang TL. Roles of Neutrophils in Glioma and Brain Metastases. *Front Immunol* (2021) 12:701383. doi: 10.3389/fimmu.2021.701383
14. Quail DF, Joyce JA. Microenvironmental Regulation of Tumor Progression and Metastasis. *Nat Med* (2013) 19(11):1423–37. doi: 10.1038/nm.3394
15. Gabrilovich DI, Ostrand-Rosenberg S, Bronte V. Coordinated Regulation of Myeloid Cells by Tumours. *Nat Rev Immunol* (2012) 12(4):253–68. doi: 10.1038/nri3175
16. Aarts CEM, Hiemstra IH, Beguin EP, Hoogendijk AJ, Bouchmal S, van Houdt M, et al. Activated Neutrophils Exert Myeloid-Derived Suppressor Cell Activity Damaging T Cells Beyond Repair. *Blood Adv* (2019) 3(22):3562–74. doi: 10.1182/bloodadvances.2019031609
17. Mi Y, Guo N, Luan J, Cheng J, Hu Z, Jiang P, et al. The Emerging Role of Myeloid-Derived Suppressor Cells in the Glioma Immune Suppressive Microenvironment. *Front Immunol* (2020) 11:737. doi: 10.3389/fimmu.2020.00737
18. Kusmartsev S, Gabrilovich DI. Inhibition of Myeloid Cell Differentiation in Cancer: The Role of Reactive Oxygen Species. *J Leukoc Biol* (2003) 74(2):186–96. doi: 10.1189/jlb.0103010
19. Gieryng A, Kaminska B. Myeloid-Derived Suppressor Cells in Gliomas. *Contemp Oncol (Pozn)* (2016) 20(5):345–51. doi: 10.5114/wo.2016.64592

20. Qian J, Luo F, Yang J, Liu J, Liu R, Wang L, et al. TLR2 Promotes Glioma Immune Evasion by Downregulating MHC Class II Molecules in Microglia. *Cancer Immunol Res* (2018) 6(10):1220–33. doi: 10.1158/2326-6066.CIR-18-0020
21. Lakshmanachetty S, Cruz-Cruz J, Hoffmeyer E, Cole AP, Mitra SS. New Insights Into the Multifaceted Role of Myeloid-Derived Suppressor Cells (MDSCs) in High-Grade Gliomas: From Metabolic Reprograming, Immunosuppression, and Therapeutic Resistance to Current Strategies for Targeting MDSCs. *Cells* (2021) 10(4):893. doi: 10.3390/cells10040893
22. Locarno CV, Simonelli M, Carenza C, Capucetti A, Stanzani E, Lorenzi E, et al. Role of Myeloid Cells in the Immunosuppressive Microenvironment in Gliomas. *Immunobiology* (2020) 225(1):151853. doi: 10.1016/j.imbio.2019.10.002
23. Kumar R, de Mooij T, Peterson TE, Kaptzan T, Johnson AJ, Daniels DJ, et al. Modulating Glioma-Mediated Myeloid-Derived Suppressor Cell Development With Sulforaphane. *PloS One* (2017) 12(6):e0179012. doi: 10.1371/journal.pone.0179012
24. Zhang X, Liu Y, Dai L, Shi G, Deng J, Luo Q, et al. BATF2 Prevents Glioblastoma Multiforme Progression by Inhibiting Recruitment of Myeloid-Derived Suppressor Cells. *Oncogene* (2021) 40(8):1516–30. doi: 10.1038/s41388-020-01627-y
25. Lee AH, Sun L, Mochizuki AY, Reynoso JG, Orpilla J, Chow F, et al. Neoadjuvant PD-1 Blockade Induces T Cell and Cdc1 Activation But Fails to Overcome the Immunosuppressive Tumor Associated Macrophages in Recurrent Glioblastoma. *Nat Commun* (2021) 12(1):6938. doi: 10.1038/s41467-021-26940-2
26. Hung AL, Maxwell R, Theodros D, Belcaid Z, Mathios D, Luksik AS, et al. TIGIT and PD-1 Dual Checkpoint Blockade Enhances Antitumor Immunity and Survival in GBM. *Oncoimmunology* (2018) 7(8):e1466769. doi: 10.1080/2162402X.2018.1466769
27. Bayik D, Zhou Y, Park C, Hong C, Vail D, Silver DJ, et al. Myeloid-Derived Suppressor Cell Subsets Drive Glioblastoma Growth in a Sex-Specific Manner. *Cancer Discov* (2020) 10(8):1210–25. doi: 10.1158/2159-8290.CD-19-1355
28. Harris MG, Hulseberg P, Ling C, Karman J, Clarkson BD, Harding JS, et al. Immune Privilege of the CNS Is Not the Consequence of Limited Antigen Sampling. *Sci Rep* (2014) 4:4422. doi: 10.1038/srep04422
29. Smolders J, Heutinck KM, Fransen NL, Remmerswaal EBM, Hombrink P, Ten Berge IJM, et al. Tissue-Resident Memory T Cells Populate the Human Brain. *Nat Commun* (2018) 9(1):4593. doi: 10.1038/s41467-018-07053-9
30. Wakim LM, Woodward-Davis A, Bevan MJ. Memory T Cells Persisting Within the Brain After Local Infection Show Functional Adaptations to Their Tissue of Residence. *Proc Natl Acad Sci USA* (2010) 107(42):17872–9. doi: 10.1073/pnas.1010201107
31. Man S, Tucky B, Cotleur A, Drazba J, Takeshita Y, Ransohoff RM. CXCL12-Induced Monocyte-Endothelial Interactions Promote Lymphocyte Transmigration Across an *In Vitro* Blood-Brain Barrier. *Sci Transl Med* (2012) 4(119):119ra14. doi: 10.1126/scitranslmed.3003197
32. Schartner JM, Hagar AR, Van Handel M, Zhang L, Nadkarni N, Badie B. Impaired Capacity for Upregulation of MHC Class II in Tumor-Associated Microglia. *Glia* (2005) 51(4):279–85. doi: 10.1002/glia.20201
33. Curtin JF, Liu N, Candolfi M, Xiong W, Assi H, Yagiz K, et al. HMGB1 Mediates Endogenous TLR2 Activation and Brain Tumor Regression. *PloS Med* (2009) 6(1):e10. doi: 10.1371/journal.pmed.1000010
34. Piccinini AM, Midwood KS. DAMPening Inflammation by Modulating TLR Signalling. *Mediators Inflamm* (2010) 2010:672395. doi: 10.1155/2010/672395
35. Yu-Ju Wu C, Chen CH, Lin CY, Feng LY, Lin YC, Wei KC, et al. CCL5 of Glioma-Associated Microglia/Macrophages Regulates Glioma Migration and Invasion *via* Calcium-Dependent Matrix Metalloproteinase 2. *Neuro Oncol* (2020) 22(2):253–66. doi: 10.1093/neuonc/noz189
36. Lu-Emerson C, Snuderl M, Kirkpatrick ND, Goveia J, Davidson C, Huang Y, et al. Increase in Tumor-Associated Macrophages After Antiangiogenic Therapy Is Associated With Poor Survival Among Patients With Recurrent Glioblastoma. *Neuro Oncol* (2013) 15(8):1079–87. doi: 10.1093/neuonc/not082
37. Landry AP, Balas M, Alli S, Spears J, Zador Z. Distinct Regional Ontogeny and Activation of Tumor Associated Macrophages in Human Glioblastoma. *Sci Rep* (2020) 10(1):19542. doi: 10.1038/s41598-020-76657-3
38. Ford AL, Goodsall AL, Hickey WF, Sedgwick JD. Normal Adult Ramified Microglia Separated From Other Central Nervous System Macrophages by Flow Cytometric Sorting. Phenotypic Differences Defined and Direct *Ex Vivo* Antigen Presentation to Myelin Basic Protein-Reactive CD4+ T Cells Compared. *J Immunol* (1995) 154(9):4309–21.
39. Jurga AM, Paleczna M, Kuter KZ. Overview of General and Discriminating Markers of Differential Microglia Phenotypes. *Front Cell Neurosci* (2020) 14:198. doi: 10.3389/fncel.2020.00198
40. Bottcher C, Schlickeiser S, Sneeboer MAM, Kunkel D, Knop A, Paza E, et al. Human Microglia Regional Heterogeneity and Phenotypes Determined by Multiplexed Single-Cell Mass Cytometry. *Nat Neurosci* (2019) 22(1):78–90. doi: 10.1038/s41593-018-0290-2
41. Muller S, Kohanbash G, Liu SJ, Alvarado B, Carrera D, Bhaduri A, et al. Single-Cell Profiling of Human Gliomas Reveals Macrophage Ontogeny as a Basis for Regional Differences in Macrophage Activation in the Tumor Microenvironment. *Genome Biol* (2017) 18(1):234. doi: 10.1186/s13059-017-1362-4
42. Solinas G, Schiarea S, Liguori M, Fabbri M, Pesce S, Zammataro L, et al. Tumor-Conditioned Macrophages Secrete Migration-Stimulating Factor: A New Marker for M2-Polarization, Influencing Tumor Cell Motility. *J Immunol* (2010) 185(1):642–52. doi: 10.4049/jimmunol.1000413
43. Chanmee T, Ontong P, Konno K, Itano N. Tumor-Associated Macrophages as Major Players in the Tumor Microenvironment. *Cancers (Basel)* (2014) 6 (3):1670–90. doi: 10.3390/cancers6031670
44. Pyonteck SM, Akkari L, Schuhmacher AJ, Bowman RL, Sevenich L, Quail DF, et al. CSF-1R Inhibition Alters Macrophage Polarization and Blocks Glioma Progression. *Nat Med* (2013) 19(10):1264–72. doi: 10.1038/nm.3337
45. Walters MJ, Ebsworth K, Berahovich RD, Penfold ME, Liu SC, Al Omran R, et al. Inhibition of CXCR7 Extends Survival Following Irradiation of Brain Tumours in Mice and Rats. *Br J Cancer* (2014) 110(5):1179–88. doi: 10.1038/bjc.2013.830
46. Su YT, Butler M, Zhang M, Zhang W, Song H, Hwang L, et al. MerTK Inhibition Decreases Immune Suppressive Glioblastoma-Associated Macrophages and Neoangiogenesis in Glioblastoma Microenvironment. *Neurooncol Adv* (2020) 2(1):vdaa065. doi: 10.1093/noajnl/vdaa065
47. Ma J, Liu L, Che G, Yu N, Dai F, You Z. The M1 Form of Tumor-Associated Macrophages in Non-Small Cell Lung Cancer Is Positively Associated With Survival Time. *BMC Cancer* (2010) 10:112. doi: 10.1186/1471-2407-10-112
48. Ait Ssi S, Chraa D, El Azhary K, Sahraoui S, Olive D, Badou A. Prognostic Gene Expression Signature in Patients With Distinct Glioma Grades. *Front Immunol* (2021) 12:685213. doi: 10.3389/fimmu.2021.685213
49. Lim M, Xia Y, Bettegowda C, Weller M. Current State of Immunotherapy for Glioblastoma. *Nat Rev Clin Oncol* (2018) 15(7):422–42. doi: 10.1038/s41571-018-0003-5
50. Lamano JB, Lamano JB, Li YD, DiDomenico JD, Choy W, Veliceasa D, et al. Glioblastoma-Derived IL6 Induces Immunosuppressive Peripheral Myeloid Cell PD-L1 and Promotes Tumor Growth. *Clin Cancer Res* (2019) 25 (12):3643–57. doi: 10.1158/1078-0432.CCR-18-2402
51. Hasan MN, Luo L, Ding D, Song S, Bhuiyan MIH, Liu R, et al. Blocking NHE1 Stimulates Glioma Tumor Immunity by Restoring OXPHOS Function of Myeloid Cells. *Theranostics* (2021) 11(3):1295–309. doi: 10.7150/thno.50150
52. Shen X, Burguillos MA, Osman AM, Frijhoff J, Carrillo-Jimenez A, Kanatani S, et al. Glioma-Induced Inhibition of Caspase-3 in Microglia Promotes a Tumor-Supportive Phenotype. *Nat Immunol* (2016) 17(11):1282–90. doi: 10.1038/ni.3545
53. Voisin P, Bouchaud V, Merle M, Diolez P, Duffy L, Flint K, et al. Microglia in Close Vicinity of Glioma Cells: Correlation Between Phenotype and Metabolic Alterations. *Front Neuroenergetics* (2010) 2:131. doi: 10.3389/fnene.2010.00131
54. Viola A, Munari F, Sanchez-Rodriguez R, Scolaro T, Castegna A. The Metabolic Signature of Macrophage Responses. *Front Immunol* (2019) 10:1462. doi: 10.3389/fimmu.2019.01462

55. Orihuela R, McPherson CA, Harry GJ. Microglial M1/M2 Polarization and Metabolic States. *Br J Pharmacol* (2016) 173(4):649–65. doi: 10.1111/bph.13139
56. Possel H, Noack H, Putzke J, Wolf G, Sies H. Selective Upregulation of Inducible Nitric Oxide Synthase (iNOS) by Lipopolysaccharide (LPS) and Cytokines in Microglia: *In Vitro* and *In Vivo* Studies. *Glia* (2000) 32(1):51–9. doi: 10.1002/1098-1136(200010)32:1<51::AID-GLIA50>3.0.CO;2-4
57. Virtuoso A, Giovannoni R, De Luca C, Gargano F, Cerasuolo M, Maggio N, et al. The Glioblastoma Microenvironment: Morphology, Metabolism, and Molecular Signature of Glial Dynamics to Discover Metabolic Rewiring Sequence. *Int J Mol Sci* (2021) 22(7):3301. doi: 10.3390/ijms22073301
58. Dong Z, Li R, Xu L, Xin K, Xu Y, Shi H, et al. Histone Hyperacetylation Mediates Enhanced IL-1beta Production in LPS/IFN-Gamma-Stimulated Macrophages. *Immunology* (2020) 160(2):183–97. doi: 10.1111/imm.13183
59. Larionova I, Kazakova E, Patysheva M, Kzhyshkowska J. Transcriptional, Epigenetic and Metabolic Programming of Tumor-Associated Macrophages. *Cancers (Basel)* (2020) 12(6):1411. doi: 10.3390/cancers12061411
60. Chen CH, Chen PY, Lin YY, Feng LY, Chen SH, Chen CY, et al. Suppression of Tumor Growth *via* IGFBP3 Depletion as a Potential Treatment in Glioma. *J Neurosurg* (2019) 132(1):168–79. doi: 10.3171/2018.8.JNS181217
61. Nemeth T, Sperandio M, Mocsai A. Neutrophils as Emerging Therapeutic Targets. *Nat Rev Drug Discov* (2020) 19(4):253–75. doi: 10.1038/s41573-019-0054-z
62. Fossati G, Ricevuti G, Edwards SW, Walker C, Dalton A, Rossi ML. Neutrophil Infiltration Into Human Gliomas. *Acta Neuropathol* (1999) 98 (4):349–54. doi: 10.1007/s004010051093
63. Coffelt SB, Wellenstein MD, de Visser KE. Neutrophils in Cancer: Neutral No More. *Nat Rev Cancer* (2016) 16(7):431–46. doi: 10.1038/nrc.2016.52
64. Ng LG, Ostuni R, Hidalgo A. Heterogeneity of Neutrophils. *Nat Rev Immunol* (2019) 19(4):255–65. doi: 10.1038/s41577-019-0141-8
65. Shaul ME, Fridlender ZG. Tumour-Associated Neutrophils in Patients With Cancer. *Nat Rev Clin Oncol* (2019) 16(10):601–20. doi: 10.1038/s41571-019-0222-4
66. Fridlender ZG, Sun J, Kim S, Kapoor V, Cheng G, Ling L, et al. Polarization of Tumor-Associated Neutrophil Phenotype by TGF-Beta: "N1" Versus "N2" TAN. *Cancer Cell* (2009) 16(3):183–94. doi: 10.1016/j.ccr.2009.06.017
67. Andzinski L, Kasnitz N, Stahnke S, Wu CF, Gereke M, von Kockritz-Blickwede M, et al. Type I IFNs Induce Anti-Tumor Polarization of Tumor Associated Neutrophils in Mice and Human. *Int J Cancer* (2016) 138 (8):1982–93. doi: 10.1002/ijc.29945
68. Sagiv JY, Michaeli J, Assi S, Mishalian I, Kisos H, Levy L, et al. Phenotypic Diversity and Plasticity in Circulating Neutrophil Subpopulations in Cancer. *Cell Rep* (2015) 10(4):562–73. doi: 10.1016/j.celrep.2014.12.039
69. Wilson CL, Jurk D, Fullard N, Banks P, Page A, Luli S, et al. NFkappaB1 Is a Suppressor of Neutrophil-Driven Hepatocellular Carcinoma. *Nat Commun* (2015) 6:6818. doi: 10.1038/ncomms7818
70. Gungor N, Knaapen AM, Munnia A, Peluso M, Haenen GR, Chiu RK, et al. Genotoxic Effects of Neutrophils and Hypochlorous Acid. *Mutagenesis* (2010) 25(2):149–54. doi: 10.1093/mutage/gep053
71. Butin-Israeli V, Bui TM, Wiesolek HL, Mascarenhas L, Lee JJ, Mehl LC, et al. Neutrophil-Induced Genomic Instability Impedes Resolution of Inflammation and Wound Healing. *J Clin Invest* (2019) 129(2):712–26. doi: 10.1172/JCI122085
72. Finisguerra V, Di Conza G, Di Matteo M, Serneels J, Costa S, Thompson AA, et al. MET is Required for the Recruitment of Anti-Tumoural Neutrophils. *Nature* (2015) 522(7556):349–53. doi: 10.1038/nature14407
73. Tecchio C, Scapini P, Pizzolo G, Cassatella MA. On the Cytokines Produced by Human Neutrophils in Tumors. *Semin Cancer Biol* (2013) 23(3):159–70. doi: 10.1016/j.semcancer.2013.02.004
74. Albrengues J, Shields MA, Ng D, Park CG, Ambrico A, Poindexter ME, et al. Neutrophil Extracellular Traps Produced During Inflammation Awaken Dormant Cancer Cells in Mice. *Science* (2018) 361(6409):eaao4227. doi: 10.1126/science.aao4227
75. Tohme S, Yazdani HO, Al-Khafaji AB, Chidi AP, Loughran P, Mowen K, et al. Neutrophil Extracellular Traps Promote the Development and Progression of Liver Metastases After Surgical Stress. *Cancer Res* (2016) 76 (6):1367–80. doi: 10.1158/0008-5472.CAN-15-1591
76. Vols S, Sionov RV, Granot Z. Always Look On the Bright Side: Anti-Tumor Functions of Neutrophils. *Curr Pharm Des* (2017) 23(32):4862–92. doi: 10.2174/1381612823666170704125420
77. Sionov RV, Fridlender ZG, Granot Z. The Multifaceted Roles Neutrophils Play in the Tumor Microenvironment. *Cancer Microenviron* (2015) 8 (3):125–58. doi: 10.1007/s12307-014-0147-5
78. Gregory AD, Houghton AM. Tumor-Associated Neutrophils: New Targets for Cancer Therapy. *Cancer Res* (2011) 71(7):2411–6. doi: 10.1158/0008-5472.CAN-10-2583
79. Wang PF, Zhang YX, Su J, Yao K, Li SW, Huang GR, et al. Neutrophil Depletion Enhances the Therapeutic Effect of PD-1 Antibody on Glioma. *Aging (Albany NY)* (2020) 12(15):15290–301. doi: 10.18632/aging.103428
80. Boeltz S, Amini P, Anders HJ, Andrade F, Bilyy R, Chatfield S, et al. To NET or Not to NET:Current Opinions and State of the Science Regarding the Formation of Neutrophil Extracellular Traps. *Cell Death Differ* (2019) 26 (3):395–408. doi: 10.1038/s41418-018-0261-x
81. Wang J. Neutrophils in Tissue Injury and Repair. *Cell Tissue Res* (2018) 371 (3):531–9. doi: 10.1007/s00441-017-2785-7
82. Munoz LE, Leppkes M, Fuchs TA, Hoffmann M, Herrmann M. Missing in Action-The Meaning of Cell Death in Tissue Damage and Inflammation. *Immunol Rev* (2017) 280(1):26–40. doi: 10.1111/imr.12569
83. Pieterse E, Rother N, Garsen M, Hofstra JM, Satchell SC, Hoffmann M, et al. Neutrophil Extracellular Traps Drive Endothelial-To-Mesenchymal Transition. *Arterioscler Thromb Vasc Biol* (2017) 37(7):1371–9. doi: 10.1161/ATVBAHA.117.309002
84. Saffarzadeh M, Juenemann C, Queisser MA, Lochnit G, Barreto G, Galuska SP, et al. Neutrophil Extracellular Traps Directly Induce Epithelial and Endothelial Cell Death: A Predominant Role of Histones. *PloS One* (2012) 7 (2):e32366. doi: 10.1371/journal.pone.0032366
85. Gupta AK, Joshi MB, Philippova M, Erne P, Hasler P, Hahn S, et al. Activated Endothelial Cells Induce Neutrophil Extracellular Traps and Are Susceptible to NETosis-Mediated Cell Death. *FEBS Lett* (2010) 584 (14):3193–7. doi: 10.1016/j.febslet.2010.06.006
86. Cools-Lartigue J, Spicer J, McDonald B, Gowing S, Chow S, Giannias B, et al. Neutrophil Extracellular Traps Sequester Circulating Tumor Cells and Promote Metastasis. *J Clin Invest* (2013) 123(8):3446–56. doi: 10.1158/1538-7445.AM2012-2972
87. Zha C, Meng X, Li L, Mi S, Qian D, Li Z, et al. Neutrophil Extracellular Traps Mediate the Crosstalk Between Glioma Progression and the Tumor Microenvironment *via* the HMGB1/RAGE/IL-8 Axis. *Cancer Biol Med* (2020) 17(1):154–68. doi: 10.20892/j.issn.2095-3941.2019.0353
88. Chiba S, Baghdadi M, Akiba H, Yoshiyama H, Kinoshita I, Dosaka-Akita H, et al. Tumor-Infiltrating DCs Suppress Nucleic Acid-Mediated Innate Immune Responses Through Interactions Between the Receptor TIM-3 and the Alarmin HMGB1. *Nat Immunol* (2012) 13(9):832–42. doi: 10.1038/ni.2376
89. Tang D, Lotze MT. Tumor Immunity Times Out: TIM-3 and HMGB1. *Nat Immunol* (2012) 13(9):808–10. doi: 10.1038/ni.2396
90. Patel J, Bozeman EN, Selvaraj P. Taming Dendritic Cells With TIM-3: Another Immunosuppressive Strategy Used by Tumors. *Immunotherapy* (2012) 4(12):1795–8. doi: 10.2217/imt.12.126
91. de Mingo Pulido A, Hanggi K, Celias DP, Gardner A, Li J, Batista-Bittencourt B, et al. The Inhibitory Receptor TIM-3 Limits Activation of the cGAS-STING Pathway in Intra-Tumoral Dendritic Cells by Suppressing Extracellular DNA Uptake. *Immunity* (2021) 54(6):1154–67.e7. doi: 10.1016/j.immuni.2021.04.019
92. Walzer T, Dalod M, Robbins SH, Zitvogel L, Vivier E. Natural-Killer Cells and Dendritic Cells: "L'union Fait La Force". *Blood* (2005) 106(7):2252–8. doi: 10.1182/blood-2005-03-1154
93. Fernandez NC, Lozier A, Flament C, Ricciardi-Castagnoli P, Bellet D, Suter M, et al. Dendritic Cells Directly Trigger NK Cell Functions: Cross-Talk Relevant in Innate Anti-Tumor Immune Responses *In Vivo*. *Nat Med* (1999) 5(4):405–11. doi: 10.1038/7403
94. Okano F, Storkus WJ, Chambers WH, Pollack IF, Okada H. Identification of a Novel HLA-A*0201-Restricted, Cytotoxic T Lymphocyte Epitope in a Human Glioma-Associated Antigen, Interleukin 13 Receptor Alpha2 Chain. *Clin Cancer Res* (2002) 8(9):2851–5.

95. Grauer O, Poschl P, Lohmeier A, Adema GJ, Bogdahn U. Toll-Like Receptor Triggered Dendritic Cell Maturation and IL-12 Secretion Are Necessary to Overcome T-Cell Inhibition by Glioma-Associated TGF-Beta2. *J Neurooncol* (2007) 82(2):151–61. doi: 10.1007/s11060-006-9274-2
96. Qiu R, Zhong Y, Li Q, Li Y, Fan H. Metabolic Remodeling in Glioma Immune Microenvironment: Intercellular Interactions Distinct From Peripheral Tumors. *Front Cell Dev Biol* (2021) 9:693215. doi: 10.3389/fcell.2021.693215
97. Li C, Deng H, Zhou Y, Ye Y, Zhao S, Liang S, et al. Expression and Clinical Significance of CXC Chemokines in the Glioblastoma Microenvironment. *Life Sci* (2020) 261:118486. doi: 10.1016/j.lfs.2020.118486
98. Xu S, Guo X, Gao X, Xue H, Zhang J, Guo X, et al. Macrophage Migration Inhibitory Factor Enhances Autophagy by Regulating ROCK1 Activity and Contributes to the Escape of Dendritic Cell Surveillance in Glioblastoma. *Int J Oncol* (2016) 49(5):2105–15. doi: 10.3892/ijo.2016.3704
99. Sheng Y, Jiang Q, Dong X, Liu J, Liu L, Wang H, et al. 3-Bromopyruvate Inhibits the Malignant Phenotype of Malignantly Transformed Macrophages and Dendritic Cells Induced by Glioma Stem Cells in the Glioma Microenvironment *via* miR-449a/MCT1. *BioMed Pharmacother* (2020) 121:109610. doi: 10.1016/j.biopha.2019.109610
100. Chirasani SR, Leukel P, Gottfried E, Hochrein J, Stadler K, Neumann B, et al. Diclofenac Inhibits Lactate Formation and Efficiently Counteracts Local Immune Suppression in a Murine Glioma Model. *Int J Cancer* (2013) 132(4):843–53. doi: 10.1002/ijc.27712
101. Mitchell D, Chintala S, Dey M. Plasmacytoid Dendritic Cell in Immunity and Cancer. *J Neuroimmunol* (2018) 322:63–73. doi: 10.1016/j.jneuroim.2018.06.012
102. Lv L, Huang J, Xi H, Zhou X. Efficacy and Safety of Dendritic Cell Vaccines for Patients With Glioblastoma: A Meta-Analysis of Randomized Controlled Trials. *Int Immunopharmacol* (2020) 83:106336. doi: 10.1016/j.intimp.2020.106336
103. Garg AD, Vandenberk L, Koks C, Verschuere T, Boon L, Van Gool SW, et al. Dendritic Cell Vaccines Based on Immunogenic Cell Death Elicit Danger Signals and T Cell-Driven Rejection of High-Grade Glioma. *Sci Transl Med* (2016) 8(328):328ra27. doi: 10.1126/scitranslmed.aae0105
104. Liau LM, Ashkan K, Tran DD, Campian JL, Trusheim JE, Cobbs CS, et al. First Results on Survival From a Large Phase 3 Clinical Trial of an Autologous Dendritic Cell Vaccine in Newly Diagnosed Glioblastoma. *J Transl Med* (2018) 16(1):142. doi: 10.1186/s12967-018-1507-6
105. Bi WL, Beroukhim R. Beating the Odds: Extreme Long-Term Survival With Glioblastoma. *Neuro Oncol* (2014) 16(9):1159–60. doi: 10.1093/neuonc/nou166

Conflict of Interest: ML has received research funding from Arbor, BMS, Accuray, Tocagen, Biohaven, Kyrin-Kyowa, Biohaven, Urogen. He also has been a consultant for Tocagen, VBI, InCephalo Therapeutics, Pyramid Bio, Merck, BMS, Insightec, Biohaven, Sanianoia, Hemispherian, Black Diamond Therapeutics, Novocure, Noxxon, and a shareholder of Egret Therapeutics.

The remaining authors declare that the research was conducted in the absence of any commercial or financial relationships that could be construed as a potential conflict of interest.

Publisher's Note: All claims expressed in this article are solely those of the authors and do not necessarily represent those of their affiliated organizations, or those of the publisher, the editors and the reviewers. Any product that may be evaluated in this article, or claim that may be made by its manufacturer, is not guaranteed or endorsed by the publisher.

frontiers | Frontiers in Immunology

ORIGINAL RESEARCH
published: 10 June 2022
doi: 10.3389/fimmu.2022.845585

The Prognostic and Immunotherapeutic Significance of AHSA1 in Pan-Cancer, and Its Relationship With the Proliferation and Metastasis of Hepatocellular Carcinoma

Wenli Li[1] *and Jun Liu*[2]*

[1] Reproductive Medicine Center, Yue Bei People's Hospital, Shantou University Medical College, Shaoguan, China,
[2] Medical Research Center, Yue Bei People's Hospital, Shantou University Medical College, Shaoguan, China

OPEN ACCESS

Edited by:
Nicolas Larmonier,
Université de Bordeaux,
France

Reviewed by:
Pulak Ranjan Nath,
National Cancer Institute (NIH),
United States
Samantha Sharma,
Indiana University Bloomington,
United States

***Correspondence:**
Jun Liu
liuyu8566@126.com

Specialty section:
This article was submitted to Cancer Immunity and Immunotherapy, a section of the journal Frontiers in Immunology

Received: 30 December 2021
Accepted: 17 May 2022
Published: 10 June 2022

Citation:
Li W and Liu J (2022) The Prognostic and Immunotherapeutic Significance of AHSA1 in Pan-Cancer, and Its Relationship With the Proliferation and Metastasis of Hepatocellular Carcinoma. Front. Immunol. 13:845585. doi: 10.3389/fimmu.2022.845585

The *AHSA1* is a main activator of ATPase of Hsp90. Hsp90 is involved in various metabolic and developmental processes of tumor cells. Although, the role of *AHSA1* in tumor cells is still unrecognized. In the current research, the RNA-seq of 33 tumors were downloaded using The Cancer Genome Atlas (TCGA) database for the analysis of *AHSA1* expression in tumors. The Kaplan-Meier method was used for the evaluation of the prognostic significance of *AHSA1* in patients with pan-cancer. Additionally, the correlation between *AHSA1* and immune cell infiltration, immune checkpoint, pyroptosis-related molecules, epithelial cell transformation-related molecules, and autophagy-related molecules were analyzed by co-expression. Furthermore, we examined the effect of *AHSA1* knockdown on cell function in Huh7 and HCCLM3 cells of hepatocellular carcinoma (HCC) cell lines.

According to the finding of this study, up-regulation of *AHSA1* expression was observed in numerous tumor tissues, and its over-expression in liver hepatocellular carcinoma (LIHC), lung adenocarcinoma (LUAD), and esophageal carcinoma (ESCA) could affect the overall survival and disease-specific survival of the patients. Meanwhile, as per the correlation analysis the expression of *AHSA1* was greatly correlated with the expression of various immune cell infiltrates, immune checkpoint inhibitors, tumor mutation load, and microsatellite instability. Moreover, this study focused on analyzing the association of *AHSA1* expression with multiple pathological stages in HCC, and confirmed that *AHSA1* was an independent prognostic factor of HCC by univariate and multivariate COX regression in TCGA and The International Cancer Genome Consortium (ICGC) cohorts. At the same time, cellular experiments proved that the *AHSA1* knockdown could decrease the proliferation activity, cell migration and invasion ability of HCC cells.

Therefore, the results of this study indicated that *AHSA1* can be used as a potential prognostic biomarker of tumors and it may have a significant role in the proliferation as well as migration of HCC cells.

Keywords: AHSA1, HCC, immune, cell migration, prognosis

INTRODUCTION

In recent decades, the malignant tumor has shown an alarming incidence and mortality rate worldwide, and it is a major threat to people's health in the 21st century (1). Although the increase of mortality rate of cancer patients in developed countries has moderated its steps in recent years, thanks to advanced prevention and treatment concepts and medical technologies, the mortality rate of cancer patients around the world still shows a prominent growth trend (2). With research development, a growing number of researchers began to pay attention to the common characteristics of various human malignant tumors, to explore the potential mechanism of tumor genesis (3). At present, pan-cancer research has been widely used to identify tumor molecular markers and signal pathways, combined with multiple omics analysis, in order to understand more comprehensively and deeply the molecular mechanism of tumor genesis and development (4–6). As a co-molecular chaperone protein, AHSA1 is currently the only ATPase activator of Hsp90 (7). AHSA1 plays a key role in regulating the molecular chaperone cycle and protein folding of Hsp90 (8). Hsp90, the acting protein of AHSA1, is a classical molecular chaperone with a highly conserved molecular structure. It can facilitate protein folding, maturation and transport of some cancer-related proteins, such as BCR-ABL, ErbB2/Neu, Akt, HIF-1α, p53 and RAF-1 (9). Lindsey B. Sheltont et al. revealed that the inhibition of *AHSA1* expression in mice models of Alzheimer's disease and *in vitro* cell models can eliminate the accumulation of Tau protein caused by Hsp90, which is expected to become a new therapeutic target for Alzheimer's disease (10). According to Jianli Shao et al, *AHSA1* mediates the invasion, proliferation, and apoptosis of tumor cells by regulating the Wnt/β-catenin pathway in osteosarcoma. At the same time, after the knockdown of AHSA1, the ATPase activity of Hsp90 decreased (11). However, current studies are limited to a few types of cancers, and the role of *AHSA1* in various types of tumors is still not understood completely. In this study, the RNA-seq from TCGA was utilized for the examination of *AHSA1* expression in a variety of human tumors. Combined with clinical follow-up data, the impact of abnormal expression of *AHSA1* on the prognosis of cancer patients was analyzed. Meanwhile, combined with correlation analysis, the possible association between *AHSA1* expression and tumor immune cell infiltration, tumor mutation load (TMB), microsatellite instability (MSI) and various pathway-related molecules were explored. In addition, this study verified the expression and prognostic role of *AHSA1* in hepatocellular carcinoma by combining data from ICGC-LIRI-JP, and verified the expression and potential function of *AHSA1* in hepatocellular carcinoma by combining cell and tissue specimens. The results of this study are helpful to understand the similarities and differences of *AHSA1* expression in a variety of tumors, reveal the potential mechanism of the interaction between *AHSA1* and tumor immunity, and demonstrate the potential function of *AHSA1* in hepatocellular carcinoma.

MATERIALS AND METHODS

Data Collection of Patients' Data Sets

The count format of 33 common tumor transcriptome data was downloaded from TCGA's official website and converted into the TPM format. The number of tumors of each type was shown on the **Table S1**. The clinical follow-up survival and staging data were downloaded at the same time. The transcriptome data of hepatocellular carcinoma was provided by the ICGC database and converted into the TPM format, and corresponding clinical data were obtained. In addition, the single-nucleotide mutation data of 33 tumors were downloaded from TCGA's official website and their tumor mutation load was calculated.

Differential Analysis and Prognostic Analysis

Transcriptome data from 33 tumors were filtered by "RMA" packs to remove the NA and duplicates, and log2 (TPM +1) conversion was performed afterward. Then, for comparing the expression differences of *AHSA1* in the normal and tumor tissues in different tumors, the Wilcoxon rank sum test was performed. Using the "SurvMiner" and "Survival" packages, the median expression values based on *AHSA1* were classified into two groups; the high risk and low-risk groups in different kinds of tumors. Their survival curves were drawn using the Kaplan-Meier method, and their statistical significance was calculated by the log-rank test.

Correlation Analysis

A comprehensive website; Tumor Immune Estimation Resource (TIMER, https://cistrome.shinyapps.io/timer/) was used for the measurement of the level of tumor immune cells infiltrating degree (12). For predicting the immune cell infiltration level from tumor transcription data there are five different methods provided by TIMER website which includes TIMER, CIBERSORT, xCell, McP-counter and EPIC. The abundance of infiltrating immune cells in tumor samples from 33 tumor types was obtained from TIMER database. The single-sample gene set enrichment analysis (ssGSEA) was performed in R package GSVA. Subsequently, the relation of *AHSA1* expression and the level of infiltration of these immune cells was calculated.

At present, TMB and MSI are considered for use as potential biomarkers to predict the efficacy of tumor immunotherapy (13, 14). The simple nucleoside variation data of level 4 processed with MuTect2 software was acquired from the TCGA database, and the TMB was calculated (15). Microsatellite instability signature for 33 tumors were obtained from reported studies (16). Reports have indicated that Epithelial-Mesenchymal Transitions (EMT), Pyroptosis and Autophagy were all associated with tumor metastasis and malignant proliferation, and the correlation between *AHSA1* and the expression of these pathway molecules was also analyzed in this study.

Protein Network Construction and Gene Enrichment Analysis

The GeneMANIA (http://genemania.org/) database finds out functionally identical genes on the basis of genomic and proteomic data (17). The GeneMANIA database was used to predict the genes that have functions similar to that of *AHSA1*. Gene oncology (GO) and Kyoto Encyclopedia of Genes and Genomes (KEGG) analyses of molecules with potential roles in AHSA1 were performed using clusterProfiler packages.

Correlation Analysis of *AHSA1* Expression and Clinical Factors

We analyzed the correlation between *AHSA1* expression and clinical stage, including pathologic stage, tumor (T) stage, histologic grade, alpha-fetoprotein (AFP) level, and vascular invasion. Meanwhile, for the further evaluation of the prognostic value of *AHSA1* in HCC patients, univariate and multivariate COX regression and Receiver Operating characteristic curve (ROC) analysis were performed respectively. In addition, we constructed a nomography based on the expression value of *AHSA1* and pathologic stage to promote the application of *AHSA1* in the evaluation of clinical prognosis of hepatocellular carcinoma, and evaluated the prediction accuracy of the nomography by calibration curve.

Cell Culture

The American Type Culture Collection (ATCC, Manassas, VA, United States) provided the normal human liver cells LO2, HCC cell lines HepG2, Huh7, and HCCLM3 for this experiment. All cells were cultured in an incubator at 37 °C with 5% CO2. Human target gene AHSA1 short hairpin RNA (shRNA) was purchased from GenScript company (https://www.genscript.com/), the sequences are as follows:

AHSA1 shRNA-1:gGGTGAAACTTCTAAGAGAAttcaagagaTTCTCTTAGAAGTTTCACCttttt, *AHSA1* shRNA-2:gGGCATGATCTTACCTACAAttcaagagaTTGTAGGTAAGATCATGCCttttt,

AHSA1 shRNA-3:gAGTCAGGAGTACAATACAAttcaagagaTTGTATTGTACTCCTGACTttttt. Huh7 and HCCLM3 cells were plated in six-well plates (4×10^5 cells/well), and cultivated in a in a 37°C, 5% CO2 incubator until they were completely adherent to the wall. Subsequently, the cells were transfected with lipo3000.

Quantitative Reverse Transcription-Polymerase Chain Reaction, RT-PCR

Four types of cell strains were used for total RNA was extraction. Reverse transcription was performed to convert the extracted RNA into cDNA using the reverse transcription kit provided by Beyotime, https://www.beyotime.com/. Exicycler 96 (BIONEER) was used to detect its fluorescence expression quantity. All results were processed with *GAPDH* for standardization. The $2^{-\Delta\Delta Ct}$ method was used to calculate the relative expression levels of genes.

Immunohistochemistry and Western Blot Analysis

Ten pairs of paraffin sections of hepatocellular carcinoma tumor tissue specimens and para-cancer specimens were provided by the Department of Pathology, North Guangdong People's Hospital. AHSA1 antibody was purchased from Proteintech Company (Article number: 14725-1-AP). Approval for this research was given by the Ethics Committee of North Guangdong People's Hospital. Western blotting was performed for the detection of post knockout changes in AHSA1 protein levels.

CCK8 Detection

HuH7 cells transfected with shRNA-*AHSA1* were digested when their level reached 90%, and then they were inoculated into 96-well culture plates with 3×10^3cells per well, and 5 multiple wells were designed for each group. Then, they were cultured in a 37°C, 5% CO2 incubator, and tested at 0h, 24h, 48h, 72h and 96h using the CCK-8 kit (WLA074, China).

Wound Healing Test

6-well plates were used for the inoculation of these cells, and after 48 hours of transfection, a 200 μl pipette tip was used to scratch the cells. The cell surface was cleaned with serum-free medium once, and the cell fragments were removed. The cells were then observed and photographed under a 100× microscope, and their positions in the photos were recorded. Subsequently, cells in each group were placed in an incubator at 37 °C with 5% CO2 for 24h and 48h, and then photographed and recorded, and the mobility of each group was calculated.

Transwell Migration and Invasion Assay

A 24-well Transwell chamber (8 μm aperture; Corning Costar, USA) was prepared overnight at 4°C with or without 100μL matrix gel substrate provided by BD Biosciences, San Jose, CA, USA. A 200ul of cell suspension containing 1×10^5cells/mL was inoculated into Transwell cells with or without matrix glue, and a culture medium (800 ul) containing 10% FBS was poured into the lower chamber. After 24h culture, cell fixation was done using 4% paraformaldehyde at room temperature for 20 minutes and staining was performed for 5 minutes with 0.5% crystal violet dye. The cell count was recorded afterwards.

RESULTS

The *AHSA1* Expression in Pan-Cancer

The mRNA expression of *AHSA1* was evaluated in pan-cancer patients according to the RNA-seq data of 33 types of TCGA tumors. The results showed that *AHSA1* was expressed at a relatively low level in normal bile duct tissue and a relatively high level in testicular germ cell tumor tissue. At the same time, the variance analysis indicated a relatively high expression of *AHSA1* in Bladder Urothelial Carcinoma (BLCA), Breast invasive carcinoma (BRCA), Cholangiocarcinoma (CHOL), Colon adenocarcinoma (COAD), Esophageal carcinoma (ESCA), Head and Neck squamous cell carcinoma (HNSC), kidney chromophobe (KICH), LIHC, Lung adenocarcinoma (LUAD), Lung squamous cell carcinoma (LUSC), Rectum adenocarcinoma (READ) and stomach adenocarcinoma (STAD), Prostate adenocarcinoma (PRAD), and uterine corpus endometrial carcinoma (UCEC) tumor tissues as compared to the corresponding para-carcinoma tissue (**Figure 1A**). Furthermore, paired comparison analysis was performed and the results of this analysis also revealed the overexpression of *AHSA1* in BLCA, BRCA, CHOL, COAD, ESCA, HNSC, LIHC, LUAD, LUSC, PRAD, READ, STAD in tumor tissues (**Figure 1B**). Considering that AHSA1 is an ATPase activator of HSP90AA1, we analyzed the expression of *HSP90AA1* in pan-cancer. Interestingly, the similar results were observed for *HSP90AA1* expression in pan-cancer (**Figures S1A, B**).

Survival Analysis

Based on the TCGA database, the Kaplan-Meier curves helped in depicting the association between abnormal expression of *AHSA1* and the general pan-cancer survival. The results indicated that the survival rate of patients with high expression levels of *AHSA1* in LIHC, LUAD, ESCA, and KIRP was worse (**Figures 2A–D**). For further evaluation of the specific effect of AHSA1 on tumor survival, the influence of abnormal *AHSA1* expression on disease-specific survival (DSS) of tumor patients was observed. The Kaplan-Meier plots showed that the abnormally increased *AHSA1* in LIHC, LUAD, ESCA and KIRP was correlated with its poor DSS (**Figures 2E–H**).

Expression of *AHSA1* and Analysis of Tumor Microenvironment

Tumor microenvironment is a complicated survival environment of tumor cells, mostly comprising of immune cells, mesenchymal environment as well as related internal and external molecular composition (18). In recent years, growing evidence indicate that the immune cell infiltration level is closely associated with the survival of tumor cells. Although previous studies have suggested the prognostic importance and expression level of *AHSA1* in various types of cancers, little is known if the abnormal expression of *AHSA1* have an influence on immune cell infiltration. In this study, the correlation between abnormal *AHSA1* expression and immune cell infiltration was evaluated using a TIMER database based on multiple immune prediction methods. The results indicated that *AHSA1* was substantially positively correlated with CD4+Th1, CD4+Th2 and MDSC cells of various tumors (**Figure 3A**). Meanwhile, *AHSA1* showed a significant positive correlation with B cells, CD4+ T cells, CD8+T cells and Myeloid dendritic cells in LIHC (**Figure 3A**). Moreover, we discussed the correlation between the *AHSA1* expression and immune checkpoint inhibitor. The results showed that *AHSA1* was significantly positively correlated with several immune checkpoint inhibitors, especially in LIHC, THCA, and THYM. Meanwhile, *AHSA1* was significantly negatively correlated with several immune checkpoint in ACC, BRCA, GBM, HNSC, LUSC, LGG, and PRAD (**Figure 3B**). In addition, *AHSA1* was significantly positively associated with *CD274*, *CD276*, and *CTLA4* in LIHC, THCA, and

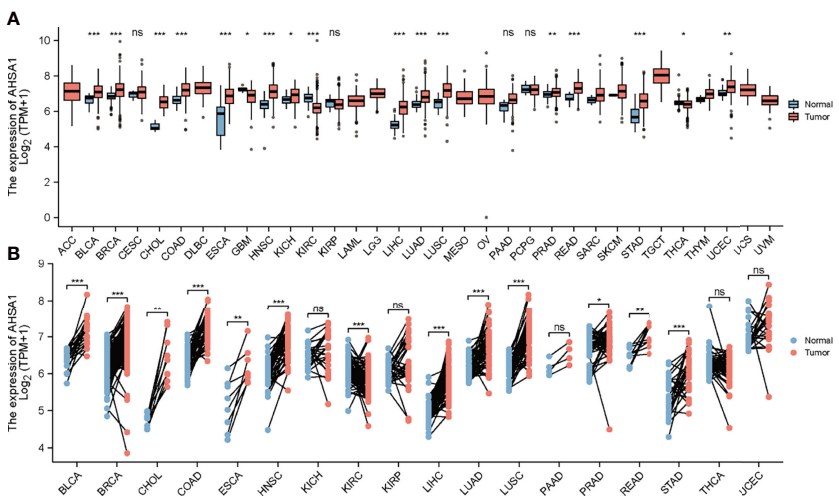

FIGURE 1 | Differential expression analysis of *AHSA1*. **(A)** Expression of *AHSA1* mRNA in pan-cancer. **(B)** The expression differences of *AHSA1* in tumor and corresponding adjacent tissues were compared with paired analysis. Mann-Whitney U test was used for this analysis, ns, p≥0.05; *p< 0.05; **p<0.01; ***p<0.001.

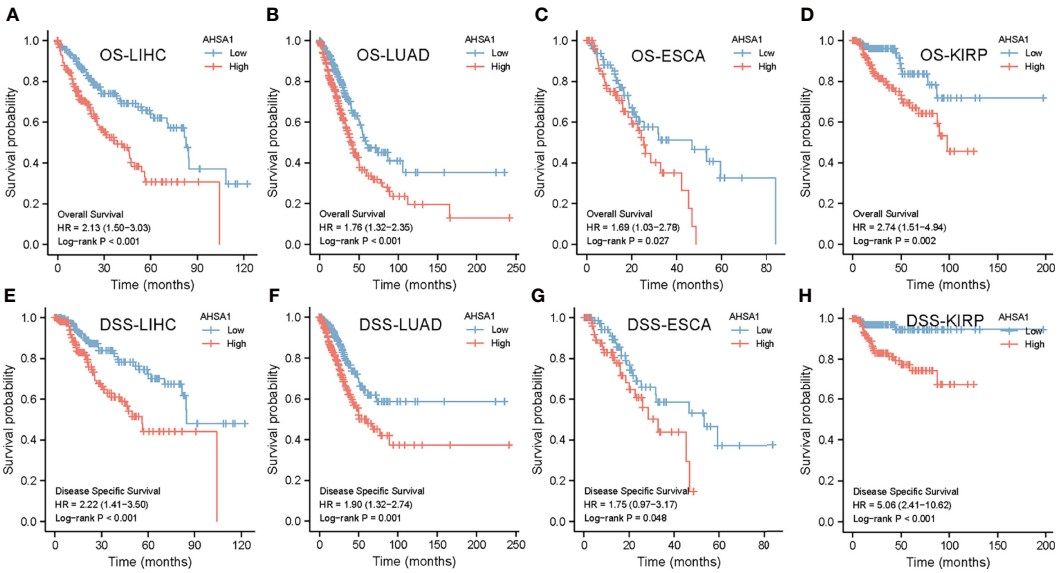

FIGURE 2 | Survival analysis of *AHSA1* in pan-cancer. The effect of *AHSA1* expression on the overall survival rate (OS) of LIHC **(A)**, LUAD **(B)**, ESCA **(C)** and KIRP **(D)** was analyzed by Kaplan-Meier method. Meanwhile, the influence of abnormal expression of *AHSA1* on disease-specific survival (DSS) of LIHC **(E)**, LUAD **(F)**, ESCA **(G)** and KIRP **(H)** was calculated.

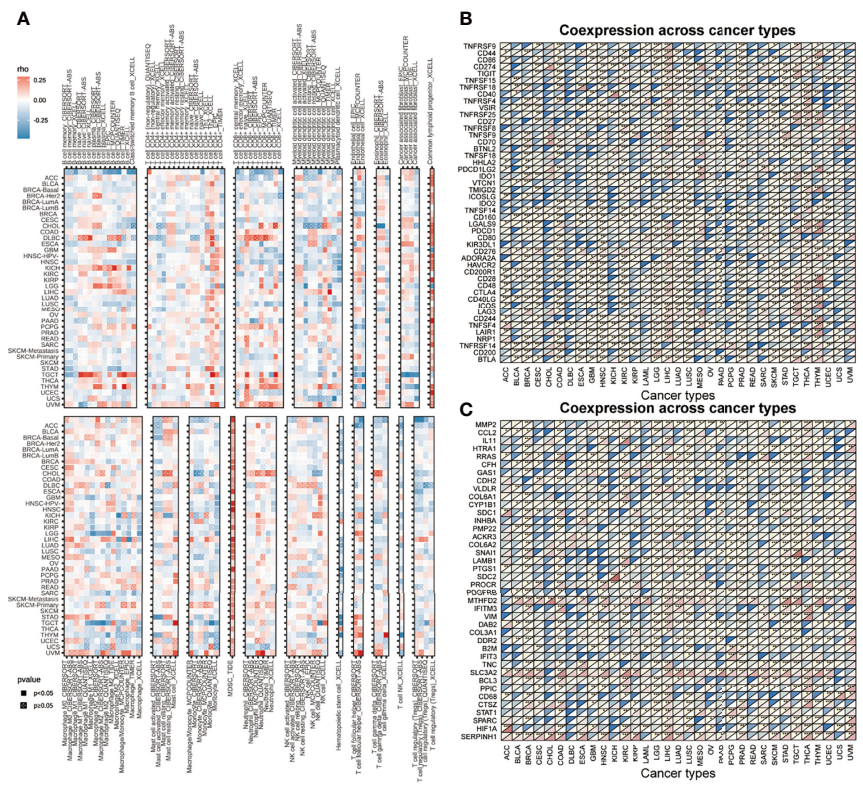

FIGURE 3 | Correlation analysis between the expression of *AHSA1* and immune cell infiltration, checkpoint inhibitors and pyroptosis-related molecules. **(A)** Correlation analysis between *AHSA1* and immune cell infiltration in pan-cancer. **(B)** Correlation analysis between the expression of *AHSA1* and immune checkpoint inhibitors. **(C)** Coexpression analysis of *AHSA1* expression and epithelial-mesenchymal transition-related molecules. *p< 0.05; **p<0.01; ***p<0.001.

TGCT (**Figure 3B**). It is understood that EMT has a significant function in tumor metastasis, which is the major cause of death. To investigate whether *AHSA1* is related to tumor metastasis, the link between *AHSA1* expression and the expression of EMT-related molecules was analyzed. Results show a significant positive correlation between the *AHSA1* and EMT-related molecules in LIHC, KIRC, and UVM (**Figure 3C**). Additionally, the *AHSA1* and *MTHFD2, SLC3A2* and *SERPINH1* showed a significant positive correlation in a wide variety of tumors. The *AHSA1* and *MMP2, CCL2, CFH*, and *CYP1B1* showed a significant negative correlation in a variety of tumors (**Figure 3C**). Pyroptosis is a new type of programmed inflammatory cell death that has a significant function in the development of tumor. Hence, the expression correlation between *AHSA1* and pyroptosis-related molecules was observed in this study. The results showed that *AHSA1* showed a significant positive correlation with pyroptosis-related molecules in BRCA, LGG, LIHC, PRAD, and THCA (**Figure 4A**). In addition, we also discussed the *AHSA1* correlation with autophagy-related molecules, the results also showed a significant positive correlation between *AHSA1* and autophagy-related molecules in BRCA, COAD, LIHC, LUAD, PAAD, PRAD and TGCT. Similar to the previous trends, *AHSA1* was significantly positively correlated with *HSP90AA1* and *HSP90AB1* (**Figure 4B**). In addition, tumor mutation load (TMB) and microsatellite instability (MSI) are known as important factors that affect tumor genesis and development. Therefore, the association between TMB or MSI and *AHSA1* expression was observed in 33 commonly known types of cancers. Results show that the *AHSA1* presented substantial relation with TMB in CESC, COAD, HNSC, KIRC, LUAD, STAD, and UCS (**Figures 4C, D**).

Molecular Interaction Network and Enrichment Analysis

To deeply understand the possible role of *AHSA1*, the molecules interacting with *AHSA1* were analyzed by GeneMANIA and comPPI. The results from GeneMANIA showed that *AHSA1* had potential interactions with *AMD1, HSP90AA1, DNAJB4* and *HSP90AB1*. Main functions included protein folding, up-regulation of DNA biosynthetic process and regulation of the metabolic processes of reactive oxygen species (**Figure 5A**). Single-sample gene set enrichment analysis (ssGSEA) algorithm was introduced to predict the infiltration levels of 24 immune cell types in HCC. The results indicated that *AHSA1* was positively correlated with T helper cells, Th2 cells, Macrophages, and iDC (**Figure 5B**). While, cytotoxic cells and Dendritic cells was negatively correlated with AHSA1 expression in HCC (**Figure 5B**). To further identify the possible role of *AHSA1*, the GO and KEGG enrichment analysis was performed on molecules that interacted with AHSA1 obtained from GeneMANIA. Cellular Component enrichment analysis showed that these molecules are mainly enriched in the cytosolic part, cell-substrate junction, cytosolic ribosome, and cytosolic small ribosomal subunit. The analysis of molecular function enrichment indicated that these molecules mostly play a role in cell adhesion molecule binding,

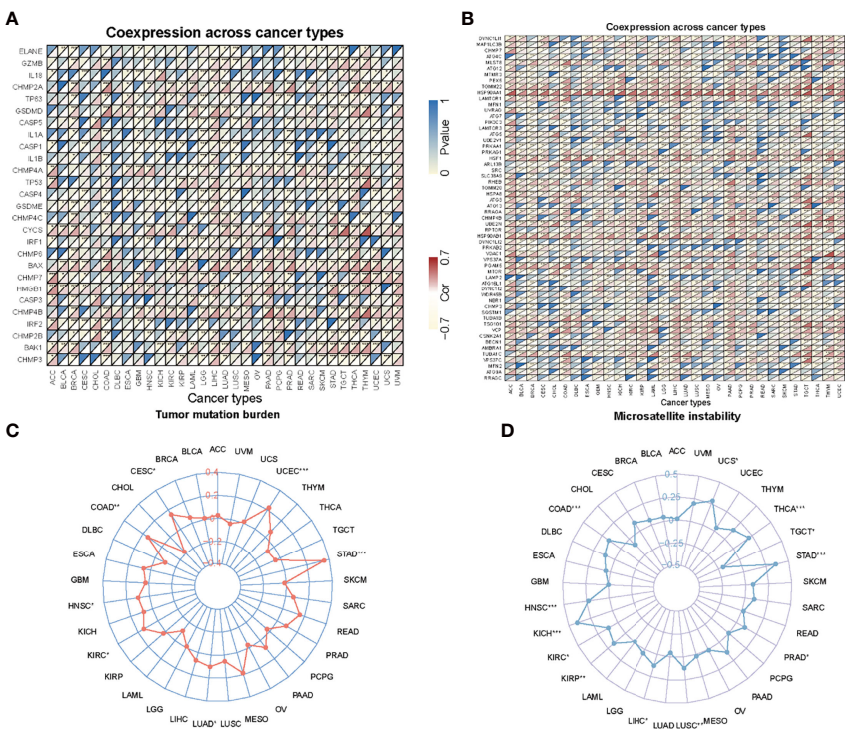

FIGURE 4 | Correlation analysis. **(A)** Correlation analysis of *AHSA1* expression and pyroptosis-related molecules. **(B)** Correlation analysis of *AHSA1* expression and autophagy-related molecules. **(C)** Correlation between *AHSA1* expression and Tumor mutation burden. **(D)** Correlation analysis of *AHSA1* expression and Microsatellite instability. *p<0.05, **p<0.01, ***p<0.001.

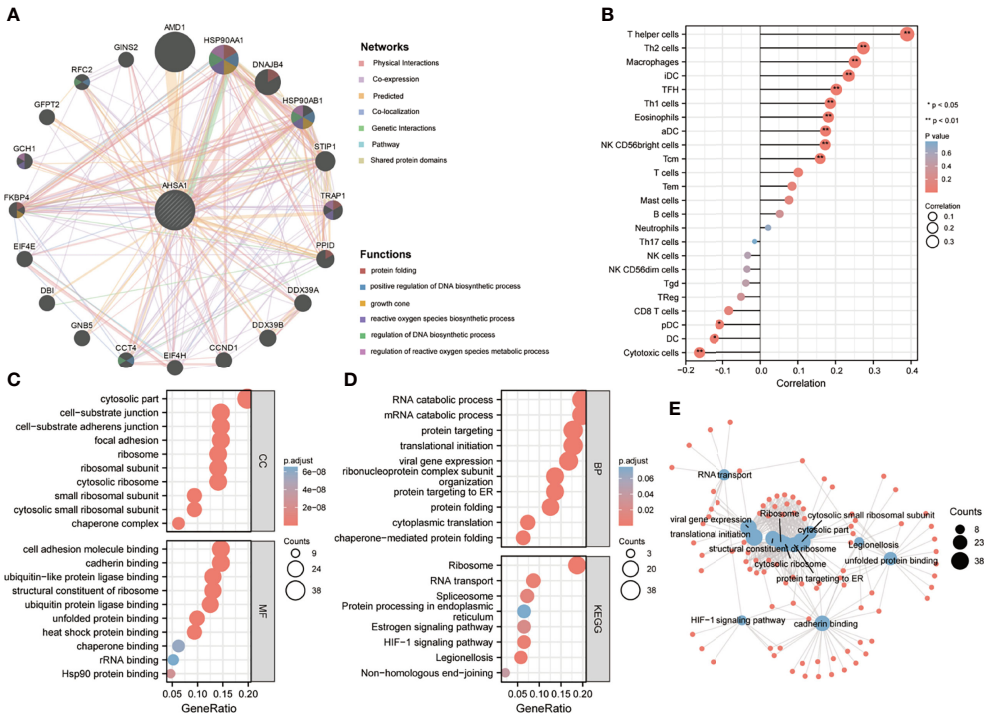

FIGURE 5 | Potential functions of *AHSA1*. **(A)** The potential interaction molecular network of *AHSA1* was created using the GeneMANIA. **(B)** The ssGSEA algorithm was employed to evaluate the abundance of immune cell infiltration in HCC. GO and KEGG functional enrichment analysis of the molecules interacted with AHSA1 **(C, D)**. **(E)** Construction of GO and KEGG interaction networks.

cadherin binding, ubiquitin-protein ligase binding, stressed protein binding, heat shock protein binding, and Hsp90 protein binding (**Figure 5C**). Enrichment analysis of biological processes showed that these molecules are mainly involved in RNA catabolic process, mRNA catabolic process, protein targeting, protein folding, and cytoplasmic translation (**Figure 5D**). KEGG analysis showed that these molecules were mainly involved in ribosome, RNA transport, Spliceosome, *HIF-1α* signaling pathway and Legionellosis (**Figure 5D**). In addition, we built an interactive relationship network between GO and KEGG, as shown in **Figure 5E**.

Clinical Correlation Analysis of AHSA1 in Hepatocellular Carcinoma

The findings of this study suggests that *AHSA1* may perform a key role in the development of hepatocellular carcinoma. Subsequently, the association between *AHSA1* expression and clinical stage was analyzed in hepatocellular carcinoma. The results indicated that *AHSA1* had a higher expression level in the higher pathologic stage (**Figure 6A**), T stage (**Figure 6B**), and histologic grade (**Figure 6C**). Meanwhile, *AHSA1* expression was also related to the expression level of AFP and vascular invasion status (**Figures 6D, E**). These findings indicate that *AHSA1* expression may be linked to the malignant pathological progression of hepatocellular carcinoma. Subsequently, we analyzed the prognostic evaluation efficacy of *AHSA1* in the overall survival rate of HCC by ROC, and the results showed that *AHSA1* showed good prognostic evaluation performance in HCC, with AUC of 0.702, 0.661 and 0.689 at 1, 3 and 5 years respectively (**Figure 6F**). We further evaluated the prognostic role of *AHSA1* in hepatocellular carcinoma by univariate and multivariate COX regression combined with clinical data, and the results showed that *AHSA1* was an independent prognostic factor of hepatocellular carcinoma (**Figure 6G**). Furthermore, in order to promote the application of *AHSA1* in clinical evaluation, we constructed a nomography (**Figure 6H**) based on the expression of *AHSA1* and the pathologic stage. At the same time, we evaluated the accuracy of the model for prognosis assessment of hepatocellular carcinoma patients after 1, 3 and 5 years by calibration curve, and according to the results, the nomography had very good accuracy, almost close to the ideal model (**Figure 6I**). For further confirmation of the value of prognosis of *AHSA1* in HCC, the expression of *AHSA1* in para-cancer and tumor tissues in the ICGC-LIRI-JP queue were analyzed. Both unpaired analysis (**Figure 7A**) and paired analysis (**Figure 7B**) showed that *AHSA1* has higher expression in HCC tumor tissues. Meanwhile, K-M curve analysis showed that HCC patients with high *AHSA1* expression in the ICGC queue had poorer survival expectations (**Figure 7C**). Meanwhile, the univariate and multi-variate COX analyses showed that *AHSA1* was an independent prognostic risk factor for HCC (**Figure 7D**). For additional verification of the expression of *AHSA1* in hepatocellular carcinoma, RT-PCR was performed to detect the mRNA expression levels of *AHSA1* in normal hepatocyte cell line LO2 along with three hepatocellular carcinoma cell lines, HCCLM3, HepG2 and Huh7. Results showed higher mRNA expression levels of *AHSA1* in hepatocellular

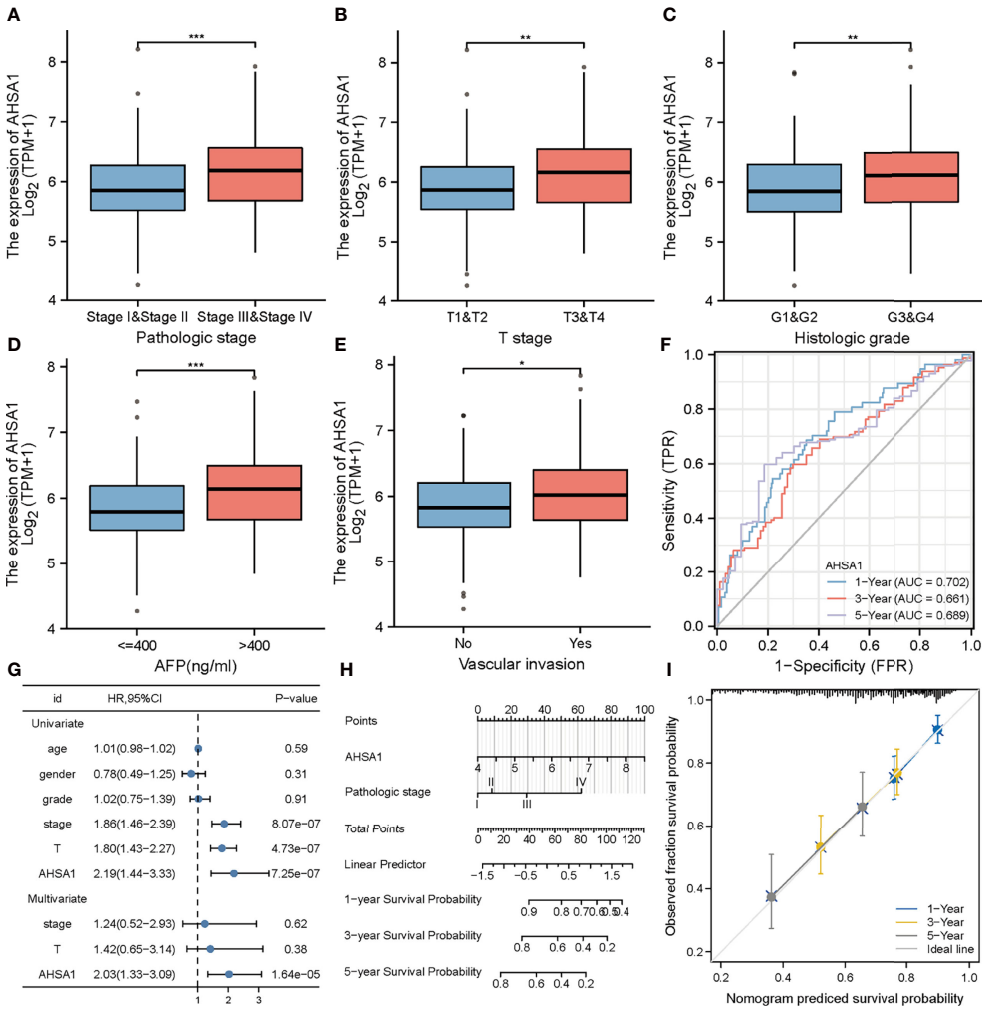

FIGURE 6 | Clinical correlation analysis of *AHSA1* in hepatocellular carcinoma. Variation analysis of *AHSA1* expression in different pathological stages **(A)**, T stage **(B)**, Histologic grade **(C)**, alpha-fetoprotein (AFP) **(D)**, Vascular invasion **(E)**. **(F)** Prognostic significance of *AHSA1* in hepatocellular carcinoma was analyzed by COX analysis. **(G)** Prognostic significance of *AHSA1* in hepatocellular carcinoma was analyzed by univariate and multivariate COX. **(H)** Nomogram based on *AHSA1* expression and pathological staging. **(I)** Correction analysis diagram of the nomogram. *p<0.05, **p<0.01, ***p<0.001.

carcinoma cells (**Figure 7E**). We also confirmed that the AHSA1 protein is expressed at a higher level in HCC cells compared to normal cells via western blot (**Figure 7F**). Subsequently, the protein expression level of AHSA1 were observed in hepatocellular tissues by immunohistochemistry, and according to the findings of this analysis, the level of protein expression of AHSA1 was greater in hepatocellular carcinoma tissues (**Figure 7G**).

The Effects of *AHSA1* on Proliferation, Migration, and Invasion of Hepatocellular Carcinoma Cells

Although the previous findings indicated that *AHSA1* was significantly over-expressed in hepatocellular carcinoma and patients with overexpression had poorer survival expectations, the role of *AHSA1* in the occurrence of hepatocellular carcinoma needs further study. Firstly, three shRNA knockout carriers of *AHSA1* were constructed and transfected into HUH7 cells. The RT-PCR and Western blot showed variations in mRNA and protein levels, respectively. According to the results, the SH2-*AHSA1* had the highest knockout efficiency (**Figures 8A, B**), and we named the carrier as sh*AHSA1*. Subsequently, we tested the changes of cell activity at different time points after transfection in three groups, namely normal cell group, negative vector group and sh*AHSA1* transfection group, using the CCK8 kit. The results showed that 48 hours after *AHSA1* knockdown, the proliferation ability of cells was significantly reduced (**Figure 8C**). In addition, after cell scratch test, we found that the healing ability of *AHSA1* knockout cells was significantly weakened (**Figures 8D, E**). Furthermore, the Transwell chamber experiment was performed to verify that the migration ability (**Figures 8F, G**) and invasion ability (**Figures 8F, H**) of Huh7 cells were significantly weakened after *AHSA1* knockout. In additional, the knockdown efficiency of *AHSA1* in HCCLM3 cells was validated by RT-PCR and Western blot (**Figures 9A, B**). CCK8

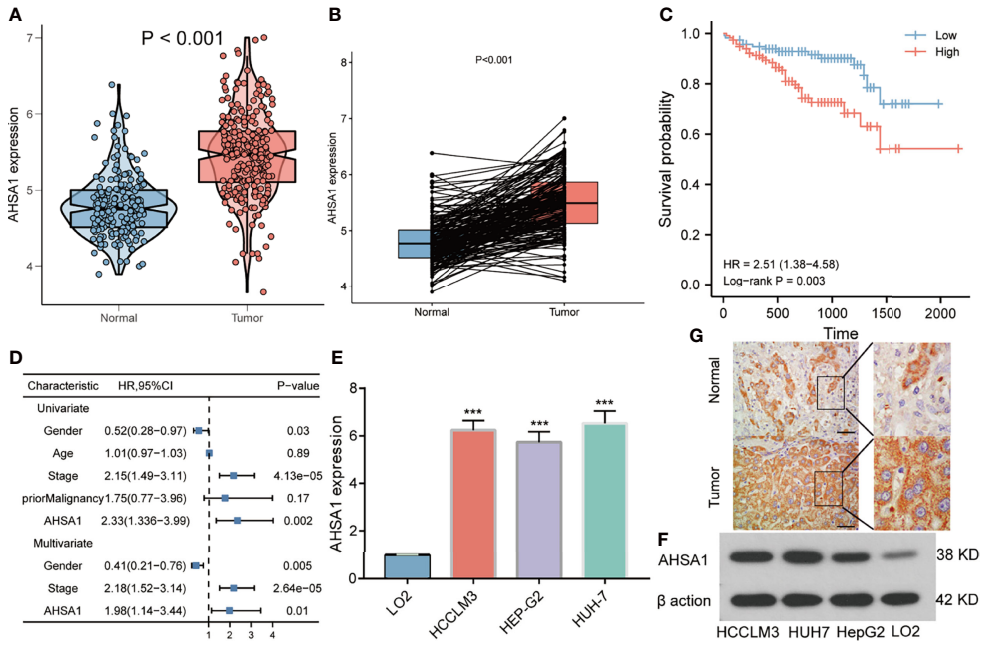

FIGURE 7 | Validation of *AHSA1* expression in hepatocellular carcinoma. **(A)** The mRNA expression of *AHSA1* in ICGC cohort. **(B)** Comparing the *AHSA1* expression in paired normal and tumor. **(C)** The relationship between *AHSA1* expression and overall survival in ICGC cohort. **(D)** Overexpression of *AHSA1* was an independent prognostic marker of HCC patients in ICGC cohort. **(E)** Relative mRNA expression of *AHSA1* in HCC cell lines. **(F)** Expression levels of AHSA1 protein in HCC cell lines. **(G)** Representative immunohistochemical analysis of *AHSA1* in HCC. ***p<0.001.

assays showed that knockdown of *AHSA1* significantly inhibited cell proliferation after 24 hours transfection in HCCLM3 cells (**Figure 9C**). Furthermore, scratch assays and transwell experiment showed that knockdown of *AHSA1* markedly reduced migration/invasion ability of HCCLM3 cell (**Figures 9D, E**). There was significant positive correlation between the mRNA expression level of *AHSA1* and *Hsp90AA1*. In order to further explore the relationship between *AHSA1* and *Hsp90AA1*, we knocked down *AHSA1* in Huh7 cells and examined the effect on *Hsp90AA1*. The rt-PCR and Western blot analysis showed that the knockdown of *AHSA1* significantly reduced the *Hsp90AA1* mRNA and protein levels (**Figures S2A, B**).

DISCUSSION

Heat Shock protein 90 (Hsp90) is a highly conserved, extensively exit molecular chaperone that has a role in the stabilizing and proper folding of at least 300 proteins (19). Reportedly, the Hsp90 protein is known to have a significant function in various cellular processes, signaling, tumor metastasis and tumor immunity (20). Hsp90 is a kind of molecular chaperone highly dependent on ATP activity, and its executive function also requires the cooperation of various auxiliary chaperone molecules. *AHSA1* can strongly stimulate the ATPase of Hsp90 and plays a significant role in the executive function of Hsp90 (21). Moreover, *AHSA1* itself is also a helper molecular chaperone involved in the maturation and stabilization of various proteins. However, systematic studies on the expression and role of *AHSA1* in tumors are still inefficient.

According to this study, based on the TCGA database, *AHSA1* was abnormally overexpressed in different types of tumors through unpaired and paired comparisons, but was expressed in low quantities in the KIRC tumor tissues. Meanwhile, by using the K-M survival analysis method, it was found that abnormally high expression of *AHSA1* in LIHC, LUAD, ESCA, and KIRP was associated with poor OS and DSS. These findings indicate that *AHSA1* may have a significant role in tumor genesis and prognosis. The tumor immune microenvironment can interact with tumor cells and play a significant function in tumor cell clearance and immune escape (22). Several reports have suggested that immune cell infiltration level in the tumor immune microenvironment is associated to tumor development and prognosis (23, 24). This study reported that the expression of *AHSA1* was significantly positively related to the infiltration level of CD4+ T cells and MDSC cells in a variety of tumors. Moreover, ssGSEA analysis also confirmed that *AHSA1* was substantially positively associated with infiltration levels of T helper cells, Th2 cells and Macrophages cells in LIHC. B Th2 cells are known to inhibit Th1 cells differentiation and IFN-γ-secreting but promote tumor cell proliferation *via* secretion of IL-4 and IL-10 (25, 26). As an important part of tumor immune microenvironment, macrophages have attracted more and more attention (27, 28). M2 macrophage can be induced to differentiate by IL-4, and promote tumorigenesis and tumor progression (29). Therefore, we preliminarily speculated that *AHSA1* might promote the tumor progression through regulating the polarization of Th2

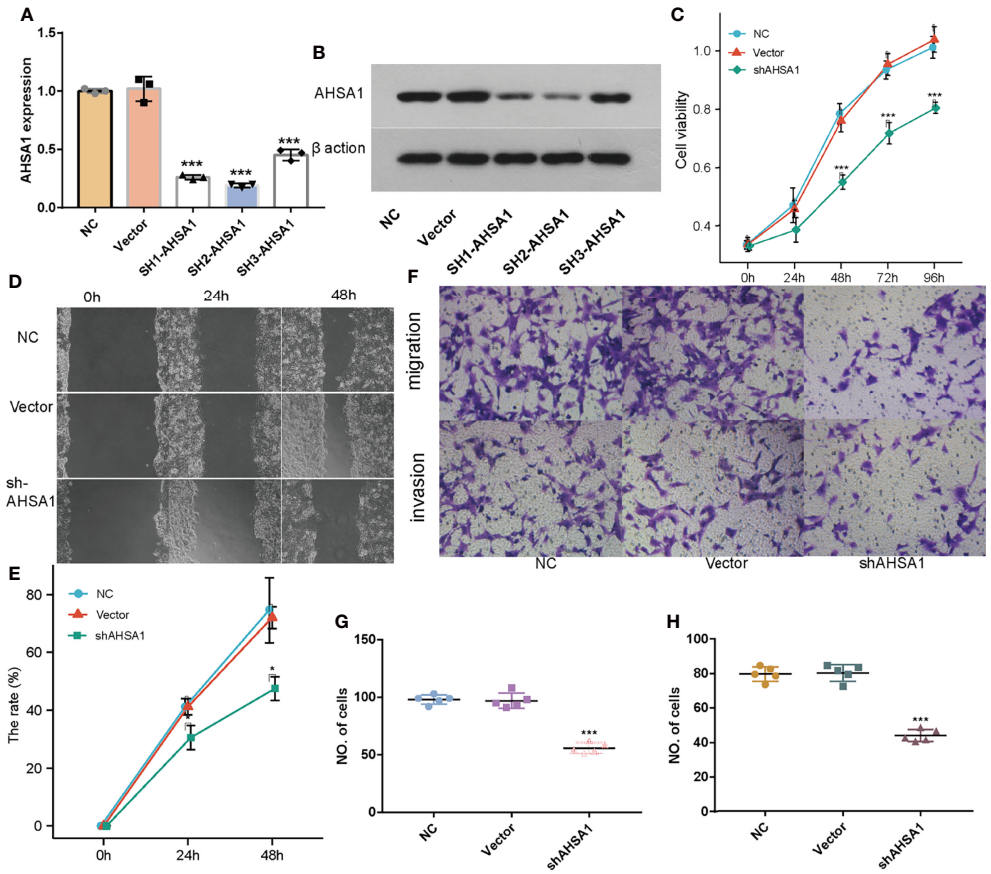

FIGURE 8 | Effects of *AHSA1* knockdown on Huh7 cell proliferation and migration. Real time PCR **(A)** and Weston blot **(B)** determine the efficiency of *AHSA1* knockdown in Huh7 cells. **(C)** Huh7 cell proliferation was detected by CCK8 assays. **(D, E)**. Cell migration ability was examined by cell scratch assay. **(F)** Tranwell analysis was preformed to determine the cell migration **(G)** and invasion **(H)**. *p<0.05, ***p<0.001.

and macrophages cells. Immune checkpoint is an important immunomodulator to maintain immune homeostasis and prevent autoimmunity (30). It consists of stimulant and inhibitory pathways, which are important for maintaining autoimmune tolerance and regulating the type, intensity, and duration of immune responses (31). The results of this study showed that *AHSA1* was substantially linked with immune checkpoints in BRCA, LIHC, and LUSC. According to these findings the *AHSA1* may play a certain role in the regulation of tumor microenvironment. Epithelial mesenchymal cell transformation, pyroptosis, and autophagy are significantly involved in the genesis, progression, and metastasis of tumors (32–34). The results of this study also indicate that *AHSA1* expression is significantly positively co-expressed with these pathway-related molecules in a variety of tumors. These results suggest that abnormal expression of *AHSA1* may be associated with tumor genesis and metastasis. Moreover, molecules with possible effects of *AHSA1* were also explored and the molecular interaction network was constructed. As expected, *AHSA1* showed strong interaction with *AMD1* and *HSP90*, which is consistent with previous reports (35). At the same time, by conducting enrichment analysis, we explained the molecules potentially interacting with *AHSA1* are mainly involved in RNA transport, spliceosome and *HIF-1α* signaling pathway. The pathways above play a significant role in tumor development (36–38). This also indicated the significant involvement of *AHSA1* in the progression of tumor. The current research highlighted that the abnormal expression of *AHSA1* was closely related to the prognosis of patients with hepatocellular carcinoma. Therefore, further analysis of the association between the expression of *AHSA1* and the clinicopathological stage was carried out, and to facilitate the application of *AHSA1* in the prognosis assessment of hepatocellular carcinoma, a nomography was constructed. Previous studies have shown that *AHSA1* inhibition can significantly inhibit the proliferation and viability of breast cancer cells (39). The results of this study showed that *AHSA1* knockdown significantly reduced the proliferation activity, migration and invasion ability of Huh7 and HCCLM3 cells. Meanwhile, *AHSA1* knockdown significantly reduced the expression of *Hsp90AA1*. And *Hsp90AA1*, as the autophagy-related genes, plays key roles in the autophagy pathway and tumorigenesis. This result suggests *AHSA1* might plays a role in regulating autophagy.

AHSA1 is abnormally upregulated in different tumor tissues, and its anomalous expression is related to the prognosis of tumors. The

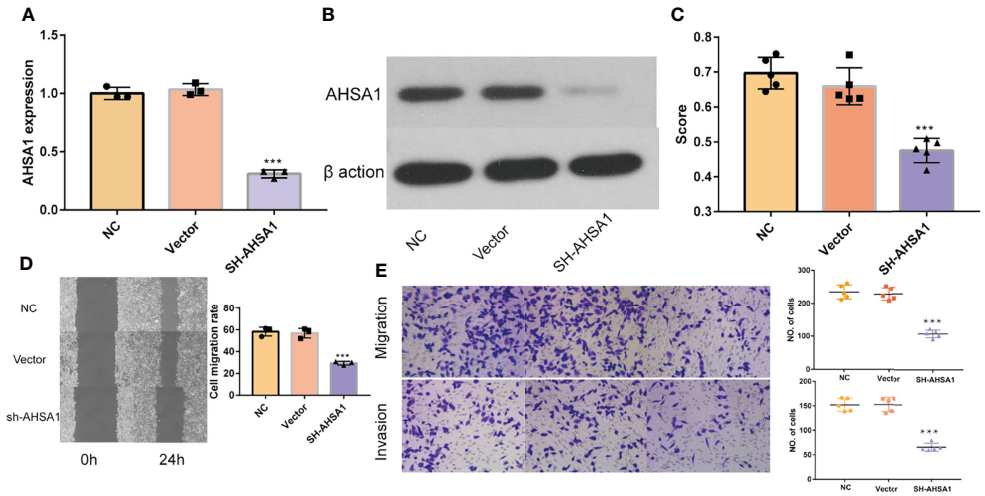

FIGURE 9 | Effects of *AHSA1* knockdown on HCCLM3 cell proliferation and migration. Real time PCR **(A)** and Weston blot **(B)** determine the efficiency of *AHSA1* knockdown in Huh7 cells. **(C)** CCK8 assays was performed to detect the cell proliferation of HCCLM3. **(D)** Scratch test was used to determine the cell migration. **(E)** Cell migration and invasion was detected by Tranwell assay. ***p<0.001.

abnormal expression of *AHSA1* is related to the infiltration of immune cells, the expression of immune checkpoints, and the expression of various tumor pathway molecules in pan-cancer. Moreover, knockdown of *AHSA1* can affect the proliferation and transformation of hepatocellular carcinoma cells. Therefore, *AHSA1* can be used as a potential prognostic biomarker.

DATA AVAILABILITY STATEMENT

The original contributions presented in the study are included in the article/**Supplementary Material**. Further inquiries can be directed to the corresponding author.

ETHICS STATEMENT

The studies involving human participants were reviewed and approved by Yue Bei People's Hospital. The patients/participants provided their written informed consent to participate in this study.

AUTHOR CONTRIBUTIONS

JL and WL both involved in drafting the manuscript. JL and WL took part in the design and data collection process of the study and are responsible for the content of the manuscript. All authors read and approved the final manuscript.

SUPPLEMENTARY MATERIAL

The Supplementary Material for this article can be found online at: https://www.frontiersin.org/articles/10.3389/fimmu.2022.845585/full#supplementary-material

Supplementary Figure 1 | Differential expression analysis of *Hsp90AA1* in Pan-cancer. **(A)** Expression of *Hsp90AA1* mRNA in pan-cancer. **(B)** The expression differences of *Hsp90AA1* in tumor and corresponding adjacent tissues were compared with paired analysis. Mann-Whitney U test was used for this analysis, ns, p≥0.05; * p< 0.05; ** p<0.01; *** p<0.001.

Supplementary Figure 2 | Real time PCR **(A)** and Weston blot **(B)** were adopted to evaluate the effects of *AHSA1* knockdown on the expression of *Hsp90AA1*. ns, p≥0.05; * p< 0.05; ** p<0.01; *** p<0.001.

REFERENCES

1. Bray F, Ferlay J, Soerjomataram I, Siegel RL, Torre LA, Jemal A. Global Cancer Statistics 2018: GLOBOCAN Estimates of Incidence and Mortality Worldwide for 36 Cancers in 185 Countries. *CA Cancer J Clin* (2018) 68 (6):394–424. doi: 10.3322/caac.21492
2. Santucci C, Carioli G, Bertuccio P, Malvezzi M, Pastorino U, Boffetta P, et al. Progress in Cancer Mortality, Incidence, and Survival: A Global Overview. *Eur J Cancer Prev* (2020) 29(5):367–81. doi: 10.1097/CEJ.0000000000000594
3. Weinstein JN, Collisson EA, Mills GB, Shaw KRM, Ozenberger BA, Ellrott K, et al. The Cancer Genome Atlas Pan-Cancer Analysis Project. *Nat Genet* (2013) 45(10):1113–20. doi: 10.1038/ng.2764
4. Saidak Z, Soudet S, Lottin M, Salle V, Sevestre M-A, Clatot F, et al. A Pan-Cancer Analysis of the Human Tumor Coagulome and its Link to the Tumor Immune Microenvironment. *Cancer Immunol Immunother* (2021) 70 (4):923–33. doi: 10.1007/s00262-020-02739-w
5. Liu J, Zhang S, Dai W, Xie C, Li J-C. A Comprehensive Prognostic and Immune Analysis of SLC41A3 in Pan-Cancer. *Front Oncol* (2020) 10:586414. doi: 10.3389/fonc.2020.586414
6. Wang Z, Zhang H, Cheng Q. PDIA4: The Basic Characteristics, Functions and its Potential Connection With Cancer. *Biomed Pharmacother* (2020) 122:109688. doi: 10.1016/j.biopha.2019.109688
7. Wolmarans A, Lee B, Spyracopoulos L, LaPointe P. The Mechanism of Hsp90 ATPase Stimulation by Aha1. *Sci Rep* (2016) 6:33179. doi: 10.1038/srep33179

8. Xu W, Beebe K, Chavez JD, Boysen M, Lu Y, Zuehlke AD, et al. Hsp90 Middle Domain Phosphorylation Initiates a Complex Conformational Program to Recruit the ATPase-Stimulating Cochaperone Aha1. *Nat Commun* (2019) 10 (1):2574. doi: 10.1038/s41467-019-10463-y
9. Trepel J, Mollapour M, Giaccone G, Neckers L. Targeting the Dynamic HSP90 Complex in Cancer. *Nat Rev Cancer* (2010) 10(8):537–49. doi: 10.1038/nrc2887
10. Shelton LB, Baker JD, Zheng D, Sullivan LE, Solanki PK, Webster JM, et al. Hsp90 Activator Aha1 Drives Production of Pathological Tau Aggregates. *Proc Natl Acad Sci USA* (2017) 114(36):9707–12. doi: 10.1073/pnas.1707039114
11. Shao J, Wang L, Zhong C, Qi R, Li Y. AHSA1 Regulates Proliferation, Apoptosis, Migration, and Invasion of Osteosarcoma. *Biomed Pharmacother* (2016) 77:45–51. doi: 10.1016/j.biopha.2015.11.008
12. Li T, Fan J, Wang B, Traugh N, Chen Q, Liu JS, et al. TIMER: A Web Server for Comprehensive Analysis of Tumor-Infiltrating Immune Cells. *Cancer Res* (2017) 77(21):e108–e10. doi: 10.1158/0008-5472.CAN-17-0307
13. Chan TA, Yarchoan M, Jaffee E, Swanton C, Quezada SA, Stenzinger A, et al. Development of Tumor Mutation Burden as an Immunotherapy Biomarker: Utility for the Oncology Clinic. *Ann Oncol* (2019) 30(1):44–56. doi: 10.1093/annonc/mdy495
14. van Velzen MJM, Derks S, van Grieken NCT, Haj Mohammad N, van Laarhoven HWM. MSI as a Predictive Factor for Treatment Outcome of Gastroesophageal Adenocarcinoma. *Cancer Treat Rev* (2020) 86:102024. doi: 10.1016/j.ctrv.2020.102024
15. Beroukhim R, Mermel CH, Porter D, Wei G, Raychaudhuri S, Donovan J, et al. The Landscape of Somatic Copy-Number Alteration Across Human Cancers. *Nature* (2010) 463(7283):899–905. doi: 10.1038/nature08822
16. Bonneville R, Krook MA, Kautto EA, Miya J, Wing MR, Chen HZ, et al. Landscape of Microsatellite Instability Across 39 Cancer Types. *JCO Precis Oncol* (2017) 2017:PO.17.00073. doi: 10.1200/PO.17.00073
17. Warde-Farley D, Donaldson SL, Comes O, Zuberi K, Badrawi R, Chao P, et al. The GeneMANIA Prediction Server: Biological Network Integration for Gene Prioritization and Predicting Gene Function. *Nucleic Acids Res* (2010) 38(Web Server issue):W214–W20. doi: 10.1093/nar/gkq537
18. Riera-Domingo C, Audigé A, Granja S, Cheng W-C, Ho P-C, Baltazar F, et al. Immunity, Hypoxia, and Metabolism-The Ménage À Trois of Cancer: Implications for Immunotherapy. *Physiol Rev* (2020) 100(1):1–102. doi: 10.1152/physrev.00018.2019
19. Schopf FH, Biebl MM, Buchner J. The HSP90 Chaperone Machinery. *Nat Rev Mol Cell Biol* (2017) 18(6):345–60. doi: 10.1038/nrm.2017.20
20. Hoter A, El-Sabban ME, Naim HY. The HSP90 Family: Structure, Regulation, Function, and Implications in Health and Disease. *Int J Mol Sci* (2018) 19 (9):2560. doi: 10.3390/ijms19092560
21. Walton-Diaz A, Khan S, Bourboulia D, Trepel JB, Neckers L, Mollapour M. Contributions of Co-Chaperones and Post-Translational Modifications Towards Hsp90 Drug Sensitivity. *Future Med Chem* (2013) 5(9):1059–71. doi: 10.4155/fmc.13.88
22. Lei X, Lei Y, Li J-K, Du W-X, Li R-G, Yang J, et al. Immune Cells Within the Tumor Microenvironment: Biological Functions and Roles in Cancer Immunotherapy. *Cancer Letters* (2020) 470:126–33. doi: 10.1016/j.canlet.2019.11.009
23. Huntington ND, Cursons J, Rautela J. The Cancer-Natural Killer Cell Immunity Cycle. *Nat Rev Cancer* (2020) 20(8):437–54. doi: 10.1038/s41568-020-0272-z
24. Engelhard VH, Rodriguez AB, Mauldin IS, Woods AN, Peske JD, Slingluff CL. Immune Cell Infiltration and Tertiary Lymphoid Structures as Determinants of Antitumor Immunity. *J Immunol* (2018) 200(2):432–42. doi: 10.4049/jimmunol.1701269
25. Lee HL, Jang JW, Lee SW, Yoo SH, Kwon JH, Nam SW, et al. Inflammatory Cytokines and Change of Th1/Th2 Balance as Prognostic Indicators for Hepatocellular Carcinoma in Patients Treated With Transarterial Chemoembolization. *Sci Rep* (2019) 9(1):3260. doi: 10.1038/s41598-019-40078-8
26. Narsale A, Moya R, Davies JD. Human CD4(+) CD25(+) CD127(hi) Cells and the Th1/Th2 Phenotype. *Clin Immunol* (2018) 188:103–12. doi: 10.1016/j.clim.2018.01.003
27. Mehla K, Singh PK. Metabolic Regulation of Macrophage Polarization in Cancer. *Trends Cancer* (2019) 5(12):822–34. doi: 10.1016/j.trecan.2019.10.007
28. Locati M, Curtale G, Mantovani A. Diversity, Mechanisms, and Significance of Macrophage Plasticity. *Annu Rev Pathol* (2020) 15:123–47. doi: 10.1146/annurev-pathmechdis-012418-012718
29. Wu K, Lin K, Li X, Yuan X, Xu P, Ni P, et al. Redefining Tumor-Associated Macrophage Subpopulations and Functions in the Tumor Microenvironment. *Front Immunol* (2020) 11:1731. doi: 10.3389/fimmu.2020.01731
30. Darvin P, Toor SM, Sasidharan Nair V, Elkord E. Immune Checkpoint Inhibitors: Recent Progress and Potential Biomarkers. *Exp Mol Med* (2018) 50(12):1–11. doi: 10.1038/s12276-018-0191-1
31. Kalbasi A, Ribas A. Tumour-Intrinsic Resistance to Immune Checkpoint Blockade. *Nat Rev Immunol* (2020) 20(1):25–39. doi: 10.1038/s41577-019-0218-4
32. Pastushenko I, Blanpain C. EMT Transition States During Tumor Progression and Metastasis. *Trends Cell Biol* (2019) 29(3):212–26. doi: 10.1016/j.tcb.2018.12.001
33. Levine B, Kroemer G. Biological Functions of Autophagy Genes: A Disease Perspective. *Cell* (2019) 176(1-2):11–42. doi: 10.1016/j.cell.2018.09.048
34. Fang Y, Tian S, Pan Y, Li W, Wang Q, Tang Y, et al. Pyroptosis: A New Frontier in Cancer. *Biomed Pharmacother* (2020) 121:109595. doi: 10.1016/j.biopha.2019.109595
35. Oroz J, Blair LJ, Zweckstetter M. Dynamic Aha1 Co-Chaperone Binding to Human Hsp90. *Protein Sci* (2019) 28(9):1545–51. doi: 10.1002/pro.3678
36. Semenza GL. HIF-1 Mediates Metabolic Responses to Intratumoral Hypoxia and Oncogenic Mutations. *J Clin Invest* (2013) 123(9):3664–71. doi: 10.1172/JCI67230
37. Lee SC-W, Abdel-Wahab O. Therapeutic Targeting of Splicing in Cancer. *Nat Med* (2016) 22(9):976–86. doi: 10.1038/nm.4165
38. Obeng EA, Stewart C, Abdel-Wahab O. Altered RNA Processing in Cancer Pathogenesis and Therapy. *Cancer Discov* (2019) 9(11):1493–510. doi: 10.1158/2159-8290.CD-19-0399
39. Ghosh S, Shinogle HE, Garg G, Vielhauer GA, Holzbeierlein JM, Dobrowsky RT, et al. Hsp90 C-Tersminal Inhibitors Exhibit Antimigratory Activity by Disrupting the Hsp90α/Aha1 Complex in PC3-MM2 Cells. *ACS Chem Biol* (2015) 10(2):577–90. doi: 10.1021/cb5008713

Conflict of Interest: The authors declare that the research was conducted in the absence of any commercial or financial relationships that could be construed as a potential conflict of interest.

frontiers | Frontiers in Immunology

REVIEW
published: 16 June 2022
doi: 10.3389/fimmu.2022.907605

Myeloid Cell Classification and Therapeutic Opportunities Within the Glioblastoma Tumor Microenvironment in the Single Cell-Omics Era

*Collin J. Larkin[1], Víctor A. Arrieta[1,2,3], Hinda Najem[1,2], Gongbo Li[1,2], Peng Zhang[1,2], Jason Miska[1,2], Peiwen Chen[1,2], Charles David James[1,2], Adam M. Sonabend[1,2] and Amy B. Heimberger[1,2]**

[1] Department of Neurological Surgery, Northwestern University Feinberg School of Medicine, Chicago, IL, United States, [2] Lou and Jean Malnati Brain Tumor Institute of the Lurie Comprehensive Cancer Center, Northwestern University Feinberg School of Medicine, Chicago, IL, United States, [3] Programa de Estudios Combinados en Medicina (PECEM), Facultad de Medicina, Universidad Nacional Autónoma de México, Mexico City, Mexico

OPEN ACCESS

Edited by:
Darya Alizadeh,
City of Hope, United States

Reviewed by:
Bozena Kaminska,
Nencki Institute of Experimental Biology (PAS), Poland
Anne Regnier-Vigouroux,
Johannes Gutenberg University Mainz, Germany

***Correspondence:**
Amy B. Heimberger
amy.heimberger@northwestern.edu

Specialty section:
This article was submitted to Cancer Immunity and Immunotherapy, a section of the journal Frontiers in Immunology

Received: 29 March 2022
Accepted: 18 May 2022
Published: 16 June 2022

Citation:
Larkin CJ, Arrieta VA, Najem H, Li G, Zhang P, Miska J, Chen P, James CD, Sonabend AM and Heimberger AB (2022) Myeloid Cell Classification and Therapeutic Opportunities Within the Glioblastoma Tumor Microenvironment in the Single Cell-Omics Era. Front. Immunol. 13:907605. doi: 10.3389/fimmu.2022.907605

The glioma tumor microenvironment (TME) is complex and heterogeneous, and multiple emerging and current technologies are being utilized for an improved comprehension and understanding of these tumors. Single cell analysis techniques such as single cell genomic and transcriptomic sequencing analysis are on the rise and play an important role in elucidating the glioma TME. These large datasets will prove useful for patient tumor characterization, including immune configuration that will ultimately influence therapeutic choices and especially immune therapies. In this review we discuss the advantages and drawbacks of these techniques while debating their role in the domain of glioma-infiltrating myeloid cells characterization and function.

Keywords: glioblastoma, immunotherapy, macrophage, tumor microenvironment, single cell analysis, transcriptomics, spatial analysis

INTRODUCTION

Gliomas are composed of multiple distinct cell populations, each playing a unique role within the tumor microenvironment (TME). Each of these cell types contains a spectrum of subtypes that increase the level of heterogeneity and complexity of these tumors. In this context, antagonistic forces promoting both tumor growth and suppression exist in the TME that influence clinical outcomes and responses to therapies. Initiatives such as The Cancer Genome Atlas (TCGA) and the GLASS consortium (1), have provided important information about the genetic variation and evolution among gliomas, leading to the molecular classification for glioblastoma (GBM) (2). However, since bulk genomic and transcriptome data averages the genetic alterations and gene expression patterns, respectively, of individual tumors, the analysis of such data has limits regarding determining the extent of cell subpopulation heterogeneity within a tumor and thus, response to therapeutic interventions. In contrast, technologies such as single-cell RNA-seq (scRNA-seq) and cytometry by time-of-flight

(CyTOF) are enabling the high-resolution characterization of glioma cellular heterogeneity (3). Single-cell analysis is proving informative about cell subpopulations in normal tissues and in treated recurrent GBM, with the latter providing insights regarding therapy-driven tumor evolution (4, 5). It is anticipated that single-cell analyses will ultimately prove informative regarding the individualization of glioma patient treatment based on knowledge of a tumor's cellular heterogeneity combined with increased understanding of cell subpopulation interactions. The myeloid compartment is the predominant subset of immune cells within the GBM microenvironment (6). This myeloid-rich environment is a hallmark of GBM, and these cells exert pro- and anti-tumor influence under different circumstances (6–8). Advances in understanding of glioma cellular heterogeneity from single cell analyses have exemplified the over-simplistic nature of the historically proposed pro-inflammatory M1 and immune suppressive M2 categories. Changes to the M1/M2 classification have been proposed by others, but without the benefit of single-cell characterization data (9). In this review, we discuss the current myeloid classification and its shortcomings, as well as how emerging single-cell technologies can be leveraged for increased understanding of glioma-infiltrating myeloid cell function in addition to impacting clinical outcomes in glioma patients.

Origins of M1/M2 Macrophage Classification

It was widely accepted for many years that the origin of tissue macrophages could be traced solely to circulating blood monocytes, which would travel to the destination tissue and differentiate into tissue-specific macrophages (i.e. microglia in the central nervous system (CNS), alveolar macrophages in the lungs, Kuppfer cells in the liver, etc.) (10–12). The current understanding is that there is a subset of tissue macrophages such as microglia derived not from circulating monocytes, but rather from stem cell populations found in the yolk sac and fetal liver during embryonic development that endure throughout life, independent of the circulating monocyte population (13–17). Evidence for this includes that these yolk sac-derived macrophages do not rely on the transcription factor c-Myb, which is necessary for differentiation of erythroid-myeloid progenitors into monocytes prior to differentiation into macrophages (18), providing a clear distinction from monocyte-derived macrophages (19, 20).

The M1/M2 classification was originally proposed to subclassify macrophages on the basis of immune activation and functional role, with M1 referring to those that are classically-activated and M2 referencing those that are alternatively activated (21). As shown by Mills et al. specifically in the context of differentiation of bone marrow-derived myeloid cells, macrophages are activated in two different ways, yielding two distinct phenotypes that have antagonistic effects on inflammation (22). Classical activation *via* stimulation with interferon (IFN)-γ, lipopolysaccharide (LPS), or granulocyte-macrophage colony-stimulating factor (GM-CSF), results in an antitumor phenotype in which numerous pro-inflammatory cytokines are produced. Alternative macrophage activation *via* interleukin (IL)-4, IL-10, IL-13, transforming growth factor (TGF)-β, and colony-stimulating factor (CSF)-1 results in the tumor-supportive phenotype characterized by macrophage production of high amounts of anti-inflammatory cytokines such as IL-10 and TGF-β (23). Tumor-supportive glioma-associated macrophages (GAMs) cells suppress inflammation, impairing the anti-tumor activity of effector cells such as T cells and natural killer (NK) cells, in addition to inducing other immunosuppressive cells such as Treg cells that ultimately support tumor growth and metastasis. A higher ratio of tumor-supportive GAMs to antitumoral GAMs is associated with a worse prognosis for cancer patients (24).

DISCUSSION

Complex Heterogeneity of Tumor-Associated Macrophages in GBM

A number of immune cell populations have been identified throughout the glioma TME, specifically macrophages, resident microglia, T and B lymphocytes, NK cells, and neutrophils, implying that the CNS is far from immune-privileged as was once thought to be the case (25–29). In fact, recent estimates suggest that 30-50% of tumor tissue is composed of monocyte-derived macrophages and microglia, which are the most numerous immune cell populations in GBM (30). The phenotypic profile of the TME immune population is subject to multiple factors dependent not only on the glioma type, but also on the location within the TME. Tumor mutational status appears to have significant impact on TME macrophage state and phenotype as well. In a comparison of isocitrate dehydrogenase (*IDH*) wild-type to *IDH* mutant gliomas, one study found that midkine (a neuroinflammatory cytokine that promotes macrophage polarization to an M2 phenotype) was preferentially upregulated in CD45+ myeloid cells of *IDH* wild-type gliomas as compared to *IDH* mutated gliomas (6). Additionally, GAMs in *IDH* wild-type tumors have been found to express higher levels of anti-inflammatory annexin A1 (ANXA1) and glycoprotein NMB (GPNMB) that have previously been found to be pro-tumorigenic (6). Regarding immune cell composition, GAMs are the most abundant in *IDH* wild-type tumors, while microglia were more common in *IDH* mutant tumors (6). These findings further highlight the need for a more granular investigation into the complex immune dynamics at play within the glioma TME.

TCGA research has revealed three molecular classifications for GBM: classical, proneural, and mesenchymal - each with distinct expression patterns that influence local macrophage polarization and gene expression (3, 25, 31, 32). Tumors of the mesenchymal subtype exhibit the highest expression of immunosuppressive genes that transcribe for galectin-3, IL-10, IL-23, and TGF-β and pro-inflammatory genes that transcribe for IL-2 and IFN (33). Conversely, recent evidence suggests that macrophages influence the phenotype of GBM cells to a mesenchymal-like state that involves the upregulation of MHC

class I and II (34). This preferential expression of pro- and anti-inflammatory genes not only promotes macrophage polarization within the TME but may also render the mesenchymal subtype of GBM more amenable to immunotherapeutic approaches. Prospective evaluation of this hypothesis requires GBM molecular classification in clinical trials that test the efficacy of immunotherapeutic treatments.

Recent work using single-cell sequencing techniques has shown significant insight into the phenotypic heterogeneity of macrophages within the glioma TME. scRNA-seq of GBM and low-grade gliomas (LGGs) has revealed that TAMs co-express canonical markers associated with antitumor and tumor-supportive macrophage polarization, with 66% of examined GAMs expressing both the immunosuppressive marker IL-10 and the pro-inflammatory marker TNF-α (35, 36). These results were consistent with the analytical techniques used, with flow cytometry revealing co-expression of immune costimulatory marker CD86 and the immunosuppressive marker CD206. The findings of macrophage co-expression of heterogeneous pro- and anti-tumor markers are corroborated by the results in a number of other studies (37–39). It is worth mentioning here that the expression of such markers can rapidly change in association with treatment, as indicated by the results of studies in which GBM patients received co-treatment with rapamycin and hydroxychloroquine or concurrent stereotactic radiotherapy with immune checkpoint blockade *via* programmed cell death protein 1 (PD-1) signal disruption (40, 41).

Recent studies have revealed transcriptional variability among monocyte-derived macrophages and microglia within the TME of glioma and brain metastases, with expression profiles not fitting into the classic M1 versus M2 polarization paradigm. One study found that high levels of traditionally "M1 markers" such as IL-6 and IL-1β were expressed by the same macrophages expressing traditionally "M2 markers" like matrix metalloproteinase (MMP)-1 and fibronectin 1 (FN1) (6). It has been shown that CD45+ myeloid cells in the GBM TME express markers of immune activation as well as immune suppression (42). A preclinical study detailed that treatment with anti-PD-1 therapy induced macrophage and microglia polarization towards a proinflammatory phenotype in glioma of $CD8^{-/-}$ mice, suggesting that the therapeutic effect of PD-1 blockade may be due to innate rather than adaptive immune system function (28). These findings underscore the complex plasticity of glioma cells to phenotypically adapt to different environments reflected in distinct transcriptional and evolutionary patterns for each patient. Nonetheless, this variability is subject to subclassification categories that may have implications for patient-specific treatments (3, 43–45).

Combined transcriptomic and proteomic approaches such as CITE-seq have demonstrated the ability to define the multidimensionality of myeloid cells and to delineate the spectrum of functions that these immune cells can display in the context of gliomas (46, 47). For instance, in applying single-cell sequencing to GAMs from human GBMs, Pombo Antunes proposed five distinct subtypes based on the activation state of the macrophage: transitory (showing markers of both monocyte and macrophage genes); phagocytic with lipid metabolism; hypoxic and glycolytic; *SEPP1*^{low}, and *SEPP1*^{high} (46). Notably, this diversity of macrophage states was recapitulated in murine gliomas analyzed with the same approach involving simultaneous proteomic and transcriptomic characterization. While this is but one way to further organize macrophage states, it may provide more utility than the existing classifications.

Another example of mouse and human data integration is an scRNA-seq study that delineated differences in the transcriptional networks between microglia and macrophages derived from non-tumor bearing mice and those derived from glioma-bearing mice. In this study, the expression of genes encoding the MHC class II molecule were increased in GAMs compared to myeloid cells isolated from non-tumor bearing mice. This difference in expression of MHC class II-associated genes was further appreciated in activated microglia from male tumor-bearing mice and GBM patients (48). Although these data show the potential antigen presentation capabilities of GAMs, scRNA-seq analysis of murine and human gliomas has also shown the immunosuppressive nature of these myeloid cells. For instance, one study showed that *ARG1/2* was upregulated predominantly in glioma-associated macrophages as opposed to microglia (49). This was further corroborated by elevated arginase-1 levels synthesized by tumor-infiltrating macrophages from mouse and human gliomas that promote the generation of polyamines and thus, T cell suppression (50).

In sum, these studies show the resolution that emerging single-cell technologies possess to characterize different transcriptional states of glioma-associated microglia and macrophages allowing the conceptualization of their complexity and heterogeneity across species.

Deconvolutional Techniques for Immune Characterization in GBM

Advanced single-cell analysis techniques like scRNA-seq and CyTOF provide an unprecedented level of resolution in characterizing the cellular composition of the TME. However, there remain several limitations with these techniques, particularly as they pertain to glioma research. CyTOF requires the selection of cell-surface markers, and although the number of detectable surface markers is rapidly growing, there is still a limitation to the absolute number that can be analyzed at one time, such that informative marker combinations can be missed due to initial marker selection. In addition, there is no standard technique for the processing of CyTOF data, leading to differences in results between labs that have performed CyTOF using the same set of markers. In particular, the randomization transformation used to better visualize CyTOF results is inherently different across analyses, and thus it has been suggested that raw data and detailed methods be provided for subsequent analysis whenever conclusions are reached from CyTOF data (51).

New results from scRNA-seq, on the other hand, are more easily compared against existing results given the vast amount of accessible online data (GBMseq, Ivy GAP, TCGA). For example,

several novel techniques have been developed recently using scRNA-seq to investigate cellular interactions and resulting transcriptomes on a single cell level in the TME such as RABID-seq and PIC-SEQ (52–54). However, considering that the transcription of a portion of the genome occurs as episodic and pulsatile bursts and that RNA collection and analysis is a snapshot in time, differential clusters of RNA expression seen during one analysis can be drastically different at another point in time (55). Similarly, phenotypic states of the same cell type as well as the immune cell composition within a TME changes with time and tumor evolution (55). Another limitation inherent to RNA expression analysis is that RNA expression does not explicitly translate to protein expression, resulting in only prediction of the potential cellular activities that might be occurring in the TME. Therefore, transcriptomics should be complemented with proteomics, functional assays, and spatial analysis. Furthermore, as a deconstructive and disruptive technique, the spatial relationships involving cell-cell interactions that influence transcriptional states are lost during the process of cell isolation, and accordingly are extrapolated from imaging data, which, even if subject of a certain degree of accuracy, is still at risk of error.

The spatial evaluation at the single-cell level along with functional information is the next step in characterizing the TME in finer detail. These will allow for more extensive investigations into the genetic and cellular changes that occur in response to therapeutic intervention within the TME, where within the TME these changes are occurring, and how best to exploit them to improve clinical response and outcomes. Previous investigations have examined the spatial distribution of immune cells throughout the infiltrating edge, proper tumor, and necrotic core of glioma, and found that there is significant heterogeneity throughout these areas in immune cell composition, distribution, and interactions (43). However, these spatial relationships between immune cells are only just starting to be further investigated in GBM undergoing microenvironmental change in response to therapy, allowing for unique opportunities for single-cell techniques to provide novel insight with the potential to advance therapeutic efficacy.

All shortcomings considered with respect to the different types of single cell analysis, the best approach for maximizing informative and accurate information yield is to utilize multiple techniques combined with spatial mapping of sample acquisition. Methods to integrate genomics, transcriptomics, and spatial measurements are emerging and have increasing influence on the way tumors are studied. Recently, Zhao et al. described a promising spatial genomic technique that not only allows for the detection of different clones of cells that harbor distinct genomic signatures, but also correlates signatures with cell location within the TME. For this particular study, spatial genomic heterogeneity was focused on tumor cells, but the approach can certainly be applied to other TME cell types such as GAMs (56). With the continuing refinement of spatial multiplex imaging technologies, detailed characterizations of the immune proteome within the TME have become possible. Using these techniques, one study found that myeloid cells localized to mesenchymal-like regions of GBM drive T cell exhaustion *via* IL-10 release, and that this T cell function was rescued with Janus kinase-signal transducer and activator of transcription (JAK/STAT) inhibition, providing a potential therapeutic opportunity (57). These techniques are allowing for the discovery of wider and more heterogeneous populations of immune cells with newly identified, previously unexploited cell phenotypes with distinct functions that influence tumor biology.

Leveraging Data From Single-Cell Technologies in Gliomas

Single cell technologies are providing opportunities to leverage data for clinical trial design and especially for treatment response interpretation (**Figure 1**). In instances where biopsy sampling of tumor prior to the initiation of treatment is possible, cellular profiles of pre-treatment specimens and corresponding on-therapy specimens obtained during surgical resection can be compared for determining the effect of treatment on TME cellular composition, as well as for determining the presence or absence of treatment anti-tumor activity. Single-cell analyses can also be used in a retrospective manner to study patient outcomes. One can conduct a retrospective analysis of tissue from patients that have received a common treatment, and in instances where tumor is collected post-mortem, the data obtained from end-stage tumors would prove informative regarding tumor evolution in response to a specific therapy. Importantly, mass cytometry and multiplex immunofluorescence can be used when specimen availability is limited to fixed tissues. In instances where frozen tissue is available, there are protocols for isolating nuclei that, in turn, enables single-nuclei RNA-seq (58). An example of this type of retrospective strategy that used fixed tissues found an association of extracellular signal-regulated kinases (ERK) 1/2 phosphorylation, an indicator of mitogen activated protein kinase (MAPK) pathway activation, with increased response and survival to adjuvant anti-PD-1 therapy in independent cohorts of recurrent GBMs (59). The integration of single-cell transcriptome analysis and multiplex immunofluorescence showed that tumors with an abundance of p-ERK contained GAMs with high major histocompatibility complex (MHC) class II gene and protein expression.

A final application of single cell analyses concerns immunoediting whereby GBM cells acquire an immune escape phenotype. Following treatment with standard-of-care temozolomide (TMZ) and radiotherapy (RT), changes in macrophage differentiation and polarization, as well as alterations in T-lymphocyte populations have been observed (60). Further, scRNA-seq data was used to investigate changes in GAM populations in response to radiotherapy specifically, finding that there was an increased ratio of macrophage: microglia as well as increased alternative activation in both populations leading to a predominantly immunosuppressive phenotype. The same study found that blocking these radiation-induced changes *via* administration of CSF-1R inhibitors significantly increased survival in preclinical models (61). Another study showed that tumors treated with neoadjuvant PD-1 immune checkpoint blockade contained

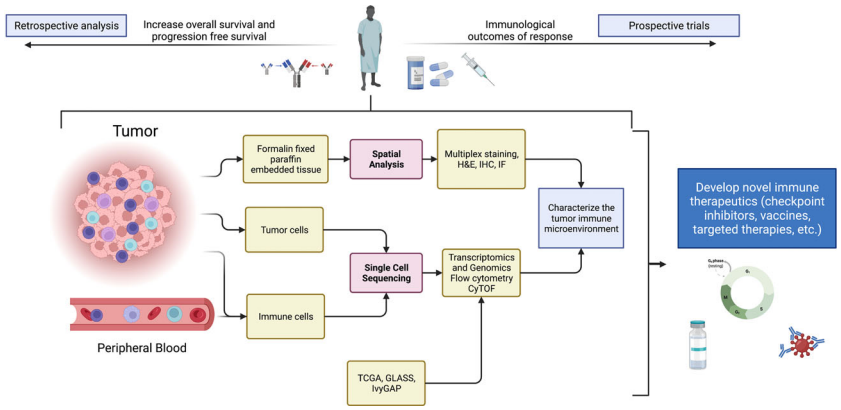

FIGURE 1 | Summary schematic detailing sources of samples, analytical techniques, and potential uses of data from single-cell technologies to improve and devise novel immune therapeutics. Specifically, single-cell technologies can be implemented in clinical studies for biomarker discovery, characterization of novel drug targets, and the study of pharmacodynamic effects of therapies in window-of-opportunity clinical trials. Created with BioRender.

higher numbers of $CD3^+$ T cells, with further analysis of the T cell receptor repertoire showing that signatures from peripheral and tumor-infiltrating T cells overlapped, suggesting that T cells from the circulation infiltrated these gliomas (62). Importantly, PD-1 blockade induced an IFN-γ gene signature in glioma-infiltrating monocytes and macrophages that was reflected by the expression of *CXCL9/10* and *PD-L1*. While the use of single-cell technologies has not yet become routine in patient care, these findings all suggest multiple applications of such single-cell techniques to provide novel avenues for therapeutic intervention.

CONCLUSION

The complexity of intratumor heterogeneity represented by diverse gene expression programs of cancer and immune cell populations in the TME has yet to be exploited for the benefit of patients. The analysis of tumor and immune cells, using single-cell technologies such as scRNA-seq and CyTOF, either before or after therapy, has the ability to dissect in detail the mechanisms of therapeutic response and resistance. In the future, we expect that integrative approaches involving the application of these methods will provide data that advance personalized treatments for cancer patients, and that will lead to improved treatment outcomes.

AUTHOR CONTRIBUTIONS

All authors have contributed significantly towards this manuscript as follows: (1) Conception and Design: AH, VA, HN, and CL; (2) Administrative Support: CL; (3) Provision of Study Materials or Patients: N/A; (4) Collection and Assembly of Data/Information: CL, VA, and HN; (5) Data Analysis and Interpretation: All authors; (6) Manuscript Writing: All authors; (7) Final Approval of Manuscript: All authors.

FUNDING

Research support was provided by the Northwestern Medicine Malnati Brain Tumor Institute of the Lurie Cancer Center, and NIH grants NS120547, CA120813, and CA221747.

REFERENCES

1. Consortium G. Glioma Through the Looking GLASS: Molecular Evolution of Diffuse Gliomas and the Glioma Longitudinal Analysis Consortium. *Neuro Oncol* (2018) 20(7):873–84. doi: 10.1093/neuonc/noy020
2. Network CGAR. Comprehensive Genomic Characterization Defines Human Glioblastoma Genes and Core Pathways. *Nature* (2008) 455(7216):1061–8. doi: 10.1038/nature07385
3. Neftel C, Laffy J, Filbin MG, Hara T, Shore ME, Rahme GJ, et al. An Integrative Model of Cellular States, Plasticity, and Genetics for Glioblastoma. *Cell* (2019) 178(4):835–49.e21. doi: 10.1016/j.cell.2019.06.024
4. Yuan GC, Cai L, Elowitz M, Enver T, Fan G, Guo G, et al. Challenges and Emerging Directions in Single-Cell Analysis. *Genome Biol* (2017) 18(1):84. doi: 10.1186/s13059-017-1218-y
5. Suvà ML, Tirosh I. Single-Cell RNA Sequencing in Cancer: Lessons Learned and Emerging Challenges. *Mol Cell* (2019) 75(1):7–12. doi: 10.1016/j.molcel.2019.05.003
6. Klemm F, Maas RR, Bowman RL, Kornete M, Soukup K, Nassiri S, et al. Interrogation of the Microenvironmental Landscape in Brain Tumors Reveals Disease-Specific Alterations of Immune Cells. *Cell* (2020) 181(7):1643–60.e17. doi: 10.1016/j.cell.2020.05.007
7. Thorsson V, Gibbs DL, Brown SD, Wolf D, Bortone DS, Ou Yang TH, et al. The Immune Landscape of Cancer. *Immunity* (2018) 48(4):812–30.e14. doi: 10.1016/j.immuni.2018.03.023
8. Friebel E, Kapolou K, Unger S, Núñez NG, Utz S, Rushing EJ, et al. Single-Cell Mapping of Human Brain Cancer Reveals Tumor-Specific Instruction of Tissue-Invading Leukocytes. *Cell* (2020) 181(7):1626–42.e20. doi: 10.1016/j.cell.2020.04.055

9. Chávez-Galán L, Olleros ML, Vesin D, Garcia I. Much More Than M1 and M2 Macrophages, There Are Also CD169+ and TCR+ Macrophages. *Front Immunol* (2015) 6(263). doi: 10.3389/fimmu.2015.00263
10. van Furth R, Cohn ZA. The Origin and Kinetics of Mononuclear Phagocytes. *J Exp Med* (1968) 128(3):415–35. doi: 10.1084/jem.128.3.415
11. Volkman A, Chang NC, Strausbauch PH, Morahan PS. Differential Effects of Chronic Monocyte Depletion on Macrophage Populations. *Lab Invest* (1983) 49(3):291–8.
12. Sawyer RT, Strausbauch PH, Volkman A. Resident Macrophage Proliferation in Mice Depleted of Blood Monocytes by Strontium-89. *Lab Invest* (1982) 46 (2):165–70.
13. Yosef N, Vadakkan TJ, Park JH, Poché RA, Thomas JL, Dickinson ME. The Phenotypic and Functional Properties of Mouse Yolk-Sac-Derived Embryonic Macrophages. *Dev Biol* (2018) 442(1):138–54. doi: 10.1016/j.ydbio.2018.07.009
14. Leid J, Carrelha J, Boukarabila H, Epelman S, Jacobsen SE, Lavine KJ. Primitive Embryonic Macrophages Are Required for Coronary Development and Maturation. *Circ Res* (2016) 118(10):1498–511. doi: 10.1161/CIRCRESAHA.115.308270
15. Hoeffel G, Ginhoux F. Fetal Monocytes and the Origins of Tissue-Resident Macrophages. *Cell Immunol* (2018) 330:5–15. doi: 10.1016/j.cellimm.2018.01.001
16. Bian Z, Gong Y, Huang T, Lee CZW, Bian L, Bai Z, et al. Deciphering Human Macrophage Development at Single-Cell Resolution. *Nature* (2020) 582 (7813):571–6. doi: 10.1038/s41586-020-2316-7
17. Ginhoux F, Greter M, Leboeuf M, Nandi S, See P, Gokhan S, et al. Fate Mapping Analysis Reveals That Adult Microglia Derive From Primitive Macrophages. *Science* (2010) 330(6005):841–5. doi: 10.1126/science.1194637
18. Hoeffel G, Chen J, Lavin Y, Low D, Almeida FF, See P, et al. C-Myb(+) Erythro-Myeloid Progenitor-Derived Fetal Monocytes Give Rise to Adult Tissue-Resident Macrophages. *Immunity* (2015) 42(4):665–78. doi: 10.1016/j.immuni.2015.03.011
19. Schulz C, Gomez Perdiguero E, Chorro L, Szabo-Rogers H, Cagnard N, Kierdorf K, et al. A Lineage of Myeloid Cells Independent of Myb and Hematopoietic Stem Cells. *Science* (2012) 336(6077):86–90. doi: 10.1126/science.1219179
20. Hettinger J, Richards DM, Hansson J, Barra MM, Joschko A-C, Krijgsveld J, et al. Origin of Monocytes and Macrophages in a Committed Progenitor. *Nat Immunol* (2013) 14(8):821–30. doi: 10.1038/ni.2638
21. Martinez FO, Gordon S. The M1 and M2 Paradigm of Macrophage Activation: Time for Reassessment. *F1000Prime Rep* (2014) 6:13–. doi: 10.12703/P6-13
22. Mills CD, Kincaid K, Alt JM, Heilman MJ. Hill AM. M-1/M-2 Macrophages and the Th1/Th2 Paradigm. *J Immunol* (2000) 164(12):6166–73. doi: 10.4049/jimmunol.164.12.6166
23. Atri C, Guerfali FZ, Laouini D. Role of Human Macrophage Polarization in Inflammation During Infectious Diseases. *Int J Mol Sci* (2018) 19(6):1801. doi: 10.3390/ijms19061801
24. Yunna C, Mengru H, Lei W, Weidong C. Macrophage M1/M2 Polarization. *Eur J Pharmacol* (2020) 877:173090. doi: 10.1016/j.ejphar.2020.173090
25. Wang Q, Hu B, Hu X, Kim H, Squatrito M, Scarpace L, et al. Tumor Evolution of Glioma-Intrinsic Gene Expression Subtypes Associates With Immunological Changes in the Microenvironment. *Cancer Cell* (2017) 32 (1):42–56.e6. doi: 10.1016/j.ccell.2017.06.003
26. Sa JK, Chang N, Lee HW, Cho HJ, Ceccarelli M, Cerulo L, et al. Transcriptional Regulatory Networks of Tumor-Associated Macrophages That Drive Malignancy in Mesenchymal Glioblastoma. *Genome Biol* (2020) 21(1):216. doi: 10.1186/s13059-020-02140-x
27. Dumas AA, Pomella N, Rosser G, Guglielmi L, Vinel C, Millner TO, et al. Microglia Promote Glioblastoma *via* mTOR-Mediated Immunosuppression of the Tumour Microenvironment. *EMBO J* (2020) 39(15):e103790. doi: 10.15252/embj.2019103790
28. Rao G, Latha K, Ott M, Sabbagh A, Marisetty A, Ling X, et al. Anti-PD-1 Induces M1 Polarization in the Glioma Microenvironment and Exerts Therapeutic Efficacy in the Absence of CD8 Cytotoxic T Cells. *Clin Cancer Res* (2020) 26(17):4699–712. doi: 10.1158/1078-0432.CCR-19-4110
29. Lee-Chang C, Rashidi A, Miska J, Zhang P, Pituch KC, Hou D, et al. Myeloid-Derived Suppressive Cells Promote B Cell-Mediated Immunosuppression *via* Transfer of PD-L1 in Glioblastoma. *Cancer Immunol Res* (2019) 7(12):1928–43. doi: 10.1158/2326-6066.CIR-19-0240
30. Chen Z, Feng X, Herting CJ, Garcia VA, Nie K, Pong WW, et al. Cellular and Molecular Identity of Tumor-Associated Macrophages in Glioblastoma. *Cancer Res* (2017) 77(9):2266–78. doi: 10.1158/0008-5472.CAN-16-2310
31. Phillips HS, Kharbanda S, Chen R, Forrest WF, Soriano RH, Wu TD, et al. Molecular Subclasses of High-Grade Glioma Predict Prognosis, Delineate a Pattern of Disease Progression, and Resemble Stages in Neurogenesis. *Cancer Cell* (2006) 9(3):157–73. doi: 10.1016/j.ccr.2006.02.019
32. Louis DN, Perry A, Wesseling P, Brat DJ, Cree IA, Figarella-Branger D, et al. The 2021 WHO Classification of Tumors of the Central Nervous System: A Summary. *Neuro Oncol* (2021) 23(8):1231–51. doi: 10.1093/neuonc/noab106
33. Doucette T, Rao G, Rao A, Shen L, Aldape K, Wei J, et al. Immune Heterogeneity of Glioblastoma Subtypes: Extrapolation From the Cancer Genome Atlas. *Cancer Immunol Res* (2013) 1(2):112–22. doi: 10.1158/2326-6066.CIR-13-0028
34. Hara T, Chanoch-Myers R, Mathewson ND, Myskiw C, Atta L, Bussema L, et al. Interactions Between Cancer Cells and Immune Cells Drive Transitions to Mesenchymal-Like States in Glioblastoma. *Cancer Cell* (2021) 39(6):779–92.e11. doi: 10.1016/j.ccell.2021.05.002
35. Müller S, Kohanbash G, Liu SJ, Alvarado B, Carrera D, Bhaduri A, et al. Single-Cell Profiling of Human Gliomas Reveals Macrophage Ontogeny as a Basis for Regional Differences in Macrophage Activation in the Tumor Microenvironment. *Genome Biol* (2017) 18(1):234. doi: 10.1186/s13059-017-1362-4
36. Degl'Innocenti A, di Leo N, Ciofani G. Genetic Hallmarks and Heterogeneity of Glioblastoma in the Single-Cell Omics Era. *Adv Ther (Weinh)* (2020) 3 (1):1900152. doi: 10.1002/adtp.201900152
37. Kaminska B, Ochocka N, Segit P. Single-Cell Omics in Dissecting Immune Microenvironment of Malignant Gliomas-Challenges and Perspectives. *Cells* (2021) 10(9):2264. doi: 10.3390/cells10092264
38. Szulzewsky F, Arora S, de Witte L, Ulas T, Markovic D, Schultze JL, et al. Human Glioblastoma-Associated Microglia/Monocytes Express a Distinct RNA Profile Compared to Human Control and Murine Samples. *Glia* (2016) 64(8):1416–36. doi: 10.1002/glia.23014
39. Szulzewsky F, Pelz A, Feng X, Synowitz M, Markovic D, Langmann T, et al. Glioma-Associated Microglia/Macrophages Display an Expression Profile Different From M1 and M2 Polarization and Highly Express Gpnmb and Spp1. *PloS One* (2015) 10(2):e0116644. doi: 10.1371/journal.pone.0116644
40. Hsu SPC, Chen YC, Chiang HC, Huang YC, Huang CC, Wang HE, et al. Rapamycin and Hydroxychloroquine Combination Alters Macrophage Polarization and Sensitizes Glioblastoma to Immune Checkpoint Inhibitors. *J Neurooncol* (2020) 146(3):417–26. doi: 10.1007/s11060-019-03360-3
41. Stessin AM, Clausi MG, Zhao Z, Lin H, Hou W, Jiang Z, et al. Repolarized Macrophages, Induced by Intermediate Stereotactic Dose Radiotherapy and Immune Checkpoint Blockade, Contribute to Long-Term Survival in Glioma-Bearing Mice. *J Neurooncol* (2020) 147(3):547–55. doi: 10.1007/s11060-020-03459-y
42. Najem H, Ott M, Kassab C, Rao A, Rao G, Marisetty A, et al. Central Nervous System Immune Interactome Is Function of Cancer Lineage, Tumor Microenvironment and STAT3 Expression. *JCI Insight* (2022) 7(9):e157612. doi: 10.1172/jci.insight.157612
43. Wang L, Babikir H, Müller S, Yagnik G, Shamardani K, Catalan F, et al. The Phenotypes of Proliferating Glioblastoma Cells Reside on a Single Axis of Variation. *Cancer Discov* (2019) 9(12):1708–19. doi: 10.1158/2159-8290.CD-19-0329
44. Tirosh I, Venteicher AS, Hebert C, Escalante LE, Patel AP, Yizhak K, et al. Single-Cell RNA-Seq Supports a Developmental Hierarchy in Human Oligodendroglioma. *Nature* (2016) 539(7628):309–13. doi: 10.1038/nature20123
45. Venteicher AS, Tirosh I, Hebert C, Yizhak K, Neftel C, Filbin MG, et al. Decoupling Genetics, Lineages, and Microenvironment in IDH-Mutant Gliomas by Single-Cell RNA-Seq. *Science* (2017) 355(6332):eaai8478. doi: 10.1126/science.aai8478
46. Pombo Antunes AR, Scheyltjens I, Lodi F, Messiaen J, Antoranz A, Duerinck J, et al. Single-Cell Profiling of Myeloid Cells in Glioblastoma Across Species and Disease Stage Reveals Macrophage Competition and Specialization. *Nat Neurosci* (2021) 24(4):595–610. doi: 10.1038/s41593-020-00789-y
47. Arrieta VA, Najem H, Petrosyan E, Lee-Chang C, Chen P, Sonabend AM, et al. The Eclectic Nature of Glioma-Infiltrating Macrophages and Microglia. *Int J Mol Sci* (2021) 22(24):13382. doi: 10.3390/ijms222413382

48. Ochocka N, Segit P, Walentynowicz KA, Wojnicki K, Cyranowski S, Swatler J, et al. Single-Cell RNA Sequencing Reveals Functional Heterogeneity of Glioma-Associated Brain Macrophages. *Nat Commun* (2021) 12(1):1151. doi: 10.1038/s41467-021-21407-w
49. Pilanc P, Wojnicki K, Roura AJ, Cyranowski S, Ellert-Miklaszewska A, Ochocka N, et al. A Novel Oral Arginase 1/2 Inhibitor Enhances the Antitumor Effect of PD-1 Inhibition in Murine Experimental Gliomas by Altering the Immunosuppressive Environment. *Front Oncol* (2021) 11:703465. doi: 10.3389/fonc.2021.703465
50. Miska J, Rashidi A, Lee-Chang C, Gao P, Lopez-Rosas A, Zhang P, et al. Polyamines Drive Myeloid Cell Survival by Buffering Intracellular pH to Promote Immunosuppression in Glioblastoma. *Sci Adv* (2021) 7(8):eabc8929. doi: 10.1126/sciadv.abc8929
51. Papoutsoglou G, Lagani V, Schmidt A, Tsirlis K, Cabrero DG, Tegnér J, et al. Challenges in the Multivariate Analysis of Mass Cytometry Data: The Effect of Randomization. *Cytometry A.* (2019) 95(11):1178–90. doi: 10.1002/cyto.a.23908
52. Clark IC, Gutiérrez-Vázquez C, Wheeler MA, Li Z, Rothhammer V, Linnerbauer M, et al. Barcoded Viral Tracing of Single-Cell Interactions in Central Nervous System Inflammation. *Science* (2021) 372(6540):eabf1230. doi: 10.1126/science.abf1230
53. Giladi A, Cohen M, Medaglia C, Baran Y, Li B, Zada M, et al. Dissecting Cellular Crosstalk by Sequencing Physically Interacting Cells. *Nat Biotechnol* (2020) 38(5):629–37. doi: 10.1038/s41587-020-0442-2
54. Cohen M, Giladi A, Barboy O, Hamon P, Li B, Zada M, et al. The Interaction of CD4(+) Helper T Cells With Dendritic Cells Shapes the Tumor Microenvironment and Immune Checkpoint Blockade Response. *Nat Cancer* (2022) 3(3):303–17. doi: 10.1038/s43018-022-00338-5
55. Dar RD, Razooky BS, Singh A, Trimeloni TV, McCollum JM, Cox CD, et al. Transcriptional Burst Frequency and Burst Size are Equally Modulated Across the Human Genome. *Proc Natl Acad Sci USA* (2012) 109(43):17454–9. doi: 10.1073/pnas.1213530109
56. Zhao T, Chiang ZD, Morriss JW, LaFave LM, Murray EM, Del Priore I, et al. Spatial Genomics Enables Multi-Modal Study of Clonal Heterogeneity in Tissues. *Nature* (2022) 601(7891):85–91. doi: 10.1038/s41586-021-04217-4
57. Ravi VM, Neidert N, Will P, Joseph K, Maier JP, Kückelhaus J, et al. T-Cell Dysfunction in the Glioblastoma Microenvironment is Mediated by Myeloid Cells Releasing Interleukin-10. *Nat Commun* (2022) 13(1):925. doi: 10.1038/s41467-022-28523-1
58. Slyper M, Porter CBM, Ashenberg O, Waldman J, Drokhlyansky E, Wakiro I, et al. A Single-Cell and Single-Nucleus RNA-Seq Toolbox for Fresh and Frozen Human Tumors. *Nat Med* (2020) 26(5):792–802. doi: 10.1038/s41591-020-0844-1
59. Arrieta VA, Chen AX, Kane JR, Kang SJ, Kassab C, Dmello C, et al. ERK1/2 Phosphorylation Predicts Survival Following Anti-PD-1 Immunotherapy in Recurrent Glioblastoma. *Nat Cancer* (2021) 2(12):1372–86. doi: 10.1038/s43018-021-00260-2
60. Ali S, Borin TF, Piranlioglu R, Ara R, Lebedyeva I, Angara K, et al. Changes in the Tumor Microenvironment and Outcome for TME-Targeting Therapy in Glioblastoma: A Pilot Study. *PloS One* (2021) 16(2):e0246646. doi: 10.1371/journal.pone.0246646
61. Akkari L, Bowman RL, Tessier J, Klemm F, Handgraaf SM, de Groot M, et al. Dynamic Changes in Glioma Macrophage Populations After Radiotherapy Reveal CSF-1R Inhibition as a Strategy to Overcome Resistance. *Sci Transl Med* (2020) 12(552):eaaw7843. doi: 10.1126/scitranslmed.aaw7843
62. Lee A, Sun L, Mochizuki A, Reynoso J, Orpilla J, Chow F, et al. Neoadjuvant PD-1 Blockade Induces T Cell and Cdc1 Activation But Fails to Overcome the Immunosuppressive Tumor Associated Macrophages in Recurrent Glioblastoma. *Res Square* (2021) 12(1):6938. doi: 10.21203/rs.3.rs-793187/av1

Conflict of Interest: The authors declare that the research was conducted in the absence of any commercial or financial relationships that could be construed as a potential conflict of interest.

frontiers | Frontiers in Immunology

REVIEW
published: 29 June 2022
doi: 10.3389/fimmu.2022.870458

Tertiary Lymphatic Structures in Primary Hepatic Carcinoma: Controversy Cannot Overshadow Hope

Weili Jia[1,2†], *Tianchen Zhang*[1,2†], *Qianyun Yao*[2], *Jianhui Li*[1,2], *Ye Nie*[1,2], *Xinjun Lei*[1,2], *Zhenzhen Mao*[1,2], *Yanfang Wang*[1,2], *Wen Shi*[1,2] *and Wenjie Song*[2*]

[1] *Xi'an Medical University, Xi'an, China,* [2] *Department of Hepatobiliary Surgery, Xijing Hospital, Fourth Military Medical University, Xi'an, China*

OPEN ACCESS

Edited by:
Nicolas Larmonier, Université de Bordeaux, France

Reviewed by:
Motoki Nakamura, Nagoya City University, Japan
Hui Li, Chongqing University, China

***Correspondence:**
Wenjie Song
wjsong@fmmu.edu.cn

†*These authors have contributed equally to this work and share first authorship*

Specialty section:
This article was submitted to Cancer Immunity and Immunotherapy, a section of the journal Frontiers in Immunology

Received: *06 February 2022*
Accepted: *30 May 2022*
Published: *29 June 2022*

Citation:
Jia W, Zhang T, Yao Q, Li J, Nie Y, Lei X, Mao Z, Wang Y, Shi W and Song W (2022) Tertiary Lymphatic Structures in Primary Hepatic Carcinoma: Controversy Cannot Overshadow Hope. Front. Immunol. 13:870458. doi: 10.3389/fimmu.2022.870458

Tertiary lymphoid structures (TLSs) are organized aggregates of immune cells found in the tumor microenvironment. TLS can influence primary hepatic carcinoma (PHC) occurrence and have an active role in cancer. TLS can promote or inhibit the growth of PHC depending on their location, and although available findings are controversial, they suggest that TLS have a protective role in PHC tissues and a non-protective role in paracancerous tissues. In addition, the cellular composition of TLS can also influence the outcome of PHC. As an immunity marker, TLS can act as a marker of immunotherapy to predict its effect and help to identify patients who will respond well to immunotherapy. Modulation of TLS formation through the use of chemokines/cytokines, immunotherapy, or induction of high endothelial vein to interfere with tumor growth has been studied extensively in PHC and other cancers. In addition, new tools such as genetic interventions, cellular crosstalk, preoperative radiotherapy, and advances in materials science have been shown to influence the prognosis of malignant tumors by modulating TLS production. These can also be used to develop PHC treatment.

Keywords: tertiary lymphoid structures (TLS), tumor-infiltrating lymphocytes (TIL), primary hepatic carcinoma (PHC), immunotherapy, cancer prognosis, immune microenvironment (IME)

1 INTRODUCTION

Tertiary lymphoid structures (TLSs), also known as tertiary lymphoid organs, ectopic lymphoid structures, induced lymphoid organs, and abnormal lymphoid appendages, are organized aggregates of immune cells such as ectopic central lymphocytes, myeloid cells, and interstitial cells for acquired immune response (1). TLS and secondary lymphoid organs (SLOs) have similar structures and functions (2). TLSs are ectopic lymphatic structures formed from long-term chronic inflammatory stimulation including viral infection, autoimmune diseases, tissue transplantation, and cancer (3). However, the prognostic role of TLS in those diseases is controversial. Previous studies have proven that TLS has a prognostic benefit in metastatic melanoma (4), invasive bladder cancer (5), non-metastatic colorectal cancer (6), endometrial cancer (7), and pancreatic cancer (8).

Conversely, there is a reported association between TLS and poor prognosis in lupus nephritis (9), rheumatoid arthritis (10), and other diseases.

Primary hepatic cancer (PHC) includes hepatocellular carcinoma (HCC), intrahepatic cholangiocarcinoma (iCCA), and mixed cancers (HCC + iCCA). HCC is the commonest histological subtype of PHC. As a cancer with an extremely high mortality rate, HCC was the sixth leading cause of cancer-related deaths in 2020 (11). The incidence of PHC is increasing yearly. According to World Health Organization projections, the number of new cases in 2040 will exceed 1.4 million, the number of deaths will exceed 1.3 million, and more than half of the cases will come from Asia (12). Surgical resection and liver transplantation are the main treatment options for early PHC. However, most patients are only diagnosed at the late stages, thus missing the best treatment opportunity (13). PHC is not sensitive to traditional radiotherapy and chemotherapy for malignant tumors. As a result, immunotherapy is one of its promising treatment methods (14). TLS are rich aggregates of immune cells and an important player in tumor immune response. Understanding TLS in PHC may help to further understand PHC immunotherapy. Therefore, this paper reviews recent studies of TLS and briefly introduces the background and concept of TLS. This manuscript focused on the dual impact of TLS distribution in PHC on prognosis, the potential value of TLS as an immune marker, and the potential of TLS formation and other TLS-related factors being treatments for PHC, which can serve as reference information for future research.

2 BACKGROUND OF TLS

2.1 Definition of TLS

TLS are lymphocyte aggregates formed in non-lymphoid tissues, which are characterized by B/T cell compartments, differentiated high-endothelial veins (HEVs), and follicular dendritic cell (FDC) networks supporting the germinal center (GC) reaction (15). In TLS, there are T-cell compartments formed by CD3+ T cells surrounding CD20+ B cells. The dominant subsets in the compartments comprise CD4+ Tfh cells (3). Generally, their composition and structure are similar to those of SLO (16) (**Figure 1**).

Tumor-infiltrating lymphocytes (TILs) are produced during the host's immune response to cancer; however, distinguishing between TILs and TLS remains difficult. Therefore, TILs and TLS are collectively referred to as TLS in this paper. Moreover, there is no approved standard TLS classification. There are several classifications of TLS by different scholars using different criteria (17–19).

2.2 TLS and SLO

In the following paragraphs, we compare TLS and SLO. SLO [including the spleen, lymph nodes (LNs), etc.] can proliferate under antigen stimulation and have an immune function—this is an important component of the immune response. They both have similar cell content, matrix composition, lymphoid chemokines, vasculature, and tissue (20). They both have similar functions including the expression of genes encoding lymphocyte chemokines and lymphotoxins (LTs). They usually contain a functional GC, which can mediate *in situ* B-cell differentiation, somatic hypermutation, oligoclonal amplification, and final antibody production (21). Even in mouse models lacking SLO, TLS have been reported to replace the function of SLO completely (22).

Although TLS and SLO have many similarities, they are not the same structures. Morphologically, TLS do not have afferent lymphatic vessels or an envelope like SLO, which means that they can be directly exposed and stimulated by the inflammatory environment. The influence of antigens and cytokines, which may cause FDCs, lymphocytes, and macromolecules to enter TLS without restriction, favor abnormal lymphocyte activation (23). This may be one of the causes of some autoimmune diseases, such as rheumatoid arthritis and lupus nephritis. In addition, TLS and SLO have different formation mechanisms. SLO are formed during embryonic development due to the interaction between lymphoid-tissue-induced cells (LTIs) and stromal cells, while physiological TLS are produced after birth due to the presence of microbiota or the immune response, which has nothing to do with pathology (24).

2.3 TLS Formation

TLS formation starts from lymphoid neogenesis (25). In the early stage of formation, innate immune cells (neutrophils, eosinophils, and monocytes) infiltrate the chronic inflammation site rapidly, and monocytes begin to differentiate into resident macrophages. Bone marrow dendritic cells gradually accumulate in leukocyte aggregates, while macrophages are excluded from the developing TLS (3, 23). Simultaneously, B cells upregulate interleukin (IL)-18, chemokine C-X-C motif ligand (CXCL)-13, heat-labile enterotoxin B (LTB), a proliferation-inducing ligand (APRIL), and other lymphoid genes to stimulate T-cell entry (25). From a morphological point of view, TLS formation and maturation can be summarized into three stages. The first stage involves T cells, B cells, and stromal cells, such as FDCs, alpha smooth muscle actin (αSMA), and fibroblasts. The second stage comprises development of polarized clusters of T cells and B cells accompanied by FDCs. The third stage comprises development of mature TLS containing GCs, proliferation of B cells, plasma cells, HEVs, and lymphatic vessels (LVs) (26). Of those, the presence of HEVs is related to the recruitment and activation of naive CD4 T cells (27, 28). LVs help to regulate the immune response around TLS (29).

Several factors regulating SLO formation at the embryonic stage overlap with those regulating TLS formation (30). Stimulation of immune cell infiltration by specific inflammatory factors in inflammatory tissues is also a condition for TLS formation (21). At the initial stage, ectopic expression of TLS-promoting factors secreted by dendritic cells plays a vital role in TLS formation (31, 32). These TLS-promoting factors can jointly recruit and activate LTIs (16). LTIs further produce IL-17, lymphotoxin α-1β-2 (LTα1β2) and bind to lymphotoxin β receptor (LTβR) expressed on lymphoid

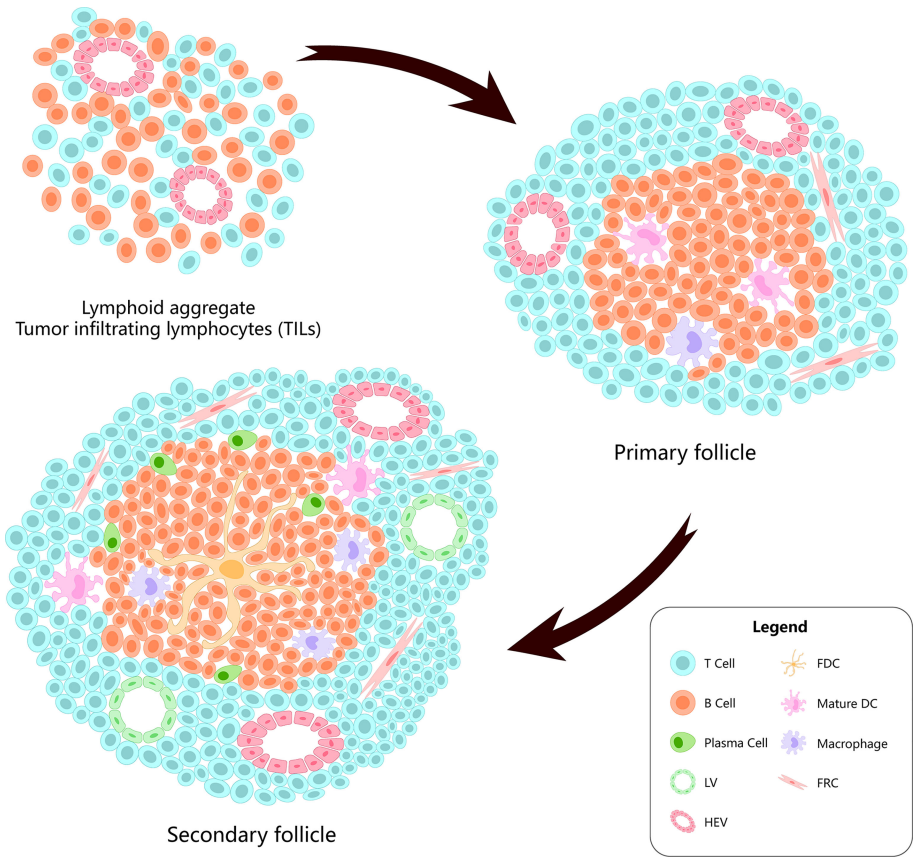

FIGURE 1 | The evolution of the tertiary lymphatic structures.

tissues to form organizers. They further continue to induce the secretion of chemokines, expression of angiogenic growth factor, and expression of adhesion factors IL-17R + stromal cells (33). Cell inflammatory factors and lymphoid chemokines (such as CXCL-13, CCL-21, CCL-19, and CXCL-12) secreted by LTIs can coordinate early recruitment of T cells and B cells and form simple aggregates (34). The secretion of vascular growth factors [such as vascular endothelial growth factor A (VEGFA) and C (VEGFC)] plays a vital role in HEV formation (16). Vascular adhesion factors [such as vascular cell adhesion molecule 1 (VCAM1) and mucosal addressin cell adhesion molecule 1 (MADCAM1)] help cells to remain in TLS for a long time (16). With continuous inflammatory stimulation, the TLSs mature. At this time, T- and B-cell compartmentalization occurs; CD21 + FDC networks appear at the TLS center and gradually form a functional GC (35). Of note, although LTIs are extremely important for SLO development in most areas of the human body, the latest evidence shows that TLS can still be formed in the absence of LTIs (36).

Generally, TLS formation is coordinated mainly by lymphoid chemokines, cytokines, and adhesion molecules (37). It is worth mentioning that TLS do not exist forever. Their existence is closely related to active tissue damage. When there is no continuous inflammatory stimulation, they dissipate after antigen clearance or tissue repair (38). Among TLS-promoting factors, IL-6 can promote TLS development in Th17 cells containing podophyllol. Meanwhile, IL-27 can limit the size and function of TLS by controlling the multiplication of Th17 cells (35, 39). Th17 cells and Th17 cytokines, such as IL-17 and IL-22, also contribute to the occurrence and development of TLS (40–43). Blocking IL-17 or podophyllin (PDPN) can inhibit the production of TLS, which may be caused by the negative regulation of PDPN neutralization in Th17 cell proliferation and differentiation (44). There is also evidence that TLS can also be formed without Th17 cytokines (45). In addition, TLS formation is also affected by B-cell activating factor (BAFF). Stimulation of myofibroblasts with Toll-like receptor agonists and cytokines can lead to the upregulation of BAFF and CXCL-13, thus promoting TLS formation (46). In addition to the above factors, tissue-specific, migrating mesenchymal stem cells, NCR3/NKp30, CD3 lymphocytes, and CD20 lymphocytes have different effects on TLS formation (47, 48).

2.4 Functions of TLS

TLS are mainly developed in non-lymphoid tissues to deal with various chronic inflammatory diseases including infection, autoimmune diseases, and cancer (49). However, they are not found in all patients, even those with the same disease (50, 51).

TLS in human solid tumors are essential for the creation of a favorable immune microenvironment to control tumor development. They are involved in the following immune processes, namely, T-cell initiation, B-cell activation, and differentiation into plasma cells, and serve as a factory for antibody secretion (52). In most cases, TLS in solid tumors are closely related to improved tumor prognosis. It can therefore be speculated that they are one of the sites of action for activated lymphocytes that partake in immune responses (53). However, although TLSs are protective in patients with infection or cancer, they are harmful in patients with autoimmune diseases and transplant rejection (54). In some autoimmune diseases, TLS are abnormal structures that produce an immune response against autoantigens. They can promote autoimmune response, stimulate local production of autoreactive T and B cells, maintain autoantibodies in the pathogenic process, and worsen the disease (55).

3 EFFECT OF TLS ON PHC PROGNOSIS

3.1 Influence of TLS Location on PHC Prognosis

Many studies have proven that TLS can be used as a cancer prognosis indicator. They are close to or in cancer lesions as immune structures; therefore, they may also play a relatively direct role in anti-tumor immune response (56). From the perspective of liver disease, chronic hepatitis caused by hepatitis B virus (HBV), hepatitis C virus (HCV), alcohol disorders, or other factors is one of the commonest causes of liver cancer, and chronic inflammation is one of the causes of TLS. Therefore, TLSs play a significant role in PHC prognosis (57, 58). In PHC, TLS are found in (intratumor TLS, iTLS) or out of the tumor (extra-tumor or peritumoral TLS, pTLS) and at the junction of the two (**Figure 2**). However, whether iTLS or pTLS is generated eventually is related to the tumor origin or disease stage. Some recent studies have also shown that HCC occurrence is significantly related to genes that promote TLS formation (59, 60). In this study, we summarized the role of TLS in PHC from existing studies (**Table 1**).

3.1.1 Role of iTLS in PHC

In HCC, iTLSs are related to a good prognosis and can reduce the risk of early recurrence of HCC. Moreover, the upregulation of iTLS-related genes can also reduce the risk of HCC recurrence in the early and middle stages, which indicates that iTLS may be related to the existence of sustained and effective anti-tumor immunity (49, 61–64). In addition, the risk of HCC recurrence is also related to TLS maturity (primary or secondary follicles and lymphoid aggregates) (61, 64). More mature TLS (lymphoid follicles) are correlated with prognosis than less mature TLS (lymphoid aggregates) (62). Moreover, TILs above 50% in the tumor parenchyma, also known as "lymphocyte-dominated cancer", have the best prognosis in HCC (65). As mentioned earlier, the dominant subpopulation in TLS is the CD4+ Tfh

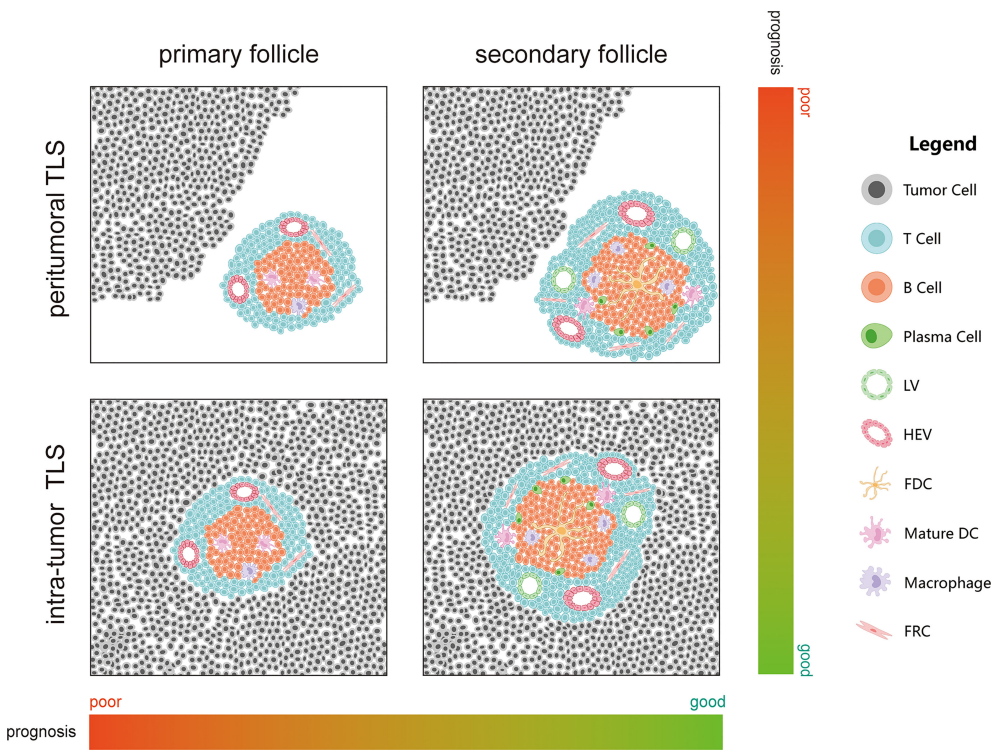

FIGURE 2 | Effect of maturation and location of tertiary lymphatic structures on cancer prognosis.

TABLE 1 | Recent research on TLS in PHC.

Time	First author	Research subjects	Conclusion
2021	Guang-Yu Ding	iCCA/TLS	iTLS contributes to a good prognosis, and pTLS is detrimental to a good prognosis.
2021	Hui Li	HCC/TLS	pTLS contributes to a good prognosis.
2020	Maxime Meylan	HCC/TLS	TLS in early HCC contributes to the development of liver cancer.
2019	Julien Calderaro	HCC/TLS	iTLS contributes to a good prognosis.
2020	Hui Li	HCC/TLS	iTLS contributes to a good prognosis.
2015	Shlomi Finkin	HCC/TLS	pTLS is detrimental to a good prognosis.
2020	Ziying Lin	HCC/TLS	iTLS contributes to a good prognosis.
2021	Fengwei Gao	HCC/TIL	TILs contribute to HCC treatment.
2021	Camila C Simoes	HCC/TIL	TILs contribute to HCC treatment.
2020	Yue Shi	HCC/TIL	TILs contribute to HCC treatment.
2019	Georgi Atanasov	HCC/TIL	TILs contribute to HCC treatment.
2015	Anthony W H Chan	HCC/TIL	TILs contribute to HCC treatment.
2020	Man Liu	HCC/TIL	TILs contribute to HCC treatment.
2019	Hyo Jeong Kang	HCC/TIL	TILs contribute to HCC treatment.
2019	Xuezhong Xu	HCC/TIL	HCC with low TIL has a worse prognosis.
2017	Wei Yao	HCC/TIL	TILs contribute to HCC treatment.
2018	Shigeki Nakagawa	HCC/TIL	HCC with low TIL has a worse prognosis.
2017	Marta Garnelo	HCC/TIL	TILs contribute to HCC treatment.
2015	Shan-Shan Jiang	HCC/TIL	TILs contribute to HCC treatment.
1998	Y Wada	HCC//TIL	TILs contribute to HCC treatment.
1995	K Shirabe	HCC/TIL	TILs contribute to HCC treatment.

cells. In patients with HCC, a decrease in circulating and/or tumor-related Tfh cells is associated with decreased disease progression and disease-free survival (DFS) (66). It has been shown that Tfh cells can drive resident CXCR5 effector T cells to produce Th1-directed responses in active TLS (67). Th1 is the most detected Th cell subset in non-cancerous tissues, and Th2, which is widely detected in patients with a poor prognosis, is considered to have a cancer-promoting effect (68–70). Th1 cells may be related to the initiation and/or maintenance of local and systemic adaptive immune responses while protecting patients from tumor invasion and metastasis (71). Some scholars believe that the response rate to immunotherapy will improve if harmful Th2 cells are modified to protective Th1 cells (72).

Studies on TILs and non-tumor hepatic lymphocyte infiltration (LILs) of HCC have shown similar results. Patients with more TILs have a better prognosis than those with fewer TILs. Contrarily, patients with more LILs in adjacent tissues have a worse prognosis than those with fewer LILs (73–75).

3.1.2 Role of pTLS in PHC

Unlike iTLS, pTLS can promote HCC occurrence (76, 77). In HCC, the TLS density of non-neoplastic liver tissue around HCC seems to be related to poor prognosis, especially late recurrence and death after HCC resection (62, 77). pTLS are also related to *de novo* HCC in patients with chronic inflammation and fibrosis or cirrhosis, and with the increase in TLS, the prevalence of HCC in such patients will also increase (62, 77). Finally, it was also found in mouse models that depletion of TLS in non-neoplastic liver parenchyma is helpful to inhibit HCC progression (77).

TLS can also be detected in early liver lesions (EHLs) such as high-grade atypical hyperplastic nodules, early liver cancer, and advanced small liver cancer (58). As the tumor progresses, these early lesions gradually transform into tumor tissue and can be regarded as paracancerous tissue. EHLs show TLS formation, immune activation, and overexpression of carcinogenic factors; however, this immune response cannot prevent cancer progression. Furthermore, the expression of such immune checkpoints and immunosuppressive molecules may lead to immune escape (58). The overall density and PD-L1 expression of immune cells in EHL are higher than those in their corresponding surrounding tissues—the average density of CD4+ T cells and CD8+ B cells increase three times (58). A high PD-L1 expression leads to immune escape of tumors and, hence, cancer progression (78, 79). The number of TLS increases with the age of the patient, and the accumulation of cancer progenitor cells in TLS is detected. These progenitor cells, which are presumably tumor-inducing cells, can imply a strong tumor-promoting effect of TLS (80). In addition, studies have shown that lymphoid neogenesis depends on LTβR signaling, and TLS can provide paracrine LTb signals to early progenitor cells to promote their growth (71). The progenitor cells expressing E-cadherin in TLS can promote HCC occurrence. After these cells are inhibited, the TLSs are suppressed, and the incidence of HCC is also reduced, which also proves that progenitor cells depend on the adaptive immune system (71). No morphologically mature TLS has been found in EHLs; most TLS in EHL lack CD21 FDCs, and their anti-tumor ability is not perfect. The occurrence of precancerous lesions can be limited by the anti-tumor ability of TLS in EHLs (58).

Coincidentally, in iCCA, the survival time of patients with TLS in the tumor's surrounding is poor, while the TLS in the intratumor area is positively correlated with a good prognosis (49). Regulatory T cells (Tregs) in TLS can inhibit endogenous anti-tumor immune response; therefore, an increase in the number of Tregs is closely related to the low survival rate of patients. This can lead to worsening of the disease and an increase in tumor infiltration by CD4+ and CD8+ T cells and macrophages (71). TLS-related Tregs can also help tumor immune escape by inhibiting the endogenous immune response against the tumor simultaneously (57, 81, 82). In

addition, compared with pTLS, although Tregs in iTLS are significantly increased, Tregs are only related to poor prognosis caused by pTLS (49). Finally, while patients with immune activity have the lowest prognostic risk, patients with immune resistance have the highest prognostic risk (49).

The findings in a study by Finkin et al. suggest that the poor prognosis is caused by pTLS (77). They used transgenic mice to explore HCC development. First, mild inflammatory response and TLS formation were observed in mice, and then, HCC appeared in these mice. The researchers first identified HCC progenitor cells with double-positive GFP and E-cadherin in TLS. Next, these progenitor cells migrated out of the cell and developed HCC outside the cell. Therefore, pTLS may play a similar role with tumor factories in HCC, leading to a poor prognosis of patients with HCC, which is not surprising.

However, the role of pTLS remains controversial. In a study by Li et al., pTLS density was related to good prognosis, that is, there was a positive correlation between high pTLS density and better overall survival (OS) and recurrence-free survival (RFS), and the survival rate of patients with a GC was higher than that of patients without a GC (81). They also observed that pTLS was significantly related to an increase in CD3+ T cells, CD8+ T cells, and CD20+ B cells in tumors, and also to a decrease in infiltration of Foxp3+, Tregs, and CD68+ macrophages (81). This is inconsistent with the increase in Tregs caused by pTLS described earlier, and a clear association has been found between Tregs and the pathogenesis of HCC and even other cancers (57, 81, 82). Tregs play a strong immunosuppressive role and promote immune escape (83, 84). The decrease in Tregs in the results suggest pTLS weakening on suppression of the tumor microenvironment (TME), which may be one of the reasons for the discrepancy between the findings by Li et al. and those of others. Regarding the specific reason for the decrease in Tregs in the study by Li et al., further research is needed. This may explain the controversial findings. In addition, previous studies have proven that CD20+ B cells can promote Tregs proliferation. Conversely, Li et al. reported that high CD20+ infiltration is accompanied by a decrease in Tregs infiltration (85–87). In fact, the role of CD20+ cells remains controversial (88). So far, it is speculated that CD20+ B cells may have a dual effect on HCC; this can be a useful point of focus for HCC treatment research.

3.2 Effect of TLS Cellular Components on PHC Prognosis

The function of TLS depends on their structure—rich in immune cells and in direct contact with cancerous tissue. Therefore, it is speculated that the cellular components of TLS have a relatively direct impact on the prognosis of PHC, and our findings seem to confirm this. In TLS, patients with high CD3, CD8, and NK cell infiltration have a better prognosis (83). High levels of CD3 and CD8 infiltration in TILs have a better prognostic value for OS. Higher levels of CD3, CD4, and CD8 imply better DFS and recurrence-free survival (RFS), while high levels of FoxP3 represent worse OS and DFS/RFS. High CD4 percentage and high CD4/CD8 ratio also affect the OS of patients. In addition, FoxP3/CD4 and FoxP3/CD8 ratios are negatively correlated with OS and DFS/RFS (89–92). Further studies have shown that there is a correlation between the density of B cells in TILs and the density of T cells, and the survival rate of patients with HCC having higher densities is higher. The co-expression of CD27 and CD40 on T cells and B cells is related to the survival rate of patients, and the density of B cells is related to the activation of T cells and NK cells and anti-tumor effects. In addition, the relationship between CD20+ mature B cells and tumor suppression is still controversial (88). However, most of the evidence so far supports that CD20+ B cells weaken tumor suppression (85–87). Studies have shown that CD39 may be involved in regulating the inhibitory ability of tumor-invasive CD8 + Tregs (93). However, high-affinity new antigens (HANs) are positively correlated with higher frequencies of CD39 and CD8 TILs, and patients with a higher HAN value have a higher anti-tumor activity (94). The activation of CD40 cells can significantly enhance the response to anti-PD-1 treatment (95). Regarding macrophages, the density of CD38 and CD68 macrophages is related to the improvement of postoperative prognosis, while the total density of CD68 macrophages is related to poor prognosis (96). High expression of reverse transcription cysteine-rich protein (RECK) was associated with more TILs and a significantly better prognosis than in patients with low RECK expression (97). The expression of T-cell activation (VISTA) protein in HCC showed cell specificity, and its expression is significantly correlated with CD8+ TILs. Patients with both VISTA+/CD8+ cells have a more favorable TME and better OS (98). FOXP3 expression in natural T cells is helpful in obtaining effective immunosuppressive ability, and FOXP3 Tregs/CD4 T cell ratio is an independent prognostic factor for OS (99, 100). Tregs promote immune escape in tumors, which inhibits the activity of T cells, bone marrow cells, and stromal cells, leading to T-cell dysfunction (83, 84). WNT/β-catenin inhibitor ICG-001 plus radiotherapy (RT) can promote CD8+ T-cell infiltration and IFN-γ production in TILs and simultaneously reduce the number of Tregs, thus contributing to HCC treatment (101, 102). Joint blockade of TIGIT and PD1 can improve the function of CD8+ TILs that do not respond to single PD1 blockade, thus inhibiting HCC development (103). A simultaneous high expression of PD-L1 and CD8+ TILs is an important prognostic factor related to immune checkpoint pathway in HCC (104). Therefore, these cellular components can be used as predictors of therapeutic effect and deserve further study.

4 THE VALUE OF TLS FOR PHC TREATMENT

4.1 The Potential Value of TLS as a Marker for Immunotherapy

Immunotherapy continues to evolve and has become one of the treatments for patients with PHC, but not all patients respond to these treatments. Therefore, the identification of appropriate biomarkers is an urgent need for the treatment of PHC. Recent

reports suggest that TLS may be an effective biomarker for immunotherapy.

In renal clear cell carcinoma and melanoma, the presence and density of TLS correlate with the responsiveness of immune checkpoint (ICP) therapy (53, 105). In breast cancer, the expression level of immune checkpoint molecules is related to the level of TILs and TLS formation (106). In addition, a strong correlation between TLS and good ICP treatment outcomes has also been observed in soft tissue sarcomas and bladder cancer (107, 108). Interestingly, immature TLS follicles are observed in most unresponsive patients; therefore, there may be a strong relationship between TLS maturity and treatment. Furthermore, in the study of sarcomas, TLS had a better prognosis in samples with high immune infiltration levels (107). Therefore, it is reasonable to assume that the stage of TLS [no follicles, primary follicles, and mature (secondary) follicles] has a direct impact on the reactivity of ICP. Regarding targeted drugs, there is also evidence to prove the biomarker value of TLS. Treatment of HER2/neu tumors with trastuzumab is associated with better DFS in TLS-enriched tumors (109). In a recent study, the appearance of TLS in immune-checkpoint-resistant PTEN-null prostate cancer is also associated with better treatment outcomes against PI3K inhibitors (110). In gastrointestinal stromal tumors (GIST), high-density TLS is associated with lower imatinib resistance, recurrence, and more favorable survival (111). Patients with drug-resistant GIST have more Tregs, which are one of the inhibitors of the immune system.

In a study on PHC immunotherapy, Vella et al. found that patients with HCC having TLS responded better to ICP therapy with carbosantinib and nivolumab (53). In another HCC study, the authors found that aspartate β-hydroxylase is an ideal tumor-associated antigen and can be used as a target for HCC immunotherapy, but its function is partly dependent on the presence of TLS (112). In addition, patients with a higher expression of TLS characteristic genes such as CCL-5, CXCL-9, CXCL-10, and CXCL-13 will also have a better response to immune checkpoint inhibitors (ICIs) (113, 114). This suggests that TLS can transform the immune microenvironment of patients to some extent, or at least there is a close relationship between the two. The former can affect the cell composition of the latter and provide a suitable environment for the T-cell-mediated ICP response and ultimately affect the effect of immunotherapy.

4.2 The Value of Modulation of TLS Formation for PHC Therapy

Tumor-associated TLSs are usually associated with a good prognosis for most cancer types; tumor-associated TLS and chronic intratumoral inflammation are associated with tumor immune tolerance, suggesting that TLS may increase cancer invasiveness (115). A successful anti-tumor immune response cannot be achieved without the synergistic effect of the body's immune cell components. TLS formation may be related to the relationship between immunosuppression and recovery of immune cell function. The recovery of cell function activates anti-cancer immune-related pathways and then induces TLS formation. After TLS formation, it can further strengthen the anti-tumor effect and improve patient survival. Many attempts to modify TLS formation as a treatment for cancer have been made; these include chemokines and immunotherapy. These approaches are further reviewed in this section.

4.2.1 TLS Regulation by Chemokines/Cytokines

Modern information technology, bioinformatics, has become a powerful tool for identifying biological phenotypes. Some recent studies have used these tools to screen TLS-related chemokine genes, which provide favorable conditions for analyzing the role of chemokines in TLS formation. The unique 12 TLS chemokines (CCL-2, CCL-3, CCL-4, CCL-5, CCL-8, CCL-18, CCL-19, CCL-21, CXCL-9, CXCL-10, CXCL-11, and CXCL-13) can affect TLS status directly and further affect patient prognosis. For example, patients with a low chemokine expression in colorectal cancer have a poor prognosis (116).

B-Lymphocyte chemokines can lead to the formation of LN-like structures, such as HEVs, interstitial cells, B cells, and T cell compartments (117). These LN structures can directly induce TLS formation, thus assisting the treatment of cancer. Different chemokines have different abilities to induce immune infiltration. For example, the CCL21 induction ability is stronger than that of CCL19 (118). CCL21, as a T-lymphocyte inducer, has been reported to recruit T cells into TLS through CCR7 to promote the formation of TLS. Some studies have found that the combined application of IL7 and CCL21 can improve the anti-tumor efficacy of various solid tumors (119). In addition, CCL21 combined with anti-CD25 monoclonal antibody can improve anti-tumor efficacy in HCC. Therefore, CCL21 may be one of the feasible targets for TLS induction and anti-PHC.

Hox antisense intergenic RNA (HOTAIR) is related to poor HCC prognosis. It can promote CCL-2 secretion and may participate in the recruitment of macrophages and bone-marrow-derived suppressor cells to the TME (120). The famous Chinese medicine Gehua Jiecheng Decoction can inhibit the expression of CCL-2 in the liver while effectively inhibiting the development of tumor cells and reducing the tumor area. In addition, the expression of inflammatory factors and angiogenesis factors in the tumor is also reduced to varying degrees to antagonize the immunosuppressive effect of the liver cancer microenvironment (121). There is also evidence that blocking CCL-2 can promote TME recovery from inhibition (122). The serum CCL-3, CCL-4, and CCL-5 levels of patients with HCC are increased and closely related to activated circulating monocytes (123, 124). The serum CCL-3 levels of patients with HCC and a good response to regorafenib chemotherapy are reduced (125). Studies have shown that CCL-5 can activate and recruit M2 macrophages in HCC, increase the proportion of M2/M1 macrophages, and promote HCC progression (126, 127). However, in a study on Biejiajian Pill and yttrium-90 (Y90) radioactive embolism (RE), CCL-5 expression was found to significantly suppress tumor cells (128, 129).

LTβR is a cell surface receptor, which is involved in apoptosis and cytokine release. Studies have shown its key role in LN

formation. LTβ deficiency leads to serious defects in the development of lymphatic organs in mice (130). Regarding the similarity between TLS and SLO, TLS can be induced or inhibited by LTβR. DCs, as a source of LT, are closely related to chemokines that contribute to TLS formation. DCs can also promote LT signaling through LTβR to achieve HEV differentiation and LN function (131). DCs promote the infiltration of immature T cells and NK cells into the TME and prolong the OS of mice when injected into their abdominal cavity (132). This proves that to induce TLS formation, the expression of chemokines can be increased through DC. LIGHT/TNFS14 is an LTβR ligand, which is expressed on immature DCs and activated T lymphocytes. By inserting the gene encoding LIGHT into attenuated *Salmonella typhimurium*, its oncolytic activity is strengthened, thus inhibiting the growth of the primary tumor and lung metastasis dissemination (133). Perhaps, attenuated or non-toxic bacteria have similar therapeutic effects with DC injections, and the advances in genetic engineering can also cause a change in required therapeutic proteins to form an artificial antibody factory in the body. In HCC, LTβR signaling is involved in the occurrence of HBV-related hepatitis and HCC (134, 135). Meanwhile, the LTβR pathway inhibits TLS formation (136). This may be achieved by regulating the production of pTLS in the liver. In addition, some studies have shown that overexpression of BCL-2 in HCC cell lines can enhance LIGHT-mediated apoptosis in Hep3BT2 cells and thus inhibit tumor cells (137). Studying the effect of LTβR in PHC tumors may bring new discoveries to the role of LTβR in PHC.

Interestingly, promoting or inhibiting TLS formation in HCC plays a favorable role in prognosis; the reason for this difference is unclear. However, we speculate that it may be related to the distribution of its own TLS inside and outside the tumor—whether the increase in TLS markers that do not exist in cancer lesions, such as chemokine CCLs in serum, can be regarded as an increase in TLS in adjacent tissues, which corresponds to the role of pTLS mentioned above. On the other hand, there is no doubt that the *in vivo* immune response requires the coordinated development of multiple factors including various complex signaling pathways, or cell-to-cell crosstalk, and these experiments on immunosuppressed mice did not obviously consider this situation. Using humanized immune mice to transplant patient-derived tumor tissue for related research may be one solution. Finally, as described above, abnormalities in the composition and function of cells in TLS can affect the disease course, which is not reported in recent studies. However, there is a recent study that verified these conjectures. The author found that upregulation of CXCL13 can promote immune escape in HCC, but under the combination of vaccine and PD-1 inhibitor, CXCL13 produced by cancer cells can recruit T lymphocytes into TLS and have a positive anti-tumor effect (112). Obviously, CXCL13 has contrary roles before and after processing. This may be explained by the aforementioned reasons. In conclusion, these results suggest that chemokines involved in TLS formation can be used in combination with various therapeutic methods. Further research on their use in induction of TLS formation or inhibitory targets to improve HCC prognosis is required.

4.2.2 TLS Regulation by Immunotherapy

There are several advances in immunotherapy in recent years. Some of them can promote TLS formation while producing therapeutic effects, which may confer dual anti-tumor effects on immunotherapy. ICIs can induce TLS formation and play an important role in the formation of TME with anti-tumor properties. In a study on the treatment of non-small cell lung cancer (NSCLC) with an ICI (nivolumab), TLS formation was observed in the samples of cases that responded to ICIs, unlike in the samples of unresponsive cases (138). Furthermore, TIL infiltration was more in biopsy samples from patients with advanced melanoma receiving anti-PD-L1 therapy (139). In addition, in another study using the allogeneic PDAC vaccine (GVAX) combined with low-dose cyclophosphamide to reduce Tregs as a treatment, upregulation of TLS infiltration after GVAX was observed (53).

As mentioned earlier, iTLS can inhibit the progression of PHC. The transcription factor CEBPA is the main regulator of liver homeostasis and bone marrow cell differentiation. Some studies have found that upregulation of CEBPA gene expression can induce the formation of iTLS in the TME and tumor suppression (140). Neoadjuvant drugs, cabozotinib and nivolumab, can also promote iTLS formation and inhibit HCC occurrence (53). In addition, ICIs are promising drugs for the treatment of advanced HCC. After HCC is treated with anti-PD-1 antibodies, TILs and patient survival (PFS and OS) increase (141). GVAX has been proven to induce iTLS formation (53). Selective internal radiotherapy can also significantly promote the recruitment/activation of effector immune cells in tumors and TIL formation (142). This shows that ICIs can convert non-immunogenic tumors into immunogenic tumors through TLS; it also suggests that the combination of ICIs and vaccine-based immunotherapy can be a potential treatment strategy.

In addition, inhibitory TME has an important influence on tumor immunity. Some scholars have found that in non-HBV/non-HCV HCC, although TILs secrete IFN-γ, they cannot kill cancer cells (143). Therefore, the conversion of inhibitory TME into immunoactive TME is a key focus for HCC treatment. Some studies have found that IL-2 can restore the anti-tumor activity of TILs (144). Activation of IL-12-mediated pathways often represent a better prognosis (145). It should be studied as a dynamic marker of the functional state of CD8 TILs. Another study also showed that the expression of TIM-3 and/or PD-1 on TILs will impair their function. They also reported that blocking TIM-3 or/and PD-1 can reverse the dysfunction of TILs in HBV-related HCC (146).

After years of research, tumor vaccine is now one of the feasible tools for induction of TLS formation. In addition to the GVAX mentioned earlier, in another study involving patients with pancreatic cancer receiving granulocyte-macrophage colony-stimulating factor (GM-CSF) vaccine, TLS was shown to regulate adaptive immunity (53). The production of TLS, which is highly related to CD8+ T cells and Th1 infiltration, can

also be observed in patients with cervical cancer treated with HPV vaccine (147). These changes are characterized by increased expression of genes related to immune activation and effector function. The study of another vaccine, Nano-sapper, reported its ability to suppress the inhibitory effect of TME in pancreatic ductal adenocarcinoma mouse tumors and induce intratumoral TLS production to improve prognosis (148). Therefore, removing inhibitory TME is key in inducing TLS and improving prognosis.

4.2.3 TLS Regulation by HEV Induction

HEV is a specialized posterior capillary vein with structural and functional differences from normal blood vessels. It is found in SLO and TLS. It affects TLS formation by mediating lymphocyte migration (53). HEV in human tumors is related mainly to increased survival rate. Tumor HEV (TU-HEV) in mice has been shown to cultivate lymphocyte-rich immune centers and enhance immune response when combined with different immunotherapy drugs, which is often considered as a key factor in TLS formation. In a retrospective study of primary breast cancer, TU-HEV density was positively correlated with DFS, metastasis-free survival, and OS (149). Therefore, it can be proven that it is of great significance for anti-tumor immune activity. Moreover, some scholars observed MECA-79-positive blood vessels in melanoma, breast cancer, ovarian cancer, colon cancer, and lung cancer samples (53). These findings were subsequently verified by other scientists and successively confirmed in kidney, stomach, pancreas, and head and neck cancers (53). In many diseases, the intensity of MECA-79 is correlated with the degree of monocyte infiltration in the lesion, and the density of MECA-79 + HEV cells is also positively correlated with clinical parameters. In primary melanoma, MECA-79 + HEV cells are associated with reduced tumor invasiveness (53). The combination of high-density MECA-79 + HEV cells and CD8+ T cells is also a prognostic factor for OS in gastric cancer (150). In addition, MECA-79 is more expressed in the normal bile duct epithelium in iCCA, which implies that MECA-79 expression is inhibited in tumor tissues and may further affect the production of HEVs and iTLS (151). Therefore, MECA-79 may be an implicit powerful target for PHC therapy.

4.3 Other Factors Related to TLS That May Affect Treatment

There are fewer studies on the generation and function of tumor TLS than on TLS therapeutic value. The tumor mutation burden (TMB) represents the number of DNA mutations per million bases (Mut/Mb) sequenced in a particular cancer. As the number of mutations and new expressions increases, these new antigens may be immunogenic and trigger T-cell responses. Initially, TMB was identified as a biomarker for ICIs, while few recent studies point it to TLS. In a study using computers to predict new antigens for pancreatic ductal adenocarcinoma, it was pointed out that the TMB of early TLS tumors is low. However, mature TLS with GCs have significantly more restrictive new antigens expressed in samples with a better prognosis (53). Some scholars have used public databases and found that tumors with a high TMB have a higher TLS density in NSCLC and melanoma based on 12 chemokine characteristics (152). Both diseases have good responsiveness to ICIs. These studies show the importance of other molecular features apart from pure TLS maturity stage and density for cancer treatment. In fact, we speculate that highly unstable tumor tissues with a high mutation probability are more likely to trigger the expression of new antigens.

Mutations in specific genes also play an important role in the occurrence and development of TLS. BRCA-mutated tumors have a strong infiltration of CD8+ T cells, and their mutations are positively correlated with high TLS scores in many tumors (including breast cancer, prostate cancer, or endometrial cancer) (53). On the other hand, some other mutations such as CTNNB1 and IDH1 are negatively correlated with high TLS scores. These mutations may directly or indirectly participate in TME formation and eventually affect TLS formation.

Various immune components in TME are mixed, and there may be some crosstalk between various effector cells (CD8+ T cells or NK cells) involved in eliminating tumors or between them and tumor cells, thus affecting their effect of fighting cancer. There is evidence supporting this. One study of HCC showed that tumor cells are able to release YWHAZ (aka 14-3-3ζ) in the TME *via* crosstalk to inhibit the anti-tumor function of tumor-infiltrating T cells (153). Blocking YWHAZ may promote HCC treatment.

Second, some researchers found that there is a difference in the transcriptional characteristics of T cells extracted from tumors with and without TLS and from the tumor TLS itself (53). Third, B cells can function as antigen-presenting cells to promote T-cellular immunity (154). In addition, the study also found that T cells in tumors seem to be a prerequisite for B-cell infiltration (53), which supports the fact that T cells are involved in the recruitment of B cells and TLS formation.

The administration of preoperative radiotherapy and chemotherapy (neoadjuvant chemotherapy, NAC) is related to the increase in TLS formation. In hepatoblastoma with a better prognosis than adenomatous *Escherichia coli* mutation, a significant increase in TLS formation can be seen in tissues before and after cisplatin chemotherapy (155). Patients with pancreatic ductal adenocarcinoma have a better prognosis after NAC, while TLS increase (156). However, during NAC, the formation of TLS is generally impaired, which is manifested by cell reduction and area reduction, but 2 weeks after treatment, their function and size normalize gradually (157). This phenomenon may be related to tumor cell death caused by radiotherapy and chemotherapy. After tumor cells die, they release the new antigens they carry, and the DC captures these antigens and triggers a stronger anti-tumor immunity.

The introduction of materials science has made biomaterials an alternative for disease treatment. Biomaterials are expected to modulate TLS formation through controlled chemokine release. Hydrogel can deliver antigen chemokines and cytokines to DCs to induce cell response (158). Research on artificial LNs has been ongoing for many years (159). Regarding future tumor therapy, the development of biomaterials will be a powerful assistant.

STING (STimulator of INterferon Genes) is a cytoplasmic DNA-sensing protein, which has strong pro-inflammatory ability in tumor-associated stromal cells and can upregulate the expression of various cytokines, which can also be a way to induce TLS formation. In melanoma, STING activation in the tumor can promote the normalization of tumor vessels, enhance lymphocyte infiltration, and promote the formation of local TLS (160). In mouse models of breast cancer, lung cancer, and melanoma, low-dose STING agonists can coordinate the promotion of tumor vascular normalization and CD8+ T cells to control tumor growth (53). The combination of STING agonists with other treatments may be a candidate for improving TLS-related anti-tumor immune response.

5 DISCUSSION

Research on TLS in PHC is still at the initial stage; there are few related studies. Regarding PHC, while the positive effect of iTLS is sure, pTLS might have a negative effect. There are several reports on the positive role of iTLS in various cancers; therefore, we can speculate that they are important in PHC. However, there are no large-scale multicenter studies on siTLS, creating the need for further research. However, there are several limitations that need to be overcome for research on TLS in PHC and even in all cancers.

First, the studies used different TLS evaluation criteria. Furthermore, the TLS determination methods were different, time consuming, subjective, and difficult to use in clinical practice. The lack of reproducible and standardized TLS identification methods is a major setback. However, the advances in artificial intelligence and computers have made it possible to standardize TLS identification, which is another powerful weapon against cancer in clinical practice. Moreover, the current TLS identification method can only be carried out using tissue biopsy. Identifying a certain feature from peripheral tissues (such as blood, digestive juice, and even excreta) will reduce patient damage and improve detection efficiency.

Second, TLS needs to be studied from a wider angle and not just as a prognostic marker. If possible, it should be used to monitor the treatment effect during a treatment intervention. Of course, less invasive inspection methods for this process would be important. Furthermore, whether the formation and composition of TLS of PHC caused by different pathogenic factors is different (such as cancer caused by HBV/HCV-related chronic hepatitis versus cancer caused by chemical factors) and whether iTLS and pTLS will transform or promote each other need further study; these will be very significant in understanding TLS evolution and disease causes.

It cannot be ignored that TLS research needs to be translated into PHC immunotherapy, which may solve the problem of the low response rate to ICIs in PHC, thus benefiting patients. As mentioned in the paper, research on both TLS and immunotherapy should be multi-faceted. It may be possible to screen sensitive patients for a certain type of immunotherapy drug or induce its generation and consumption to regulate the efficacy of immunotherapy. Combination therapy is also a potential effective treatment. However, more in-depth mechanism research and verification *via* large-scale *in vivo* and *in vitro* experiments are required.

Finally, the defects in immunodeficient mice used in TLS research are not suitable for investigating the controversial TLS effects in PHC. Further research should focus on how to reconstruct the complex TME of tumor tissue in the human body while considering the interaction of various factors in the body's immunity.

AUTHOR CONTRIBUTIONS

WJ and TZ have made similar contributions to the design and conception of review. QY has carefully reviewed the first draft of the article. JL, YN, WShi, and XL contributed to the discussion. WSong supervised all aspects of the literature review design and manuscript writing. All authors contributed to the article and approved the submitted version.

FUNDING

This study was supported by the National Natural Science Foundation of China (81672716).

ACKNOWLEDGMENTS

We would like to thank Editage (www.editage.cn) for English language editing.

REFERENCES

1. Barone F, Gardner DH, Nayar S, Steinthal N, Buckley CD, Luther SA. Stromal Fibroblasts in Tertiary Lymphoid Structures: A Novel Target in Chronic Inflammation. *Front Immunol* (2016) 7:477. doi: 10.3389/fimmu.2016.00477
2. Neyt K, Perros F, GeurtsvanKessel CH, Hammad H, Lambrecht BN. Tertiary Lymphoid Organs in Infection and Autoimmunity. *Trends Immunol* (2012) 33:297–305. doi: 10.1016/j.it.2012.04.006
3. van de Walle T, Vaccaro A, Ramachandran M, Pietilä I, Essand M, Dimberg A. Tertiary Lymphoid Structures in the Central Nervous System: Implications for Glioblastoma. *Front Immunol* (2021) 12:724739. doi: 10.3389/fimmu.2021.724739
4. Lynch KT, Young SJ, Meneveau MO, Wages NA, Engelhard VH, Slingluff CL, et al. Heterogeneity in Tertiary Lymphoid Structure B-Cells Correlates With Patient Survival in Metastatic Melanoma. *J Immunother Cancer* (2021) 9:e002273. doi: 10.1136/jitc-2020-002273
5. Zhou L, Xu B, Liu Y, Wang Z. Tertiary Lymphoid Structure Signatures are Associated With Survival and Immunotherapy Response in Muscle-Invasive Bladder Cancer. *Oncoimmunology* (2021) 10:1915574. doi: 10.1080/2162402X.2021.1915574
6. Posch F, Silina K, Leibl S, Mündlein A, Moch H, Siebenhüner A, et al. Maturation of Tertiary Lymphoid Structures and Recurrence of Stage II and III Colorectal Cancer. *Oncoimmunology* (2018) 7:e1378844. doi: 10.1080/2162402X.2017.1378844

7. Qin M, Hamanishi J, Ukita M, Yamanoi K, Takamatsu S, Abiko K, et al. Tertiary Lymphoid Structures are Associated With Favorable Survival Outcomes in Patients With Endometrial Cancer. *Cancer Immunol Immunother* (2021) 71:1431–42. doi: 10.1007/s00262-021-03093-1
8. Hiraoka N, Ino Y, Yamazaki-Itoh R, Kanai Y, Kosuge T, Shimada K. Intratumoral Tertiary Lymphoid Organ is a Favourable Prognosticator in Patients With Pancreatic Cancer. *Br J Cancer* (2015) 112:1782–90. doi: 10.1038/bjc.2015.145
9. Jamaly S, Rakaee M, Abdi R, Tsokos GC, Fenton KA. Interplay of Immune and Kidney Resident Cells in the Formation of Tertiary Lymphoid Structures in Lupus Nephritis. *Autoimmun Rev* (2021) 20:102980. doi: 10.1016/j.autrev.2021.102980
10. Bombardieri M, Lewis M, Pitzalis C. Ectopic Lymphoid Neogenesis in Rheumatic Autoimmune Diseases. *Nat Rev Rheumatol* (2017) 13:141–54. doi: 10.1038/nrrheum.2016.217
11. Sung H, Ferlay J, Siegel RL, Laversanne M, Soerjomataram I, Jemal A, et al. Global Cancer Statistics 2020: GLOBOCAN Estimates of Incidence and Mortality Worldwide for 36 Cancers in 185 Countries. *CA Cancer J Clin* (2021) 71:209–49. doi: 10.3322/caac.21660
12. Ferlay J, Laversanne M, Ervik M, Lam F, Colombet M, Mery L, et al. *Global Cancer Observatory: Cancer Tomorrow* (2020). Available at: https://gco.iarc.fr/tomorrow.
13. Cheng W, Li H-L, Xi S-Y, Zhang X-F, Zhu Y, Xing Le, et al. Growth Differentiation Factor 1-Induced Tumour Plasticity Provides a Therapeutic Window for Immunotherapy in Hepatocellular Carcinoma. *Nat Commun* (2021) 12:7142. doi: 10.1038/s41467-021-27525-9
14. Xing R, Gao J, Cui Q, Wang Q. Strategies to Improve the Antitumor Effect of Immunotherapy for Hepatocellular Carcinoma. *Front Immunol* (2021) 12:783236. doi: 10.3389/fimmu.2021.783236
15. Bombardieri M, Barone F, Lucchesi D, Nayar S, van den Berg WB, Proctor G, et al. Inducible Tertiary Lymphoid Structures, Autoimmunity, and Exocrine Dysfunction in a Novel Model of Salivary Gland Inflammation in C57BL/6 Mice. *J Immunol* (2012) 189:3767–76. doi: 10.4049/jimmunol.1201216
16. Jacquelot N, Teller J, Nut Sl, Belz Gt. Tertiary Lymphoid Structures and B Lymphocytes in Cancer Prognosis and Response to Immunotherapies. *Oncoimmunology* (2021) 10:1900508. doi: 10.1080/2162402X.2021.1900508
17. Kim JH, Seo M-K, Lee JA, Yoo S-Y, Oh HJ, Kang H, et al. Genomic and Transcriptomic Characterization of Heterogeneous Immune Subgroups of Microsatellite Instability-High Colorectal Cancers. *J Immunother Cancer* (2021) 9:e003414. doi: 10.1136/jitc-2021-003414
18. Qin M, Jin Y, Pan L-Y. Tertiary Lymphoid Structure and B-Cell-Related Pathways: A Potential Target in Tumor Immunotherapy. *Oncol Lett* (2021) 22:836. doi: 10.3892/ol.2021.13097
19. Benzerdjeb N, Dartigues P, Kepenekian V, Valmary-Degano S, Mery E, Avérous G, et al. Tertiary Lymphoid Structures in Epithelioid Malignant Peritoneal Mesothelioma Are Associated With Neoadjuvant Chemotherapy, But Not With Prognosis. *Virchows Arch* (2021) 479:765–72. doi: 10.1007/s00428-021-03099-1
20. Ruddle NH. High Endothelial Venules and Lymphatic Vessels in Tertiary Lymphoid Organs: Characteristics, Functions, and Regulation. *Front Immunol* (2016) 7:491. doi: 10.3389/fimmu.2016.00491
21. Nerviani A, Pitzalis C. Role of Chemokines in Ectopic Lymphoid Structures Formation in Autoimmunity and Cancer. *J Leukoc Biol* (2018) 104:333–41. doi: 10.1002/JLB.3MR0218-062R
22. Hutloff A. T Follicular Helper-Like Cells in Inflamed Non-Lymphoid Tissues. *Front Immunol* (2018) 9:1707. doi: 10.3389/fimmu.2018.01707
23. Aloisi F, Pujol-Borrell R. Lymphoid Neogenesis in Chronic Inflammatory Diseases. *Nat Rev Immunol* (2006) 6:205–17. doi: 10.1038/nri1786
24. Buckley CD, Barone F, Nayar S, Bénézech C, Caamaño J. Stromal Cells in Chronic Inflammation and Tertiary Lymphoid Organ Formation. *Annu Rev Immunol* (2015) 33:715–45. doi: 10.1146/annurev-immunol-032713-120252
25. Coleby R, Lucchesi D, Pontarini E, Pitzalis C, Bombardieri M. Stepwise Changes in the Murine Salivary Gland Immune Response During Virally-Induced Ectopic Lymphoid Structure Formation. *Clin Exp Rheumatol* (2021) 39(Suppl 133):39–48. doi: 10.55563/clinexprheumatol/gb7pfc
26. Dieudé M, Kaci I, Hébert M-J. The Impact of Programmed Cell Death on the Formation of Tertiary Lymphoid Structures. *Front Immunol* (2021) 12:696311. doi: 10.3389/fimmu.2021.696311
27. Hu D, Mohanta SK, Yin C, Peng L, Ma Z, Srikakulapu P, et al. Artery Tertiary Lymphoid Organs Control Aorta Immunity and Protect Against Atherosclerosis *via* Vascular Smooth Muscle Cell Lymphotoxin β Receptors. *Immunity* (2015) 42:1100–15. doi: 10.1016/j.immuni.2015.05.015
28. Schrama D, thor Straten P, Fischer WH, McLellan AD, Bröcker EB, Reisfeld RA, et al. Targeting of Lymphotoxin-Alpha to the Tumor Elicits an Efficient Immune Response Associated With Induction of Peripheral Lymphoid-Like Tissue. *Immunity* (2001) 14:111–21. doi: 10.1016/s1074-7613(01)00094-2
29. Li W, Gauthier JM, Tong AY, Terada Y, Higashikubo R, Frye CC, et al. Lymphatic Drainage From Bronchus-Associated Lymphoid Tissue in Tolerant Lung Allografts Promotes Peripheral Tolerance. *J Clin Invest* (2020)130:6718–27. doi: 10.1172/JCI136057
30. Germain C, Gnjatic S, Dieu-Nosjean M-C. Tertiary Lymphoid Structure-Associated B Cells are Key Players in Anti-Tumor Immunity. *Front Immunol* (2015) 6:67. doi: 10.3389/fimmu.2015.00067
31. Luo S, Zhu R, Yu T, Fan H, Hu Y, Mohanta SK, et al. Chronic Inflammation: A Common Promoter in Tertiary Lymphoid Organ Neogenesis. *Front Immunol* (2019) 10:2938. doi: 10.3389/fimmu.2019.02938
32. Corsiero E, Bombardieri M, Manzo A, Bugatti S, Uguccioni M, Pitzalis C. Role of Lymphoid Chemokines in the Development of Functional Ectopic Lymphoid Structures in Rheumatic Autoimmune Diseases. *Immunol Lett* (2012) 145:62–7. doi: 10.1016/j.imlet.2012.04.013
33. Aoyama S, Nakagawa R, Mulé JJ, Mailloux AW. Inducible Tertiary Lymphoid Structures: Promise and Challenges for Translating a New Class of Immunotherapy. *Front Immunol* (2021) 12:675538. doi: 10.3389/fimmu.2021.675538
34. Stranford S, Ruddle NH. Follicular Dendritic Cells, Conduits, Lymphatic Vessels, and High Endothelial Venules in Tertiary Lymphoid Organs: Parallels With Lymph Node Stroma. *Front Immunol* (2012) 3:350. doi: 10.3389/fimmu.2012.00350
35. Hill DG, Ward A, Nicholson LB, Jones GW. Emerging Roles for IL-6 Family Cytokines as Positive and Negative Regulators of Ectopic Lymphoid Structures. *Cytokine* (2021) 146:155650. doi: 10.1016/j.cyto.2021.155650
36. Berteloot L, Molina TJ, Bruneau J, Picard C, Barlogis V, Secq V, et al. Alternative Pathways for the Development of Lymphoid Structures in Humans. *Proc Natl Acad Sci USA* (2021) 118:e2108082118. doi: 10.1073/pnas.2108082118
37. Mebius RE. Organogenesis of Lymphoid Tissues. *Nat Rev Immunol* (2003) 3:292–303. doi: 10.1038/nri1054
38. Corsiero E, Delvecchio FR, Bombardieri M, Pitzalis C. B Cells in the Formation of Tertiary Lymphoid Organs in Autoimmunity, Transplantation and Tumorigenesis. *Curr Opin Immunol* (2019) 57:46–52. doi: 10.1016/j.coi.2019.01.004
39. Lucchesi D, Coleby R, Pontarini E, Prediletto E, Rivellese F, Hill DG, et al. Impaired Interleukin-27-Mediated Control of CD4+ T Cell Function Impact on Ectopic Lymphoid Structure Formation in Patients With Sjögren's Syndrome. *Arthritis Rheumatol* (2020) 72:1559–70. doi: 10.1002/art.41289
40. Grogan JL, Ouyang W. A Role for Th17 Cells in the Regulation of Tertiary Lymphoid Follicles. *Eur J Immunol* (2012) 42:2255–62. doi: 10.1002/eji.201242656
41. Luo R, Cheng Y, Chang D, Liu T, Liu L, Pei G, et al. Tertiary Lymphoid Organs are Associated With the Progression of Kidney Damage and Regulated by Interleukin-17A. *Theranostics* (2021) 11:117–31. doi: 10.7150/thno.48624
42. Gassen RB, Fazolo T, Nascimento de Freitas D, Borges TJ, Lima K, Antunes GL, et al. IL-21 Treatment Recovers Follicular Helper T Cells and Neutralizing Antibody Production in Respiratory Syncytial Virus Infection. *Immunol Cell Biol* (2021) 99:309–22. doi: 10.1111/imcb.12418
43. Pontarini E, Murray-Brown WJ, Croia C, Lucchesi D, Conway J, Rivellese F, et al. Unique Expansion of IL-21+ Tfh and Tph Cells Under Control of ICOS Identifies Sjögren's Syndrome With Ectopic Germinal Centres and MALT Lymphoma. *Ann Rheum Dis* (2020) 79:1588–99. doi: 10.1136/annrheumdis-2020-217646
44. Zhu M, Yang H, Lu Y, Yang H, Tang Y, Li L, et al. Cardiac Ectopic Lymphoid Follicle Formation in Viral Myocarditis Involving the Regulation of

Podoplanin in Th17 Cell Differentiation. *FASEB J* (2021) 35:e21975. doi: 10.1096/fj.202101050RR
45. Fleige H, Haas JD, Stahl FR, Willenzon S, Prinz I, Förster R. Induction of BALT in the Absence of IL-17. *Nat Immunol* (2011) 13:1; author reply 2. doi: 10.1038/ni.2167
46. Ciccia F, Rizzo A, Maugeri R, Alessandro R, Croci S, Guggino G, et al. Ectopic Expression of CXCL13, BAFF, APRIL and LT-β Is Associated With Artery Tertiary Lymphoid Organs in Giant Cell Arteritis. *Ann Rheum Dis* (2017) 76:235–43. doi: 10.1136/annrheumdis-2016-209217
47. Pontarini E, Sciacca E, Grigoriadou S, Rivellese F, Lucchesi D, Fossati-Jimack L, et al. NKp30 Receptor Upregulation in Salivary Glands of Sjögren's Syndrome Characterizes Ectopic Lymphoid Structures and Is Restricted by Rituximab Treatment. *Front Immunol* (2021) 12:706737. doi: 10.3389/fimmu.2021.706737
48. Dorraji SE, Hovd A-MK, Kanapathippillai P, Bakland G, Eilertsen GØ, Figenschau SL, et al. Mesenchymal Stem Cells and T Cells in the Formation of Tertiary Lymphoid Structures in Lupus Nephritis. *Sci Rep* (2018) 8:7861. doi: 10.1038/s41598-018-26265-z
49. Zhao H, Wang H, Zhou Q, Ren X. Insights Into Tertiary Lymphoid Structures in the Solid Tumor Microenvironment: Anti-Tumor Mechanism, Functional Regulation, and Immunotherapeutic Strategies. *Cancer Biol Med* (2021) 18:981–91. doi: 10.20892/j.issn.2095-3941.2020.0569
50. Lee YH, Sato Y, Saito M, Fukuma S, Saito M, Yamamoto S, et al. Advanced Tertiary Lymphoid Tissues in Protocol Biopsies are Associated With Progressive Graft Dysfunction in Kidney Transplant Recipients. *J Am Soc Nephrol* (2022) 33:186–200. doi: 10.1681/ASN.2021050715
51. Werner F, Wagner C, Simon M, Glatz K, Mertz KD, Läubli H, et al. A Standardized Analysis of Tertiary Lymphoid Structures in Human Melanoma: Disease Progression- and Tumor Site-Associated Changes With Germinal Center Alteration. *Front Immunol* (2021) 12:675146. doi: 10.3389/fimmu.2021.675146
52. Teillaud J-L, Dieu-Nosjean M-C. Tertiary Lymphoid Structures: An Anti-Tumor School for Adaptive Immune Cells and an Antibody Factory to Fight Cancer? *Front Immunol* (2017) 8:830. doi: 10.3389/fimmu.2017.00830
53. Vella G, Guelfi S, Bergers G. High Endothelial Venules: A Vascular Perspective on Tertiary Lymphoid Structures in Cancer. *Front Immunol* (2021) 12:736670. doi: 10.3389/fimmu.2021.736670
54. Pitzalis C, Jones GW, Bombardieri M, Jones SA. Ectopic Lymphoid-Like Structures in Infection, Cancer and Autoimmunity. *Nat Rev Immunol* (2014) 14:447–62. doi: 10.1038/nri3700
55. Sautès-Fridman C, Petitprez F, Calderaro J, Fridman WH. Tertiary Lymphoid Structures in the Era of Cancer Immunotherapy. *Nat Rev Cancer* (2019) 19:307–25. doi: 10.1038/s41568-019-0144-6
56. Dieu-Nosjean M-C, Goc J, Giraldo NA, Sautès-Fridman C, Fridman WH. Tertiary Lymphoid Structures in Cancer and Beyond. *Trends Immunol* (2014) 35:571–80. doi: 10.1016/j.it.2014.09.006
57. Pikarsky E, Heikenwalder M. Focal and Local: Ectopic Lymphoid Structures and Aggregates of Myeloid and Other Immune Cells in Liver. *Gastroenterology* (2016) 151:780–3. doi: 10.1053/j.gastro.2016.09.029
58. Meylan M, Petitprez F, Lacroix L, Tommaso LD, Roncalli M, Bougoüin A, et al. Early Hepatic Lesions Display Immature Tertiary Lymphoid Structures and Show Elevated Expression of Immune Inhibitory and Immunosuppressive Molecules. *Clin Cancer Res* (2020) 26:4381–9. doi: 10.1158/1078-0432.CCR-19-2929
59. Nie Y, Li J, Wu W, Guo D, Lei X, Zhang T, et al. A Novel Nine-lncRNA Risk Signature Correlates With Immunotherapy in Hepatocellular Carcinoma. *Front Oncol* (2021) 11:706915. doi: 10.3389/fonc.2021.706915
60. Zhang Y, Gao C, Cao F, Wu Y, Chen S, Han X, et al. Pan-Cancer Analysis of IGF-1 and IGF-1R as Potential Prognostic Biomarkers and Immunotherapy Targets. *Front Oncol* (2021) 11:755341. doi: 10.3389/fonc.2021.755341
61. Calderaro J, Petitprez F, Becht E, Laurent A, Hirsch TZ, Rousseau B, et al. Intra-Tumoral Tertiary Lymphoid Structures are Associated With a Low Risk of Early Recurrence of Hepatocellular Carcinoma. *J Hepatol* (2019) 70:58–65. doi: 10.1016/j.jhep.2018.09.003
62. Shen Y-C, Hsu C-L, Jeng Y-M, Ho M-C, Ho C-M, Yeh C-P, et al. Reliability of a Single-Region Sample to Evaluate Tumor Immune Microenvironment in Hepatocellular Carcinoma. *J Hepatol* (2020) 72:489–97. doi: 10.1016/j.jhep.2019.09.032
63. Luo M, Lin Y, Liang R, Li Y, Ge L. Clinical Significance of the HHLA2 Protein in Hepatocellular Carcinoma and the Tumor Microenvironment. *J Inflammation Res* (2021) 14:4217–28. doi: 10.2147/JIR.S324336
64. Li H, Wang J, Liu H, Lan T, Xu L, Wang G, et al. Existence of Intratumoral Tertiary Lymphoid Structures Is Associated With Immune Cells Infiltration and Predicts Better Prognosis in Early-Stage Hepatocellular Carcinoma. *Aging (Albany NY)* (2020) 12:3451–72. doi: 10.18632/aging.102821
65. Gao F, Xie K, Xiang Q, Qin Y, Chen P, Wan H, et al. The Density of Tumor-Infiltrating Lymphocytes and Prognosis in Resectable Hepatocellular Carcinoma: A Two-Phase Study. *Aging (Albany NY)* (2021) 13:9665–78. doi: 10.18632/aging.202710
66. Jia Y, Zeng Z, Li Y, Li Z, Jin L, Zhang Z, et al. Impaired Function of CD4+ T Follicular Helper (Tfh) Cells Associated With Hepatocellular Carcinoma Progression. *PloS One* (2015) 10:e0117458. doi: 10.1371/journal.pone.0117458
67. Noël G, Fontsa ML, Garaud S, Silva PD, de Wind A, Van den Eynden GG, et al. Functional Th1-Oriented T Follicular Helper Cells That Infiltrate Human Breast Cancer Promote Effective Adaptive Immunity. *J Clin Invest* (2021) 131:e139905. doi: 10.1172/JCI139905
68. Becht E, Goc J, Germain C, Giraldo NA, Dieu-Nosjean M-C, Sautès-Fridman C, et al. Shaping of an Effective Immune Microenvironment to and by Cancer Cells. *Cancer Immunol Immunother* (2014) 63:991–7. doi: 10.1007/s00262-014-1590-3
69. Roulleaux Dugage M, Jones RL, Trent J, Champiat S, Dumont S. Beyond the Driver Mutation: Immunotherapies in Gastrointestinal Stromal Tumors. *Front Immunol* (2021) 12:715727. doi: 10.3389/fimmu.2021.715727
70. Gao S, Hsu T-W, Li MO. Immunity Beyond Cancer Cells: Perspective From Tumor Tissue. *Trends Cancer* (2021) 7:1010–9. doi: 10.1016/j.trecan.2021.06.007
71. Sautès-Fridman C, Fridman WH. TLS in Tumors: What Lies Within. *Trends Immunol* (2016) 37:1–2. doi: 10.1016/j.it.2015.12.001
72. Frafjord A, Buer L, Hammarström C, Aamodt H, Woldbæk PR, Brustugun OT, et al. The Immune Landscape of Human Primary Lung Tumors Is Th2 Skewed. *Front Immunol* (2021) 12:764596. doi: 10.3389/fimmu.2021.764596
73. Cariani E, Pilli M, Zerbini A, Rota C, Olivani A, Pelosi G, et al. Immunological and Molecular Correlates of Disease Recurrence After Liver Resection for Hepatocellular Carcinoma. *PloS One* (2012) 7:e32493. doi: 10.1371/journal.pone.0032493
74. Xin H, Liang D, Zhang M, Ren D, Chen H, Zhang H, et al. The CD68+ Macrophages to CD8+ T-Cell Ratio is Associated With Clinical Outcomes in Hepatitis B Virus (HBV)-Related Hepatocellular Carcinoma. *HPB* (2021) 23:1061–71. doi: 10.1016/j.hpb.2020.11.002
75. Kang HJ, Oh J-H, Chun S-M, Kim D, Ryu Y-M, Hwang HS, et al. Immunogenomic Landscape of Hepatocellular Carcinoma With Immune Cell Stroma and EBV-Positive Tumor-Infiltrating Lymphocytes. *J Hepatol* (2019) 71:91–103. doi: 10.1016/j.jhep.2019.03.018
76. Patman G. Ectopic Lymphoid Structures Promote Carcinogenesis in the Liver. *Nat Rev Gastroenterol Hepatol* (2015) 12:671–1. doi: 10.1038/nrgastro.2015.192
77. Finkin S, Yuan D, Stein I, Taniguchi K, Weber A, Unger K, et al. Ectopic Lymphoid Structures Function as Microniches for Tumor Progenitor Cells in Hepatocellular Carcinoma. *Nat Immunol* (2015) 16:1235–44. doi: 10.1038/ni.3290
78. Dong H, Strome SE, Salomao DR, Tamura H, Hirano F, Flies DB, et al. Tumor-Associated B7-H1 Promotes T-Cell Apoptosis: A Potential Mechanism of Immune Evasion. *Nat Med* (2002) 8:793–800. doi: 10.1038/nm730
79. Brown JA, Dorfman DM, Ma F-R, Sullivan EL, Munoz O, Wood CR, et al. Blockade of Programmed Death-1 Ligands on Dendritic Cells Enhances T Cell Activation and Cytokine Production. *J Immunol* (2003) 170:1257–66. doi: 10.4049/jimmunol.170.3.1257
80. Svinarenko M, Katz S-F, Tharehalli U, Mulaw MA, Maier HJ, Sunami Y, et al. An IKK/NF-κb Activation/p53 Deletion Sequence Drives Liver Carcinogenesis and Tumor Differentiation. *Cancers (Basel)* (2019) 11:1410. doi: 10.3390/cancers11101410

81. Li H, Liu H, Fu H, Li J, Xu L, Wang G, et al. Peritumoral Tertiary Lymphoid Structures Correlate With Protective Immunity and Improved Prognosis in Patients With Hepatocellular Carcinoma. *Front Immunol* (2021) 12:648812. doi: 10.3389/fimmu.2021.648812
82. Zhao H-Q, Li W-M, Lu Z-Q, Yao Y-M. Roles of Tregs in Development of Hepatocellular Carcinoma: A Meta-Analysis. *World J Gastroenterol* (2014) 20:7971–8. doi: 10.3748/wjg.v20.i24.7971
83. Schoenberg MB, Li X, Li X, Han Y, Hao J, Miksch RC, et al. The Predictive Value of Tumor Infiltrating Leukocytes in Hepatocellular Carcinoma: A Systematic Review and Meta-Analysis. *Eur J Surg Oncol* (2021) 47:2561–70. doi: 10.1016/j.ejso.2021.04.042
84. Liu S, Zhou B, Wu L, Sun Y, Chen J, Liu S. Single-Cell Differential Splicing Analysis Reveals High Heterogeneity of Liver Tumor-Infiltrating T Cells. *Sci Rep* (2021) 11:5325. doi: 10.1038/s41598-021-84693-w
85. Ratanatharathorn V, Pavletic S, Uberti JP. Clinical Applications of Rituximab in Allogeneic Stem Cell Transplantation: Anti-Tumor and Immunomodulatory Effects. *Cancer Treat Rev* (2009) 35:653–61. doi: 10.1016/j.ctrv.2009.07.004
86. Zhang Y, Morgan R, Podack ER, Rosenblatt J. B Cell Regulation of Anti-Tumor Immune Response. *Immunol Res* (2013) 57:115–24. doi: 10.1007/s12026-013-8472-1
87. Luu VP, Vazquez MI, Zlotnik A. B Cells Participate in Tolerance and Autoimmunity Through Cytokine Production. *Autoimmunity* (2014) 47:1–12. doi: 10.3109/08916934.2013.856006
88. Garnelo M, Tan A, Her Z, Yeong J, Lim CJ, Chen J, et al. Interaction Between Tumour-Infiltrating B Cells and T Cells Controls the Progression of Hepatocellular Carcinoma. *Gut* (2017) 66:342–51. doi: 10.1136/gutjnl-2015-310814
89. Schoenberg MB, Hao J, Bucher JN, Miksch RC, Anger HJW, Mayer B, et al. Perivascular Tumor-Infiltrating Leukocyte Scoring for Prognosis of Resected Hepatocellular Carcinoma Patients. *Cancers (Basel)* (2018) 10:E389. doi: 10.3390/cancers10100389
90. Yao W, He J-C, Yang Y, Wang J-M, Qian Y-W, Yang T, et al. The Prognostic Value of Tumor-Infiltrating Lymphocytes in Hepatocellular Carcinoma: A Systematic Review and Meta-Analysis. *Sci Rep* (2017) 7:7525. doi: 10.1038/s41598-017-08128-1
91. Ding W, Xu X, Qian Y, Xue W, Wang Y, Du J, et al. Prognostic Value of Tumor-Infiltrating Lymphocytes in Hepatocellular Carcinoma: A Meta-Analysis. *Med (Baltimore)* (2018) 97:e13301. doi: 10.1097/MD.0000000000013301
92. El-Rebey HS, Abdou AG, Sultan MM, Ibrahim SH, Holah NS. The Profile and Role of Tumor-Infiltrating Lymphocytes in Hepatocellular Carcinoma: An Immunohistochemical Study. *Appl Immunohistochem Mol Morphol* (2021) 29:188–200. doi: 10.1097/PAI.0000000000000865
93. Timperi E, Barnaba V. CD39 Regulation and Functions in T Cells. *Int J Mol Sci* (2021) 22:8068. doi: 10.3390/ijms22158068
94. Liu T, Tan J, Wu M, Fan W, Wei J, Zhu B, et al. High-Affinity Neoantigens Correlate With Better Prognosis and Trigger Potent Antihepatocellular Carcinoma (HCC) Activity by Activating CD39+CD8+ T Cells. *Gut* (2021) 70:1965–77. doi: 10.1136/gutjnl-2020-322196
95. Diggs LP, Ruf B, Ma C, Heinrich B, Cui L, Zhang Q, et al. CD40-Mediated Immune Cell Activation Enhances Response to Anti-PD-1 in Murine Intrahepatic Cholangiocarcinoma. *J Hepatol* (2021) 74:1145–54. doi: 10.1016/j.jhep.2020.11.037
96. Lam JH, Ng HHM, Lim CJ, Sim XN, Malavasi F, Li H, et al. Expression of CD38 on Macrophages Predicts Improved Prognosis in Hepatocellular Carcinoma. *Front Immunol* (2019) 10:2093. doi: 10.3389/fimmu.2019.02093
97. Dong Z-R, Chen Z-Q, Yang X-Y, Ding Z-N, Liu K-X, Yan L-J, et al. RECK Expression is Associated With Angiogenesis and Immunogenic Tumor Microenvironment in Hepatocellular Carcinoma, and Is a Prognostic Factor for Better Survival. *J Cancer* (2021) 12:3827–40. doi: 10.7150/jca.56167
98. Zhang M, Pang H-J, Zhao W, Li Y-F, Yan L-X, Dong Z-Y, et al. VISTA Expression Associated With CD8 Confers a Favorable Immune Microenvironment and Better Overall Survival in Hepatocellular Carcinoma. *BMC Cancer* (2018) 18:511. doi: 10.1186/s12885-018-4435-1
99. Li X-F, Dai D, Song X-Y, Liu J-J, Zhu L, Zhu X, et al. A Different Representation of Natural T Cells and Natural Killer Cells Between Tumor-Infiltrating and Periphery Lymphocytes in Human Hepatocellular Carcinoma. *Oncol Lett* (2017) 13:3291–8. doi: 10.3892/ol.2017.5808
100. Tu J-F, Ding Y-H, Ying X-H, Wu F-Z, Zhou X-M, Zhang D-K, et al. Regulatory T Cells, Especially ICOS+ FOXP3+ Regulatory T Cells, are Increased in the Hepatocellular Carcinoma Microenvironment and Predict Reduced Survival. *Sci Rep* (2016) 6:35056. doi: 10.1038/srep35056
101. Huang Y, Sheng H, Xiao Y, Hu W, Zhang Z, Chen Y, et al. Wnt/β-Catenin Inhibitor ICG-001 Enhances the Antitumor Efficacy of Radiotherapy by Increasing Radiation-Induced DNA Damage and Improving Tumor Immune Microenvironment in Hepatocellular Carcinoma. *Radiother Oncol* (2021) 162:34–44. doi: 10.1016/j.radonc.2021.06.034
102. Teng C-F, Li T-C, Wang T, Liao D-C, Wen Y-H, Wu T-H, et al. Increased Infiltration of Regulatory T Cells in Hepatocellular Carcinoma of Patients With Hepatitis B Virus Pre-S2 Mutant. *Sci Rep* (2021) 11:1136. doi: 10.1038/s41598-020-80935-5
103. Ge Z, Zhou G, Campos Carrascosa L, Gausvik E, Boor PPC, Noordam L, et al. TIGIT and PD1 Co-Blockade Restores *Ex Vivo* Functions of Human Tumor-Infiltrating CD8+ T Cells in Hepatocellular Carcinoma. *Cell Mol Gastroenterol Hepatol* (2021) 12:443–64. doi: 10.1016/j.jcmgh.2021.03.003
104. Chang H, Jung W, Kim A, Kim HK, Kim WB, Kim JH, et al. Expression and Prognostic Significance of Programmed Death Protein 1 and Programmed Death Ligand-1, and Cytotoxic T Lymphocyte-Associated Molecule-4 in Hepatocellular Carcinoma. *APMIS* (2017) 125:690–8. doi: 10.1111/apm.12703
105. Xu W, Ma C, Liu W, Anwaier A, Tian X, Shi G, et al. Prognostic Value, DNA Variation and Immunologic Features of a Tertiary Lymphoid Structure-Related Chemokine Signature in Clear Cell Renal Cell Carcinoma. *Cancer Immunol Immunother* (2022) published online. doi: 10.1007/s00262-021-03123-y
106. Solinas C, Garaud S, De Silva P, Boisson A, Van den Eynden G, de Wind A, et al. Immune Checkpoint Molecules on Tumor-Infiltrating Lymphocytes and Their Association With Tertiary Lymphoid Structures in Human Breast Cancer. *Front Immunol* (2017) 8:1412. doi: 10.3389/fimmu.2017.01412
107. Petitprez F, de Reyniès A, Keung EZ, Chen TW-W, Sun C-M, Calderaro J, et al. B Cells are Associated With Survival and Immunotherapy Response in Sarcoma. *Nature* (2020) 577:556–60. doi: 10.1038/s41586-019-1906-8
108. Groeneveld CS, Fontugne J, Cabel L, Bernard-Pierrot I, Radvanyi F, Allory Y, et al. Tertiary Lymphoid Structures Marker CXCL13 Is Associated With Better Survival for Patients With Advanced-Stage Bladder Cancer Treated With Immunotherapy. *Eur J Cancer* (2021) 148:181–9. doi: 10.1016/j.ejca.2021.01.036
109. Lee HJ, Kim JY, Park IA, Song IH, Yu JH, Ahn J-H, et al. Prognostic Significance of Tumor-Infiltrating Lymphocytes and the Tertiary Lymphoid Structures in HER2-Positive Breast Cancer Treated With Adjuvant Trastuzumab. *Am J Clin Pathol* (2015) 144:278–88. doi: 10.1309/AJCPIXUYDVZ0RZ3G
110. Qi Z, Xu Z, Zhang L, Zou Y, Li J, Yan W, et al. Overcoming Resistance to Immune Checkpoint Therapy in PTEN-Null Prostate Cancer by Intermittent Anti-PI3Kα/β/δ Treatment. *Nat Commun* (2022) 13:182. doi: 10.1038/s41467-021-27833-0
111. Lin Q, Tao P, Wang J, Ma L, Jiang Q, Li J, et al. Tumor-Associated Tertiary Lymphoid Structure Predicts Postoperative Outcomes in Patients With Primary Gastrointestinal Stromal Tumors. *Oncoimmunology* (2020) 9:1747339. doi: 10.1080/2162402X.2020.1747339
112. Bai X, Zhou Y, Yokota Y, Matsumoto Y, Zhai B, Maarouf N, et al. Adaptive Antitumor Immune Response Stimulated by Bio-Nanoparticle Based Vaccine and Checkpoint Blockade. *J Exp Clin Cancer Res* (2022) 41:132. doi: 10.1186/s13046-022-02307-3
113. Hsu C-L, Ou D-L, Bai L-Y, Chen C-W, Lin L, Huang S-F, et al. Exploring Markers of Exhausted CD8 T Cells to Predict Response to Immune Checkpoint Inhibitor Therapy for Hepatocellular Carcinoma. *Liver Cancer* (2021) 10:346–59. doi: 10.1159/000515305
114. Tan AT, Meng F, Jin J, Zhang J-Y, Wang S-Y, Shi L, et al. Immunological Alterations After Immunotherapy With Short Lived HBV-TCR T Cells Associates With Long-Term Treatment Response in HBV-HCC. *Hepatol Commun* (2021) 6:841–54. doi: 10.1002/hep4.1857

115. Wang S, Xie K, Liu T. Cancer Immunotherapies: From Efficacy to Resistance Mechanisms – Not Only Checkpoint Matters. *Front Immunol* (2021) 12:690112. doi: 10.3389/fimmu.2021.690112
116. Tokunaga R, Nakagawa S, Sakamoto Y, Nakamura K, Naseem M, Izumi D, et al. 12-Chemokine Signature, a Predictor of Tumor Recurrence in Colorectal Cancer. *Int J Cancer* (2020) 147:532–41. doi: 10.1002/ijc.32982
117. Luther SA, Lopez T, Bai W, Hanahan D, Cyster JG. BLC Expression in Pancreatic Islets Causes B Cell Recruitment and Lymphotoxin-Dependent Lymphoid Neogenesis. *Immunity* (2000) 12:471–81. doi: 10.1016/s1074-7613(00)80199-5
118. Luther SA, Bidgol A, Hargreaves DC, Schmidt A, Xu Y, Paniyadi J, et al. Differing Activities of Homeostatic Chemokines CCL19, CCL21, and CXCL12 in Lymphocyte and Dendritic Cell Recruitment and Lymphoid Neogenesis. *J Immunol* (2002) 169:424–33. doi: 10.4049/jimmunol.169.1.424
119. Luo H, Su J, Sun R, Sun Y, Wang Y, Dong Y, et al. Coexpression of IL7 and CCL21 Increases Efficacy of CAR-T Cells in Solid Tumors Without Requiring Preconditioned Lymphodepletion. *Clin Cancer Res* (2020) 26:5494–505. doi: 10.1158/1078-0432.CCR-20-0777
120. Fujisaka Y, Iwata T, Tamai K, Nakamura M, Mochizuki M, Shibuya R, et al. Long non-Coding RNA HOTAIR Up-Regulates Chemokine (C-C Motif) Ligand 2 and Promotes Proliferation of Macrophages and Myeloid-Derived Suppressor Cells in Hepatocellular Carcinoma Cell Lines. *Oncol Lett* (2018) 15:509–14. doi: 10.3892/ol.2017.7322
121. Cheng C, Shou Q, Lang J, Jin L, Liu X, Tang D, et al. Gehua Jiecheng Decoction Inhibits Diethylnitrosamine-Induced Hepatocellular Carcinoma in Mice by Improving Tumor Immunosuppression Microenvironment. *Front Pharmacol* (2020) 11:809. doi: 10.3389/fphar.2020.00809
122. Li X, Yao W, Yuan Y, Chen P, Li B, Li J, et al. Targeting of Tumour-Infiltrating Macrophages *via* CCL2/CCR2 Signalling as a Therapeutic Strategy Against Hepatocellular Carcinoma. *Gut* (2017) 66:157–67. doi: 10.1136/gutjnl-2015-310514
123. Ponziani FR, Bhoori S, Castelli C, Putignani L, Rivoltini L, Del Chierico F, et al. Hepatocellular Carcinoma Is Associated With Gut Microbiota Profile and Inflammation in Nonalcoholic Fatty Liver Disease. *Hepatology* (2019) 69:107–20. doi: 10.1002/hep.30036
124. Sadeghi M, Lahdou I, Oweira H, Daniel V, Terness P, Schmidt J, et al. Serum Levels of Chemokines CCL4 and CCL5 in Cirrhotic Patients Indicate the Presence of Hepatocellular Carcinoma. *Br J Cancer* (2015) 113:756–62. doi: 10.1038/bjc.2015.227
125. Teufel M, Seidel H, Köchert K, Meinhardt G, Finn RS, Llovet JM, et al. Biomarkers Associated With Response to Regorafenib in Patients With Hepatocellular Carcinoma. *Gastroenterology* (2019) 156:1731–41. doi: 10.1053/j.gastro.2019.01.261
126. Cao P, Ma B, Sun D, Zhang W, Qiu J, Qin L, et al. Hsa_Circ_0003410 Promotes Hepatocellular Carcinoma Progression by Increasing the Ratio of M2/M1 Macrophages Through the miR-139-3p/CCL5 Axis. *Cancer Sci* (2021) 113:634–47. doi: 10.1111/cas.15238
127. Lu C, Rong D, Hui B, He X, Jiang W, Xu Y, et al. CircETFA Upregulates CCL5 by Sponging miR-612 and Recruiting EIF4A3 to Promote Hepatocellular Carcinoma. *Cell Death Discov* (2021) 7:321. doi: 10.1038/s41420-021-00710-x
128. Chew V, Lee YH, Pan L, Nasir NJM, Lim CJ, Chua C, et al. Immune Activation Underlies a Sustained Clinical Response to Yttrium-90 Radioembolisation in Hepatocellular Carcinoma. *Gut* (2019) 68:335–46. doi: 10.1136/gutjnl-2017-315485
129. Yang X, Sun J, Wen B, Wang Y, Zhang M, Chen W, et al. Biejiajian Pill Promotes the Infiltration of CD8+ T Cells in Hepatocellular Carcinoma by Regulating the Expression of CCL5. *Front Pharmacol* (2021) 12:771046. doi: 10.3389/fphar.2021.771046
130. Koni PA, Sacca R, Lawton P, Browning JL, Ruddle NH, Flavell RA. Distinct Roles in Lymphoid Organogenesis for Lymphotoxins Alpha and Beta Revealed in Lymphotoxin Beta-Deficient Mice. *Immunity* (1997) 6:491–500. doi: 10.1016/s1074-7613(00)80292-7
131. Moussion C, Girard J-P. Dendritic Cells Control Lymphocyte Entry to Lymph Nodes Through High Endothelial Venules. *Nature* (2011) 479:542–6. doi: 10.1038/nature10540
132. Chen L, Taylor JL, Sabins NC, Lowe DB, Qu Y, You Z, et al. Extranodal Induction of Therapeutic Immunity in the Tumor Microenvironment After Intratumoral Delivery of Tbet Gene-Modified Dendritic Cells. *Cancer Gene Ther* (2013) 20:469–77. doi: 10.1038/cgt.2013.42
133. Loeffler M, Le'Negrate G, Krajewska M, Reed JC. Attenuated Salmonella Engineered to Produce Human Cytokine LIGHT Inhibit Tumor Growth. *Proc Natl Acad Sci U.S.A.* (2007) 104:12879–83. doi: 10.1073/pnas.0701959104
134. Wolf MJ, Adili A, Piotrowitz K, Abdullah Z, Boege Y, Stemmer K, et al. Metabolic Activation of Intrahepatic CD8+ T Cells and NKT Cells Causes Nonalcoholic Steatohepatitis and Liver Cancer *via* Cross-Talk With Hepatocytes. *Cancer Cell* (2014) 26:549–64. doi: 10.1016/j.ccell.2014.09.003
135. Zhu Q, Li N, Li F, Sang J, Deng H, Han Q, et al. Association of LTBR Polymorphisms With Chronic Hepatitis B Virus Infection and Hepatitis B Virus-Related Hepatocellular Carcinoma. *Int Immunopharmacol* (2017) 49:126–31. doi: 10.1016/j.intimp.2017.05.031
136. Conlon TM, John-Schuster G, Heide D, Pfister D, Lehmann M, Hu Y, et al. Inhibition of Ltβr Signalling Activates WNT-Induced Regeneration in Lung. *Nature* (2020) 588:151–6. doi: 10.1038/s41586-020-2882-8
137. Mc C, Tl H, Ty L, Sl H. Overexpression of Bcl-2 Enhances LIGHT- and Interferon-Gamma -Mediated Apoptosis in Hep3BT2 Cells. *J Biol Chem* (2000) 275:38794–801. doi: 10.1074/jbc.M003292200
138. Cottrell TR, Thompson ED, Forde PM, Stein JE, Duffield AS, Anagnostou V, et al. Pathologic Features of Response to Neoadjuvant Anti-PD-1 in Resected non-Small-Cell Lung Carcinoma: A Proposal for Quantitative Immune-Related Pathologic Response Criteria (irPRC). *Ann Oncol* (2018) 29:1853–60. doi: 10.1093/annonc/mdy218
139. Stein JE, Soni A, Danilova L, Cottrell TR, Gajewski TF, Hodi FS, et al. Major Pathologic Response on Biopsy (MPRbx) in Patients With Advanced Melanoma Treated With Anti-PD-1: Evidence for an Early, on-Therapy Biomarker of Response. *Ann Oncol* (2019) 30:589–96. doi: 10.1093/annonc/mdz019
140. Huang K-W, Tan CP, Reebye V, Chee CE, Zacharoulis D, Habib R, et al. MTL-CEBPA Combined With Immunotherapy or RFA Enhances Immunological Anti-Tumor Response in Preclinical Models. *Int J Mol Sci* (2021) 22:9168. doi: 10.3390/ijms22179168
141. Morita M, Nishida N, Sakai K, Aoki T, Chishina H, Takita M, et al. Immunological Microenvironment Predicts the Survival of the Patients With Hepatocellular Carcinoma Treated With Anti-PD-1 Antibody. *Liver Cancer* (2021) 10:380–93. doi: 10.1159/000516899
142. Craciun L, de Wind R, Demetter P, Lucidi V, Bohlok A, Michiels S, et al. Retrospective Analysis of the Immunogenic Effects of Intra-Arterial Locoregional Therapies in Hepatocellular Carcinoma: A Rationale for Combining Selective Internal Radiation Therapy (SIRT) and Immunotherapy. *BMC Cancer* (2020) 20:135. doi: 10.1186/s12885-020-6613-1
143. Schoenberg MB, Zhu T, Hao J, Bucher JN, Li X, Li X, et al. Highly Differential Count of Circulating and Tumor Infiltrating Immune Cells in Patients With non-HCV/non-HBV Hepatocellular Carcinoma. *Cancer Immunol Immunother* (2021) 71:1103–33. doi: 10.1007/s00262-021-03061-9
144. Shi Y, Men X, Li X, Yang Z, Wen H. Research Progress and Clinical Prospect of Immunocytotherapy for the Treatment of Hepatocellular Carcinoma. *Int Immunopharmacol* (2020) 82:106351. doi: 10.1016/j.intimp.2020.106351
145. Li Z, Chen G, Cai Z, Dong X, Qiu L, Xu H, et al. Genomic and Transcriptional Profiling of Tumor Infiltrated CD8+ T Cells Revealed Functional Heterogeneity of Antitumor Immunity in Hepatocellular Carcinoma. *Oncoimmunology* (2019) 8:e1538436. doi: 10.1080/2162402X.2018.1538436
146. Liu F, Zeng G, Zhou S, He X, Sun N, Zhu X, et al. Blocking Tim-3 or/and PD-1 Reverses Dysfunction of Tumor-Infiltrating Lymphocytes in HBV-Related Hepatocellular Carcinoma. *Bull Cancer* (2018) 105:493–501. doi: 10.1016/j.bulcan.2018.01.018
147. Maldonado L, Teague JE, Morrow MP, Jotova I, Wu TC, Wang C, et al. Intramuscular Therapeutic Vaccination Targeting HPV16 Induces T Cell Responses That Localize in Mucosal Lesions. *Sci Transl Med* (2014) 6:221ra13. doi: 10.1126/scitranslmed.3007323
148. Huang Y, Chen Y, Zhou S, Chen L, Wang J, Pei Y, et al. Dual-Mechanism Based CTLs Infiltration Enhancement Initiated by Nano-Sapper Potentiates Immunotherapy Against Immune-Excluded Tumors. *Nat Commun* (2020) 11:622. doi: 10.1038/s41467-020-14425-7

149. Martinet L, Filleron T, Le Guellec S, Rochaix P, Garrido I, Girard J-P. High Endothelial Venule Blood Vessels for Tumor-Infiltrating Lymphocytes Are Associated With Lymphotoxin β-Producing Dendritic Cells in Human Breast Cancer. *J Immunol* (2013) 191:2001–8. doi: 10.4049/jimmunol.1300872
150. Hong SA, Hwang HW, Kim MK, Lee TJ, Yim K, Won HS, et al. High Endothelial Venule With Concomitant High CD8+ Tumor-Infiltrating Lymphocytes Is Associated With a Favorable Prognosis in Resected Gastric Cancer. *J Clin Med* (2020) 9:E2628. doi: 10.3390/jcm9082628
151. Hoshino H, Ohta M, Ito M, Uchimura K, Sakai Y, Uehara T, et al. Apical Membrane Expression of Distinct Sulfated Glycans Represents a Novel Marker of Cholangiolocellular Carcinoma. *Lab Invest* (2016) 96:1246–55. doi: 10.1038/labinvest.2016.104
152. Lin Z, Huang L, Li S, Gu J, Cui X, Zhou Y. Pan-Cancer Analysis of Genomic Properties and Clinical Outcome Associated With Tumor Tertiary Lymphoid Structure. *Sci Rep* (2020) 10:21530. doi: 10.1038/s41598-020-78560-3
153. Wang X, Shen H, Zhangyuan G, Huang R, Zhang W, He Q, et al. 14-3-3ζ Delivered by Hepatocellular Carcinoma-Derived Exosomes Impaired Anti-Tumor Function of Tumor-Infiltrating T Lymphocytes. *Cell Death Dis* (2018) 9:159. doi: 10.1038/s41419-017-0180-7
154. Delvecchio FR, Goulart MR, Fincham REA, Bombadieri M. Kocher Hm. *B Cells Pancreatic Cancer Stroma. World J Gastroenterol* (2022) 28:1088–101. doi: 10.3748/wjg.v28.i11.1088
155. Morcrette G, Hirsch TZ, Badour E, Pilet J, Caruso S, Calderaro J, et al. APC Germline Hepatoblastomas Demonstrate Cisplatin-Induced Intratumor Tertiary Lymphoid Structures. *Oncoimmunology* (2019) 8:e1583547. doi: 10.1080/2162402X.2019.1583547
156. Kuwabara S, Tsuchikawa T, Nakamura T, Hatanaka Y, Hatanaka KC, Sasaki K, et al. Prognostic Relevance of Tertiary Lymphoid Organs Following Neoadjuvant Chemoradiotherapy in Pancreatic Ductal Adenocarcinoma. *Cancer Sci* (2019) 110:1853–62. doi: 10.1111/cas.14023
157. Boivin G, Kalambaden P, Faget J, Rusakiewicz S, Montay-Gruel P, Meylan E, et al. Cellular Composition and Contribution of Tertiary Lymphoid Structures to Tumor Immune Infiltration and Modulation by Radiation Therapy. *Front Oncol* (2018) 8:256. doi: 10.3389/fonc.2018.00256
158. Singh A, Peppas NA. Hydrogels and Scaffolds for Immunomodulation. *Adv Mater* (2014) 26:6530–41. doi: 10.1002/adma.201402105
159. Okamoto N, Chihara R, Shimizu C, Nishimoto S, Watanabe T. Artificial Lymph Nodes Induce Potent Secondary Immune Responses in Naive and Immunodeficient Mice. *J Clin Invest* (2007) 117:997–1007. doi: 10.1172/JCI30379
160. Chelvanambi M, Fecek RJ, Taylor JL, Storkus WJ. STING Agonist-Based Treatment Promotes Vascular Normalization and Tertiary Lymphoid Structure Formation in the Therapeutic Melanoma Microenvironment. *J Immunother Cancer* (2021) 9:e001906. doi: 10.1136/jitc-2020-001906

Conflict of Interest: The authors declare that the research was conducted in the absence of any commercial or financial relationships that could be construed as a potential conflict of interest.

Publisher's Note: All claims expressed in this article are solely those of the authors and do not necessarily represent those of their affiliated organizations, or those of the publisher, the editors and the reviewers. Any product that may be evaluated in this article, or claim that may be made by its manufacturer, is not guaranteed or endorsed by the publisher.

frontiers | Frontiers in Immunology

ORIGINAL RESEARCH
published: 22 July 2022
doi: 10.3389/fimmu.2022.932298

TIE-2 Signaling Activation by Angiopoietin 2 On Myeloid-Derived Suppressor Cells Promotes Melanoma-Specific T-cell Inhibition

*Amélie Marguier[1], Caroline Laheurte[1,2], Benoît Lecoester[1], Marine Malfroy[1], Laura Boullerot[1,2], Adeline Renaudin[2], Evan Seffar[1], Abhishek Kumar[1], Charlée Nardin[1,3], François Aubin[1,3] and Olivier Adotevi[1,2,4]**

[1] Univ. Bourgogne Franche-Comté, INSERM, EFS BFC, UMR1098, RIGHT Interactions Greffon-Hôte Tumeur/Ingénierie Cellulaire et Génique, Besançon, France, [2] INSERM CIC-1431, Clinical Investigation Center in Biotherapy, Plateforme de Biomonitoring, Besançon, France, [3] Department of Dermatology, University Hospital of Besançon, Besançon, France, [4] Service Oncologie médicale, CHU Besançon, Besançon, France

OPEN ACCESS

Edited by:
Nicolas Larmonier, Université de Bordeaux, France

Reviewed by:
Arantzazu Alfranca, Hospital de la Princesa, Spain
Emeric Limagne, Centre Georges François Leclerc, France

***Correspondence:**
Olivier Adotevi
olivier.adotevi@univ-fcomte.fr

Specialty section:
This article was submitted to Cancer Immunity and Immunotherapy, a section of the journal Frontiers in Immunology

Received: 29 April 2022
Accepted: 23 June 2022
Published: 22 July 2022

Citation:
Marguier A, Laheurte C, Lecoester B, Malfroy M, Boullerot L, Renaudin A, Seffar E, Kumar A, Nardin C, Aubin F and Adotevi O (2022) TIE-2 Signaling Activation by Angiopoietin 2 On Myeloid-Derived Suppressor Cells Promotes Melanoma-Specific T-cell Inhibition. Front. Immunol. 13:932298. doi: 10.3389/fimmu.2022.932298

Myeloid-derived suppressor cells (MDSCs) are a heterogeneous group of immune suppressive cells detected in several human cancers. In this study, we investigated the features and immune suppressive function of a novel subset of monocytic MDSC overexpressing TIE-2 (TIE-2$^+$ M-MDSC), the receptor for the pro-angiogenic factor angiopoietin 2 (ANGPT2). We showed that patients with melanoma exhibited a higher circulating rate of TIE-2$^+$ M-MDSCs, especially in advanced stages, as compared to healthy donors. The distribution of the TIE-2$^+$ M-MDSC rate toward the melanoma stage correlated with the serum level of ANGPT2. TIE-2$^+$ M-MDSC from melanoma patients overexpressed immune suppressive molecules such as PD-L1, CD73, TGF-β, and IL-10, suggesting a highly immunosuppressive phenotype. The exposition of these cells to ANGPT2 increased the expression of most of these molecules, mainly Arginase 1. Hence, we observed a profound impairment of melanoma-specific T-cell responses in patients harboring high levels of TIE-2$^+$ M-MDSC along with ANGPT2. This was confirmed by *in vitro* experiments indicating that the addition of ANGPT2 increased the ability of TIE-2$^+$ M-MDSC to suppress antitumor T-cell function. Furthermore, by using TIE-2 kinase-specific inhibitors such as regorafenib or rebastinib, we demonstrated that an active TIE-2 signaling was required for optimal suppressive activity of these cells after ANGPT2 exposition. Collectively, these results support that TIE-2$^+$ M-MDSC/ANGPT2 axis represents a potential immune escape mechanism in melanoma.

Keywords: ANGPT2, tumor antigen, melanoma, tie-2, M-MDSCs

BACKGROUND

Myeloid-derived suppressor cells (MDSCs) are a heterogeneous group of immature myeloid origin with immunosuppressive properties. Physiologically, MDSCs play a fundamental role in the resolution of inflammation and the maintenance of immune homeostasis (1). However, MDSCs are massively accumulated in pathological conditions such as inflammation or cancer (2, 3). These

cells represent one critical immune escape mechanism developed by tumor, and evidence supports the detrimental role of tumor-induced MDSC in many cancers (2, 4–6). M-MDSC are also involved in metastasis formation and treatment resistance (4, 7).

Although there are heterogeneous populations, MDSCs are classified into two subtypes, monocytic (M-MDSC) and polymorphonuclear (PMN-MDSC), which resemble monocyte and neutrophil, respectively (6). M-MDSCs are characterized by the expression of CD11b, CD14, CD33, and HLA-DR$^{-/low}$, while PMN-MDSCs are characterized by the expression of CD11b, CD15, CD33, and CD66b (6, 8). These suppressive cells are involved in the tumor escape to immune attack through several mechanisms (9) such as the production of inhibitory cytokines (10, 11), Arginase 1 (Arg1) (12), and reactive oxygen species (2) and the regulation of adenosine mechanism by ectonucleotidase CD39 and CD73 (13).

We recently described that a subtype of M-MDSC expresses TIE-2, a receptor of the proangiogenic factor Angiopoietin 2 (TIE-2$^+$ M-MDSC) (14). TIE-2 is a tyrosine kinase receptor expressed mainly by endothelial cells, cancer cells, and some immune cells like monocytes (15, 16). This receptor has many ligands in the angiopoietin family, notably ANGPT2. ANGPT2 is expressed by endothelial cells, cancer cells, and some immune cells depending on the hypoxia context or upon stimulation by different cytokines or growth factors such as TNF-α, TGF-β, and VEGF (17–20). The ANGPT2/TIE-2 axis was implicated in angiogenesis and tumor progression (21, 22) due to its role in the permeabilization of the blood vessels and the activation of TIE-2$^+$-expressing monocytes (TEMs). TEMs are present in high quantity in the tumor microenvironment and blood vessels (23). In many cancers, it has been described that TEMs suppress T-cell proliferation and are implicated in neovascularization. Moreover, the immunosuppressive functions of TEMs are enhanced by the ANGPT2 stimulation. Inhibition of TIE-2 in myeloid cells induced a decrease in tumor volume and metastasis in lung cancer (23–28). In lung cancer, we identified a high rate of TIE-2$^+$ M-MDSC and ANGPT2 in the metastatic stage, which are associated with a poor prognosis. Furthermore, ANGPT2 enhances immunosuppressive functions of TIE-2$^+$ M-MDSC against antitumor response (14).

In this study, we investigated the TIE-2$^+$ M-MDSC in patients with melanoma and their suppressive function against tumor-specific T cells. We also analyzed the expression of different proteins implicated in the immunosuppressive function of M-MDSC.

METHODS

Patients

A total of 156 patients with melanoma were included at the University Hospital of Besançon (Besançon, France) between October 2011 and January 2016 in the LYTELOMEL cohort. Patients with cancer stages I to IV were enrolled before any anticancer therapy. All patients were included with informed consent in accordance with the French laws and after approval by the local and national ethics committees. The main clinical characteristics of the patients are summarized in **Supplementary Table S1**. Blood samples were collected before any anticancer therapy. Peripheral blood mononuclear cells (PBMCs) were isolated by density gradient separation on Ficoll Unisep tubes (Eurobio, Les Ulis, France) and frozen until use. Blood cells were also collected from 40 anonymous healthy donors (HDs) at the Etablissement Français du Sang (EFS, Besançon, France) with informed consent and following EFS guidelines.

Flow Cytometry

To discriminate living from dead cells, PBMCs were first washed in 1× phosphate-buffered saline (PBS) (Gibco, Grand Island, NY, USA) and stained with eFluor 506 viability dye according to the manufacturer's instructions (eBioscience, San Diego, CA, USA).

For M-MDSC analysis, samples were surface-stained in the dark for 30 min at 4°C with a mixture of the following antibodies: HLA-DR, CD14, CD33, CD11b, and TIE-2 plus lineage cocktail [(Lin) composed of CD19, CD56, and CD3].

For characterization of the MDSC phenotype, samples were surface-stained in the dark for 30 min at 4°C with different antibodies: HLA-DR, CD14, PD-L1, CD39, and CD73. Cells were fixed and permeabilized using eBioscience Foxp3/Transcription factor staining buffer set, according to the manufacturer's instructions. After permeabilization, antibodies against IL-10, LAP, Arg1, NOS2, or COX2 were added for 30 min at 4°C and washed.

Samples were acquired on a FACS BD Canto II (BD Biosciences, San Jose, CA, USA) and analyzed with KALUZA analysis software (Beckman Coulter, Brea, CA, USA).

ANGPT2 Measurement

The patients' serum was collected and frozen until use. ANGPT2 was measured in patients' serum by ELISA assay (R&D Systems, Minneapolis, MN, USA) according to the manufacturer's instructions. The values were represented in pg/ml.

Synthetic Peptides

A previously described mixture of eight pan MHC class II-restricted peptides derived from human telomerase (hTERT) (29, 30) and a mixture of overlapping 15-mer peptides derived from NY-ESO1 were used to analyze circulating CD4$^+$ T-cell response against tumor-associated antigens (TAAs). For studying CD8$^+$ T-cell response, a mixture of 12 MHC class I-restricted peptides derived from hTERT and a mixture of 5 peptides derived from NY-ESO1 were used.

hTERT MHC class II-restricted derived peptides were purchased from JPT (Berlin, Germany) (purity >80%), and NY-ESO1 MHC class II-restricted derived peptides were purchased from CTL (Cellular Technology Ltd., Shaker Heights, OH, USA). TERT and NY-ESO1 MHC class I-restricted peptides were purchased from ProImmune (Oxford, UK) (purity > 90%). To assess antiviral T-cell immunity, peptide mixtures derived from influenza virus, Epstein–Barr virus, and cytomegalovirus were used (PA-CEF-001).

Assessment of Spontaneous T-Cell Responses Against Tumor-Associated Antigens by IFN-γ ELISpot

T-cell responses were assessed by IFNγ ELISpot assay after a short *in vitro* stimulation as described previously (29, 30). For *in vitro* stimulation, at day 0, Ficoll-isolated PBMCs were plated at 1.10^6 cells/well for 6 days in 48-well plates with different peptide mixtures derived from hTERT and NY-ESO-1: 5 µg/ml of hTERT HLA class II, 1 µg/ml of hTERT HLA class I, or 1µg/ml of NY-ESO1. Recombinant interleukins IL-7 (5 ng/ml; PeproTech, Cranbury, NJ, USA) and IL-2 (20 UI/ml; Novartis, Basel, Switzerland) were added on days 1 and 3, respectively. On day 7, specific T-cell responses were measured by IFNγ ELISpot according to the manufacturer's instructions (Diaclone, Besançon, France). Briefly, cells were incubated at 1.10^5 cells/well in X-Vivo 15 medium (Lonza, Basel, Switzerland) in a 96-well ELISpot plate with the relevant peptides for 15 h. Cells cultured with medium and phorbol myristate acetate (PMA; 1 ng/ml)/ionomycin (500 ng/ml) were used as negative and positive controls, respectively. Spots were revealed, and spot-forming cells were counted using the C.T.L Immunospot System (Cellular Technology Ltd). Responses were considered positive when IFNγ spot numbers were twice those of the medium control and >10.

ANGPT2/TIE-2$^+$ Axis *In Vitro* Inhibition Assay

PBMCs from melanoma patients with TIE-2$^+$ M-MDSC were assessed for T-cell response in the absence or presence of ANGPT2. Briefly, T-cell responses were evaluated by IFN-γ ELISpot, as described above. To analyze ANGPT2/TIE-2$^+$ axis inhibition, 300 ng/ml of recombinant ANGPT2 was added on days 0 and 3 of the *in vitro* stimulation. In some cases, TIE-2 inhibitors—5 nM of rebastinib (MedChemExpress, Monmouth Junction, NJ, USA; DCC-2036), 50 nM of Regorafenib (Selleck, Munich, Germany; SE-S1178), or tyrosine kinase inhibitor 10 nM of dasatinib (Sigma-Aldrich, St. Louis, MO, USA; SML2589)—were added to the culture at days 0 and 3.

Real-Time Quantitative Reverse Transcriptase PCR

Cells were collected in RLT buffer (Qiagen, Valencia, CA, USA), and total mRNAs were extracted using RNAeasy Mini Kit according to the manufacturer's instructions (Qiagen). Total mRNA was reverse transcribed using the TaqMan gene expression assay for IL-10 (Hs00961622_m1), TEK (Hs00945150_m1), STAT3 (Hs00374280_m1), CD39 (Hs00969556_m1), CD73 (Hs00159686_m1), and Arg1 (Hs00163660_m1) (Thermo Fisher Scientific, Waltham, MA, USA) and the CFX96 Real-Time PCR Detection System (Bio-Rad, Hercules, CA, USA).

Statistical Analysis

Without further indication, the data are presented as the mean and their associated SD. For two-group comparisons, the non-parametric Student's t-test was used. For the survival analysis, the threshold values were calculated with the Restricted Cubic Spline method: 4.85% for TIE-2$^+$ M-MDSC and 439.5 pg/ml for ANGPT2. Overall survival (OS) was calculated from the date of study enrollment to the date of death from any cause. Patients known to be alive were censored at the time of their last follow-up assessment. Information about patients' outcomes was collected up to 7 years after their inclusion. OS was estimated using the Kaplan–Meier method described using median or rate at specific time points with 95% CI and compared among the groups with the log-rank test. All analyses were performed using Prism 7 GraphPad™ Software and R software version 2.15.2 (R Development Core Team; http://www.r-project.org). All tests were two-sided, and p-values lower than 0.05 were considered statistically significant (*$p < 0.05$, **$p < 0.01$, ***$p < 0.001$, ****$p < 0.0001$).

RESULTS

Accumulation of TIE-2$^+$ Monocytic Myeloid-Derived Suppressor Cells in Patients With Advanced Melanoma

TIE-2 expressing M-MDSCs (TIE-2$^+$ M-MDSC) were analyzed by flow cytometry in peripheral blood from melanoma patients (n = 81) and HDs (n = 22) as control. The phenotype of M-MDSC was Lineage$^-$ (CD3$^-$, CD19$^-$, and CD56$^-$), HLA-DR^{low}, CD11b$^+$, CD33$^+$, and CD14$^+$, as previously described (31) (**Figure 1A**). A higher circulating rate of TIE-2$^+$ M-MDSC was observed in melanoma patients than in HDs (7.3% vs 1.5%, $p < 0.0001$), and this rate was significantly more increased in advanced stages (**Figures 1B, C** and **Supplementary Table 1**). Moreover, most advanced patients displayed high levels of circulating TIE-2$^+$ M-MDSC (>5%) as compared to stage I/II patients (**Figure 1C**). Accordingly, a higher amount of serum ANGPT2, the ligand of TIE-2, was shown in melanoma patients and especially in advanced stages (**Figures 1D, E**). As expected, we found that a high level of TIE-2$^+$ M-MDSC (>4.85%) was associated with lower OS as compared to patients with TIE-2^{low} M-MDSC (55% vs 80% alive at 24 months, $p = 0.0078$) (**Figure 1E**). A higher amount of ANGPT2 was also associated with poor outcomes in melanoma (70% vs 87% alive at 24 months, $p = 0.065$), in line with the literature (31–34) (**Figure 1F**). Accordingly, patients exhibiting both TIE-2$^+$ M-MDSC/ANGPT2^{high} profiles had a bad prognosis, and their median OS was 7 months versus not reached in the group TIE-2$^+$ M-MDSC/ANGPT2^{low} ($p = 0.019$) (**Figure 1G**). This negative impact associated with a high TIE-2$^+$ M-MDSC/ANGPT2 environment was mainly related to advanced stages since patients who belonged to stages I and II often had an overall lower level of circulating TIE-2$^+$ M-MDSC or ANGPT2 (**Supplementary Figures 1A, B**).

A High Rate of TIE-2$^+$ Monocytic Myeloid-Derived Suppressor Cells is Associated with An Impairment of Melanoma-Specific T-Cell Responses

The above results suggest that the deleterious effect of TIE-2$^+$ M-MDSC may be related to their inhibitory effect on antitumor

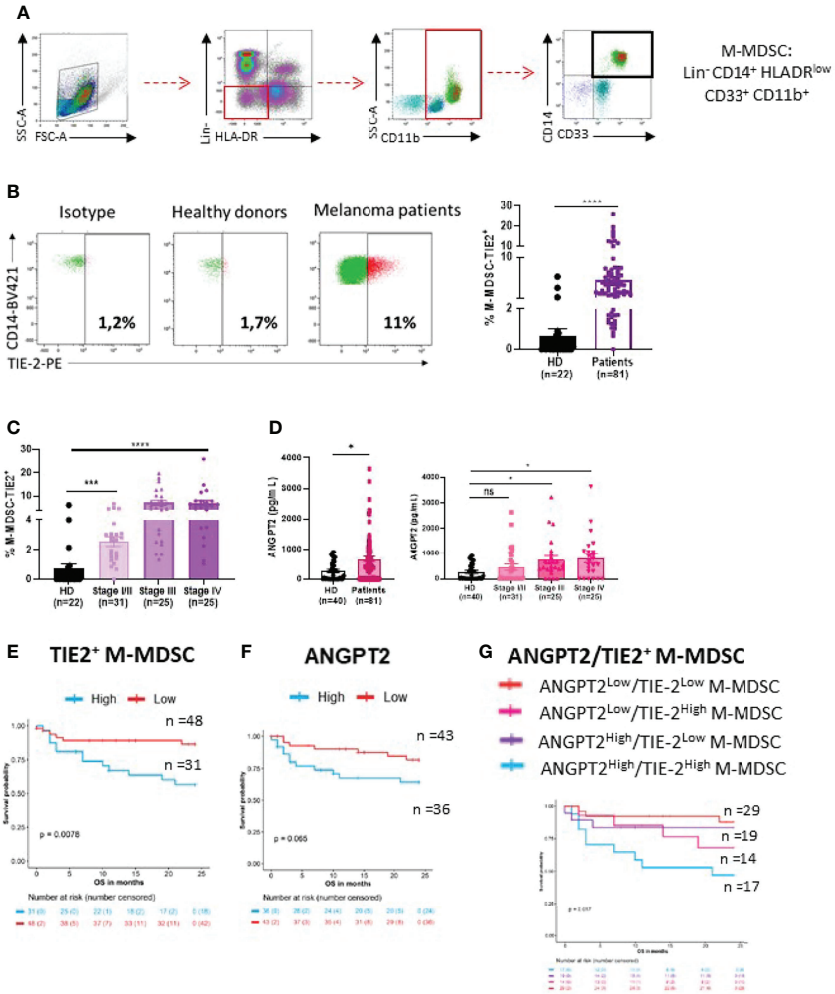

FIGURE 1 | Distribution of TIE-2$^+$ M-MDSC and ANGPT2 in melanoma patients. **(A)** Gating strategy of M-MDSC (Lineage$^-$, HLA-DR^{low}, CD11b$^+$, CD33$^+$ and CD14$^+$). **(B)** Left, representative dot plot of TIE-2 expressed on M-MDSC from 1 healthy donor (HD) versus 1 melanoma patient gated with isotype; right, percentage of TIE-2$^+$ M-MDSC in HD (n = 22) and in patients (n = 81) (Student's t-test, ****p < 0.0001). **(C)** Percentage of TIE-2$^+$ M-MDSC according to melanoma disease stages (Student's t-test, ***p<0.001, ****p < 0.0001). **(D)** Left, level of ANGPT2 serum measured in HD (n = 22) and patient (n = 81); right, according to the disease stage (Student's t-test, *p < 0.01). **(E–G)** Association between overall survival (OS) and percentage of TIE-2$^+$ M-MDSC **(E)**, ANGPT2 concentration **(F)**, and the combination of both parameters **(G)**. **(E)** Kaplan–Meier curves according to percentage of TIE-2$^+$ M-MDSC in overall population (p = 0.0079). Thresholds were determined according to the restricted cubic spline method (4.85%). **(F)** Kaplan–Meier curves according to concentration of ANGPT2 in overall population (p = 0.062). Thresholds were determined according to the restricted cubic spline method (439.5 pg/ml). **(G)** Patients were classified into 4 distinct groups according to the level of TIE-2$^+$ M-MDSC and ANGPT2 concentration. Kaplan–Meier curves for the 4 groups in overall population (p = 0.017). ns, no signigicant.

T-cell responses, as previously described (14). To investigate this purpose, we measured spontaneous T-cell responses directed against a mixture of peptides derived from hTERT and NY-ESO-1, two tumor antigens highly expressed in melanoma or with virus-derived peptides used as non-tumor antigens (36–38). The frequencies of responder patients to hTERT and NY-ESO1 measured by INF-γ ELISpot assay were 46% (37/80) and 27.3% of patients (21/77), respectively (**Figure 2A**). Overall, 47% of patients responded to at least one antigen, and 16% responded against the two antigens. The frequency of immune responders against one and two melanoma-associated antigens was equivalent regardless of the melanoma stage (**Figures 2B, C**). In contrast to stage I/II patients, we found that in the advanced stage III/IV group, non-responder patients exhibited a high level of TIE-2$^+$ M-MDSC than responder patients (8.4 vs 5.4%, p < 0.03). A similar trend was found with mean fluorescence intensity (MFI) value of TIE-2 expression on M-MDSC: mean MFI 816 vs 1,001 in immune responders and non-responders, respectively (** p < 0.01) (**Figure 2D**). Similar trends were made with the ANGPT2 level in these two groups of localized or advanced patients (**Figure 2E**). As a result, we found that the majority of patients (>90%) had functional melanoma-specific T-cell responses in the group of patients with TIE-2$^+$ M-MDSC/ANGPT2^{low}

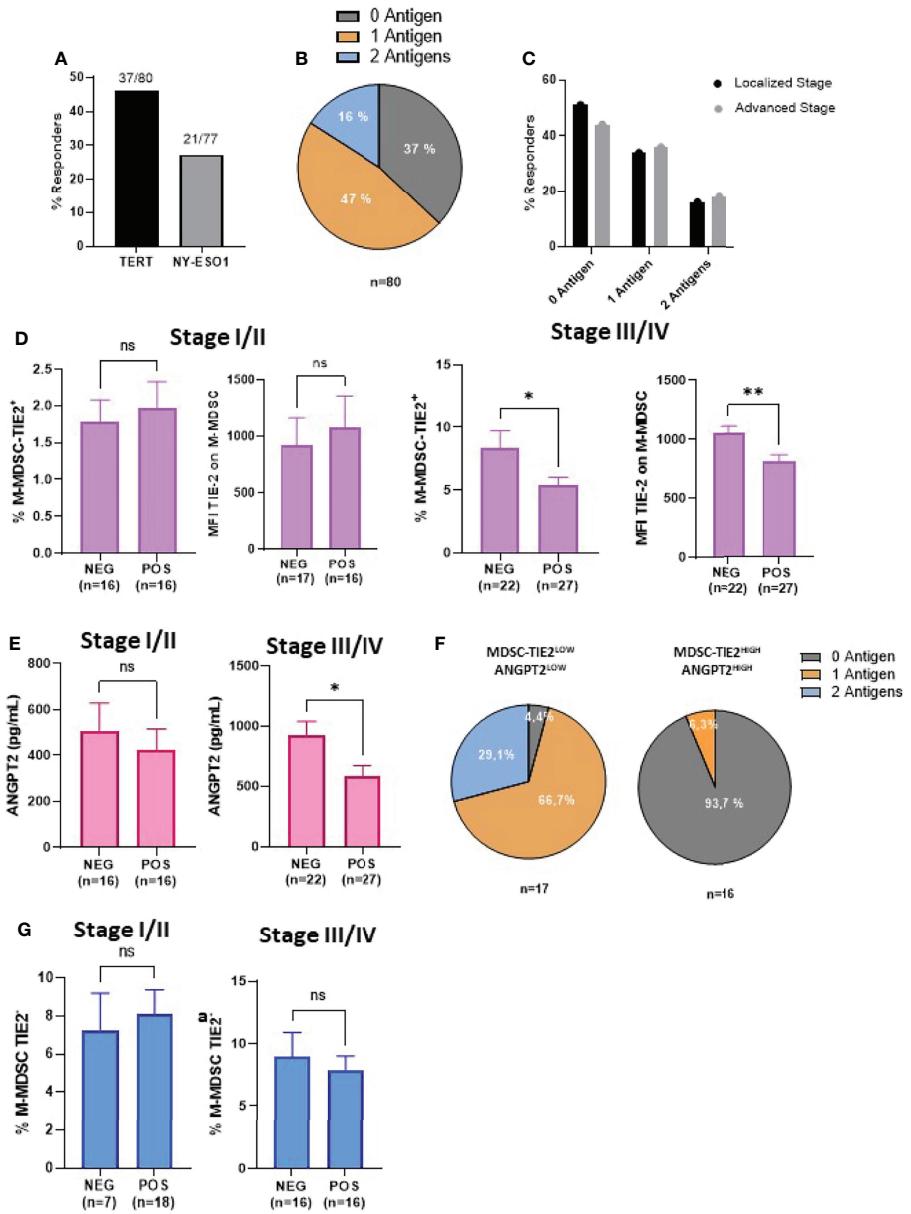

FIGURE 2 | Correlation between TIE-2^{+} M-MDSC/ANGPT2 and antitumor-specific T-cell responses in melanoma patients. **(A)** Frequency of patients exhibiting spontaneous T-cell responses against TERT (37/80) or NY-ESO1 (21/77) antigens by IFN-γ ELISpot assay. **(B)** Distribution of patients according to their antitumor responding responses against 0, 1, or 2 antigens (n = 80). **(C)** Responders' frequency to 0, 1, or 2 antigens between localized or advanced stages. **(D)** TIE-2^{+} M-MDSC percentage and TIE-2 MFI expression according to antitumor T-cell response negative (NEG) or positive (POS) in localized stage (I–II) (left) and in advanced stage (III–IV) (right) (Student's t-test, * $p < 0.1$). **(E)** ANGPT2 concentration according to antitumor T-cell response negative (NEG) or positive (POS) in localized stage (I–II) (left) and in advanced stage (III–IV) (right) (Student's t-test, *$p < 0.1$, **$p < 0.01$). **(F)** Distribution of antitumor T-cell responses in TIE-2^{high} M-MDSCs, ANGPT2^{high} (n = 16) vs TIE-2^{low} M-MDSCs, and ANGPT2^{low} (n = 17). **(G)** TIE-2^{neg} M-MDSC percentage according to antitumor T-cell response negative (NEG) or positive (POS) in localized stage (I–II) (left) and in advanced stage (III–IV) (right) (Student's t-test, *$p < 0.1$). ns, no signigicant.

profile, whereas only 6% of patients with TIE-2^{+} M-MDSC/ANGPT2^{high} had a preexisting antitumor T-cell response (**Figure 2F**).

Of note is that no obvious relationship was shown between the antiviral T-cell responses and TIE-2^{+} M-MDSC or ANGPT2 (**Supplementary Figures 2A–C**). Furthermore, no correlation was observed between TIE-2^{neg} M-MDSC and melanoma-specific T-cell response in this population (**Figure 2G**). Thus, a high level of TIE-2^{+} M-MDSC/ANGPT2 in peripheral blood is associated with impaired antitumor T-cell responses in advanced melanoma, suggesting that this proangiogenic pathway may suppress tumor-specific T cell in melanoma.

ANGPT2 Increases Immune Suppressive Features of TIE-2^{+} Monocytic Myeloid-Derived Suppressor Cells

To scrutinize the inhibitory role of the TIE-2^{+} M-MDSC/ANGPT2 axis, we analyzed the expression of inhibitory pathways related to suppressive cells (2, 10–13, 39) on TIE-2^{+} M-MDSCs using flow cytometry. We showed that TIE-2^{+} M-MDSCs expressed a higher level of PD-L1 and CD73 but not of CD39 than TIE-2^{neg} M-MDSC (**Figures 3A–C**). Next, we performed intracellular staining of suppressive factors such as Arg1, IL-10, and TGF-β on TIE-2^{+} versus TIE-2^{neg} M-MDSC. Although increased IL-10 and TGF-β expression levels were detected on TIE-2^{+} M-MDSC, no obvious change was observed for Arg1 expression (**Figures 3D–F**). In contrast, the expression of iNOS and COX2 appeared lower in TIE-2^{+} as compared to TIE-2^{neg} M-MDSC (**Figures 3G, H**). We demonstrated that the *in vitro* exposition of TIE-2^{+} M-MDSC to recombinant ANGPT2 stimulation enhanced the expression of most of these inhibitory pathways, mainly PD-L1 and Arg1, but did not influence the expression of iNOS and COX2 in TIE-2^{+} M-MDSC. As expected, ANGPT2 had no effect on TIE-2^{neg} M-MDSC (**Figure 3I** and **Supplementary Figure 3A**), suggesting the upregulation of these suppressive factors involved in TIE-2 signaling. Furthermore, we showed that ANGPT2 treatment of M-MDSC TIE-2 also upregulated transcripts such as Arg1, TIE-2, and CD39 in line

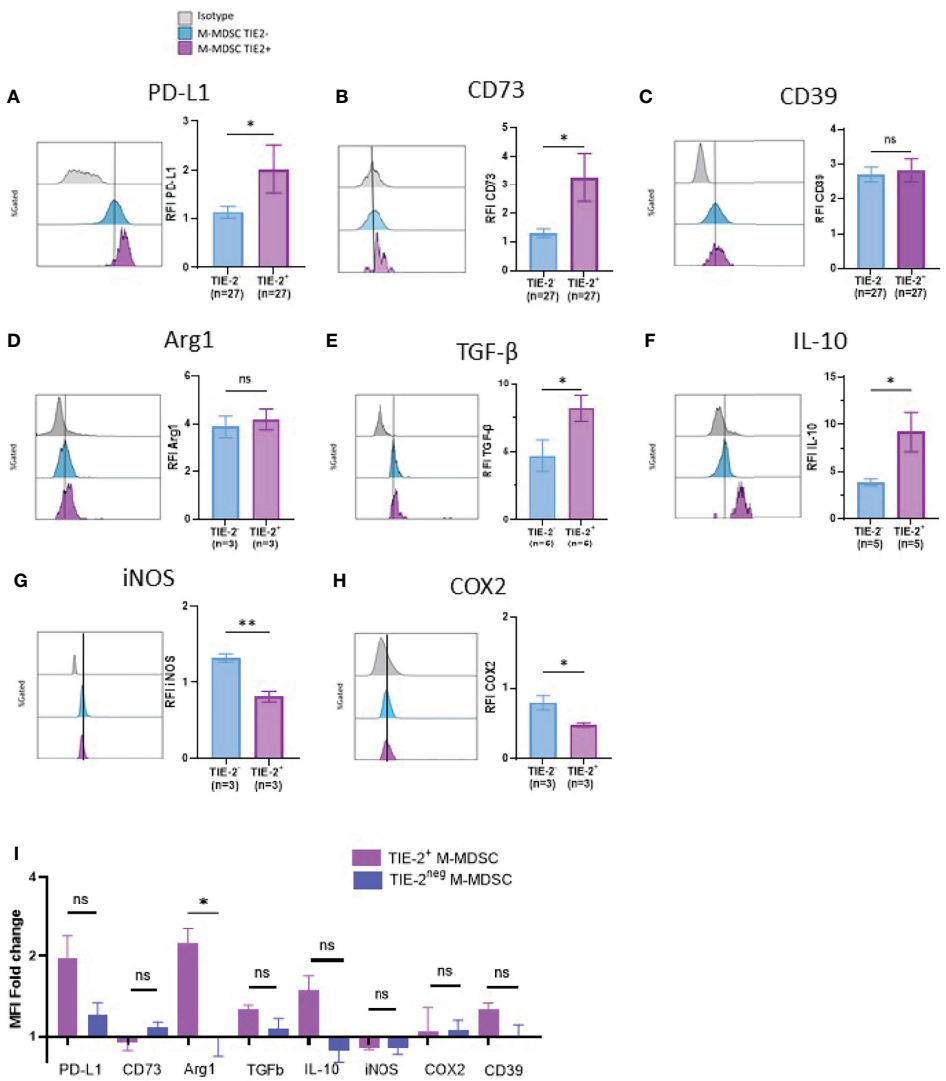

FIGURE 3 | Immune suppressive factors of TIE-2^{+} M-MDSC. **(A–H)** Expression of different proteins (PD-L1, CD39, CD73, Arg1, TGF-β, IL-10, iNOS, and COX2) was studied in TIE-2^{+} M-MDSC (TIE-2^{+}) and TIE-2^{-} M-MDSC (TIE-2^{-}). Left, histogram overlay from one representative patient of the mean fluorescence intensity (MFI) of different proteins; right, relative fluorescence intensity (RFI) of these proteins (Mann–Whitney test, *p < 0.1). **(I)** TIE-2^{+} M-MDSC enriched melanoma patients' peripheral blood mononuclear cells (PBMCs) were stimulated or not with 300 ng/ml of ANGPT2 overnight, and the expression of the different immunosuppressive proteins was analyzed by flow cytometry. Histograms of the MFI fold change. ns, no signigicant.

with protein level (**Supplementary Figure 3B**). Thus, ANGPT2 enhances suppressive pathways in TIE-2^{+} M-MDSC.

ANGPT2/TIE-2 Signaling on Monocytic Myeloid-Derived Suppressor Cells Inhibits IFN-γ Production by Melanoma-Specific T Cells

To study the involvement of ANGPT2/TIE-2^{+} M-MDSC in the inhibition of antitumor T-cell function, we first performed *in vitro* stimulation on PBMCs from patients with elevated levels of TIE-2^{+} M-MDSCs in the presence or not of recombinant ANGPT2 (**Figure 4A**). Immune responder patients were selected, and hTERT and NY-ESO1 derived HLA class I binding peptides were used for T-cell stimulation. As shown in **Figure 4B**, IFN-γ production of tumor-specific CD8 T-cell responses significantly decreased in the presence of ANGPT2. Similar results were obtained against tumor-specific CD4 T-cell response (**Supplementary Figure 4**). In contrast, ANGPT2 had no effect on tumor-specific T-cell response in the context of TIE-2^{low} M-MDSC patients (**Figures 4C, D**).

To demonstrate that ANGPT2 acts through TIE-2^{+} signaling, we performed similarly *in vitro* stimulation experiments in the presence or not of TIE-2 kinase inhibitors such as rebastinib and regorafenib (40–42). Dasatinib, a BCR-ABL kinase inhibitor, was used as a control (**Figure 4E**). The results showed that, in contrast to dasatinib, the addition of both regorafenib and rebastinib effectively restored the IFN-γ production by tumor-specific T cells inactivated by ANGPT2 exposition (**Figure 4F**). In the absence of ANGPT2, the TIE-2 inhibitors did not affect IFN-γ production by melanoma-specific T cells (**Figure 4G**). Thus, TIE-2^{+} signaling activation on M-MDSC through ANGPT2 binding inhibits IFN-γ secretion by tumor-reactive T-cells.

DISCUSSION

In this study, we showed that circulating TIE-2^{+} M-MDSC in melanoma patients displayed high immunosuppressive patterns than the TIE-2^{neg} counterpart and were accumulated in

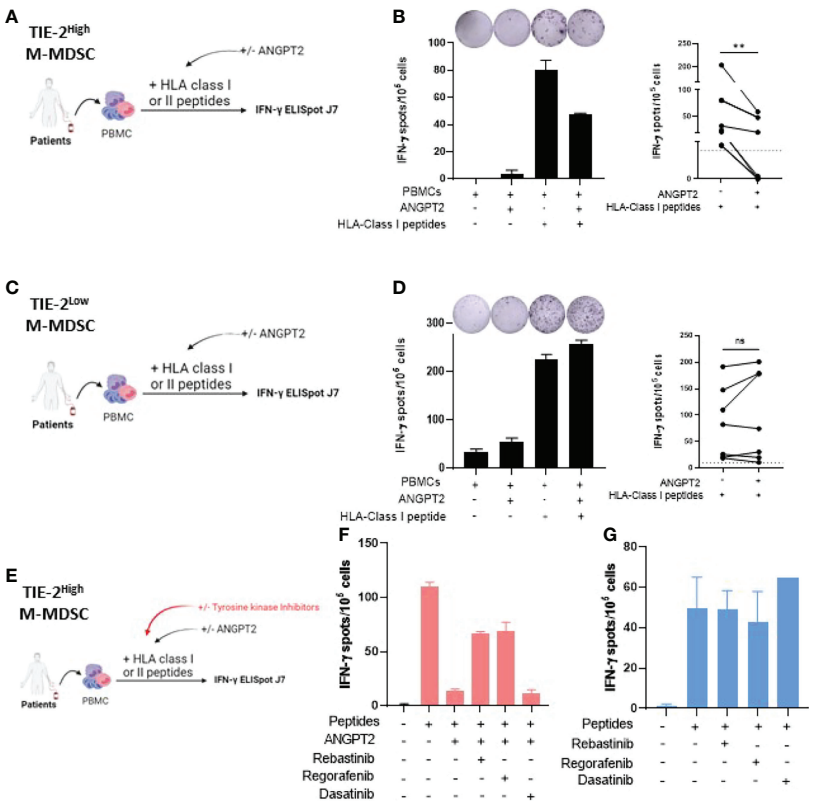

FIGURE 4 | Effect of ANGPT2/TIE-2 signaling on M-MDSC on antitumor responses. **(A)** Peripheral blood mononuclear cells (PBMCs) from melanoma patients with TIE-2^{high} M-MDSC were stimulated with TERT class I peptides in presence or not of 300 ng/ml of ANGPT2, and an IFN-γ ELISpot assay was performed. **(B)** Left, IFN-γ T-cell responses of one representative example of patient; right, histograms from 6 patients (Wilcoxon test, **p < 0.01). **(C)** PBMCs from melanoma patients with TIE-2^{low} M-MDSC were stimulated with TERT class I peptides in presence or not of 300 ng/ml of ANGPT2, and an IFN-γ ELISpot assay was performed. **(D)** Left, IFN-γ T-cell responses of one representative example of patient; right, histograms from 8 patients (Wilcoxon test, **p < 0.01). **(E)** PBMCs from melanoma patients with TIE-2^{high} M-MDSC were stimulated with TERT class I or class II peptides in presence or not of ANGPT2 and in presence or not of TIE-2 inhibitors, and then an IFN-γ ELISpot was performed. **(F)** Histograms of IFN-γ T-cell responses in presence of ANGPT2 (n = 6). **(G)** Histograms of IFN-γ T-cell responses in the absence of ANGPT2 (n = 6). ns, no signigicant. ns, no signigicant.

advanced stages. The high rate of these cells was associated with low melanoma-specific T-cell responses, and ANGPT2 increases the ability of TIE-2^+ M-MDSC to suppress melanoma-specific T-cell functions. We demonstrated that the involvement of TIE-2 kinase activation in T-cell inhibition is mediated by TIE-2^+ M-MDSC. As a result, a high level of TIE-2^+ M-MDSC together with ANGPT2 in peripheral blood was associated with a very poor prognosis.

These results confirmed the negative impact on clinical outcomes in melanoma as we previously reported in lung cancer patients (14). This population of TIE-2^+ M-MDSC is distinct from the previously described TEMs, which are characterized by the expression of $CD16^+$, $CD14^{low}$, $HLADR^+$, and $CD62L^-$ (43). These cells were previously found in the tumor microenvironment and peripheral blood (23).

Here, we found that TIE-2 expression on M-MDSC enhances the suppressive features of M-MDSC such as the overexpression of PD-L1, CD73, IL-10, and TGF-β, which are proteins involved in their inhibitory roles (44–46). The addition of ANGPT2 also enhances the expression of many of these inhibitory pathways including Arg1, which is known to promote essential amino acid L-arginine depletion and in turn suppresses T cells. This effect was also described in TEMs, which overexpressed IL-10 after ANGPT2 stimulation (25). In contrast, the expression of other immune-suppressive molecules, such as iNOS and COX2, was not influenced by TIE-2 kinase signaling. Similar observations were previously reported in the case of TEMs in a mouse tumor model by using transcriptomic analysis. The authors showed a high level of Arg1 transcript but lower COX2 and iNOS in TEMs (47).

These phenotypic changes of M-MDSC mediated by TIE-2 signaling after ANGPT2 stimulation toward a highly immunosuppressive role were thereby confirmed by the functional profiling. Hence, in line with our previous report (14), we showed the effect of ANGPT2 stimulation enhanced the capacity of TIE-2^+ M-MDSC to suppress melanoma-specific T-cell function *in vitro*. This is also in accordance with the complete impairment of spontaneous anti-melanoma T-cell responses observed in melanoma patients harboring both ANGPT2 and TIE-2^+ M-MDSC-rich blood.

Although the precise mechanism by which TIE-2 intracellular pathway mediates IFN-γ production by T cells is not yet elucidated, we demonstrated that this involved an active TIE-2 signaling, since the use of TIE-2 kinase-specific inhibitors restored this ability of tumor-specific T-cells. In our experiments, we cannot exclude the possible participation of TEMs in the inhibitory role exerted by ANGPT2 on T-cell responses. Nevertheless, our preliminary finding by using co-culture of antitumor T-cell clone with TIE-2^+ cells sorted from PBMCs suggests that M-MDSC displayed more suppressive capacity than TEMs. However, these observations deserve future investigations.

In conclusion, this study in melanoma shows the ability of TIE-2^+ M-MDSC to suppress antitumor T-cell function through ANGPT2 stimulation. Together with our first report, our results support that TIE-2^+ M-MDSC/ANGPT2 signature represents a tumor escape mechanism across human cancers. Our finding also encourages combining TIE-2 inhibitors with immunotherapy in melanoma.

DATA AVAILABILITY STATEMENT

The raw data supporting the conclusions of this article will be made available by the authors upon reasonable request.

ETHICS STATEMENT

The studies involving human participants were reviewed and approved by CPP EST-II (France). The patients/participants provided their written informed consent to participate in this study.

AUTHOR CONTRIBUTIONS

AM, BL, MM, LB, and AR realized experiment. All authors provided inputs on the data analyses. AM, CL. and OA wrote the first draft of the manuscript. All authors contributed to the article and approved the submitted version.

FUNDING

This work was supported by La ligue contre le cancer (Grand Est, call for projets 2020, OPE= 2021-0009) and by the Région Bourgogne Franche-Comté (Grand ISIT 2019).

ACKNOWLEDGMENTS

We thank all the patients, the medical doctors, and the nurses from the oncologic Department and Dermatology Department of the University Hospital of Besançon. We also thank the Biomonitoring platform of CIC-1431 and the French Blood Establishment (EFS).

SUPPLEMENTARY MATERIAL

The Supplementary Material for this article can be found online at: https://www.frontiersin.org/articles/10.3389/fimmu.2022.932298/full#supplementary-material

Supplementary Table 1 | Melanoma patients' main clinical characteristics.

Supplementary Figure 1 | Overall survival of ANGPT2/TIE-2^+ M-MDSC according to the melanoma disease stage. **(A)** Association between overall survival (OS) and the percentage of TIE-2^+ M-MDSC according to the melanoma disease stage. Kaplan–Meier curves according to percentage of TIE-2^+ M-MDSC in localized stage (I-II, p = 0.71) and in advanced stage (III-IV, p = 0.18). Threshold were determined according to the Restrictped Cubic Spline method (4.85%). **(B)** Association between OS and the concentration of ANGPT2. Kaplan–Meier curves according to concentration of ANGPT2 in localized stage (p = 0.33) and in advanced stage (p = 0.067). Threshold were determined according to the Restricted Cubic Spline method (439.5 pg/mL). **(C)** Patients were classified into 2 distinct groups according to the level of TIE-

2^+ M-MDSC and ANGPT2 concentration in advanced stage. Kaplan–Meier curves for the 2 groups in advanced stages (p = 0.043).

Supplementary Figure 2 | Correlation between TIE-2^+ M-MDSC/ANGPT2 and anti-viral T cell responses in melanoma patients. **(A)** TIE-2^+ M-MDSCs percentage according to antiviral T cells response negative (NEG) or positive (POS) in localized stage (I-II) (right) and in advanced stage (III-IV) (left) (Student T test *p <0,1). **(B)** ANGPT2 concentration according to antiviral T cells response negative (NEG) or positive (POS) in localized stage (I-II) (right) and in advanced stage (III-IV) (left) (Student T test * p <0,1). **(C)** TIE-2^{neg} M-MDSCs percentage according to antiviral T cells response negative (NEG) or positive (POS) in localized stage (I-II) (right) and in advanced stage (III-IV) (left) (Student T test *p <0,1)

Supplementary Figure 3 | Immune suppressive factors of TIE-2^+M-MDSC. **(A)** MFI expression of different proteins (PD-L1, CD39, CD73, Arg1, TGF-β, IL-10, iNOS and COX2) studied in TIE-2^+ M-MDSC and in TIE-2^{neg} M-MDSC after or not exposition to ANGPT2. **(B)** mRNA expression of different gene (TIE-2, CD73, Arg1, IL-10, STAT3 and CD39) were analyzed by RT-qPCR in TIE-2^{High} and TIE-2^{Low} M-MDSC and the fold change after ANGPT2 exposition was calculated.

Supplementary Figure 4 | Effect of ANGPT2/TIE-2 signaling on M-MDSC on anti-tumor responses. PBMCs from melanoma patients with TIE2^{High} M-MDSC were stimulated with TERT class II peptides in presence or not of 300 ng/mL ANGPT2 and an IFN-γ ELISpot assay was performed. IFN-γ T cell responses, in left, one representative example of patient; in right, histograms from 6 patients respectively (Wilcoxon test **p< 0,01; *p<0,1).

REFERENCES

1. Veglia F, Perego M, Gabrilovich D. Myeloid-Derived Suppressor Cells Coming of Age. *Nat Immunol* (2018) 19(2):108–19. doi: 10.1038/s41590-017-0022-x
2. Gabrilovich DI. Myeloid-Derived Suppressor Cells. *Cancer Immunol Res* (2017) 5(1):3–8. doi: 10.1158/2326-6066.CIR-16-0297
3. Zitvogel L, Pietrocola F, Kroemer G. Nutrition, Inflammation and Cancer. *Nat Immunol* (2017) 18(8):843–50. doi: 10.1038/ni.3754
4. Solito S, Marigo I, Pinton L, Damuzzo V, Mandruzzato S, Bronte V. Myeloid-Derived Suppressor Cell Heterogeneity in Human Cancers. *Ann New York Acad Sci* (2014) 1319(1):47–65. doi: 10.1111/nyas.12469
5. Condamine T, Ramachandran I, Youn J-I, Gabrilovich DI, et al. Regulation of Tumor Metastasis by Myeloid-Derived Suppressor Cells. *Annu Rev Med* (2015) 66(1):97–110. doi: 10.1146/annurev-med-051013-052304
6. Marvel D, Gabrilovich DI. Myeloid-Derived Suppressor Cells in the Tumor Microenvironment: Expect the Unexpected. *J Clin Invest* (2015) 125(9):3356–64. doi: 10.1172/JCI80005
7. Xie F, Ling L, van Dam H, Zhou F, Zhang L. TGF-β Signaling in Cancer Metastasis. *Acta Biochim Biophys Sin* (2018) 50(1):121–32. doi: 10.1093/abbs/gmx123
8. Ostrand-Rosenberg S, Fenselau C. Myeloid-Derived Suppressor Cells: Immune-Suppressive Cells That Impair Antitumor Immunity and Are Sculpted by Their Environment. *J Immunol* (2018) 200(2):422–31. doi: 10.4049/jimmunol.1701019
9. Kumar V, Patel S, Tcyganov E, Gabrilovich DI. The Nature of Myeloid-Derived Suppressor Cells in the Tumor Microenvironment. *Trends Immunol* (2016) 37(3):208–20. doi: 10.1016/j.it.2016.01.004
10. Huang B, Pan P-Y, Li Q, Sato AI, Levy DE, Bromberg J, et al. Gr-1+CD115+ Immature Myeloid Suppressor Cells Mediate the Development of Tumor-Induced T Regulatory Cells and T-Cell Anergy in Tumor-Bearing Host. *Cancer Res* (2006) 66(2):1123–31. doi: 10.1158/0008-5472.CAN-05-1299
11. Beury DW, Parker KH, Nyandjo M, Sinha P, Carter KA, Ostrand-Rosenberg S. Cross-Talk Among Myeloid-Derived Suppressor Cells, Macrophages, and Tumor Cells Impacts the Inflammatory Milieu of Solid Tumors. *J Leuk Biol* (2014) 96(6):1109–18. doi: 10.1189/jlb.3A0414-210R
12. Wang R, Green DR. Metabolic Checkpoints in Activated T Cells. *Nat Immunol* (2012) 13(10):907–15. doi: 10.1038/ni.2386
13. Hoskin DW, Mader JS, Furlong SJ, Conrad DM, Blay J. Inhibition of T Cell and Natural Killer Cell Function by Adenosine and its Contribution to Immune Evasion by Tumor Cells (Review). *Int J Oncol* (2008) 32(3):527–35. doi: 10.3892/ijo.32.3.527
14. Joseph ELM, Laheurte C, Jary M, Boullerot L, Asgarov K, Gravelin E, et al. Immunoregulation and Clinical Implications of ANGPT2/TIE2+ M-MDSC Signature in Non–Small Cell Lung Cancer. *Cancer Immunol Res* (2020) 8 (2):268–79. doi: 10.1158/2326-6066.CIR-19-0326
15. Dumont DJ, et al. Tek, a Novel Tyrosine Kinase Gene Located on Mouse Chromosome 4, is Expressed in Endothelial Cells and Their Presumptive Precursors. *Oncogene* (1992) 7(8):1471–80.
16. Duran CL, Borriello L, Karagiannis GS, Entenberg D, Oktay MH, Condeelis JS, et al. Targeting Tie2 in the Tumor Microenvironment: From Angiogenesis to Dissemination. *Cancers* (2021) 13(22):5730. doi: 10.3390/cancers13225730
17. Oh H, Takagi H, Suzuma K, Otani A, Matsumura M, Honda Y. Hypoxia and Vascular Endothelial Growth Factor Selectively Up-Regulate Angiopoietin-2 in Bovine Microvascular Endothelial Cells *. *J Biol Chem* (1999) 274 (22):15732–9. doi: 10.1074/jbc.274.22.15732
18. Pichiule P, Chavez JC, LaManna JC. Hypoxic Regulation of Angiopoietin-2 Expression in Endothelial Cells *. *J Biol Chem* (2004) 279(13):12171–80. doi: 10.1074/jbc.M305146200
19. De Luca A, Gallo M, Aldinucci D, Ribatti D, Lamura L, D'Alessio A, et al. Role of the EGFR Ligand/Receptor System in the Secretion of Angiogenic Factors in Mesenchymal Stem Cells. *J Cell Physiol* (2011) 226(8):2131–8. doi: 10.1002/jcp.22548
20. Chen J-X, Chen Y, DeBusk L, Lin W, Lin PC. Dual Functional Roles of Tie-2/Angiopoietin in TNF-α-Mediated Angiogenesis. *Am J Physiol Heart Circulatory Physiol* (2004) 287(1):H187–95. doi: 10.1152/ajpheart.01058.2003
21. Kinnen A, Klaschik S, Neumann C, Egger E-K, Mustea A, Soehle M, et al. Gene Expression in the Angiopoietin/TIE Axis is Altered in Peripheral Tissue of Ovarian Cancer Patients: A Prospective Observational Study. *Life Sci* (2021) 274:119345. doi: 10.1016/j.lfs.2021.119345
22. Hou Y, Jia H, Cao Y, Zhang S, Zhang X, Wei P, et al. LncRNA EPIC1 Promotes Tumor Angiogenesis *via* Activating the Ang2/Tie2 Axis in non-Small Cell Lung Cancer. *Life Sci* (2021) 267:118933. doi: 10.1016/j.lfs.2020.118933
23. De Palma M, Venneri MA, Galli R, Sergi LS, Politi LS, Sampaolesi M, et al. Tie2 Identifies a Hematopoietic Lineage of Proangiogenic Monocytes Required for Tumor Vessel Formation and a Mesenchymal Population of Pericyte Progenitors. *Cancer Cell* (2005) 8(3):211–26. doi: 10.1016/j.ccr.2005.08.002
24. De Palma M, Murdoch C, Venneri MA, Naldini L, Lewis CE. Tie2-Expressing Monocytes: Regulation of Tumor Angiogenesis and Therapeutic Implications. *Trends Immunol* (2007) 28(12):519–24. doi: 10.1016/j.it.2007.09.004
25. Coffelt SB, Chen Y-Y, Muthana M, Welford AF, Tal AO, Scholz A, et al. Angiopoietin 2 Stimulates TIE2-Expressing Monocytes To Suppress T Cell Activation and To Promote Regulatory T Cell Expansion. *J Immunol* (2011) 186(7):4183–90. doi: 10.4049/jimmunol.1002802
26. Mazzieri R, Pucci F, Moi D, Zonari E, Ranghetti A, Berti A, et al. Targeting the ANG2/TIE2 Axis Inhibits Tumor Growth and Metastasis by Impairing Angiogenesis and Disabling Rebounds of Proangiogenic Myeloid Cells. *Cancer Cell* (2011) 19(4):512–26. doi: 10.1016/j.ccr.2011.02.005
27. Turrini R, Pabois A, Xenarios I, Coukos G, Delaloye J-F, Doucey M-A. TIE-2 Expressing Monocytes in Human Cancers. *Oncoimmunology* (2017) 6(4): e1303585. doi: 10.1080/2162402X.2017.1303585
28. Atanasov G, Pötner C, Aust G, Schierle K, Dietel C, Benzing C, et al. TIE2-Expressing Monocytes and M2-Polarized Macrophages Impact Survival and Correlate With Angiogenesis in Adenocarcinoma of the Pancreas. *Oncotarget* (2018) 9(51):29715–26. doi: 10.18632/oncotarget.25690
29. Godet Y, Fabre E, Dosset M, Lamuraglia M, Levionnois E, Ravel P, et al. Analysis of Spontaneous Tumor-Specific CD4 T-Cell Immunity in Lung Cancer Using Promiscuous HLA-DR Telomerase-Derived Epitopes: Potential Synergistic Effect With Chemotherapy Response. *Clin Cancer Res* (2012) 18(10):2943–53. doi: 10.1158/1078-0432.CCR-11-3185
30. Laheurte C, Galaine J, Beziaud L, Dosset M, Kerzerho J, Jacquemard C, et al. Immunoprevalence and Magnitude of HLA-DP4 Versus HLA-DR-Restricted Spontaneous CD4+ Th1 Responses Against Telomerase in Cancer Patients. *OncoImmunology* (2016) 5(5):e1137416. doi: 10.1080/2162402X.2015.1137416

31. Bronte V, Brandau S, Chen S-H, Colombo MP, Frey AB, Greten TF, et al. Recommendations for Myeloid-Derived Suppressor Cell Nomenclature and Characterization Standards. *Nat Commun* (2016) 7:12150. doi: 10.1038/ncomms12150
32. Helfrich I, Edler L, Sucker A, Thomas M, Christian S, Schadendorf D, et al. Angiopoietin-2 Levels Are Associated With Disease Progression in Metastatic Malignant Melanoma. *Clin Cancer Res* (2009) 15(4):1384–92. doi: 10.1158/1078-0432.CCR-08-1615
33. Xu Y, Zhang Y, Wang Z, Chen N, Zhou J, Liu L. The Role of Serum Angiopoietin-2 Levels in Progression and Prognosis of Lung Cancer: A Meta-Analysis. *Medicine* (2017) 96(37):e8063. doi: 10.1097/MD.0000000000008063
34. Pari AAA, Singhal M, Hübers C, Mogler C, Schieb B, Gampp A, et al. Tumor Cell–Derived Angiopoietin-2 Promotes Metastasis in Melanoma. *Cancer Res* (2020) 80(12):2586–98. doi: 10.1158/0008-5472.CAN-19-2660
35. Jary M, Hasanova R, Vienot A, Asgarov K, Loyon R, Tirole C, et al. Molecular Description of ANGPT2 Associated Colorectal Carcinoma. *Int J Cancer* (2020) 147(7):2007–18. doi: 10.1002/ijc.32993
36. Nardin C, Laheurte C, Puzenat E, Boullerot L, Ramseyer M, Marguier A, et al. Naturally Occurring Telomerase-Specific CD4 T-Cell Immunity in Melanoma. *J Invest Dermatol* (2022) 142(2):435–44. doi: 10.1016/j.jid.2021.07.160
37. Lee S, Opresko P, Pappo A, Kirkwood JM, Bahrami A. Association of TERT Promoter Mutations With Telomerase Expression in Melanoma. *Pigment Cell Melanoma Res* (2016) 29(3):391–3. doi: 10.1111/pcmr.12471
38. Aung PP, Liu Y-C, Ballester LY, Robbins PF, Rosenberg SA, Lee C-CR. Expression of NY-ESO-1 in Primary and Metastatic Melanoma. *Hum Pathol* (2014) 45(2):259–67. doi: 10.1016/j.humpath.2013.05.029
39. Noman MZ, Desantis G, Janji B, Hasmim M, Karray S, Dessen P, et al. PD-L1 is a Novel Direct Target of HIF-1α, and its Blockade Under Hypoxia Enhanced MDSC-Mediated T Cell Activation. *J Exp Med* (2014) 211(5):781–90. doi: 10.1084/jem.20131916
40. Todesca P, Marzi L, Critelli RM, Cuffari B, Caporali C, Turco L, et al. Angiopoietin-2/Tie2 Inhibition by Regorafenib Associates With Striking Response in a Patient With Aggressive Hepatocellular Carcinoma. *Hepatology* (2019) 70(2):745–7. doi: 10.1002/hep.30588
41. Mross K, Frost A, Steinbild S, Hedbom S, Büchert M, Fasol U, et al. A Phase I Dose–Escalation Study of Regorafenib (BAY 73–4506), an Inhibitor of Oncogenic, Angiogenic, and Stromal Kinases, in Patients With Advanced Solid Tumors. *Clin Cancer Res* (2012) 18(9):2658–67. doi: 10.1158/1078-0432.CCR-11-1900
42. Harney AS, Karagiannis GS, Pignatelli J, Smith BD, Kadioglu E, Wise SC, et al. The Selective Tie2 Inhibitor Rebastinib Blocks Recruitment and Function of Tie2Hi Macrophages in Breast Cancer and Pancreatic Neuroendocrine Tumors. *Mol Cancer Ther* (2017) 16(11):2486–501. doi: 10.1158/1535-7163.MCT-17-0241
43. Venneri MA, Palma MD, Ponzoni M, Pucci F, Scielzo C, Zonari E, et al. Identification of Proangiogenic TIE2-Expressing Monocytes (TEMs) in Human Peripheral Blood and Cancer. *Blood* (2007) 109(12):5276–85. doi: 10.1182/blood-2006-10-053504
44. Okła K, Rajtak A, Czerwonka A, Bobiński M, Wawruszak A, Tarkowski R, et al. Accumulation of Blood-Circulating PD-L1-Expressing M-MDSCs and Monocytes/Macrophages in Pretreatment Ovarian Cancer Patients is Associated With Soluble PD-L1. *J Trans Med* (2020) 18:220. doi: 10.1186/s12967-020-02389-7
45. Li J, Wang L, Chen X, Li L, Li Y, Ping Y, et al. CD39/CD73 Upregulation on Myeloid-Derived Suppressor Cells *via* TGF-β-mTOR-HIF-1 Signaling in Patients With non-Small Cell Lung Cancer. *Oncoimmunology* (2017) 6(6):e1320011. doi: 10.1080/2162402X.2017.1320011
46. Mao Y, Sarhan D, Steven A, Seliger B, Kiessling R, Lundqvist A, et al. Inhibition of Tumor-Derived Prostaglandin-E2 Blocks the Induction of Myeloid-Derived Suppressor Cells and Recovers Natural Killer Cell Activity. *Clin Cancer Res* (2014) 20(15):4096–106. doi: 10.1158/1078-0432.CCR-14-0635
47. Pucci F, Venneri MA, Biziato D, Nonis A, Moi D, Sica A, et al. A Distinguishing Gene Signature Shared by Tumor-Infiltrating Tie2-Expressing Monocytes, Blood "Resident" Monocytes, and Embryonic Macrophages Suggests Common Functions and Developmental Relationships. *Blood* (2009) 114(4):901–14. doi: 10.1182/blood-2009-01-200931

Conflict of Interest: The authors declare that the research was conducted in the absence of any commercial or financial relationships that could be construed as a potential conflict of interest.

frontiers | Frontiers in Immunology

TYPE Original Research
PUBLISHED 10 August 2022
DOI 10.3389/fimmu.2022.889075

OPEN ACCESS

EDITED BY
Darya Alizadeh,
City of Hope, United States

REVIEWED BY
Hiroaki Shime,
Nagoya City University, Japan
Sabrin Albeituni,
St. Jude Children's Research Hospital, United States

*CORRESPONDENCE
Panayotis Verginis
pverginis@uoc.gr

SPECIALTY SECTION
This article was submitted to Cancer Immunity and Immunotherapy, a section of the journal Frontiers in Immunology

RECEIVED 03 March 2022
ACCEPTED 07 July 2022
PUBLISHED 10 August 2022

CITATION
Papafragkos I, Grigoriou M, Boon L, Kloetgen A, Hatzioannou A and Verginis P (2022) Ablation of NLRP3 inflammasome rewires MDSC function and promotes tumor regression. *Front. Immunol.* 13:889075. doi: 10.3389/fimmu.2022.889075

Ablation of NLRP3 inflammasome rewires MDSC function and promotes tumor regression

Iosif Papafragkos[1,2], Maria Grigoriou[3], Louis Boon[4], Andreas Kloetgen[5], Aikaterini Hatzioannou[6] and Panayotis Verginis[1,2,3,6]*

[1]Laboratory of Immune Regulation and Tolerance, Division of Basic Sciences, University of Crete Medical School, Heraklion, Greece, [2]Institute of Molecular Biology and Biotechnology, Foundation for Research and Technology, Heraklion, Greece, [3]Center of Clinical, Experimental Surgery and Translational Research, Biomedical Research Foundation Academy of Athens, Athens, Greece, [4]JJP Biologics, Warsaw, Poland, [5]Department of Computational Biology of Infection Research, Helmholtz Centre for Infection Research, Braunschweig, Germany, [6]Institute for Clinical Chemistry and Laboratory Medicine, Faculty of Medicine, Technische Universität Dresden, Dresden, Germany

Myeloid-derived suppressor cells (MDSCs) are myeloid precursors that exert potent immunosuppressive properties in cancer. Despite the extensive knowledge on mechanisms implicated in mobilization, recruitment, and function of MDSCs, their therapeutic targeting remains an unmet need in cancer immunotherapy, suggesting that unappreciated mechanisms of MDSC-mediated suppression exist. Herein, we demonstrate an important role of NLRP3 inflammasome in the functional properties of MDSCs in tumor-bearing hosts. Specifically, *Nlrp3*-deficient mice exhibited reduced tumor growth compared to wild-type animals and induction of robust anti-tumor immunity, accompanied by re-wiring of the MDSC compartment. Interestingly, both monocytic (M-MDSCs) and granulocytic (G-MDSCs) subsets from *Nlrp3*$^{-/-}$ mice displayed impaired suppressive activity and demonstrated significant transcriptomic alterations supporting the loss-of-function and associated with metabolic re-programming. Finally, therapeutic targeting of NLRP3 inhibited tumor development and re-programmed the MDSC compartment. These findings propose that targeting NLRP3 in MDSCs could overcome tumor-induced tolerance and may provide new checkpoints of cancer immunotherapy.

KEYWORDS

myeloid-derived suppressor cells (MDSCs), inflammasome, cancer immunotherapy, tumor immunity, tumor resistance

Introduction

The advent of immune checkpoint inhibitors (ICI) has revolutionized cancer immunotherapy. However, despite the enormous success, a significant proportion of patients do not respond (1), while responses are frequently accompanied by life-threatening autoimmune-related adverse events (irAEs) (2). Mounting evidence suggests that tumoral resistance and development of irAEs are dependent on the immunosuppressive nature of the tumor microenvironment (TME). It is therefore of paramount importance to delineate unappreciated mechanisms of resistance in order to design novel treatments aiming to confer robust and durable anti-tumor immunity. Accomplishment of this goal has been hampered by the multiple and complex immune suppressive networks operating during tumor development promoting tumor immune evasion (3). Myeloid-derived suppressor cells (MDSCs) are bone marrow (BM) progenitors of dendritic cells (DCs), macrophages, and neutrophils, composed by monocytic (M-MDSCs) and granulocytic (G-MDSCs) subsets (4). MDSCs constitute a major component of the tumor-induced immunosuppressive circuit since they are significantly enriched in the periphery and the TME of patients with solid tumors and hematologic malignancies (5) while MDSC presence is associated with poor prognosis as well as metastasis and is also linked to resistance to chemotherapy and immunotherapy (6, 7). Multiple mechanisms have been attributed to MDSC-mediated inhibition of anti-tumor immune responses, ranging from secretion of immunosuppressive mediators to direct cell-to-cell contact (6, 8). In preclinical models, targeting of such mechanism has generated promising results by promoting tumor regression and development of potent anti-tumor immunity. For example, targeting of autophagy pathway in M-MDSCs promoted the antigen-presenting properties of these cells and enhanced the anti-tumor immunity in a mouse model of melanoma (9). Furthermore, treatment with all-trans retinoic acid (ATRA) induced the differentiation of M-MDSCs into macrophages and DCs and killed G-MDSCs in both mice and humans (10–12). In addition, treatment of mice with fatty acid transporter 2 (FATP2) (13) or cyclooxygenase 2 (COX2) (14, 15) has been shown to interfere with MDSC expansion and to significantly attenuate tumor development. Finally, targeting of protein kinase R-like ER kinase (PERK) pathway induced the maturation of M-MDSCs and attenuated their function (16). However, the clinical translation of these findings remains in its infancy. Therefore, shedding light into mechanisms that mediate expansion and activation as well as arrest of differentiation of MDSCs may facilitate the design of new therapeutic target for immunotherapy in solid tumors and hematologic malignancies.

Chronic inflammation constitutes a hallmark of cancer. Inflammasomes and their effectors such as IL-1β and IL-18 significantly contribute to establishment of inflammation, while the TME is enriched in damage-associated molecular patterns (DAMPs) that have been shown to drive inflammasome activation in both immune and cancer cells. Among the best-studied inflammasomes, the NOD-like receptor family, pyrin domain containing-3 protein (NLRP3), has shown to be activated by DAMPs, followed by assembly of the NLRP3 complex and activation of caspase-1 in order to promote maturation of IL-1β and IL-18 cytokines (17, 18). Alternatively, sensing of cytoplasmic lipopolysaccharide (LPS) or Gram-negative bacteria induce inflammasome activation in a non-canonical manner, involving activation of caspase-11 upon type I IFN signaling, which, in turn, promotes IL-1β maturation and release through activation of the NLRP3/caspase-1 pathway (19). Although presence of IL-1β has been closely linked to tumor progression and metastasis in various types of cancer (20), the role of NLRP3 inflammasome activation remains controversial, suggesting that other functional roles of inflammasome, beyond secretion of pro-inflammatory mediators, may exist. Importantly, the impact of activation of NLRP3 in cancer cells versus the host cells during tumor immune surveillance remain ill defined. Considering that accumulating evidence proposes an important role of NLRP3 in chemotherapy success through induction of anti-tumor immunity (21, 22), while other studies highlight that activation of NLRP3 inflammasome impedes the effectiveness of ICI immunotherapy (23), it is necessary to unravel the molecular mechanism *via* which the inflammasome pathway imprints on anti-tumor immunity and effectiveness of immunotherapy.

Herein, we demonstrate that *Nlrp3* deficiency led to diminished tumor development, which was accompanied by a robust anti-tumor immunity and re-arrangement of the MDSC compartment. Both M-MDSCs and G-MDSCs from tumor-inoculated *Nlrp3*$^{-/-}$ mice lost their ability to suppress T-cell activation and proliferation and demonstrated an extensive transcriptomic reprogramming enriched in inflammatory and metabolic pathways. Notably, therapeutic inhibition of inflammasome significantly decreased tumor development and re-arranged the MDSC subsets, mirroring the effect described in *Nlrp3*$^{-/-}$ animals. Overall, uncovering of mechanisms that mediate tumor immune evasion may facilitate the development of new therapeutic opportunities for cancer patients.

Methods

TCGA survival analysis

Survival and gene expression information were downloaded from the TCGA data portal (https://portal.gdc.cancer.gov/) for SKCM (skin cutaneous melanoma) and LUSC (lung squamous cell carcinoma) datasets. We specifically downloaded preprocessed expression data using the quantile-normalized FPKM values. Next, patients were either stratified by expression of NLRP3 or the NLRP3-inflammasome-related

gene set as defined by Ju et al. (24). For the NLRP3 inflammasome gene set, we defined a module score inspired by Seurat single-cell analysis (25), using each patient's average expression of all NLRP3 inflammasome gene-set genes subtracted by the average expression of all genes. For survival analysis, we used the bottom and top 33% of patients with either NLRP3 expression or NLRP3 inflammasome module score. Statistical evaluation and Kaplan–Meier plot representation were performed with the R package survminer version 0.4.9, using the log-rank test for *p*-value estimation and 95% confidence interval of patient survival.

Animals

C57BL/6J mice were purchased from the Jackson Laboratory; *Nlrp3*-deficient (*Nlrp3*$^{-/-}$) mice (on a C57BL/6 background) were kindly provided by Jürg Tschopp (Department of Biochemistry, Center of Immunity and Infection, University of Lausanne, Switzerland) (26). Disruption of the mouse *Nlrp3* gene was based on the insertion of an EGFP cassette, which was accompanied by SV40 poly(A) tail, fused in frame with the ATG of exon 2. A PGK-neo selection cassette was also inserted in intron 2, which was flanked by two loxP sites and was deleted by the backcrossing of the mice, with the targeting vector, with a Cre-expressing strain (C57BL/6) resulting in a *Nlrp3*$^{-/-}$ mouse on a C57BL/6 background. Foxp3^{EGFP}.KI mice (on a C57BL/6 background) were kindly provided by Alexander Rudensky (Department of Immunology, Memorial Sloan-Kettering Cancer Center, New York, USA).

All mice were maintained in the animal facility of the Biomedical Research Foundation of the Academy of Athens [BRFAA] and Institute of Molecular Biology and Biotechnology Institute [IMBB]. All procedures were in accordance with institutional guidelines and were approved by the Institutional Committee of Protocol Evaluation of the BRFAA and the Institutional Committee of Protocol Evaluation of the IMBB together with the Directorates of Agricultural Economy and Veterinary, Region of Crete, Greece (14/10/2020 Heraklion, Greece, protocol 234446). Unless indicated otherwise, all experiments used sex- and age-matched mice aged between 6 and 12 weeks.

PCR Genotyping

Nlrp3-deficient mice were screened by PCR genotyping on tail genomic DNA using the following primers: 5'GCTCAGGACATACGTCTGGA3' (forward in intron 1) and 5'TGAGGTCCACATCTTCAAGG3' (reverse in exon 2). *Nlrp3*$^{+/+}$ (wild type) mice gave a product of 327 base pairs (bp), whereas *Nlrp3*$^{-/-}$ mice did not give any PCR product. The program used for the PCR genotyping is as follows: 94°C (3 min), 30 × [94°C (30 s), 58°C (30 s), 72°C (1 min)], and 72°C (5 min).

Cell lines and primary cell culture

The murine melanoma cancer cell line B16.F10 and the murine Lewis Lung carcinoma (LLC) cell line that were used for the solid tumor induction models were kindly provided by A. Eliopoulos (Medical School, National and Kapodistrian University of Athens, Athens, Greece) and were negative for *Mycoplasma* spp., tested by PCR.

B16.F10 and LLC cancer cells were cultured at 37°C under 5% CO_2 in RPMI-1640 (GlutaMAX^{TM}, Gibco, #61870) medium supplemented with 10% heat-inactivated fetal bovine serum (FBS, Gibco, #10270), 100 U/ml penicillin–streptomycin (10,000 U/ml, Gibco, #15140), and 50 μM 2-mercaptoethanol (50 mM, Gibco, #31350). Cells were split when they were 90%–100% confluent. All experiments were performed with early passage (p2–3) cells.

Splenocytes and sorted MDSCs were obtained as described below. Mouse splenocytes and MDSCs were grown in RPMI-1640 culture medium containing 10% heat-inactivated FBS, 100 U/ml penicillin–streptomycin, and 50 μM 2-mercaptoethanol. The stimuli at the cultures were added where indicated, as mentioned below.

Solid tumor induction and *in vivo* immunotherapy administration protocols

The transplantation of solid tumors in the tumor models was performed as described previously (27). Briefly, mice were implanted subcutaneously, at the back, with 3×10^5 B16.F10 melanoma or LLC cells (viability assessed by Trypan blue exclusion). Tumor volume was monitored during the days indicated in the legends of corresponding curves. The tumor growth was monitored by measurement of two perpendicular diameters of palpable tumors every day by a caliper and was calculated using the equation $\frac{(length \times width^2)}{2}$. Mice were sacrificed and analysis was performed 15 days after tumor induction or as indicated each time. Mice with tumors larger than 1,100 mm^3 were euthanized. Mice that manifested tumor ulceration were excluded for the experimental processes. At the endpoint of each experiment, the tumor weight was also determined.

For the application of the combinational therapy protocol, each mouse was treated with anti-CTLA-4 Ab (clone 4F10, Bioceros LB) at 100 μg per 100-μl dose and anti-PD-1 Ab (clone RMP1–14, Bioceros LB) at 200 μg per 100-μl dose intraperitoneally (i.p.) every 3 days after tumor implantation,

whereas NLRP3 inhibitor (MCC950, Sigma-Aldrich, #5.38120.0001) was administered at 10 mg/kg dose to each mouse by i.p. injection every other day. Control mouse cohort was administered PBS on the same days.

Tissue dissociation and sample preparation

For the analysis of tumor-infiltrating lymphocytes (TILs), single-cell suspensions were generated by dissecting and dissociating tumor tissue in the presence of collagenase D (1 mg ml^{-1}, Roche) and DNase I (0.25 mg ml^{-1}, Sigma), diluted in RPMI-1640 medium (Gibco), for 45 min at 37°C and then were homogenized and strained passing through a 40-μm pore size cell strainer (BD Falcon). For the analysis and isolation of different immune populations, single-cell suspensions from spleen and lymph nodes (LNs) were prepared by homogenization of the tissue and passing through a 40-μm pore size cell strainer. Isolated femoral and tibial bones from the hindlimbs were flushed with ice-cold 5% FBS in PBS for BM single-cell suspensions. Single-cell suspensions from spleen and BM were prepared after erythrocyte lysis with red blood cell lysis buffer.

Flow cytometry, cell sorting, and quantification

For extracellular marker staining, single-cell suspensions from TILs, spleen, LNs, or BM were incubated for 20 min at 4°C with the following anti-mouse conjugated antibodies: CD45-PerCP/Cy5.5 (BioLegend, clone 30-F11, #103132, diluted 1:200), CD11c-PE/Cy7 (BioLegend, clone N418, #117318, diluted 1:200), CD11b-Brialliant Violet 510 (BioLegend, clone M1/70, #101263, diluted 1:200), CD11b-PE (BD Pharmingen, clone M1/70, #553311, diluted 1:200), Gr1-Pacific Blue (BioLegend, clone RB6-8C5, #108430, diluted 1:200), Gr1-Brilliant Violet 421 (BioLegend, clone RB6-8C5, #108434, diluted 1:200), Gr1-PE (eBioscience, clone RB6-8C5, #12-5931-82, diluted 1:200), Ly6G-PE (BioLegend, clone 1A8, #127608, diluted 1:200), Ly6C-Brilliant Violet 421 (BioLegend, clone RB6-8C5, #108430, diluted 1:200), CD8a-PE/Cy7 (BioLegend, clone 53-6.7, #100722, diluted 1:200), CD8a-PE (BioLegend, clone 53-6.7, #100708, diluted 1:200), CD4-PE (BioLegend, clone RM4-4, #116006, diluted 1:200), NK-1.1-APC (BioLegend, clone PK136, #108710, diluted 1:200), CD16/32-PE (BioLegend, clone 93, #101308, diluted 1:200), CD16/32-PerCP/Cy5.5 (BioLegend, clone 93, #101323, diluted 1:200), TER-119/Erythroid Cells-PE (BioLegend, clone TER-119, #116208, diluted 1:200), CD45R/B220-PE (BioLegend, clone RA3-6B2, #103208, diluted 1:200), Ly-6A/E (Sca-1)-APC (BioLegend, clone E13-161.7, #122512, diluted 1:200), CD117 (c-kit)-PE/Cy7 (BioLegend, clone 2B8, #105813, diluted 1:200), CD34-Brilliant Violet 421 (BioLegend, clone MEC14.7, #119321, diluted 1:200), CD44-PerCP/Cy5.5 (BioLegend, clone IM7, #103032, diluted 1:200), and CD25-PE (BioLegend, clone 3C7, #101904, diluted 1:200). Dead cells in cultured splenocytes were stained by the addition of 7-AAD Viability Staining Solution (BioLegend, #420404). For NLRP3-APC (R&D Systems, clone 768319, #IC7578A, diluted 1:25) and IL-1β-FITC (R&D Systems, clone 166931, #IC4013F, diluted 1:50) intracellular staining, cells were stained for the extracellular markers, and then permeabilized and stained using the intracellular Fixation & Permeabilization buffer set (eBioscience) according to the vendor's instructions. Rat IgG1 kappa Isotype Control-APC (eBioscience, clone eBRG1, #17-4301-81, diluted 1:100) and Rat IgG2b kappa Isotype Control-FITC (eBioscience, clone eB149/10H5, # 11-4031-82, diluted 1:100) were used as controls for NLRP3 and IL-1β, respectively. For IFN-γ intracellular staining, tumor cells were incubated with 50 ng ml^{-1} of phorbol 12-myristate 13-acetate (PMA, Sigma-Aldrich), 2 μg ml^{-1} of ionomycin (Sigma-Aldrich), and brefeldin (1/1,000; Becton Dickinson Biosciences) for 4 h at 37°C and 5% CO_2, stained for extracellular markers, and fixed and stained for IFN-γ (BioLegend, clone XMG1.2, #505808, diluted 1:50) or Rat IgG2a kappa Isotype Control-PE (eBioscience, clone eBR2a, #12-4321-81, diluted 1:50) using Foxp3 Transcription Factor Staining Buffer Set (eBioscience) according to the manufacturer's instructions. All samples were analyzed using FACS ARIA III (BD Biosciences) and FACS Canto II (BD Biosciences). Flow cytometry data were analyzed with FlowJo v.8.7 and 10.8.1 software. MDSCs were sorted on a FACS ARIA III (BD Biosciences) and the BD FACSDIVA v8.0.1 software (BD Biosciences). Cell purity was above 95%.

Calculation of TIL numbers per gram of tumor tissue was performed, by flow cytometry, upon tumor tissue isolation, weighing, digestion, and suspension in a 0.1 g/100 μl volume of 5% FBS in PBS prior to staining.

Inflammasome activation assays

Splenocytes as well as sorted splenic MDSCs from naïve and tumor-bearing mice were isolated as previously described. We seeded 5×10^5 splenocytes or 1×10^5 MDSCs per well in 96-well flat-bottom and 96-well round-bottom plates, respectively, and stimulated them for 24 h with 1 μg/ml LPS from *Escherichia coli* O55:B5 (Sigma, L2880). The next day, 1 h before the ending of the stimulation time, the culture medium was supplemented with 5 mM adenosine 5'-triphosphate disodium salt hydrate (ATP) inflammasome activator (Jena Bioscience, NU-1010-1G). Supernatants were removed and analyzed using Mouse IL-1

beta/IL-1F2 Quantikine ELISA Kit (R&D Systems, MLB00C), according to the manufacturer's instructions, and cultured cells were prepared for staining of extracellular and intracellular markers, as described above.

MCC950-mediated inflammasome inhibition assays

Total splenocytes from naïve mice were seeded 5×10^5 cells per well in 96-well flat-bottom plates and stimulated for 24 h with 1 μg/ml LPS (Sigma, L2880). The following day, in the medium from the overnight culture was added water for injection (control) or MCC950 NLRP3 inhibitor (2 μM) (Sigma-Aldrich, 5381200001) for the indicated time points. One hour before the end of priming, cells were stimulated with ATP inflammasome activator (Jena Bioscience, NU-1010-1G). Supernatants were removed and used for mouse IL-1β ELISA and cultured splenocytes were prepared for 7-AAD viability staining, as described above.

In vitro suppression assay

For the suppression assay of MDSC subsets, $CD4^+Foxp3^-$ effector T cells (Teff) were sorted from the LNs of naïve $Foxp3^{EGFP}$.KI mice, as previously described, and stained with the division-tracking dye CellTrace Violet (CTV, Invitrogen, #C34557) according to the manufacturer's protocol. A total of 75×10^3 labeled Teff cells were then seeded in 96-well round-bottom plate in each well. M-MDSC ($CD11b^{high}Ly6C^+Ly6G^-$) and G-MDSC ($CD11b^{high}Ly6C^-Ly6G^+$) subsets sorted from the spleens of WT or *Nlrp3*$^{-/-}$ B16.F10 inoculated mice were added at the culture, at a ratio Teff/M-MDSCs 1:1 and Teff/G-MDSCs 3:1. Then, Dynabeads mouse T-activator conjugated with monoclonal antibody (mAb) to the invariant signaling protein CD3 plus mAb to CD28 (Gibco, #11456D) were supplemented into culture, at a ratio of one bead per one Teff cell. Cells were cultured in DMEM (Gibco, #11965) supplemented with 10% heat-inactivated FBS, 100 U/ml penicillin–streptomycin, and 50 μM 2-mercaptoethanol. As positive and negative controls, we used Teff cells cultured with or without anti-CD3/anti-CD28 activation beads, respectively. The plate was incubated at 37°C under 5% CO_2 for 64 h and then cultured cells were prepared for staining of extracellular markers, as described above, for the determination of proliferation and activation of Teff cells with flow cytometry analysis.

Enzyme-linked immunosorbent assay

Tumor homogenates were generated in PBS that was supplemented with a cocktail of protease inhibitors (Roche) using a pestle inside an Eppendorf. The conditioned media of cultured splenocytes and MDSCs from *in vitro* cultures were also collected. The homogenates and cell culture supernatants were centrifuged and were assayed for mouse IL-1β using the Mouse IL-1 beta/IL-1F2 Quantikine ELISA Kit (R&D Systems, MLB00C), according to the manufacturer's instructions.

RNA-seq library preparation

M-MDSCs and G-MDSCs were sorted from spleens of B16.F10 melanoma-bearing WT and *Nrlp3*$^{-/-}$ mice, and total RNA was extracted using the Macherey-Nagel NucleoSpin RNA kit as described by the manufacturer's protocol (NucleoSpin® RNA). Each RNA sample was representative of one mouse.

NGS libraries were generated using 300 ng of total RNA as input on average with the QuantSeq 3′ mRNA-Seq Library Prep Kit FWD for Illumina kit from Lexogen according to manufacturer's protocol, using 15 or 17 cycles of amplification. Libraries were sequenced on Illumina Nextseq 500 on 1 × 75 High flowcell.

RNA sequencing pipeline

Fastq files were downloaded from Illumina-BaseSpace and mapped to mm10 genes (iGenomes UCSC/mm10) using hisat2 version 2.1.0 (–score-min L 0,-0.5) (28). Gene counts were computed with htseq-count (-s yes, version 0.11.2) (29).

Further processing was performed with the R Bioconductor (Bioconductor) package edgeR v.3.14.0 (edgeR). Reads were normalized for intra- and inter-sample variances using the functions "calcNormFactors" and "estimateTagwiseDisp", and further by the gene length as per Ensembl V103 Genes annotations, resulting in fragments per kilobase per million (FPKM) for each gene. Differential gene expression analysis was performed as previously described (30). Genes with FDR< 0.05 and fold change $|FC| > 1.5$ were considered statistically significant. Heatmaps and boxplots were created in R with an in-house developed script that is based on the ggplot package.

Enrichment analysis

Significant differentially expressed genes (DEGs) were used for gene ontology (GO) analysis using the g:Profiler web-server. Gene set enrichment analysis (GSEA) was also performed in order to reveal enriched signatures in our gene sets based on the Molecular Signatures Database (MSigDB) v7.4. Gene sets were ranked by taking the –log10 transform of the *p*-value multiplied by the FC. Significantly upregulated genes were at the top and significantly downregulated genes were at the bottom of the

ranked list. GSEA pre-ranked analysis was then performed using the remapped Mouse Gene Symbol dataset and collapsing probe sets while keeping only the max probe value. The rest of the parameters were left to default. Enrichment was considered significant FDR (q-value)<5%.

Data analysis and statistics

Data are presented as mean ± S.D., as bar graphs represent the mean and standard deviation (SD) between biologically independent mouse samples or technical repeats, as indicated each time. For statistical analysis, all data were analyzed using Prism 8 (GraphPad Software, Inc., La Jolla, USA). Data were analyzed using the two-tailed, parametric, unpaired Student's t test or the two-tailed, nonparametric Mann–Whitney test, as appropriate after testing for normality of the values with the F test, with 95% confidence intervals. For multiple-group comparisons, the one-way ANOVA test and Tukey's multiple comparison test were performed. Kaplan–Meier statistics were done with the log(rank) (Mantel–Cox) test. The p-value of<0.05 was considered to be statistically significant for each dataset.

Results

NLRP3 inflammasome pathway genes are associated with survival in melanoma and lung cancer patients

Despite the established role of inflammasome pathway in the orchestration of an inflammatory response, through release of pro-inflammatory cytokines IL-1β and IL-18, its role in cancer development, progression, and immunotherapy response remains contradictive. To investigate the impact of NLRP3 inflammasome in the progression of LUSC and SKCM, Kaplan–Meier survival analysis was performed based on high and low NLRP3 gene expression or NLRP3 pathway gene-set expression [median expression of the 30 pathway genes as defined by Ju et al. (24), Supplementary Figure 1A], using the top/bottom 33% of samples with the highest/lowest expression, respectively. Patients with the lowest expression of both NLRP3 gene and its pathway gene set were found to display prolonged survival of LUSC patients (p = 0.068 and p = 0.047, respectively, Figures 1A, B, left panels). In accordance, low expression of the NLRP3 pathway gene set was also associated with prolonged survival of SKCM patients (p = 0.059, Figure 1A, right upper panel), whereas in these patients, low expression of NLRP3 gene was associated with increased morbidity rate (p = 0.004, Figure 1B, right lower panel). In summary, these data indicate that differential expression of NLRP3 pathway genes is associated with survival probability of cancer patients and extend the findings that NLRP3 inflammasome may have pro- and anti-tumorigenic roles.

Nlrp3-deficient mice exhibit attenuated tumor development and re-arranged MDSC compartment

To examine the functional importance of NLRP3 pathway during tumor development, we utilized the *Nlrp3*-deficient mice (*Nlrp3*$^{-/-}$), in which the *Nlrp3* gene has been disrupted by the insertion of an EGFP cassette (Supplementary Figure 2A). Effective inactivation of NLRP3 inflammasome was confirmed by the absence of IL-1β in culture supernatants of LPS/ATP-stimulated splenocytes from *Nlrp3*$^{-/-}$ animals compared to WT mice (Supplementary Figure 2B). Furthermore, *Nlrp3*$^{-/-}$ animals did not exhibit significant alterations in the composition of lymphoid (Supplementary Figures 2C, D) and myeloid compartments (Supplementary Figures 2E, F) compared to WT mice at the steady state, suggesting that inactivation of *Nlrp3* gene does not disturb the immune homeostasis.

Therefore, this model allows us to study the role of the NLRP3 pathway in host cells through implantation of NLRP3-sufficient tumor cell line. To this end, upon inoculation with B16.F10 melanoma cells, *Nlrp3*$^{-/-}$ mice exhibited significantly reduced tumor growth compared to WT mice, as assessed by the measurement of tumor volume and weight (Figure 2A). The tumor-suppressive effect of NLRP3 deficiency was not restricted only to the melanoma model, since inoculation with the LLC cell line demonstrated significantly decreased tumor growth in *Nlrp3*$^{-/-}$ animals (Figure 2B). Tumor regression in melanoma-bearing *Nlrp3*$^{-/-}$ mice was accompanied by significantly increased frequencies of tumor-infiltrating CD45^{+} leukocytes (Figure 2C), CD8^{+} lymphocytes, which exhibited elevated IFN-γ expression, and NK1.1^{+} cells, as well as increased frequencies of CD4^{+} T cells, compared to WT mice (Figures 2D, E). These findings were further confirmed upon extrapolation of cell subset frequencies to respective numbers per gram of tumor tissue (Supplementary Figure 3A). Interestingly, CD11c^{-}CD11b^{+}Gr1^{+} MDSCs frequencies were comparable between WT and *Nlrp3*$^{-/-}$ mice (Figure 3A), whereas assessment of MDSC subsets revealed an increased accumulation of CD11b^{high}Ly6C^{+}Ly6G^{-} M-MDSCs and markedly decreased levels of CD11b^{high}Ly6C^{-}Ly6G^{+} G-MDSCs into the tumor site of *Nlrp3*$^{-/-}$ mice (Figure 3B). The MDSC subset re-arrangement was also evident in the spleen of tumor-inoculated WT and *Nlrp3*$^{-/-}$ mice (Figures 3C, D). Overall, these findings indicate an important role of NLRP3 in the suppression of anti-tumor immune responses and tumor development, associated with a major rewiring of the MDSC compartment.

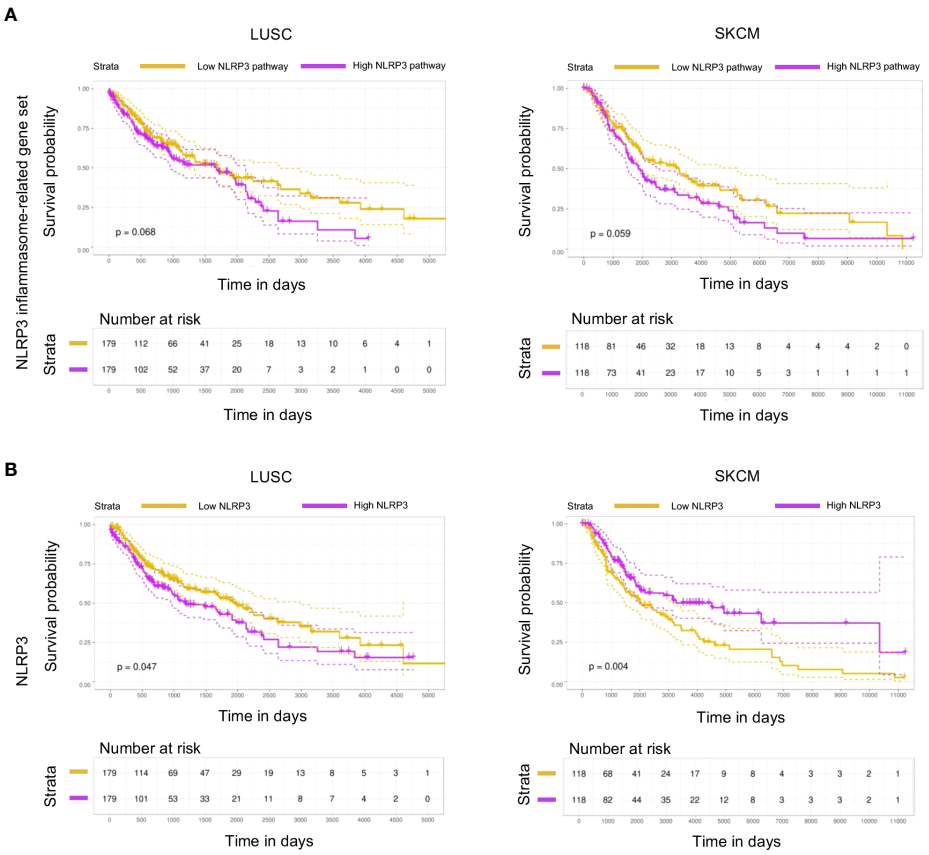

FIGURE 1
NLRP3 expression is associated with survival in melanoma and lung cancer patients. **(A,B)** Kaplan–Meier plot with patients-at-risk table showing overall survival of TCGA datasets LUSC (lung squamous cell carcinoma; left) and SKCM (skin cutaneous melanoma; right), with patients stratified by NLRP3 inflammasome-related gene set **(A)** and NLRP3 **(B)** expression using top and bottom 33% of stratified patients. Gene-set stratification is based on the median expression of all 30 containing genes. Dotted lines represent 95% confidence intervals. Statistical evaluation was performed using the log-rank test.

Enhanced activation of NLRP3/pro-IL-1β axis in the myeloid compartment of tumor-bearing mice

Based on the established expression of NLRP3 in the myeloid compartment (31) combined with the enhanced accumulation of MDSCs compared to other myeloid cell subsets in the TME (Figure 4A and Supplementary Figure 4A) and the extended re-arrangement of MDSC subsets in the tumor-inoculated *Nlrp3*$^{-/-}$ mice, we sought to determine the NLRP3 and pro-IL-1β expression in the MDSC population during tumor development. To this end, MDSCs demonstrated enhanced expression of NLRP3, which was accompanied by increased expression of pro-IL-1β, in spleen of melanoma-bearing animals, compared to isotype controls (Figure 4B). This was also confirmed to M-MDSC and G-MDSC subpopulations (Figures 4C, D), with the latter to express higher levels of both NLRP3 and pro-IL-1β (Supplementary Figure 4B).

Next, we asked whether NLRP3 inflammasome is functionally active in MDSCs, and to address this, we exposed them to cellular insults that include "priming" signal with a TLR agonist, such as LPS, and an activation stimulus, such as ATP. Flow cytometry analysis demonstrated robust expression of NLRP3 and pro-IL-1β in MDSCs from spleens of naïve mice (Figure 4E) as well as in highly pure MDSCs isolated from tumor-bearing mice (Figure 4F), and this is accompanied by increased levels of secreted IL-1β as determined in culture supernatants (Figure 4G). Overall, these data indicate that the NLRP3 inflammasome pathway is activated and functional in MDSCs during tumor development.

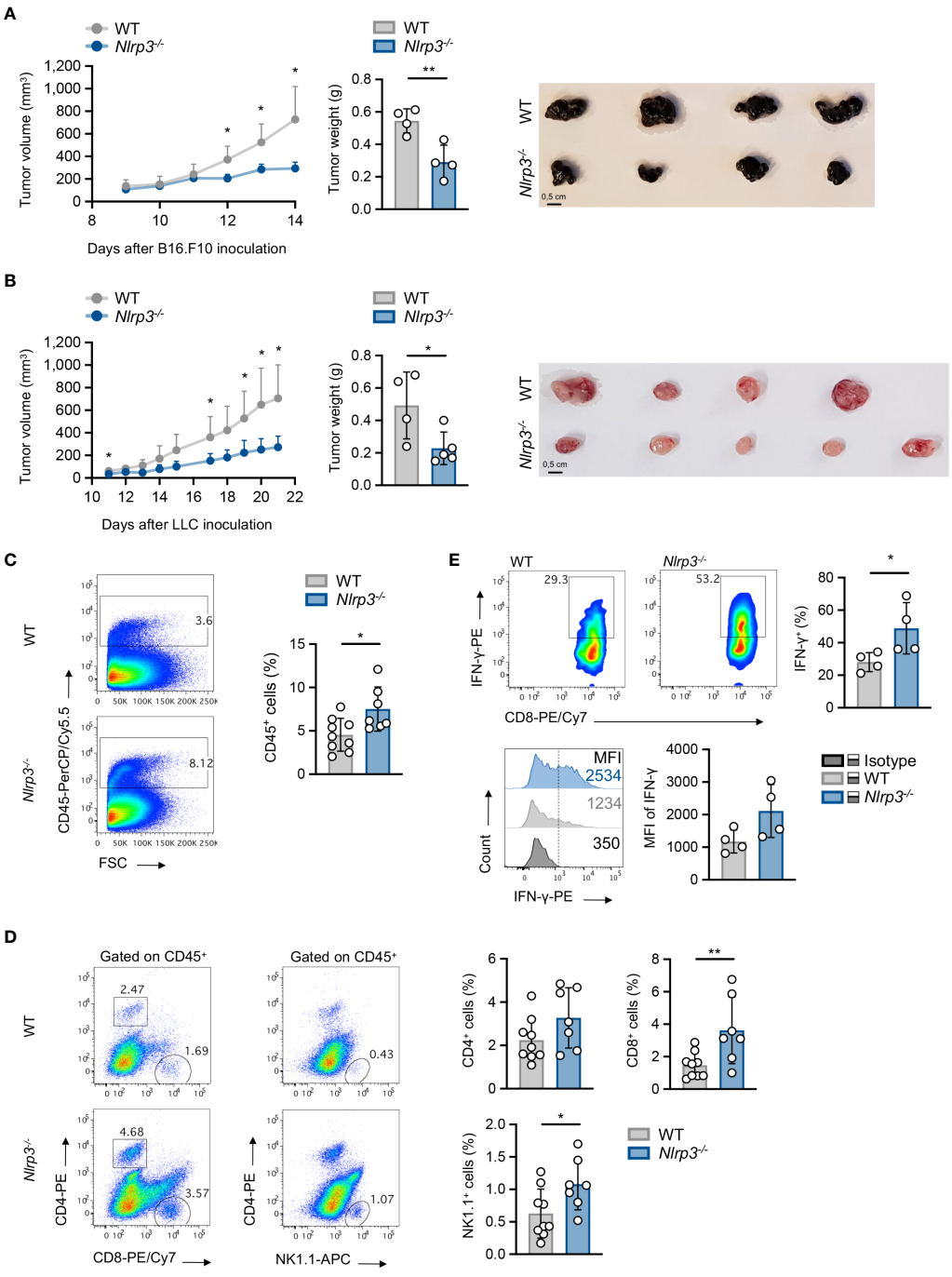

FIGURE 2
Nlrp3 deficiency promotes tumor regression and anti-tumor immunity. **(A)** Tumor volume curve of WT (n = 4) and *Nlrp3*$^{-/-}$ (n = 4) mice 9–14 days after B16.F10 inoculation, tumor weight on day 14, and representative image of excised melanoma tumors. **(B)** Tumor volume curve of WT (n = 4) and *Nlrp3*$^{-/-}$ (n = 5) mice 11–21 days after LLC inoculation, tumor weight on day 21, and representative image of excised LLC tumors. **(C)** Representative fluorescence-activated cell sorting (FACS) plots and percentages of intratumoral CD45$^+$ cells of WT (n = 9) and *Nlrp3*$^{-/-}$ (n = 7) mice 15 days after B16.F10 inoculation. **(D)** Gating strategy and frequencies of intratumoral CD4$^+$, CD8$^+$, and NK1.1$^+$ cells in CD45$^+$ population of WT (n = 9) and *Nlrp3*$^{-/-}$ (n = 7) mice 15 days after B16.F10 inoculation. **(E)** Representative FACS plots and frequencies of CD8$^+$ IFN-γ$^+$ cells from CD45$^+$ tumor-infiltrating cells of WT (n = 4) and Nlrp3$^{-/-}$ (n = 4) mice 15 days after B16.F10 inoculation, and representative overlay and mean fluorescence intensity (MFI) of IFN-γ produced by CD8$^+$ cells after *in vitro* activation. Data are shown as mean (± S.D.). Representative data from at least two independent experiments are shown. Statistical significance was obtained by unpaired Student's t-test. Symbols: (*), $p \leq 0.05$; (**), $p \leq 0.01$, n = biologically independent mouse samples.

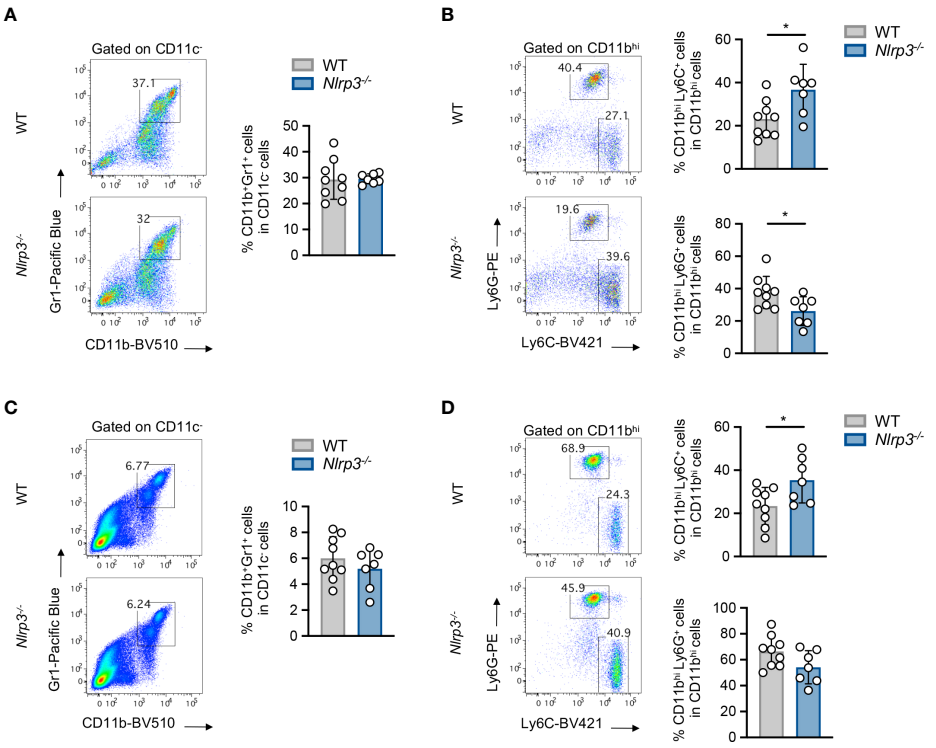

FIGURE 3
Nlrp3 deficiency re-arranges the MDSC compartment. **(A, B)** Representative FACS plots and frequencies of intratumoral MDSC population **(A)** and MDSC subpopulations **(B)**, M-MDSCs and G-MDSCs, of WT (n = 9) and *Nlrp3*$^{-/-}$ (n = 7) mice 15 days after B16.F10 inoculation. **(C, D)** Representative FACS plots and frequencies of spleen-infiltrating MDSC population **(C)** and MDSC subpopulations **(D)**, M-MDSCs and G-MDSCs, of WT (n = 9) and *Nlrp3*$^{-/-}$ (n = 7) mice on day 15 after B16.F10 inoculation. Data are shown as mean ($\pm$ S.D.). Representative data from four independent experiments are shown. Statistical significance was obtained by unpaired Student's t-test. Symbols: (*), $p \leq 0.05$, n = biologically independent mouse samples.

Decreased frequencies of granulocyte-myeloid progenitors in the BM of *Nlrp3*$^{-/-}$ mice

MDSCs are BM-derived cells, and recent evidence highlights the importance of BM hematopoiesis and in particular of myeloid progenitors in shaping of anti-tumor immunity (32). Thus, we asked whether *Nlrp3*$^{-/-}$ animals present alterations of BM progenitors during tumor growth, which may affect the generation of MDSC subsets. To this end, flow cytometry analysis revealed that tumor-bearing *Nlrp3*$^{-/-}$ mice did not exhibit significant differences in frequencies of hematopoietic progenitors (LSKs; Lin$^-$cKit$^+$Sca1$^+$) in their BM as compared to the tumor-bearing WT group (Supplementary Figures 5A, B). In line with this, assessment of total myeloid progenitor frequencies (MyPs; Lin$^-$cKit$^+$Sca1$^-$) did not demonstrate any significant difference between *Nlrp3*$^{-/-}$ and WT mice (Supplementary Figures 5C, D) with granulocyte macrophage progenitors (GMPs; Lin$^-$cKit$^+$Sca1$^-$CD16/32$^+$CD34$^+$) to be decreased in *Nlrp3*$^{-/-}$ mice while common myeloid progenitors (CMPs; Lin$^-$cKit$^+$Sca1$^-$CD16/32$^-$CD34$^+$) were not affected (Supplementary Figures 5C, E). To conclude, these data suggest that *Nlrp3*$^{-/-}$ mice did not exhibit differences in the hematopoietic progenitors but granulocyte progenitors are decreased in tumor-bearing animals.

Transcriptomic re-programming of both M- and G-MDSCs in tumor-bearing *Nlrp3*$^{-/-}$ animals

To investigate the molecular mechanisms *via* which NLRP3 deficiency imprints on the re-wiring of MDSC subsets, highly pure M-MDSCs and G-MDSCs isolated from spleen of B16.F10-bearing *Nlrp3*$^{-/-}$ and WT mice were subjected to mRNA sequencing (mRNA-seq) and gene expression analysis. A combined principal component analysis (PCA) of all RNA-seq samples showed clustering by both factors, subpopulation and species. While PC1, explaining 46.08% of the total variance, separates G-MDSCs from M-MDSCs, PC2, explaining 15.84% of the total variance, differentiates pure deficient samples from control samples (Supplementary Figure 6A).

Specifically, transcriptomic analysis in M-MDSCs revealed 992 DEGs ($|FC| \geq 1.5$, FDR< 0.05) between *Nlrp3*$^{-/-}$ and WT melanoma-bearing animals (Figure 5A) with 318 and 674 genes

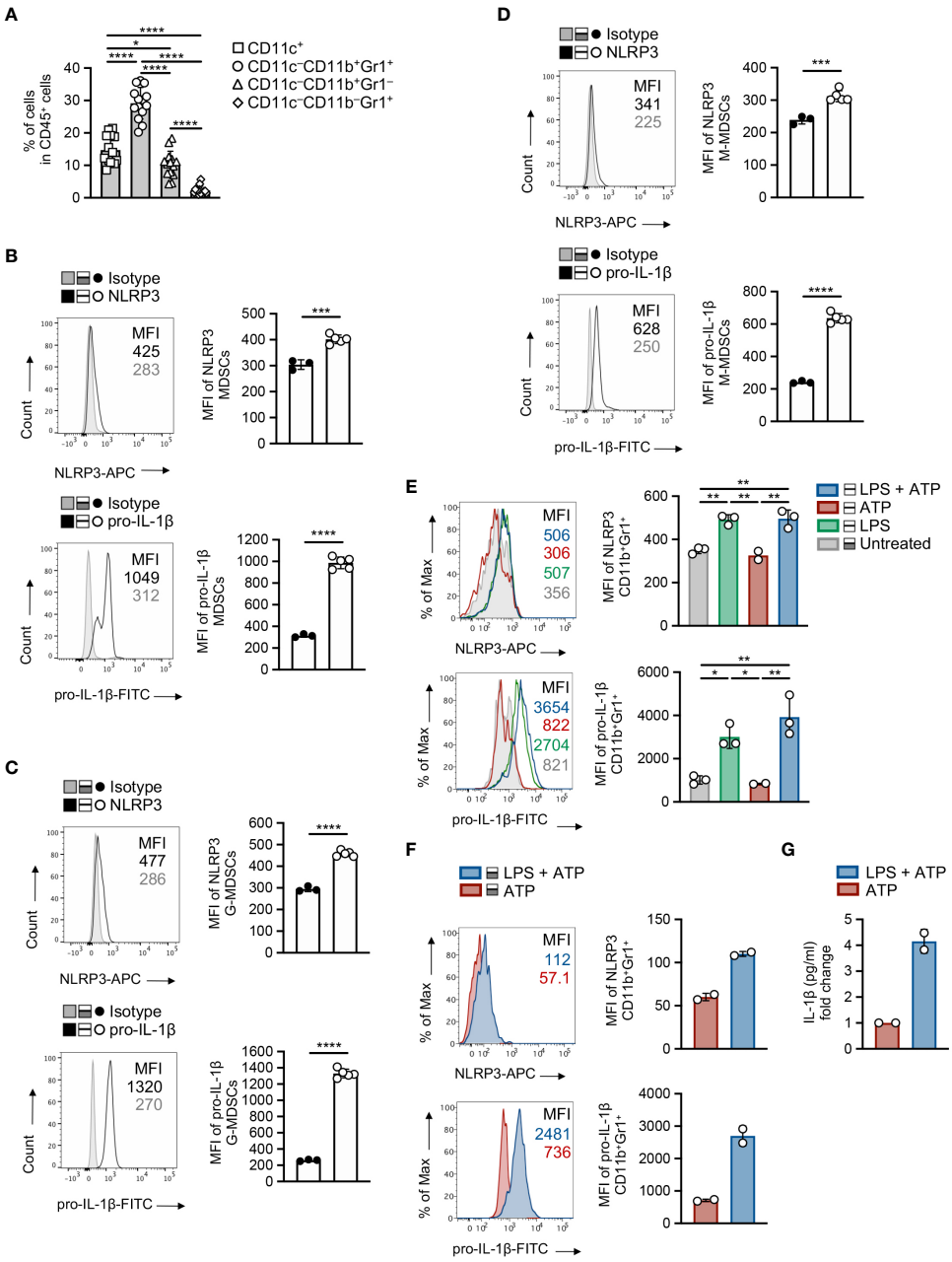

FIGURE 4
MDSCs exhibit increased activation of NLRP3 during tumor development. **(A)** Frequencies of intratumoral myeloid cell subsets in CD45$^+$ population on day 15 of B16.F10 melanoma tumors (n = 14), determined by flow cytometric analysis. **(B)** Representative histogram overlays of NLRP3 and pro-IL-1β expression and plots of NLRP3 (n = 5) and pro-IL-1β (n = 5) MFI of spleen-infiltrating MDSCs, compared to isotype controls (n = 3), on day 15 after B16.F10 inoculation. **(C, D)** Representative histogram overlays of NLRP3 and pro-IL-1β expression and plots of NLRP3 (n = 5) and pro-IL-1β (n = 5) MFI of spleen-infiltrating G-MDSCs **(C)** and M-MDSCs **(D)**, compared to isotype controls (n = 3), as in **(B)**. **(E, F)** Representative histogram overlays of NLRP3 and pro-IL-1β expression and quantitative plots of MFI of NLRP3 and pro-IL-1β MFI with quantitative plots of NLRP3 and pro-IL-1β MFI in WT splenocytes from naïve mice (n = 3) gated on MDSCs **(E)** and sorted MDSCs from the spleens of tumor-bearing mice (n = 2) **(F)**, primed with LPS (1 μg/ml) and stimulated for NLRP3 activity by ATP (5 mM). **(G)** Quantification of IL-1β levels (pg ml^{-1}) in the supernatants of LPS and/or ATP stimulated sorted MDSCs (n = 2), determined by ELISA (graph shows the fold change relative to ATP). Data from one experiment are shown **(F, G)**. Data are shown as mean (± S.D.). Representative data from at least two **(A–E)** independent experiments are shown. Statistical significance was obtained by unpaired Student's t-test or one-way ANOVA with Tukey's multiple comparison test (a, e). Symbols: (*), $p \leq 0.05$; (**), (***), $p \leq 0.001$, $p \leq 0.01$; (****), $p \leq 0.0001$, n = biologically independent mouse samples.

to be up- and downregulated, respectively (Supplementary Figure 6B). Pathway analysis of DEGs performed on Gene Ontology terms demonstrated that M-MDSCs from *Nlrp3*$^{-/-}$ mice exhibited an inflammatory phenotype consisting of pathways involved in the interferon-alpha production, myeloid cell differentiation, and the response to DNA damage and repair pathways (Figure 5B). Importantly, transcription factors that have been closely linked to the suppressive activity of MDSCs

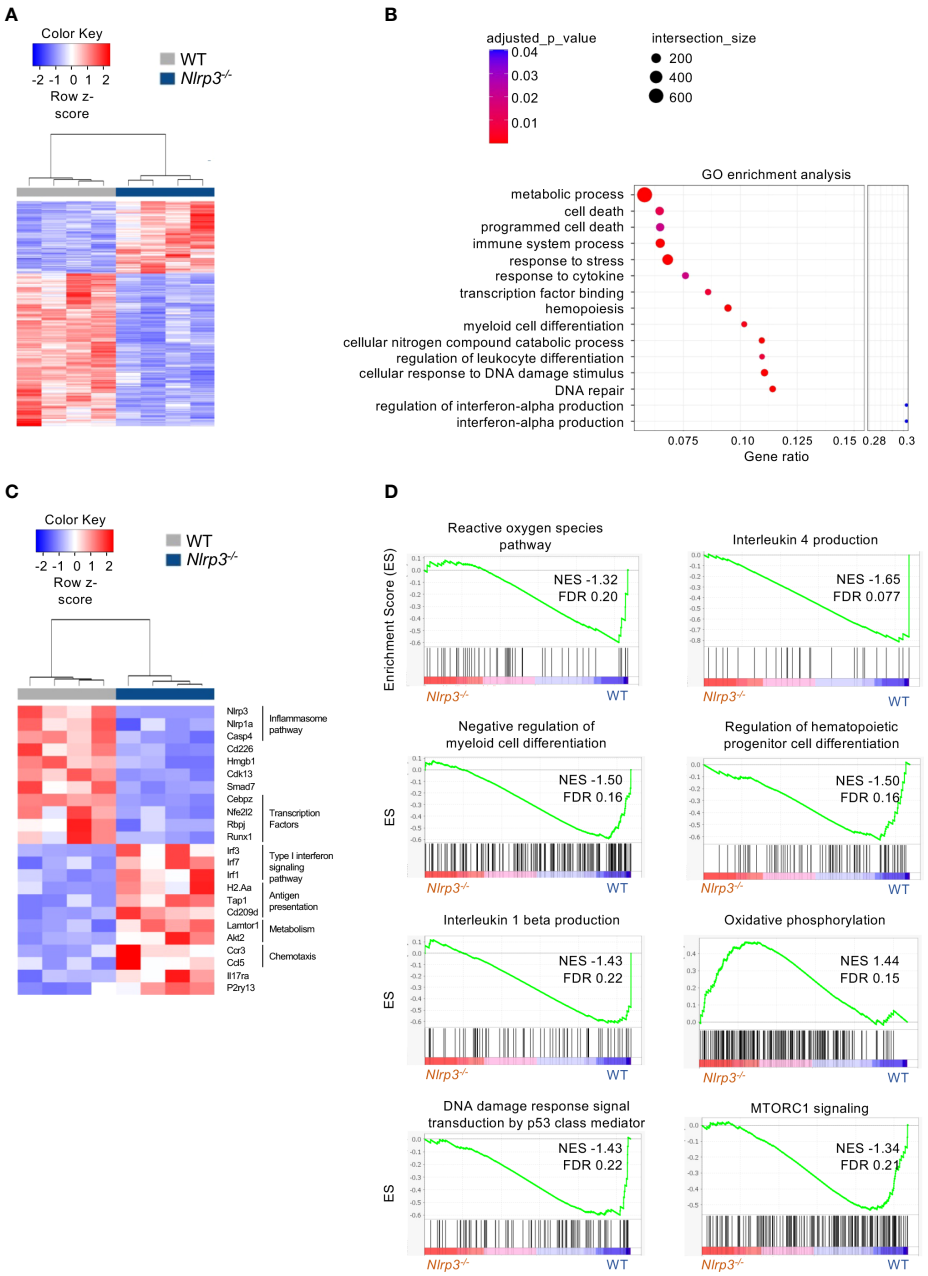

FIGURE 5
Extensive transcriptomic re-programming of *Nlrp3*$^{-/-}$ M-MDSCs. **(A)** Heatmap of DEGs from M-MDSCs from tumor-bearing *Nlrp3*$^{-/-}$ (n = 4) and WT (n = 4) mice. **(B)** Pathway analysis of DEGs from *Nlrp3*$^{-/-}$ vs. WT. **(C)** Heatmap of selected DEGs from M-MDSCs from tumor-bearing *Nlrp3*$^{-/-}$ and WT mice. **(D)** GSEA plot showing the enrichment of "Reactive oxygen species pathway" (NES –1.32, FDR 0.20), "Interleukin 4 production" (NES –1.65, FDR 0.077), "Negative regulation of myeloid cell differentiation" (NES –1.50, FDR 0.16), "Regulation of hematopoietic progenitor cell differentiation" (NES –1.50, FDR 0.16), "Interleukin 1-beta production" (NES –1.43, FDR 0.22), "Oxidative phosphorylation" (NES 1.44, FDR 0.15), "DNA damage response signal transduction by p53 class mediator" (NES –1.43, FDR 0.22), and "MTORC1 signaling" (NES –1.34, FDR 0.21) gene set.

(16, 33) (i.e., Cebpz, NF-E2-related factor 2) were downregulated in *Nlrp3*-deficient M-MDSCs (Figure 5C). Furthermore, genes associated with the antigen presentation process (*H2Aa*, *Tap1*, and *Cd209d*), as well as genes related to metabolic processes (*Lamtor1*, *Akt2*) were increased in M-MDSCs from *Nlrp3*$^{-/-}$ mice (Figure 5C). In support, GSEA, based on the Molecular Signatures Database (MSigDB) Hallmark and Gene Ontology gene set collections, revealed that *Nlrp3*-deficient M-MDSCs were metabolically re-programmed since they demonstrate enriched expression of transcripts related to the "oxidative phosphorylation" (NES 1.44, FDR 0.15) gene set, but were negatively correlated with "mTORC1 signaling" (NES −1.34, FDR 0.21) and "reactive oxygen species" (NES −1.32, FDR 0.20) (Figure 5D).

Regarding the G-MDSCs, differential expression analysis revealed 1,521 DEGs (|FC| > 1.5, FDR< 0.05) between tumor-bearing *Nlrp3*-deficient and WT mice (Figure 6A), with 466 and 1,055 genes to be up- and downregulated, respectively (Supplementary Figure 6B). Pathway analysis showed an enrichment in tumor necrosis factor (TNF)-alpha/NF-kB as well as the mTOR and AKT signaling pathways (Figure 6B), consistent with an inflammatory re-programming of *Nlrp3*-deficient G-MDSCs. Interestingly, expression of oxidized low-density lipoprotein receptor 1 gene (*Olr1*, also known as LOX-1), a signature gene in G-MDSCs (34), was downregulated in *Nlrp3*-deficient cells (Figure 6C). In addition, expression of *Cd274* gene (known as PDL1), closely linked to tumor immune evasion (35, 36), was downregulated in *Nlrp3*$^{-/-}$ G-MDSCs (Figure 6C). Notably, type I interferon genes were upregulated in G-MDSCs from *Nlrp3*$^{-/-}$ mice consistent with loss of suppressive function (32) (Figure 6C). Finally, GSEA revealed a metabolic rewiring in *Nlrp3*-deficient G-MDSCs as evident by the negative enrichment of the "regulation of response to reactive oxygen species" (NES −1.51, FDR 0.16) gene set (Figure 6D), which was further supported by the upregulation of superoxide dismutase 2 (*Sod2*) expression, an antioxidant enzyme crucial for mtROS scavenging (37), which is known to be highly expressed in mature neutrophils (38) (Figure 6C). Conclusively, these findings support an extensive transcriptomic re-programming of both M- and G-MDSCs in *Nlrp3*$^{-/-}$ tumor-inoculated animals, consistent with an inflammatory and less-suppressive phenotype.

Nlrp3-deficient MDSC subsets demonstrated impaired suppressive activity

To provide evidence for the functional re-programming of MDSC subsets in *Nlrp3*-deficient mice as suggested by the transcriptomic analysis, we set up an *in vitro* suppression assay. To this end, highly pure M-MDSCs and G-MDSCs were isolated from the spleens of melanoma-bearing *Nlrp3*$^{-/-}$ and WT animals and co-cultured with CellTrace Violet (CTV)-labeled T effector ($CD4^+Foxp3^-$) cells sorted from naïve $Foxp3^{GFP}$ mice in the presence of anti-CD3/anti-CD28 activation beads (Figure 7A). Both MDSC subsets from *Nlrp3*$^{-/-}$ mice displayed reduced suppressive ability compared with their WT counterparts as evidenced by decreased CTV dilution (Figure 7B). Furthermore, absence of T-cell suppression by *Nlrp3*$^{-/-}$ MDSC subsets was accompanied by enhanced activation of T cells as demonstrated by the CD25 and CD44 expression (Figure 7B). Overall, these data reveal that NLRP3 deficiency attenuates the suppressive activity of MDSC subsets.

Therapeutic targeting of NLRP3 inflammasome attenuates tumor growth and re-arranges the MDSC compartment

Considering that immunotherapy has demonstrated impressive results, yet in a small proportion of cancer patients, we sought to investigate whether pharmacologic inhibition of NLRP3 inflammasome in combination with ICI immunotherapy may demonstrate a synergistic therapeutic effect in tumor-bearing animals. For this reason, we first examined whether the MCC950 inhibitor, which prevents ATP hydrolysis, thus preserving an inactive conformation of NLRP3 inflammasome (39, 40), could efficiently inhibit NLRP3 inflammasome in primary splenocytes from naïve mice. Indeed, treatment with MCC950 of LPS-exposed splenocytes demonstrated a significant reduction of IL-1β secretion in culture supernatants confirming the potency to inhibit NLRP3 inflammasome (Supplementary Figure 7B). In the meantime, MCC950 did not demonstrate cytotoxic effects since assessment of 7-AAD expression by flow cytometry showed no differences between treated and non-treated cells (Supplementary Figure 7A).

In order to examine the therapeutic efficacy of MCC950 *in vivo* and whether it may possess a synergistic effect if combined with immune checkpoint immunotherapy, WT animals were inoculated with B16.F10 melanoma cells and treated with MCC950 alone or in combination with anti-PD-1 and anti-CTLA-4 monoclonal antibodies (Figure 8A). Strikingly, systemic pharmacological inhibition of NLRP3 inflammasome significantly reduced tumor growth in tumor-bearing compared to control-treated mice (Figure 8B). However, no significant differences in tumor growth were observed between MCC950-treated mice and those that received the combination treatment protocol (MCC950 + anti-PD-1/anti-CTLA-4 ICIs) (Figure 8B). The therapeutic effect of MCC950 was accompanied by modulation of the myeloid compartment and specifically a significant reduction of both MDSCs and $CD11c^+$ DCs was observed (Figure 8C). Of interest, DC frequencies were further reduced in mice treated with the combination of MCC950 inhibitor and anti-PD-1/anti-CTLA-4 antibodies compared to MCC950 alone (Figure 8C). Importantly, pharmacologic MCC950-mediated inflammasome

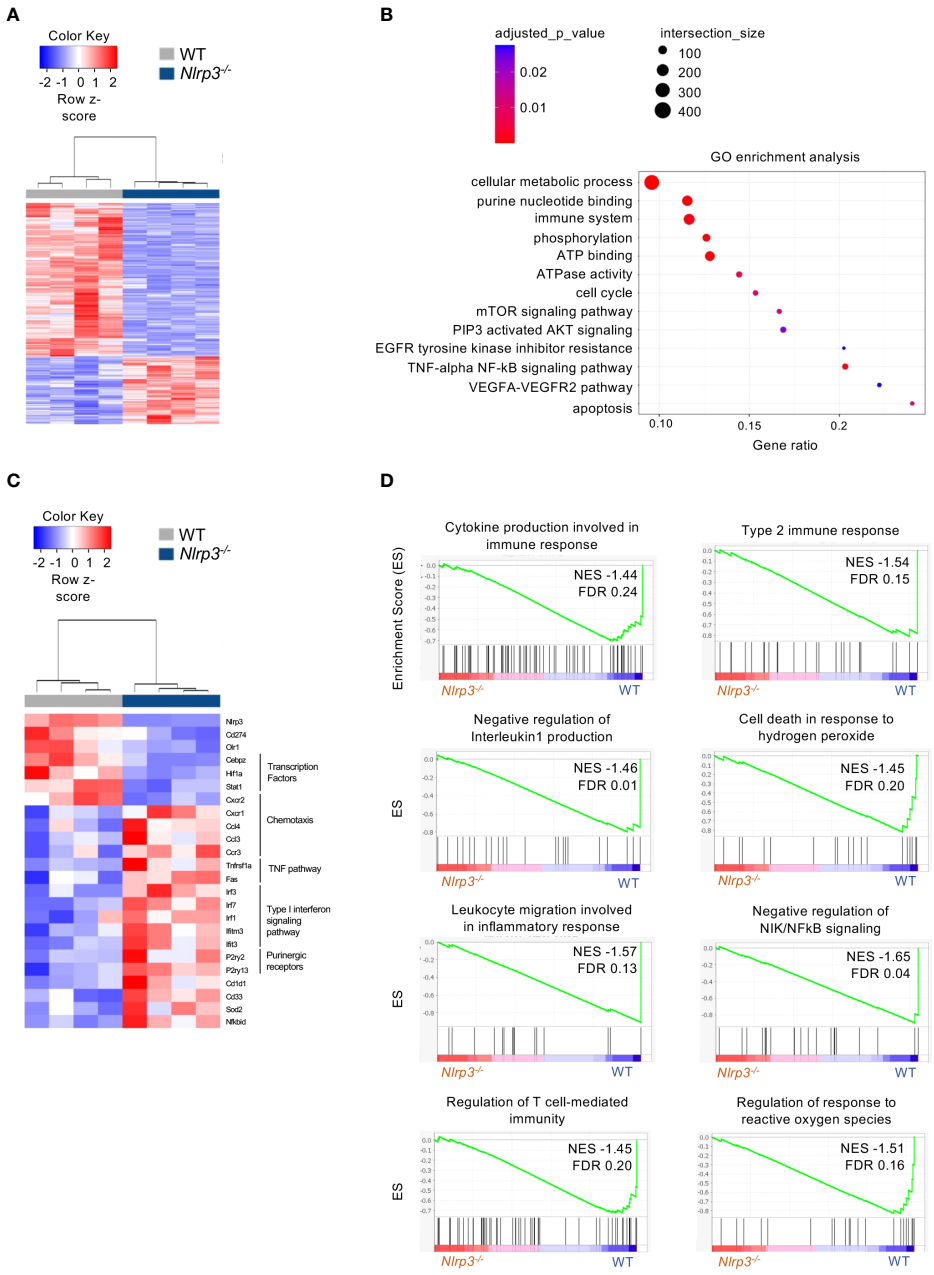

FIGURE 6
NLRP3 deficiency induces a transcriptional re-wiring to G-MDSCs. **(A)** Heatmap of DEGs from G-MDSCs from tumor-bearing *Nlrp3*$^{-/-}$ (n = 4) and WT (n = 4) mice. **(B)** Pathway analysis of DEGs from *Nlrp3*$^{-/-}$ vs. WT. **(C)** Heatmap of selected DEGs from G-MDSCs from tumor-bearing *Nlrp3*$^{-/-}$ and WT mice. **(D)** GSEA plot showing the enrichment of "Cytokine production involved in immune response" (NES –1.44, FDR 0.24), "Type 2 immune response" (NES –1.54, FDR 0.15), "Negative regulation of interleukin 1 production" (NES –1.46, FDR 0.01), "Cell death in response to hydrogen peroxide" (NES –1.45, FDR 0.20), "Leukocyte migration involved in inflammatory response" (NES –1.57, FDR 0.13), "Negative regulation of NIK/NFkB signaling" (NES –1.65, FDR 0.04), "Regulation of T cell-mediated immunity" (NES –1.45, FDR 0.20), and "Regulation of response to reactive oxygen species" (NES –1.51, FDR 0.16) gene set.

inhibition resulted in a significant increase in the spleen M-MDSCs and subsequent reduction of G-MDSCs as compared to the control-treated group (Figure 8D), recapitulating the results obtained in *Nlrp3*$^{-/-}$ tumor-inoculated animals. Collectively, therapeutic targeting of NLPR3 in tumor-bearing mice results in tumor regression and re-programming of the MDSC compartment, while no synergistic effect in combination with ICIs was observed.

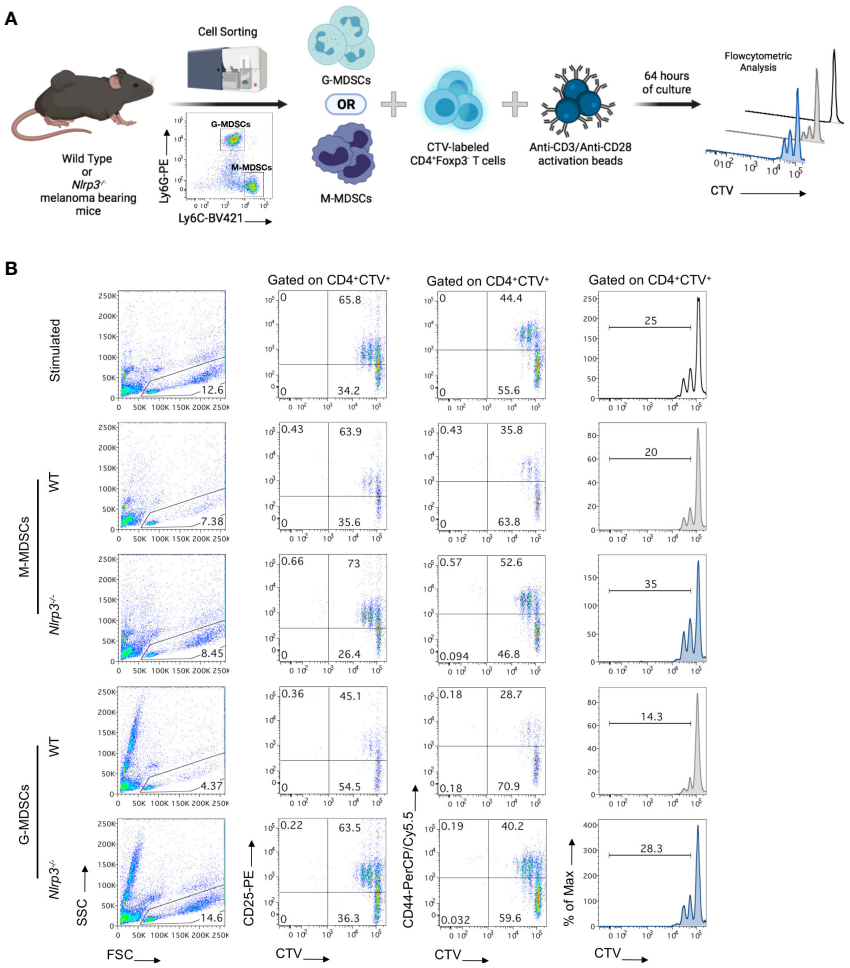

FIGURE 7
MDSC subsets from *Nlrp3*$^{-/-}$ mice exhibit an impaired suppressive function. **(A)** Schematic representation of the *in vitro* experimental setup for the evaluation of the suppressive ability of MDSC subsets. M-MDSCs and G-MDSCs were sorted from the spleen of WT (n = 2) and *Nlrp3*$^{-/-}$ (n = 2) melanoma-bearing mice and were co-cultured, at different ratios, with CellTrace Violet (CTV)-labeled T effectors (CD4^{+}Foxp3^{-}) cells, isolated from the lymph nodes (LNs) of Foxp3^{GFP} naïve mice and activated by anti-CD3/anti-CD28 monoclonal antibodies. Suppressive activity of MDSC subsets was estimated 64 h later by flow cytometry. **(B)** Representative FACS plots showing the percentages of lymphocytes according to FSC and SSC, frequencies of CD4^{+}CTV^{+}CD25^{+} and CD4^{+}CTV^{+}CD44^{+} populations, and histograms of CTV MFI dilution of different culture conditions (T:M-MDSCs 1:1; T:G-MDSCs 3:1). Histogram plots were gated on CD4^{+}CTV^{+} cells and thus represent Teff cell proliferation. Numbers in histograms represent percentages of proliferated cells. Representative data from two independent mouse samples (n) are shown. Illustration created with BioRender.com.

Discussion

Inflammation is considered one of the most important hallmarks of cancer. However, as of today, therapeutic attempts in targeting the various inflammatory mediators that abundantly presented in the TME has shown limited success, highlighting the existence of unappreciated mechanisms of pro-tumorigenic inflammation. Herein, we reveal that targeting of the NLRP3 inflammasome in host cells, promotes tumor regression and induces re-wiring of the MDSCs, which constitute a major mechanism of tumor immune evasion. Specifically, we report a phenotypic, transcriptomic and functional re-programming between the monocytic and granulocytic subsets of MDSCs, upon *Nlrp3* deletion, during tumor development. Finally, pharmacologic inhibition of inflammasome, attenuates tumor growth and re-programs the MDSC compartment in a similar fashion to genetic silencing of *Nlrp3*.

Our findings are consistent with a pro-tumorigenic role of NLRP3 expression. This is in agreement with several studies, demonstrating that NLRP3 activation promoted tumor development in experimental models (41–47) and is associated with susceptibility to melanoma (48) and with poor survival in patients with advanced colorectal cancer (49) or development of

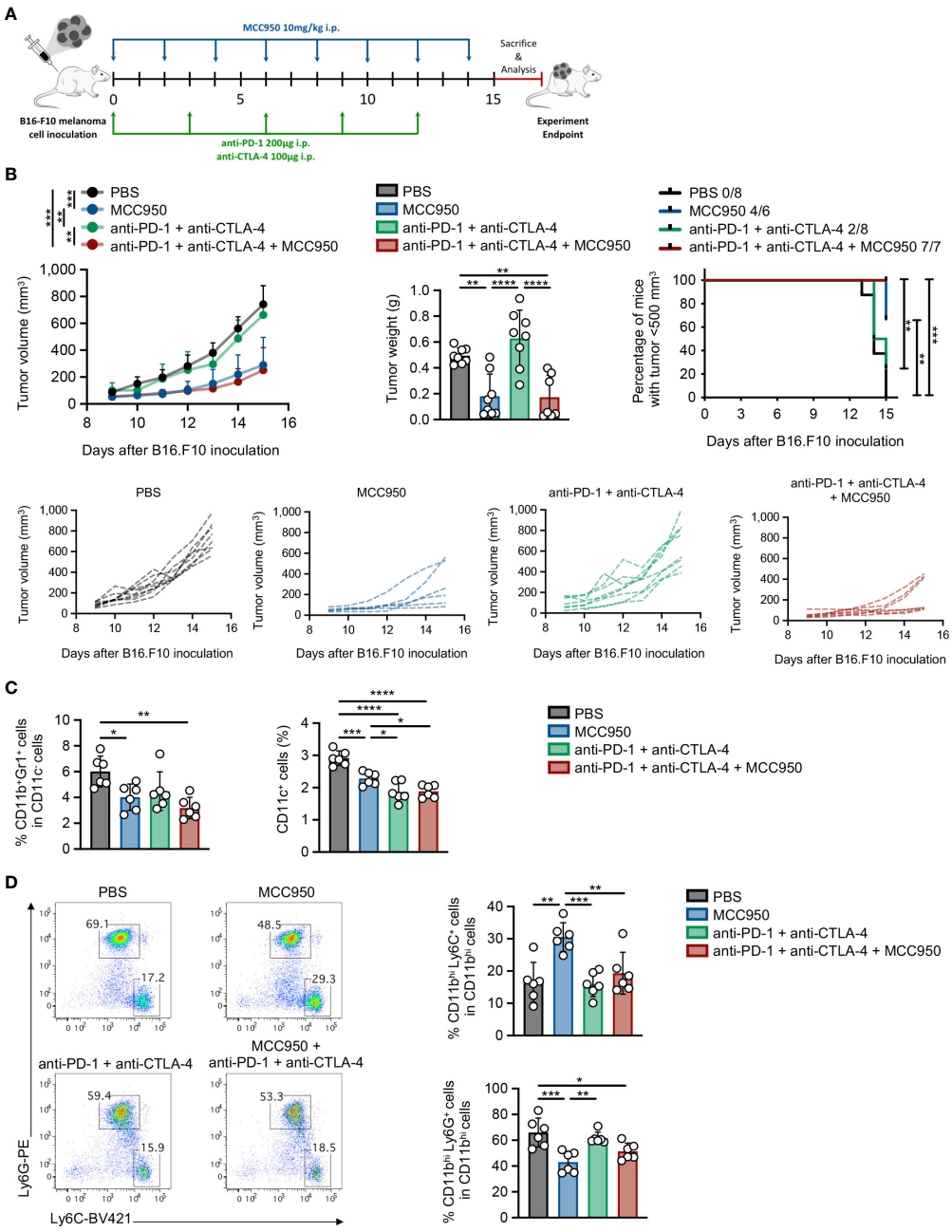

FIGURE 8
Pharmacologic inhibition of NLRP3 attenuates tumor growth and re-programs the MDSC compartment. **(A)** Experimental protocol for immunotherapy administration. B16.F10 melanoma-bearing C57BL/6J mice were treated with MCC950, anti-PD-1, and anti-CTLA-4 immune checkpoint inhibitors, or PBS as shown. Analysis was performed 15 days after tumor induction. **(B)** Tumor volume curve 9–15 days after B16.F10 inoculation, tumor weight on the experiment endpoint, and percentage of mice bearing tumors<500 mm^3, with the ratio showing the number of mice with tumor<500 mm^3/total injected mice (PBS: n = 8; MCC950: n = 8; anti-PD-1/anti-CTLA-4: n = 8; MCC950 + anti-PD-1/anti-CTLA-4: n = 7). **(C)** Frequencies of MDSCs and DCs in spleen tissue of B16.F10 melanoma-bearing C57BL/6J mice treated with the indicated treatments (PBS: n = 6; MCC950: n = 6; anti-PD-1/anti-CTLA-4: n = 6; MCC950 + anti-PD-1/anti-CTLA-4: n = 6), determined by flow cytometric analysis. **(D)** Representative FACS plots and frequencies of spleen-infiltrating M-MDSCs and G-MDSCs subsets of B16.F10 melanoma-bearing C57BL/6J mice treated with the indicated treatments (PBS: n = 6; MCC950: n = 6; anti-PD-1/anti-CTLA-4: n = 6; MCC950 + anti-PD-1/anti-CTLA-4: n = 6), determined by flow cytometric analysis. Data are shown as mean (± S.D.). Data from one **(C, D)** and representative data from two **(B)** independent experiments are shown. Statistical significance was obtained by one-way ANOVA with Tukey's multiple comparison test or log(rank) test **(B)**. Symbols: (*), $p \leq 0.05$; (**), $p \leq 0.01$; (***), $p \leq 0.001$; (****), $p \leq 0.0001$, n = biologically independent mouse samples.

various hematologic malignancies (47, 50). Despite these findings, an anti-tumorigenic role of NLRP3 has also been described as for example in NLRP3-deficient animals that showed increased susceptibility to colitis-associated cancer induced by dextran sulfate sodium (DSS) (51). In this line, a single-nucleotide polymorphism in *Nlrp3* gene Q705K (rs35829419) was correlated with decreased survival in colorectal cancer patients (52) and was also mapped at high frequency in patients with pancreatic cancer (53). Our TCGA analysis also revealed a contrasting correlation of NLRP3 expression and survival in patients with melanoma and lung cancer, building upon the proposed dual role of NLRP3 in cancer. In line with this, a previous pan-cancer analysis of NLRP3-related genes revealed that 15 types of cancer out of the 24 types analyzed demonstrated differential expression of NLRP3 signatures compared to normal samples and also showed that NLRP3 score could serve as an independent prognostic factor in SKCM (24). What determines the pro- versus the anti-tumorigenic role of NLRP3 remains obscure. It is possible that in the inflammatory context of the TME, the cell type in which NLRP3 operates, the genetic background, and the tumor cell per se possess a decisive role on NLRP3 activation and function during tumor development. Accordingly, activation of NLRP3 in cancer-associated fibroblasts (CAFs) (43) or macrophages (44) promoted tumor growth and metastasis supporting its pro-tumorigenic role, whereas sensing of dying tumors by DCs led to activation of NLRP3 followed by IL-1β secretion, which showed to be required for priming of tumor-specific IFN-γ-producing cytotoxic T lymphocytes promoting anti-tumor immunity consistent with an anti-tumorigenic role of NLRP3 in this cell subset (21). Finally, targeting NLRP3 expression in B16.F10 melanoma cells attenuated tumor growth and limited the expansion of MDSCs (54). Of note, in the latter study, *Nlrp3*$^{-/-}$ did not exhibit significant differences regarding B16.F10 melanoma cell growth compared to WT animals, in contrast to what we report. This discrepancy may account for the different strains of *Nlrp3*$^{-/-}$ mice used and/or the different melanoma cell numbers and method of injections (mixing with Matrigel) used in the two studies. Although studies with conditional targeting of *Nlrp3* in diverse cell types of the TME are still lacking, understanding the inflammasome role in an individual cell population that orchestrates the tumor immune evasion processes will provide further insights into the functional importance of this pathway and may introduce novel therapeutic targets.

Accumulating evidence in both preclinical models and patients with malignancies have established an important role of MDSCs in impeding tumor immune surveillance (5, 6, 8). Furthermore, MDSC-mediated suppression is an important mechanism of immunotherapy resistance. Therefore, major efforts over the last decade were placed for MDSC targeting to enhance anti-tumor immunity and immunotherapy responses (8, 55, 56). However, the heterogeneous nature of MDSCs and the limited knowledge on mechanisms *via* which may exert their function in the diverse tumor settings prevented such attempts. Our results demonstrate that the NLRP3/IL-1β pathway is activated in MDSCs in melanoma-bearing animals. Importantly, NLRP3 deficiency shifted the balance between M- and G-MDSCs frequencies, and transcriptomic analysis revealed that in the absence of *Nlrp3*, both MDSC subsets exhibited a robust re-programming highlighted by enrichment in type I IFN signature, inflammatory pathway signaling antigen processing and presentation transcripts, which has been closely linked to the functional properties of MDSCs. In addition, M-MDSCs showed enrichment in mTOR signaling, antigen processing, and presentation transcripts, which is in line with the findings by Alissafi et al. in which autophagy-deficient M-MDSCs upregulated the antigen presentation machinery and MHC-II expression promoting anti-tumor immunity (9). Moreover, G-MDSCs from *Nlrp3*$^{-/-}$ mice not only downregulated *Lox1* and *Pdl1* expression, which are associated with G-MDSC identity (34) and tumor immune evasion (35, 36), respectively, but also demonstrated enrichment in type I IFN signatures, which is linked to re-programming of granulocytic cells in the TME (32). Furthermore, the differential expression analysis from our RNA-seq data did not reveal any difference in the gene expression of Arginase-1 (Arg-1) and nitric oxide synthase 2 (Nos2) immunosuppressive factors, in both MDSC subsets. However, *Nlrp3* deficiency downregulated the expression of Stat-1 and hypoxia-inducible factor (Hif) 1a in G-MDSCs, which are transcription factors related to the immunosuppressive properties of MDSCs mainly by regulating *Arg-1* and *Nos2* expression (57–59). Notably, the transcriptomic re-wiring of MDSC subsets in *Nlrp3*$^{-/-}$ mice was accompanied by loss of function in both subsets as demonstrated by their inability to suppress T-cell responses *in vitro*.

So far, NLPR3 activation has been shown to be involved in the mobilization and expansion/activation of MDSCs through IL-1β secretion, while NLRP3 or IL-1β inhibition limited the MDSC presence in the TME (20). Moreover, the progression of melanoma was found to be associated with elevated concentrations of IL-1β as compared to patients with stable disease, and enrichment of circulating monocytic MDSCs significantly correlated with a decreased progression free survival of melanoma patients (60). Interestingly, our results show that IL-1β is not decreased in the TME of melanoma-bearing *Nlrp3*$^{-/-}$ animals (data not shown), indicating that NLRP3 ablation may promote tumor regression and MDSC subset re-programming *via* an IL-1β-independent mechanism. Thus, IL-1β may be secreted in an inflammasome-independent fashion (61) or other inflammasome products like IL-18 are likely to explain these findings. In support, IL-18 has been shown to enhance the immunosuppressive properties of M-MDSCs and to promote their accumulation in the TME (62). Alternatively, NLRP3 may exert cell-intrinsic signaling, which could instruct the differentiation of MDSCs not only in the periphery but also in the BM. Indeed, our results point to

decreased frequencies of GMPs in the BM of *Nlrp3*$^{-/-}$ mice, which may be a result of the reduced inflammation due to tumor regression or could be explained by an intrinsic effect due to the absence of NLRP3, which may imprint on MDSC generation and subset differentiation. These hypotheses need to be thoroughly investigated considering that NLRP3 expression is established in human and mouse HSPCs and its involvement in hematopoiesis is emerging (63).

Several stimuli have been reported to activate NLRP3, ranging from pathogen-associated molecular patterns and DAMPs leading to NFkB activation, to stressogenic molecules and pathways such as reactive oxygen species, hypoxia, and extracellular ATP (17). Our results demonstrated that extracellular ATP induces the functional activation of NLRP3 in tumor-induced MDSCs *ex vivo*, accompanied by IL-1β release. The mechanisms, however, leading to NLRP3 activation in MDSCs during tumor development remain obscure. The TME is characterized by hypoxic conditions, which may drive NLRP3 activation in infiltrated cells including MDSCs. However, expression of the hypoxia-inducible transcription factor Hif1a is downregulated in G-MDSCs from *Nlrp3*-deficient mice. In addition, tumor dying cells release large amounts of ATP, which mediate NLRP3 activation (21). Consistent with this, the transcriptomic profile of *Nlrp3*$^{-/-}$ G-MDSCs has shown upregulation of *P2ry2* and *P2ry13* purinergic receptor genes. Furthermore, recently, Treg cells showed to release large amounts of ATP, upon apoptosis in the TME (64), which may, in turn, activate the inflammasome in other cells in close proximity like MDSCs. This may be envisioned as a resistance mechanism in which therapeutic targeting of one suppressive axis (i.e., Tregs) may empower a second one (i.e., MDSCs) to cope with tumor immune evasion. In support of this hypothesis chemotherapy-induced cathepsin B release demonstrated to activate NLRP3 inflammasome in MDSCs, curtailing anti-tumor immunity (65). In contrast, ATP released from tumor cells (21) or perforin released from CD8$^+$ cytotoxic T lymphocytes (CTLs) (66) activated NLRP3 in antigen-presenting cells (APCs) and promoted immunity against tumors. Overall, identification of pathways that lead to NLRP3 activation in MDSCs may provide novel insights into the specific targeting of inflammasome and its products to these potent suppressive cells.

One of the mechanisms of acquired resistance to immunotherapy is the immunosuppressive circuit in the TME, which blunts the induction of anti-tumor immune responses. ICIs revolutionized cancer treatment but still a significant percentage of patients fail to respond (1). Whether inflammasome activation contributes to immunotherapy resistance and whether its targeting could augment therapeutic efficacy is not fully understood. Our data show that pharmacologic inhibition of inflammasome induces regression of melanoma growth and re-programs the MDSC compartment in a similar fashion to *Nlrp3*-deficient mice. Of interest, the combination of the NLRP3 inhibitor with anti-CTLA-4/anti-PD-1 did not demonstrate a significant synergistic effect in regard to tumor growth but only in the frequencies of MDSC subsets. The extent of inflammation involvement in the enhancement of immunotherapy efficacy is unexplored. In this line, pharmacologic targeting of inflammasome de-repression, through disruption of the transmembrane protein TMEM176b, augments the therapeutic efficacy of anti-CTLA4/anti-PD1 by unleashing inflammasome activation (67). The inflammatory context and the cell type where anti-CTLA-4/anti-PD-1-mediated NLRP3 activation takes place to instruct anti-tumor immunity remain to be determined.

In conclusion, our findings place inflammasome in the therapeutic quiver of cancer, while further efforts should be aimed at overcoming immunotherapy resistance in combinatorial regimens incorporating inflammasome inhibitors.

Data availability statement

The datasets presented in this study can be found in online repositories. The names of the repository/repositories and accession number(s) can be found below: Gene Expression Omnibus (GEO accession number: GSE188973).

Ethics statement

The animal study was reviewed and approved by Institutional Committee of Protocol Evaluation of the IMBB together with the Directorates of Agricultural Economy and Veterinary, Region of Crete, Greece (14/10/2020 Heraklion, Greece, protocol 234446).

Author contributions

IP designed and performed experiments, analysed the data, generated the figures and wrote the manuscript. MG performed bioinformatic analysis of RNA-seq data and interpretation. LB generated and provided critical reagents. AK performed the TCGA survival analysis and edited the manuscript. AH performed experiments, analysed data and critically edited the manuscript. PV designed and supervised the study, performed the data analysis and wrote the manuscript. All authors contributed to the article and approved the submitted version.

Acknowledgments

We thank all the members of the P. Verginis laboratory for helpful discussions. We thank Efrosyni Markaki for assisting with experiments, and Pavlos Alexakos and Hara Roumpaki for technical assistance on animal handling and maintenance, in the animal facility of the Biomedical Research Foundation of the Academy of Athens [BRFAA] and Institute of Molecular Biology and Biotechnology Institute [IMBB], respectively. We also thank Anastasia Apostolidou and Hara Vlata for technical assistance

on flow cytometry and cell sorting at BRFAA and IMBB, respectively, and Vasiliki Theodorou and Emmanuel Dialynas for assistance with the transcriptomic analysis. This work was supported by grants from the Greek General Secretariat of Research and Technology Aristeia II 3468, the T2EDK-02288, MDS-TARGET to P.V., and the COST Action Mye-EUNITER (BM1404, http://www.mye-euniter.eu), as part of the European Union Framework Program Horizon 2020.

Conflict of interest

The authors declare that the research was conducted in the absence of any commercial or financial relationships that could be construed as a potential conflict of interest.

Publisher's note

Supplementary material

The Supplementary Material for this article can be found online at: https://www.frontiersin.org/articles/10.3389/fimmu.2022.889075/full#supplementary-material

References

1. Pitt JM, Vétizou M, Daillère R, Roberti MP, Yamazaki T, Routy B, et al. Resistance mechanisms to immune-checkpoint blockade in cancer: Tumor-intrinsic and -extrinsic factors. *Immunity* (2016) 44:1255–69. doi: 10.1016/j.immuni.2016.06.001

2. Michot JM, Bigenwald C, Champiat S, Collins M, Carbonnel F, Postel-Vinay S, et al. Immune-related adverse events with immune checkpoint blockade: A comprehensive review. *Eur J Cancer* (2016) 54:139–48. doi: 10.1016/j.ejca.2015.11.016

3. Chen DS, Mellman I. Oncology meets immunology: The cancer-immunity cycle. *Immunity* (2013) 39:1–10. doi: 10.1016/j.immuni.2013.07.012

4. Bronte V, Brandau S, Chen SH, Colombo MP, Frey AB, Greten TF, et al. Recommendations for myeloid-derived suppressor cell nomenclature and characterization standards. *Nat Commun* (2016) 7:12150. doi: 10.1038/ncomms12150

5. Papafragkos I, Markaki E, Kalpadakis C, Verginis P. Decoding the myeloid-derived suppressor cells in lymphoid malignancies. *J Clin Med* (2021) 10:3462. doi: 10.3390/jcm10163462

6. Marvel D, Gabrilovich DI. Myeloid-derived suppressor cells in the tumor microenvironment: Expect the unexpected. *J Clin Invest* (2015) 125:3356–64. doi: 10.1172/JCI80005

7. Veglia F, Sanseviero E, Gabrilovich DI. Myeloid-derived suppressor cells in the era of increasing myeloid cell diversity. *Nat Rev Immunol* (2021) 21:485–98. doi: 10.1038/s41577-020-00490-y

8. Hatziioannou A, Alissafi T, Verginis P. Myeloid-derived suppressor cells and T regulatory cells in tumors: Unraveling the dark side of the force. *J Leukoc Biol* (2017) 102:407–21. doi: 10.1189/jlb.5vmr1116-493r

9. Alissafi T, Hatzioannou A, Mintzas K, Barouni RM, Banos A, Sormendi S, et al. Autophagy orchestrates the regulatory program of tumor-associated myeloid-derived suppressor cells. *J Clin Invest* (2018) 128:3840–52. doi: 10.1172/JCI120888

10. Nefedova Y, Fishman M, Sherman S, Wang X, Beg AA, Gabrilovich DI. Mechanism of all-trans retinoic acid effect on tumor-associated myeloid-derived suppressor cells. *Cancer Res* (2007) 67:11021 LP–11028. doi: 10.1158/0008-5472.CAN-07-2593

11. Kusmartsev S, Cheng F, Yu B, Nefedova Y, Sotomayor E, Lush R, et al. All-Trans-Retinoic acid eliminates immature myeloid cells from tumor-bearing mice and improves the effect of vaccination. *Cancer Res* (2003) 63:4441 LP – 4449.

12. Iclozan C, Antonia S, Chiappori A, Chen D-T, Gabrilovich D. Therapeutic regulation of myeloid-derived suppressor cells and immune response to cancer vaccine in patients with extensive stage small cell lung cancer. *Cancer Immunol Immunother* (2013) 62:909–18. doi: 10.1007/s00262-013-1396-8

13. Veglia F, Tyurin VA, Blasi M, De Leo A, Kossenkov AV, Donthireddy L, et al. Fatty acid transport protein 2 reprograms neutrophils in cancer. *Nature* (2019) 569:73–8. doi: 10.1038/s41586-019-1118-2

14. Fujita M, Kohanbash G, Fellows-Mayle W, Hamilton RL, Komohara Y, Decker SA, et al. COX-2 blockade suppresses gliomagenesis by inhibiting myeloid-derived suppressor cells. *Cancer Res* (2011) 71:2664 LP – 2674. doi: 10.1158/0008-5472.CAN-10-3055

15. Rodriguez PC, Hernandez CP, Quiceno D, Dubinett SM, Zabaleta J, Ochoa JB, et al. Arginase I in myeloid suppressor cells is induced by COX-2 in lung carcinoma. *J Exp Med* (2005) 202:931–9. doi: 10.1084/jem.20050715

16. Mohamed E, Sierra RA, Trillo-Tinoco J, Cao Y, Innamarato P, Payne KK, et al. The unfolded protein response mediator PERK governs myeloid cell-driven immunosuppression in tumors through inhibition of STING signaling. *Immunity* (2020) 52:668–682.e7. doi: 10.1016/j.immuni.2020.03.004

17. Swanson KV, Deng M, Ting JP-Y. The NLRP3 inflammasome: Molecular activation and regulation to therapeutics. *Nat Rev Immunol* (2019) 19:477–89. doi: 10.1038/s41577-019-0165-0

18. Paik S, Kim JK, Silwal P, Sasakawa C, Jo E-K. An update on the regulatory mechanisms of NLRP3 inflammasome activation. *Cell Mol Immunol* (2021) 18:1141–60. doi: 10.1038/s41423-021-00670-3

19. He Y, Hara H, Núñez G. Mechanism and regulation of NLRP3 inflammasome activation. *Trends Biochem Sci* (2016) 41:1012–21. doi: 10.1016/j.tibs.2016.09.002

20. Karki R, Kanneganti T-D. Diverging inflammasome signals in tumorigenesis and potential targeting. *Nat Rev Cancer* (2019) 19:197–214. doi: 10.1038/s41568-019-0123-y

21. Ghiringhelli F, Apetoh L, Tesniere A, Aymeric L, Ma Y, Ortiz C, et al. Activation of the NLRP3 inflammasome in dendritic cells induces IL-1β–dependent adaptive immunity against tumors. *Nat Med* (2009) 15:1170–8. doi: 10.1038/nm.2028

22. Huang Y, Wang H, Hao Y, Lin H, Dong M, Ye J, et al. Myeloid PTEN promotes chemotherapy-induced NLRP3-inflammasome activation and antitumour immunity. *Nat Cell Biol* (2020) 22:716–27. doi: 10.1038/s41556-020-0510-3

23. Theivanthiran B, Evans KS, DeVito NC, Plebanek M, Sturdivant M, Wachsmuth LP, et al. A tumor-intrinsic PD-L1/NLRP3 inflammasome signaling pathway drives resistance to anti–PD-1 immunotherapy. *J Clin Invest* (2020) 130:2570–86. doi: 10.1172/JCI133055

24. Ju M, Bi J, Wei Q, Jiang L, Guan Q, Zhang M, et al. Pan-cancer analysis of NLRP3 inflammasome with potential implications in prognosis and immunotherapy in human cancer. *Brief Bioinform* (2021) 22:bbaa345. doi: 10.1093/bib/bbaa345

25. Stuart T, Butler A, Hoffman P, Hafemeister C, Papalexi E, Mauck WMIII, et al. Comprehensive integration of single-cell data. *Cell* (2019) 177:1888–1902.e21. doi: 10.1016/j.cell.2019.05.031

26. Martinon F, Pétrilli V, Mayor A, Tardivel A, Tschopp J. Gout-associated uric acid crystals activate the NALP3 inflammasome. *Nature* (2006) 440:237–41. doi: 10.1038/nature04516

27. Hatzioannou A, Banos A, Sakelaropoulos T, Fedonidis C, Vidali MS, Köhne M, et al. An intrinsic role of IL-33 in treg cell–mediated tumor immunoevasion. *Nat Immunol* (2020) 21:75–85. doi: 10.1038/s41590-019-0555-2

28. Kim D, Langmead B, Salzberg SL. HISAT: A fast spliced aligner with low memory requirements. *Nat Methods* (2015) 12:357–60. doi: 10.1038/nmeth.3317

29. Anders S, Pyl PT, Huber W. HTSeq-a Python framework to work with high-throughput sequencing data. *Bioinformatics* (2015) 31:166–9. doi: 10.1093/bioinformatics/btu638

30. Alissafi T, Kalafati L, Lazari M, Filia A, Kloukina I, Manifava M, et al. Mitochondrial oxidative damage underlies regulatory T cell defects in autoimmunity. *Cell Metab* (2020) 32:591–604.e7. doi: 10.1016/j.cmet.2020.07.001

31. Guarda G, Zenger M, Yazdi AS, Schroder K, Ferrero I, Menu P, et al. Differential expression of NLRP3 among hematopoietic cells. *J Immunol* (2011) 186:2529 LP – 2534. doi: 10.4049/jimmunol.1002720

32. Kalafati L, Kourtzelis I, Schulte-Schrepping J, Li X, Hatzioannou A, Grinenko T, et al. Innate immune training of granulopoiesis promotes anti-tumor activity. *Cell* (2020) 183:771–785.e12. doi: 10.1016/j.cell.2020.09.058

33. Thevenot PT, Sierra RA, Raber PL, Al-Khami AA, Trillo-Tinoco J, Zarreii P, et al. The stress-response sensor chop regulates the function and accumulation of myeloid-derived suppressor cells in tumors. *Immunity* (2014) 41:389–401. doi: 10.1016/j.immuni.2014.08.015

34. Condamine T, Dominguez GA, Youn JI, Kossenkov AV, Mony S, Alicea-Torres K, et al. Lectin-type oxidized LDL receptor-1 distinguishes population of human polymorphonuclear myeloid-derived suppressor cells in cancer patients. *Sci Immunol* (2016) 1:aaf8943. doi: 10.1126/sciimmunol.aaf8943

35. Lau J, Cheung J, Navarro A, Lianoglou S, Haley B, Totpal K, et al. Tumour and host cell PD-L1 is required to mediate suppression of anti-tumour immunity in mice. *Nat Commun* (2017) 8:14572. doi: 10.1038/ncomms14572

36. Zou W, Chen L. Inhibitory B7-family molecules in the tumour microenvironment. *Nat Rev Immunol* (2008) 8:467–77. doi: 10.1038/nri2326

37. Sies H, Jones DP. Reactive oxygen species (ROS) as pleiotropic physiological signalling agents. *Nat Rev Mol Cell Biol* (2020) 21:363–83. doi: 10.1038/s41580-020-0230-3

38. Youn J-I, Collazo M, Shalova IN, Biswas SK, Gabrilovich DI. Characterization of the nature of granulocytic myeloid-derived suppressor cells in tumor-bearing mice. *J Leukoc Biol* (2012) 91:167–81. doi: 10.1189/jlb.0311177

39. Coll RC, Hill JR, Day CJ, Zamoshnikova A, Boucher D, Massey NL, et al. MCC950 directly targets the NLRP3 ATP-hydrolysis motif for inflammasome inhibition. *Nat Chem Biol* (2019) 15:556–9. doi: 10.1038/s41589-019-0277-7

40. Coll RC, Robertson AAB, Chae JJ, Higgins SC, Muñoz-Planillo R, Inserra MC, et al. A small-molecule inhibitor of the NLRP3 inflammasome for the treatment of inflammatory diseases. *Nat Med* (2015) 21:248–55. doi: 10.1038/nm.3806

41. Guo B, Fu S, Zhang J, Liu B, Li Z. Targeting Inflammasome/IL-1 pathways for cancer immunotherapy. *Sci Rep* (2016) 6:36107. doi: 10.1038/srep36107

42. Kaplanov I, Carmi Y, Kornetsky R, Shemesh A, Shurin GV, Shurin MR, et al. Blocking IL-1β reverses the immunosuppression in mouse breast cancer and synergizes with anti–PD-1 for tumor abrogation. *Proc Natl Acad Sci* (2019) 116:1361 LP – 1369. doi: 10.1073/pnas.1812266115

43. Ershaid N, Sharon Y, Doron H, Raz Y, Shani O, Cohen N, et al. NLRP3 inflammasome in fibroblasts links tissue damage with inflammation in breast cancer progression and metastasis. *Nat Commun* (2019) 10:4375. doi: 10.1038/s41467-019-12370-8

44. Daley D, Mani VR, Mohan N, Akkad N, Pandian GSDB, Savadkar S, et al. NLRP3 signaling drives macrophage-induced adaptive immune suppression in pancreatic carcinoma. *J Exp Med* (2017) 214:1711–24. doi: 10.1084/jem.20161707

45. Weichand B, Popp R, Dziumbla S, Mora J, Strack E, Elwakeel E, et al. S1PR1 on tumor-associated macrophages promotes lymphangiogenesis and metastasis *via* NLRP3/IL-1β. *J Exp Med* (2017) 214:2695–713. doi: 10.1084/jem.20160392

46. Chow MT, Sceneay J, Paget C, Wong CSF, Duret H, Tschopp J, et al. NLRP3 suppresses NK cell–mediated responses to carcinogen-induced tumors and metastases. *Cancer Res* (2012) 72:5721 LP – 5732. doi: 10.1158/0008-5472.CAN-12-0509

47. Hamarsheh S, Osswald L, Saller BS, Unger S, De Feo D, Vinnakota JM, et al. Oncogenic KrasG12D causes myeloproliferation *via* NLRP3 inflammasome activation. *Nat Commun* (2020) 11:1659. doi: 10.1038/s41467-020-15497-1

48. Okamoto M, Liu W, Luo Y, Tanaka A, Cai X, Norris DA, et al. Constitutively active inflammasome in human melanoma cells mediating autoinflammation *via* caspase-1 processing and secretion of interleukin-1β *. *J Biol Chem* (2010) 285:6477–88. doi: 10.1074/jbc.M109.064907

49. Shi F, Wei B, Lan T, Xiao Y, Quan X, Chen J, et al. Low NLRP3 expression predicts a better prognosis of colorectal cancer. *Biosci Rep* (2021) 41:BSR20210280. doi: 10.1042/BSR20210280

50. Zhao X, Zhang C, Hua M, Wang R, Zhong C, Yu J, et al. NLRP3 inflammasome activation plays a carcinogenic role through effector cytokine IL-18 in lymphoma. *Oncotarget* (2017) 8:108571–83. doi: 10.18632/oncotarget.21010

51. Allen IC, TeKippe EM, Woodford R-MT, Uronis JM, Holl EK, Rogers AB, et al. The NLRP3 inflammasome functions as a negative regulator of tumorigenesis during colitis-associated cancer. *J Exp Med* (2010) 207:1045–56. doi: 10.1084/jem.20100050

52. Ungerbäck J, Belenki D, Jawad ul-Hassan A, Fredrikson M, Fransén K, Elander N, et al. Genetic variation and alterations of genes involved in Nfκb/TNFAIP3- and NLRP3-inflammasome signaling affect susceptibility and outcome of colorectal cancer. *Carcinogenesis* (2012) 33:2126–34. doi: 10.1093/carcin/bgs256

53. Miskiewicz A, Szparecki G, Durlik M, Rydzewska G, Ziobrowski I, Górska R. The Q705K and F359L single-nucleotide polymorphisms of NOD-like receptor signaling pathway: Association with chronic pancreatitis, pancreatic cancer, and periodontitis. *Arch Immunol Ther Exp (Warsz)* (2015) 63:485–94. doi: 10.1007/s00005-015-0355-9

54. Tengesdal IW, Menon DR, Osborne DG, Neff CP, Powers NE, Gamboni F, et al. Targeting tumor-derived NLRP3 reduces melanoma progression by limiting MDSCs expansion. *Proc Natl Acad Sci* (2021) 118:e2000915118. doi: 10.1073/pnas.2000915118

55. Draghiciu O, Lubbers J, Nijman HW, Daemen T. Myeloid derived suppressor cells–an overview of combat strategies to increase immunotherapy efficacy. *Oncoimmunology* (2015) 4:e954829. doi: 10.4161/21624011.2014.954829

56. Nakamura K, Smyth MJ. Myeloid immunosuppression and immune checkpoints in the tumor microenvironment. *Cell Mol Immunol* (2020) 17:1–12. doi: 10.1038/s41423-019-0306-1

57. Kusmartsev S, Gabrilovich DI. STAT1 signaling regulates tumor-associated macrophage-mediated T cell deletion. *J Immunol* (2005) 174:4880 LP – 4891. doi: 10.4049/jimmunol.174.8.4880

58. Corzo CA, Condamine T, Lu L, Cotter MJ, Youn J-I, Cheng P, et al. HIF-1α regulates function and differentiation of myeloid-derived suppressor cells in the tumor microenvironment. *J Exp Med* (2010) 207:2439–53. doi: 10.1084/jem.20100587

59. Doedens AL, Stockmann C, Rubinstein MP, Liao D, Zhang N, DeNardo DG, et al. Macrophage expression of hypoxia-inducible factor-1α suppresses T-cell function and promotes tumor progression. *Cancer Res* (2010) 70:7465–75. doi: 10.1158/0008-5472.CAN-10-1439

60. Jiang H, Gebhardt C, Umansky L, Beckhove P, Schulze TJ, Utikal J, et al. Elevated chronic inflammatory factors and myeloid-derived suppressor cells indicate poor prognosis in advanced melanoma patients. *Int J Cancer* (2015) 136:2352–60. doi: 10.1002/ijc.29297

61. Jain A, Irizarry-Caro RA, McDaniel MM, Chawla AS, Carroll KR, Overcast GR, et al. T Cells instruct myeloid cells to produce inflammasome-independent IL-1β and cause autoimmunity. *Nat Immunol* (2020) 21:65–74. doi: 10.1038/s41590-019-0559-y

62. Lim HX, Hong H-J, Cho D, Kim TS. IL-18 enhances immunosuppressive responses by promoting differentiation into monocytic myeloid-derived suppressor cells. *J Immunol* (2014) 193:5453 LP – 5460. doi: 10.4049/jimmunol.1401282

63. Ratajczak MZ, Bujko K, Cymer M, Thapa A, Adamiak M, Ratajczak J, et al. The Nlrp3 inflammasome as a "Rising star" in studies of normal and malignant hematopoiesis. *Leukemia* (2020) 34:1512–23. doi: 10.1038/s41375-020-0827-8

64. Maj T, Wang W, Crespo J, Zhang H, Wang W, Wei S, et al. Oxidative stress controls regulatory T cell apoptosis and suppressor activity and PD-L1-Blockade resistance in tumor. *Nat Immunol* (2017) 18:1332–41. doi: 10.1038/ni.3868

65. Bruchard M, Mignot G, Derangère V, Chalmin F, Chevriaux A, Végran F, et al. Chemotherapy-triggered cathepsin b release in myeloid-derived suppressor cells activates the Nlrp3 inflammasome and promotes tumor growth. *Nat Med* (2013) 19:57–64. doi: 10.1038/nm.2999

66. Yao Y, Chen S, Cao M, Fan X, Yang T, Huang Y, et al. Antigen-specific CD8+ T cell feedback activates NLRP3 inflammasome in antigen-presenting cells through perforin. *Nat Commun* (2017) 8:15402. doi: 10.1038/ncomms15402

67. Segovia M, Russo S, Jeldres M, Mahmoud YD, Perez V, Duhalde M, et al. Targeting TMEM176B enhances antitumor immunity and augments the efficacy of immune checkpoint blockers by unleashing inflammasome activation. *Cancer Cell* (2019) 35:767–781.e6. doi: 10.1016/j.ccell.2019.04.003

frontiers | Frontiers in Immunology

TYPE Original Research
PUBLISHED 18 January 2023
DOI 10.3389/fimmu.2022.947136

OPEN ACCESS

EDITED BY
Nicolas Larmonier,
Université de Bordeaux, France

REVIEWED BY
Gustavo Pedraza-Alva,
Institute of Biotechnology, National Autonomous University of Mexico, Mexico
Haili Qian,
Chinese Academy of Medical Sciences and Peking Union Medical College, China

*CORRESPONDENCE
Zhi Zhang
zhi1969@163.com
Xuemei Zhang
zhangxuemei@ncst.edu.cn

†These authors have contributed equally to this work and share first authorship

SPECIALTY SECTION
This article was submitted to Cancer Immunity and Immunotherapy, a section of the journal Frontiers in Immunology

RECEIVED 18 May 2022
ACCEPTED 28 December 2022
PUBLISHED 18 January 2023

CITATION
Liu J, Fu N, Yang Z, Li A, Wu H, Jin Y, Song Q, Ji S, Xu H, Zhang Z and Zhang X (2023) The genetic and epigenetic regulation of *CD55* and its pathway analysis in colon cancer. *Front. Immunol.* 13:947136. doi: 10.3389/fimmu.2022.947136

The genetic and epigenetic regulation of *CD55* and its pathway analysis in colon cancer

Jiawei Liu[1,2†], Ning Fu[2†], Zhenbang Yang[3], Ang Li[3], Hongjiao Wu[3], Ye Jin[2], Qinqin Song[1], Shanshan Ji[1], Hongxue Xu[3], Zhi Zhang[1*] and Xuemei Zhang[2,3*]

[1]Affiliated Tangshan Gongren Hospital, North China University of Science and Technology, Tangshan, China, [2]College of Life Science, North China University of Science and Technology, Tangshan, China, [3]School of Public Health, North China University of Science and Technology, Tangshan, China

Background: *CD55* plays an important role in the development of colon cancer. This study aims to evaluate the expression of *CD55* in colon cancer and discover how it is regulated by transcriptional factors and miRNA.

Methods: The expression of *CD55* was explored by TIMER2.0, UALCAN, and Human Protein Atlas (HPA) databases. TRANSFAC and Contra v3 were used to predict the potential binding sites of transcription factors in the *CD55* promoter. TargetScan and starBase v2.0 were used to predict the potential binding ability of miRNAs to the 3′ untranslated region (3′UTR) of *CD55*. SurvivalMeth was used to explore the differentially methylated sites in the *CD55* promoter. Western blotting was used to detect the expression of *TFCP2* and *CD55*. Dual-luciferase reporter assay and chromatin immunoprecipitation (ChIP) assay were performed to determine the targeting relationship of *TFCP2*, *NF-κB*, or miR-27a-3p with *CD55*. *CD55*-related genes were explored by constructing a protein–protein interaction (PPI) network and performing pathway analysis by Gene Ontology (GO) and Kyoto Encyclopedia of Genes and Genomes (KEGG).

Results: *CD55* was highly expressed in colon cancer tissues. The mRNA and protein expression levels of *TFCP2* were reduced by si-*TFCP2*. *NF-κB* mRNA was obviously reduced by *NF-κB* inhibitor and increased by *NF-κB* activator. *CD55* protein was also inhibited by miR-27a-3p. Dual-luciferase reporter assays showed that after knocking down *TFCP2* or inhibiting *NF-κB*, the promoter activity of *CD55* was decreased by 21% and 70%, respectively; after activating *NF-κB*, the promoter activity of *CD55* increased by 2.3 times. As *TFCP2* or *NF-κB* binding site was mutated, the transcriptional activity of *CD55* was significantly decreased. ChIP assay showed that *TFCP2* and *NF-κB* combined to the promoter of *CD55*. The luciferase activity of *CD55* 3′UTR decreased after being co-transfected with miR-27a-3p mimics and increased by miR-27a-3p antagomir. As the miR-27a-3p binding site was mutated, we did not find any significant effect of miR-27a-3p on reporter activity. PPI network assay revealed a set of *CD55*-related genes, which included *CFP*, *CFB*, *C4A*, and *C4B*. GO and KEGG analyses revealed that the target genes occur more frequently in immune-related pathways.

Conclusion: Our results indicated that *CD55* is regulated by *TFCP2*, *NF-κB*, miR-27a-3p, and several immune-related genes, which in turn affects colon cancer.

KEYWORDS

complement, *CD55*, colon cancer, *NF-κB*, MiR-27a-3p

1 Introduction

According to GLOBOCAN 2020, colorectal cancer (CRC) ranks third in terms of morbidity and mortality in the world, presenting a serious threat to human health. Also, over the past decade, the rate of decline in CRC mortality has slowed (1). The incidence of CRC is known to be significantly influenced by early-life exposures (2). Thus, it is essential to find effective molecular targets for colon cancer treatment.

Gene expression is a highly regulated process. Given the complexity of gene regulation, it is not surprising that many human diseases, including various cancers, are caused by defective gene regulation. Transcription factors (TFs) are known to regulate chromatin and transcription by recognizing specific DNA sequences and subsequently forming a complex (3). MicroRNAs (miRNAs) are endogenous, and small non-coding RNAs are implicated in nearly all known physiological and pathological processes, such as cell proliferation, differentiation, and apoptosis. Importantly, miRNAs act as important regulators of several genes at the post-transcriptional level in almost all kinds of cancer cells. Multiple studies have reported that miRNAs exhibit aberrant expression in a variety of cancers.

DNA methylation is an epigenetic mechanism that tends to be crucial in the regulation of gene expression (4–6). Gene expression can be affected by the bonding of the methyl group to the cytosine nucleotide. DNA methylation in the promoter region of genes is often associated with the repression of transcription (7). The DNA methylation level in tumor tissues is mostly reported to be lower than that in normal adjacent tissues. During the development of cancer, the level of hypomethylation of genomic DNA increases as lesions progress from benign cell proliferation to aggressive cancer (8).

The complement system is a crucial element of innate immunity, and it also plays an essential role in the regulation of adaptive immunity (9). The activation of the complement system promotes cell proliferation in various cancers (10). *CD55*, also known as decay-accelerating factor (*DAF*), is one of the membrane-bound complement regulatory proteins (*mCRPs*) that play a key role in maintaining the homeostasis of the complement system. Dho and his colleagues found that *CD55* was over-expressed in metastatic colon cancer tissues, and inhibition of *CD55* could restrain colon cancer tumorigenesis and metastasis (11). The high expression of *CD55* has a significantly decreased 7-year survival rate for colon cancer (12). Comprehensive bioinformatics analysis has also shown that *CD55* was positively correlated with infiltration levels of $CD8^+$ T cells, neutrophils, and dendritic cells in colon cancer, suggesting its potential role in tumor immune regulation (13).

Since *CD55* might be used as a prognostic indicator and a therapeutic target in colon cancer, we investigated the possible mechanism of the regulation of *CD55* in colon cancer and its impact on the molecular and immunological characteristics of colon cancer.

2 Materials and methods

2.1 The expression analysis of *CD55* and miR-27a

TIMER2.0 (http://timer.cistrome.org/) is a web server freely available to the research community. It consists of three main components: immunization, exploration, and estimation. The "Diff Exp" component allows users to compare gene expression differences between multiple tumor and normal tissues. In this study, we used TIMER2.0 to analyze the expression difference of *CD55* between cancer tissues and normal tissues in a pan-cancer way. We analyzed the expression level of *CD55* in colorectal cancer and its association with different histopathological types by UALCAN (http://ualcan.path.uab.edu), which contains cancer OMICS data. The protein expression of *CD55* in human normal colon tissue and colon cancer tissue was verified by Human Protein Atlas (HPA; https://www.proteinatlas.org/). The HPA database, an antibody-based approach combined with transcriptomic data to outline global expression profiles, is the largest and most comprehensive public database of the spatial distribution of proteins in human tissues and cells (14). We downloaded the available miRNA data from the Gene Expression Omnibus (GEO) database (GSE48267 and GSE59856). We used the Limma program to analyze the expression of miR-27a in colorectal cancer.

2.2 *In silico* analysis of *CD55* regulatory region

From *CD55*, 2 kb of 5′ flanking region and 3′ untranslated region (3′UTR) was downloaded from the National Center for Biotechnology Information (NCBI) database. Transcription factor binding sites in the promoter of *CD55* were predicted by using the TRANSFAC program (http://gene-regulation.com) and ConTra v3 online web tool (http://bioit2.irc.ugent.be/contra/v3/). "Vertebrates" was chosen as "Matrix groups", and "cut-offs" was set to "minimize

the sum of both error rates". The potential miRNA binding sites in 3′ UTR of *CD55* were screened using TargetScanHuman 7.2 (https://www.targetscan.org/vert_72/) and starBase v2.0 (https://starbase.sysu.edu.cn/starbase2/index.php).

2.3 Cell lines and reagents

Human colon cancer cells HCT-116 and LOVO were provided by Procell (Wuhan, China). All plasmids (pGL3-Basic, pRL-SV40, and psiCHECK-2 plasmid) were purchased from Promega (Madison, WI, USA). The si-*TFCP2*, miR-27a-3p mimics, and miR-27a-3p antagomir were synthesized by GenePharma (Shanghai, China). The sequences of si-*TFCP2* were 5′-GCU AAU CCA ACU CAA CUA ATT-3′ and 5′-UUA GUU GAG UUG GAU UAG CTT-3′. The sequences of siRNA control were 5′-UUC UCC GAA CGU GUC ACG UTT-3′ and 5′-ACG UGA CAC GUU CGG AGA ATT-3′. The sequences of miR-27a-3p mimics were 5′-UUC ACA GUG GCU AAG UUC CGC-3′ and 5′-GGA ACU UAG CCA CUG UGA AUU-3′. The sequences of mimics control were 5′-UUC UCC GAA CGU GUC ACG UTT-3′ and 5′-ACG UGA CAC GUU CGG AGA ATT-3′. The sequence of miR-27a-3p antagomir was 5′-GCG GAA CUU AGC CAC UGU GAA-3′. The sequence of antagomir control was 5′-CAG UAC UUU UGU GUA CAA-3′. *NF-κB* inhibitor (B5556) and *NF-κB* activator (TNFα) (HZ-1014) were purchased from Sigma-Aldrich (New Jersey, USA) and ProteinTech (Chicago, USA), respectively.

2.4 Construction of *CD55* promoter and 3′UTR plasmid

The primer pair used to amplify the promoter of *CD55* (1,963 bp) was *CD55*-PF (5′-GG GGTACC CCT CTC TAT GAA GGG CA-3′)/*CD55*-PR (5′-CCC AAGCTT GGG GAC GGC GGG AAC CAC GAC-3′) with protective bases and the recognition sites (underlined bases) of *Kpn*I or *Hin*dIII in each primer. This PCR product was then cloned into a pGL3-Basic plasmid. The PCR primers to amplify the fragment of 3′UTR (1,237 bp) were $CD55_{3'UTR}$-PF (5′-CCG CTCGAG TGC CTT CAT TTA GGA TGC TTT CA-3′) and $CD55_{3'UTR}$-PR (5′-GTAA GCGGCCGC TTT ACA GTG AAA TGC CAT GAA CG-3′), of which protective bases and recognition sites (underlined) of *Xho*I and *Not*I sites were added. The 3′UTR PCR product was then cloned into a psiCHECK-2 plasmid. Successful plasmids were then designed wild-type plasmids as pGL3-$CD55_{pro}$-Wt and psi-$CD55_{3'UTR}$-Wt. The *CD55* promoter fragment containing *TFCP2* or *NF-κB* binding sites was synthesized to generate mutant type (pGL3-$CD55_{pro}$-*TFCP2*-Mut and pGL3-$CD55_{pro}$-*NF-κB*-Mut) by Sangon Biotech (Shanghai, China). The *CD55* 3′UTR fragment containing miR-27a-3p binding sites was also synthesized to generate a mutant type (psi-$CD55_{3'UTR}$-Mut).

2.5 Cell culture and treatment

Human colon cancer cells were cultured in complete Dulbecco's modified Eagle's medium (DMEM; Thermo Fisher Scientific, Waltham, MA, USA) with 10% fetal bovine serum (FBS; Thermo Fisher Scientific, USA), 1% penicillin–streptomycin (100 U/ml of penicillin and 100 mg/ml of streptomycin, P&S; Thermo Fisher Scientific, USA) in an atmosphere with 5% CO_2 at 37°C. Cells were transfected with Lipofectamine 2000 reagent (Thermo Fisher Scientific, USA), according to the manufacturer's instructions. For *TFCP2* binding analysis, 500 ng of pGL3-$CD55_{pro}$/pGL3-$CD55_{mut}$ plasmid and 0.5 ng of pRL-SV40 plasmid were co-transfected with si-*TFCP2* or negative control into HCT116 cells for 24 h. For *NF-κB* binding analysis, colon cancer cells were transfected with 500 ng of pGL3-$CD55_{pro}$/pGL3-$CD55_{mut}$ and 0.5 ng of pRL-SV40 for 24 h and then treated with or without 20 μM of *NF-κB* inhibitor/50 ng of *NF-κB* activator for another 24 h. For miRNA binding analysis, 30 ng of psi-$CD55_{3'UTR}$-Wt/psi-$CD55_{3'UTR}$-Mut was co-transfected with 100 nM of miR-27a-3p mimics/control or 20 nM of miR-27a-3p antagomir/control into HCT116 cells for 24 h.

2.6 cDNA synthesis and qRT-PCR

Total RNA was extracted from HCT116 cells using TRIzol reagent (Thermo Fisher Scientific, USA) and was then reversely transcribed into cDNA with RevertAid First Strand cDNA Synthesis Kit (Thermo Fisher Scientific, USA). *TFCP2* mRNA was detected using Power SYBR Green PCR Master Mix (Thermo Fisher Scientific, USA) in ABIPRISM® 7900HT Fast Real-Time PCR System (Applied Biosystems, Foster City, CA, USA). The amplification procedure was 50°C for 2 min and 95°C for 2 min, followed by 45 cycles of 95°C for 15 s and 60°C for 2 min. *GAPDH* was used as the reference gene. The primer pairs for the amplification of *TFCP2*, *NF-κB*, and *GAPDH* were *TFCP2*-PF/*TFCP2*-PR (5′-TCA CGT ATG TCA ATA ACT CCC CA-3′/5′-GTG TGG TTG GTA AGA GGT T-3′), *NF-κB*-PF/*NF-κB*-PR (5′-AAC AGA GAG GAT TTC GTT TCC G-3′/5′-TTT GAC CTG AGG GTA AGA CTT CT-3′), and *GAPDH*-PF/*GAPDH*-PR (5′-ACA ACT TTG GTA TCG TGG AAG G-3′/5′-GCC CAT CAC GCC ACA GTT TC-3′). Three repetitions were performed for each reaction. The relative mRNA expression was analyzed using the $2^{-\Delta\Delta Ct}$ method.

2.7 Dual-luciferase reporter assay

Colon cancer cells were plated at 2×10^5 cells per well into 24-well plates. When cells reached 70%–80% confluence, each plasmid was then transfected into cells. After 24 h, cells were collected, and luciferase and Renilla reporter signals were detected using the Dual-luciferase Reporter Assay System (Promega, USA) by GloMax® 20/20 Luminometer (Promega, USA).

2.8 Western blotting analysis

The colon cancer cells were lysed with radioimmunoprecipitation assay (RIPA) buffer (Thermo Fisher Scientific, USA). After being quantified and denatured, samples were separated by 10% sodium dodecyl sulfate–polyacrylamide gel electrophoresis (SDS-PAGE) and then transferred to a polyvinylidene difluoride (PVDF) membrane (Millipore, Billerica, MA, USA). After being blocked for 1 h with 5%

skimmed milk in TBST at room temperature, the membrane was incubated with the primary antibody overnight at 4°C and then washed and incubated with horseradish peroxidase (HRP)-conjugated secondary antibody for 1 h at room temperature. Specific protein was then developed by using enhanced chemiluminescence (ECL) luminescence reagents (Amersham, UK). The densitometry analysis was performed using ImageJ (National Institutes of Health, USA). β-Actin was applied as a reference control. The following primary antibodies were used: anti–*CD55* (1:10,000 dilution; ab133684; Abcam, Cambridge, UK), anti–*NF-κB p65* (1:5,000 dilution; ab32536; Abcam), and anti–*TFCP2* (1:5,000 dilution; 15203-1-AP; ProteinTech).

2.9 Chromatin immunoprecipitation assay

LOVO cells (2×10^6) were plated in a 6-mm dish for the chromatin immunoprecipitation (ChIP) experiment by using a ChIP Assay kit (Thermo Fisher Scientific, USA) following the manufacturer's protocol. To verify if *NF-κB* or *TFCP2* binds to the promoter of *CD55*, a total of 5 µg of sheared DNA was used for chromatin immunoprecipitation using anti-*NF-κB* (1:250 dilution; ab32536; Abcam) or anti–*TFCP2* antibody (1:250 dilution; 15203-1-AP; ProteinTech). The immunoprecipitated DNA was then amplified using specific primers to analyze the transcription factor binding site of *CD55*. The *CD55* promoter-specific primers were described as follows: *NF-κB* site-PF/*NF-κB* site-PR (5′-CGT GTG GGG TGA GTA GGG-3′/5′-ATG CTG GTG AGC GGC GAG-3′) and *TFCP2* site-PF/*TFCP2* site-PR (5′-CGT CTT GTT TGT CCC ACC C-3′/5′-GCA GTA AGC AGA AGC CTC G-3′).

2.10 Cell viability detection by CCK8 assay

Cell viability was analyzed by Cell Counting Kit 8 (CCK8; Dojindo, Kumamoto, Japan) according to the manufacturer's protocol. Cells were seeded and cultured at a density of 5×10^3/well into 96-well microplates. After psi-*CD55*3′UTR-Wt was co-transfected with miR-27a-3p mimics or mimics control for 24 h, 10 µl of CCK8 reagent was added and cultured for 30 mins. All experiments were performed in triplicate. The absorbance was measured at 450 nm using a microplate reader (Multiskan FC, Thermo Fisher Scientific, USA).

2.11 PPI network construction of *CD55*-related proteins

STRING consortium 2022 (https://string-db.org) aims to integrate all known and predicted associations between proteins, including both physical interactions and functional associations. We set the network type to "full STRING network", the required score to "high confidence (0.700)", and the size cutoff to "no more than 20 interactors" to obtain the *CD55*-related protein. We used the Cytoscape 3.9.1 platform to construct the protein interaction network (protein–protein interaction (PPI) network) and analyze the network characteristics.

2.12 GO and KEGG analyses of *CD55*-related genes

We used the "ggplot2" R package and DAVID 6.8 (http://www.david.niaid.nih.gov) database to conduct Gene Ontology (GO) and Kyoto Encyclopedia of Genes and Genomes (KEGG) analysis of *CD55*-related proteins ($p < 0.05$). We performed the visualization of GO and KEGG enrichment by R version 3.6.1.

2.13 The detection of methylation modification of *CD55* and its effect on the prognosis of colon cancer patients

SurvivalMeth (http://bio-bigdata.hrbmu.edu.cn/survivalmeth/) investigates the effect of DNA methylation-related functional elements on prognosis, which was developed by Harbin Medical University. We analyzed the methylation sites and their effect on the survival time of colon cancer patients of *CD55* by using SurvivalMeth.

2.14 Statistical analyses

All analyses were performed with R version 3.6.1 and its appropriate packages. Statistical graphs were produced in GraphPad Prism 8. Statistical significance of the Wilcoxon rank sum test or t-test was used for two-group comparisons. All statistical tests were two-sided, and $p < 0.05$ was considered to be statistically significant.

3 Results

3.1 The expression analysis of *CD55* in colorectal cancer tissues

Using the TIMER2.0 online program, we found that *CD55* was highly expressed in a variety of solid cancers, including colorectal cancer (Figure 1A). There are two pathological types of colorectal cancer tissues, adenocarcinoma and mucinous adenocarcinoma. Using the UALCAN database, we evaluated the expression of *CD55* in colorectal cancer tissues and its relationship with different pathological types and found that *CD55* was highly expressed in either colorectal adenocarcinoma or mucinous adenocarcinoma when compared with that in adjacent normal tissues. Additionally, the average level of *CD55* in mucinous adenocarcinoma tissue is significantly higher than that in adenocarcinoma tissue (Figures 1B–E). Immunohistochemical images from the HPA database showed that the expression *CD55* was higher in colorectal cancer than in adjacent normal tissue (Figure 1F).

3.2 Transcriptional regulation of *CD55*

To predict the potential TF binding sites of *CD55*, we used TRANSFAC online program, and it generated eight transcriptional factors, including *COMP1*, *Hand1/E47*, *CDP CR1*, *Pax-4*, *TFCP2*, *Nkx2-5*, *c-Rel*, and *NF-κB* (Table 1). According to the core binding characteristic

10.3389/fimmu.2022.947136

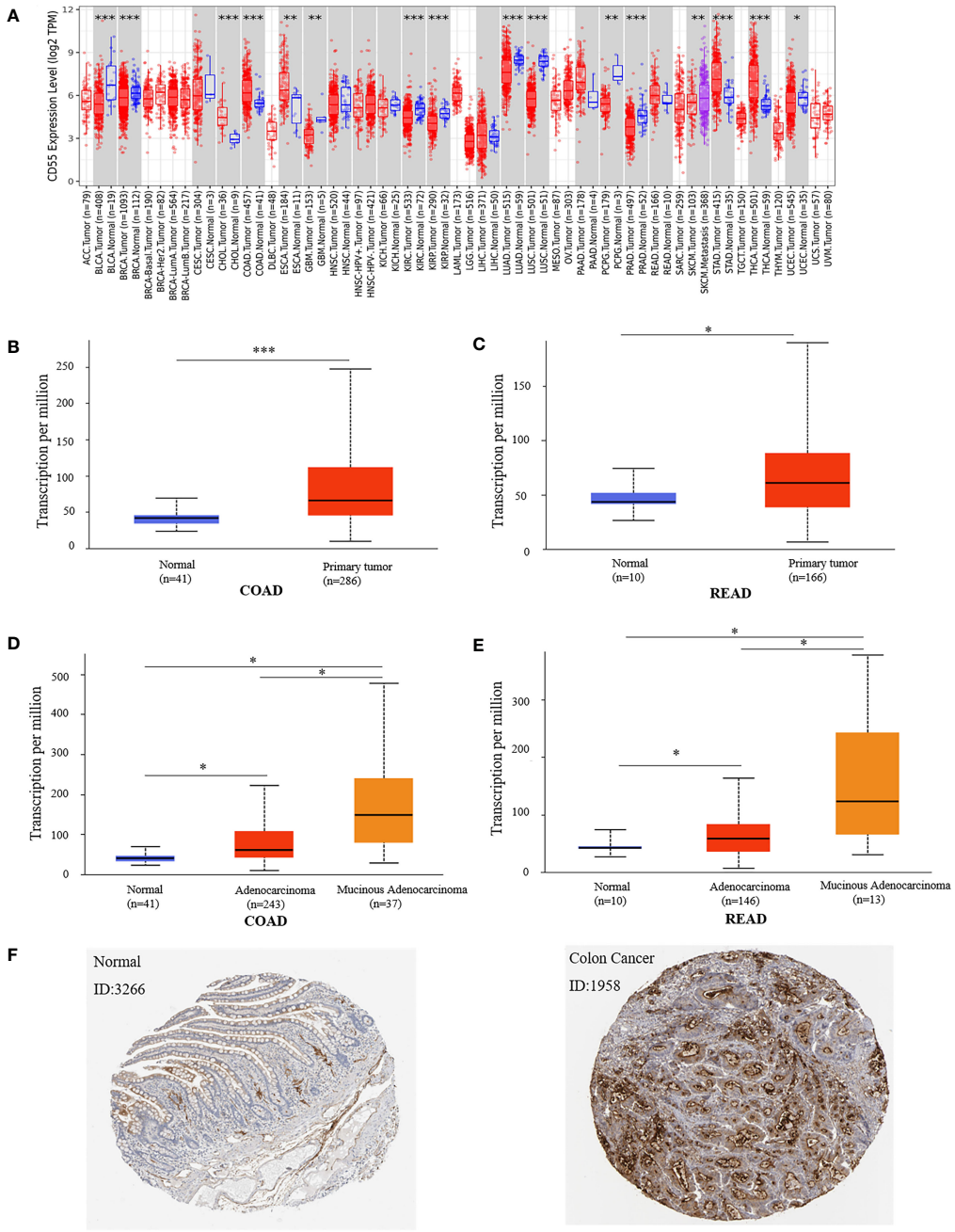

FIGURE 1
Expression of *CD55* in colon cancer tissue and adjacent normal tissue. **(A)** *CD55* expression levels in different tumor types from TCGA database were determined by TIMER2.0. **(B, C)** Quantification of *CD55* expression levels in colorectal cancer (COAD, colon adenocarcinoma; READ, rectal adenocarcinoma) and paired adjacent normal tissues. **(D, E)** Quantification of *CD55* expression in different pathological types of colorectal cancer. **(F)** Protein levels of *CD55* in colorectal cancer and normal tissues by HPA database (*$p < 0.05$, **$p < 0.01$, ***$p < 0.001$). TCGA, The Cancer Genome Atlas.

of these TFs provided by the Contra v3 database, we found that *TFCP2* and *NF-κB* were the most likely to bind to *CD55* (Figures 2A–C).

To confirm the regulation of *TFCP2* to the expression of *CD55*, we used *TFCP2* siRNA to treat HCT116 cells. We found that *TFCP2* siRNA effectively reduced the expression of *TFCP2* (Figures 3A, B). Dual-luciferase reporter assay showed that the reporter activity of pGL3-$CD55_{pro}$-Wt with *TFCP2* knockdown decreased by 21% compared with that without *TFCP2* knockdown ($p < 0.05$) (Figure 3C). After the *TFCP2* binding site was mutated, the promoter activity of *CD55* was reduced by 66% (Figure 3G).

We also evaluated the effect of *NF-κB* on the promoter activity of *CD55*. We found that the expression of *NF-κB* was significantly decreased by the *NF-κB* inhibitor and increased by the *NF-κB* activator (Figure 3D). The luciferase reporter analysis showed that the promoter activity of *CD55* was decreased by 70% due to the *NF-κB* inhibitor ($p < 0.01$) (Figure 3E). The transcriptional activity of *CD55* was activated by the *NF-κB* activator; however, after we mutated the binding site of *NF-κB*, we did not see the effect of the *NF-κB* activator on the luciferase reporter activity (Figure 3F). After the *NF-κB* binding site was mutated, the promoter activity of *CD55* was reduced by 42% (Figure 3G).

TABLE 1 The potential binding transcription factors of the *CD55*.

Factor name	Core match	Matrix match	Sequence
COMP1	1.00	0.82	ctgtagGATTGgctccagcaatgg
Hand/E47	1.00	0.96	ctagCCAGAcccagat
CDP CR1	1.00	0.93	cccaTCAATg
Pax-4	0.93	0.84	tgggtTGATGggtgcagcaaa
Pax-4	0.90	0.88	agcacTCAAGcgcggggatgc
TFCP2	0.95	0.9	CTTGGtgacgc
Nkx2-5	1.00	1.00	caTAATTa
NF-κB	1.00	1.00	GGGAAttccc
c-Rel	1.00	1.00	GGAAAttccc
NF-κB	1.00	1.00	gggaaGCCCC

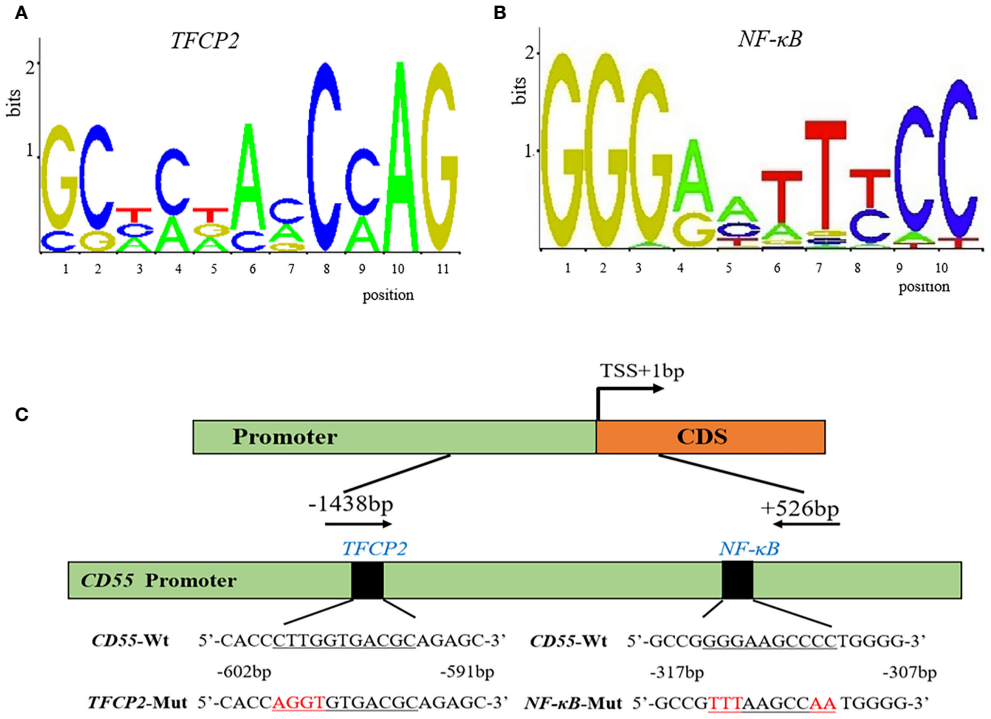

FIGURE 2
The potential binding sites and the diagram of the *CD55* promoter. **(A, B)** The potential conserved sequence of *TFCP2* and *NF-κB* binding site in the promoter of *CD55* by Contra v3. **(C)** A diagram of the *CD55* promoter region that was cloned in the luciferase reporter vector.

ChIP assay presented that *TFCP2* and *NF-κB* were combined to the promoter of *CD55* (Figure 3H), which further supported the binding capability of *TFCP2* and *NF-κB* to the promoter of *CD55*.

3.3 Regulation of *CD55* 3′UTR activity

Through TargetScan and starBase v2.0 database, we found that there was one potential binding site of miR-27a-3p in the 3′UTR of *CD55* (Figure 4A). Using the dataset from GEO, we found that miR-27a was downregulated in colorectal cancer (Figure 4B). We then conducted a CCK8 assay to see the effect of miR-27a on cell proliferation and found that miR-27a inhibited cell proliferation by 37.8%. We constructed luciferase reporter plasmid of *CD55* 3′UTR with or without mutated miR-27a-3p binding site. By co-transfecting with miR-27a-3p mimics or its mimics control into HCT116 or using an antagomir of miR-27a-3p or its antagomir control, we found that the luciferase reporter activity of *CD55* 3′UTR reduced by 56% by miR-27a-3p mimics and increased by 33% by miR-27a-3p antagomir ($p < 0.001$) (Figure 4C). Next, after transfecting miR-27a-3p mimics

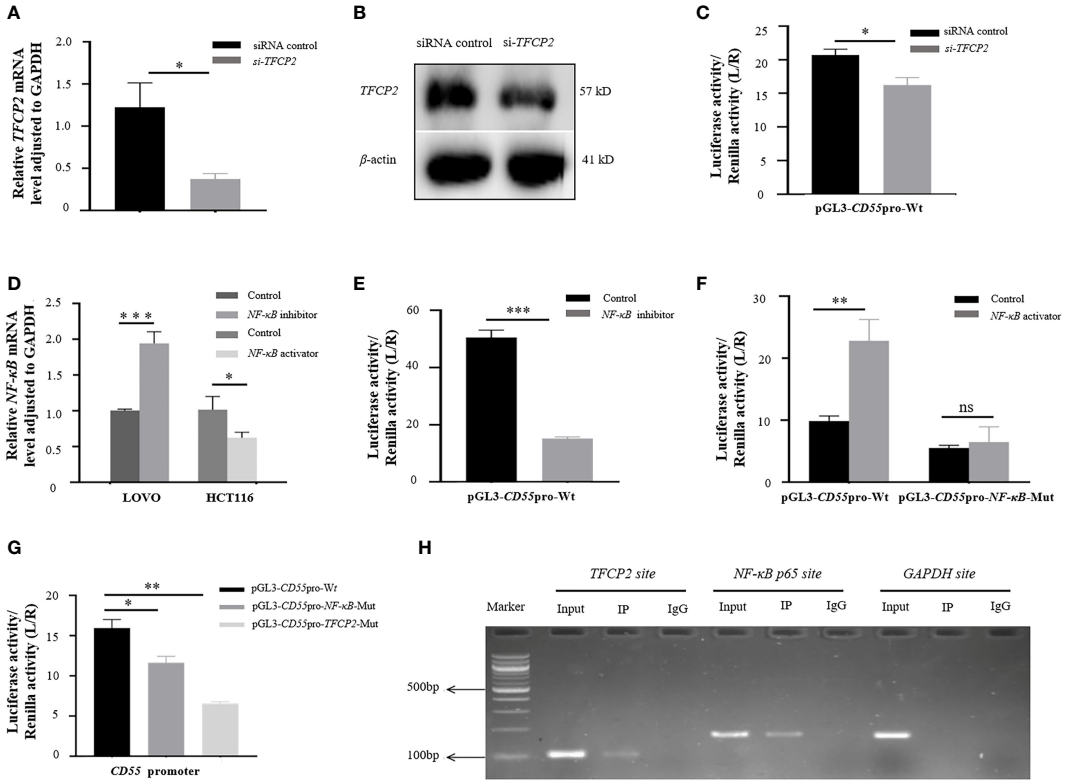

FIGURE 3
The regulation of transcription factors to the promoter of *CD55*. **(A)** The mRNA level of *TFCP2* by RT-PCR after HCT116 cells transfected with si-*TFCP2* or siRNA control for 24 h. **(B)** The protein expression of *TFCP2* by Western blotting after HCT116 cells transfected with si-*TFCP2* or siRNA control for 48 h. **(C)** Dual-luciferase assay of pGL3-$CD55_{pro}$-Wt in HCT116 cells after co-transfected with si-*TFCP2*. **(D)** The mRNA level of *NF-κB* in HCT116 cells treated with *NF-κB* inhibitor and that in LOVO cells treated with *NF-κB* activator for 24 h. **(E)** The luciferase activity of pGL3-$CD55_{pro}$-Wt in HCT116 cells treated with or without *NF-κB* inhibitor. **(F)** The luciferase activity of pGL3-$CD55_{pro}$-Wt and pGL3-$CD55_{pro}$-*NF-κB*-Mut in LOVO cells treated with or without *NF-κB* activator (TNFα). **(G)** *CD55* promoter activity assay in pGL3-$CD55_{pro}$-Wt, pGL3-$CD55_{pro}$-*NF-κB*-Mut, and pGL3-$CD55_{pro}$-*TFCP2*-Mut plasmids. Luciferase activity was normalized to Renilla luciferase activity (L/R). **(H)** The binding of *TFCP2* and *NF-κB* to the promoter of *CD55* by ChIP. IgG from rabbits served as a control (*$p < 0.05$, **$p < 0.01$, ***$p < 0.001$, ns, no significance). ChIP, chromatin immunoprecipitation.

into HCT116, we found that *CD55* was upregulated by miR-27a-3p (Figure 4D).

3.4 *CD55* was regulated by methylation modification

SurvivalMeth presented that three methylation sites (cg00797651, cg22048546, and cg25771140) appeared in the promoter of *CD55*. Among these sites, cg00797651 has a lower DNA methylation level in tumor samples than in normal samples ($p < 0.01$) (Figure 5A). Then, we divided the samples into high- and low-risk groups by differentially methylated sites and compared the methylation level of CpGs between the two groups. We found that the high-risk group had lower methylation levels (Figures 5B, C).

3.5 Protein–protein interaction network analysis of *CD55*-related proteins and their functional annotation

We constructed a PPI regulatory network for *CD55*-related proteins using the STRING database. When setting the size cutoff to "no more than 20 interactors", *CFP*, *CFB*, *C4A*, *C4B*, *C5AR1*, *C3*, *C3AR1*, *C2*, *EGF*, *LCK*, *CD59*, *PIGA*, *PGAP1*, *ICAM1*, *EMR2*, and *CD97* proteins were incorporated (Figure 6). The top three GO enrichment involved in complement activation and apoptotic cell clearance at the biological process level was as follows: extracellular exosome, extracellular space, and plasma membrane at the cellular component level, and complement binding, endopeptidase inhibitor activity, and complement receptor activity at the molecular function level (Figure 7A; Table 2). KEGG pathway enrichment analysis showed that these genes were significantly enriched in complement and coagulation cascade pathways, *Staphylococcus aureus* infection pathways, coronavirus disease–COVID-19, alcoholic liver disease pathways, pertussis pathways, etc. (Figure 7B; Table 3).

4 Discussion

The complement system in humans remains on standby and constantly on high alert for any potential intruders (15). The membrane complement regulatory proteins (*CD35*, *CD46*, *CD55*, and *CD59*) are important regulators of the complement system and are widely expressed on the surface of cells. In addition to the normal cells and tissues, the mCRPs also protect malignant cells from

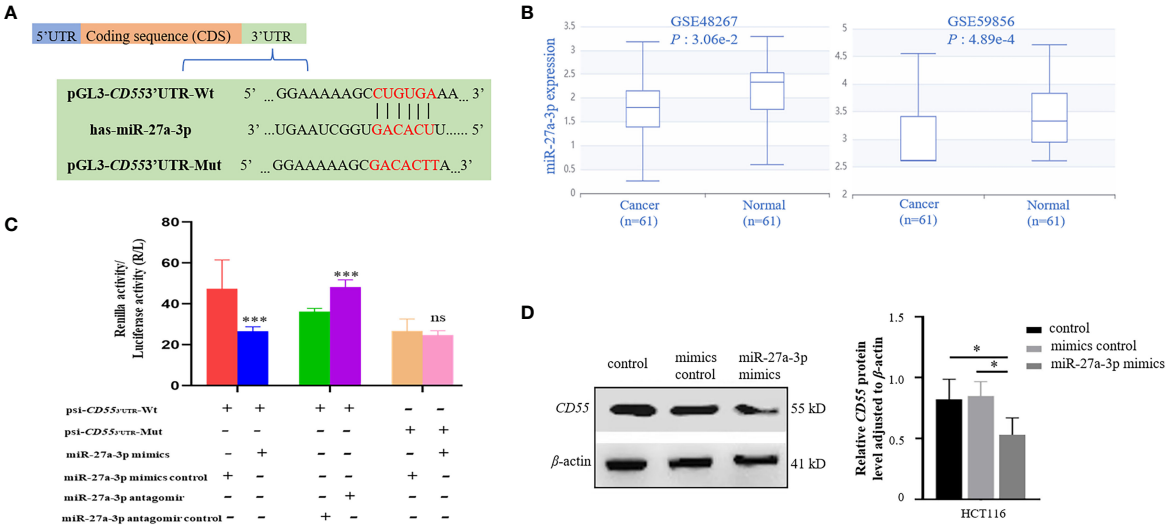

FIGURE 4
Binding and regulation of miRNA to *CD55* 3′UTR. **(A)** TargetScan and starBase v2.0 database predicted miR-27a-3p binding site in the 3′UTR of *CD55*. **(B)** The differential expression of miR-27a in two colon cancer GEO datasets ($p < 0.05$). **(C)** Verification of the potential binding of miR-27a-3p mimics or antagomir with *CD55* using luciferase reporter assay. The luciferase reporter activity of *CD55* 3′UTR reduced by miR-27a-3p mimics and increased miR-27a-3p antagomir ($p < 0.001$). The relative luciferase activity was normalized to the Renilla luciferase activity. Each experiment was performed in triplicate. Data are presented as the mean value ± SD (*$p < 0.05$; **$p < 0.01$; ***$p < 0.001$, ns, no significance). **(D)** The protein expression of *CD55* in HCT116 cells determined by Western blotting and densitometry analysis after cells were transfected with or without miR-27a-3p mimics (negative control) or with mimics control for 48 h (*$p < 0.05$). GEO, Gene Expression Omnibus.

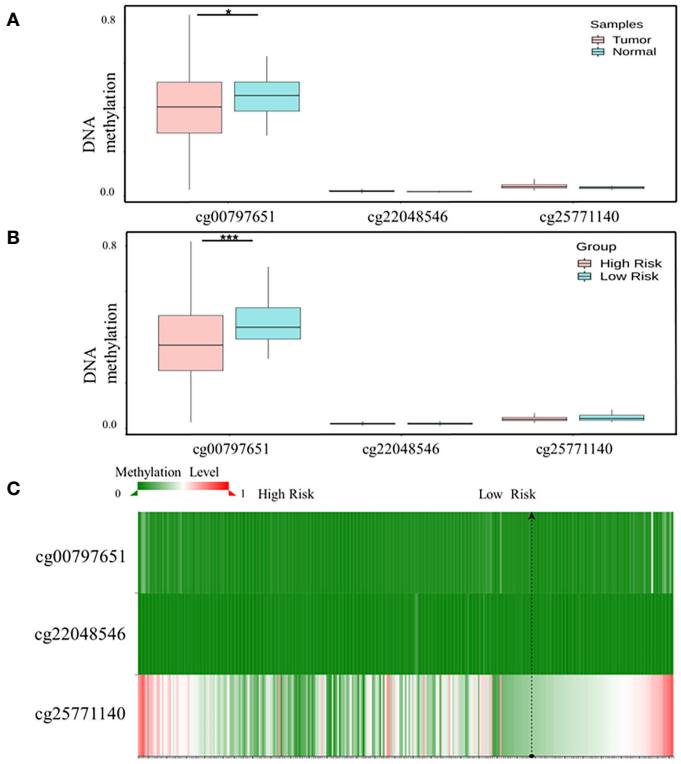

FIGURE 5
Methylation modification of *CD55* promoter in colon cancer. **(A)** The cg sites of *CD55* promoter region in COAD by SurvivalMeth. **(B)** The methylation level of CpGs in high- and low-risk groups. **(C)** The heatmap of three cg sites and their methylation level (*$p < 0.05$, ***$p < 0.001$). COAD, colon adenocarcinoma.

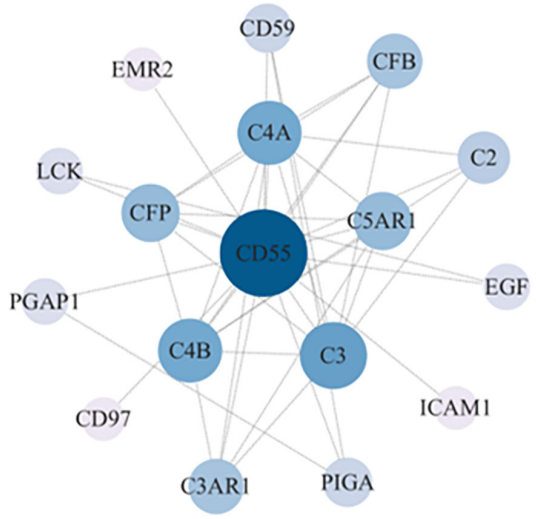

FIGURE 6
CD55 PPI network analysis. The PPI network of *CD55* and related proteins were visualized by the STRING database. PPI, protein–protein interaction.

complement attack (16). For example, all hematopoietic cells, as well as endothelial and epithelial tissues, express *CD55*/*DAF* (17, 18). In comparison to the surrounding normal tissues, *CD55*/*DAF* is often expressed at substantially higher levels in a variety of malignant cells, including cells of CRC (19). The findings of the present study are consistent with those of the previous studies.

According to the UALCAN program, CRC tissues had higher levels of *CD55* than normal tissue, which is supported by the data from the IHC and HPA databases (20). Notably, high expression of *CD55* can also promote the dissemination of tumor cells in circulation. Blocking or downregulating *CD55* may be an important step in advancing the efficacy of monoclonal antibody (mAb) immunotherapy for cancer (16).

Transcription factor CP2 (*TFCP2*) belongs to the *TFCP2*/*Grainyhead* family. The ubiquitous expression of *TFCP2* suggests its involvement in comprehensive cellular functions and diseases such as cancer, Alzheimer's disease, and AIDS (21). Previous studies have identified *TFCP2* as a pro-cancer factor in hepatocellular carcinoma (22), pancreatic cancer (23), breast cancer (24), and CRC (25). Additionally, *TFCP2* acts as a tumor suppressor, inhibiting the development of melanoma (26). Using the TRANSFAC online program, we found that *TFCP2* potentially binds to the promoter of *CD55*. To verify this, we conducted a dual-luciferase reporter assay. After knocking down *TFCP2* by siRNA, we found that the promoter activity of *CD55* reduced by 21%; however, after the mutated *TFCP2* binding site, it reduced by 66%. RNA interference (RNAi) is a natural process of target mRNA degradation. After we used si-*TFCP2*, the expression *TFCP2* was decreased by more than 50%; however, *TFCP2* could still bind to the promoter of *CD55*. After we mutated the binding site of *TFCP2*, *TFCP2* hardly binds to the promoter of *CD55* to regulate the expression of *CD55*. We then performed a ChIP assay

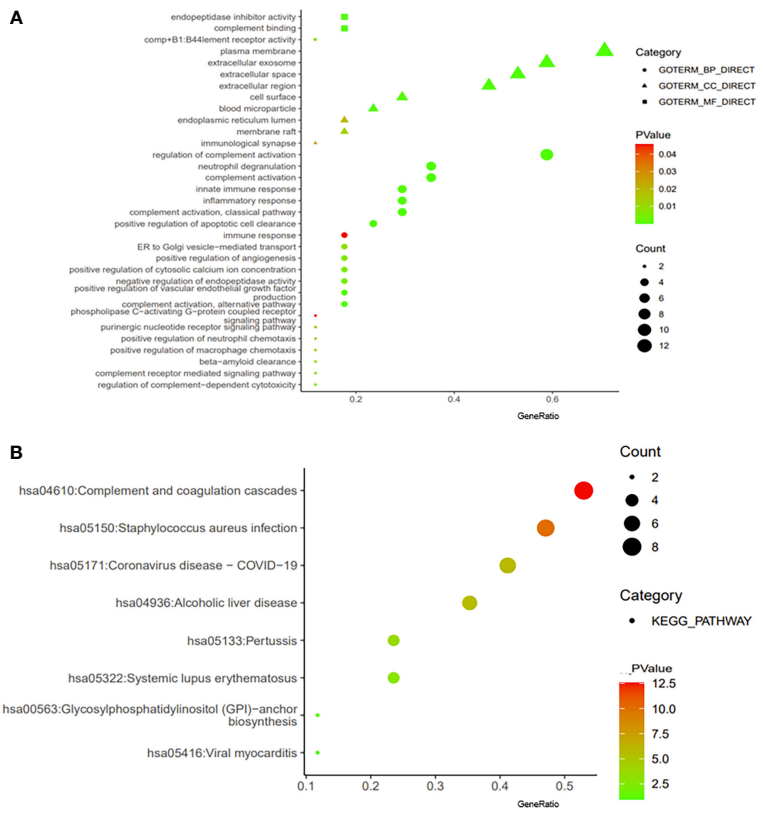

FIGURE 7
Enrichment analysis of *CD55*. The visualization of GO enrichment analysis **(A)** and KEGG enrichment analysis **(B)** of *CD55* by DAVID 6.8. GO, Gene Ontology; KEGG, Kyoto Encyclopedia of Genes and Genomes.

TABLE 2 GO pathway enrichment analysis.

GO	ID	Description	*p*-Value	Gene ID
BP	GO:0030449	Regulation of complement activation	1.02E−17	*C4B*, *C3*, *C4A*, *C5AR1*, *C3AR1*, *CD59*, *CFP*, *CD55*, *CFB*, *C2*
BP	GO:006956	Complement activation	4.96E−09	*C4B*, *C3*, *C4A*, *CFP*, *CFB*, *C2*
BP	GO:2000427	Positive regulation of apoptotic cell clearance	6.02E−09	*C4B*, *C3*, *C4A*, *C2*
CC	GO:0070062	Extracellular exosome	2.76E−06	*C4B*, *C3*, *C4A*, *LCK*, *EGF*, *CD59*, *CD55*, *CFB*, *ICAM1*, *C2*
CC	GO:0005615	Extracellular space	1.14E−05	*C4B*, *C3*, *C4A*, *EGF*, *CD59*, *CFP*, *CFB*, *ICAM1*, *C2*
CC	GO:0005886	Plasma membrane	3.35E−05	*C4B*, *C3*, *C4A*, *LCK*, *EGF*, *C5AR1*, *C3AR1*, *CD59*, *CFP*, *CD55*, *CFB*, *ICAM1*
MF	GO:0001848	Complement binding	7.74E−06	*C4B*, *CD59*, *CFB*
MF	GO:0004866	Endopeptidase inhibitor activity	4.80E−04	*C4B*, *C3*, *C4A*
MF	GO:0004875	Complement receptor activity	0.01	*C5AR1*, *C3AR1*

GO, Gene Ontology; BP, biological process; MF, molecular function; CC, cellular component.

TABLE 3 KEGG pathway enrichment analysis.

ID	Description	*p*-Value	Gene ID
hsa04610	Complement and coagulation cascades	2.96E−13	*C4B*, *C3*, *C4A*, *C5AR1*, *C3AR1*, *CD59*, *CD55*, *CFB*, *C2*
hsa05150	*Staphylococcus aureus* infection	8.36E−11	*C4B*, *C3*, *C4A*, *C5AR1*, *C3AR1*, *CFB*, *ICAM1*, *C2*
hsa05171	Coronavirus disease–COVID-19	1.27E−06	*C4B*, *C3*, *C4A*, *C5AR1*, *C3AR1*, *CFB*, *C2*
hsa04936	Alcoholic liver disease	2.70E−06	*C4B*, *C3*, *C4A*, *C5AR1*, *C3AR1*, *C2*
hsa05133	Pertussis	2.67E−04	*C4B*, *C3*, *C4A*, *C2*

KEGG, Kyoto Encyclopedia of Genes and Genomes.

and found that *TFCP2* directly binds to the promoter of *CD55* in colon cancer cells.

Nuclear factor-kappa B (*NF-κB*), belonging to the *Rel/NF-κB* family, regulates innate and adaptive immune responses (27). *NF-κB* is involved in tumorigenesis by regulating some important cell cycle-related genes, promoting cell proliferation, and inhibiting cell death (28). Using the TRANSFAC program, we found that *NF-κB* might bind to the promoter of *CD55*, which was subsequently confirmed by the dual-luciferase reporter assay. Colorectal cancer is a typical inflammation-dependent cancer (29, 30). *NF-κB* signaling is shown to link inflammation and the development of cancer (31). Moreover, ChIP provided clear evidence to support this finding.

MiRNAs are small non-coding regulatory RNAs (ncRNAs) that inhibit gene expression at a post-transcriptional level by binding to the 3′UTR of target mRNAs (32). Minor changes in miRNA have significant effects on gene expression (33). The dysregulation of miRNA was found in colon cancer tissues (34). Studies have shown that miR-27a-3p targets *BTG1* to affect the biological phenotype of colorectal and ovarian cancer cells (35, 36). Additionally, in colon cancer cells, wild-type *p53* downregulated the expression of miR-27a-3p (37). In the current study, through TargetScanHuman 7.2, we predicted that miR-27a-3p targeted the 3′UTR of *CD55*. Subsequently, *CD55* was confirmed as a direct target of miR-27a-3p by a dual-luciferase reporter gene assay. It is reasonable to speculate that miR-27a-3p affects colon cancer cells by targeting *CD55*.

DNA methylation is a form of epigenetic modification. Aberrant DNA methylation has been identified as an important aspect of promoting CRC pathogenesis by silencing tumor suppressor genes. Studies have found that DNA hypermethylation could promote CRC metastasis by regulating *CEBPB* and *TFCP2* (38). Using the SurvivalMeth program, we found that the promoter region of *CD55* does have hypermethylation sites in colon cancer tissues. However, we did not find any overlap between hypomethylation sites in colorectal cancer cells and any of the putative binding sites identified on the *CD55* promoter or impaired *NF-κB* binding to the *CD55* promoter. Future research is still required to identify the mechanism.

The PPI network showed that *CD55* and the key complement system components *C3*, *C4A*, and *C4B* are closely related to colon cancer. Studies have shown that C3 is also an immune-related core differential protein in colon adenocarcinoma (COAD) and is negatively correlated with the overall survival of COAD patients (39). Recent studies proposed that deficiency or pharmacological blockade of *C5aR1* significantly impeded tumorigenesis of CRC, and the over-expression of *C5aR1* contributed to the poor prognosis of CRC patients (40, 41). *CFP* plays a positive role in regulating the natural immune system in alternative pathways, and it is associated with immune infiltration in gastric cancer and lung cancer (42). We speculated that *CFP* and *CD55* might be involved in the immune infiltration of tumor cells in colon cancer. This evidence

indicated that *CD55* promoted cancer by regulating complement activation either directly or indirectly (43).

In conclusion, the expression of *CD55* in colon cancer was associated with the genetic regulation of *TFCP2*, *NF-κB*, epigenetic regulation of miR-27a-3p, and methylation modification. The genes associated with *CD55* are probably involved in immune-related pathways in colon cancer. This study provides a theoretical basis and insight into the development of biomarkers for future research in the field of colon cancer.

Data availability statement

The datasets presented in this study can be found in online repositories. The names of the repository/repositories and accession number(s) can be found in the article/supplementary material.

Author contributions

JL and NF: conceptualization, writing—original draft, and validation. ZY, AL, HW, YJ, HX, and QS: methodology and validation. AL and SJ: software and data curation. ZZ and XZ: supervision, writing—review and editing, and project administration. XZ: funding acquisition. All authors contributed to the article and approved the submitted version.

Funding

This study was supported by the Key Project of the Natural Science Foundation of Hebei province of China (grant number H2017209233).

Acknowledgments

The manuscript has previously appeared in a preprint: (44).

Conflict of interest

The authors declare that the research was conducted in the absence of any commercial or financial relationships that could be construed as a potential conflict of interest.

Publisher's note

References

1. Siegel RL, Miller KD, Jemal A. Cancer statistics, 2020. *CA: Cancer J Clin* (2020) 70 (1):7–30. doi: 10.3322/caac.21590

2. Siegel RL, Torre LA, Soerjomataram I, Hayes RB, Bray F, Weber TK, et al. Global patterns and trends in colorectal cancer incidence in young adults. *Gut* (2019) 68 (12):2179–85. doi: 10.1136/gutjnl-2019-319511

3. Lambert SA, Jolma A, Campitelli LF, Das PK, Yin Y, Albu M, et al. The human transcription factors. *Cell* (2018) 172(4):650–65. doi: 10.1016/j.cell.2018.01.029

4. Feinberg AP, Vogelstein B. Hypomethylation distinguishes genes of some human cancers from their normal counterparts. *Nature* (1983) 301(5895):89–92. doi: 10.1038/301089a0

5. Razin A, Riggs AD. DNA Methylation and gene function. *Sci (New York NY)* (1980) 210(4470):604–10. doi: 10.1126/science.6254144

6. Felsenfeld G, McGhee J. Methylation and gene control. *Nature* (1982) 296 (5858):602–3. doi: 10.1038/296602a0

7. Matharu N, Ahituv N. Modulating gene regulation to treat genetic disorders. *Nat Rev Drug Discovery* (2020) 19(11):757–75. doi: 10.1038/s41573-020-0083-7

8. Esteller M. Epigenetics in cancer. *New Engl J Med* (2008) 358(11):1148–59. doi: 10.1056/NEJMra072067

9. Dunkelberger JR, Song WC. Complement and its role in innate and adaptive immune responses. *Cell Res* (2010) 20(1):34–50. doi: 10.1038/cr.2009.139

10. Afshar-Kharghan V. The role of the complement system in cancer. *J Clin Invest* (2017) 127(3):780–9. doi: 10.1172/jci90962

11. Dho SH, Cho EH, Lee JY, Lee SY, Jung SH, Kim LK, et al. A novel therapeutic anti –CD55 monoclonal antibody inhibits the proliferation and metastasis of colorectal cancer cells. *Oncol Rep* (2019) 42(6):2686–93. doi: 10.3892/or.2019.7337

12. Durrant LG, Chapman MA, Buckley DJ, Spendlove I, Robins RA, Armitage NC. Enhanced expression of the complement regulatory protein CD55 predicts a poor prognosis in colorectal cancer patients. *Cancer immunol immunother CII* (2003) 52 (10):638–42. doi: 10.1007/s00262-003-0402-y

13. Bao D, Zhang C, Li L, Wang H, Li Q, Ni L, et al. Integrative analysis of complement system to prognosis and immune infiltrating in colon cancer and gastric cancer. *Front Oncol* (2020) 10:553297. doi: 10.3389/fonc.2020.553297

14. Thul PJ, Lindskog C. The human protein atlas: A spatial map of the human proteome. *Protein Sci Publ Protein Soc* (2018) 27(1):233–44. doi: 10.1002/pro.3307

15. Liszewski MK, Farries TC, Lublin DM, Rooney IA, Atkinson JP. Control of the complement system. *Adv Immunol* (1996) 61:201–83. doi: 10.1016/s0065-2776(08)60868-8

16. Gorter A, Meri S. Immune evasion of tumor cells using membrane-bound complement regulatory proteins. *Immunol Today* (1999) 20(12):576–82. doi: 10.1016/s0167-5699(99)01537-6

17. Medof ME, Walter EI, Rutgers JL, Knowles DM, Nussenzweig V. Identification of the complement decay-accelerating factor (DAF) on epithelium and glandular cells and in body fluids. *J Exp Med* (1987) 165(3):848–64. doi: 10.1084/jem.165.3.848

18. Asch AS, Kinoshita T, Jaffe EA, Nussenzweig V. Decay-accelerating factor is present on cultured human umbilical vein endothelial cells. *J Exp Med* (1986) 163(1):221–6. doi: 10.1084/jem.163.1.221

19. Li L, Spendlove I, Morgan J, Durrant LG. CD55 is over-expressed in the tumour environment. *Br J Cancer* (2001) 84(1):80–6. doi: 10.1054/bjoc.2000.1570

20. Shang Y, Chai N, Gu Y, Ding L, Yang Y, Zhou J, et al. Systematic immunohistochemical analysis of the expression of CD46, CD55, and CD59 in colon cancer. *Arch Pathol Lab Med* (2014) 138(7):910–9. doi: 10.5858/arpa.2013-0064-OA

21. Veljkovic J, Hansen U. Lineage-specific and ubiquitous biological roles of the mammalian transcription factor LSF. *Gene* (2004) 343(1):23–40. doi: 10.1016/j.gene.2004.08.010

22. Santhekadur PK, Rajasekaran D, Siddiq A, Gredler R, Chen D, Schaus SE, et al. The transcription factor LSF: a novel oncogene for hepatocellular carcinoma. *Am J Cancer Res* (2012) 2(3):269–85.

23. Yuedi D, Yuankun C, Jiaying Z, Han L, Yueqi W, Houbao L, et al. TFCP2 activates beta-catenin/TCF signaling in the progression of pancreatic cancer. *Oncotarget* (2017) 8 (41):70538–49. doi: 10.18632/oncotarget.19741

24. Zhao Y, Kaushik N, Kang JH, Kaushik NK, Son SH, Uddin N, et al. A feedback loop comprising EGF/TGFα sustains TFCP2-mediated breast cancer progression. *Cancer Res* (2020) 80(11):2217–29. doi: 10.1158/0008-5472.Can-19-2908

25. Shao K, Pu W, Zhang J, Guo S, Qian F, Glurich I, et al. DNA Hypermethylation contributes to colorectal cancer metastasis by regulating the binding of CEBPB and TFCP2 to the CPEB1 promoter. *Clin Epigenet* (2021) 13(1):89. doi: 10.1186/s13148-021-01071-z

26. Kotarba G, Krzywinska E, Grabowska AI, Taracha A, Wilanowski T. TFCP2/TFCP2L1/UBP1 transcription factors in cancer. *Cancer Lett* (2018) 420:72–9. doi: 10.1016/j.canlet.2018.01.078

27. Liang Y, Zhou Y, Shen P. NF-kappaB and its regulation on the immune system. *Cell Mol Immunol* (2004) 1(5):343–50.

28. Naugler WE, Karin M. NF-kappaB and cancer-identifying targets and mechanisms. *Curr Opin Genet Dev* (2008) 18(1):19–26. doi: 10.1016/j.gde.2008.01.020

29. Coussens LM, Werb Z. Inflammation and cancer. *Nature* (2002) 420(6917):860–7. doi: 10.1038/nature01322

30. Grivennikov SI, Greten FR, Karin M. Immunity, inflammation, and cancer. *Cell* (2010) 140(6):883–99. doi: 10.1016/j.cell.2010.01.025

31. Taniguchi K, Karin M. NF-κB, inflammation, immunity and cancer: coming of age. *Nat Rev Immunol* (2018) 18(5):309–24. doi: 10.1038/nri.2017.142

32. Lee YS, Dutta A. MicroRNAs in cancer. *Annu Rev Pathol* (2009) 4:199–227. doi: 10.1146/annurev.pathol.4.110807.092222

33. Cao Y, Hu J, Fang Y, Chen Q, Li H. Association between a functional variant in microRNA-27a and susceptibility to colorectal cancer in a Chinese han population. *Genet Mol Res GMR* (2014) 13(3):7420–7. doi: 10.4238/2014.September.12.8

34. Xi Y, Formentini A, Chien M, Weir DB, Russo JJ, Ju J, et al. Prognostic values of microRNAs in colorectal cancer. *biomark Insights* (2006) 2:113–21. doi: 10.1177/117727190600100009

35. Choo KB, Soon YL, Nguyen PN, Hiew MS, Huang CJ. MicroRNA-5p and -3p co-expression and cross-targeting in colon cancer cells. *J Biomed Sci* (2014) 21(1):95. doi: 10.1186/s12929-014-0095-x

36. Su C, Huang DP, Liu JW, Liu WY, Cao YO. miR-27a-3p regulates proliferation and apoptosis of colon cancer cells by potentially targeting BTG1. *Oncol Lett* (2019) 18 (3):2825–34. doi: 10.3892/ol.2019.10629

37. Li E, Han K, Zhou X. microRNA-27a-3p down-regulation inhibits malignant biological behaviors of ovarian cancer by targeting BTG1. *Open Med (Wars)* (2019) 14:577–85. doi: 10.1515/med-2019-0065

38. Xi Y, Shalgi R, Fodstad O, Pilpel Y, Ju J. Differentially regulated micro-RNAs and actively translated messenger RNA transcripts by tumor suppressor p53 in colon cancer. *Clin Cancer Res an Off J Am Assoc Cancer Res* (2006) 12(7 Pt 1):2014–24. doi: 10.1158/1078-0432.Ccr-05-1853

39. Liang JZ, Liang XL, Zhong LY, Wu CT, Zhang J, Wang Y. Comparative proteome identifies complement component 3-mediated immune response as key difference of colon adenocarcinoma and rectal adenocarcinoma. *Front Oncol* (2020) 10:617890. doi: 10.3389/fonc.2020.617890

40. Ding P, Li L, Li L, Lv X, Zhou D, Wang Q, et al. C5aR1 is a master regulator in colorectal tumorigenesis *via* immune modulation. *Theranostics* (2020) 10(19):8619–32. doi: 10.7150/thno.45058

41. Ding P, Xu Y, Li L, Lv X, Li L, Chen J, et al. Intracellular complement C5a/C5aR1 stabilizes β-catenin to promote colorectal tumorigenesis. *Cell Rep* (2022) 39(9):110851. doi: 10.1016/j.celrep.2022.110851

42. Cui G, Geng L, Zhu L, Lin Z, Liu X, Miao Z, et al. CFP is a prognostic biomarker and correlated with immune infiltrates in gastric cancer and lung cancer. *J Cancer* (2021) 12(11):3378–90. doi: 10.7150/jca.50832

43. Geller A, Yan J. The role of membrane bound complement regulatory proteins in tumor development and cancer immunotherapy. *Front Immunol* (2019) 10:1074. doi: 10.3389/fimmu.2019.01074

44. Liu J, Fu N, Wu H, Jin Y, Li A, Song Q, et al. The genetic and epigenetic regulation of CD55 and its pathway analysis in colon cancer. *Res Square* (2022). doi: 10.21203/rs.3.rs-1583620/v1

Frontiers in Immunology

Explores novel approaches and diagnoses to treat immune disorders.

The official journal of the International Union of Immunological Societies (IUIS) and the most cited in its field, leading the way for research across basic, translational and clinical immunology.

Discover the latest Research Topics

See more →

Frontiers

Avenue du Tribunal-Fédéral 34
1005 Lausanne, Switzerland
frontiersin.org

Contact us

+41 (0)21 510 17 00
frontiersin.org/about/contact